Solid–Liquid Separation

Solid–Liquid Separation

Fourth Edition

Editor

Ladislav Svarovsky, Dipl Ing, PhD, CEng, FIChem E

Professor of Chemical Engineering, FPS Institute, England and
University of Pardubice, Czech Republic

BUTTERWORTH HEINEMANN

OXFORD AUCKLAND BOSTON JOHANNESBURG MELBOURNE NEW DELHI

Butterworth-Heinemann
Linacre House, Jordan Hill, Oxford OX2 8DP
225 Wildwood Avenue, Woburn, MA 01801-2041
A division of Reed Educational and Professional Publishing Ltd

 A member of the Reed Elsevier plc group

First published 1977
Reprinted 1979
Second edition 1981
Third edition 1990
Reprinted 1991
Fourth edition 2000

British Library Cataloguing in Publication Data
A catalogue record for this book is available from the British Library

Library of Congress Cataloguing in Publication Data
A catalogue record for this book is available from the Library of Congress

ISBN 0 7506 4568 7

Typeset in India at Integra Software Services Pvt Ltd, Pondicherry 605005

Contents

Preface to the fourth edition

My book now enters a new millennium and does so in a much revised form. The first edition, published in 1977, had developed from a course manual for our short course on the same subject which started in 1974 and has run annually ever since. Both the course and later the book had answered a call from Frank Tiller ('The Crisis in Filtration Technology', *Filtration & Separation*, November/December, 1973). It was thanks to his clear message initially and his personal encouragement later that I found myself so much in the midst of a subject that has prospered ever since.

In the past the course was given as a four-day course called Solid–Liquid Separation annually in Bradford and occasionally abroad, and also as an in-house course in many companies worldwide. It has developed into an 'equipment users' course, with the Butterworth's book written specifically for it. The more recent version of the course is an open, three-day course entitled Filtration, Separation and Washing, with even more emphasis on practical application and with more time given to solids washing.

This edition of the book reflects those recent changes in the course. The reduction in the course duration, brought about by the need to accommodate the ever-busier industrialist, has sharpened our focus on the really practical and useful aspects of solid–liquid separation. A discerning reader will notice our reluctance to propagate 'academic nonsense' which dominates some areas of filtration and separation, its only practical use often being to obtain promotion points for its authors. Our course has flourished for over a quarter of a century by staying close to industrial practice and using only as much theory as necessary to understand the rules of equipment design and scale-up. I have now spent 30 years consulting in this and other closely related subjects, and my criterion for including equations on the course is whether I have ever needed them in consulting. I have tried to apply this to the book too, although, naturally, the book does have to go a little deeper than the course.

I will make it easier for the reviewers by outlining here what's new in this fourth edition. Firstly, there are the classics among the chapters, which have been left virtually untouched because they serve well and are timeless. This includes Wim Pearson's equipment selection chapter, Lawrence Loff's filter media and the two-part chapter on Coagulation and Flocculation by Mike Hughes and Ken Ives.

Secondly, some chapters have been omitted either because the topics are better dealt with in conjunction with equipment (e.g. filter aids) or the topic has never been warmly embraced by course participants and no longer warrants a separate chapter (although it is still covered in other parts of the book, such as in the Introduction), for example Magnetic Separation, Flotation and Deep Bed Filtration.

Thirdly, there are those chapters which only needed minor updating and amendments. These include Characterization of Particles Suspended in Liquids, Efficiency of Separation of Particles from Fluids, Hydrocyclones, Separation by Centrifugal Sedimentation, Filtration Fundamentals, Methods for Limiting Cake Growth, Pressure Filtration, Particle–Fluid Interaction, Thermodynamics of Solid–Liquid Separation.

Fouthly, there are some major revisions or total rewrites such as Introduction to Solid–Liquid Separation, Gravity Clarification and Thickening, Vacuum Filtration, Centrifugal Filtration and Countercurrent Washing.

And finally, there are the brand new chapters, such as Cake Washing and Separator Series and Networks, the introduction of which reflects the growing interest in industry.

Every time there is a new edition I find it exciting and this is no exception. I believe it is necessary to break some new ground and lay down the basics for the new century and millennium. Only until the next edition, of course.

L. S.

Preface to the first edition

It is with great pleasure and excitement that I introduce this work consisting of contributions from myself and several leading specialists. In my opinion it is nearly impossible for a single author to cover in depth most of the field of solid–liquid separation; not only because the field is very wide—it extends over very different branches of technology—but also because the range of equipment and principles involved is enormous. That is why I regard myself as very fortunate to have had the benefit of the co-operation of a group of contributors with whom I have worked over the past two years on post-experience courses for industry.

The contributors include consultants, academics and industrialists who, despite their inevitably varied approaches, have produced a book of surprisingly compact and coherent structure. All those who have ever ventured into editing a multi-author publication of this kind will know what a headache it can be to ensure that everyone meets the given deadlines; I have been fortunate in this respect too, as the high level of discipline and responsibility of the contributors has made my task relatively easy.

The book comprises chapters on basic fundamentals, on principles and on equipment, as well as on various important aspects of solid–liquid separation such as filter aids, washing, flocculation, etc. The emphasis is on the use of equipment rather than on its design, although the latter is not ignored; consequently, the book will probably be most useful to chemical engineers and process engineers, particularly those in plant operation, plant design or equipment testing and commissioning. I hope that we have managed to strike a good balance between practical and academic considerations as both are equally important and cannot be separated. The book can be used as a textbook for both undergraduate and postgraduate teaching and for the post-experience courses from which it originated.

My long list of acknowledgements and thanks must start with the contributors because without them this book would never have been possible. I am therefore indebted to Dr M. A. Hughes, a colleague at Bradford University; Professor K. J. Ives of University College, London; Dr D. G. Osborne of Anglo-American Corporation Ltd., Coal Division, Republic of South Africa; Mr A. L. Masters of Johns–Manville (Great Britain) Ltd.; Mr H. G. W. Pierson of Pierson & Co. (Manchester) Ltd.; Dr R. J. Wakeman of University

of Exeter; and Dr K. Zeitsch of Alfa–Laval Separationstechnik GmbH, Germany.

My own contributions naturally reflect my professional career and experience, both of which have been greatly influenced by a number of people. The late Professor J. Pulkrábek gave me the initial encouragement and opportunity in the field now called environmental engineering; Dr J. Smolik, also at the Technical University of Prague, first introduced me to particle–fluid separation and the work with him gave me a firm basis of knowledge in particle technology on which I have been building ever since. In Bradford, I have had the benefit of support and encouragement from Dr J. C. Williams together with a close association with Dr T. Allen, whose expertise in particle size measurement (and also in technical writing) has greatly benefited my own progress. I am also grateful to Professor C. Hanson and Professor W. L. Wilkinson both of whom have backed and encouraged my work in solid–liquid separation.

I must also acknowledge the useful work of a long string of undergraduate, postgraduate and extra-mural students who over the past few years have worked with me on various projects related to particle separation. Thanks are also due to many industrialists who have shared their experience with me and contributed indirectly to this publication. I am grateful to Professor Mullin, the series editor, for his guidelines and comments with regard to the manuscript.

Last but not least I am indebted to my own family who patiently suffered the inevitable reduction in my attention during the preparation of this book. My wife's engineering and computing expertise has enhanced my work and this is greatly appreciated.

L. S.

1 Introduction to solid–liquid separation

L. Svarovsky

FPS Institute, England and University of Pardubice, Czech Republic

Separation technology now has a dominant role in the chemical process industries. According to Ruthven, the editor of the recently published *Encyclopedia of Separation Technology*[1], separation has a dominant role in the chemical process industries. Since the mid-1990s, approximately half the capital investment and over half of the operating costs were associated with separation processes. This of course includes both the separation of chemical species and that of phases, with solid–liquid separation being part of the latter but often closely associated with the former.

That the importance of separation is to grow even further is certain. There are three main reasons for this:

1 the ever-increasing demands on product purity, particularly in the pharmaceutical, biotechnology and food industries,
2 the gradual reduction in the quality of raw materials, this being a particularly serious problem in mineral processing,
3 the growing demands for environmental acceptability of waste materials.

Solid–liquid separation plays an important role in separation. The abovementioned, two-volume *Encyclopedia of Separation Technology* has eight whole chapters on different aspects of it, including two, on Filtration and on Sedimentation, by the present author.

Most of the process industries in which particulate slurries are handled use some form of solid–liquid separation within their flowsheets. It is used in many processes with the aim of:

1 recovering and dewatering the valuable solids (this may be followed by washing),
2 recovering and cleaning the liquid,
3 separating the two phases from each other before recycling/reusing both,
4 separating the two phases, for environmental reasons, for example, before disposing of either or of both.

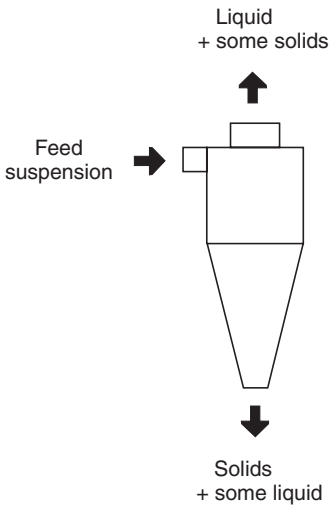

Figure 1.1 A schematic diagram of a separator

Similarly to other unit operations in chemical engineering such as mass or heat transfer, solid–liquid separation is never complete. Typically (see *Figure 1.1*) there may be some fine solids leaving in the overflow/filtrate stream and there will certainly be some liquid entrained with the bulk of the solids leaving through the underflow/cake. One of the important concerns in this subject is therefore the question, how complete is the separation achieved with a given piece of equipment under a given set of operating conditions?

The separation of the solids is usually expressed as mass recovery or 'total efficiency' (in filtration this is also known as 'retention') as dealt with in depth in chapter 3, whilst the separation of the liquid is usually characterized by the moisture content of the cake or concentration of solids in the underflow. Separation efficiencies of the solids and the liquid are best considered separately because different applications place different emphasis on the two: in thickening, for example, the emphasis is on the high efficiency for the liquid (i.e. high solids content in cakes or underflows), whilst in recovery or clarification, high efficiency for the solids is required. If the emphasis placed on the two efficiencies is equal then they can be combined in one criterion, the entropy index, discussed in Part II, chapter 18.

There are several processes in and aspects of solid–liquid separation which, due to their special role, require special attention. One such process closely married to solid–liquid separation is solid–solid separation by particle size, particle shape, solids density or affinity to water. The purpose here is to use the solid–liquid separation processes to remove only one fraction of the solids or only one mineral from a mixture.

Taking first the separation by particle size, this is clearly based on the size dependent nature of some solid–liquid separation principles and equipment

such as hydrocyclones or sedimenting centrifuges. Solids are 'classified' by the separation process and the feed is either split into coarse and fine fractions (with the fine fraction usually remaining in suspension) or only a tail removed from either end of the size distribution (de-gritting or de-sliming). Even in cases when solids classification is not required it may still be desirable before the solid–liquid separation stage in order that the material in each size range may be treated by the type of equipment best suited to it. The grade efficiency concept is used extensively here, the major concern being the steepness of the curve because it determines the amount of misplaced material (fines in the coarse product and coarse particles in the fine product), see chapter 3.

Gravity sedimentation equipment, hydrocyclones, sedimenting centrifuges or flotation cells have also been extensively used in mineral processing for separation of minerals according to density or affinity to water. In such separations, the efficiency is expressed by the Tromp curve which, similar to the grade efficiency curve, shows probability of separation as a function of material density or mineral composition. The steepness of the curve is a measure of the sharpness of the separation.

Another process closely related to solid–liquid separation is washing of solids. This is used to replace the mother liquor in the solids stream, in a cake form or as a suspension, with a wash liquid. The growing importance of this process is due to the demands for increasing purity of the products combined with the increasingly poorer raw materials available and growing requirements for environmental acceptability of wastes. Washing may often represent a dominant portion of the installation cost because it is usually multi-staged. The suitability of different equipment for solid–liquid separation to washing varies widely and there are three ways of doing it: by cake washing, by reslurrying and by successive dilution. Cake washing is potentially the most efficient, it may be advantageous to enhance it by compression and several models exist to describe and predict cake washing performance on the basis of a minimum of experimental measurements, see chapter 10.

Washing generally often has to be done in several stages and can be co-current or countercurrent. Chapter 15 deals with countercurrent washing arrangements as ways of saving on wash liquid requirement.

Dewatering is another process identified as part of solid–liquid separation and its aim is simply to reduce the moisture content of filter cakes or sediments. The most widely used ways of achieving this are mechanical compression of cakes, air displacement under vacuum or pressure, and drainage in a gravitational or centrifugal system. Other dewatering methods include shearing of cakes (sequential or simultaneous, by vibration, for example) or exposing cakes to other forms of energy such as sound or radio waves, all while under vacuum. Dewatering of cakes can also be enhanced by the addition of dewatering aids to the suspensions, in the form of surfactants which reduce surface tension. Dewatering of sludges in belt presses can be enhanced with electro-osmosis and with addition of polymers[2].

In dewatering by mechanical compression, the necesary prerequisite is the compressibility of the cake and this is usually expressed by one of two widely used empirical equations which relate average cake porosity ε_{av} to the final applied pressure across the cake Δp_c:

$$\varepsilon_{av} = (1 - a)\varepsilon_o(\Delta p_c)^a \tag{1.1}$$

$$\varepsilon_{av} = \varepsilon_o - b \log(\Delta p_c) \tag{1.2}$$

where a, b and ε_o are material-dependent constants.

In dewatering by air (or other gas) displacement, see *Figure 12.1* in chapter 12, the important issues are the threshold pressure which has to be exceeded in order that air may enter the filter cake, the irreducible saturation level which gives the least moisture content achievable by air displacement, and finally kinetic dewatering characteristics. Similarly, in dewatering by gravity or centrifugal action, the irreducible saturation and kinetic dewatering characteristics have to be known for effective equipment design and scale-up.

Before reviewing the available technology for solid–liquid separation it is important to consider briefly the methods of pretreatment of the suspensions for improved equipment performance.

1.1 Pretreatment of suspensions

As the title suggests, solid–liquid separation is the separation of two phases, solid and liquid, from a suspension. The technology for carrying out this process is often referred to as 'mechanical separation' because the separation is accomplished by purely physical means. This does not preclude chemical or thermal pretreatment which is increasingly used to enhance the separation that follows. Although some slurries separate perfectly well without chemical or physical conditioning, most slurries and pulps of a widely varying nature can benefit from pretreatment, whether the separation is by sedimentation (gravity or centrifugal), filtration or flotation. The chemical pretreatment is considered briefly here and in much more detail in chapter 4.

A conditioning effect can be obtained using several processes such as coagulation and flocculation, addition of inert filter aids, crystallization, freezing, temperature or pH adjustment, thermal treatment and ageing. Only the first two operations are considered in more detail here due to their importance and wide use.

1.1.1 Coagulation and flocculation (chapter 4)

The two words are often used interchangeably because both processes lead to increases of the effective particle size with the accompanying benefits of higher settling or flotation rates, higher permeability of filtration cakes, or

better particle retention in deep bed filters. There is, however, a subtle difference between coagulation and flocculation.

Coagulation is a process which brings particles into contact to form agglomerates. The suspension is 'de-stabilized' by addition of inorganic chemicals such as hydrolysis coagulants like alum or ferric salts, or lime, and the subsequent agglomeration can produce particles up to 1 mm in size. Some of the coagulants simply neutralize the surface charges on the primary particles, others suppress the double layer ('indifferent' electrolytes such as NaCl, $MgSO_4$) or some even combine with the particles through hydrogen bridging or complex formation.

Flocculation uses flocculating agents, usually in the form of natural or synthetic polyelectrolytes of high molecular weight, which interconnect and enmesh the colloidal particles into giant flocs up to 10 mm in size. Flocculating agents have undergone very fast development in the past three decades and this has led to a remarkable improvement in the use and performance of many types of separation equipment. As such agents are relatively expensive the correct dosage is critical and has to be carefully optimized. Overdosage is not merely uneconomic but may inhibit the flocculation process by coating the particles completely, with the subsequent restabilization of the suspension, or cause operating problems such as blinding of filter media or mud-balling and underdrain constriction in sand filters. Overdosage may also greatly increase the volume of sludge for disposal. Optimum dosage has been found to correspond to a situation when about one-half of the surface area of the particles is covered with polymer. As surface charges are also affected by pH, the control of it is therefore also essential in pretreatment.

The natural process of bringing the particles (and also the polyelectrolytes) together by Brownian motion (called 'perikinetic flocculation') is often assisted by 'orthokinetic flocculation' which increases particle collisions through the motion of the fluid and velocity gradients in the flow. This is the idea behind the use of in-line mixers or paddle-type flocculators in front of some separation equipment such as gravity clarifiers. The rate of flocculation in clarifiers is also increased by recycling of the flocs in order to increase the rate of particle–particle collisions through the increase in solids concentration.

The type of floc required depends very much on the separation process which follows. Rotary vacuum filtration, for example, requires evenly sized, small, strong flocs, with capture of ultra-fines within the floc to prevent cloth binding and cloudy filtrates. The flocs should not be subject to sedimentation in the vat or breakage by the agitator. Such flocs are not likely to cause localized air breakthrough, cake collapse, shrinkage or cracking in the dewatering stage.

In filtration operations which use gravity settling initially, such as the belt presses, large and loosely packing flocs are required. The resulting free-draining sediment can then be subjected to a controlled breakdown over a period of time, ultimately leading to a complete collapse of the cake due to mechanical squeezing between the belts.

In gravity thickening, large and relatively fragile flocs are needed, in order to allow high settling rates and fast collapse in the compression zone.

The optimum flocculant type and dosage depend on many factors such as solids concentration, particle size distribution, surface chemistry, electrolyte content and pH value, and the effect of these is very complex. The flocculant selection and optimization of dosage therefore require extensive experimentation with only some general guidance as to the ionic charge or molecular weight (or chain length) required. Anionic flocculants, for example, are known to perform well on coal slurries because the relatively high levels of calcium ions and hydrogen bonding provide salt linkages for the anchorage of the polymer anionic groups to the coal surface. Zero potential often does not seem to be involved because neutral (non-ionic) or even 'wrong' polyelectrolytes (cationic rather than anionic, or vice versa) can be quite effective.

1.1.2 Addition of inert aids prior to filtration, sedimentation or magnetic separation

Filter aids are rigid, porous and highly permeable powders which are added to the feed suspensions to extend the applicability of surface filtration. Very dilute or very fine and slimey suspensions are normally too difficult to filter by cake filtration due to fast pressure build-up and medium blinding, but the addition of filter aids can alleviate such problems. They can be used in either or both of the following modes of operation:

1 to form a pre-coat (which then acts as a filter medium) on a coarse support material called a septum, or
2 to be mixed with the feed suspensions as 'body feed' in order to increase the permeability of the resulting cake.

In the pre-coat mode, filter aids allow filtration of very fine or compressible solids from suspensions of 5% or higher solids concentration on a 'rotary drum pre-coat filter'. This modification of the rotary drum vacuum filter uses an advancing knife to skim off the separated solids and the uppermost layer of the thick pre-coat continuously, until the whole of the pre-coat is removed and a new layer has to be applied. This makes it possible to discharge very thin cakes as well as that part of the pre-coat which has been penetrated into by the solids and partially blinded.

In the pre-coat and body feed modes, filter aids allow application of surface filtration to clarification of liquids, i.e. filtration and very dilute suspensions of less than 0.1% by volume, such as those normally treated by deep bed filters or centrifugal clarifiers. Filter aids are used in this mode mostly with pressure filters although not exclusively so. A pre-coat is first formed by passing through the filter a suspension of the filter aid. This is followed by filtration of the feed liquid, which may have the filter aid mixed with it as

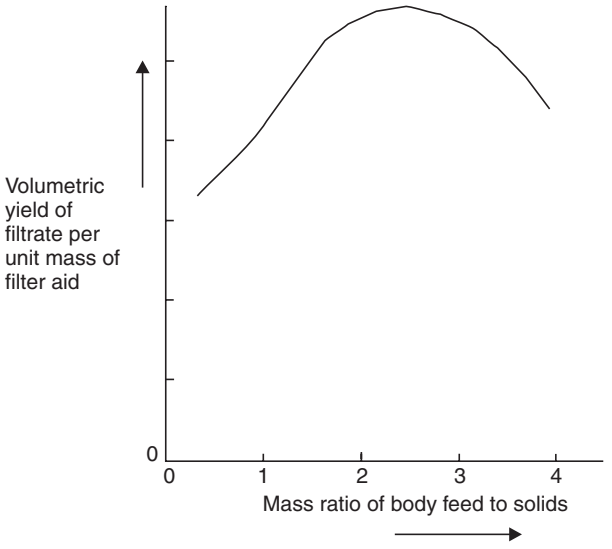

Figure 1.2 Optimization of body feed for maximum filtrate yield

'body feed' in order to improve the permeability of the resulting cake. The proportion of the filter aid to be added as body feed is of the same order as the amount of contaminant solids in the feed liquid and this of course limits the application of such systems to low concentrations. Recovery and regeneration of filter aids from the cakes is normally not practised except in a few very large installations where it might become economical.

Materials suitable as filter aids include diatomaceous earth, expanded perilitic rock, asbestos, cellulose, non-activated carbon, ashes, ground chalk or mixtures of those materials. Whilst mineral filter aids have been well established in industry for many decades, those based on organic, self-replenishing raw or even waste materials such as cellulose, wood fibres or plant fibres have been increasing in use[3]. The best situation is when a cheap or reject material can be found elsewhere in the process and is suitable for using as a filter aid, at little or no extra cost.

The amount of body feed is subject to optimization which has to be based on experiments but can be modelled mathematically[4]. The criterion for the optimization depends on the purpose of the filtration. Maximum yield of filtrate per unit mass of filter aid, as depicted in *Figure 1.2*, is probably the most common but least cake resistance[4]; longest cycle, fastest flow, or maximum utilization of cake space are other criteria which each require a different rate of body feed addition[5]. The tests to be carried out for such optimization normally use laboratory or pilot scale filters and have to include variation of the filtration parameters such as pressure or cake thickness in the optimization.

If the filter aid material has the right properties to benefit the filtration process, there is always an optimum similar to that in *Figure 2.1*. This

is because the addition of filter aid always improves performance at low feed-to-solids ratios but at high values the aid begins to dominate the process as the filtration performance approaches that of the pure filter aid (see the experimental filtrate yield curve in the example below, m/h). The rate of improvement levels off and, when expressed per mass or cost of the aid material, it is no longer economical or worthwhile. The optimum is between these two ends and this is best demonstrated in an example.

Example of filter aid optimization

20 m^3/h of a suspension containing 1 kg/m^3 solids are to be clarified. A pre-coat of 0.5 kg/m^2 of filter aid is needed at the start of each cycle and body feed has to be added during filtration. A cycle time of 1 h is to be used. The table in *Figure 1.3* gives experimental filtrate yields for different ratios of body feed to the solids in the original suspension.

(a) Complete the table and plot the second graph.
(b) Determine the optimum filtrate yield per kg of filter aid and the corresponding filter area.

Solution

body feed to solids (kg/kg)	filtrate yield per cycle (m/h)	filtration area for 20 m^3/h (m^2)	body feed required (kg/h)	pre-coat required (kg/h)	total filter aid required (kg/h)	filtrate yield per kg of aid (m/kg)
0.00	0.42	47.62	0.00	23.81	23.81	0.0176
0.50	0.98					
1.00	1.47					
1.50	1.80					
2.00	1.95					

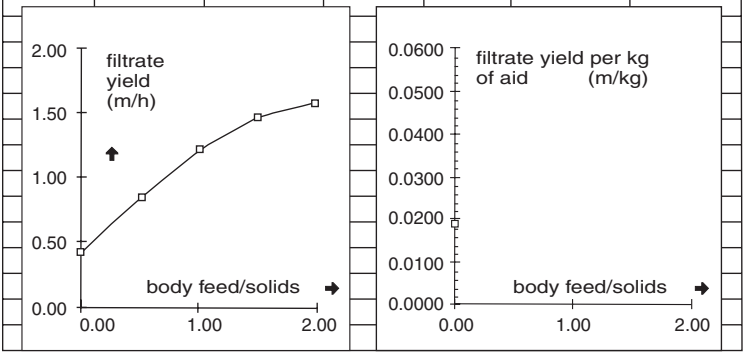

Figure 1.3

Starting with the *second row*,

column 3, the filtration area is $20/0.98 = 20.41\ m^2$

column 4, body feed required is $0.5 \times 20 = 10$ kg/h

column 5, pre-coat required is $0.5 \times 20.41 = 10.20$ kg/h
column 6, total fiter aid is $10.00 + 10.20 = 20.20$ kg/h
column 7, filtrate yield/kg is $0.98/20.20 = 0.0485$ m/kg
and the rest of the table is completed accordingly.

Referring to the tabulated data and the diagram of filtrate yield/kg of aid in *Figure 1.4*, the maximum on the curve is at the body feed/solids ratio of one, i.e.

optimum filtrate yield = **0.0548 m/kg** ($\equiv m^3/m^2kg$)
and filter area = **13.61 m²**

body feed to solids (kg/kg)	filtrate yield per cycle (m/h)	filtration area for 20 m^3/h (m^2)	body feed required (kg/h)	pre-coat required (kg/h)	total filter aid required (kg/h)	filtrate yield per kg of aid (m/kg)
0.00	0.42	47.62	0.00	23.81	23.81	0.0176
0.50	0.98	20.41	10.00	10.20	20.20	0.0485
1.00	1.47	13.61	20.00	6.80	26.80	0.0548
1.50	1.80	11.11	30.00	5.56	35.56	0.0506
2.00	1.95	10.26	40.00	5.13	45.13	0.0432

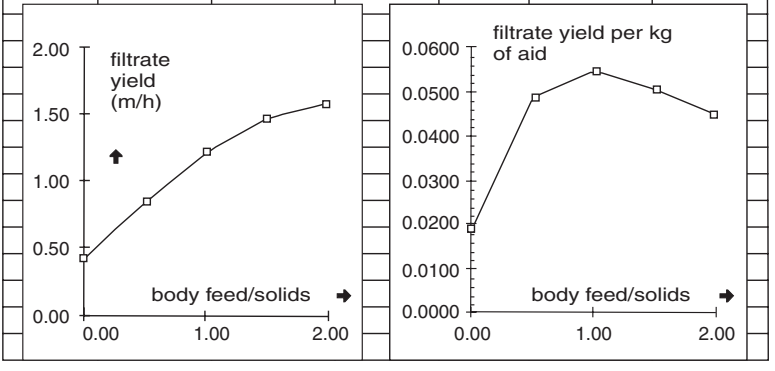

Figure 1.4

Aids can also be added prior to other separation processes. In sedimentation, for example, slow- or non-settling colloidal materials can be flocculated with sand or other cheap and dense solids, thereby making the agglomerates much more settleable. Probably the most famous process based on a similar principle is the Sirofloc process first developed in Australia by CSIRO (Australia) at around 1980[6], and with at least three water treatment plants now operating in UK. CSIRO (Australia) in conjunction with AUSTEP Pty Ltd have gained much experience in the operation of wet drum separators when incorporated in the 'Sirofloc' process for water treatment[7].

The Sirofloc process removes turbidity (algae, bacteria, colloidal matter) and dissolved coloured material from contaminated underground and surface waters or waste waters by flocculation with reusable magnetite particles (a waste product of some iron processing plants). The magnetite particles from 1 to 10 microns in size have great adsorptive powers and important magnetic

properties. The particles are treated to give them positively charged surfaces which then attract the negatively charged impurities. Agglomeration takes place, the particles are magnetized and the aggregates settle out very quickly by gravity or are separated on relatively cheap and robust magnetic drums[8]. Organic polyelectrolytes may also be used to achieve the aggregation in turbid waters which do not respond to magnetite alone.

A somewhat similar but high-tech process, the magnetically assisted chemical separation process, is discussed in section 2.2.

1.2 Equipment and principles

Figure 1.5 gives the general classification of equipment and principles of solid–liquid separation. There are two separate main groups of equipment which differ in the way the particles are collected.

In the first group of sedimentation and flotation, the liquid is constrained in a stationary or rotating vessel and the particles move freely within the liquid. The separation is due to mass forces acting on the particles because of an external or internal field of acceleration that might be the gravity field, centrifugal field or magnetic field. The separation process does not end by the arrival of the particles onto a collecting surface. If the process is to be continuous, the collected particles have to be transported and discharged from the separator vessel. If gravity or centrifugal fields are used (except in the case of flotation), a density difference must exist between the solids and the suspending liquid for the separation to take place. On the whole, the principles in this group can result in continuously operating equipment which often turns out to be cheaper than filtration. Gravity sedimentation or flotation should therefore be looked at as possible alternatives in the early stages of equipment selection.

The second group, loosely called filtration, constrains the particles by a medium and the liquid is allowed to flow freely through the medium. Density difference is not necessary in this group but a truly continuous operation is either not easy or impossible to achieve and the costs might be high.

Figure 1.5 lists the conventional separation processes as a further subdivision of the two main classes but it also shows some relatively novel methods developed in recent years. A brief description of the processes in *Figure 1.5* is given in the following, in the order from left to right. Note that where a separate chapter is devoted to the class of equipment in question, the chapter number is given in the section title. Equipment not covered in separate chapters is given somewhat more space here.

1.2.1 Flotation

Flotation is a gravity separation process based on the attachment of air or gas bubbles to solid (or liquid) particles, which are then carried to the liquid

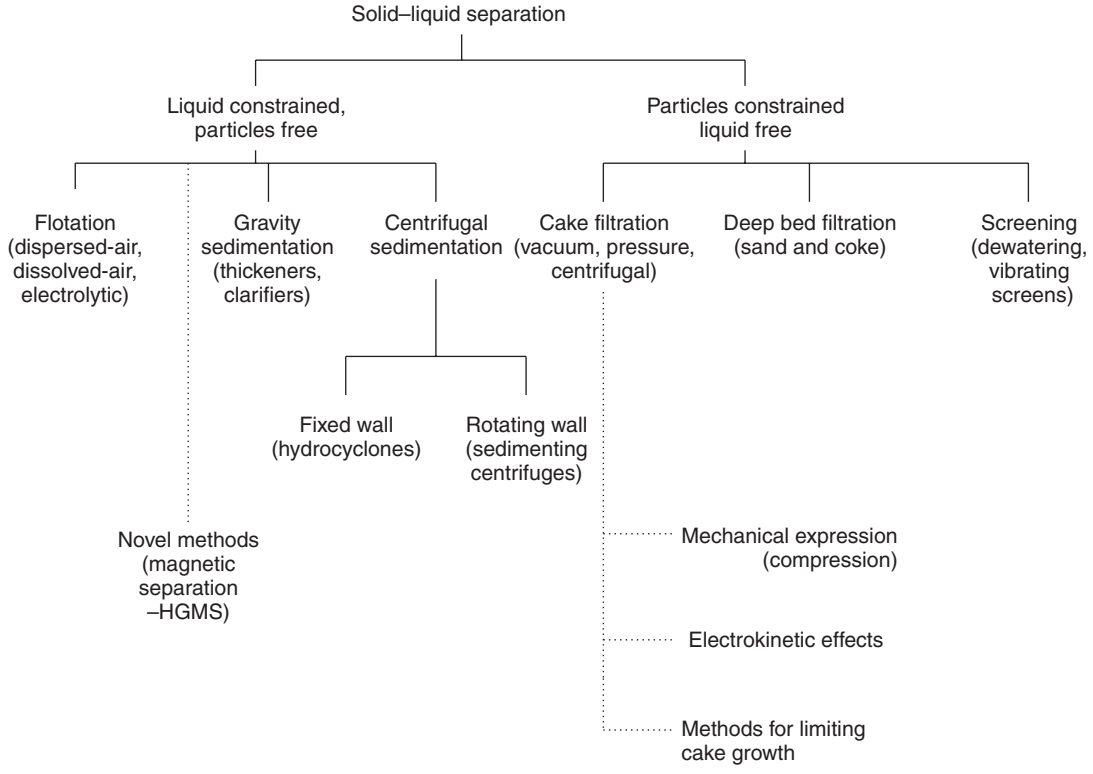

Figure 1.5 Classification of solid–liquid separation processes

surface, where they accumulate as a 'float' and can be skimmed off. The process consists of two stages: the production of suitably small bubbles and their attachment to the particles. Depending on the method of bubble production, flotation is classified as dispersed air, dissolved air or electrolytic. The particles to be floated have to be hydrophobic.

Dispersed air flotation generates the bubbles by injection of air combined with agitation (froth flotation) or by bubbling air through porous media (foam flotation). The size of bubbles is rather large (typically 1 mm), capable of floating large and heavy particles. Dispersed air flotation has been used for many years in mineral processing to concentrate base metals, as a solid–solid separation process where one mineral is hydrophobic (i.e. floats) while the other is hydrophillic (i.e. sinks).

Dissolved air (and electrolytic) flotation has made considerable inroads into solid–liquid separation because it can be applied to fine suspensions. It offers a viable alternative to gravity sedimentation because it can operate at much higher overflow rates and use smaller, more compact equipment of lower capital cost (but higher operating cost). Dissolved air flotation (see *Figure 1.6*) is based on the higher solubility of air in water as the pressure increases. Part or all of the feed is recycled through a saturator vessel where the water is saturated with air at high pressure. The air-saturated water is then mixed with the incoming feed where the pressure is reduced so that fine air bubbles appear and become available for flotation. The bubbles produced are typically less than 100 or even 60 microns in size and can therefore float fine solids. The typical overflow rates (sometimes called 'hydraulic loading') per unit plan area of the flotation cell are from 1.5 to 17 metres per hour. Most industrial applications of dissolved air flotation are in waste water treatment where the particles might often be hydrophobic (oily) by nature.

In electrolytic flotation (electroflotation), hydrogen and oxygen gas bubbles are generated by electrolysis. The bubbles produced can be smaller than 30 microns. Instead of the saturator, an expensive rectifier system is required. The flotation unit is very similar to the dissolved air unit, and in fact the same

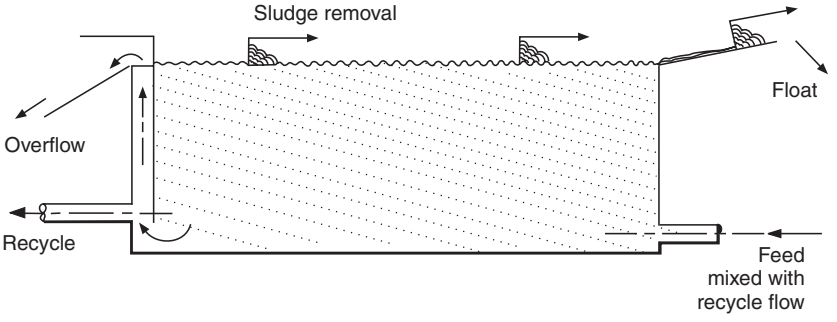

Figure 1.6 A schematic diagram of a dissolved air flotation cell with partial recycle saturation

unit can be used for either, having electrodes in one case and an external recycle saturation system in the other. As with the dissolved air units, a flocculation stage normally precedes the flotation stage.

1.2.2 Magnetic separation

The use of a magnetic field is an obvious means of removing ferromagnetic particles from a suspension. In mineral processing, permanent magnets have been used for removing tramp iron and for concentrating magnetic ores. Ceramic magnets, metal-alloy magnets or magnetized steel balls are useful when placed into the flow for separation of small ferromagnetic particles from hydraulic fluids. These 'filters' are generally cleaned manually by withdrawing the entire assembly.

Continuous magnetic separators such as the wet drum separators are widely used for beneficiation of ores and for recycling of magnetite or ferrosilicon from the heavy media pulps used for coal washing[9], or in the Sirofloc process[5,6] in water treatment, as discussed in section 1.1.2. Wet drum separators are robust and surprisingly cheap to install and operate. The wet drum separator is the major workhorse but little is published on the efficiency of such devices. Suleski, for example, discusses a specific manufacturer's product[8].

Wet drum separators can be operated with concurrent rotation or counter-rotation. Concurrent rotation is better for separation of magnetics from non-magnetics whilst counter-rotation is more efficient for high recoveries: drum operated at 20 m^3/hour per metre of drum width recovering magnetite particles of 50 microns would have a leakage of 50–200 ml/m^3 (ppm).

Magnetic ion exchangers can also be recovered from slurries[10] after appropriate reactions by wet drum separators. Ion exchange resins and other adsorbents have been made in the form of magnetic beads by incorporation of suitable oxides into the monomer mixes before polymerization. (Resins used: Sirotherm, Siromag; amount of magnetic oxide: 10–15% of the volume of the bead.) A pilot drum 300 mm dia, 150 mm wide was used to separate magnetic resins from water, mineral slimes and biological sludges, beads 420–1000 microns. Full scale drum 750 mm dia, 2700 mm wide should be able to process 70 cu.m/h.

Much stronger magnetic fields and gradients can be produced by the High Gradient Magnetic Separators (HGMS) which have enjoyed considerable attention recently. They can be used for separation of very fine and weakly paramagnetic particles on a large scale. The design and operation of the HGMS is in many ways similar to deep bed filters. The 'filtration' takes place through a canister (*Figure 1.7*) full of loosely packed, fine steel wool which is placed in a uniform magnetic field generated by an electromagnet. After the filtration stage, the field is switched off and backwash takes place to remove the particles separated on the steel wool.

The main advantage of HGMS is their high efficiency of separation even at relatively high flow rates and minimum pressure drops across the filter. The

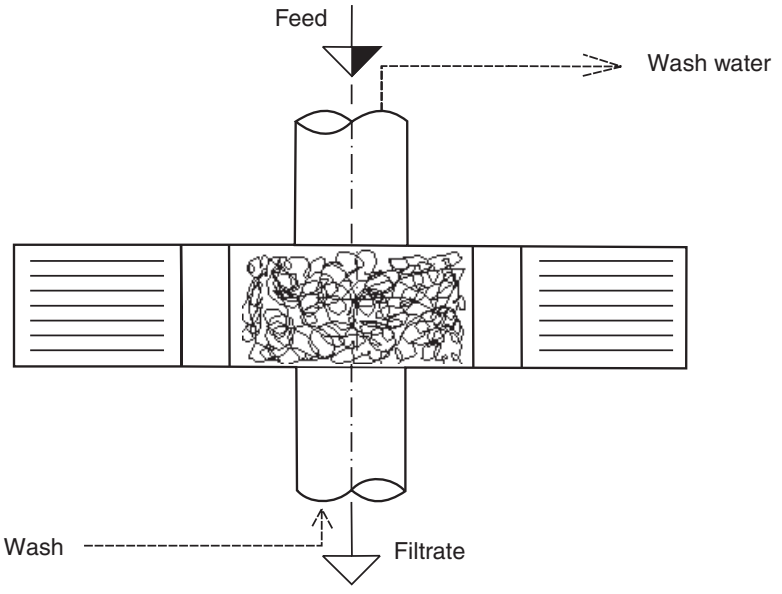

Figure 1.7 A schematic diagram of a high gradient magnetic separator

capital cost is very high, however, and only large installations are attractive economically.

There is a wide range of either actual or potential use of HGMS in industry: brightening of caolin clay (by removal of feebly magnetic contaminants); purification of boiler feed water in power generation; nuclear water polishing; process water treatment in steel mills and paper making; separation of red blood cells; and also waste water treatment, where non-magnetic solids can be separated by seeding (and flocculation) with finely ground magnetite.

A magnetically assisted chemical separation process[11] has recently been developed by Argonne National Laboratory for cleaning waste streams containing low concentrations of hazardous metals or radioactive elements. It uses small magnetic particles (ranging from 30 nm to 25 μm), with a chemical coating of selective chemical extractants which extract specific metals or radionuclides even in acidic or caustic conditions. The particles are either rare earth or ferromagnetic, embedded in polymer. The coatings include CMPO, TBP, amines, phosphonic acid, crown ethers, cryptands, polyethylene imine, silicotitanates etc.

As can be seen from *Figure 1.8*, extraction takes place onto the coating in a stirred tank and the particles are then separated in a magnetic field (e.g. using a magnet or an HGMS). A stripping process removes the contaminant-laden coating which is then separated from the particles and these are then recycled into the extraction stage. The process is claimed to be simpler, more versatile, cheaper and more compact than the conventional processes of solvent extraction or ion exchange.

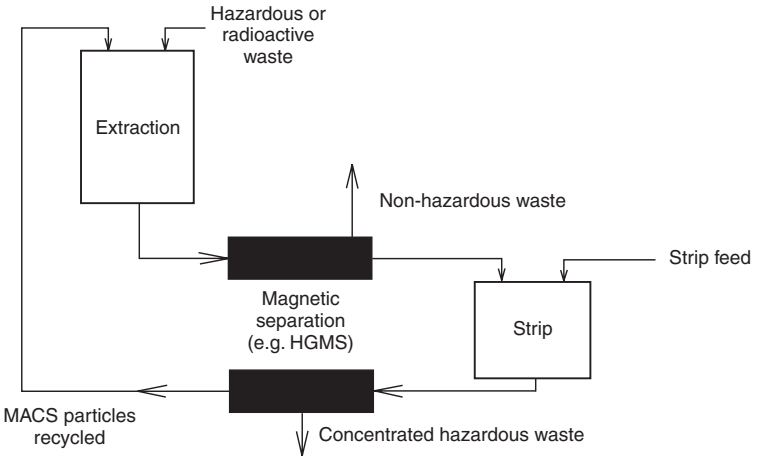

Figure 1.8 A schematic diagram of a magnetically assisted chemical separation process[11]

1.2.3 Gravity sedimentation (chapter 5)

The available gravity sedimentation equipment can be divided into batch operated settling tanks and continuously operated thickeners or clarifiers. The batch settling tanks are still used where relatively small quantities of liquids are to be treated such as, for example, in spent lubrication oil reclamation and cleaning. The bulk of the processing by gravity sedimentation is, however, in continuously operated thickeners and clarifiers.

If the primary purpose is to produce the solids in a highly concentrated slurry then the process is called thickening and the equipment is known as the gravity thickener. The feed to a thickener is usually more concentrated than to a clarifier, the primary purpose of which is to clarify the feed. A correctly designed and operated thickener, however, can accomplish both clarification and thickening in one stage.

The most commonly used thickener is the circular basin type. The flocculant-treated feed slurry enters through the central feed well which dispersed the feed gently into the thickener. The overflow is collected in a trough around the periphery of the basin. Raking mechanisms, slowly turning around the centre column, promote solids consolidation in the compression zone and aid solids discharge through the bottom central opening.

Thickener types vary with the application. Deep cone type compression tanks are used for coal washery slurries, so that the highly flocculated sediment can be compacted by the weight of the material. The tray thickener is a series of circular thickeners stacked around a common central shaft, each having its own raking mechanism. The lamella type thickener affords space saving through the use of flat or corrugated inclined plates (or tubes) in the settling tank to promote solids contacting and settling along and down the plates.

Gravity clarifiers are built with more emphasis on the clarity of the overflow and the feed concentrations are generally lower than those of most thickeners. Clarifiers are more often rectangular basins with feed at one end and overflow at the other. Settled solids are pushed to a discharge trench by slowly-moving paddles or blades on a chain mechanism. As with thickeners, the feed suspensions to clarifiers are flocculated to increase settling rates (these usually range from 1 to 8 m per hour). The bulk of applications for gravity clarifiers is in the water industry, where the common types are the 'one pass' clarifiers which incorporate paddle type flocculators, the sludge blanket clarifiers based on fluidization of a blanket of flocculated solids, and the solids recirculating clarifiers, where the settled solids are fed back to mix with the incoming raw water. The newer developments include the lamella clarification in the so-called rapid settling clarifiers.

1.2.4 Hydrocyclones (chapter 6)

The separation action of hydrocyclones is based on the effect of centrifugal forces. In contrast to sedimenting centrifuges, however, hydrocyclones do not have any rotating parts and the necessary vortex action is produced by pumping the fluid tangentially into a mono-cylindrical body. The cylindrical part is closed on top by a cover, through which the liquid overflow pipe (often called 'vortex finder') protrudes some distance into the cyclone body. The underflow, which carries most of the solids, leaves through the opening in the apex of the cone. There have been many different designs in use in some specialized fields but for separation of granular solids, the above described, conventional design is still the best.

The diameters of individual cyclones range from 10 mm to 2.5 m, cut sizes for most solids range from 2 to 250 microns, flow rates (capacities) of single units range from 0.1 to 7200 cubic metres per hour. The operating pressure drops vary from 0.34 to 6 bar, with smaller units usually operated at higher pressures than the large ones.

If hydrocyclones are to be used to produce thick underflows, the total mass recovery of the feed solids has to be sacrificed because throttling the underflow orifice inevitably leads to some loss of the solids to the overflow. A hydrocyclone as a single unit cannot therefore be used for both clarification and thickening at the same time. Typically the underflow concentrations that can be achieved with hydrocyclones are up to 50% by volume or more. In this they compare favourably with gravity thickeners and hydrocyclone systems are often used to replace the much larger and more expensive gravity thickeners.

Another application of hydrocyclones is for solid–solid separation by particle size. As the grade efficiency of a cyclone increases with particle size, it can be used to split the feed solids into fine and coarse fractions. This may be a process requirement, by which coarse and fine solids are separated to follow different routes in the plant, such as, for example, in closed circuit wet

grinding where the oversize particles are returned to the mill for further grinding. Most frequently in this category, hydrocyclones are used either to remove coarse particles from the product (in a de-gritting or 'refining' operation) or to remove fine particles from the product (in a de-sliming or 'washing' operation). Hydrocyclones are also used as classifiers simply to improve the performance of other filtration or separation equipment.

In heavy media separation, the use of hydrocyclones is for solid–solid separation by solid density as required in mining and mineral processing. The density of the suspending medium is chosen to be between the densities of the two minerals to be separated and the cyclone is then used as a 'sink-and-float' separator.

Another important use of hydrocyclones in heavy media separation plants is for densification (= thickening) of the recovered and cleaned medium. Very fine solid suspensions of magnetite or ferrosilicon are used to obtain a heavy medium because there are no liquids of such high densities that are necessary.

Hydrocyclones can also be used for washing of solids by arranging several stages in a counter-current arrangement similar to that used with gravity thickeners, see chapter 15. Such systems are found in the production of potato or corn starch, or in the chemical industry.

The conventional hydrocyclone has been subjected to considerable development to improve its characteristics. Sharpness of cut, for example, can be improved by injection of clean liquid into the flow near the apex of the cone. Another way is to operate the cyclone upside down so that the solids are separated into a container above the cyclone and subsequently fall back into the cyclone to be washed again. There is also some evidence that a flat bottom hydrocyclone can give better sharpness of cut.

In order to make use of the high efficiency of separation of small diameter hydrocyclones, most manufacturers offer multiple arrangements of varying design. Series arrangements, with or without recycles, can be used to improve any performance characteristic of hydrocyclones, see chapter 16.

1.2.5 Sedimenting centrifuges (chapter 7)

A sedimenting centrifuge is an imperforate bowl into which a suspension is fed and which is rotated at high speed. The liquid is removed through a skimming tube or over a weir while the solids either remain in the bowl or are intermittently (or continuously) discharged from the bowl. There are different types of industrial sedimenting centrifuges, classified according to the design of the bowl and of the solids discharge mechanism: tabular, multi-chamber, imperforate basket, scroll type and disc centrifuges. The disc centrifuges are further divided into solids retaining, solids ejecting and nozzle types. The tubular, multi-chamber and solids retaining disc centrifuges are only suitable as liquid clarifiers because the bowls have to be cleaned manually. The imperforate basket type and the solids ejecting disc type are suitable for

moderate feed concentrations and have intermittent solids discharge during which the feed may have to be briefly interrupted. Only the nozzle disc type and the scroll type centrifuges are truly continuous in both the operation and solids discharge, the latter being suitable for particularly high feed solids concentrations of up to 50% volume.

Most of the centrifuge types are capable of giving cut sizes well into the sub-micron region. The scroll type gives a cut size in the region of about 2 microns with materials such as clay, silica or similar. It is widely used in the chemical industry, in coal preparation and other mineral processing applications. It is also often used for dewatering of coarse solids like PVC particles of size in excess of 100 microns. The most usual design of the scroll centrifuge is one in which the solids and the liquid move in a counter-current fashion in the bowl. A relatively recent, co-current design offers certain advantages, mostly because it requires lower speeds for the same separation duty.

Sedimentation centrifuges, due to the lack of shear in the flow, are suitable for flocculation and suitable agents are often added to the feed upstream of the centrifuge. In solid–liquid separation, centrifuges are often compared with the Rolls-Royces in the car industry: they perform well but the capital and running costs are high.

1.2.6 Cake filtration (chapter 9)

Cake filtration is based on passing a suspension through a permeable, relatively thin medium (chapter 8). The solids are deposited in the form of a cake on the upstream side of the medium. As soon as the first layer of cake is formed, the subsequent filtration takes place on top of this cake and the medium provides only a supporting function. These so-called 'surface filters' are best used for filtration of suspensions of solids concentrations in excess of 1% by volume in order to minimize medium blinding which occurs in the filtration of dilute suspensions. If cake filtration is to be applied to clarification of liquids, which implies low feed concentrations of solids, addition of filter aids is usually necessary—see section 2.2.

Depending on the way the required pressure drop across the filter medium is generated, surface filters are classified into vacuum, pressure and centrifugal filters. Gravity static head is rarely used in cake filtration, except perhaps for the initial dewatering of highly flocculated sludges in belt presses.

In vacuum filters (chapter 13), the driving force for filtration results from the application of a suction on the filtrate side of the medium. Although the theoretical pressure drop available for vacuum filtration is 100 kPa, in practice it is often limited to 70 or 80 kPa.

In applications where the proportion of fine particles in the feed slurry is low, a simple and relatively cheap vacuum filter can yield cakes with moisture contents comparable to those discharged by pressure filters. Furthermore, this category includes the only truly continuous filters built in large sizes that can provide for washing, drying and other process requirements.

Vacuum filters are available in a variety of types and are usually classified as either batch operated or continuous. One important distinguishing feature is the position of the filtration area with respect to gravity. A number of vacuum filter types use a horizontal filtering surface with the cake forming on top. This arrangement offers the following advantages:

1 Gravity settling can take place before the vacuum is applied. In many cases this may prevent excessive blinding of the cloth due to action of the coarser particles forming a pre-coat.
2 Heavy or coarse materials can be filtered without problems due to settling.
3 Fine particle penetration through the medium can be tolerated because the filtrate can be recycled back onto the belt.
4 Top-feed filters are ideal for cake washing, cake dewatering and other process operations such as leaching.
5 A high degree of control can be exercised over cake formation. Allowances can be made for changed feed and/or different cake quality requirements. This is particularly true of the horizontal belt vacuum filters. With these units the relative proportions of the belt allocated to filtration, washing, drying, etc., as well as the belt speed and vacuum quality, can be altered easily to suit process changes.

There are, however, two major drawbacks:

1 Such filters usually require large floor areas.
2 Their capital cost is high.

Saving in floor area as well as in installation cost can be made by using a filter with vertical or other non-horizontal filtration surfaces but at the cost of losing most, if not all, of the above listed five advantages of horizontal filters.

The driving force for filtration in pressure filters (chapter 12) is the liquid pressure developed by pumping or by the force of gas pressure in the feed vessel. The most important feature of pressure filters is that they can generate pressure drops across the medium in excess of 1 bar, which is the theoretical limit of vacuum filters. Whilst the use of high pressure drops is often advantageous, leading to higher outputs, drier cakes or greater clarity of the overflow, this is not necessarily always the case. For compressible solids, an increase in pressure drop leads to a decrease in permeability of the cake and hence reduced filtration rate relative to a given pressure drop. This reduction in permeability may be so significant as to nullify or even overtake the advantage of using high pressures in the first place and there is no reason for using the generally more expensive pressure filtration hardware. Whilst a simple liquid pump may be cheaper than a vacuum pump needed with vacuum filters, if air displacement dewatering is to follow filtration in pressure filters, an air compressor has to be used which is expensive. Pressure

filters can treat feeds with concentrations up to 10% solids and having large proportions of difficult to handle fine particles.

Excluding variable chamber presses, which rely on mechanical squeezing of the cake and which are dealt with in the following section, presssure filters may be grouped into two categories, plate-and-frame filter presses and pressure vessels containing filter elements.

A great majority of the pressure filters are batch operated but there have been some relatively recent developments of continuous pressure filters. It is obvious that a rotary drum or rotary disc vacuum filter can be adapted to pressure by enclosing it in a pressure cover but the disadvantages of this measure are equally obvious. The enclosure is a pressure vessel which is heavy and expensive, the progress of filtration cannot be watched and the removal of the cake from the vessel is the most difficult problem of the whole design. Other complications of the design are caused by the necessity of arranging for two or more differential pressures between the inside and outside of the filter, which require a troublesome system of pressure regulating valves.

This short review of pressure filters would not be complete without a mention of cartridge filters. These use an easily replaceable cartridge made of paper, cloth or various membranes of pore size down to 0.2 microns. Cartridge filtration is nearly always limited to liquid polishing, i.e. removing very low amounts of solids, in order to keep the frequency of cartridge replacement down. Cartridge filters are used to polish power fluids, lubrication oils, juices or pharmaceutical liquids.

The third type of driving force used in cake filtration is the centrifugal force, in the centrifugal filters (chapter 14). A centrifugal filter consists of a rotating perforate basket, fitted with a filter cloth or other medium. The action of the centrifugal field leads to two effects: it creates a pressure drop across the filter medium, due to the centrifugal head of the suspension layer rotating in the basket, and it also pulls the liquid out of the cake and medium. The latter effect makes the centrifugal filters ideally suitable for dewatering duties and these indeed represent the bulk of their industrial applications. The range of particle size and the feed is from 10 microns to 10 mm, with most machines used in the coarser part of the range.

Centrifugal filters can be classified into two fundamentally different classes: discontinuously fed, fixed bed machines, and continuously fed, moving bed machines.

Starting with the fixed bed, batch or cyclic centrifuges, these have a cylindrical screen onto which the feed suspension is fed and the cake is stationary. This feature makes it possible to separate relatively finer particles than in the continuous moving bed machines. The perforate basket (or ‘three point’) centrifuge and the peeler type centrifuge are examples in this category.

The continuously fed, moving bed machines use a metal screen instead of filter cloth and this makes them suitable for dewatering of coarse solids only. The baskets are either conical, with or without a scroll (or a vibration device) to aid the movement of the solids across the screen, or cylindrical, in the

pusher centrifuges. The pusher centrifuges use a reciprocating piston to push the solids along the basket. They require high feed concentrations of the solids to enable the formation of a sufficiently rigid cake to transmit the thrust of the piston. By the very nature of their operation, the pusher centrifuges are suitable for washing, particularly in their multi-stage screen versions.

1.2.7 Mechanical expression (chapter 12, sections 12.2.5 and 12.3.5)

Mechanical squeezing of the cake in the so-called variable chamber filters has been used relatively recently to lower the moisture content of the final cake. This is obviously applicable only to cakes that are compressible. Many filters are available in which some form of mechanical expression of the cake is used either to follow a conventional filtration process or to replace it.

There are basically three ways to achieve this mechanical expression: with an inflatable diaphragm, with a compression belt or in a screw conveyor of reducing pitch or diameter.

An inflatable diaphragm or membrane has been used in membrane plate presses which are closely related to the conventional plate and frame presses. A pressure filtration period is followed by compression with the hydraulically operated membrane or by a hydraulically operated ram if flexible rim seals are fitted. This principle is also used in vertical presses that use either one or two endless cloth belts indexing between plates. Inflatable membrane is also used on a cylindrical filtration surface with or without a preceding pressure filtration stage, in the so-called tube presses.

Compression belts or rollers are sometimes added to conventional vacuum drum or belt filters but the most significant application is in the recently popular belt presses. These are usually horizontal belt filters (with one exception of a vertical belt press) which initially use gravity dewatering of the highly flocculated feeds, followed by compression with a second belt which gradually moves closer to the primary belt and squeezes the cake. The cake is also sheared by going through a series of meander rollers and this also aids dewatering.

The third category includes ‘screw presses’. These consist of a single or double screw conveyor, which has perforated walls. The solids being conveyed are squeezed due to a gradual reduction in the pitch or diameter of the screw. Screw presses are mostly used for dewatering of rough organic materials.

1.2.8 Methods of limiting cake growth (chapter 11)

The most important disadvantage of conventional cake filtration is the declining rate due to the increasing pressure drop caused by the growth of the cake on the filter medium. The flow rate of the liquid through the medium can be maintained high if no or little cake is allowed to form on the medium. This leads to the thickening of the slurry on the upstream part of the medium and the filters based on this principle are sometimes called filter thickeners.

There are several ways of limiting cake growth and these are classified into five groups as follows:

1 Removal of cake by mass forces (gravity or centrifugal), or by electrophoretic forces tangential to or away from the filter medium.
2 Mechanical removal of the cake by brushes, liquid jets or scrapers.
3 Dislodging of the cake by intermittent reverse flow.
4 Prevention of cake deposition by vibration.
5 Cross-flow filtration by moving the slurry tangentially to the filter medium so that the cake is continuously sheared off.

The extent of the commercial exploitation of the above listed principles in the available equipment varies but cross-flow filtration is certainly the one exploited most of all. There are two distinctly different groups of equipment in this category. American and European 'dynamic filters' use rotating elements to generate the necessary shear in the flow. The feed suspension is pumped through a number of stages where it gradually thickens until it is discharged as a thick paste. It is not clear whether these filters actually save energy because the higher filtration velocities are at the expense of high torques required by the rotating elements. There is, however, a saving in the size of the filter required for a given duty.

The second way of shearing the cake off the medium is by pumping the suspension across the surface at high speeds. This principle first originated in reverse osmosis and ultrafiltration where much closer membranes are used than in cross-flow filtration. The suspension is pumped through a long, porous pipe under pressure and it gradually thickens until it is discharged at the end. The pores in the medium get gradually fouled and have to be regularly cleaned by back-flushing or chemical treatment.

Cross-flow filtration and the other methods for limiting cake growth are still undergoing development and will gradually find wider application in industry.

1.2.9 Deep bed filtration

Deep bed filtration is fundamentally different from cake filtration both in its principle and its application. The filter medium is a deep bed of pore size much greater than the particles it is meant to remove. No cake should form on the face of the medium but particles penetrate into the medium where they separate due to gravity settling, diffusion and inertial forces. Attachment to the medium is due to molecular and electrostatic forces. Sand is the most common medium and multi-media filters also use garnet and anthracite. The filtration process is cyclic because when the bed is full of solids and the pressure drop across the bed is excessive, the flow is interrupted and solids are backwashed from the bed (this is sometimes aided by air scouring or wash jets).

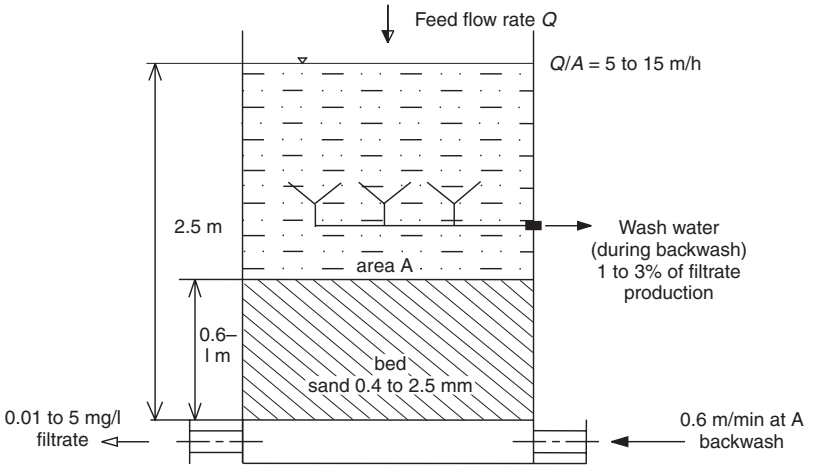

Figure 1.9 A downflow filter in potable water treatment showing the typical operating conditions

In order to keep the frequency of backwash and the wash water demand down, deep bed filtration is usually applied only to very dilute suspensions of solids concentrations less than 0.1% by volume. Deep bed filters were originally developed for potable water treatment (see the typical operating conditions of a downflow filter in *Figure 1.9*) as the final polishing process following chemical pretreatment and sedimentation. They are also increasingly applied in industrial waste water treatment under somewhat harsher operating conditions of higher solids loadings and more difficult backwashing of the media.

Most deep bed filters are gravity fed but there are also some pressure types in use. The most common arrangement is the downflow filter, with backwash in the upward direction in order to fluidize the bed. The stratification of the particles that make up the bed, caused by the fluidization (fines on top), is not desirable, however. The solids holding capacity of the bed is best utilized if the filtration flow encounters progressively finer sand particles. This is achieved in the upflow filters, where the fluidization due to backwash produces the correct stratification in the bed. Both the filtration flow and the backwash take place in the same direction and the disadvantage is that the wash goes to the 'clean side' of the filter.

The trend in the use of deep bed filters in water treatment is to eliminate conventional flocculators and sedimentation tanks, and to employ the filter as a 'flocculation reactor' for direct filtration of low turbidity waters. The constraints of batch operation can be removed by using one of the available continuous filters which provide continuous backwashing of a portion of the medium. Such systems include moving bed filters, radial flow filters or travelling backwash filters. Further development of continuous deep bed filters is most likely.

1.2.10 Screening

Screening is an operation by which particles are introduced to a screen of a given aperture size and thus have an opportunity of either passing through if they are smaller than the apertures, or being retained on the screen if they are larger. The bulk of the screens in industry are used for size grading but they are also used in a dewatering function, often combined with washing.

Virtually any type of screen can be used for dewatering but some screens have been designed specifically for this purpose. The DSM sieve bend is a good example of a stationary screen suitable for dewatering duties, see *Figure 1.10*. It consists of a curved, wedge wire deck with the wires or bars at right angles to the feed. The feed suspension is distributed on the top, across the full width of the screen. Coarse screens are gravity fed, whilst finer ones are pressure fed through a set of nozzles. Polyurethane surface or woven wire cloth have also been used in place of the wedge wire. The applications include thickening mineral, organic or waste slurries, starch fibre washing, paper pulp fibre screening and many other similar operations. The effective cut size varies from 40 to 2000 microns.

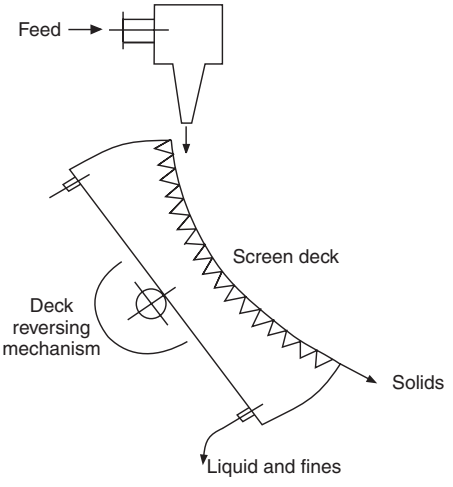

Figure 1.10 Schematic diagram of a sieve bend

Other dewatering screens include high frequency electromagnetic screens and resonance screens such as the Fordertechnik screen and the Elliptex dewaterizer (ref. 12, chapter 8) which also use a wedge wire deck but give a larger minimum effective cut size, generally above 200 microns. Other types include gyratory screens, rotary screens or band screens.

1.2.11 Electrokinetic effects

The application of direct current (d.c.) potential in filtration or sedimentation is known to have a beneficial effect on the separation. Although this has been

known and studied since the beginning of the 19th century, its practical application and development have only recently accelerated and commercial application is likely in the near future.

There are several effects due to the existence of the double layer on the surface of most particles suspended in liquids, and they can all be used to measure the so-called zeta potential. A simplified summary of the effects is given in *Table 1.1* and further explanation and definitions are given in section 4.4.3.

Table 1.1 Electrokinetic effects

Fluid	*Particles*	*Electric field*	*Effect*
Still	Moving	Applied	Electrophoresis
Still	Moving	Measured	Sedimentation (or migration) potential
Moving	Still	Applied	Electro-osmosis
Moving	Still	Measured	Streaming potential
Still	Still	Applied	Electro-osmotic pressure

The best known effect is electrophoresis. This term is given to the migration of small particles suspended in a polar liquid, in an electric field, towards an electrode. If a sample of the suspension is placed in a suitably designed cell (with a d.c. potential applied across the cell) and the particles are observed through a microscope, they can all be seen to move in one direction, towards one of the two electrodes. All the particles, regardless of their size, appear to move at the same velocity (as both the electrostatic force and resistance to particle motion depend on particle surface) and this velocity can be easily measured.

The second effect, which often accompanies electrophoresis, is electro-osmosis. This is the transport of the liquid past a surface or through a porous solid, which is electrically charged but immovable, towards the electrode with the same sign of charge as that of the surface. It can be said that electrophoresis reverts to electro-osmotic flow when the charged particles are made immovable, and, if the electro-osmotic flow is forcibly prevented, pressure builds up and is called electro-osmotic pressure.

1.2.11.1 Electrophoretic settling and electro-osmotic dewatering

This is a straightforward use of electrophoresis when settling velocities are enhanced by placing one electrode (usually negative and perforated) floating on top of the slurry and another at the bottom of the tank. Furthermore, electro-osmosis thickens the settled sludge at the same time. The settling consists in fact of three successive processes. In the first, suspended particles

settle with the resultant velocity of the gravitational and the electrophoretic components. In the second process, the sludge is thickened by compression and electro-osmosis. In the third process, when compression due to gravity is completed, the sludge is thickened only by electro-osmosis.

Enhancement of gravity settling by electrophoresis is also used with liquid–liquid dispersions in solvent extraction and for the separation of oil–water emulsions. Electro-osmosis on its own is a well-tested method for the gathering of ground water to facilitate its removal from foundations and other sites in civil engineering. It can also be applied to the dewatering of filter cakes as described in the following.

1.2.11.2 Electrokinetic filtration

Electrophoresis and electro-osmosis can also be used to enhance conventional cake filtration. Electrodes of suitable polarity are placed on either side of the filter medium (as most particles carry negative charge, the electrode upstream of the medium is usually positive) so that the incoming particles move towards the upstream electrode, away from the medium. The electric field can cause the suspended particles to form a more open cake or, in the extreme, to prevent cake formation altogether by keeping all particles away from the medium.

There is an additional pressure drop across the cake developed by electro-osmosis which leads to increased flow rates through the cake (and further dewatering at the end of the filtration cycle). The filtration theory proposed for electrofiltration assumes the simple superposition of electro-osmotic pressure on the hydraulic pressure drop.

Whether the recent growth in the theoretical and experimental study of the electrokinetic effects applied to solid–liquid separation will lead to greater commercial use remains to be seen; to date, there are only two commercial electrofilters on the market known to the author. However, electrofiltration is certainly an area of potential development.

1.3 The spectrum of particle size

This book deals with processes that can, between them, deal with particle size spanning several orders of magnitude. *Figure 1.11* shows the spectrum of particle size and where various common materials lie on the scale. It also gives the broad ranges of application of the membrane separation, filtration and screening processes (the right-hand side group in *Figure 1.5*), the separation efficiency of which is, within their respective range of application, more-or-less independent of particle size. The efficiency of the group on the left in *Figure 1.5* is highly size dependent (most of the separators in that group are often referred to as ‘dynamic separators’) and it is characterized by the ‘grade efficiency curve’, as further explained in chapter 3. *Figure 1.12* shows

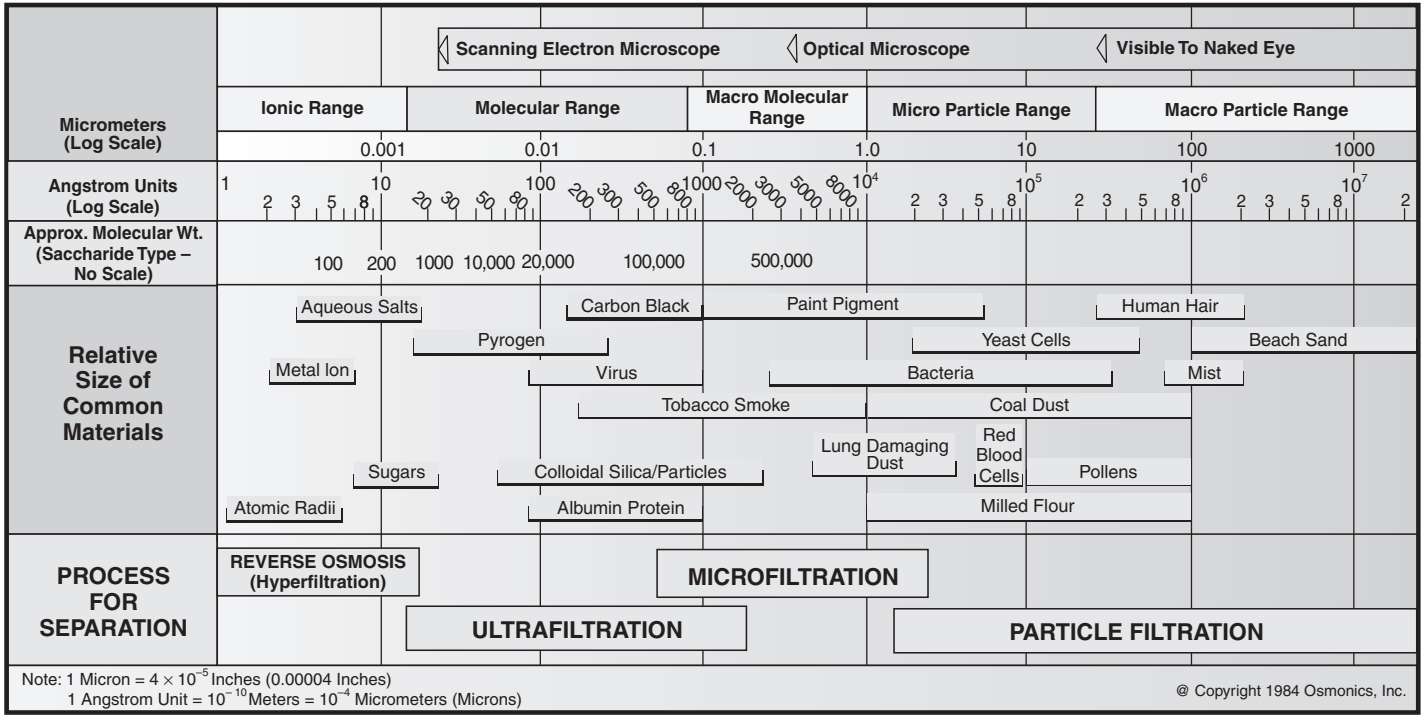

Figure 1.11 The spectrum of particle size. Note: $1\,\mu m = 4 \times 10^{-5}$ in; $1\text{Å} = 10^{-10}$ m $= 10^{-4}\,\mu m$ (Courtesy of Osmonics, Inc.)

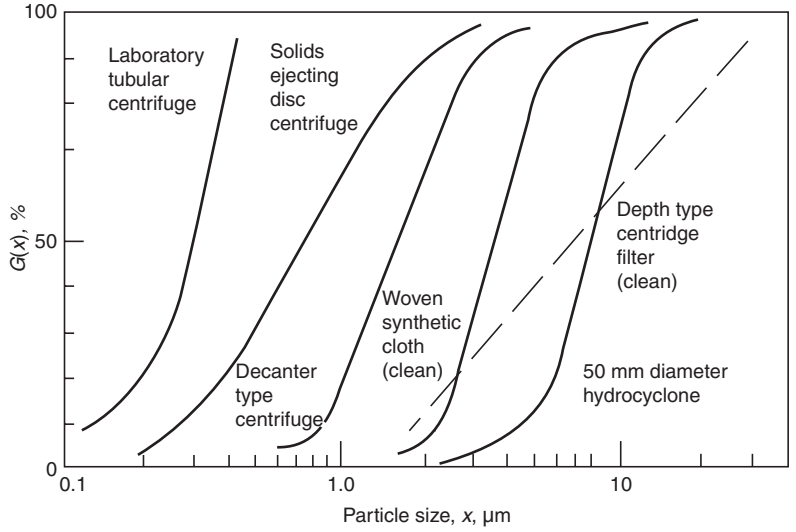

Figure 1.12 The grade efficiency curves of various types of equipment

such curves for some types of equipment used at the fine end of the particle size spectrum.

This book aims to cover the whole of the size spectrum shown in *Figure 1.11* but, inevitably, the greater emphasis is given to a somewhat narrower range, most frequently encountered in the chemical and process industries, approximately between 0.05 and 500 μm.

References

1. Ruthven, D. M. (Ed.), *Encyclopedia of Separation Technology*, John Wiley & Sons, New York (1997)
2. Smollen, M. and Kafaar, A., Development of electro-osmotic sludge dewatering technology, WRC Report No. 427/1/95, CSIR, Stellenbosch, January 1995, ISBN 1 86845 163 1
3. Gerdes, E., 'Precoat filtration with organic filter aids', *Filtration & Separation*, 1040–1043 (December 1997)
4. Heertjes, P. M. and Zuideveld, P. L., 'Clarification of liquids using filter aids—Part III. Cake resistance in surface filtration', *Powder Technology*, **19**, 45–64 (1978)
5. Walton, H. G., 'Diatomite filtration—optimising the body feed', *Filtration & Separation*, May/June 237–238, (1982)
6. CSIRO, Magnetic Water Treatment, International News, Water & Waste Treatment, September, 4 (1980)
7. Anderson, N. J. *et al*., 'Colour and turbidity removal with reusable magnetite particles, VI Pilot plan operation', *Water Res*., **17** (10), 1235–1243 (1983)
8. Suleski, J., 'New magnets and tank designs for magnetic wet drum separators', *World Min*., April, 60–61 (1972)

9. Oberteuffer, J. A., 'Magnetic separation, a review', *IEEE Trans. Magn.*, **10**, June, 223–238 (1974)
10. Swinton, E. A., 'Separation of ion exchangers from slurries by magnetic drum separators, Part 5', paper 39 in: G. A. Davies (Ed.), *Separation Processes in Hydrometallurgy*, Ellis Horwood Ltd, Chichester, 408–420 (1987)
11. Nunez, L. and Kaminski, M. D., 'Magnetically assisted chemical separation process', *Filtration & Separation*, May, 349–352 (1998)
12. Svarovsky, L. (Ed.), *Solid–Liquid Separation* (3rd edn), Butterworths, London (1990)

Bibliography

Fujisaki, K. and Nagami, S., 'Dissolved-gas flotation of waste activated sludge by use of carbon dioxide', Proceedings Volume I, World Filtration Congress 8, European Federation of Chemical Engineering Event No. 607, organised by The Filtration Society and Elsevier Science, The Brighton Centre, Brighton, UK, 3–7 April 2000, 119–122 (2000)

Glasgow, G. D. E and Stevenson, D. G., 'Flow rate changes in drinking water filtration—comparison of a mathematical model and experiment observation', Proceedings Volume I, World Filtration Congress 8, European Federation of Chemical Engineering Event No. 607, organised by The Filtration Society and Elsevier Science, The Brighton Centre, Brighton, UK, 3–7 April 2000, 127–130 (2000)

Herdem, S., Abbasov, T., Memmedov, A. and Koksal, M., 'On the coagulation and detachment processes of particles in magnetic field', Proceedings Volume II, World Filtration Congress 8, European Federation of Chemical Engineering Event No. 607, organised by The Filtration Society and Elsevier Science, The Brighton Centre, Brighton, UK, 3–7 April 2000, 781–784 (2000)

Jegatheesan, V., Vigneswaran, S., Ngo, H. H. and Aim, R. B., 'Particle detachment in deep bed filtration', Proceedings Volume II, World Filtration Congress 8, European Federation of Chemical Engineering Event No. 607, organised by The Filtration Society and Elsevier Science, The Brighton Centre, Brighton, UK, 3–7 April 2000, 823–826 (2000)

Mackie, R. I., Khan, S. M. M. A. and Stoecker, O., 'Modelling of headloss development in deep-bed filtration', Proceedings Volume II, World Filtration Congress 8, European Federation of Chemical Engineering Event No. 607, organised by The Filtration Society and Elsevier Science, The Brighton Centre, Brighton, UK, 3–7 April 2000, 835–838 (2000)

2

Characterization of particles suspended in liquids

L. Svarovsky

FPS Institute, England and University of Pardubice, Czech Republic

2.1 Introduction, the reasons for particle characterization

Particle characterization, i.e. the description of the primary properties of particles in a particulate system, underlies all work in particle technology. Primary particle properties such as the particle size distribution, particle shape, density, surface properties and others, together with the primary properties of the liquid (viscosity and density) and also with the concentration and the state of dispersion, govern the other, secondary properties such as the settling velocities of the particles, the permeability of a bed or the specific resistance of a filter cake. Knowledge of these properties is vital in the design and operation of equipment for solid–liquid separation.

One could of course argue that it may be not only simpler but often more reliable to measure the secondary properties directly without reference to the primary properties; this is of course done in practice but the ultimate aim is to be able to predict the secondary properties from the primary ones. After all, in fluid dynamics for example, we do not test the pipe resistance to flow every time we need to design a piece of pipework, we measure the primary properties of the liquid (viscosity and density) and of the pipeline (roughness) and determine the resistance from known relationships. As the relationships in solid–liquid separation are rather complex and in many cases not yet available, primary particle properties are mainly used for only a qualitative assessment of the behaviour of suspensions, for example as a selection guide. Taking particle size for instance, the finer the particle size the more difficult is the separation but the concentration of solids also plays an important role. Lloyd and Ward[1] have given a very informative diagram, presented in a slightly modified form in *Figure 2.1*, which shows schematically the range of solid–liquid separation equipment for different particle sizes.

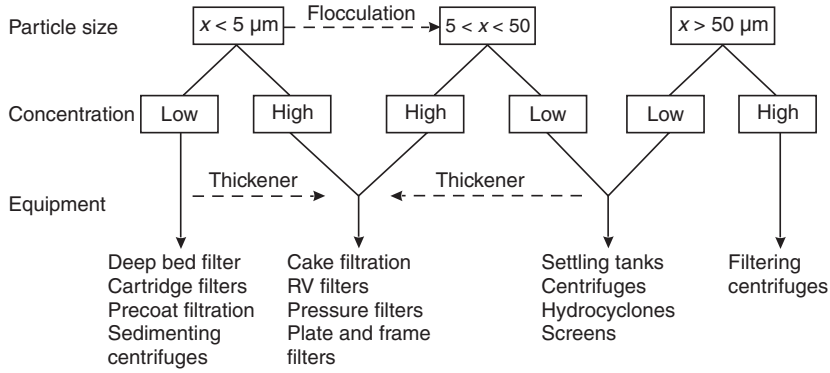

Figure 2.1 Particle size as a guide in the selection of solid–liquid separation equipment[1]

The particle size greatly affects the permeability, or specific resistance, of packed beds (as can be clearly seen from equation 9.36, the specific cake resistance (α) is given by

$$\alpha \sim 1/x^2$$

where x is the particle size, because the specific surface of the particles making up the bed is inversely proportional to particle size), hence particle size can be used for a qualitative assessment of the permeability. In sedimentation, Stokes' diameter (as defined later) plays an important role in 'free settling' applications and in the Sigma theory used for sedimenting centrifuges (see chapter 7).

There are many properties of particulate systems other than those relevant to solid–liquid separation, which depend strongly on particle size: the activity of drugs, the setting time of cement, and the hiding power of pigments, to name just a few.

The characterization of solid particles, most of which are, in practice, irregular in shape, is usually made by analysing the particle size (the measure of size most relevant to the particle property which is under investigation) and its distribution. Other characteristic properties of the solid material may be included in the measure of size determined, for example Stokes' diameter combines size, density and shape all in one parameter; they can be characterized separately if necessary. British Standard BS2955 attempts to define shape qualitatively; a quantitative measure of particle shape can be obtained indirectly by analysing two or more measures of particle size and looking at different 'shape coefficients' that relate to those sizes.

Before a technique can be selected for particle size analysis, two important decisions have to be made about the variables we measure: i.e. the measure of particle size x and the type of size distribution Φ required.

2.2 Definitions of particle size

An irregular particle can be described by a number of sizes depending on what dimension or property is measured. There are basically three groups of sizes: 'equivalent sphere diameters', 'equivalent circle diameters' and 'statistical diameters'.

The first group of sizes are the diameters of a sphere which would have the same property as the particle itself (e.g. the same volume, the same projected area, the same settling velocity etc.)—see *Table 2.1*.

Table 2.1 A list of definitions of 'equivalent sphere diameters'

Symbol	*Name*	*Equivalent property of a sphere*
x_v	Volume diameter	Volume
x_s	Surface diameter	Surface
x_{sv}	Surface volume diameter	Surface to volume ratio
x_d	Drag diameter	Resistance to motion in the same fluid at the same velocity
x_f	Free-falling diameter	Free-falling speed in the same liquid, same particle density
x_{St}	Stokes' diameter	Free-falling speed, if Stokes' Law is used ($Re < 0.2$)
x_A	Sieve diameter	Passing through the same square aperture

The second group of sizes are the diameters of a circle that would have the same property as the projected outline of the particles—see *Table 2.2*.

Table 2.2 A list of definitions of 'equivalent circle diameters'

Symbol	*Name*	*Equivalent property of a circle*
x_a	Projected area diameter	Projected area if the particle is resting in a stable position
x_p	Projected area diameter	Projected area if the particle is randomly orientated
x_c	Perimeter diameter	Perimeter of the outline

The third group of sizes, the 'statistical diameters' are obtained when a linear dimension is measured (by microscopy) parallel to a fixed direction—see *Table 2.3*.

Different methods of particle size measurement determine different measures of size (see the list in *Table 2.7*) and great care must be taken when

Table 2.3 A list of definitions of 'statistical diameters'

Symbol	*Name*	*Dimension measured*
x_F	Feret's diameter	Distance between two tangents on opposite sides of the particle
x_M	Martin's diameter	Length of the line which bisects the image of the particle
x_{SH}	Shear diameter	Particle width obtained with an image shearing eyepiece
x_{CH}	Maximum chord diameter	Maximum length of a line limited by the contour of the particle

making a selection as to what size is most relevant to the property or process which is to be controlled. For example, in those methods of solid–liquid separation in which particle motion relative to the fluid is the governing mechanism (gravity or centrifugal sedimentation, hydrocyclones) it is of course most relevant to use a method which measures the free-falling diameter or, more often, the Stokes' diameter (sedimentation or fluid classification methods). In filtration on the other hand, it is the surface volume diameter (which is measured, for example, by permeametry) which is most relevant to the mechanism of separation.

2.3 Types of particle size distribution

For a given particulate matter, four different types of particle size distribution are defined (see *Figure 2.2a*). These are:

1 particle size distribution by number $f_N(x)$;
2 particle size distribution by length (not used in practice) $f_L(x)$;
3 particle size distribution by surface $f_S(x)$;
4 particle size distribution by mass (or volume) $f_M(x)$.

These distributions are related but conversion from one to another is possible only when the shape factor is constant, i.e. the particle shape is independent of size.

The following relationships show the basis of such conversions:

$$f_L(x) = k_1 x f_N(x) \tag{2.1}$$

$$f_S(x) = k_2 x^2 f_N(x) \tag{2.2}$$

$$f_M(x) = k_3 x^3 f_N(x) \tag{2.3}$$

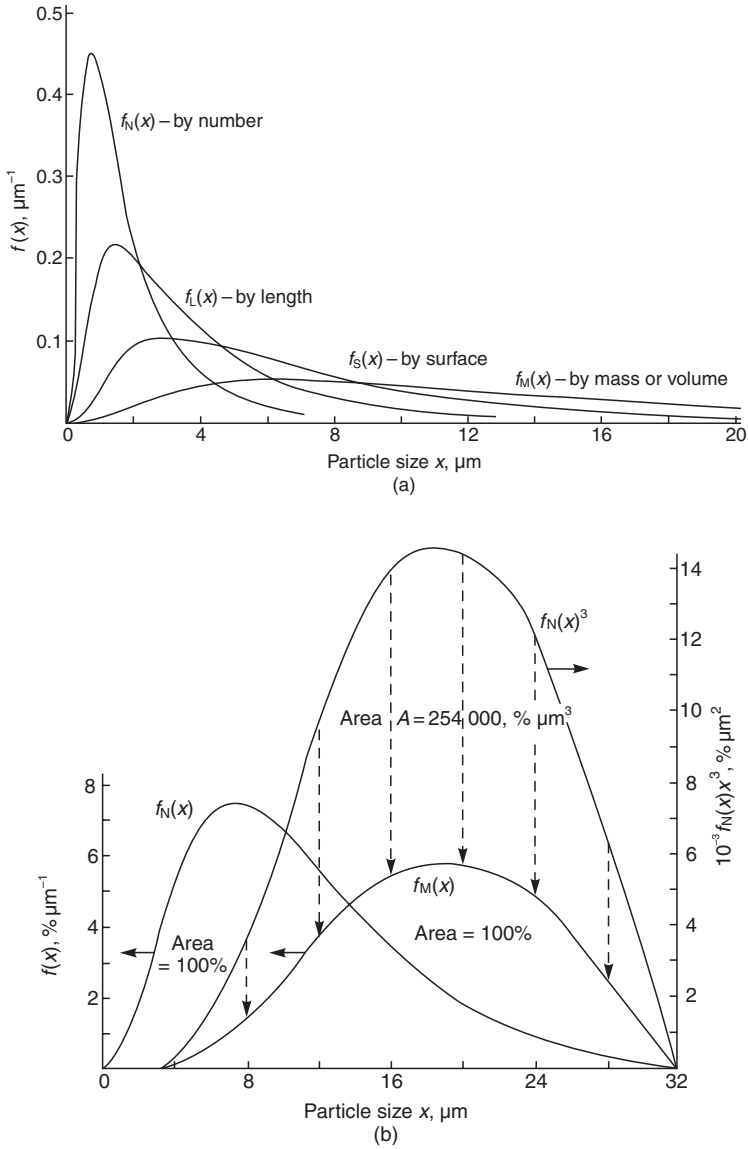

Figure 2.2 (a) Four particle size distributions of a given particle population; (b) Example of conversion of f_N to f_M (particle size distribution by number to particle size distribution by mass)

The constants k_1, k_2 and k_3 contain a shape factor which may often be particle-size-dependent; this makes an accurate conversion impossible without a full quantitative knowledge of the shape factor's dependence on particle size. If the shape of the particles does not vary with size, the constants

k_1, k_2 and k_3 can easily be found because, by definition of the distribution frequency

$$\int_0^\infty f(x)\,\mathrm{d}x = 1 \tag{2.4}$$

the areas under the curves of frequency against particle size should be equal to one. The actual procedure is best shown in the example in *Figure 2.2b* where the particle size distribution frequency by number, $f_N(x)$, is converted to a distribution by mass, $f_M(x)$, by multiplication of the values of f_N, corresponding to different sizes x, by x^3 (following equation 2.3). The resulting curve of $x^3 f_N(x)$ is then simply scaled down by a factor

$$k_3 = \frac{1}{\int_0^\infty x^3 f_N(x)\,\mathrm{d}x} = \frac{1}{A} \tag{2.5}$$

in order to give $f_M(x)$.

If the data are in a cumulative form, as cumulative percentage undersize or oversize (see section 2.5), conversions between the different particle size distributions can be made without having to differentiate the curves to obtain the size frequencies, as follows.

If, for example, the cumulative percentage undersize by surface in *Figure 2.3* is to be converted into a distribution by mass (a procedure often needed when using a photosedimentometer—see section 2.7 on methods), equations 2.2 and 2.3 combined give:

$$f_M(x) = k\,x f_S(x) \tag{2.6}$$

which if integrated for all particle sizes up to a given size x_1

$$\int_0^{x_1} f_M(x)\,\mathrm{d}x = k \int_0^{x_1} x f_S(x)\,\mathrm{d}x \tag{2.7}$$

gives

$$F_M(x_1) = k \int_0^{F_S(x_1)} x\,\mathrm{d}F_S(x) \tag{2.8}$$

where F denotes the cumulative percentage such that

$$f_S(x) = \frac{\mathrm{d}F_S(x)}{\mathrm{d}x} \tag{2.9}$$

Equation 2.8 forms the basis for the conversion because

$$\int_0^{F_s(x_1)} x\,\mathrm{d}F_S(x)$$

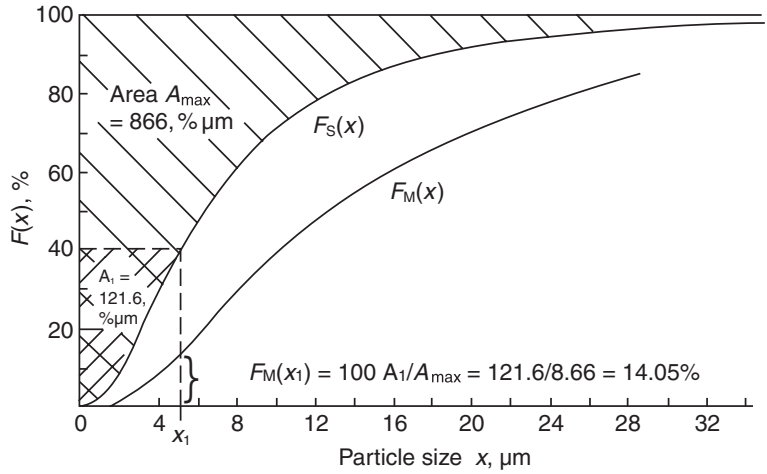

Figure 2.3 Example of conversion of F_S to F_M (surface to mass)

is simply the area A_1 under the curve up to the point corresponding to x_1 but integrated with respect to the vertical axis $F_S(x)$ as shown in *Figure 2.3*.

Hence,

$$F_M(x_1) = k A_1 \tag{2.10}$$

and k may be found from the condition that

$$k A_{max} = 1 \tag{2.11}$$

where

$$A_{max} = \int_0^1 x \, dF_S(x)$$

This conversion is carried out step by step as indicated in *Figure 2.3* and the resulting $F_M(x)$ can be plotted on the same graph.

To conclude this section, it must be emphasized that the conversions described above are to be avoided whenever possible (because of inherent errors in such procedures), by using a method which gives the desired type of distribution directly. Different methods give different particle size distributions (see *Table 2.7*, section 2.7) and the selection of a method is made on the basis of *both* the particle size and the type of distribution required. In most applications in solid–fluid separation, it is the particle size distribution by mass that is of interest because, usually, we are interested in gravimetric efficiencies and mass balances. There are, however, cases such as liquid clarification where the turbidity of the overflow is of importance (clarification of beer etc.) and particle size distribution by surface or even by number is more relevant.

2.4 Measures of central tendency

There are a great number of different average or mean sizes which can be defined for a given particle size distribution. The purpose of such measures of central tendency is to represent a population of particles by a single figure; this of course gives no indication of the width of the distribution but it may sometimes provide a useful guide for process control. The following relationships and definitions are based on general mathematical concepts, applied here specifically to particulate systems.

There are three most important measures of central tendency for a given size distribution (by a given quantity Φ)—see *Figure 2.4*: the mode, the median and the mean.

The mode is the most commonly occurring size, i.e. the size corresponding to the peak on the size distribution frequency curve. Some distributions may have more than one peak and are commonly referred to as multimodal distributions. The median or the 50% size is the size such that half the particles (by the given quantity Φ) are larger and half are smaller, i.e. the size which divides the area under the distribution frequency curve into two halves. The median is most easily determined from the cumulative percentage curves (see section 2.5) where it corresponds to 50%.

There are many mean diameters that can be defined for a given particle size distribution; their definition is, in a general form

$$g(\bar{x}) = \int_0^\infty g(x) f(x)\,\mathrm{d}x \tag{2.12}$$

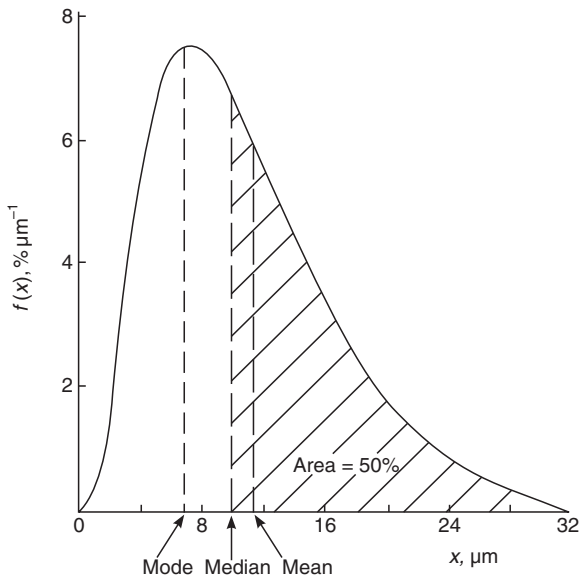

Figure 2.4 The mode, median and mean of a size distribution

where $f(x)$ is the particle size distribution frequency either by number, length, area or mass, whichever may be of interest, and $g(x)$ is a certain function of particle size x. Depending on the form of this function we have several types of mean diameters $\bar{x}$ as shown in *Table 2.4*.

Table 2.4 Types of mean diameter $\bar{x}$

Form of g(x)	*Name of mean diameter $\bar{x}$*
$g(x) = x$	arithmetic mean, $\bar{x}_a$
$g(x) = x^2$	quadratic mean, $\bar{x}_q$
$g(x) = x^3$	cubic mean, $\bar{x}_c$
$g(x) = \log x$	geometric mean, $\bar{x}_g$
$g(x) = 1/x$	harmonic mean, $\bar{x}_h$

Comparing equation 2.12 for the arithmetic mean ($g(x) = x$), quadratic mean ($g(x) = x^2$) and cubic mean ($g(x) = x^3$) with equations 2.1, 2.2 and 2.3 respectively, it may be shown that, for example, the number arithmetic mean relates the total length (if all particles are placed next to each other in a line) to the total number in the population and is therefore known as the number length mean x_{NL}; *Table 2.5* summarizes these relationships.

Evaluation of the various means required for a given size distribution is based on equation 2.12 which may also be written as

$$g(\bar{x}) = \int_0^1 g(x)\,\mathrm{d}F \tag{2.13}$$

because (similarly to equation 2.9)

$$f(x) = \mathrm{d}F/\mathrm{d}x \tag{2.14}$$

If either $f(x)$ or $F(x)$ are available as analytical functions (see section 2.5), the desired mean diameters are evaluated by integration following equation 2.12.

Table 2.5

$\bar{x}_{a\,number} = x_{NL}$	number length mean
$\bar{x}_{q\,number} = x_{NS}$	number surface mean
$\bar{x}_{c\,number} = x_{NV}$	number volume (or mass) mean
$\bar{x}_{a\,length} = x_{LS}$	length surface mean
$\bar{x}_{q\,length} = x_{LV}$	length volume (or mass) mean
$\bar{x}_{a\,surface} = x_{SV}$	surface volume (or mass) mean
$\bar{x}_{a\,volume} = x_{VM}$	volume (or mass) moment mean

For example, if the arithmetic mean of a log–normal distribution (see equation 2.24, section 2.5) is required, equation 2.12 becomes

$$\bar{x}_a = A \int_0^\infty x \exp\left(-b \ln^2 \frac{x}{x_m}\right) dx$$

where

$$A = \left(\frac{b}{\pi}\right)^{1/2} \frac{\exp(-1/4b)}{x_m}$$

b is a constant (known as the steepness constant, see equation 2.25) and

x_m is the mode (see section 2.5).

After integration this reduces to

$$\bar{x}_a = x_m \exp(3/4b)$$

or

$$\bar{x}_a = x_m c^{-3/2} \tag{2.15}$$

where

$$c = \exp(-1/2b) \tag{2.16}$$

If, however, no analytical function is fitted and the particle size distribution is in the form of a graph or a table, evaluation of mean diameters can best be done graphically.

As discussed in section 2.5, most particle size measurement techniques yield the cumulative percentage distribution $F(x)$, and these can be used in equation 2.13 directly as follows; if $F(x)$ is plotted against $g(x)$ for a number of corresponding sizes, $g(\bar{x})$ is then represented by the area under the curve with respect to the $F(x)$ axis as illustrated in *Figure 2.5*. The mean is

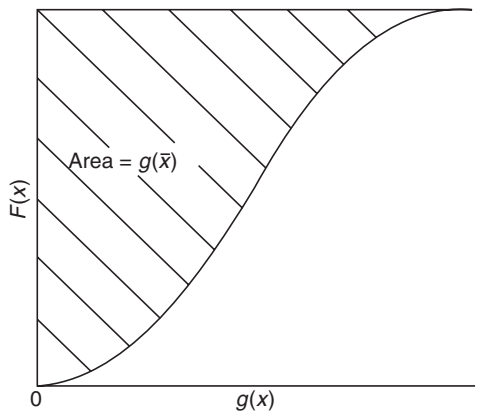

Figure 2.5 Evaluation of a mean $\bar{x}$ from the cumulative percentage $F(x)$

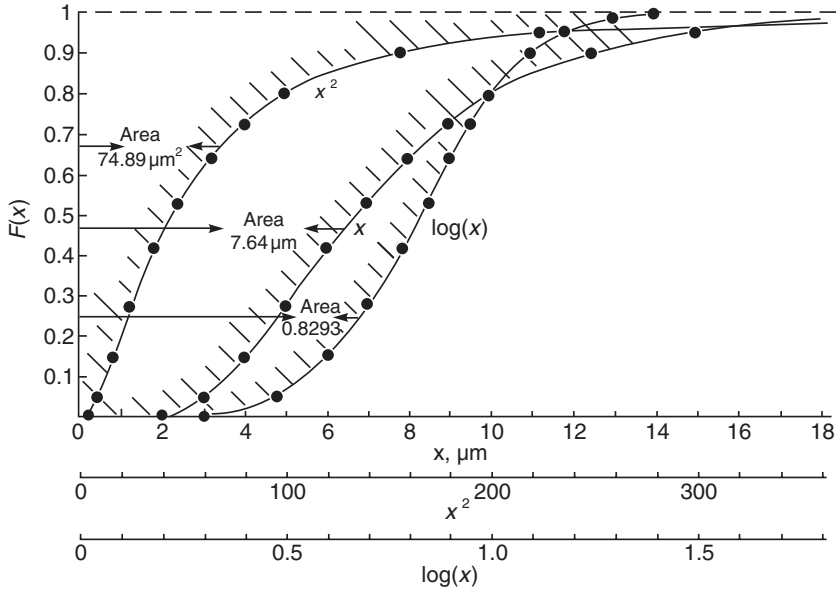

Figure 2.6 Example of graphical evaluation of arithmetic, quadratic and geometric means

evaluated from this area using the corresponding equation for $g(x)$—see *Table 2.4*.

It is immaterial whether $F(x)$ is plotted as percentage oversize or undersize.

Table 2.6 and *Figure 2.6* give an example of such a graphical evaluation of $\bar{x}_a$, $\bar{x}_q$ and $\bar{x}_g$. Experimental values of the cumulative percentage $F(x)$ are given in *Table 2.6*. For evaluation of the arithmetic mean $\bar{x}_a$, $F(x)$ is plotted against x and the area measured, giving $g(\bar{x}_a) = \bar{x}_a = 7.64\,\mu m$ (see *Figure 2.6*). The quadratic mean $\bar{x}_q$ is determined from a plot of $F(x)$ against x^2; the area is $g(\bar{x}_q) = \bar{x}_q^2 = 74.89\,\mu m^2$ thus $\bar{x}_q = 8.65\,\mu m$. Similarly, the geometric mean $\bar{x}_g$ may be calculated from the corresponding area on the plot of $F(x)$ against $\log x$, giving $g(\bar{x}_g) = \log \bar{x}_g = 0.8293$ and $\bar{x}_g = 6.75\,\mu m$.

There are a great number of different mean sizes and a question arises which of those is to be chosen to represent the population. The selection is of course based on the application, namely what property is of importance and should be represented. In liquid filtration for example, it is the surface volume mean x_{sv} (surface arithmetic mean $\bar{x}_{a\,surface}$) because the resistance to flow through packed beds depends on the specific surface of the particles that make up the bed (see equation 9.36). It can be shown that x_{sv} is equal to the mass harmonic mean $\bar{x}_h$ (see Appendix 2.2). For distributions that follow closely the log–normal equation (see section 2.5) the geometric mean $\bar{x}_g$ is equal to the median.

Table 2.6

Cumulative percentage undersize, %	*Particle size x,* μm	x^2, μm^2	log *x*
0.7	2	4	0.30
5.0	3	9	0.48
15.0	4	16	0.60
27.5	5	25	0.70
42.0	6	36	0.78
53.0	7	49	0.85
64.0	8	64	0.90
72.5	9	81	0.95
80.0	10	100	1.00
90.0	12.5	156	1.10
95.0	15	225	1.18
98.5	20	400	1.30
99.6	25	625	1.40

In conclusion it has to be emphasized that it is always best to represent a population of particles by the actual size distribution curve and only in cases when this is not possible or feasible should one resort to using a single number, a measure of central tendency, for characterizing a particulate system; in such cases care must be taken to select the type of mean size most relevant to the given application; some guidance is given in Appendix 2.1.

2.5 Presentation of data

Particle size distributions are presented either in an analytical form (as a function) or as a set of data in a table or a diagram. The distributions are given as either frequencies $f(x)$ or cumulative frequencies (expressed as fractions or percentages) $F(x)$ which mutually correspond because the frequency curve can be obtained by differentiation of the cumulative curve

$$f(x) = \mathrm{d}F(x)/\mathrm{d}x \tag{2.17}$$

or, vice versa, the cumulative curve $F(x)$ can be obtained by integration of the frequency $f(x)$, i.e.

$$F(x) = \int f(x)\,\mathrm{d}x \tag{2.18}$$

The area under the frequency curve is by definition equal to 1 (see *Figure 2.7*) so that $F(x)$ goes from 0 to 1 or 100%. The cumulative percentages are

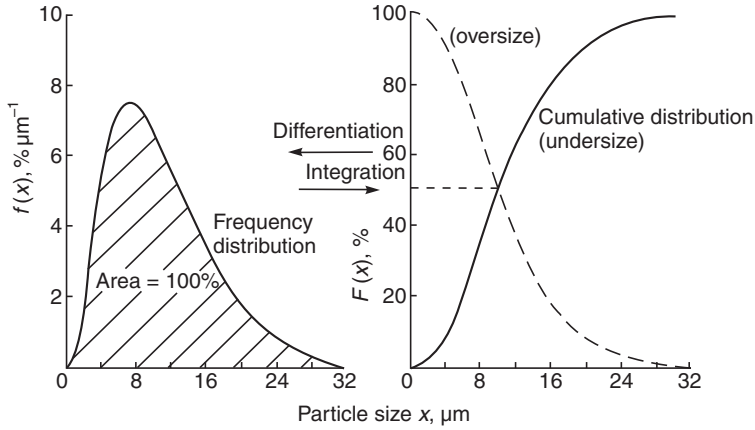

Figure 2.7 Relationship between frequency and cumulative distributions

given as either oversize or undersize, which mutually correspond because (see *Figure 2.7*)

$$F(x)_{\text{oversize}} = 1 - F(x)_{\text{undersize}} \tag{2.19}$$

Most particle size analysis methods do not produce continuous frequency curves but give percentages in a few ranges of particle size (e.g. with sieving). Many textbooks recommend that such information may be plotted as a histogram, which is a step-like frequency distribution curve. Such a plot is a very crude approximation of the actual, continuous frequency curve and a smooth curve cannot be accurately drawn through histograms. The preferred method is to plot the data cumulatively as percentages undersize or oversize and, as these points do lie on the actual distributions, a smooth curve may be drawn through them. If a distribution frequency curve is required, it should be obtained by differentiation of the cumulative plots, rather than directly from histograms.

Differentiation is often unnecessary because the required data processing (such as grade efficiency evaluation—see section 3.2.2—or evaluation of mean diameters) may be made using the cumulative plots directly. The main advantage of the distribution frequency curve is, however, that it gives a good illustration of the size spectrum particularly if it happens to be multimodal, i.e. if it has more than one local maximum.

Owing to the gradual increase in the availability and capacity of computers, it is becoming more and more convenient and feasible to fit an analytical function to the experimental particle size distribution data and then handle this function mathematically in further treatment. It is for example very much easier to evaluate mean sizes from analytical functions than from experimental data. Apart from the many curve-fitting techniques available, use can also be made of special graph papers which exist for many of the common

analytical functions used. A brief review of the functions available is given in the following. Most of them are two-parameter functions but some three-parameter equations are also shown, the latter being of course more general and more likely to fit closely the practical empirical data. All of the functions should be treated as empirical equations as they very rarely have any theoretical relation to the process in which the particles were produced.

2.5.1 Normal distributions

The normal distribution is a symmetrical bell-shaped curve referred to in statistics as a Gaussian curve. It is a two-parameter function, one parameter is the mean, $\bar{x}_a$ which due to the symmetry of the curve coincides with the mode and median, and the other is the standard deviation σ, which is a measure of the width of the distribution. The normal distribution of particle size is given by

$$\frac{dF}{dx} = \frac{1}{\sigma\sqrt{(2\pi)}} \exp\left(\frac{(x - \bar{x}_a)^2}{2\sigma^2}\right) \tag{2.20}$$

Graph papers are available on which the integral function to equation 2.20 ($F(x)$) is plotted against particle size x; normal distributions give straight lines on such a grid and the two parameters for equation 2.20 can be easily determined; the mean (which is also the median) corresponds to 50%, the standard deviation is the 84% size minus the 50% size.

Real powders and suspensions rarely fit normal distributions closely because in practice most particle size distributions are skewed. The main theoretical criticism of the normal distribution is that it extends into the region of negative size.

2.5.2 Log–normal distribution

The log–normal distribution is probably the most widely used type of function; it is again a two-parameter function, it is skewed to the right and it gives equal probability to ratios of sizes rather than to size differences, as in the normal distribution. The log–normal distribution equation is obtained from the normal distribution in equation 2.20 by substitution of $\ln x$ for x, $\ln x_g$ for $\bar{x}_a$ and $\ln \sigma_g$ for σ, i.e.

$$\frac{dF}{d(\ln x)} = \frac{x\,dF}{dx} = \frac{1}{\ln \sigma_g \sqrt{(2\pi)}} \exp\left(-\frac{(\ln x - \ln x_g)^2}{2 \ln^2 \sigma_g}\right) \tag{2.21}$$

As the plot of $dF/d(\ln x)$ against $\ln x$ is a normal distribution and, therefore, symmetrical, it follows from the definitions of the geometric mean (equation 2.12 and *Table 2.4*) that x_g represents the geometric mean of the distribution dF/dx. It can be shown mathematically that x_g is in this case equal to the median x_{50}.

As equation 2.21 does not explicitly express dF/dx, it is often given in a different form where x from the left-hand side of the equation is absorbed into the exponential term in the right-hand side and the substitution

$$\ln x_m = \ln x_g - \ln^2 \sigma_g \tag{2.22}$$

is made so that equation 2.21 becomes

$$\frac{dF}{dx} = \frac{1}{x_m \ln \sigma_g \sqrt{(2\pi)}} \exp(-\ln^2 \sigma_g/2) \exp\left(-\frac{(\ln x - \ln x_m)^2}{2 \ln^2 \sigma_g}\right) \tag{2.23}$$

This form of equation 2.21 is mathematically more convenient because the variable x only appears once in it; x_m represents the mode because it is the size at which dF/dx has its maximum.

Equation 2.23 may be re-written as[2]

$$dF(x) = A \exp\left(-b \ln^2 \frac{x}{x_m}\right) dx \tag{2.24}$$

where

$$A = \left(\frac{b}{\pi}\right)^{1/2} \frac{\exp(-1/4b)}{x_m} \tag{2.25}$$

and b is a new parameter called the steepness constant, and replaces σ_g:

$$b = \frac{1}{2 \ln^2 \sigma_g} \tag{2.26}$$

The relationship between the mode and the median in equation 2.22 assumes the form

$$x_m = c x_g \tag{2.27}$$

where

$$c = \exp\left(-\frac{1}{2b}\right)$$

(see equation 2.16).

Graph papers are available on which the integral function $F(x)$ is plotted against $\ln x$ and distributions that follow the log–normal law give straight lines. The evaluation of the two necessary parameters from the plots can be done in two somewhat different ways.

The conventional method, quoted in many textbooks[3], is based on equation 2.21. The median size $x_{50} = x_g$ is read off the chart, σ_g is the ratio of the 84% size to the 50% size. Equation 2.22 may be used for evaluation of the mode and the mean (arithmetic) may be calculated from its definition (equation 2.12 with equation 2.22)

$$\ln \bar{x}_a = \ln x_g + 0.5 \ln^2 \sigma_g \tag{2.28}$$

Similar equations exist for other types of means (x_q, x_c, x_h).

The second method is based on equation 2.24 and the parameters x_m and b may be determined either from x_g and σ_g (found as described above) using equations 2.22 and 2.26 or directly from a graph paper which is furnished with two additional scales of b and c (see *Figure 2.8*); the mode x_m is then determined from equation 2.27. This method offers the advantage of a mathematically simpler equation (equation 2.24) together with simpler equations for the various mean diameters (derived from the definitions in equation 2.12 with equation 2.24)

$$x_m = cx_g \tag{2.27}^*$$

$$\bar{x}_a = c^{-1/2}x_g \tag{2.29}$$

$$\bar{x}_q = c^{-1}x_g \tag{2.30}$$

$$\bar{x}_c = c^{-3/2}x_g \tag{2.31}$$

$$\bar{x}_h = c^{1/2}x_g \tag{2.32}$$

Example 2.1

The data given in *Table 2.6*, when plotted in *Figure 2.8*, give a straight line. The parameters for the conventional form of the log–normal equation (equation 2.21) are $x_g = 6.75$ and

$$\sigma_g = x_{84\%}/x_{50\%} = 11.15/6.75 = 1.65$$

The mode is, according to equation 2.22

$$x_m = \text{antilog}(\ln 6.75 - \ln^2 1.65) = 5.27\,\mu\text{m}$$

and the mean, according to equation 2.28

$$\bar{x}_a = \text{antilog}(\ln 6.75 + 0.5\ln^2 1.65) = 7.65\,\mu\text{m}$$

If the additional scales in *Figure 2.8* are used for parameter determination, then $b = 2.0$ and $c = 0.78$, giving, according to equation 2.27

$$x_m = 0.78 \times 6.75 = 5.27\,\mu\text{m}$$

and the complete size distribution function is then

$$\mathrm{d}F(x) = 0.134\exp\left[-2\ln^2\left(\frac{x}{5.27}\right)\right]\mathrm{d}x$$

with $A = 0.134$ determined from b and equation 2.25.

Equations 2.29 to 2.32 give

$$\bar{x}_a = 6.75/\sqrt{(0.78)} = 7.64\,\mu\text{m}$$

$$\bar{x}_q = 6.75/0.78 = 8.65\,\mu\text{m}$$

$$\bar{x}_c = 6.75/\sqrt{(0.78)^3} = 9.80\,\mu\text{m}$$

$$\bar{x}_h = 6.75\sqrt{(0.78)} = 5.96\,\mu\text{m}$$

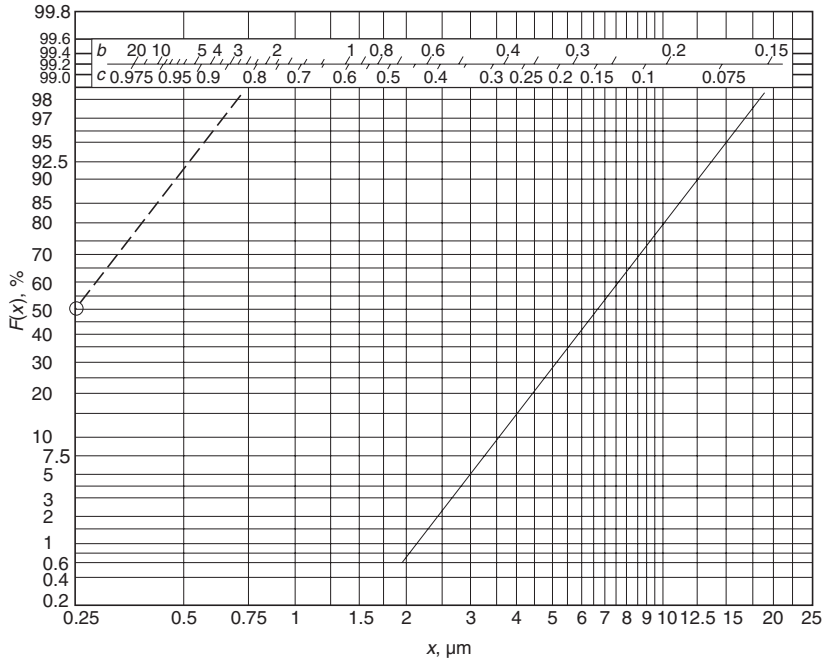

Figure 2.8 Log–probability paper furnished with two additional scales

Another important advantage of log–normal distributions is the easy conversion from one type of size distribution to another. It can be shown mathematically that all four particle size distributions, by number, length, surface and volume (mass), when plotted on log-probability paper are parallel lines with equal linear spacing, as can be seen in *Figure 2.9*, because

$$x_{\text{g length}} = x_{\text{g number}} \times \frac{1}{c} \tag{2.33}$$

and also

$$x_{\text{g surface}} = x_{\text{g length}} \times \frac{1}{c} \tag{2.34}$$

$$x_{\text{g mass}} = x_{\text{g surface}} \times \frac{1}{c} \tag{2.35}$$

Equations 2.33, 2.34 and 2.35 are derived from equations 2.1, 2.2, 2.3 and 2.24. As the lines in *Figure 2.9* are parallel, equations 2.33, 2.34 and 2.35 must also apply to all mean sizes and to the mode; the steepness constant b (or geometric standard deviation σ_g) remain the same and only x_m (or x_g) varies in equation 2.24 (or 2.21) so that the expressions for the four size distributions can be written easily from one set of experimental data (bearing in mind the

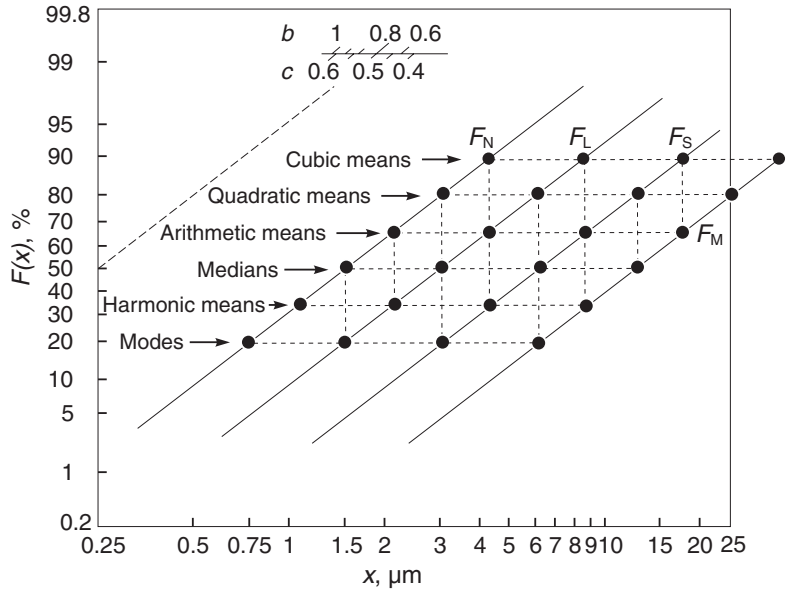

Figure 2.9 The four particle size distributions shown in Figure 2.2(a) plotted as cumulative percentages on log-probability paper; note the relationships between various means

assumptions involved in the conversions as discussed in section 2.3). *Figure 2.9* gives an example and also shows graphically the relationships between the different mean values.

Although the log–normal distribution is primarily a two-parameter function, one or even two extra parameters can be added to define the lower and/or the upper bound to the range of values of the variable[4] (this being the case in many practical size distributions).

2.5.3 The Rosin–Rammler distribution

The Rosin–Rammler distribution function is another equation widely used in particle size measurement. It is a two-parameter function, usually given as cumulative percentage oversize:

$$F(x) = \exp\left[-\left(\frac{x}{x_R}\right)^n\right] \tag{2.36}$$

where x_R is a constant giving a measure of the particle size range present and n is another constant characteristic of the material under analysis and gives a measure of the steepness of the cumulative curve. The frequency distribution is obtained by differentiation of equation 2.36.

Equation 2.36 can be reduced to

$$\log\left(\ln\frac{1}{F(x)}\right) = n\log x - n\log x_{\mathrm{R}} \tag{2.37}$$

which gives a straight line if $\log(\ln 1/F(x))$ is plotted against $\ln x$. This is the basis for the Rosin–Rammler graph paper; x_{R} can be easily found from the plot in the Rosin–Rammler graph paper because it is the size corresponding to $100/\mathrm{e} = 36.8\%$ and n is the slope of the line.

Rosin–Rammler charts from German sources contain edge scales, which with the aid of a parallel rule allow direct estimation of n. For accurate work, the use of large size (32.5×25.4 cm) charts designed by Harris[5] is recommended.

The various mean sizes available may be easily calculated from the Rosin–Rammler equation; they all involve the Gamma functions[3] which can be readily evaluated from mathematical tables.

2.5.4 Harris's three-parameter equation

Harris[6] introduced a three-parameter equation which is very versatile and fits most empirical size distributions that I have come across[7]. He showed that most of the widely used two-parameter equations are in fact special cases of the equation

$$F(x) = \left[1 - \left(\frac{x}{x_0}\right)^s\right]^r \tag{2.38}$$

where $F(x)$ is cumulative percentage oversize, x_0 is the maximum size in the sample, s is a parameter concerned with the slope of the log–ln plot in the fine size region and r is a parameter concerned with the shape of the log–ln plot in the coarse region. Using the same transformation as for the Rosin–Rammler equation (equation 2.37) we get from equation 2.38

$$\log\left(\ln\frac{1}{F(x)}\right) = \log r + \log\left(\ln\frac{1}{1-(x/x_0)^s}\right) \tag{2.39}$$

Harris developed a procedure for parameter determination based on equation 2.39 and it is similar in the region of extremely fine particles ($x/x_0 \ll 1$) to the Rosin–Rammler plot because for $x/x_0 \ll 1$:

$$\log\ln\frac{1}{1-(x/x_0)^s} \simeq s\log x - s\log x_0 \tag{2.40}$$

(compare with equation 2.37).

The procedure makes use of the standard Rosin–Rammler plot (which is usually curved in the coarse region) which is overlaid with a transparent tracing of several standard curves of $F(x) = (x/x_0)^s$ (Gates–Gaudin–Schuhman

equation as a special case of equation 2.38) furnished with an extra scale of r values; s is estimated from the slope of the fine end of the distribution and the values of x_0 and r are obtained from the relative shifts of the axes in the x and y directions respectively.

Harris's three-parameter equation is very flexible and can be closely fitted to most uni-modal distributions. As its mathematical form lends itself easily to further treatment it has been used in a relatively involved evaluation of results from scanning centrifugal sedimentation instruments for particle size analysis[7].

2.5.5 Other equations available

There is a wide range of other equations available for modelling particle size distributions, e.g. the Weibull function, the Gaudin–Meloy equation, Pearson's equations and many others. Harris presented a very comprehensive review of these[8] and after a very detailed study found that most of the well known distribution equations are in fact special cases of

$$\frac{\mathrm{d}F}{\mathrm{d}x} = c' x^{\alpha} \left[1 - \left(\frac{x}{x_0} \right)^{\gamma} \right]^{x_0^{\gamma}\beta'} \tag{2.41}$$

where c', α, β', γ and x_0 are parameters.

For the normal and the log–normal distributions, for example, $\alpha = 0$, $\gamma = 2$ and $x_0 \to \infty$: for the Rosin–Rammler distribution, $\alpha = n - 1$, $\gamma = n$ and $x_0 \to \infty$, and for Harris's three-parameter equation $\alpha = s - 1$, $x_0^{\gamma}\beta' = r - 1$ and $\gamma = s$.

2.6 Sampling

It is often said that particle size analysis can be only as good as the sampling technique used for collecting the sample. As all laboratory techniques (and also some on-line techniques) use a small sample taken from a production stream in which particle stratification or segregation often takes place, the correct sampling technique is critical for the accuracy of the eventual particle size analysis data.

There are two basic 'golden' rules of sampling:

1 sampling should be made preferably from a moving stream (this applies to both powders *and* suspensions);
2 a sample of the whole of the stream should be taken for many short periods rather than part of the stream for the whole of the time.

It is very likely that a sample collected from the main production stream is going to be too large for most particle size analysis techniques; the

problem is then to ensure a good subdivision of the sample into several fractions, all representing closely the original sample. In liquids this is usually done by sampling a stirred suspension with a syringe. This is satisfactory for fine suspensions but with coarser suspensions concentration gradients and the stratification of particles resulting from the centrifugal motion of the liquid caused by the stirring action may lead to appreciable deviations in both the size distribution and concentration of solids in the sample. Burt *et al.*[9] developed a suspension sampler for such subdivisions of coarse suspensions, which divides a sample of from 10 to 100 ml into ten fractions; Burt found it to give significantly better results than the syringe withdrawal.

If the second rule cannot be satisfied for some reason and a small sample has to be withdrawn continuously from a moving suspension, then some thought has to be given to a sampling condition referred to as 'isokinetic sampling'. This is based on the aspiration of a sample of the suspension from the main stream through a sampling probe (with the sampling nozzle pointing towards the direction of flow) so that the velocity of flow into the nozzle is identical with the undisturbed local stream velocity. Isokinetic sampling is designed to ensure an accurate representation of the coarse particles in the sample because at higher or lower sampling rates than isokinetic, the proportion of coarse particles in the sample would, because of inertial effects, be lower or higher respectively.

Fine particles have a low inertia compared with the drag force, and follow the flow closely whatever the sampling rate.

Whilst isokinetic sampling is usually critical in dust-laden gas[10] sampling it does not have to be observed in most applications of liquid suspension sampling because of the high liquid viscosities. An inertia parameter (Stokes' number) is usually used to assess the necessity of isokinetic sampling; Parker[11] suggested the range of

$$0.05 < \Psi < 50 \tag{2.42}$$

outside of which isokinetic sampling is not critical.

The inertia parameter used is the ratio between the particle stopping distance and the diameter of the sampling nozzle D so that

$$\Psi = \frac{ux^2\rho_s}{18\mu D} \tag{2.43}$$

where u is velocity of flow, ρ_s is the density of solids and μ is the viscosity of the suspending liquid.

Equation 2.43, using the lower limit of $\Psi = 0.05$, gives $x_{\text{critical}} \simeq 60\,\mu\text{m}$ for $u = 1\,\text{m s}^{-1}$, $D = 1\,\text{cm}$, $\mu = 0.001$ (water) and $\rho_s = 2600\,\text{kg m}^{-3}$ (silica). It can therefore be concluded that isokinetic sampling of liquid suspensions only becomes important if the suspensions contain very coarse particles (in our example, coarser than 60 μm); equations 2.42 and 2.43 can be used to assess the necessity of isokinetic sampling for any given conditions.

For sampling of powders in a dry form, Allen[12] reviewed and tested most methods available and found the spinning riffler to be the best.

2.7 Laboratory measurement of particle size

There is an abundance of methods available for the measurement of particle size distributions and many excellent textbooks exist[3] which review the field in great depth. Because of the limited scope of this chapter only a short review of the methods particularly relevant to solid–liquid systems is given.

Table 2.7 gives a schematic review of the methods available, the size ranges covered and the types of particle size and size distribution measured. This information is given in order to assist an engineer faced with the problem of selection of the best method for a given application—only a preliminary selection can be attempted using *Table 2.7*, because it was impossible to list all the important factors influencing the choice, these are:

1 type of equivalent diameter required;
2 quantity to be measured (number, surface, mass);
3 size range;
4 quantity of sample available;
5 number of points on the distribution (or perhaps just some measure of central tendency) required;
6 number and frequency of analyses required;
7 operator's involvement and degree of experience necessary;
8 cost of accessories such as sample preparation, evaluation of data etc.;
9 degree of automation required.

It should be noted that many of these factors are inter-related and their relative importance varies in different applications.

As was stated in the introduction, Stokes' diameter x_{St} is usually used to characterize particle size in those applications where it is the behaviour of particles in liquids that determines the separation efficiency and other operational characteristics of the separators (e.g. in sedimentation, centrifugation and hydrocyclones). Methods that measure Stokes' diameter, such as sedimentation or fluid classification, have therefore been used extensively in this field. Although preference is naturally given to wet methods, air classification is also widely used.

Most of gravity sedimentation techniques use an initially homogeneous suspension in which particles are allowed to settle under the influence of gravity. Two basic modes of operation can be found in practice: the fraction of particles which have a given settling velocity is determined from either the concentration measurements at a certain depth below the surface in a sedimentation cell (incremental techniques) or from measurements of the total mass of solids accumulated at the bottom (cumulative techniques).

Table 2.7 Classification of laboratory methods of particle size measurement*

Method	*Approximate size range, μm*	*Type of particle size—see Tables 2.1, 2.2, 2.3*	*Type of size distribution*
Sieving (wet or dry)			
Woven wire	37–4000	x_A	by mass
Electro-formed	5–120		
Microscopy			
Optical	0.8–150	x_a, x_F, x_M	by number
Electron	0.001–5	x_{SH}, x_{CH}	
Gravity sedimentation			
Incremental (except photosedimentation)	2–100	x_{St}, x_f	by mass (by surface)
Cumulative	2–100	x_{St}, x_f	by mass
Centrifugal sedimentation			
Two layer—incremental —cumulative	0.01–10	x_{St}, x_f	by mass
Homogeneous—incremental			
Flow classification			
Gravity elutriation (dry)	5–100	x_{St}, x_f	by mass
Centrifugal elutriation (dry)	2–50	x_{St}, x_f	by mass
Impactors (dry)	0.3–50	x_{St}, x_f	by mass or by number
Cyclonic (wet or dry)	5–50	x_{St}, x_f	by mass
Coulter principle (wet)	0.8–200	x_v	by number or by volume
Particle counters (wet or dry)	0.3–100 or 2–9000	x_p, x_s	by number
Field flow fractionation	1 nm–100 μm	x_d	depends on detector
Hydrodynamic chromatography	0.01–50	x_d	depends on detector
Fraunhofer diffraction (laser)	1–2000	equivalent laser diameter	by volume
Mie theory light scattering (laser)	0.1–40	equivalent laser diameter	by volume
Photon correlation spectroscopy	0.003–3	equivalent laser diameter	by number
Scanning infrared laser	3–100	chord length	by number
Aerodynamic sizing in nozzle flow	0.5–30	x_d	by number
Mesh obscuration method	5–25	x_A	by number
Laser Doppler phase shift	1–10 000	equivalent laser diameter	mean only
Time-of-transition	2–1200	equivalent laser diameter	by number
Surface area determination		x_{SV}	mean only (surface volume)
Permeametry			
Hindered settling			
Gas diffusion			
Gas adsorption			
Adsorption from solution			
Flow microcalorimetry			

* For details of the newer methods in the latter part of this table, consult Lloyd[15].

Sedimentation balances and β back-scattering techniques have been used for the cumulative measurements while sampling (Andreasen pipette method) or the absorption of radiation (photosedimentation or use of X-rays) are most frequently used for the incremental measurements. It seems that the incremental techniques, because of their advantages of easy operation and evaluation, and relatively simple instrumentation, have somewhat wider application.

Stokes' law is used for the evaluation of particle sizes corresponding to the setting velocities of the appropriate mass fractions measured; this law gives the well known equation

$$x_{\mathrm{St}} = \sqrt{\left(\frac{18\mu v}{\Delta\rho g}\right)} \tag{2.44}$$

which requires knowledge of the liquid viscosity, μ; the difference between the density of solids and of the liquid, $\Delta\rho$; and the acceleration due to gravity g. There are many applications in which μ and $\Delta\rho$ are difficult to determine with a sufficient degree of certainty, say when the density of the solids varies with particle size, and in such cases the conversion from the settling velocity, ν, to the particle size x_{St} in equation 2.44 is simply not carried out and the results are left in the form of the distribution of settling velocities (usually by mass). Equation 2.44 requires SI units or units in any other consistent system; many experienced particle size analysts use and remember its more convenient but dimensionally inconsistent form

$$x_{\mathrm{St}} \simeq 175\sqrt{\frac{\mu\nu}{\Delta\rho}} \tag{2.45}$$

where the units are x_{St}, μm; μ, P; ν, cm min^{-1} and $\Delta\rho$, g cm^3. (The constant in equation 2.45 is, more accurately, 174.90.)

All of the gravity sedimentation techniques, with the exception of photosedimentometers which detect the projected area of the particles (which in turn is proportional to particle surface) measure size distribution by mass. Photosedimentometers can only give useful results for particles coarser than around 5 μm because for finer particles the wavelength of light becomes comparable to the particle size, the laws of geometric optics break down and the so-called light extinction coefficient becomes highly size dependent.

In centrifugal sedimentation the days of bottle or tube-type centrifuges seem to be over and the disc centrifuge almost entirely dominates the field. In addition to equipment which uses the homogeneous technique, some disc centrifuges are also designed to use a 'line start' or 'two layer' technique where a thin layer of suspension is introduced on top of a clear suspending fluid. This mode of operation leads to very simple evaluation of results but suffers from an effect called streaming, which results from particles breaking through the initial interface in 'streams'. This can be overcome by various means but observation by an operator is always required. A more serious disadvantage of the line start technique is that it is inherently unstable because at all times after the start of the analysis density inversions occur (higher

suspension densities at small radii than 'lower down' at greater radii). Both the line start and the homogeneous mode of operation may be used either cumulatively or incrementally and the latter is again more frequent in use.

Instruments working with initially homogeneous suspensions are very simple in operation but evaluation of the results is mathematically complicated. Unlike the gravity settling, particles here settle along radial, i.e. diverging paths and this continuous dilution effect obscures the fall in concentrations resulting from particles falling out of the suspension. Several evaluation methods have been suggested including a semi-automated analogue evaluation[13] designed for an X-ray centrifugal sedimentometer. An equivalent to the Andreasen pipette method in gravity sedimentation is the Simcar centrifuge or the recently introduced Ladal Pipette Centrifuge[14] where samples are withdrawn at different times from a given depth in a rotating suspension. The latter offers increased versatility (0.01 to 5 μm) and requires only a small sample of 1 to 2 g.

In centrifugal sedimentation the basic equation for the conversion of settling velocity to particle size is analogous to equation 2.44:

$$x_{St} = \sqrt{\left(\frac{18\mu \ln R/R_0}{\Delta\rho\omega^2 t}\right)} \tag{2.46}$$

where R is the radius of the measurement zone, R_0 is the radius of the liquid surface, ω is angular speed and t is time from the start of the analysis.

Equation 2.46 becomes:

$$x_{St} = 5477\sqrt{\left(\frac{\mu \ln (R/R_0)}{\Delta\rho\omega^2 t}\right)} \tag{2.47}$$

where the units are μ, P; $\Delta\rho$, g cm^{-3}; ω, s^{-1} and t, min.

Finally it should be pointed out that equations 2.44 and 2.46 have a limited application to small sizes (the minimum is 1 μm in a gravity field and much smaller in a centrifugal field depending on the speed of rotation) when Brownian motion effectively slows down settling rates and to large sizes when, for Reynolds numbers greater than about 0.2, increasing deviations from Stokes' law occur.

Elutriation and fluid classification methods are also highly relevant to solid–liquid separation problems—they use the same or similar mechanisms for analysis as many separators. Use is made here of the size-dependent nature of dynamic separation processes and most of these methods are based on the analytical cut size defined in chapter 3, 'Efficiency of Separation'.

In cake filtration, where the surface volume diameter is of interest, methods for surface area determination are relevant (these measure only mean sizes) particularly, permeametry, gas diffusion and hindered settling methods.

Other methods of particle size measurement are also widely used in the characterization of suspensions, e.g. particle counters or the Coulter principle in filter rating, microscopy for general particle investigations and screening for coarse solids (above 75 μm).

Table 2.7, particularly the lower part, also contains some more recent additions to the available laboratory measurement methods. Many of these methods involve the use of a laser and the interaction between its light output and an assembly of particles. Most of these methods give a fast response and are thus suitable for automation and for application of the statistical measurement control techniques (see section 2.9). It cannot be said, however, that any of the newer methods are particularly suitable in solid–liquid separation; their increasing popularity in industry owes more to their speed and ease of use than to their fundamental suitability for solid–liquid applications. Only a very brief account of the newer methods is given below, in the same order as they appear in *Table 2.7*, and for further reading and details the reader is referred to Lloyd.[15]

In field flow fractionation, a sample is injected into a narrow channel where stratification according to particle size takes place under the effects of gravity or centrifugal fields. The coarse particles are eluted from the channel later than the fine ones due to the flow being slower lower down, near the wall, where the coarse fraction prevails. The concentration at the outlet of the channel is monitored over time using a variety of detectors, mostly based on light extinction.

Hydrodynamic chromatography relies on different particle velocities in laminar flow through capillaries or packed columns. Larger particles move faster with the flow than do fine ones because they are, on average, further away from the capillary wall. The operation and the equipment are the same as in liquid chromatography: colloidal particles are injected into a column packed with beads and a suitable detector (ultraviolet light detector or a spectrophotometer) monitors the flow from the column. Both field flow fractionation and hydrodynamic chromatography are most suitable for nearly mono-sized particle systems.

A number of expensive but very powerful analysers available on the market are based on Fraunhofer diffraction. An assembly of particles in a liquid or in a gas are illuminated by an expanded laser beam and the particle size distribution is derived from the measurement of the spatial distribution of the diffraction patterns on a flat detector behind the sample.

A similar principle but different hardware and software are used in the Mie theory light-scattering-based laser analysers, extending the range into the submicron region.

Photon correlation spectroscopy measures the interference between coherent light and fine particles diffusing in a liquid. The interference is modulated by the random motion of the particles which depends on their size; a correlation computer evaluates the size distribution from the autocorrelation function of the signal measured in one or more defined scattering directions.

The scanning infrared laser method sends an oscillating laser beam into a suspension and detects back-scattered infrared light. The random chords within particles are thus measured and this information is related to the particle size distribution of the suspension. This method can be used to

measure more concentrated suspensions than can most other light-based methods.

The equivalent aerodynamic diameter of dry powder or aerosol particles can be measured using aerodynamic sizing in nozzle flow. This measures the transit times between two focussed laser beams in accelerated air flow seeded with particles.

The mesh obscuration method is a quick way of, for example, measuring the size of the contaminant in lubricating liquids. The contaminated fluid is passed through a fully characterized filter mesh and the development of a pressure drop is monitored. The number of particles larger than the mesh size is deduced from the pressure drop; three filter mesh units are used in series.

A mean particle size can be measured using laser Doppler phase shift. Two laser beams cross in a measurement volume and scattered light is measured; in addition to the usual velocity measurement obtained from the frequency shift, the phase shift can provide the mean particle size.

Finally, the recently proposed time-of-transition method scans a focussed, narrow laser beam in a measurement zone, in a circular fashion. The interaction pulses are detected by a photodiode behind the beam. The pulse width is a measure of particle size, and particle shape analysis is also possible.

2.8 On-line measurement techniques

Automation of process control has created a need for continuous monitoring of the particle size of particulate matter in process streams. Some ‘on-line’ particle size analysis instrumentation has been developed recently to meet this need; it can initiate regulatory or shut-down signals in control systems. The basic requirements for such instrumentation are that it must operate automatically and continuously under preset instructions, and the response time from observation to readout must be so short as to be nearly instantaneous.

This relatively new range of techniques follows the general pattern found in the whole subject of particle size measurement: a variety of techniques differing in

1 principle;
2 suitability for different systems, materials and particle sizes;
3 the types of particle diameters they measure;
4 the number of points on the distribution they are capable of determining;
5 degree of truly ‘on-stream’ operation.

Some methods only give a measure of central tendency (a mean diameter), others give one or more points on the size distribution. They may be truly on-line in operating on the whole process stream, or they may need a partial sample stream taken off the main stream or they may merely be automated rapid-response batch techniques.

On-line measurement is a buoyant area which is undergoing fast growth. Reviews in the literature become quickly out of date; there are two excellent review papers published by Hinde and Lloyd[16] and by Stanley-Wood[17], the latter also listing some methods that are merely fast-response laboratory techniques.

Equipment may be broadly divided into two categories: 'stream scanning' and 'field scanning'. Stream scanning is generally applied to dilute systems; the particles are sent in single file past a detecting device, i.e. a particle counter based on the Coulter method, a light interruption or scattering method, or the Langer acoustic method. All of these require a small sample withdrawn continuously from the main stream, with all the associated sampling problems.

Field scanning usually applies to concentrated systems in which some size-dependent behaviour of the bulk material is monitored and the particle size is deduced from theoretical or calibrated relationships. Ultrasonic attenuation, echo measurements, laser attenuation, on-line viscometry, electronic noise correlation techniques, X-ray attenuation and X-ray fluorescence are examples of such field scanning methods. Most relevant to solid–liquid separation problems are those field scanning instruments which deduce particle size from the separation efficiency of some separational equipment, using the concept of the analytical cut size (see chapter 3 'Efficiency of Separation of Particles from Fluids'). Firstly, there are automatic wet sieving machines, one developed by Hinde and Lloyd[16] and another described by Schönert *et al.*[18] Secondly, the separation performance of hydrocyclones which may already form parts of some industrial plants, has been suggested as a means of giving an indication of changes in particle size in the feed suspension[19]; particle size measurement is thus reduced to solids concentration measurement.

The use of cyclones or other separators, in the sampling mode, for on-line particle size measurement is now well established in both dry[20–23] and wet applications[24,25]. This involves taking a continuous sample stream through a small cyclone or hydroclone under a given set of operating conditions, and monitoring the recovery of the cyclone. The task of particle size measurement is thus reduced to measurement of solids concentrations in two material streams.

A similar idea forms the basis for the operation of the Mintex/RSM slurry analyser[26,35] based on the work of Holland-Batt[27]; the slurry is pumped through a single-turn helical tube of rectangular cross-section and β-ray attenuation measurements before the helix and at different positions just after the helix (where particle stratification occurs due to centrifugal forces) yield a point on size distribution data. The instrument requires calibration, which can be made at any selected reference size in the range of 10 to 105 μm.

2.9 Statistical measurement control

The recent proliferation of fast and convenient instruments for particle size analysis has brought with it, for the first time in this subject, a practical

opportunity to apply the techniques of statistical measurement control. Repeat analyses with such instruments are easy and statistical techniques can thus be used to evaluate precision and accuracy, and keep the measurement under statistical control. We can no longer justify making comparisons or conclusions on the basis of one or two measurements, as was so often the case in the past.

A measurement process is said to be under statistical control when all the critical parameters and conditions are under sufficient control such that any variation in data from repeated measurements does not change over an extended period of time. The variation (scatter) must also be demonstrated to occur in a random fashion. The best way of checking this is to use control charts[28–34] in which the mean values and standard deviations of replicate measurements are plotted against time and the data are checked to be within statistically derived limits.

The replicate measurements (at least two each time) are made over a prolonged period of time (at least 40 times), on a 'check-standard' sample which must remain constant and homogeneous during the measurement cycle. Software packages are available to assist in the evaluation of results and in plotting the control charts, and any measurements outside the control limits are automatically highlighted. Visual inspection of the charts may reveal systematic trends on drifts. The variability is then analysed, its causes identified and brought under control and reduced.

Apart from data on precision (repeatability, reproducibility), control charts may be used to check or monitor accuracy, i.e. to what extent the measured value of a quantity (such as the mean particle size, for example) agrees with the accepted value for that quantity, bearing in mind that the 'true value' is never known. In testing accuracy, the standard test powders available on the market[33] may be used.

It is beyond the scope of this book to give more than a quick review of this important subject. The interest in and application of the statistical-measurement control techniques in particle size measurement, however, are certain to continue to grow in the future.

Appendix 2.1 The choice of a mean particle size

As shown in section 2.4, there is a bewildering variety of different definitions of 'mean' particle size. Most textbooks quote the definitions either in the form of summations or as integrals, the latter being more appropriate if the particle size distributions are generated as continuous curves. Few textbooks, however, give any hints as to which of the definitions are to be used and when. This is a serious omission because the correct choice of the most appropriate mean is vital in most applications.

As can be seen from *Figure 2.A1.1*, two different size distributions may have one mean the same (arithmetic mean in the example) but all the other

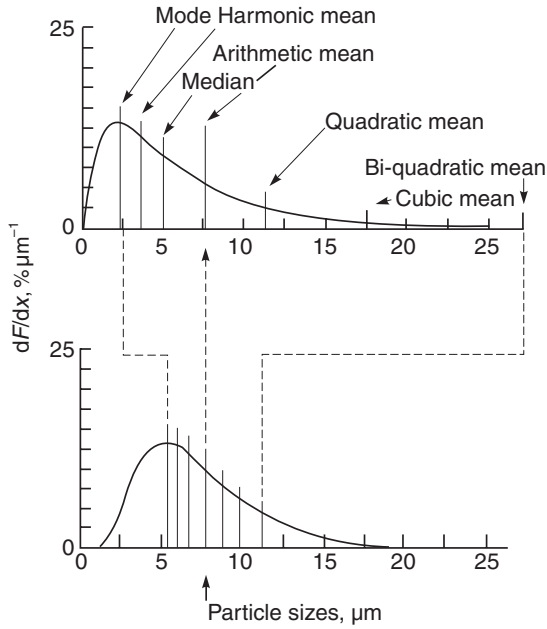

Figure 2.A1.1 Two different size distributions with the same arithmetic mean

means may be different. Thus, if the comparison is made on the basis of that one mean (arithmetic in this case), the distributions would be judged to be the same. If any of the other means were chosen, the conclusion would be very different: according to the higher order means such as the quadratic or cubic means, the top distribution in *Figure 2.A1.1* is the coarser of the two, whilst according to the median or harmonic mean the top distribution is finer. The wrong choice of the mean may, therefore, lead to incorrect or misleading conclusions and examples of this may be found in many branches of particle technology.

The mean particle size is rarely quoted in isolation: it is usually related to some application and used as a single number to represent the full size distribution. It represents the distribution by some property which is vital to the application or process under study; if two size distributions have the same mean, the two materials are likely to behave in the process in the same way.

It is, therefore, the application which governs the selection of the most appropriate mean. Usually, enough is known about the process under study to be able to identify some fundamentals which can then be used as a starting point. The fundamental relations may be oversimplified or inadequate to describe the process fully, but it is still better to use these relations than to pick the mean definition out of a hat!

Two examples of some simple fundamentals used in the selection of the most relevant mean in solid–liquid separation are given below.

Example 2.A1.1

Application: flow through packed beds (e.g. cake resistance in filtration, cake washing or dewatering)

If the particle size distribution in *Table 2.6* (plotted in *Figure 2.8*) is by mass and the material forms a filtration cake, what is the value and definition of the mean to be used when correlating particle size with specific cake resistance?

Solution

Firstly, the decision about the definition of the mean has to be made. Equation 9.36 gives a fundamental relationship which can be used here

$$\alpha = \frac{K_o S_0{}^2}{\rho_s} \frac{(1-\epsilon)}{\epsilon^3} \tag{2.A1.1}$$

where α is the specific cake resistance, K_0 is a constant, S_0 is the volume specific area of the solids making up the cake and ϵ is the voidage of the cake.

We can relate the specific surface to particle size but no simple relationship exists for the voidage. All we can do here is to assume that ϵ is constant, independent of particle size; the task is then to represent the particle population by a mono-size system (mean size) which has the same S_0 as the real population.

It can be shown that, for a sphere, the specific surface is

$$S_0 = 6/\bar{x}$$

and this is to be equal to the total surface/total volume of the real distribution. The mean $\bar{x}$ is then calculated as

$$\bar{x} = \frac{6 \cdot \text{total volume}}{\text{total surface}}$$

i.e.

$$\bar{x} = \frac{\Sigma x_i S_i}{\Sigma S_i}$$

where S_i is the surface area of a particle of size x_i.

Analytically, this can be written as

$$\bar{x} = \int_0^1 x \, \mathrm{d}F_{\text{surface}}$$

which is the definition of the arithmetic mean of the distribution by surface $\bar{x}_a$ (equation 2.13 and *Table 2.4*).

The remaining task is to determine $\bar{x}_a$ from the distribution by surface; our size distribution is by mass, however, and a conversion has to be made. Rather than converting the whole distribution (from mass to surface) in this case, because the distribution is log–normal (see *Figure 2.8*), we can use the fact that the arithmetic mean by surface is equal to the harmonic mean by mass

(see Appendix 2.2). The harmonic mean of the above distribution was determined in this example (*Example 2.1*) as 5.96 μm which is the mean size to be used in correlation with the specific cake resistance.

Example 2.A1.2

Application: mass recovery of solids in a dynamic separator such as a gravity settling tank or a sedimenting centrifuge

Which of the two particle size distributions given in *Table 2.A1.1*, if suspended in a liquid, would you expect to give higher mass recovery in a gravity settling tank and why?

The two samples are of the same solid, i.e. are of the same solids density (greater than that of the liquid), suspended in the same liquid and the settling tank is run at identical operating conditions (same residence time, temperature, etc.) for both samples. The two distributions were determined by sedimentation and are given as per cent by mass.

Table 2.A1.1 Two particle size distributions determined by sedimentation (in per cent by mass)

Particle size, μm	*Sample 1, % undersize*	*Sample 2, % undersize*
20	7.94	33.05
30	27.45	50.00
40	49.01	62.22
60	78.37	77.34
90	94.46	88.27
130	99.01	94.37
170	99.79	96.97
210	99.95	98.24
230	100.00	100.00

Solution

The above problem lies in determining which of the two distributions given is coarser, for the purpose of recovery in gravity settling tanks. Let us derive, from some simple first principles, the definition of a mean to be used in this problem as a criterion for the comparison.

Total recovery of any separator can be obtained by processing the feed size distribution (cumulative) $F(x)$ with the operating grade efficiency curve $G(x)$ of the separator. Mathematically, this can be written as

$$E_T = \int_0^1 G(x)\,\mathrm{d}F \tag{2.A1.2}$$

A simple, plug-flow model of the separation in a settling tank without flocculation gives the grade efficiency in the following form

$$G(x) = \frac{u_t A}{Q}$$

where A is the settling area, Q is the suspension flow rate and u_t is the terminal settling velocity of particle size x.

Assuming Stokes' law for the terminal settling velocity

$$u_t = \frac{x^2 \Delta \rho g}{18 \mu}$$

The above three equations, when combined, give the total recovery as

$$E_T = \frac{A \Delta \rho g}{18 Q \mu} \cdot \int_0^1 x^2 \, dF$$

where the integral is, of course, the definition of the quadratic mean, of the particle size distribution by mass because E_T is by mass (see equation 2.13 and *Table 2.4*).

The relevant mean to be used in the comparison of the two particle size distributions of this example is, therefore, the quadratic mean of the mass distribution. The graphical method outlined in section 2.4, when applied to the data given in the above example, yields the plots in *Figure 2.A1.2*. As the question does not require numerical answers, it is merely necessary to decide from the plots which of the two would give the greater area between the curve and the y axis.

As shown in *Figure 2.A1.2*, the deduction can be made from a simple comparison of the cross-hatched areas; as area A is greater than area B it follows that the quadratic mean of sample 2 is coarser than that of sample 1 and the recovery with sample 2 would, therefore, be greater.

This conclusion is, of course, subject to the assumptions made in the above derivation, but the example is merely used to illustrate the method and more realistic (and more complicated) assumptions may be used if necessary.

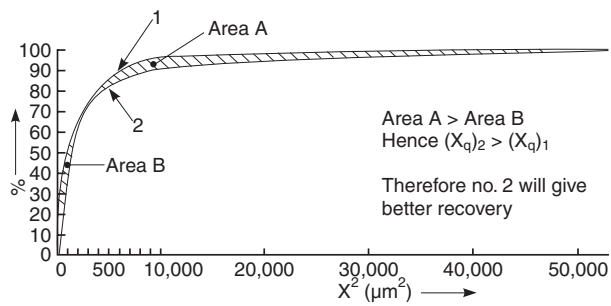

Figure 2.A1.2 Plots of F against X^2 to determine the quadratic means

Appendix 2.2 Can the Arithmetic Mean of the Surface Distribution (Surface–Volume Diameter) be Determined from the Mass Distribution?

The distributions by surface and mass can be related by the following equation (from equations 2.2 and 2.3)

$$f_{\mathrm{m}}(x) = k\,x f_{\mathrm{s}}(x)$$

This can be written explicitly for f_{s}, but by substituting $\mathrm{d}F$ for f

$$\mathrm{d}F_{\mathrm{s}} = \mathrm{d}F_{\mathrm{m}}/(k\,x)$$

By definition, the arithmetic mean of the surface distribution (see equation 2.13 and *Table 2.4*) is

$$(\bar{x}_a)_{\mathrm{S}} = \frac{1}{k}\int_0^1 \mathrm{d}F_{\mathrm{M}}$$

which, after substitution, gives

$$(\bar{x}_a)_{\mathrm{S}} = \int_0^1 x\,\mathrm{d}F_{\mathrm{S}}$$

i.e. the integral is equal to 1 and

$$(\bar{x}_{\mathrm{a}})_{\mathrm{S}} = \frac{1}{k}$$

The constant k may be determined from the equation for $\mathrm{d}F_{\mathrm{S}}$, after integration of both sides from 0 to 1:

$$k = \int_0^1 \frac{1}{x}\,\mathrm{d}F_{\mathrm{M}}$$

which is the definition of the harmonic mean of the mass distribution. Therefore, $(\bar{x}_{\mathrm{a}})_{\mathrm{S}} = (\bar{x}_h)_{\mathrm{M}}$ for any shape of the distribution, but only if k is a constant and not a function of x (i.e. the shape factor is independent of particle size).

References

1. Lloyd, P. J. and Ward, A. S., *Filtration and Separation*, **12**, 250 (1975)
2. Svarovsky, L., *Powder Technology*, **7**, 351–352 (1973)
3. Allen, T., *Particle Size Measurement*, 2nd edn. Chapman and Hall, London, (1975)
4. Aitchison, J. and Brown, J. A. C., *The Log–normal Distribution*, Cambridge Univ. Press, London, (1957)
5. Harris, C. C., *Powder Technology*, **5**, 39–42 (1971/72)
6. Harris, C. C., *Trans. SME*, **244**, No. 6, 187–190 (1969)
7. Svarovsky, L. and Friedova, J., *Powder Technology*, **5**, 273–277 (1971/72)
8. Harris, C. C., *Trans. SME*, **241**, 343–358 (1968)

9. Burt, M. W. G., Fewtrell, C. A. and Whatron, R. A., *Powder Technology*, **7**, No. 6 327–330 (1973)
10. Svarovsky, L., *Chemistry and Industry*, No. 15, 7 August 1976, 626–630 (1976)
11. Parker, G. J., *Atmospheric Environment*, **2**, 477–490 (1968)
12. Allen, T. and Khan, A. A., *Chem. Eng.* **238**, CE 108–112 (1970)
13. Svarovsky, L. and Svarovska, J., *Partikelmesstechnik*, Dechema-Monographien, Nr. 1589–1615, Band 79, 293–308, Dechema, Frankfurt-am-Main (1976) and Svarovsky, L. and Svarovska, J., *J. Phys. D: Appl. Phys.*, **8**, 181–190 (1975)
14. Allen, T. and Svarovsky, L., *Partikelmesstechnik*, Dechema-Monographien, Nr. 1589–1615, Band 79, 279–291, Dechema, Frankfurt-am-Main (1976)
15. Lloyd, P. J. (Ed.), *Particle Size Analysis*, Wiley, Chichester (1988)
16. Hinde, A. L. and Lloyd, P. J. D., *Powder Technology*, **12**, 37–50 (1975)
17. Stanley-Wood, N. G., *Control & Instrumentation*, **7**, No. 1, 30–35 (1975)
18. Schönert, K., Schwenk, W. and Steier, K., *J. Aufbereit. Verfahrenstech*, **7**, 368–372 (1974)
19. Lynch, A. J., Rao, T. C. and Whiten, N. J., *Proc. Australasian Inst. Mining Met.*, **223**, 71–73 (1967)
20. Nakajima, Y., Gotoh, K. and Tanaka, T., *I&EC Fundamentals*, **6**, No. 4, 587–592 (1967)
21. Svarovsky, L. and Hadi, R. S., 'A new on-line particle size analyser for fine powders', *Proc. Int. Symp. on Fine Particle Processing*, Vol. 1, Chap. 19, (Ed. P. Somasundaran), AIME, Las Vegas, 366–379 (1980)
22. Svarovsky, L., *Method and Apparatus for Monitoring Particle Size*, University Research Ltd., U.S. Patent No. 4179934, British Patent No. 1578157, German Patent DE 2932987 C2
23. Svarovsky, L. and Hadi, R. S., 'A new, simple and sensitive on-line particle size analyser for fine powders suspended in gases', *Proc. 2nd European Symposium on Particle Characterization* (Nuremberg), 343–359 (1979) (also by R. S. Hadi)
24. *Bestobell Cyclometric Sizer*, Bestobell Mobrey, Slough
25. Svarovsky, L., *Hydrocyclones*, Holt, Rinehart and Winston, London (1984)
26. *The Y1308/RSM Slurry Sizer*, Carter Group Ltd., Slough
27. Holland-Batt, A. B., *Inst. Mining and Metall.*, **77**, C185 (1968)
28. *ASTM Manual on Presentation of Data and Control Chart Analysis*, ASTM Publication No. STP 15D, Philadelphia (1985)
29. Belanger, B., *Measurement Assurance Programs, Part I: General Introduction*, NBS Special Publ. No. 676–I (1984)
30. *Statistical Quality Control Handbook*, AT&T, Delmar Printing Co., Charlotte, NC (1984)
31. Feigenbaum, A. V., *Total Quality Control*, McGraw-Hill, New York (1983)
32. Speitel, K., 'Measurement Assurance', in *Handbook of Industrial Engineering*, Wiley, New York (1982)
33. *BCR Test Powders*, Community Bureau of Reference, Rue de la Loi 200, B–1049 Brussels, Belgium (also available from the National Physical Laboratory, Teddington)
34. Wood, B., Ph. D. Thesis, University of Bradford (1988)
35. *MINTEK/TOPIC 2/2 Monitoring wet mill performance with the Mintek/R.S.M/ Slurry Sizer*, Cartner Group Ltd., Slough
36. Putnam, R., 'Optimizing grinding mill loading by particle size analysis', *Mining Congress J.*, **Sept.**, 68–74 (1973)

Further reading

Allen, T., *Particle Size Measurement (Powder Technology Series)*, 5th edn, Chapman & Hall (November 1997), ISBN: 0 41275 350 2

Bernhardt, I. C., *Particle Size Analysis—Classification and Sedimentation Methods*, Chapman & Hall (September 1994), ISBN: 0 41255 880 7

Gy, P. and Royle, A. G. (translator), *Sampling for Analytical Purposes*, John Wiley & Sons Ltd (abridged 153 pages) (July 1998), ISBN: 0 47197 956 2

Kaye, B. H., *Characterization of Powders and Aerosols*, John Wiley & Sons Ltd (January 1999), ISBN: 3 52728 853 8

Ortega-Rivas, E. and Svarovsky, L., 'A direct combined method for measuring particle size distribution in obtaining grade efficiency curves', *Powder Handling and Processing*, Vol. 6, No. 4, 401–404 (October/December 1994) also in: *Processing Part IV, Trans Tech Publications*, ISBN 0 87849 124 4, Clausthal-Zellerfeld, 31–34 (2000)

Ortega-Rivas, E. and Svarovsky, L., 'Centrifugal air classification as a tool for narrowing the spread of particle size distributions of powders', Bulk Solids Handling, Vol. 14, No. 4, 811–813 (October/December 1994) also in: *Processing Part I, Trans Tech Publications*, ISBN 0 87849 121 X, Clausthal-Zellerfeld, 193–195 (2000)

3

Efficiency of separation of particles from fluids

L. Svarovsky

FPS Institute, England and University of Pardubice, Czech Republic

3.1 Introduction

Imperfection in the performance of any real separation equipment can be characterized by the separation efficiency. In this chapter basic definitions are given together with the relationships between the efficiency and particle size distributions of various combinations of the feed, underflow or overflow product streams. Practical considerations for grade efficiency testing and total efficiency prediction are given, together with worked examples.

The so-called 'grade efficiency concept' studied here is applicable to those principles of and equipment for solid–liquid separation whose separational performance does not change with time if all operational variables are kept constant. Hydrocyclones, sedimenting centrifuges or gravitational clarifiers are examples of such equipment; the concept is not widely used in filtration because there the efficiency changes with the amount of solids collected either on the face of the filter medium (in cake filtration) or within the medium itself (in deep bed filtration). Even in filtration, however, it is interesting to determine the grade efficiency of the clean medium which governs the initial retention characteristics of the filter and can be used for filter rating (see the example given in *Figure 3.4*).

As the efficiency of separation is very often particle-size dependent, some separational equipment can be, and often is, also used for the classification of solids. This is the area where the grade efficiency concept was first developed; it is now also widely used in gas cleaning.

Hence there are three major operations in which this concept is applicable:

1 solid–liquid separation;
2 solid–gas separation (gas cleaning and dust control);
3 solid–solid separation (often called classification of powders) with liquid or gas as a medium.

3.2 Basic definitions and mass balance equations

A single-stage separational apparatus can be schematically drawn as in *Figure 3.1*, where:

M is the mass flow rate of the feed (in kg s^{-1})
M_c is the mass flow rate of the coarse material in the underflow (in kg s^{-1})
M_f is the mass flow rate of the fine material in the overflow (in kg s^{-1})
$dF(x)/dx$ is the size distribution frequency of the feed
$dF_c(x)/dx$ is the size distribution frequency of the coarse material
$dF_f(x)/dx$ is the size distribution frequency of the fine material
x is the particle size
Q is the volumetric flow rate of the feed suspension (in $m^3\,s^{-1}$)
O is the volumetric flow rate of the overflow suspension (in $m^3\,s^{-1}$)
U is the volumetric flow rate of the underflow suspension (in $m^3\,s^{-1}$).

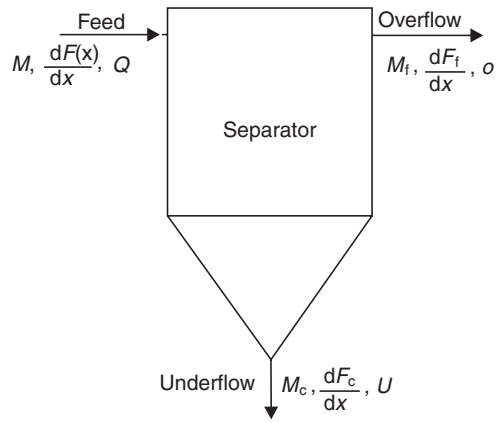

Figure 3.1 Schematic diagram of a separator

The total mass of the feed must be equal to the sum of the total masses of the products if there is no accumulation of material in the equipment, i.e.

$$M = M_c + M_f \tag{3.1}$$

Mass balance must also apply to any size fractions present in the feed if there is no change in particle size of the solids inside the separator (no agglomeration or comminution). Hence for particles of size between x_1 and x_2:

$$(M)_{x_1/x_2} = (M_c)_{x_1/x_2} + (M_f)_{x_1/x_2} \tag{3.2}$$

and also for each particle size x present in the feed:

$$(M)_x = (M_c)_x + (M_f)_x \tag{3.3}$$

By definition, the particle size distribution frequency gives the fraction of particles of size x in the sample. The total mass of particles of size x in the feed for example is therefore the total mass of the feed M multiplied by the appropriate fraction $\mathrm{d}F/\mathrm{d}x$ so that equation 3.3 becomes:

$$M\frac{\mathrm{d}F}{\mathrm{d}x} = M_\mathrm{c}\frac{\mathrm{d}F_\mathrm{c}}{\mathrm{d}x} + M_\mathrm{f}\frac{\mathrm{d}F_\mathrm{f}}{\mathrm{d}x} \tag{3.4}$$

3.2.1 Total efficiency

If a total (or overall) efficiency E_T is now defined as simply the ratio of the mass M_c of all particles separated to the mass M of all solids fed into the separator, i.e.

$$E_\mathrm{T} = \frac{M_\mathrm{c}}{M} \tag{3.5}$$

or, if mass balance in equation 3.1 applies:

$$E_\mathrm{T} = 1 - \frac{M_\mathrm{f}}{M} \tag{3.6}$$

equation 3.4 can be rewritten as:

$$\frac{\mathrm{d}F}{\mathrm{d}x} = E_\mathrm{T}\frac{\mathrm{d}F_\mathrm{c}}{\mathrm{d}x} + (1 - E_\mathrm{T})\frac{\mathrm{d}F_\mathrm{f}}{\mathrm{d}x} \tag{3.7}$$

which relates the particle size distributions of the feed, the coarse product and the fine product. The same relationship holds for particle fractions between x_1 and x_2

$$F(x_2) - F(x_1) = E_\mathrm{T}[F_\mathrm{c}(x_2) - F_\mathrm{c}(x_1)] + (1 - E_\mathrm{T})[F_\mathrm{f}(x_2) - F_\mathrm{f}(x_1)] \tag{3.8}$$

as well as for cumulative percentages corresponding to any size x

$$F(x) = E_\mathrm{T}F_\mathrm{c}(x) + (1 - E_\mathrm{T})F_\mathrm{f}(x) \tag{3.9}$$

(Note that equations 3.8 and 3.9 are obtained by integration of equation 3.7.) The mass balance in equation 3.9 (or 3.7) allows the calculation of any one missing size distribution provided the other distributions and the total efficiency are known, i.e.

$F(x)$ from E_T, $F_\mathrm{c}(x)$ and $F_\mathrm{f}(x)$
$F_\mathrm{f}(x)$ from E_T, $F_\mathrm{c}(x)$ and $F(x)$
$F_\mathrm{c}(x)$ from E_T, $F_\mathrm{f}(x)$ and $F(x)$

or even E_T from $F(x)$, $F_\mathrm{c}(x)$ and $F_\mathrm{f}(x)$. The last combination is the basis of the analysis of errors in particle size distribution data (and of sampling) because equation 3.9 can be written in the form:

$$E_\mathrm{T} = \frac{F(x) - F_\mathrm{f}(x)}{F_\mathrm{c}(x) - F_\mathrm{f}(x)} \tag{3.10}$$

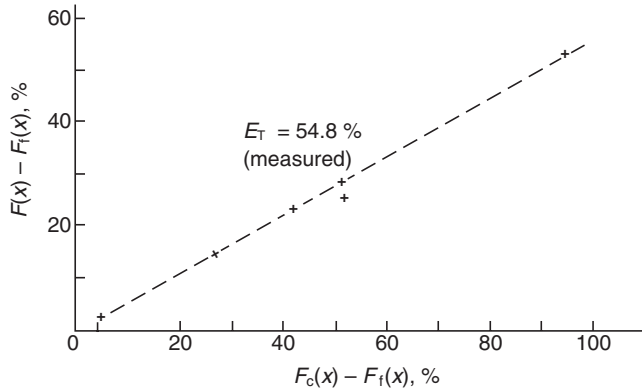

Figure 3.2 Example of scatter in the mass balance of particle size distribution data

If the differences $F(x) - F_f(x)$ and $F_c(x) - F_f(x)$ are plotted against each other for different sizes x, a straight line with a slope of E_T should be obtained. Because of the errors in particle size measurement, however, there may be a considerable scatter in the results. *Figure 3.2* shows a practical example of a test with a hydrocyclone; the line is drawn at a slope of the actual (measured) total efficiency, which of course is also subject to measurement error.

Note that the cumulative percentages in equations 3.8, 3.9 and 3.10 can be either 'oversize' or 'undersize' as long as the same type is used for all the distributions in the given equation. As to the quantity considered, equation 3.7 applies to particle size distributions by mass, surface or number simply because, for example:

$$\left(\frac{dF}{dx}\right)_{\text{by mass}} = kx^3\left(\frac{dF}{dx}\right)_{\text{by number}} \tag{3.11}$$

and as this is also true for the coarse and fine products (with the same constant k), x^3k will cancel out in equation 3.7. This does not necessarily apply to equations 3.8, 3.9 and 3.10 because the constant k in equation 3.11 may be particle-size dependent (when the particle shape factor varies with size) and may complicate the integration of equation 3.7. Only when the particle shape factor is constant throughout the size range in question, will equations 3.8, 3.9 and 3.10 also apply to particle size distributions other than those by mass.

3.2.2 Grade efficiency

As the performance of most available separational equipment is highly size dependent (and hence different sizes are separated with different efficiency), the total efficiency E_T defined in equation 3.5 (or 3.6) depends very much on the size distribution of the feed solids and is, therefore, unsuitable as a general criterion of efficiency. Thus values of total efficiency quoted in

manufacturers' literature may result in misleading conclusions about the separational capability of equipment unless they are accompanied by the full particle size distribution of the feed solids (and the method of size analysis), the density of the solids and the operational data such as flow rate, temperature, type of fluid, solids input concentration, etc. A single value of the total efficiency cannot be used to deduce the separation capability of the equipment for any materials other than the actual test materials.

If, however, the mass efficiency is found for every particle size x, a curve referred to as the gravimetric grade efficiency function $G(x)$ is obtained which is normally independent of the solids size distribution and density and is constant for a particular set of operating conditions, e.g. fluid viscosity, flow rate and often also solids concentration. It is necessary, however, that the chosen characteristic particle size is a decisive factor in the principle of separation used in the equipment.

If, for instance, the separation effect is influenced only by the mobility of particles in fluids, the terminal settling velocity or Stokes' diameter could be used for the size x and the method of particle size analysis would be chosen accordingly (sedimentation or elutriation).

To make a given grade efficiency curve applicable to solid–fluid density differences $\Delta\rho_2$ and liquid viscosities μ_2 other than those quoted with the curve ($\Delta\rho_1$, μ_1), conversion of the particle size scale can be made assuming Stokes' law, from which

$$\frac{x_1}{x_2} = \sqrt{\left(\frac{\mu_1 \Delta\rho_2}{\mu_2 \Delta\rho_1}\right)} \tag{3.12}$$

This conversion, however, has to be made with caution and should be avoided wherever possible, not only because of the hidden assumptions in Stokes' law, but also because of the likely changes in the flow patterns in the separator under different viscosities.

Figure 3.3 shows a typical grade efficiency curve for a sedimenting (tubular) centrifuge, and *Figure 3.4* the curves for a depth and a surface-type cartridge filter (clean medium). The grade efficiency curves are usually S-shaped in devices that use either screening (cake filtration, strainers) or particle dynamics in which the body forces acting on the particles (which are proportional to x^3) such as inertia, gravity or centrifugal forces are opposed by drag forces (which are proportional to x^2).

Note that the S-shaped grade efficiency curves do not necessarily start from the origin—in applications with a considerable underflow to throughput ratio (by volume) R_f, the grade efficiency curves tend to the value $G(x) = R_f$ as $x \to 0$. This is a result of the splitting of the flow, or 'dead flux' that carries even the finest solids into the underflow in proportion to the volumetric split of the feed. Section 3.4 discusses possible modifications to the efficiency definitions which account for the volumetric split and illustrate only the net separation effect. Such 'reduced efficiencies' are widely used for hydrocyclones and nozzle-type disc centrifuges where large diluted underflows occur.

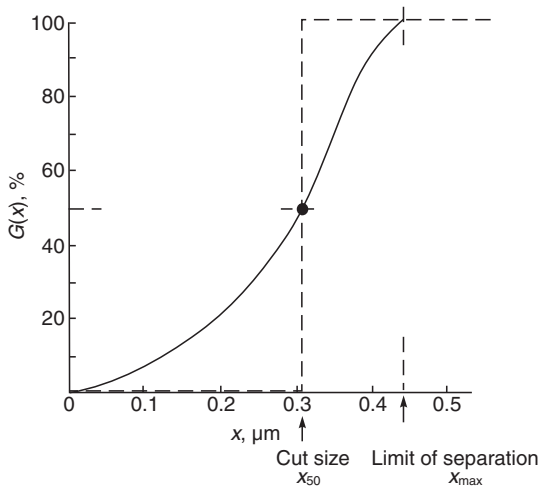

Figure 3.3 A typical grade efficiency curve for a tubular centrifuge, with definitions of x_{50} and x_{max}

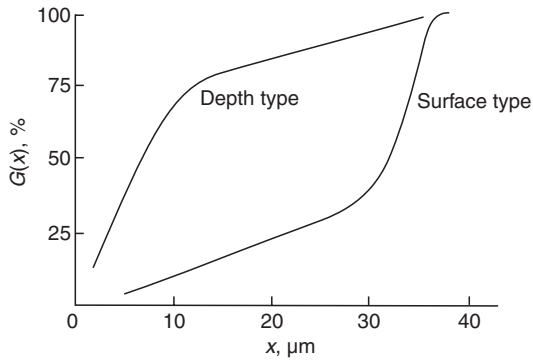

Figure 3.4 Typical grade efficiency curves for two types of cartridge filters (clean medium)[1]

The value of the grade efficiency has the character of probability. This may be explained by considering the following: if only one particle of certain size x enters the separator, it will either be separated or it will pass through with the fluid. The grade efficiency will, therefore, be either 100% or 0%. If two particles of the same size enter the separator, the grade efficiency may be 100, 50 or 0% depending upon whether the separator will separate both, one or no particles. If a great number of particles of the same characteristic size enter the separator, a certain probable value of the number of separated particles will be reached.

This probability (not certainty) of the value of the grade efficiency occurs because different particles (of the same size) experience different conditions

when passing through the separator. The finite dimensions of the input and output of the separator, uneven conditions for separation at different points in the separator and finally the different surface properties of particles (of the same size) influence the separation process to a great extent and are the reason for the probability character of the grade efficiency values.

It is for these same reasons that the grade efficiency value cannot be determined by a physically exact calculation. If, under certain simplifying assumptions, such a calculation is carried out, the results have to be corrected by coefficients determined experimentally, values of which may be very different from 100% according to the degree of the simplification adopted. Such a procedure can be used with separators that employ inertia principles, sedimentation, centrifugation, etc., where the particle trajectories in the separator can be estimated.

3.2.2.1 Important points on the grade efficiency curve

3.2.2.1.1 Cut size

A graph of the grade efficiency function is sometimes called the partition probability curve because it gives the probability with which any particular size in the feed will separate or leave with the fluid. The size corresponding to 50% probability is called the equiprobable size x_{50} and is often taken as the 'cut' size of the particular equipment (see *Figure 3.3*). Determination of this cut size (which is independent of the feed material) requires a knowledge of the whole grade efficiency curve. There are, however, two other simpler definitions of a cut size, but these give values not necessarily equal to x_{50}.

The so-called *analytical cut size* x_a is the size such that ideally the feed solids would be split according to size (with no misplaced material) in the proportions given by the total efficiency E_T. In other words the analytical cut size corresponds to the percentage equal to E_T on the cumulative particle size distribution oversize $F(x)$ of the feed material (see *Figure 3.5a*), i.e.

$$F(x_a) = E_T \tag{3.13}$$

It is clear from the definition of x_a that it would be equal to x_{50} if the grade efficiency were a step function (the broken line in *Figure 3.3*) giving an

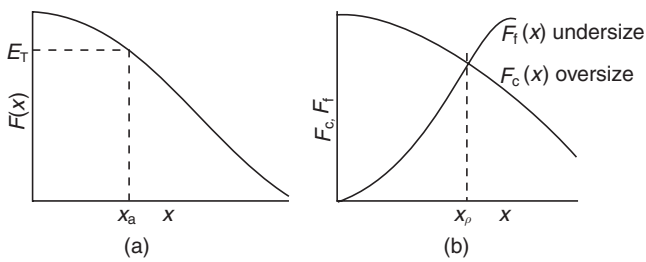

Figure 3.5 Definitions of the analytical cut size x_a and of x_ρ

ideally sharp classification of solids (the nearest to this is screening with a uniform aperture size); the two cut sizes would also be equal even for a non-ideal classification if both the coarse and fine products contained an equal quantity of misplaced material (i.e. material consisting of particles finer than x_a in the coarse product or particles coarser than x_a in the fine product). This of course leads to a practical conclusion that the analytical cut size x_a can be used as an estimate of x_{50} in those cases where the classification is very sharp with little misplaced material. The analytical cut size is widely used in particle size measurement.

In some applications, when E_T is unknown, another cut size x_ρ is sometimes used, defined as the size x at which the cumulative percentage undersize of the coarse fraction is equal to the cumulative frequency oversize of the fines (or vice versa), see *Figure 3.5b*. This cut size, however, is even more sensitive to the changes in the feed size distribution than the analytical cut size.

Further discussion of the cut size and its determination is given in section 3.3.1.5.

3.2.2.1.2 Limit of separation

There is always a value of particle size x above which the grade efficiency is 100% for all x. This is the size x_{max} of the largest particle remaining in the overflow after the separation (maximum particle size that would have a chance to escape) and will be called 'limit of separation' in the following (see *Figure 3.3*).

If the particle trajectories in the separator can be approximated, the most unfavourable conditions of separation are taken for determining this limit of separation. Examples of doing this may be found in theories of separation in centrifuges or settling tanks.

In practice, however, it is often difficult to determine the limit of separation accurately; in that case the size corresponding to 98% efficiency is measured thus giving a more easily defined point. This size x_{98}, sometimes called 'the approximate limit of separation' is widely used, for example in filter rating.

3.2.2.1.3 Sharpness of cut

When the principles of and equipment for the separation of solids from fluids are applied to solids classification, it is desirable to minimize the amount of misplaced material. This is related to the general slope of the grade efficiency curve which can be expressed in terms of a 'sharpness index' defined in many different ways: sometimes simply as the slope of the tangent to the curve at x_{50} or, more often, as a ratio of two sizes corresponding to two different percentages on the grade efficiency curve on either side of 50%, i.e. for example:

$$H_{25/75} = x_{25}/x_{75} \tag{3.14}$$

or

$$H_{10/90} = x_{10}/x_{90} \tag{3.14a}$$

or

$$H_{35/65} = x_{35}/x_{65} \tag{3.14b}$$

or alternatively, the reciprocal values of these.

3.3 Basic relationships between E_T, $G(x)$ and the particle size distributions of the products

From the definition in section 3.2.2, the grade efficiency is

$$G(x) = (M_c)_x/(M)_x \tag{3.15}$$

which by the same argument as that following equation 3.3 in section 3.2 is

$$G(x) = \frac{M_c}{M}\frac{dF_c/dx}{dF/dx} \tag{3.16}$$

Using equation 3.5, which defines the total efficiency

$$G(x) = E_T\frac{dF_c}{dF} \tag{3.17}$$

Equation 3.17 (or 3.16) shows how the grade efficiency can be obtained from the size distribution data of the feed and the coarse product, and the total efficiency E_T. It is apparent from equation 3.17 that the particle size distributions of the feed and the coarse product can be by mass, surface area or number as long as they are both by the same quantity as E_T. This is because the size-dependent shape factor would cancel out in the ratio (see equation 3.11). The evaluation of $G(x)$ is shown graphically in *Figure 3.6* where the curves of dF/dx and $E_T\,dF_c/dx$ are plotted in the same diagram. The grade efficiency $G(x)$ is then the ratio of the two values for any particle size x.

Most particle size analysis equipment, however, gives the cumulative size distribution $F(x)$ which is the integral function of the size frequency and has, therefore, to be differentiated in order to obtain the size frequency. This differentiation of two curves (feed and coarse product) can be avoided by

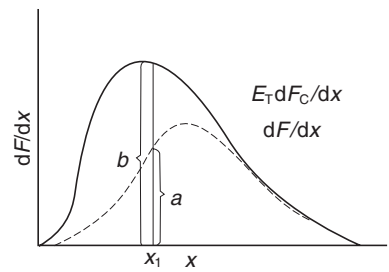

Figure 3.6 Determination of $G(x)$ from E_T, dF/dx and dF_c/dx. $G(x_1) = a/b$

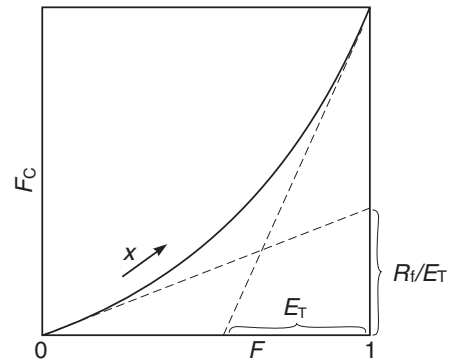

Figure 3.7 Determination of $G(x)$ from E_T, $F(x)$ and $F_c(x)$ (% undersize). ($G(x_1)$ is the slope of the line at x_1 multiplied by E_T)

using the cumulative distributions directly according to equation 3.17. This is shown graphically in *Figure 3.7* by plotting the values of $F(x)$ and $F_c(x)$ against each other for every particle size x and differentiating the curve.

The values of $dF_c(x)/dF(x)$ are then, according to equation 3.17, multiplied by E_T to obtain $G(x)$. Multiplication by E_T can be, of course, done before the differentiation:

$$G(x) = \frac{d[E_T F_c(x)]}{dF(x)} \tag{3.18}$$

Note that it is of great help in practical evaluations to know the limiting values of the slope dF_c/dF; a maximum grade efficiency of 1 leads to (see equation 3.17)

$$dF_c/dF = 1/E_T$$

and the minimum grade efficiency equal to R_f leads to

$$dF_c/dF = R_f/E_T$$

If lines of slopes $1/E_T$ (for $x \to \infty$) and R_f/E_T (for $x \to 0$) are plotted in *Figure 3.7* through the diagonally opposite corners of the square corresponding to $x = \infty$ and $x = 0$, they provide the two limiting asymptotes and make it easier to draw a curve through the set of often scattered points (see the example in section 3.3.1.1).

The grade efficiency can also be obtained from the size distributions of the feed $F(x)$ and the fine product $F_f(x)$ or from the fine and coarse products, $F_f(x)$ and $F_c(x)$ from the following relationships, obtained by combining equations 3.17 and 3.7 (mass balance)

$$G(x) = 1 - (1 - E_T)\frac{dF_f(x)}{dF(x)} \tag{3.19}$$

or

$$\frac{1}{G(x)} = 1 + \left(\frac{1}{E_T} - 1\right)\frac{dF_f(x)}{dF_c(x)} \tag{3.20}$$

Equations 3.19 and 3.20 can be used with either the size frequencies or the cumulative percentages as is obvious from their mathematical form and is similar to the case of equation 3.17 described above. The following sections show the use of the basic relationships given above and are based entirely on the cumulative size distributions of products because this in practice leads to more accurate results.

3.3.1 Grade efficiency testing and evaluation

From the definition of the grade efficiency it is the efficiency of a separator if a mono-sized material is used as the feed. Such a mono-disperse powder can be prepared, but only with difficulty and in small quantities. If this material was used in the separator, the total efficiency obtained would give a single point on the grade efficiency curve corresponding to the given particle size.

This procedure could be repeated with several other mono-sized fractions of different sizes until enough points on the efficiency curve were obtained. This procedure would be time consuming and expensive. It is for this reason that, as an alternative, equations 3.17, 3.19 and 3.20 are used for grade efficiency testing, depending upon which two out of the three particle size distributions of the materials involved are available. Such an experiment, with a poly-disperse material as the feed, enables us to estimate the grade efficiency in one experiment.

Some experience is necessary in the choice of a suitable feed material. It is first of all necessary that the particles of the feed entering the separator do not agglomerate since the agglomerates would then be separated as larger particles and subsequently broken down to the original particles when the particle size analysis was carried out. The grade efficiency obtained would not correspond to the actual performance of the separator and would give higher values for smaller particles. The feed solids must therefore be well dispersed in the liquid and the concentration should be sufficiently low, say one or two per cent by volume at the most, for the number of impacts and interactions between particles to be small. Apart from particle interactions leading to hindered settling, higher concentrations of particles cause changes in the flow patterns in the separator thus affecting its performance. Tests at higher concentrations can, of course, also be carried out but the results cannot be reliably applied to materials and concentrations other than those used in the tests.

Depending on the actual arrangement of the testing rig, two of the three material streams involved (feed, coarse or fine product) are analysed for the grade efficiency determination and the appropriate equation 3.17, 3.19 or 3.20 used for evaluation. The most frequent combination is the feed and coarse

product because of the convenience of their collection and size determination; it is not unusual to analyse all three materials because this provides a useful check on the mass balance and on the overall accuracy of the results (see section 3.2.1, equation 3.10).

The total efficiency can be determined from three different combinations of the material streams involved (equation 3.5 combined with the mass balance in equation 3.1); the mass flow rates of the solids are usually determined by measuring the total volumetric flow rates and the corresponding solids concentrations; the mass flow rate is, of course, the product of the two. The combination giving the smallest standard deviation of E_T (if all the variables are subject to random errors only) is that of the overflow and underflow streams. (The same conclusion applies to the testing of $G(x)$.)

The evaluation of the grade efficiency may be carried out graphically, in a table or using a computer. Tabular procedures usually do not give results of great accuracy often because only a relatively low number of points are available. The graphical methods are most versatile and instructive, and examples of these are given in the following sections. Simple computer programs can be written to carry out the task and these may save a great deal of time and effort in routine work. The author has successfully used a simple computing technique of fitting a second-order polynomial through three adjacent points in the appropriate square diagram and computing the differentiation for the middle point; this is done successively through the range of data, starting and finishing in diagonally opposite corners of the square diagram. This technique provides results which correspond very favourably with those obtained by graphical methods even if the number of data points available is as low as four or five.

Examples of grade efficiency evaluations from different combinations of the measured data are given in the following sub-sections 3.3.1.1–3.3.1.4. These are all based on a single test in which all three streams were analysed for particle size distribution and the total efficiency was also measured.

Example 3.1

A hydrocyclone was tested at certain operating conditions with a suspension of clay in water. Using the data given below and in *Table 3.1*, evaluate the grade efficiency curve for the given operating conditions, and as a function of particle size for a density difference $(\rho_s - \rho_l)$ of 1000 kg m^{-3}.

3.3.1.1 Evaluation of $G(x)$ from $F(x)$, $F_c(x)$ and E_T

Equation 3.17 is used to evaluate $G(x)$; $F_c(x)$ is plotted against $F(x)$ in a square diagram in *Figure 3.8* and the corresponding sizes marked beside each of the five points. Limiting lines are plotted, one at a slope of $R_f/E_T = 0.482$ through the point corresponding to $x = 0$ in the top right-hand corner, the other at a slope

Table 3.1

Particle size of test powder, μm	*Feed material* $F(x)$, *% oversize*	*Coarse product* $F_c(x)$, *% oversize*	*Fine product* $F_f(x)$, *% oversize*
40	1	2	0.1
20	12	22	0.2
10	31	55	5
4	48	71	20
2	62	80	38

Data: Density of solids $\rho_s = 2640\,\text{kg m}^{-3}$
Density of water $\rho_l = 1000\,\text{kg m}^{-3}$
Underflow-to-throughput ratio $R_f = 26.4\%$ v/v
Total efficiency $E_T = 54.8\%$

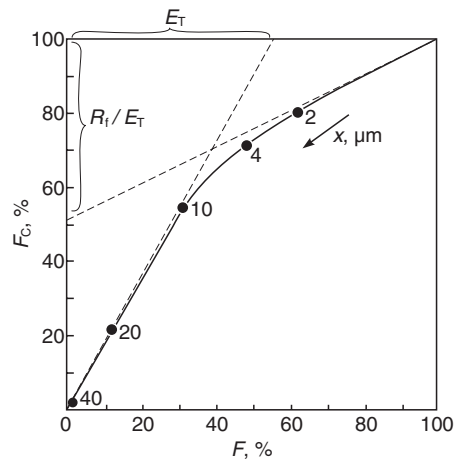

Figure 3.8 An example of $G(x)$ determination from F_c, F (both oversize) and E_T

of $1/E_T = 1.825$ through the point of $x = \infty$ in the bottom left-hand corner of the square diagram. A curve is drawn through the data points so that it is asymptotic to the limiting lines. Tangents are then drawn to the curve at each data point in turn and their slopes measured. Following equation 3.17, the measured gradients are multiplied by E_T thus giving the values of $G(x)$ for the test powder—see *Table 3.2*, column 3 for results (section 3.3.1.3). For a particle size of 4 μm for example, the slope measured is 0.777, thus

$$G(4) = 0.777 \times 54.8 = 42.6\%$$

If the grade efficiency curve is now to be plotted against particle size for a material with a density difference of $(\rho_s - \rho_l) = 1000\,\text{kg m}^{-3}$, equation 3.12

Table 3.2

Particle size of test powder ($\rho_s - \rho_l =$ 1640 kg m^{-3}), μm	*Particle size* ($\rho_s - \rho_l =$ 1000 kg m^{-3}), μm	*G*(*x*) *from* *F*, F_c, E_T, %	*G*(*x*) *from* *F*, F_f, E_T, %	*G*(*x*) *from* F_c, F_f, E_T, %	*G*(*x*) *average,* %	*G*(*x*) *from* F_c, F_f, *F*, %
40	51.2	100.0	100.0	100.0	100.0	(91.2)
20	25.6	98.0	100.0	100.0	99.3	97.5
10	12.8	72.2	73.3	68.4	71.3	68.5
4	5.1	42.6	50.3	42.8	45.2	42.7
2	2.6	33.5	37.7	34.1	35.1	34.9
0	0	26.4	26.4	26.4	26.4	26.4

is used to determine the particle size scale conversion. The size of particle which has the same grade efficiency as a particle of 4 μm in the test powder (assuming the viscosity remains the same) is given by

$$x_1 = x_2\sqrt{\left(\frac{\Delta\rho_2}{\Delta\rho_1}\right)} = 4\sqrt{\frac{1640}{1000}} = 5.1\ \mu\text{m}$$

Figure 3.9 shows the resulting grade efficiency curve, which must go through the point of 26.4% ($= R_f$) at $x = 0$.

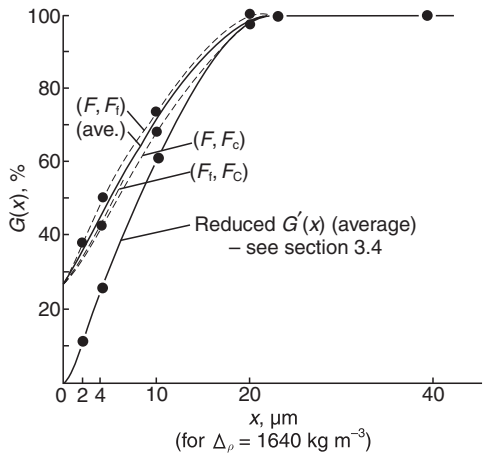

Figure 3.9 Plots of $G(x)$ from Table 3.2, columns 3–6 and the reduced grade efficiency $G'(x)$ from equation 3.34

Note that since particle size analysis data are subject to relatively large errors, the plot in *Figure 3.8* may show a considerable scatter. At best, a smooth curve is drawn through the scattered data points; the limiting lines provide useful guide-lines for this.

3.3.1.2 Evaluation of $G(x)$ from $F(x)$, $F_f(x)$ and E_T

If $F_f(x)$ is measured instead of $F_c(x)$, the following procedure can be adopted for the evaluation of $G(x)$. The evaluation is based on equation 3.19; $F_f(x)$ is plotted against $F(x)$ in a square diagram (*Figure 3.10*) in the same way as $F_c(x)$ in section 3.3.1.1. One limiting line is the x-axis ($F_f(x) = 0$) so that equation 3.19 gives $G(\infty) = 1$, the other, for the condition $G(0) = R_f$ at $x = 0$ has a slope of

$$\frac{(1 - R_f)}{(1 - E_T)}$$

and is drawn through the top right-hand corner of the diagram; the data line should again be asymptotic to both lines.

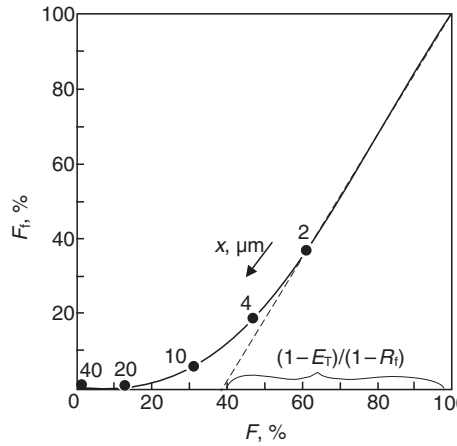

Figure 3.10 Determination of $G(x)$ from E_T, $F(x)$ and $F_f(x)$

Tangents are then drawn to the curve at each data point in turn and their slopes measured. Following equation 3.19, the measured gradients are multiplied by $(1 - E_T)$ and then subtracted from 1 to give $G(x)$. For example, if the slope at 4 µm is 1.1

$$G(4) = 1 - (1 - 0.548)1.1 = 0.503 = 50.3\%$$

The resulting $G(x)$ (*Table 3.2*, column 4) is plotted in *Figure 3.9* and, as it applies to the same test as $G(x)$ from section 3.3.1.1, the two should be comparable.

The conversion of particle sizes is not given here as it is described in section 3.3.1.1.

3.3.1.3 Evaluation of $G(x)$ from $F_c(x)$, $F_f(x)$ and E_T

If the size distributions of the products $F_c(x)$ and $F_f(x)$ are measured, equation 3.20 is used to evaluate $G(x)$. Values of dF_f/dF_c are again obtained from a

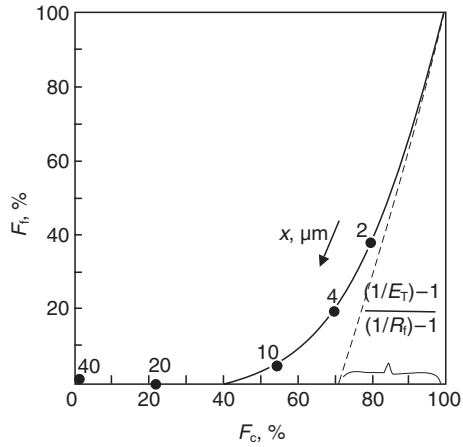

Figure 3.11 Determination of $G(x)$ from E_T, $F_f(x)$ and $F_c(x)$

square diagram—*Figure 3.11*—by drawing tangents to the curve plotted through the set of data points. The limiting lines in this case are the x-axis ($F_f(x) = 0$) for $x = \infty$ and a line at a slope of

$$\frac{(1/R_f) - 1}{(1/E_T) - 1}$$

drawn through the point corresponding to $x = 0$, in this case the top right-hand corner. The slopes measured, corresponding to given particle sizes, are then processed according to equation 3.20 so that for example, if the slope at 4 μm is 1.62, then

$$\frac{1}{G(x)} = 1 + \left(\frac{1}{0.548} - 1\right)1.62 = 2.336$$

hence

$$G(x) = 0.428 = 42.8\%$$

The rest of the results are shown in *Table 3.2*, column 5; the conversion of particle sizes is the same as in section 3.3.1.1. *Figure 3.9* shows the points from columns 3, 4 and 5 of *Table 3.2* all plotted in the same graph, and the full line represents the average $G(x)$ from column 6. The scatter of points in *Figure 3.9* gives some indication of the effect of errors in particle size analysis—doing all three analyses and evaluations as in this example, somewhat improves the accuracy of the resulting function. The best way of reducing random errors is of course repetition of the tests.

3.3.1.4 Evaluation of $G(x)$ from $F(x)$, $F_c(x)$ and $F_f(x)$

The grade efficiency curve can be determined from particle size analyses of the three streams alone, without the need to measure E_T

The basic equation for this may be derived from equation 3.9 by elimination of E_T using equation 3.17, this gives

$$G(x) = \left(\frac{F(x) - F_f(x)}{F_c(x) - F_f(x)}\right)\left(\frac{dF_c(x)}{dF(x)}\right) \tag{3.21}$$

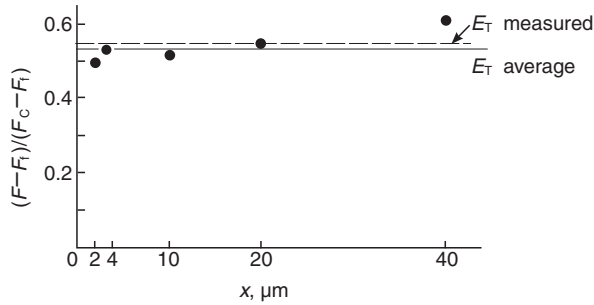

Figure 3.12 Variation in E_T derived from the mass balance of the particle size distributions of the three material streams

which is in fact identical to equation 3.17 if equation 3.10 is substituted for E_T; as a result of the inaccuracy of particle size measurement and sampling, there is always a scatter in these 'derived' values of E_T if plotted against particle size x—see *Figure 3.12* for the example given previously (see also *Table 3.3*). The average value of E_T derived from the mass balance of the particle size analysis data using equation 3.10 is 53.7% and is in fact lower than the value of E_T measured directly, 54.8%; this indicates the errors in the measurement of the data for the evaluation of both of these values.

Equation 3.21 suggests $G(x)$ can be determined from the individual 'derived' values for the total efficiency together with the slopes dF_c/dF which can be determined graphically as described in section 3.3.1.1; column 7 in *Table 3.2* gives the results which are not very different from the results from the three previous sections (except for the point for $x = 40\,\mu m$ where the mass balance from the particle size distributions is at its worst—see *Figure 3.12*).

3.3.1.5 Simple evaluation of the cut size

If the complex separation performance of a size-dependent separator (best shown by a full grade efficiency curve) has for some reason to be described by a single number, in most applications it is best to use the concept of a cut size. In such a case, the cut size has to be unique and, if possible, independent of the size distribution of the feed solids, so that it characterizes only the machine run under the chosen conditions of operation. As the whole of the grade efficiency curve usually satisfies this condition, it is best to define the cut size as corresponding to a unique point on the curve. The equiprobable size x_{50} is probably best suited for this purpose and it is certainly the best of the three definitions of cut size reviewed here (section 3.2.2.1).

A simple way has recently been suggested[1] of determining x_{50} without the need for the whole grade efficiency curve. If $G(x)$ in equation 3.17 is equal to 0.5, it can be shown that the cut size x_{50} corresponds to the point on a plot of $(F - 2E_T F_c)$ at which:

$$\frac{d}{dx}(F - 2E_T F_c) = 0 \tag{3.22}$$

which corresponds to the maximum.

Alternative combinations of the material streams (equations 3.19 and 3.20) give:

$$\frac{d}{dx}[F - 2(1 - E_T)F_f] = 0 \tag{3.23}$$

and

$$\frac{d}{dx}\left[F_c - \frac{1 - E_T}{E_T}F_f\right] = 0 \tag{3.24}$$

Equations 3.22, 3.23 and 3.24 require plotting the composite functions of two solid size distributions and the total efficiency and finding the maximum (see the worked example elsewhere[2]), which requires no differentiation and can be performed easily in industrial production situations. Naturally, the test information necessary for this calculation is the same as for the grade efficiency curve itself: two particle size distributions and the total efficiency E_T.

The values of the other two commonly used cut sizes, the analytical cut size x_a and the 'curve intersection' cut size x_ρ (as defined in section 3.2.2.1.1) are always different from x_{50}, unless x_{50} is equal to the median of the feed size distribution x_g when all three coincide; the difference between x_{50}, and x_a and x_ρ increases as the median of the feed moves towards either end of the grade efficiency curve. This is best shown in the plot of $G(x)$ against $F(x)$ in *Figure 3.13*, from which it can be seen that both x_a and x_ρ are always on the same side of x_{50} as the median x_g of the feed, with x_a being always closest to x_{50}, hence:

if $x_g < x_{50}$

$$x_g < x_\rho < x_a < x_{50}$$

if $x_g = x_{50}$

$$x_g = x_\rho = x_a = x_{50}$$

and if $x_g > x_{50}$

$$x_g > x_\rho > x_a > x_{50}$$

Theoretical conversion of the easily obtainable analytical cut size x_a into the equiprobable size x_{50} is possible if both the feed size distribution and the grade efficiency curve can be approximated by an analytical function. Thus for example if both of the above-mentioned functions are log-normal it can be shown that the total efficiency E_T can be determined analytically from the following expression[3]

$$E_T = \frac{1}{2} + \frac{1}{2}\,\mathrm{erf}\,\frac{\ln x_g - \ln x_{50}}{\sqrt{(2)}\sqrt{(\ln^2 \sigma_g + \ln^2 \sigma_{gs})}} \tag{3.25}$$

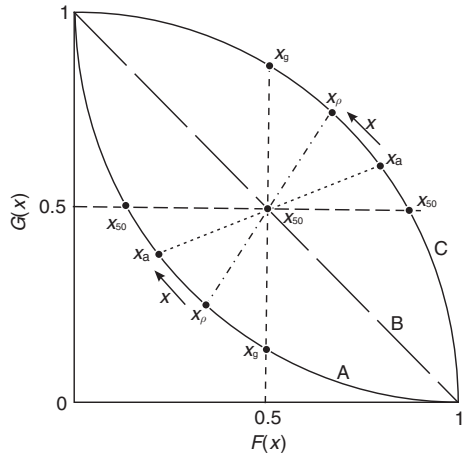

Figure 3.13 Plot of $G(x)$ against $F(x)$ for three different feed size distributions $F(x)$, showing the relative position of the three cut sizes x_{50}, x_a and x_ρ with respect to the feed median x_g. Curve A—fine feed, i.e. $x_g < x_{50}$. Curve B—$x_g = x_{50}$. Curve C—coarse feed, i.e. $x_g > x_{50}$

where

x_g and σ_g are the median and geometric standard deviation of the feed size distribution respectively,
x_{50} and σ_{gs} are the equiprobable size (cut size) and the geometric standard deviation of the grade efficiency function respectively, and the erf function is defined as

$$\mathrm{erf}(z) = \frac{2}{\sqrt{\pi}} \int_0^z \mathrm{e}^{-t^2} \mathrm{d}t \tag{3.26}$$

Equation 3.25 can be solved using tables of the erf function. There are also some analytical approximations available which obviate the use of tables.

By definition of the analytical cut size x_a the cumulative percentage oversize of the feed at x_a is equal to the total efficiency E_T (equation 3.13) and hence, by integration of equation 2.21,

$$\frac{1}{2} - \frac{1}{2} \mathrm{erf} \frac{\ln x_a - \ln x_g}{\sqrt{2} \ln \sigma_g} = E_T \tag{3.27}$$

Equation 3.27, in combination with equation 3.25, gives the final conversion formula

$$\frac{x_{50}}{x_g} = \left(\frac{x_a}{x_g}\right) \sqrt{\left[\left(1 + \frac{\ln \sigma_{gs}}{\ln \sigma_g}\right)^2\right]} \tag{3.28}$$

The above equation can be used to calculate the true cut size x_{50} from the known size distribution of the feed defined by x_g and σ_g and from the simply

Table 3.3 Three different log–normal size distributions (feed) with the same $\sigma_g = 2.05$ and medians 10, 15 and 20 μm processed by a log–normal grade efficiency of $\sigma_g = 1.65$ and $x_{50} = 10\,\mu m$

Feed median x_g, μm	*10*	*15*	*20*
E_T, %	50.0	67.8	78.6
x_{50}	10.0	10.0	10.0
x_a	10.0	10.8	11.3
x_ρ	10.0	12.0	14.0

measured analytical cut size x_a providing that an estimate of the geometric standard deviation σ_{gs} of the separator grade efficiency curve is available. Such information can be found in the literature. Gibson[4], for example, has recently given values of σ_{gs} for a disc centrifuge and a hydrocyclone under different operating conditions.

Better still, equation 3.25 can be used directly to calculate x_{50} from E_T but this involves the inverse of the error function.

Table 3.3 gives examples of three sets of E_T, x_{50}, x_a and x_ρ calculated for three different log–normal feed size distributions if processed by a log–normal grade efficiency. It can be clearly seen that, as predicted earlier in this section (*Figure 3.13*), the closer is the feed median to x_{50} the better is the agreement between x_{50}, x_a and x_ρ. x_a and x_ρ are always on the same side of x_{50} as the feed median x_g. The values of E_T were calculated from equation 3.25 such as, for example, for $x_g = 20$

$$E_T = \frac{1}{2} + \frac{1}{2}\,\text{erf}\,\frac{\ln 20 - \ln 10}{\sqrt{(2)}\sqrt{(\ln^2 2.05 + \ln^2 1.65)}}$$
$$= \frac{1}{2} + \frac{1}{2}\,\text{erf}\,0.56$$
$$= 78.6\%$$

using standard tables of the erf function defined in equation 3.26. The analytical cut size x_a was calculated using equation 3.28, which for $x_g = 20$ again gives

$$x_a = 20 \times \left(\frac{10}{20}\right) \frac{1}{\sqrt{\left(1 + \left(\frac{\ln 1.65}{\ln 2.05}\right)^2\right)}}$$
$$= 11.33\,\mu m$$

There is no simple way to determine the 'intersection' cut size x_ρ so this was done by calculating the size distributions of the products and finding their cross-over point as required by the definition shown in *Figure 3.5*.

Similar correction factors can be derived for other types of analytical functions that describe the feed and the grade efficiency curve.

3.3.2 Total efficiency determination from the grade efficiency and the size distribution of the feed

If the grade efficiency curve can be regarded as a characteristic parameter of a separator for particular conditions (flow rate, viscosity of liquid etc.), this curve can be used to determine the total efficiency that can be expected to be obtained with a particular feed material under the same conditions. The size distribution $dF(x)/dx$ of the feed material must be known, then, from equation 3.17:

$$G(x)\,dF = E_T\,dF_c \tag{3.29}$$

which after integration in the given size range $0-x_{max}$ gives

$$\int_0^1 G(x)\,dF = E_T \int_0^1 dF_c \tag{3.30}$$

since the value of the total efficiency is a constant for a given application.

From the definition of the particle size distribution

$$\int_0^1 dF_c = 1 \tag{3.31}$$

which makes the integral on the right-hand side of equation 3.30 equal to 1. Hence the total efficiency is

$$E_T = \int_0^1 G(x)\,dF \tag{3.32}$$

Evaluation of the integral can be carried out graphically, in a table or using a computer.

For graphical evaluation the values of $G(x)$ and F are plotted against each other (for every size x) in a square diagram—see *Figure 3.14*—and the area under the curve is found. The total efficiency is a ratio of this area to the area of the square (which would represent a total efficiency of 100% if $G(x)$ were 100% for all particle sizes).

If the size frequency curve dF/dx is to be used, the evaluation is carried out according to the modified equation 3.19:

$$E_T = \int_0^\infty G(x)\frac{dF(x)}{dx}\,dx \tag{3.33}$$

which represents multiplication of the values of $G(x)$ and dF/dx for every size x and then integration of the resulting curve.

If a digital computer is to be used, linear interpolation between the points in a plot of $G(x)$ against $F(x)$ may not give very accurate results because of the limited number of points on both the size distribution and the grade efficiency curve. The author has successfully used a technique for this integration that first finds parameters for a polynomial that can be fitted through every three adjacent points and then integrates the function obtained in this way step by step.

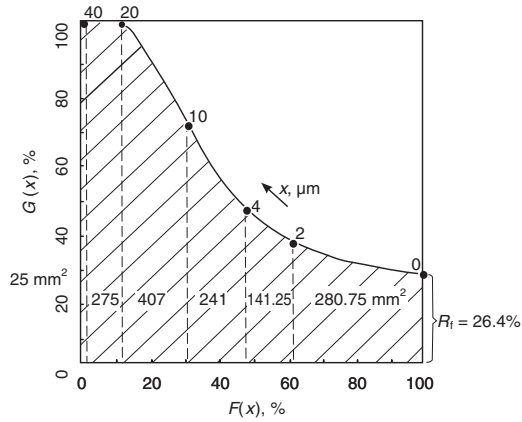

Figure 3.14 Prediction of E_T and $F_c(x)$ from $G(x)$ and $F(x)$ Total area (shaded) is 1370 mm^2, the area of the square is 2500 mm^2, hence $E_T = 1370/2500 = 0.548$ $F_c(2) = (280.75/2500)(1/0.548) = 0.205 = 20.5\%$ undersize or 79.5% oversize $F_c(4) = (280.75 + 141.25)/(1/0.548) = 30.8\%$ undersize or 69.2% oversize etc.

If both the feed size distribution $F(x)$ and the grade efficiency curve $G(x)$ can be approximated by an analytical function, the integration in equation 3.32 can be done analytically. Equation 3.25 can, for example, be used for log–normal functions—see section 3.3.1.5.

Example 3.2

Estimate the total efficiency that can be expected with a hydrocyclone which is identical with the one tested in section 3.3.1 and operated under the same conditions as in example 3.1, with feed material of a size distribution $F(x)$ as given in *Table 3.2*. Use the average grade efficiency curve obtained from the tests in section 3.3.1, column 6 in *Table 3.2*.

The solution is based on equation 3.32; *Figure 3.14* gives the required plot and yields, after integration of the curve (shaded area) $E_T = 54.8\%$ which is identical with the measured value given in section 3.3.1.

3.3.3 Determination of the size distribution of the products from the grade efficiency and the size distribution of the feed

Apart from the total efficiency of a separator, the quality of the products can also be predicted provided that the grade efficiency curve is known for the particular conditions of separation.

For determination of the size distribution of the coarse product equation 3.29 may be rearranged as

$$\mathrm{d}F_c(x) = \frac{G(x)}{E_T}\mathrm{d}F(x) \tag{3.34}$$

from which the value of $F_c(x_1)$ for any x_1 may be evaluated by integration

$$F_c(x_1) = \frac{1}{E_T} \int_0^{F(x_1)} G(x)\, dF(x) \tag{3.35}$$

provided that the total efficiency has already been found as in the previous section. Equation 3.35 may be evaluated graphically in a similar way to the total efficiency, but in this case the integration is carried out up to several different values of x until enough points on the cumulative size distribution of the coarse product are obtained—see *Figure 3.14* for an example.

If a size frequency curve dF/dx is to be used instead of the cumulative curve, the evaluation is simpler since, according to equation 3.31

$$dF_c/dx = \frac{1}{E_T} G(x) \frac{dF(x)}{dx} \tag{3.36}$$

i.e. the product of the grade efficiency and the size distribution for any x divided by the total efficiency gives the size frequency distribution of the coarse product.

For determination of the size distribution of the fine product, the procedure is very similar. From equations 3.11 and 3.16

$$dF_f(x) = \frac{1 - G(x)}{1 - E_T}\, dF(x) \tag{3.37}$$

which after integration gives

$$F_f(x_1) = \frac{1}{1 - E_T} \int_0^{F(x_1)} [1 - G(x)]\, dF(x) \tag{3.38}$$

or for dealing with size frequency curves

$$\frac{dF_f(x)}{dx} = \frac{1 - G(x)}{1 - E_T} \frac{dF(x)}{dx} \tag{3.39}$$

These two equations 3.38 and 3.39 may be evaluated in a similar manner to equations 3.35 and 3.36.

Example 3.3

Taking the data given in example 3.1, equation 3.35 is used for prediction of the particle size distribution of the separated coarse product. *Figure 3.14* shows the graphical method of solving the equation step by step where each integration is performed up to a given particle size x and the area obtained as a fraction of the total area under the curve gives the required cumulative percentage $F_c(x_1)$.

For the size distribution of the fine product in the overflow, equation 3.38 is used directly; graphically, *Figure 3.14* can also be used for this except that in this case the areas above the curve are integrated. Alternatively, if the coarse product distribution has been worked out first, the mass balance in equation

Table 3.4

Particle size, μm	*Coarse product* $F_c(x)$, %	*Fine product* $F_f(x)$, %
40	1.8	0.0
20	22.0	0.0
10	51.6	6.0
4	69.2	22.2
2	79.5	40.7

3.9 can be used to evaluate the fine product size distribution instead. *Table 3.4* gives the resulting size distribution worked out from the data given in example 3.1, which constitute the results of the tests in section 3.3.1. There are, of course, some discrepancies between the measured data in *Table 3.1* and the predicted values in *Table 3.4*; this is due to inaccurate mass balance in the experimental data (a result of measurement errors).

Note that as the total efficiency is needed for a prediction of the size distributions of the products, it must always be evaluated first using the method given in section 3.3.2.

3.4 Modifications of efficiency definitions for applications with an appreciable underflow-to-throughput ratio

3.4.1 Reduced efficiency

As was pointed out in section 3.2.2, in applications with an appreciable and diluted underflow, a 'reduced' efficiency concept is used if one wants to look at the net separation effect alone. The necessity for this modified efficiency springs from the simple fact that, as there is always some liquid accompanying the solids in the underflow, the total flow is split into two streams so that a certain 'guaranteed' efficiency is always achieved as a result of this split. In other words, the separator functions as a flow divider and divides the solids too, in at least as large a ratio as R_f the volumetric ratio of underflow to throughput. When looking at the performance of separators, it is then desirable to observe the net separation effect, i.e. to subtract the contribution of the dead flux. This gave rise to a number of possible new definitions of efficiency, reviewed by Tenbergen and Rietema[5]. The best and most widely used formula is one due to Kelsall[6] and also Mayer[7].

$$E'_T = \frac{E_T - R_f}{1 - R_f} \tag{3.40}$$

where

E'_T is the so-called 'reduced' total efficiency
E_T is the total efficiency as defined by equation 3.5 (ratio of mass flow rates of solids) and
$R_f = U/Q$ is the underflow-to-throughput ratio (by volume) which is the minimum efficiency due to dead flux.

It can be seen that equation 3.40 satisfies the basic requirements for a definition of net efficiency in that it gives zero for conditions of no separation when $E_T = R_f$ and one for complete separation of solids when $E_T = 1$.

The grade efficiency curve $G(x)$, which in its unmodified form (defined by equation 3.15) also obscures the existence of a volumetric split of the flow, can be modified in the same way:

$$G'(x) = \frac{G(x) - R_f}{1 - R_f} \tag{3.41}$$

which represents a net separation effect and, for inertial separation, goes through the origin since $G'(0) = 0$ (whereas $G(0) = R_f$, see *Figure 3.9*).

The size corresponding to $G'(x) = 50\%$ is used as the 'reduced' cut size x'_{50}.

This 'reduced' efficiency concept is widely used in hydrocyclones; the effect of this modification on the shape of the grade efficiency curve is shown in *Figure 3.9* which uses the average curve of $G(x)$ from *Table 3.2* (see section 3.3.1). It should be noted that the basic relationship between the total and grade efficiencies (equation 3.32) also holds for reduced efficiencies, so that:

$$E'_T = \int_0^1 G'(x)\,\mathrm{d}F \tag{3.42}$$

Note that the product size distributions cannot be calculated without the knowledge of R_f because equation 3.17 does not hold for $G'(x)$ and E'_T.

It is interesting to find that the often used clarification number[8] is in fact equal to the reduced total efficiency E'_T because it can be shown from the definition of E'_T that

$$E'_T = \frac{C - C_0}{C} \text{ (the clarification number)} \tag{3.43}$$

(equations 3.42 and 3.43 indicate that C_o is not affected by R_f if $G'(x)$ is not) or, alternatively:

$$E'_T = \left(\frac{C_u - C}{C}\right)\left(\frac{R_f}{1 - R_f}\right) \tag{3.44}$$

or

$$E'_{\mathrm{T}} = \frac{C_{\mathrm{u}} - C_{\mathrm{o}}}{C_{\mathrm{u}} - C_{\mathrm{o}} + (C_{\mathrm{o}}/R_{\mathrm{f}})} \tag{3.45}$$

which offers three alternatives for convenient measurement of the reduced efficiency from the measurement of the concentration of solids C, C_{u} and C_{o} in the feed, underflow and overflow respectively, and of the volumetric split R_{f}.

3.4.2 Other definitions of efficiency

As was explained in chapter 1, solid–liquid separation is often assessed by considering the solids recovery *and* the moisture content of the recovered solids simultaneously, with their relative importance varying with application. If a single parameter which combines both of these criteria together is required, some efficiency definitions originally proposed for powder classification may be used, as below. In this case it is advantageous to redefine the description of the three streams involved as follows:

M_{F} is the mass flow rate of the feed suspension
M_{O} is the mass flow rate of the overflow suspension
M_{U} is the mass flow rate of the underflow suspension
y_{F} is mass fraction of solids in the feed
y_{O} is mass fraction of solids in the overflow
y_{U} is mass fraction of solids in the underflow

In terms of the three mass fractions y_{F}, y_{U} and y_{O}, Newton[9] efficiency E_{N} is defined as:

$$E_{\mathrm{N}} = \frac{(y_{\mathrm{U}} - y_{\mathrm{F}})(y_{\mathrm{F}} - y_{\mathrm{O}})}{y_{\mathrm{F}}(1 - y_{\mathrm{F}})(y_{\mathrm{U}} - y_{\mathrm{O}})} \tag{3.46}$$

which can be rewritten in another form:

$$E_{\mathrm{N}} = \frac{M_{\mathrm{U}} \cdot y_{\mathrm{U}}}{M_{\mathrm{F}} \cdot y_{\mathrm{F}}} - \frac{M_{\mathrm{U}}(1 - y_{\mathrm{U}})}{M_{\mathrm{F}}(1 - y_{\mathrm{F}})} \tag{3.47}$$

The latter form of Newton efficiency shows the physical significance because it is clearly the mass recovery of the solids E_{T} minus the undesirable 'recovery' of liquid, both in the underflow. This efficiency definition was selected as the best available by Tengbergen[5] but, more recently, Ogawa *et al.*[10] have pointed out that it gives uneven sensitivity to small changes in the mass fractions of solids in either the underflow or in the overflow (as can be seen from equation 3.46). In order to make the sensitivity more uniform over the whole range of possible values of y_{U} and y_{O}, Ogawa *et al.* derived

another definition for separation efficiency, using the information theory, in the following form:

$$E_0 = 1 - \frac{(y_F - y_O)\phi(y_U) + (y_U - y_F)\phi(y_O)}{(y_U - y_O)\phi(y_F)} \tag{3.48}$$

where

$$\phi(y) = -y \ln y - (1 - y) \ln (1 - y) \tag{3.49}$$

Although this definition is an improvement on Newton efficiency with regard to the above-mentioned sensitivity, it is very complicated algebraically (it fails to satisfy one of the criteria laid down by Tengbergen[5] in that it should be simple) and it is therefore doubtful that it will be used in practice.

A far simpler solution to the sensitivity problem is in another possible definition in the form[11]:

$$E_s = \frac{(y_U - y_F)(y_F - y_O)}{(1 - y_F)y_F} \tag{3.50}$$

which gives a completely uniform sensitivity to changes in y_U and y_O over the whole range (as equation 3.50 is a straight line for either $E_s = f(y_U)$ or $E_s = f(y_O)$). The physical significance of E_s can be shown from equation 3.50: it is a product of

$$\frac{y_U - y_F}{y_F}$$

(equal to the relative improvement in the solids content of the underflow) and

$$\frac{(1 - y_O) - (1 - y_F)}{1 - y_F}$$

(equal to the relative improvement in water content of the overflow).

The three efficiency definitions quoted in this section suffer from the same disadvantage as for the total gravimetric efficiency in section 3.2.1 because their values for any specific equipment depend on the size distribution of the feed solids and they are therefore unsuitable as a general criterion of efficiency. This is, of course, unless they could be used in a differential form defined in the same way but for different particle sizes in turn; only Newton efficiency can be rearranged for that purpose[5].

It is fitting to end this review of efficiency definitions with a rather speculative but theoretically very basic definition. The thermodynamic efficiency may be defined as the basic energy of mixing of the solids in a fluid, in relation to the work done in a separator to 'unmix' the suspension. The former is as yet impossible to establish because little is known quantitatively about the thermodynamics of solid–fluid systems and the thermodynamic efficiency

therefore remains a purely theoretical concept which might be worth studying in the future (see chapter 18, Part 2).

3.5 A new method of testing separators

This section describes a new and simple experimental method[12] for obtaining the reduced cut size and the rest of the reduced grade efficiency curve of an operating separator. The method relies on feeding a known and fully characterized slurry to the separator under test, and on measuring only two solids concentrations (in the feed and in the overflow), one static pressure differential (or some other flow rate-dependent variable) and the slurry temperature. These measurements are best done and logged by a personal computer, and, for hydrocyclones, have to be repeated at two different pressure settings.

The new method eliminates the need for sampling, particle size determinations (except that of the feed suspension but this is only done once for a whole string of experiments) or flow rate measurements. This makes the tests simpler than the conventional test methods and also capable of being performed by simple, on-line instrumentation and a computer.

In this section, the underlying theory is fully developed and its application demonstrated on a specific case of testing a small diameter hydrocyclone used for monitoring very fine particle size in industrial slurries.[13]

3.5.1 Introduction

Testing the grade efficiencies of separators is a tedious and time-consuming task. It is still very much needed, however, particularly when investigating the effect of feed concentration of solids where, for most separators, the scale-up theory still requires experimentally determined constants.

The conventional test method (see section 3.3.1) requires sampling of at least two of the material streams involved. This is followed by full particle size analyses (and concentration measurements) of these samples and, also, by flow rate measurements for the necessary determination of the total solids recovery to underflow. Alternatively, the total solids recovery can be evaluated from the particle size distributions in all three streams around the separator, see section 3.3.1.4.

The grade efficiency curves that are evaluated from such conventional tests are subject to large, random variations because all errors of sampling, particle size measurements and concentration measurements are propagated into the final result.

In our ongoing search for new methods of on-line particle size analysis and in developing one based on a hydrocyclone[13], we have discovered an elegant way of simplifying the grade efficiency testing which also, at the same time, gives more reproducible results than the conventional tests. The theory and an example of use of the test method are given in the following.

3.5.2 Grade efficiency of a separator

For any separator with a size-dependent performance, such as a hydrocyclone, a sedimenting centrifuge or a settling vessel, the grade efficiency varies with particle size, and a graphical representation of this is called the grade efficiency curve (see section 3.2.2). As the value of the grade efficiency has the character of probability, it is sometimes referred to as the partition probability; the curve then becomes the partition probability curve or Tromp curve.

In practice, the grade efficiency curve is a continuous function of particle size x—see *Figure 3.15*, which gives a typical grade efficiency curve for a hydrocyclone. The preferred definition of particle size in grade efficiency testing of separators is the equivalent Stokes diameter as measured by laboratory methods involving gravitational or centrifugal sedimentation. This incorporates the effects of particle density, shape and fluid viscosity on particle–fluid interaction, within the validity of Stokes' law, see chapter 2.

The effect of flow splitting (or 'dead flux') in applications with appreciable and dilute underflow, as is common with some separators, is to modify the shape of the grade efficiency curve to make it appear as if the performance of the separator were better than it actually is. As shown in *Figure 3.15*, the curve does not start from the origin (as it should for inertial separation) but has an intercept, the value of which is usually equal to the underflow-to-throughput ratio R_f. This is because the very fine particles simply follow the flow and are split between the underflow and the overflow in the same ratio as the fluid. The R_f ratio is defined as the fraction of the volumetric feed rate which turns up in the underflow, i.e. the underflow rate, divided by the feed rate.

In order to remove the effect of flow splitting from the efficiency definition, so that it describes only the true 'centrifugal efficiency', the grade efficiency is 'reduced' by equation 3.41.

This forces the curve to pass through the origin as indicated by the second curve, $G'(x)$ in *Figure 3.15*. The reduced grade efficiency curve can, for some separators, be approximated by an analytical expression such as the one used in this method—see equation 3.51 in the following section.

While it provides the most comprehensive description of separation efficiency, the grade efficiency curve is rather clumsy for correlation with operating variables or for simple equipment comparisons. Such applications call for a single number, independent of the size of the feed solids, as a measure of efficiency. This is available in the form of the 'cut size' x_{50} which is defined as the size corresponding to 50% on the grade efficiency curve $G(x)$—see *Figure 3.15*. Most mathematical descriptions of the performance of separators, however, are in terms of the reduced cut size x'_{50} (also shown in *Figure 3.15*) and defined as the size corresponding to 50% on the reduced grade efficiency curve $G'(x)$.

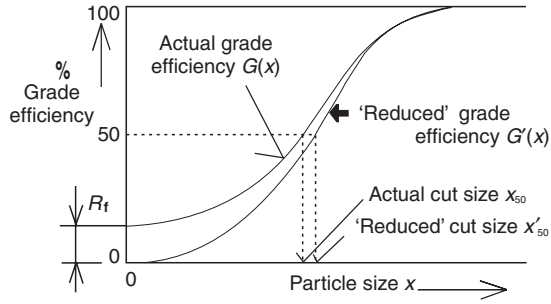

Figure 3.15 Grade efficiency curves for a hydrocyclone

3.5.3 The theory

The reduced grade efficiency curves of separators can often be fitted by a cumulative log–normal function in the following form[14]:

$$G'(x) = 0.5 + 0.5\,\mathrm{erf}\left[\frac{\ln(x) - \ln(x'_{50})}{\sqrt{2}\ln(\sigma_s)}\right] \tag{3.51}$$

where the erf function is defined as:

$$\mathrm{erf}(z) = \frac{2}{\sqrt{\pi}}\int_0^z e^{-t^2}\mathrm{d}t \tag{3.52}$$

and erf(z) can be evaluated using tables, series or analytical approximations. Note that parameters x_{50} and σ_s can be determined from a plot of the reduced grade efficiency curve in a log–probability graph paper or by using a curve-fitting package such as the one in ref. 15.

Once the actual grade efficiency curve is known for a given set of operating conditions, the total efficiency E_T (recovery of solids into the underflow) expected with a particular feed of a cumulative particle size distribution $F(x)$ can be predicted using the integral in equation 3.32. Total efficiency E_T can also be reduced to account for the splitting of the flow by equation 3.40, in direct analogy with equation 3.15 for the grade efficiency. Equation 3.42 then applies to the reduced efficiencies, as equation 3.32 applies to actual efficiencies.

According to the present method, the particle size distribution of the feed solids must be capable of being closely approximated by the log–normal distribution in the following form, analogous to equation 3.51 (as cumulative fraction undersize):

$$F(x) = 0.5 + 0.5\,\mathrm{erf}\left[\frac{\ln(x) - \ln(x_g)}{\sqrt{2}\ln(\sigma_g)}\right] \tag{3.53}$$

where the erf function is again defined in equation 3.52, and x_g and σ_g are parameters defining the particle size distribution (x_g is the median and σ_g is the geometric standard deviation which defines the spread).

The total reduced efficiency E'_T can then be predicted from $G'(x)$ and $F(x)$ by integration (equation 3.42) and this, using equations 3.51 and 3.53, leads to the following formula:

$$E'_T = 0.5 + 0.5 \operatorname{erf}\left[\frac{\ln(x_g) - \ln(x'_{50})}{\sqrt{2}\sqrt{\ln^2(\sigma_g) + \ln^2(\sigma_s)}}\right] \tag{3.54}$$

The total reduced efficiency E'_T can also be evaluated directly from the feed solids concentration c and the solids concentration in the overflow c_o using equation 3.43. Conveniently, equation 3.43 does not require the knowledge of the flow ratio R_f. It is the combination of equations 3.43 and 3.54, by eliminating E'_T, which forms the basis of the present method:

$$1 - \frac{c_o}{c} = 0.5 + 0.5 \operatorname{erf}\left[\frac{\ln(x_g) - \ln(x'_{50})}{\sqrt{2}\sqrt{\ln^2(\sigma_g) + \ln^2(\sigma_s)}}\right] \tag{3.55}$$

In the above equation, the response of the separator to the operating conditions, in terms of the cut size x'_{50} and the standard geometric deviation of the reduced grade efficiency σ_s, can be found experimentally by using a feed of a known particle size distribution (described by x_g and σ_g in equation 3.53 above), and by monitoring the two concentrations c and c_o.

As one equation is not enough for calculating the two parameters, another equation has to be generated. This is done by changing the operating conditions whilst feeding the separator with the same slurry. With hydrocyclones, for example, equation 3.55 can be duplicated by taking measurements at two different pressure drops but, as the cut size changes with pressure drop, a fundamental model describing such change also has to be available. It is assumed here, however, that the value of σ_s does not change with a small change in pressure drop.

3.5.4 Practical use of the method

The sequence of the measurement, preferably controlled by a computer, is to take the readings of c and c_o at one pressure drop (result set 1), then switch to another pressure drop and repeat the measurement (set 2). *Figure 3.16* shows a schematic diagram of the measurement positions, with all of the readings being capable of being taken and logged by a computer. The concentration readings are from two separate and suitably calibrated densitometers such as gamma gauges, vibrating U-tube density meters or ultrasonic devices.

It is also possible to use just one densitometer and re-route periodically and alternately the feed and overflow streams through it. This is best done by solenoid or motorized valves, controlled by the computer (see an example in *Figure 3.17* described below).

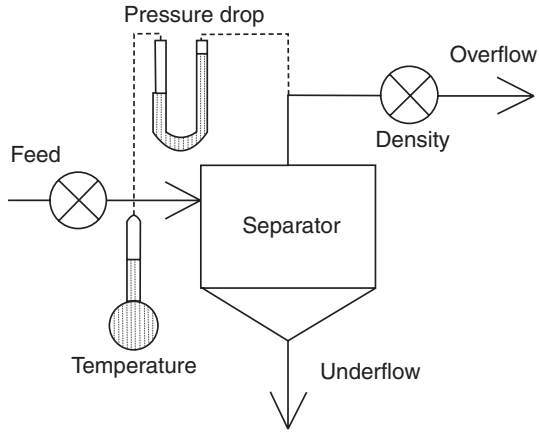

Figure 3.16 A schematic diagram of the measurement positions

The evaluation of results is done with a computer that uses a mathematical model of the separator function and the following simple algorithm for the evaluation of the two unknown parameters x'_{50} and σ_s:

1 assume σ_s and evaluate $(x'_{50})_1$ from equation 10 and the result set 1,
2 change Δ_p and calculate x'_{50} from the result set 2,
3 use a fundamental model which should link the two values of x'_{50} and if it does not, keep changing σ_s and recalculating the two values of x'_{50} until it does,
4 print or display the two final values of x'_{50}, each corresponding to a different pressure drop, and the one common value of σ_s.

Given the simplicity of the above calculations and the speed of personal computers, the calculations are done virtually instantaneously. The only delay in the measurement is through the necessity of switching to another pressure drop and the need to establish steady-state operation after the change. This is, however, quite short (a few seconds) with hydrocyclones because the residence time of the fluid inside is typically less than 1 second.

According to the present test method, the feed slurry containing the test solids is recirculated through a specially built and instrumented test rig (containing the separator under test) such as the one shown schematically in *Figure 3.17* and further described in the following section. The small step change in pressure drop required can be easily introduced by using a solenoid or motorized valve, or by changing the speed of the supply pump. The change can be initiated by the controlling computer.

The only particle size analysis required by the present method is that of the test solids in the feed stream. This is done off-line, using laboratory analytical equipment, and repeated many times to reduce errors.

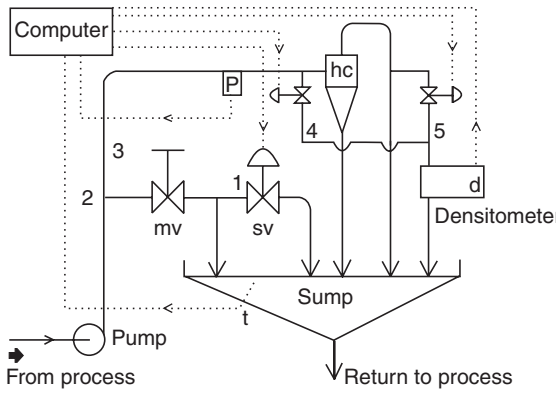

Figure 3.17 A schematic diagram of the experimental set-up

3.5.5 Experimental apparatus

In the experimental rig shown in *Figure 3.17* that we used to test a 10 mm stainless steel 'Doxie' hydrocyclone from Dorr–Oliver, the change from one operating pressure to another was achieved by switching on or off the solenoid valve (sv) in the by-pass line 1. This is, however, only possible when the test solids contain only very fine particles, which do not separate significantly in the T-junction 2 that splits the pumped flow into the hydrocyclone feed line 3 and the by-pass line 1. In the case of coarser slurries used in testing larger hydrocyclones, this arrangement would not be acceptable and the change in the operating pressure drop might better be achieved by changing the speed of the supply pump.

It may also be noted from *Figure 3.17* that, in this example, only one densitometer is used and the two streams to be measured (the sample stream 4 from the feed stream 3 and the sample stream 5 from the overflow 6) are switched through it alternately, with a delay in between to allow each sample stream to reach the sensor head of the instrument. A vibrating U-tube density meter is used in the example. Note also that both of the streams taken through the densitometer have to be well de-aerated and this is achieved by venting the lines and routing them in such a way that de-aeration takes place by gravity.

3.5.6 Example of test results

Figure 3.18 shows the particle size distribution, by mass, of the solids used in the tests (chalk), as obtained with the Ladal Pipette Centrifuge and the Andreasen Pipette Method. As can be seen from the log–probability plot, the distribution is very nearly log–normal and thus suitable for testing the performance of the hydrocyclone. Furthermore, the medium size of the chalk (3.9 microns) is within the range of cut sizes expected from the hydrocyclone (2 to 4 microns) which is a requirement for effective separator testing.

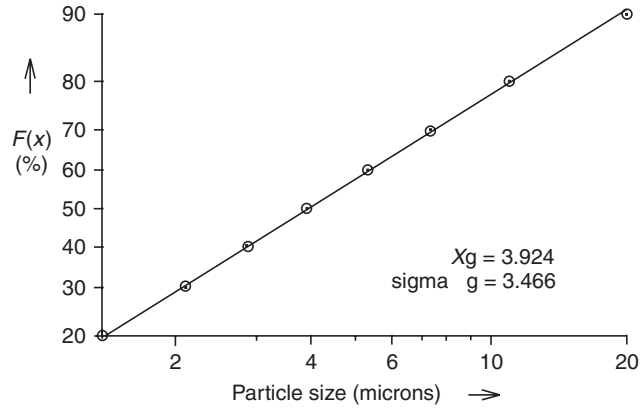

Figure 3.18 Particle size distribution by mass of the test powder (chalk)

The most important effect to be tested in hydrocyclones is that of the feed solids concentration. The range covered was from 0 to 20% by volume. An IBM-compatible personal computer was used to control the rig and log the data, using a specially developed program that included the necessary algorithms mentioned previously.

Besides the feed solids concentration c, there is a whole host of variables affecting hydrocyclone performance and these are conveniently grouped together in dimensionless groups. A model based on the use of such groups has been published before[16] and the present method is based on an adaptation of this model to small diameter hydrocyclones.

Whilst with larger hydrocyclones the resistance coefficient called the Euler number, Eu, depends on the Reynolds number, for very small hydrocyclones (such as the one used in this work) it is practically constant. We felt justified, therefore, in using such a combination of Eu with Stk (instead of a straight product of Stk·Eu as derived from first principles, equation 6.12), which would obviate the need to measure flow rates on the rig and, therefore, greatly simplify the testing procedure.

The main equation relating the relevant dimensionless groups is as follows:

$$\mathrm{Stk}'_{50} \cdot \sqrt{\mathrm{Eu}} = k_1 \cdot \exp(k_2 c) + k_3 \tag{3.56}$$

where the dimensionless groups are defined in chapter 6, equations 6.9 to 6.11.

The left-hand term in equation 3.56, $\mathrm{Stk}'_{50} \cdot \sqrt{\mathrm{Eu}}$, is a dimensionless group that has its theoretical basis in the turbulent two-phase flow theory for hydrocyclones (equation 4.21 in ref. 16), whilst the right-hand side is a semi-empirical expression of the effect of feed concentration, which has its roots in the theory of hindered settling.[17]

The test rig described previously was run with the chalk slurry at several solids concentrations ranging up to 20% by volume, with duplicated measurements

at each concentration. The range of reduced cut sizes measured was from 2 microns at low concentrations to 5 microns at 20%. The geometric standard deviation of the reduced grade efficiency curve varied between 1.8 and 2.5. The above results agree with those obtained with the conventional test methods.[18,19]

Figure 3.19 shows the results in dimensionless form and the best fit curve obtained by the minimum sum of squares method. This provided the constants for equation 3.56, with the following values (if c is in % v/v):

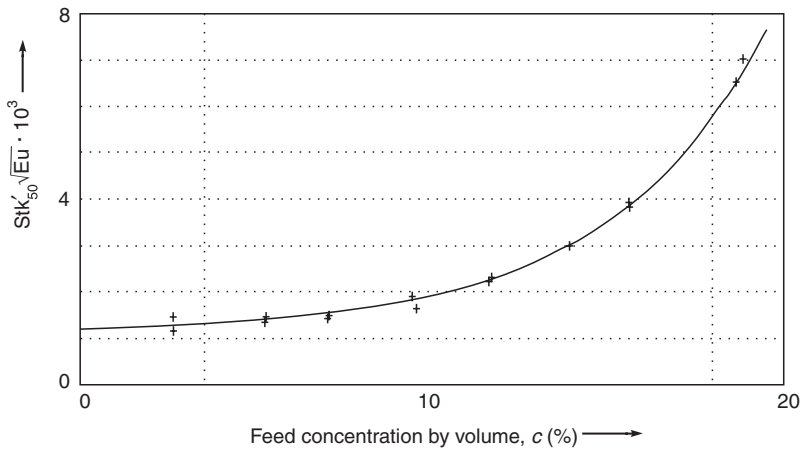

Figure 3.19 Test data obtained with a 10 mm hydrocyclone

$$k_1 = 0.083419 \times 10^{-3},$$
$$k_2 = 0.22359 \text{ and}$$
$$k_3 = 1.1335 \times 10^{-3}.$$

Equation 3.56 then represents the performance of the hydrocyclone within the range of operating conditions used in its testing. Equation 3.56 can then be employed, for example, as a model for particle size measurement of unknown slurries pumped through the same rig as used in testing the hydrocyclone.

3.5.7 Conclusions

The advantages of the new method for testing separators can be summarized as follows:

1 testing of separators is greatly simplified and speeded up, compared to conventional methods, and the method can be used in research and development,
2 a personal computer can be used to automatically control the measurement, to take multiple readings of each variable (for improved accuracy) and to log and evaluate the data,

3 errors of sampling, concentration measurement, flow rate measurement and particle size measurement normally present in conventional testing are either reduced or completely eliminated,
4 the same equipment and method can be used for on-line monitoring of the median particle size and of the spread of the distribution in the feed slurry.[20,21]

Any suitable feed solids material may be used for the testing but it has to be one with a mono-modal particle size distribution that approximately follows the log–normal law. This requirement is not too limiting because the test material is a matter of choice.

The new test method was recently used by the authors in the course of the development of a new, hydrocyclone-based, on-line monitor of particle size in fine suspensions.[13,20,21]

Nomenclature

c	is mass concentration of solids in the feed
c_o	is mass concentration of solids in the overflow
D	is the internal diameter of a hydrocyclone
E_T	is the total coarse efficiency (or recovery)
E'_T	is the reduced total efficiency defined in equation 3.5
Eu	is Euler number as defined in equation 3.12
$F(x)$	is the cumulative percentage undersize in the feed
$G(x)$	is the actual grade efficiency function (curve)
$G'(x)$	is the reduced grade efficiency function, equation 3.1
R_f	is the underflow-to-throughput ratio (by volume)
Q	is the volumetric flow rate of the feed
Stk'_{50}	is Stokes number as defined in equation 3.13
v	is characteristic velocity as defined in equation 3.14
x	is particle size as a variable
x_g	is the mass median of the feed solids $[F(x_g) = 0.50]$
x'_{50}	is the reduced cut size $[G'(x'_{50}) = 0.50]$
Δ_p	is static pressure drop across the hydrocyclone
μ	is liquid viscosity
ρ	is liquid density
ρ_s	is solids density
σ_g	is the geometric standard deviation of $F(x)$
σ_s	is the geometric standard deviation of $G'(x)$

References

1. Trawinski, H., *Aufbereitungs–Technik*, **17** (5), 449–459 (1975)
2. Svarovsky, L., *'Measurement of efficiency of gas cleaning equipment', Proc. Filtration Society's Conference on Filtration*, Olympia, London, September 20–22 (1977) Also in: *Filtration and Separation*, **15** (4), 355–359 (1978)
3. Allander, C. G., *Staub–Reinhaltung Der Luft*, **18** (1), 15–17 (1958)
4. Gibson, K., '*Large scale tests on sedimenting centrifuges and hydrocyclones for mathematical modelling of efficiency', Proc. of the Symposium on Solid–Liquid Separation Practice*, Yorkshire Branch of the I. Chem. E., Leeds, England, March 27–29 (1979), pp. 1–10
5. Van Ebbenhorst Tengbergen, H. J. and Rietema, K., 'Efficiency of Phase Separations'. In *Cyclones in Industry*, Rietema, K. and Verver, C. G., (Eds) Elsevier, Amsterdam (1961)
6. Kelsall, D. F., '*The theory and applications of the hydrocyclones*'. In Pool and Doyle: *Solid–liquid Separation*, H.M.S.O., London (1966)
7. Mayer, F. W., *Zement-Kalk-Gips* **19**, No. 6, 259–268 (1966)
8. Fontein, F. J., Van Kooy, J. G. and Leniger, H. A., *Brit. Chem. Engng*, **7**, 410 (1962)
9. Newton, H. W., *Rock Product*, **35** (26), 26–30 (1932)
10. Ogawa, K., Ito, S. and Kishino, H., *J. Chem. Engng of Japan*, **11** (1), 44–47 (1976)
11. Svarovsky, L., *The efficiency of separation processes*. In R. J. Wakeman, *Progress in Filtration and Separation*, Elsevier, Amsterdam (1979)
12. Svarovsky, L. and Svarovsky, J., 'A new method of testing hydrocyclone grade efficiencies', paper given at the 4th International Conference on Hydrocyclones, Southampton, 23–25 September 1992 and published in a book edited by L. Svarovsky and M. T. Thew, *Hydrocyclones: Analysis and Applications, Vol. 12 Fluid Mechanics and its Applications*, Kluwer Academic Publishers, Dordrecht, 135–145 (1992)
13. Svarovsky, L. and Svarovsky, J. 'A new method and apparatus for monitoring of particle size distributions in industrial processes', *Particle Size Analysis 1991*, Loughborough, 17–19 September 1991 (published in the proceedings)
14. Gibson, K., 'Large scale tests on sedimenting centrifuges and hydrocyclones for mathematical modelling of efficiency', 1–10, in *Proc. Symp. on Solid–liquid Separation Practice*, Yorkshire Branch of the I. Chem. E., Leeds, 27–29 March 1979
15. Interactive Data Plotting, Catalogue of In-Company Short Courses, Books and Particle Technology Software, FPS, The Lares, Maple Avenue, Cooden, Bexhill-on-Sea, TN39 4ST, 2000
16. Svarovsky, L., *Hydrocyclones*, Holt Rinehart and Winston, London (1984)
17. Davies, L., Dollimore, D. and McBridge, G. B., *Powder Technology*, 16, 45, (1977)
18. Svarovsky, L., 'Evaluation of clarification performance of a two-stage hydrocyclone system', 2nd International Conf. on Hydrocyclones, Bath, 19–21 September 1984, Paper J2, Proceedings published by BHRA, Cranfield, (1984)
19. Svarovsky, L., 'Evaluation of small diameter hydrocyclones', I.Chem.E. Symposium on Solid/Liquids Separation Practice and the Influence of New Techniques, Leeds, 3–5 April 1984, Paper 24, 193–205, Inst. of Chemical Engineers, Yorkshire Branch (1984)
20. Svarovsky, L. and Svarovsky, J. 'In-situ testing of plant separators and their subsequent use for on-line monitoring of particle size', AFS Seminar and Expo,

System Approach to Separation and Filtration Process Equipment, Chicago, Illinois USA, 3–6 May 1993, paper published in '*Advances in Filtration and Separation Technology*', W. W-F Leung (Ed.), Vol. 7, AFS 1993, 56–60

21. Svarovsky, L. and Svarovsky, J. 'In-situ testing of plant separators and their subsequent use for on-line monitoring of particle size', paper presented at the 21st Conference of the Slovak Society of Chemical Engineering, Vyhne, Slovakia, 23–26 May 1994, paper published in the proceedings, 123–126

4 Coagulation and flocculation Part I

M. A. Hughes

Department of Chemical Engineering, University of Bradford

4.1 Introduction

Solids which have to be separated from liquids vary both in size and morphology as well as chemical nature. The term 'colloid' is generally applied to those particles which are smaller than 1 μm and a dispersion of these particles in a fluid is called a 'sol'. Particles of less than 0.2 μm are called 'super' colloids and, although colloids are larger than molecules, they are too small to be seen under a microscope. Alexander and Johnson[1] classify colloid particles as those in the size range 10^{-6} to 10^{-9} m. Dispersions of larger particles are called 'suspensions'. The size limits mentioned above are only arbitrary and colloidal properties can be exhibited by suspensions. The separation of the very small particles in sols present more problems than do larger particles, hence techniques have been developed which cause agglomeration of the small particles and thus simplify the separation techniques.

Colloidal dispersions can be altered by treatment of the solid–liquid interface by the addition of either electrolytes or surface-active agents and, of course, adjustment of the physical conditions may lead to crystal growth and a change in the particle size and interfacial area. Procedures which lead to increased sol stability (i.e. which lead to uniform dispersion of the particles in the liquid) are called 'peptizing', 'stabilizing' or 'deflocculating' procedures whereas those which lead to breakdown of the sol (i.e. which cause the particles and liquid to separate out) are termed 'coagulating' or 'flocculating' procedures. The terms 'coagulation' and 'flocculation' are used widely to mean the same thing, but in the water treatment industry they refer to quite different processes (see later).

Dispersions can be classified into either lyophilic or lyophobic colloids. In the former the solid shows a marked affinity for water or some other dispersion medium so that sols are formed spontaneously on mixing. Lyophobic colloids exhibit a low affinity for the host medium. Examples of

these colloids are clays, hydrated oxides etc. Examples of lyophilic colloids are macromolecules such as proteins, humic acids etc.

Lyophobic sols can be formed by chemical means or by mechanical mixing and it is this group of sols which is particularly sensitive to the addition of electrolytes to a bulk phase, being readily persuaded to flocculate upon such additions. Lyophilic colloids are less sensitive to the addition of electrolytes and very high concentrations of the electrolyte salts are necessary for precipitation.

A basic requirement for the formation of large particles is for smaller ones to 'come together'. The simplest picture of the approach of two charged spherical particles is given in *Figure 4.1*. We shall see that all particles carry a residual charge and a negatively charged particle is shown in *Figure 4.1* although positively charged particles are possible. Attracting forces such as the London and van der Waals forces are opposed by the interaction of like charges distributed over each particle. If the charge on the particle can be reduced then close approach is possible.

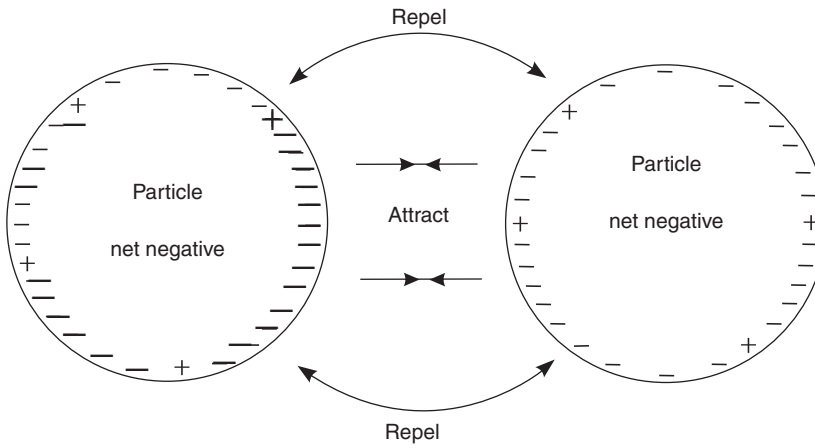

Figure 4.1 The approach of two like-charged particles

The total interaction between colloidal particles is discussed by Verwey and Overbeek[2] and Osipow[3]. A simplified approach is to consider the curves of energy against distance shown in *Figure 4.2a* and *4.2b* for repulsion and attraction respectively; these curves may be combined to give resultant interaction curves of the type shown in *Figure 4.3*.

The effect of thermal motion must also be included in the system since this will oppose any attraction which the particles may have for each other. Thus for a dispersion to be stable the potential energy maximum in the resultant curve must be considerably greater than kT (where k is the Boltzmann constant and T the absolute temperature). In *Figure 4.3* curves A, B, C and D therefore represent stable sol conditions whereas curves E, F and G represent instability. The height of the maximum on the potential energy

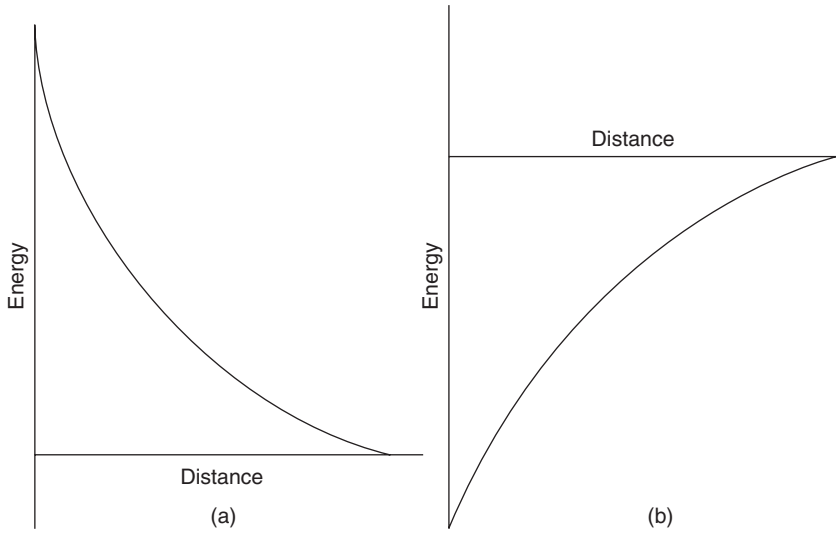

Figure 4.2 (a) Repulsion curve and (b) attraction curve for two like-charged particles approaching each other

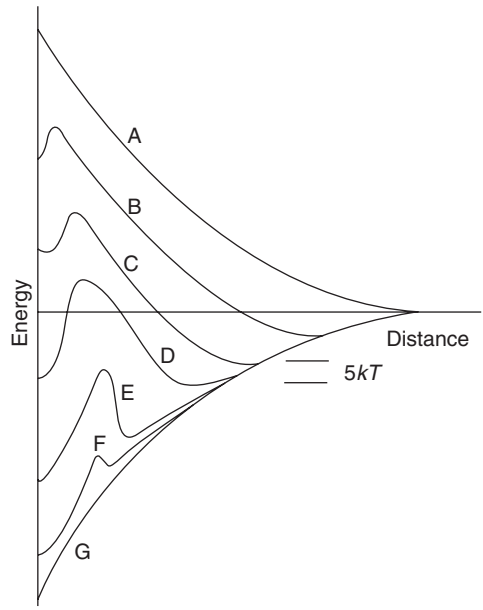

Figure 4.3 Resultant energy curves for particles approaching each other. Curves A, B, C and D demonstrate net repulsion, curves E, F and G demonstrate net attraction. Secondary minima occur in curves D, E and F; meta-instability may result at this separation distance

curve is an indicator of the rate of flocculation and this height is determined by the potential drop on the double layer which surrounds the particle and extends into the bulk which contains the electrolyte.

Indeed, the charge surrounding a particle is a key to the flocculation process. It is now necessary to consider the origin of this charge and its distribution at and near to the solid–liquid interface.

4.2 The colloidal model

4.2.1 The net charge on a solid

Most naturally occurring and man-made particles carry a residual charge on their solid surface, usually this is a net negative charge, as in the case of minerals and clays, although it can be net positive, as in the case of sewage sludge. There are three mechanisms which can cause this charge.

Mechanism 1

In crystalline materials the lattice is defective because of, e.g. Schottky defects[4] and thus a net excess of anions (negative) or cations (positive) exists at the surface. The net charge is compensated by an equivalent ionic charge at the surface and, on contact with water, the crystal releases the compensating ions to form a double layer. This behaviour is typical of ion-exchange materials such as zeolites, clays etc.

Mechanism 2

Some solids may be classified as sparingly soluble ionic crystals. When these are dispersed in water they exist in equilibrium with a concentration of the product ions, the concentration being determined from the solubility product. The potential of the solid (ψ_0) is determined from the Nernst equilibrium condition; for colloidal silver iodide for example, this gives

$$\psi_{0\,(\mathrm{AgI})} = A + \left(\frac{RT}{F}\right) \ln C_{\mathrm{Ag}^+} \tag{4.1}$$

or

$$\psi_{0\,(\mathrm{AgI})} = B - \left(\frac{RT}{F}\right) \ln C_{\mathrm{I}^-} \tag{4.2}$$

where A and B are constants, C is the concentration (activity) and F is Faraday's constant.

In general the potential of this type of solid is

$$\psi_0 = \left(\frac{RT}{vF}\right) \ln\left(\frac{C}{C_0}\right) \tag{4.3}$$

where v is the valency and C_0 is the zero point charge concentration. Of particular importance to the technologist is the behaviour of metal oxides and

hydroxides which are notoriously difficult to separate from liquid phases, in the latter case the ions which determine the potential are H^+ and OH^-. We expect these systems to be especially sensitive to bulk electrolytes and to the pH of the bulk phase.

Mechanism 3

A third method by which net surface charge is generated is through the adsorption of specific ions from solution. In particular the adsorption can occur via a hydrogen-bonding mechanism where large organic molecules are adsorbed. Such agents are useful in reverting particles which are originally positively charged to negatively charged particles in order that the classical flocculation procedures devised for negatively charged solids may be used.

4.2.2 The double layer

The colloidal model for a net electronegative particle is shown in *Figure 4.4*. The layer of negative charge is surrounded by positive charges to give the double layer, the charge extends into the bulk but becomes more diffuse and random (a Boltzmann distribution is assumed). Certain potentials may be identified. A shear layer exists, which is the plane of slip between the double layer and the bulk media and the Nernst potential is the potential which exists between the shear plane and the solid surface. The zeta potential, ζ, is of especial importance since this is the potential which can be measured; it is the potential existing between the shear plane and the bulk phase.

A number of models exist which account for the double layer. The Gouy–Chapman model[4–6] was the first to indicate the way in which the potential, ψ, varies with the distance, x, into the bulk. The model is summarized in equation 4.4.

$$\frac{d\psi}{dx} = -\left(\frac{8\pi nkT}{\varepsilon}\right)^{1/2}\left[\exp\left(\frac{ve\psi}{kT}\right) - \exp\left(-\frac{ve\psi}{kT}\right)\right] \tag{4.4}$$

where

k is the Boltzmann constant
v is the valency of the ion with opposite charge to that on the surface
n is the bulk concentration of this last ion
ε is the dielectric constant of the bulk liquid phase
ψ is the double layer potential at a distance x from the surface
e is the electronic charge.

Integration of equation 4.4 can lead to a simple statement in which the double layer potential varies with x, thus

$$\psi = \psi_0 \exp(-\mathscr{H}x) \tag{4.5}$$

where $\mathscr{H}$ is the Debye–Huckel function

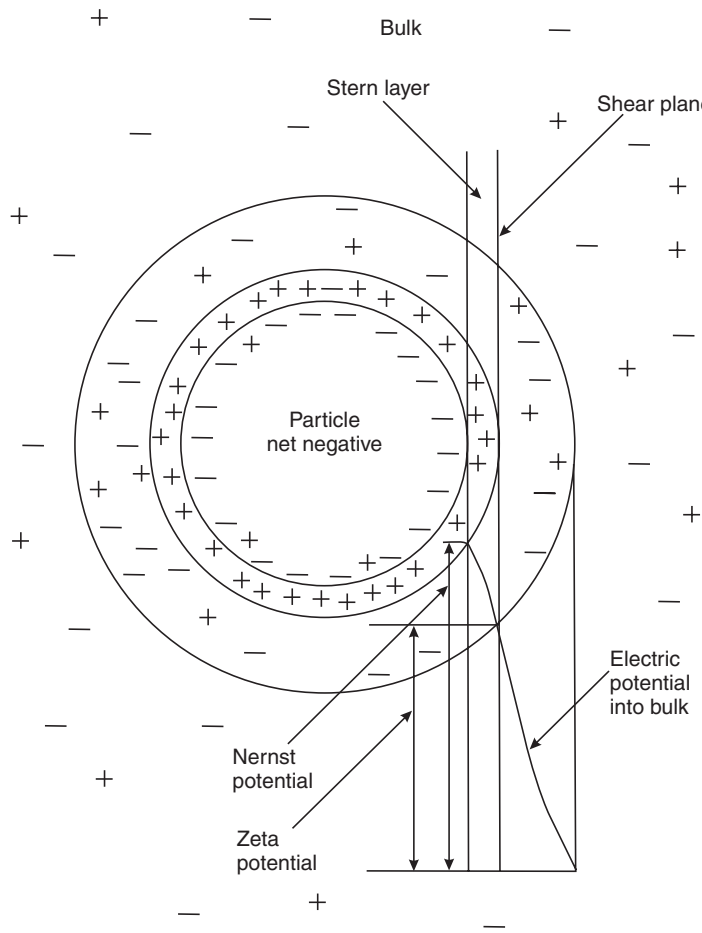

Figure 4.4 The colloidal model

$$\mathscr{H} = \sqrt{\left(\frac{8\pi e^2 N^2 I}{1000\varepsilon RT}\right)} \tag{4.6}$$

in which N is Avogadro's number and I is ionic strength. Thus the potential of a charged surface falls away exponentially with increasing distance into the bulk phase. The potential is almost zero at a distance $x = 3/\mathscr{H}$ from the surface and then beyond this distance the ions in solution experience no effect from the surface charge.

An expression for the charge density on the surface, σ, can be developed as in equation 4.7

$$\sigma = \left(\frac{\varepsilon\pi kT}{2}\right)^{1/2}\left[\exp\left(\frac{ve\psi_0}{2kT}\right) - \exp\left(-\frac{ve\psi_0}{2kT}\right)\right] \tag{4.7}$$

Stern[7] improved on the Gouy–Chapman model by allowing for finite ionic size in the double layer. The total charge density then becomes,

$$\sigma = \sigma_s + \sigma_g \tag{4.8}$$

where σ_g is the charge density as given by the Gouy model above, with ψ_0 replaced by ψ_δ which is the potential at the Stern layer (see *Figure 4.4*), and σ_s is the absorbed charge per unit area due to the Stern layer. The complete expression for the Stern model then becomes

$$\sigma = n\sigma_m\left[n + A\exp\left(-\frac{ve\psi_\delta}{kT} - \phi\right)\right]^{-1} + \left(\frac{\varepsilon nkT}{2\pi}\right)^{1/2}\left[\exp\left(\frac{ve\psi_\delta}{2kT}\right) - \exp\left(-\frac{ve\psi_\delta}{2kT}\right)\right] \tag{4.9}$$

where

σ_m is a charge corresponding to a monolayer of counter ions
A is the frequency factor
ϕ is van der Waals energy.

The equation is complicated but represents the best model to date.

4.2.3 Compression of the double layer

It can be shown that for small colloid particles of low charge, and in the presence of electrolytes, the thickness of the double layer, d, is approximated by the reciprocal of the Debye–Huckle function, $\mathscr{H}$ (equation 4.6). For water at 298 K, the thickness becomes

$$d = \frac{2.3 \times 10^{-9}}{\sqrt{I}}\,\text{cm} \tag{4.10}$$

It is seen to be dependent on the ionic strength and for some practical situations *Table 4.1* reflects this last fact. Consequently, the addition of

Table 4.1 Estimates of double layer thickness around a particle in various media

Medium	$d = 1/\mathscr{H}$, *nm*
Distilled water	900
10^{-4}_{M} NaCl	31
10^{-4}_{M} $MgSO_4$	15
River Thames water	4
Sea water	0.4

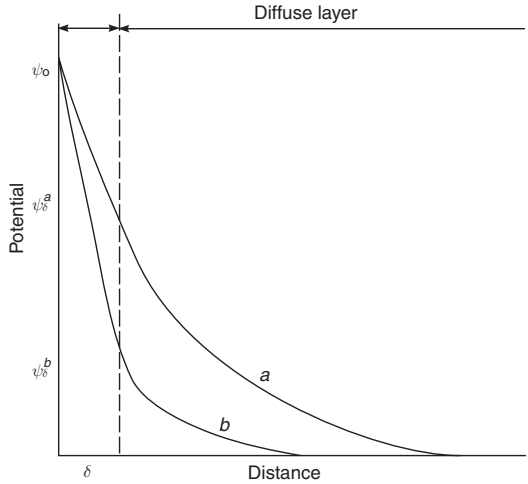

Figure 4.5 The Stern model for the electric double layer showing compression from (a) low to (b) high ionic strength

various electrolytes at increasing concentrations compresses the double layer as shown in *Figure 4.5*. The double layer becomes very small on the addition of high valency salts in appreciable concentrations.

Thus one effect of the addition of indifferent electrolytes (that is, where electrolyte ions are not adsorbed on the surface) to the sol may be to reduce the double layer thickness and thus to promote closer approach of particles and consequent aggregation (see section 4.4).

4.2.4 The rate of aggregation

The process of aggregation is seen to require a low charge on each particle and a collision event. Assuming that electrical repulsion is absent, as a result of pretreatment with electrolyte, then the rate of aggregation depends on Brownian motion. In the assumed absence of velocity gradients, induced by e.g. stirring, we have the case of perikinetic aggregation or flocculation when Brownian motion alone dictates the rate.

According to the theory of von Smoluchowski[8,9] the most rapid aggregation will occur when every contact leads to the adherence of one particle to another. So the rate of perikinetic flocculation or aggregation is given by

$$-\frac{\mathrm{d}n}{\mathrm{d}t} = k_\mathrm{p} n^2 \tag{4.11}$$

in which n is the number of particles present in a given volume and k_p is a specific rate constant. Hence on integration

$$n = \frac{n_0}{1 + k_\mathrm{p} n_0 t} \tag{4.12}$$

then it follows that

$$t_{1/2} = \frac{1}{k_p n_0} \tag{4.13}$$

where $t_{1/2}$ is the half life.

The half life for particles, $t_{1/2}$, is the time taken for the initial number of particles to be reduced to one half and is related to the diffusion constant, D, the effective radius of the particles, r (assumed spherical) and n_0, the number of particles of radius r_0 initially present:

$$t_{1/2} = \frac{1}{8\pi D r n_0} \tag{4.14}$$

Taking the diffusion constant as

$$D = \frac{kT}{6\pi\eta r_0} \tag{4.15}$$

where η is the viscosity of the liquid bulk phase, then

$$t_{1/2} = \frac{3\eta}{4kTn_0} \tag{4.16}$$

Taking as an example water at $T = 298\,\mathrm{K}$

$$t_{1/2} \approx \frac{2 \cdot 10^{11}}{n_0} \tag{4.17}$$

The more highly concentrated the sols, the faster the aggregation.

The rate constant k_p is also given by

$$k_p = \frac{4kT}{3\eta} \tag{4.18}$$

which demonstrates the effect of the thermal energy kT as reflected in the Brownian motion of the particles.

Equation 4.14 may be altered for the case of slow aggregation in which only a fraction β of the collisions leads to adherence between particles:

$$t_{1/2} = \frac{1}{8\pi D r n_0 \beta} \tag{4.19}$$

Further analysis of slow coagulation is made in terms of the energy barrier, E^*, which exists for collisions. The coagulation is slowed down by a stability factor W which is given by

$$W = 2\int_2^\infty \frac{\mathrm{d}s}{s^2} \exp\left(\frac{E^*}{kT}\right) \tag{4.20}$$

where $s = p/r$ and p is the distance between particles. Equation 4.20 approximates to

$$W \approx \frac{1}{2\kappa r} \exp\left(\frac{E^*_{\max}}{kT}\right) \tag{4.21}$$

where κ is the Debye–Huckel function now given by

$$\kappa = \sqrt{\left(\frac{4\pi e^2 \Sigma n_{i0}\, z_i^2}{\varepsilon kT}\right)} \tag{4.22}$$

n_{i0} is the concentration of ions of type i in the bulk phase and z_i is the valency. Now since $E^*_{\max}$ can be evaluated, from the theory of Verwey and Overbeek[2], the dependence of the stability factor W on the electrolyte concentration and valency can be predicted. It can thus be shown that a 2:2 electrolyte provides less hindrance to the aggregation rate than does a 1:1 electrolyte at the same concentration.

Gregory[10] observes that Brownian motion alone is unlikely to produce aggregates of an acceptable size (say 1 mm) which leads to useful flocs in a reasonable time. In any case, if aggregates of many particles are formed by this mechanism the consequent reduction in particle numbers dramatically alters the rate to a very slow value.

Stirring a dispersion can cause an increase in flocculation rate—orthokinetic flocculation. At low energy inputs collisions of particles are induced through induced velocity gradients; obviously at high shear rates the aggregates break up again. Now, if every collision leads to an aggregate then equation 4.11 becomes, for orthokinetic flocculation,

$$-\frac{\mathrm{d}n}{\mathrm{d}t} = \frac{2}{3} G d^3 n^2 \tag{4.23}$$

in which d is the diameter of the particle and G is the shear rate (s^{-1}).

Now as particles and aggregates collide, the probability of such collisions is increased through the energy imparted to the host fluid and so the reduced particle concentration (and hence reduced rate through equation 4.11) is partially offset. It also follows that

$$\frac{\text{orthokinetic rate}}{\text{perikinetic rate}} = \frac{G\eta d^3}{2kT} \tag{4.24}$$

Gregory points out that if the shear rate, $10\,s^{-1}$, is used to describe gentle agitation, the two rates are equal when the particle diameter is around 1 μm but orthokinetic flocculation becomes more significant with larger particles and higher shear rates.

4.3 Electrokinetic phenomena and the zeta potential

It has already been said that a practical way to characterize the double layer is to measure the zeta potential, ζ. Several techniques are possible; these come within the category of electrokinetic phenomena.

In electrophoresis a potential gradient is applied to a dispersion and the movement of the charged particles relative to the stationary bulk phase is measured. Sedimentation potential is the reverse of the above; the

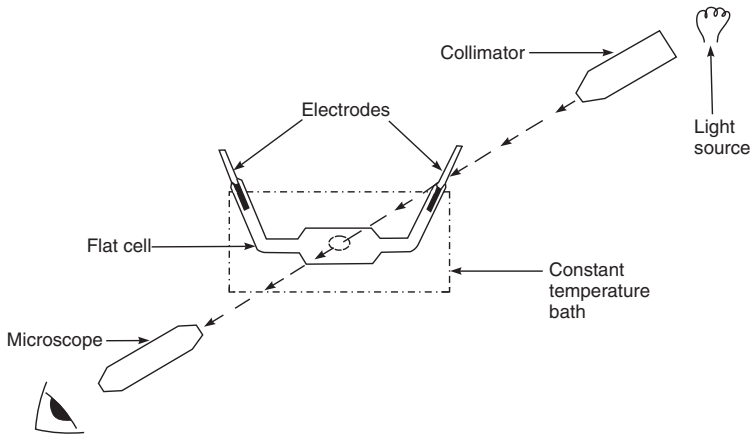

Figure 4.6 Schematic diagram of apparatus for measuring the electro-phoretic effect. The flat cell contains the dispersion of particles and these are subjected to an applied d.c. voltage across the electrodes. A light beam is focused into the flat cell at the predetermined stationary layer and the movement of the practicles is observed through the microscope

potential which is developed when the charged particles precipitate through the stationary liquid is measured.

In electro-osmosis the charged solid is held stationary (possibly in the form of a plug), a potential gradient is applied, and the bulk liquid phase moves. Pressure is then applied until it just counters the flow, and this is the electro-osmotic pressure. Streaming potential is the opposite of electro-osmosis: the potential gradient generated when the bulk liquid phase is forced through the stationary charged solid is measured.

Commercial apparatus is available for the measurement of electrokinetic phenomena[11]. One such apparatus, to measure the electrophoretic effect, is shown in *Figure 4.6*. Observation cells are available in two forms, either cylindrical or flat; generally the flat cell is more robust. The potential is applied at platinized black electrodes and care must be taken to ensure that such electrodes do not become polarized during the measurements. The particles are observed through the microscope which must be focused into the stationary layer of the bulk phase, otherwise 'cell wall effects' will enhance or slow down the true velocity, V_{E}, of the charged particles. The velocity of the particles is obtained by timing the passage of a number of individual particles across the calibrated grid set in the lens of the microscope and so an average V_E is obtained.

Kruyt[12] has related the electro-osmotic velocity of flow to the double layer potential at the shear plane and to the applied external field. The double layer must satisfy the relation

$$\nabla^2\psi = -\frac{4\pi Z}{\varepsilon} \tag{4.25}$$

where

∇^2 is the Laplace operator
ψ is the double layer potential at a distance x from the surface
Z is the net space charge per unit volume at point x, and
ε is the dielectric constant of the medium.

When an external field E is applied, a volume of the bulk liquid of thickness $\mathrm{d}x$ is subject to a force

$$F = EZ\,\mathrm{d}x \tag{4.26}$$

A number of layers adjacent to the shear layer will be moving at different velocities and will exert viscous drag on the latter. Consider a layer at position x from the surface; the drag force on this layer is

$$F_x = -\eta\left(\frac{\partial v}{\partial x}\right)_x \tag{4.27}$$

and at $x + \mathrm{d}x$ the drag force is

$$F_{x+\mathrm{d}x} = -\eta\left(\frac{\partial v}{\partial x}\right)_{x+\mathrm{d}x} \tag{4.28}$$

Therefore the net frictional force on the layer is

$$F' = \eta\left(\frac{\partial v}{\partial x}\right)_{x+\mathrm{d}x} - \eta\left(\frac{\partial v}{\partial x}\right)_x \tag{4.29}$$

In the steady state the total force on the layer is zero so that

$$EZ\,\mathrm{d}x = \eta\left(\frac{\partial^2 v}{\partial x^2}\right)\mathrm{d}x \tag{4.30}$$

Since at a plane surface

$$\nabla^2\psi = \left(\frac{\partial^2\psi}{\partial x^2}\right) \tag{4.31}$$

then

$$Z = -\frac{\nabla^2\psi\varepsilon}{4\pi} = -\frac{\varepsilon}{4\pi}\left(\frac{\partial^2\psi}{\partial x^2}\right) \tag{4.32}$$

and

$$-\frac{E\varepsilon}{4\pi}\left(\frac{\partial^2\psi}{\partial x^2}\right) = \eta\left(\frac{\partial^2 v}{\partial x^2}\right) \tag{4.33}$$

Equation 4.33 is now integrated over the whole liquid from the shear plane to infinity to give

$$-\frac{E\varepsilon\,\mathrm{d}\psi}{4\pi\,\mathrm{d}x} = \eta\frac{\mathrm{d}v}{\mathrm{d}x} + C \tag{4.34}$$

where E is zero when

$$\left(\frac{\partial\psi}{\partial x}\right)_{x=\infty} = 0 \quad \left(\frac{\partial v}{\partial x}\right)_{x=\infty} = 0$$

Further integration of equation 4.34 gives

$$-\left(\frac{E\varepsilon}{4\pi}\right)\psi = \eta v + C' \tag{4.35}$$

At $x = \infty, \psi = 0$ and $v = V_E$ where V_E is the true electro-osmotic velocity. Also at the shear plane $v = 0$ and $\psi = \zeta$ so that,

$$V_E = \frac{\varepsilon E \zeta}{4\pi\eta} \tag{4.36}$$

Equation 4.36 is used to determine ζ when V_E is measured (as described previously) and E, ε and η are known.

4.4 Practical applications of the zeta potential

If the zeta potential is an indicator of the electrical state of the double layer then when the value of ζ approaches zero the sols should become unstable, and this should lead to clarification. This has often been demonstrated where inorganic electrolytes have been used to lower the zeta potential of industrial wastes, municipal wastes and paper processing slurries[13].

Riddick[14] has commented that the zeta potential is the most significant controlling factor in the achievement of coagulation, although it should not be regarded as the only parameter to be adjusted to produce the desired clarification. His remarks are pertinent to water clarification.

4.4.1 Coagulation

La Mer[15] has suggested that the term 'coagulation' should be restricted to the chemical destabilization of sols whereby electrolytes are added to a sol so as to reduce the charge on the particles and allow close approach and aggregation. This is also adopted by the industry concerned with water treatment. A 'primary coagulant' then becomes the salt which is added to achieve the effect.

The useful practical effect consequent upon the addition of indifferent electrolytes is now discussed.

Schulze[16, 17] showed that certain lyophobic colloids became unstable and flocculated on the addition of electrolytes. The multivalent ions, e.g. Al^{3+} and Fe^{3+}, were very effective for net negatively charged particles. The Schulze–Hardy rule states that the coagulation effect is determined by the valency of the ion with opposite charge to that of the sol. *Figure 4.7* gives typical ζ measurements for a sol with an initial net charge of -25 mV

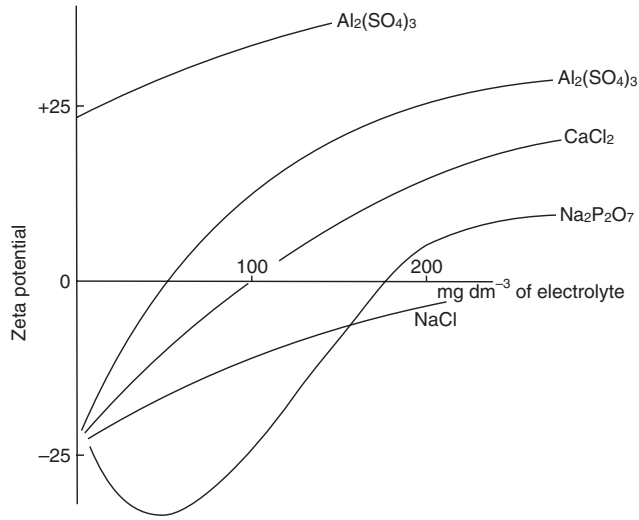

Figure 4.7 The changes in zeta potential when electrolytes are added. A 2.3 electrolyte, $Al_2(SO_4)_3$, is the most effective in reducing the initial negative zeta potential to zero.

dosed with small quantities (up to $\sim 250\,\text{mg dm}^{-3}$) of various electrolytes (1:1, 1:2 and 2:3 types). An aluminium salt is seen to be the most effective and optimum dose is around $60\,\text{mg dm}^{-3}$. Note that the charge can be reversed from net negative to net positive. Of course, the addition of aluminium to already net positively charged sols only acts to increase the sol charge. A 1:3 electrolyte, e.g. $FeCl_3$, would be as effective as the aluminium salt.

It is now readily explained why primary coagulation is achieved when a sol is treated with either lime/alum (when net negatively charged sols coagulate) or with phosphates (when net positively charged sols coagulate).

The general dosage range for a useful primary coagulant is about $100–400\,\text{mg dm}^{-3}$.

Of particular interest is the effect of sodium metaphosphate (CALGON is a common coagulating agent and is made up from the sodium salts of meta- and pyro-phosphoric acids). In the case of *Figure 4.7*, the immediate effect of the metaphosphate is further to increase the negative ζ potential of the particles *then* the potential becomes more positive as the concentration of this electrolyte is increased. In this case the first additions lead to adsorption of $P_2O_7^{4-}$ ions on the surface but then the ionic strength effect takes over generating a reduction in the ζ potential towards zero as the ionic strength increases. The metaphosphate-type anions must be useful in treatment of a colloid with any initial positive ζ potential.

In fact, it can be shown that the critical coagulation concentration (c_f), which is the concentration of specifically adsorbing counter ions required to

Table 4.2 Critical coagulation concentrations for colloids, according to Freundlich[18]

Electrolyte added	c_f *value*, mmol dm^{-3}		
Negatively Charged Colloids			
	As_2S_3 sol	*Au sol*	*Pt sol*
NaCl	51.0	24.0	2.5
KCl	49.5	—	2.2
$CaCl_2$	0.65	0.41	—
$BaCl_2$	0.69	0.35	0.058
$Al(NO_3)_3$	0.095	—	—
$\frac{1}{2}Al_2(SO_4)_3$	0.096	0.009	0.013
Positively Charged Colloids			
	Fe_2O_3 sol	*Al_2O_3 sol*	
NaCl	9.25	77.0	
KCl	9.0	80.0	
$\frac{1}{2}BaCl_2$	9.65	—	
K_2SO_4	—	0.28	
K_2CrO_4	—	0.60	
$K_3[Fe(CN)_6]$	—	0.10	
$K_4[Fe(CN)_6]$	—	0.08	

cause coagulation (usually a narrow range of concentrations), is inversely proportional to the sixth power of the charge on the ion. Lists of critical coagulation concentrations for electrolytes and sols exist[18]—see also *Table 4.2*. The c_f value depends to some extent on the nature of the sol and the usual quoted ratio of coagulating powers of ions of different charges, e.g. ~ 1:100:1000 for uni-: di-: tri-, is seen to be only approximate. Other factors besides the effect of the charge on the appropriate ion of the indifferent electrolyte dictate sol stability. Thus adsorption of the ion of the same charge as the colloid, hydration of the ions in solution, and hydration of the surface of the particle may all influence stability of dispersions of colloids. An empirical relationship is usually found for the plots of log c_f against charge, and this is usually linear—see *Figure 4.8*.

Careful mixing of colloids of opposite charge can lead to coagulation and flocculation. However this is difficult to control, as the desired flocculation of say a positively charged colloid by addition of the negative one can easily be redispersed when the charge passes through zero only to become negative because of excess of the second colloid.

Natural clays, usually charged negative, might be used to coagulate a positively charged sol.

As stated above, the indifferent electrolyte effect is altered and possibly enhanced when the ions of that electrolyte undergo hydrolysis in the aqueous

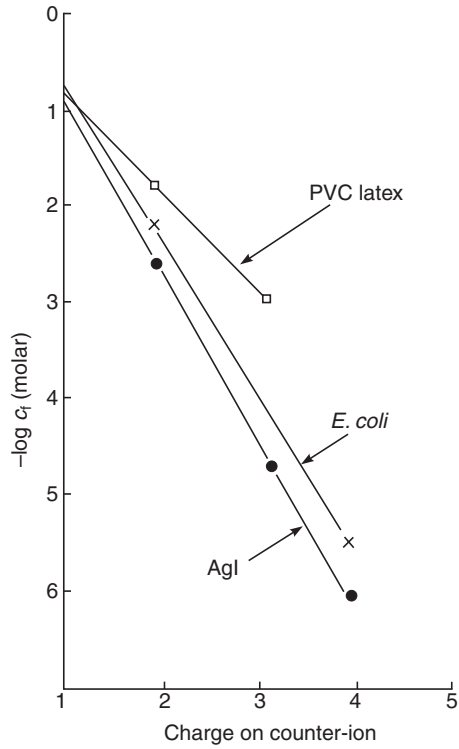

Figure 4.8 Variation of the critical flocculation concentration (c_f) with counter-ion charge

phase. We will now deal with cations in solution and the effect of the pH of the aqueous phase.

In the first place some cations and anions are not significantly hydrolysed at pHs in the range 1–14; these include common alkali metals such as Na^+ and K^+ and common anions like Cl^- and SO_4^{2-}. Of course, they will be hydrated and certain of these ions have a structuring or destructuring effect on the water. The Li^+ ion, in particular, structures water strongly and it would be of interest to study its effect on the double layer.

More important effects in practical coagulation are observed with ions which hydrolyse. The species and relevant stability constants can be pursued[19].

Of particular importance are the metal cations in solution and especially the species associated with aluminium, iron, silicon, magnesium and calcium. Of these, aluminium, iron and silicon hydrolyse the most readily (see *Table 4.3*), i.e. they give hydrolysis species even in acid media. Taking aluminium as an example, a variety of species have been proposed ranging from hydrated Al^{3+} ions through $(Al_8(OH)_{20})^{4+}$, $(Al_6(OH)_{15})^{3+}$, $(Al(OH)_2)^+$ to $(Al(OH)_4)^-$ and the insoluble hydrated oxide $Al_2O_3\,nH_2O$; the amounts of these species are

Table 4.3 First hydrolysis constants for metals, and the pH at which precipitation occurs with approximately 0.02 mol dm^{-3} concentration of metal[19]

Ion	$-\log_{10} K_n^*$	*pH for precipitation*
Fe^{3+}	2.22	2.0
Ce^{4+}	~0.7	2.7
Cu^{2+}	7.5	5.3
Cr^{3+}	3.82	5.3
Fe^{2+}	9.5	5.5
Co^{2+}	9.6	6.8
Mg^{2+}	11.4	10.5

$^*K_n$ refers to the first hydrolysis step of the type $M^{n+} + H_2O \rightleftharpoons MOH^{(n-1)+} + H^+$.

dependent on pH and on the total aluminium concentration. Hall[20] treats the variation of ζ potential with pH in the system water/kaolinite dispersions to which aluminium has been added. The situation is complex but the kaolinite appears to form a layer of amorphous hydroxide on the surface even under conditions where coagulation is not possible, e.g. at pH less than 6–5. At higher pH values the amorphous oxide precipitates in the bulk of the solution and then the ζ potential of the aluminium hydroxide is a function of a polynuclear ion, e.g. $Al_6(OH)_{15}^{3+}$. The ζ potential is now at a maximum positive value and yet coagulation is efficient.

The relative ease of hydrolysis of certain metal species in increasingly acid media can be observed from a listing of the point of charge (p.z.c.) given by Gregory[10] for a series of hydrous oxides—oxide and p.z.c.—$SiO_2(2), TiO_2(6), Fe_2O_3(8.5), Al_2O_3(9), MgO(12)$. The p.z.c. is the characteristic pH value at which the oxide surface has no net charge, and it results from a series of reactions between the surface and the hydroxyl and hydrogen ions in solution, as illustrated in *Figure 4.9*.

Another measure of the above effect is the well-known phenomenon that Fe^{3+} in solution begins to precipitate hydrated ferric oxides at fairly low pH, e.g. typically at a pH of 1.8.

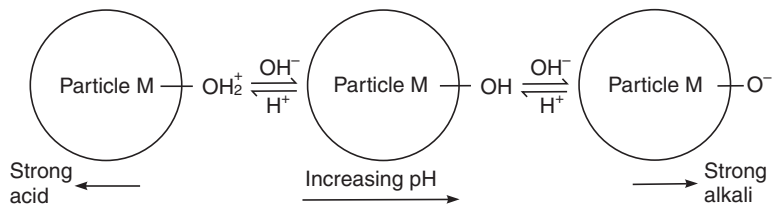

Figure 4.9 The changing character of the hydrous oxide surface as the bulk phase pH is altered

Consequently, there must be a mechanism other than the effect of double layer compression whereby these hydrous oxides ($Al_2O_3nH_2O$, $Fe_2O_3nH_2O$ etc.) aid the growth of aggregates. The hydrous oxides proceed to gather aggregates, trapping aggregate particles in a network of hydrous oxide polymers. Riddick[14] considers that this progress is very fast involving times of up to a few seconds. Eventually this 'floc gathering' process, which can be aided by natural silica or added silica and by polyelectrolytes (see section 4.5) leads to efficient flocculation; the total process takes up to 15–30 minutes after application of the initial aluminium ion dose.

From the above, it is clear that the ageing of these flocs is important; a certain period is needed in a process for optimum floc size to be reached, thus leading to an easily separated solid. Further ageing may or may not have an adverse effect. In the latter case the floc becomes destabilized and might lead to some redispersion. Obviously care must be taken when flocs are separated out and then further treated; for example, a precipitate might be 'washed' in some instances and this may lead to alteration of the floc characteristics and some redispersion.

The chemistry of the aqueous phase and all the complexes which are possible is too detailed to be covered here and the reader should refer to standard texts on this subject.

4.4.2 Flotation

There is also a close relationship between the zeta potential and the efficient flotation of solids by purposely designed organic molecules which carry either positive or negative charge. The reader is referred to the work of Aplan and de Bruyn[21]. In general, anionic collectors are effective on positive surfaces and cationic collectors react with negative surfaces. If the material to be collected already has a charge close to zero then no collector is likely to be effective. Many applications exist in the minerals treatment industries.

4.5 Flocculation by polyelectrolytes

The term 'flocculation' may be taken to cover those processes whereby small particles or small groups of particles form large aggregates. In the water industry the term is especially reserved for the formation of large flocs when the dispersion is stirred and aged in holding tanks. The term is also used for the dramatic effect when polyelectrolytes are added and a large stable floc is formed very quickly. 'Perikinetic flocculation' is a term reserved for floc formation brought about by Brownian motion alone whilst 'orthokinetic flocculation' is used to describe flocculation achieved by imparting velocity gradients to the dispersion through stirring. Orthokinetic flocculation is described in Part II by Ives. Perikinetic flocculation is touched upon in section 4.2.4.

One of the greatest advances in solid–liquid separation has been the development of polymers with remarkable abilities to flocculate sols when added in only trace quantities. Indeed, these polyelectrolytes may be used to supplement or replace the primary coagulants previously mentioned. Although they are considerably more expensive than primary coagulants the dose rate is much lower, typically 0.1–0.15 mg dm^{-3} of substrate to be treated. Already widely used in the mining industries, polyelectrolytes are now being considered for solid–liquid treatment applied to sewage.

4.5.1 The chemical nature of synthetic polyelectrolytes

The types of synthetic polymer which are considered useful are summarized in *Table 4.4*. It is observed that they fall into three main classes, non-ionic, anionic and cationic. Obviously the anionic/cationic character can be altered

Table 4.4 Monomers and polyelectroytes

MONOMERS

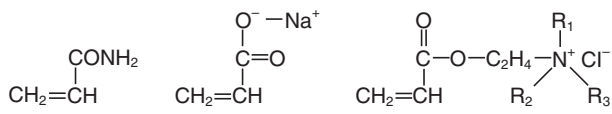

Acrylamide | Sodium acrylate | Polyquaternaryester

POLYMERS

Nonionic	Polyacrylamides	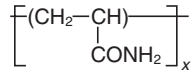
	Polyethylenoxide	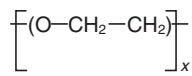
Aninonic	Acrylamide co-polymer	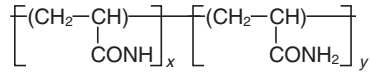
	Polyacrylics	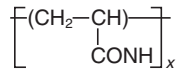
Cationics	Polyamines	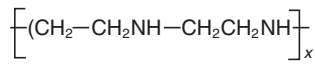
	Acrylamide co-polymers	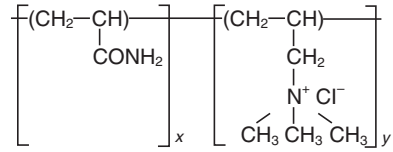
		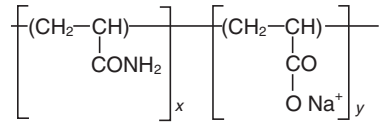

at will by co-polymerization of the various monomers and any one product is then characterized by

1 its average molecular weight and
2 the charge density distribution within the polymer molecule.

Molecular weights can be classified according to high $\simeq 20 \times 10^6$, medium $\simeq 10 \times 10^6$, low $\simeq 5 \times 10^6$ and very low $< 1 \times 10^6$. A detailed description of the chemistry of polyelectrolytes has been given by Schwoyer[22].

4.5.2 Mode of action and application

The mechanism of flocculation by polyelectrolytes is considered to involve the two processes of surface charge neutralization and bridging. If the first mechanism is to be effective then one must take care to choose a polyelectrolyte whose charge is of the opposite sign to the charge on the particles. The charge density on the polymer will be an important measure of its capacity to flocculate. The process of charge neutralization and bridging then proceeds as shown in *Figure 4.10*.

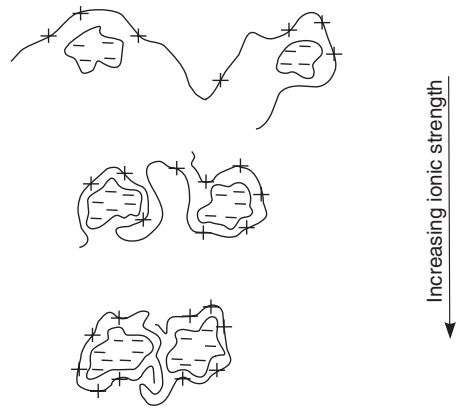

Figure 4.10 Flocculation by charge neutralization and bridging. (A cationic polymer is used to collect particles with a net negative charge)

The correct choice of polyelectrolyte is best made after laboratory trials on samples of the liquor to be clarified. Usually, for a given charge density, the polymer with highest molecular weight will give the fastest sedimentation rate. It will always be necessary to determine the optimum dosage for the best results, especially where an expensive chemical is in use.

Efficient use of the expensive agent is assured if a proper dosing system is adopted. The polymers are supplied either as solids or liquids and obviously, for efficient dosing at such low levels, the solid products must be taken up into some liquid to give a concentrate feed for the dosing plant. The Dow Chemical

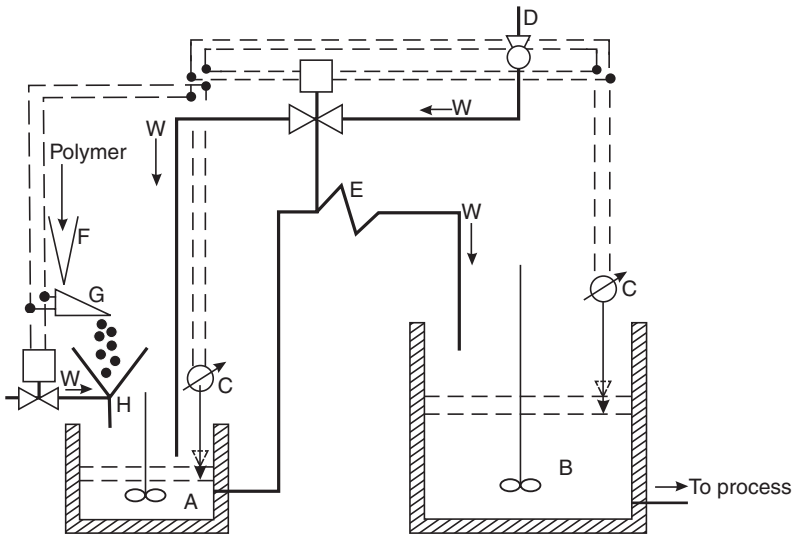

Figure 4.11 Schematic layout of a dilution system for a solid polyelectrolyte polymer. The polymer in hopper F is fed to a vibrator G which discharges into a dispenser H fed with water W. Tank A, (volume 1–2 m^3) provides the first mixing and the product is fed through the mixing device E (fed with water from pump D) into tank B where the final mixing takes place. The solution is now fed to the process line. Automatic level controls are provided at C and are connected to valves and pumps as shown

Company[23] have given diagrams of typical automatic dosing systems, where the polymer is a solid, and one such system is reproduced in *Figure 4.11*. Further useful practical points concerning efficient polyelectrolyte usage are listed:

1 add the polyelectrolyte to the main stream in a very dilute solution (< 0.1 %);
2 add as near as possible to the point where flocculation is required;
3 add at points of local turbulence;
4 add in stages at different points;
5 add across the whole of the stream to be treated;
6 avoid turbulence subsequent to floc formation;
7 at high solids concentrations, add recycled or other dilution water to the system;
8 at low solids concentrations, recycle settled solids into the stream.

It will be gathered from the above that subsequent treatment of the flocs may lead to break up, indeed it is best to regard the flocculation of hydrophilic sols as reversible. Different techniques used for the physical separation of the flocs from the suspension liquid have shown that if belt presses are used then fragile flocs should be treated carefully, with the pressure being applied only gradually; even filter presses have provided problems in the past. Centrifu-

ging would require a strong floc; high molecular weight polyelectrolytes are useful here, otherwise it is usual to employ polyelectrolytes of medium to low molecular weights but with high charge density.

4.5.3 Some examples of polyelectrolytes in action

The most important class of polymers are those anionic polyelectrolytes containing carboxyl groups. High molecular weight anionics (> 1 000 000), with low charge density, have many uses as flocculants for water and waste water.

Those cationic polymers in use for water treatment are nearly all based upon quaternized aminoesters or amino amides. Few non-ionic polyelectrolytes are used in water treatment and true non-ionic types are difficult to prepare. Polyacrylamides containing less than 1% hydrolysable groups are available. High molecular weight poly(ethyleneoxides) are used in flotation processes.

In recent years, work has been carried out on combinations of flocculants with other chemicals to achieve highly efficient solid/water separation.

Field[24] showed that a combined anionic flocculant/cationic coagulent system, at constant coagulent dose, performs better on coal-tailings than when flocculant alone is used. In general, it is the type of solid–liquid processes in use which dictate the *molecular weight* of the chosen electrolyte—see *Table 4.5*. On the other hand, the *chemical type* necessary generally depends on the slurry characteristics, i.e. solid chemical surface type, particle size distribution, the dissolved electrolytes and the pH.

Table 4.5 Choice of molecular weight for different processing techniques

Process type	*Molecular weight range*
Sedimentation and centrifugation	High (in conjunction with highly cationic electrolyte for overflow clarity)
Vacuum filtration	Medium to high
Pressure filtration	Low to medium
Pressure belt filtration	Medium to high (in conjunction with low molecular weight, high cationic electrolyte)
Low solids clarification	Very low to high

Some of the major applications of polyelectrolytes are given in *Table 4.6*.

4.6 Other considerations

It cannot be claimed that this chapter is an exhaustive coverage of all those chemicals which are used to improve solid–liquid separations. For example, the potato starch which is commercially available has found wide use. This naturally occurring polymer with a molecular weight of about 1 000 000 is

Table 4.6 Polyelectrolyte use in solid–liquid separation

Substrate to be treated	*Class of electrolyte*	*Typical dosage, per tonne of dry solids*
Water (potable)	High molecular weight polyacrylamides of low toxicity with usage of non-ionic, cationic, anionic	Must not exceed 0.5 ppm w/v
	Modified starches (organic coagulents may be used in conjunction)	Average 0.1 ppm w/v
Effluents		1–10 kg
Textiles	Low molecular weight, highly cationic—followed by anionic	
Sewage sludge	High molecular weight polyacrylamides	1–4 kg
Paper pulp	High molecular weight cationic or anionic polyacrylamides for retention and drainage of paper stock	
	Dual component systems exist involving low molecular weight cationic first then high molecular weight anionic polyacrylamides to badge the floc	Up to 9.5 kg
	The new Hydrcol® system involves first the addition of cationic polyacrylamides then a modified bentonite to produce 'super coagulation'	
Mineral slurries		0.03 kg
Iron ore tailings	Medium molecular weight anionic polyacrylamide plus highly cationic coagulent	
Clayey coal tailings	Medium molecular weight anionic polyacrylamide plus highly cationic coagulent	0.03–0.05 kg
Acid leach liquors (Cu, U, Zn, Au, etc.)	Non-ionic or slightly anionic/cationic polyacrylamides also sulphonic acid polymers	0.03–0.15 kg
Alkali leach liquors (U, Bayer Process Al)	Highly anionic polyacrylamide	0.03–0.175 kg
Mine 'run-off' water, low solids	Highly cationic polyamine or anionic polyacrylamides plus highly cationic coagulents	1 ppm w/v
Coal slurries		
Frothed slimes	Medium to high anionic polyacrylamides	0.03–0.05 kg
Coal tailings	Low to medium/high anionic polyacrylamides	0.04–0.06 kg

Hydrocol® is a registered trademark of Allied Colloids Limited, Bradford.

made up of glucose units and operates in its neutral form through hydrogen bonding, and by suitable chemical pretreatment, starches bearing positive or negative charges can be made.

Other important water soluble polymers (biopolymers) include a variety of naturally occurring gums, e.g. Guar, Acacia (Gum Arabic), Tragacanth, Xanthan, etc. Guar gum, in particular, has found use as a food thickener as well as a flocculating agent in the minerals industry; it also has important industrial properties as an agent for friction reduction.

Flocculating agents may also be used in a selective manner to recover one solid which is in suspension with another unwanted material. In one sense this is like the selective flotation practised in the mining industry and has great potential where there is now a continuing interest in the recycling of valuable materials from waste.

Finally, a comment must be made on the toxicity of the substances used for chemical pretreatment in solid–liquid separation. Some polyelectrolyte products may contain monomers as impurities and Croll *et al.*[25] have reported residues of acrylamide in water. Acrylamide has a high chronic toxicity, being a neurotoxin, and accumulation of the monomer in treated drinking water is guarded against. Primary coagulants in the form of inorganic salts are less toxic but nevertheless certain countries have standards for the final effluent from a mining complex which must not be exceeded. Hawley[26] reports Canadian regulations for aluminium sulphate, ferric sulphate and ferric chloride.

References

1. Alexander, A. E. and Johnson, P., *Colloid Science*, p. 129, University Press, Oxford (1950)
2. Verwey, E. J. W. and Overbeck, J. Th. G., *Theory of the Stability of Lyophobic Colloids*, Elsevier, New York (1948)
3. Osipow, L. I., *Surface Chemistry*, Reinhold, New York (1963)
4. Chapman, D. D., *Phil. Mag.*, **11**, 425 (1906)
5. Gouy, G., *J. Physique*, **9**, 457 (1910)
6. Gouy, G., *Annls Phys.*, **7**, 129 (1917)
7. Stern, O., Z. *Elektrochem.*, **30**, 508 (1924)
8. von Smoluchowski, M. *Phys. Z.*, **17**, 557, 585 (1916)
9. von Smoluchowski, M., *Phys. Chem.*, **92**, 129 (1917)
10. Gregory, J., *Effluent and Water Treatment Journal*, **516**, (1977)
11. Szwarestajn, E. and Jain, S. C., *Indian Pulp and Paper*, **27**, 3 (1973)
12. Kryut, H. R., *Colloid Science*, Vol. 1, Elsevier, New York (1952)
13. Calver, J. V. M., *The Research Association for the Paper and Board, Printing and Packaging Industries, Bibliography No. 727* (1974)
14. Riddick, T. M., *Effluent and Water Treatment Journal*, **563**, (1964)
15. La Mer, V. K., *J. Colloid Science*, **19**, 291 (1964)
16. Schulze, H., *J. Prackt. Chem.*, **25**, 431 (1882)

17. Schulze, H., *J. Prakt. Chem.*, **27**, 320 (1883)
18. Freundlich, H., *Colloid and Capillary Chemistry*, Methuen (1926)
19. *Stability Constants Handbook,* Parts I and II, Publ. Chem. Soc., London (1957)
20. Hall, E. S., *J. Appl. Chem.*, **197**, (1965)
21. Fuerstenau, D. W. (Ed.), *Froth Flotation*, Vol. 170, p. 91, AIMM and Pet. Eng., New York (1962)
22. Schwoyer, W. L. K. (Ed.), *Polyelectrolytes for Water and Waste Water Treatment*, CRC Press, Boca Raton, FL (1981)
23. *Handbook on Separan*, Dow Chemical Co., Horgen, Switzerland (1976)
24. Field, R. J., *Coal Preparation*, **4**, 79 (1987)
25. Croll, B. T., Arkell, G. M. and Hodge, R. P. J., *Water Research*, **8**, 989 (1974)
26. Hawley, J. R., *The Use, Characteristics and Toxicity of Mine-Mill Reagents in the Province of Ontario*, Ministry of the Environment, Ontario, Canada (1972)

Bibliography

Akers, R. J., *Flocculation and Coagulation*, Chapman & Hall, London, ISBN: 0 41215 160 X (1999)

Bikales, N. M. (Ed.), *Water-soluble polymers. Polymer Science and Technology*, Vol. 2, Plenum Press, New York (1973)

Blaser, S. 'Break-up of flocs in contraction and swirling flows', *Colloid and Surfaces, A: Physiochem. and Eng. Asp*., **Vol. 166**, No. 1–3 (2000)

Dobias, B. (Ed.), *Coagulation and Flocculation*, Marcel Dekker, New York, ISBN: 0 82478 797 8 (1993)

Dongsheng, W., 'Particle speciation analysis of inorganic polymer flocculants: An examination by photon correlation spectroscopy', *Colloid and Surfaces, A: Physiochem. and Eng. Asp*., **Vol. 166**, No. 1–3 (2000)

Fan, A. and Somasundaran, P., 'A study of dual polymer flocculation', *Colloid and Surfaces, A: Physiochem. and Eng. Asp*., **Vol. 162**, No. 1–3 (January 2000)

Finch, C. A. (Ed.), *The Chemistry and Technology of Water Soluble Polymers*, Plenum Press, New York (1983)

Karmakar, N. C., Sastry, B. S. and Singh, R. P., 'Flocculation and settling characteristics of copper ore fines suspension from a concentration plant', *CIM Bulletin*, **Vol. 92**, No. 1035 (October 1999)

Larsson, A., 'Flocculation of cationic polymers and nanosized particles', *Colloid and Surfaces, A: Physiochem. and Eng. Asp*., **Vol. 159**, No. 1 (November 1999)

Lee., S. J., Chu, C. P. and Lee, D. J., 'Effects of polyelectrolyte flocculation on filter cake characteristics', Proceedings Volume II, World Filtration Congress 8, European Federation of Chemical Engineering Event No. 607, organised by The Filtration Society and Elsevier Science, The Brighton Centre, Brighton, UK, 3–7 April 2000, 1236–1239 (2000)

Manttari, M. and Nystrom, M., 'Influence of flocculants on the performance of a ceramic capillary filter', *Filtration & Separation*, January, 75–80 (1996)

Molyneux, P., *Water-soluble Polymers: Properties and Behaviour*, Vol. 1, CRC Press, Boca Raton, FL (1985)

Moody, G. M., 'Pre-treatment chemicals', *Filtration & Separation*, April, 329–336 (1995)

Rachas, I. and Taylor, P., 'The displacement of adsorbed polymer from silica surfaces by the addition of a nonionic surfactant', *Colloid and Surfaces, A: Physiochem. and Eng. Asp*., **Vol. 161**, No. 2 (December 1999)

Russel, W., 'Distinguishing between dynamic yielding and wall slip in a weakly flocculated colloidal dispersion', *Colloid and Surfaces, A: Physiochem. and Eng. Asp*., **Vol. 161**, No. 2 (December 1999)

Seppanen, R., 'Heteroflocculation of kaolin pre-treated with oppositely charged polyelectrolytes', *Colloid and Surfaces, A: Physiochem. and Eng. Asp*., **Vol. 164**, No. 2–3 (December 2000)

Tao, D., Groppo, J. G. and Parekh, B. K., 'Enhanced ultrafine coal dewatering using flocculation filtration processes', *Minerals Engineering*, **Vol. 13**, No. 2 (February 2000)

Weir, S. and Moody, G. M., 'Trends in the development of flocculants as aids to solid/liquid separation', Proceedings Volume II, World Filtration Congress 8, European Federation of Chemical Engineering Event No. 607, organised by The Filtration Society and Elsevier Science, The Brighton Centre, Brighton, UK, 3–7 April 2000, 1223–1226 (2000)

Coagulation and flocculation Part II—Orthokinetic flocculation

K. J. Ives

Professor of Public Health Engineering, University College London

Nomenclature

A	Area perpendicular to flow	m^2
A_p	Projected area of stirrer blade normal to motion	m^2
C	Floc volume concentration	—
C_D	Drag coefficient	—
C_s	Suspended solids concentration	$g\ m^{-3}$
c	Chezy coefficient	$m^{\frac{1}{2}}\ s^{-1}$
D	Grain or bubble diameter	m
d	Tube diameter	m
F	Filtrability number	—
f	Pipe friction factor	—
G	Mean velocity gradient	s^{-1}
H	Head loss	m
H_B	Baffle head loss	m
H_f	Friction head loss	m
h	Distance of sampling point below water level	m
i, j, k	Labels for i-, j- and k-particles, respectively	—
k_B	Boltzmann's constant	$J\ K^{-1}$
L	Length	m
N_i, N_j	Number concentration of i- and j-particles, respectively	m^{-3}
N_o, N_t	Number concentration of original and time t particles, respectively	m^{-3}
P	Power dissipated in fluid motion	W
p	Upper limit aggregate size label	—
Q	Volumetric flow rate of liquid	$m^3\ s^{-1}$
q	Sludge bleed flow	$m^3\ s^{-1}$
R	Hydraulic radius	m
r_i, r_j	Radius of i- and j-particles, respectively	m
T	Kelvin temperature	K
T_q	Torque	Nm
t	Time	s

u	Velocity of liquid motion in the x-direction	$m\,s^{-1}$
V	Volume of liquid	m^3
V_a	Volume of air	m^3
v	Velocity of liquid being stirred, or flowing in flocculator	$m\,s^{-1}$
v_a	Apparent velocity of setting of particles	$m\,s^{-1}$
v_h	Hindered velocity of settling of particles	$m\,s^{-1}$
v_p	Velocity of stirrer blade	$m\,s^{-1}$
v_s	Settling velocity of single particle	$m\,s^{-1}$
x	Dimension in the directon of liquid motion	m
z	Dimension across the velocity gradient	m
β	Collision efficiency factor	—
Δp	Pressure drop	Nm^{-2}
ε	Porosity of granular media	—
μ	Dynamic viscosity of liquid	$kg\,m^{-1}s^{-1}$
ρ	Density of liquid	$kg\,m^{-3}$
ρ_s	Density of particle, or floc	$kg\,m^{-3}$
ω	Angular velocity	$rad\,s^{-1}$

4.7 Introduction

It is commonly observed that gentle stirring promotes flocculation of particles which have been destablized and which may have commenced to aggregate by Brownian motion (see Part I of this chapter). This is due to the velocity gradients which are induced in the liquid causing relative motion and therefore collisions between the particles which are present. Such flocculation caused by fluid motion is called 'orthokinetic', to differentiate it from that caused by Brownian motion, called 'perikinetic'.

A simple theory of flocculation kinetics can be derived for a constant velocity gradient (i.e. a uniform shear field, as for a Newtonian fluid shear stress, is proportional to velocity gradient). Such constant velocity gradients are difficult to achieve in practice, as they require parallel flat plates separated by a small gap moving at constant relative velocity. The closest experimental form has been in the annular gap between coaxian rotating cylinders (Couette apparatuses)[1,2]. Consequently, the theory has been extended to velocity gradients created in turbulent flow conditions, such as paddle stirrers, baffled channels, oscillating paddles, fluidized beds etc.

4.8 Theory

4.8.1 Constant velocity gradient (uniform shear field)

As relative motion is the cause of particle collisions, it is useful to treat one particle (j) as a collector, being stationary in a constant velocity gradient

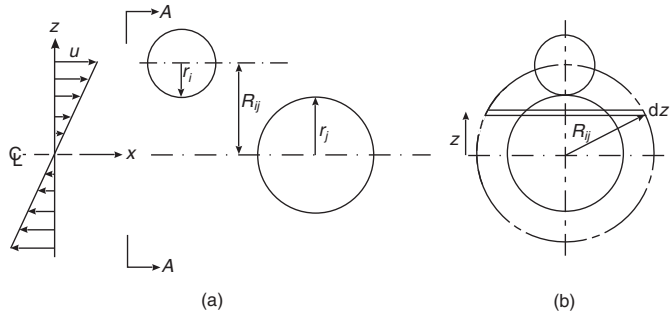

Figure 4.12 Definition sketch for orthokinetic flocculation. (a) Uniform shear field. (b) End view A-A

du/dz (*Figure 4.12*). The liquid contains other particles (i), which will move relative to j if they are not on the centre line through j.

It is assumed that the uniform shear field is unperturbed by the presence of the particles and therefore the path of the i-particles is rectilinear. Although Arp and Mason[3] have shown that the curvature of the stream lines around the particles may appear to have a small effect, van de Ven and Mason[4] have shown that rolling of particles around one another does significantly reduce the collection efficiency of collisions. However, as a simplification each collision is assumed to result in an effective collection, i.e. flocculation with no electrical or hydrodynamic barriers. This simplification can be later adjusted by a collision efficiency factor $\beta \leq 1.0$ to take into account a proportion of ineffective collisions.

With reference to *Figure 4.12*, i-particles above the centre line (positive z) move in the direction x. If their centres lie within the hemi-cylinder radius R_{ij} $(= r_j + r_j)$, they will collide with the j-particle. Their velocities relative to the j-particle will depend on their distance z from the x-plane, and will equal $z(\mathrm{d}u/\mathrm{d}z)$.

The liquid flowing through the upper hemi-cylinder, relative to the j-particle, is the sum of all flow through the elements of height $\mathrm{d}z$.

$$\text{Element flow} = \text{area} \times \text{velocity}$$

$$\mathrm{d}Q = 2\left[\sqrt{\left(R_{ij}^2 - z^2\right)}\right] \mathrm{d}z z(\mathrm{d}u/\mathrm{d}z) \tag{4.37}$$

Total flow in the upper hemi-cylinder relative to j

$$Q_{\frac{1}{2}} = 2(\mathrm{d}u/\mathrm{d}z) \int_0^{R_{ij}} z\left[\sqrt{\left(R_{ij}^2 - z^2\right)}\right] \mathrm{d}z \tag{4.38}$$

There is an identical flow through the lower hemi-cylinder in the negative x-direction, so the total liquid flow relative to j is:

$$Q = 4(\mathrm{d}u/\mathrm{d}z) \int_0^{R_{ij}} z\left[\sqrt{\left(R_{ij}^2 - z^2\right)}\right] \mathrm{d}z \tag{4.39}$$

which, integrated, becomes:

$$Q = \frac{4}{3}(\mathrm{d}u/\mathrm{d}z)R_{ij}^3 \tag{4.40}$$

Q is the volumetric flow rate $\mathrm{d}V/\mathrm{d}t$, so for N_i particles per unit volume, the rate of collision of i-particles with the j-particle is:

$$N_i(\mathrm{d}V/\mathrm{d}t) = \frac{4}{3}N_i(\mathrm{d}u/\mathrm{d}z)R_{ij}^3 \tag{4.41}$$

If there are N_j j-particles per unit volume, then the total collision rate is:

$$\mathrm{d}N_{ij}/\mathrm{d}t = N_iN_j(\mathrm{d}V/\mathrm{d}t) = \frac{4}{3}N_iN_j(\mathrm{d}u/\mathrm{d}z)R_{ij}^3 \tag{4.42}$$

This is the simple Smoluchowski equation of orthokinetic flocculation, and shows that the rate of flocculation is second-order with respect to concentration, depends linearly on the velocity gradient and is proportional to the third power of the collision radius. Consequently, in these simple terms theory states that the rate of flocculation can be increased by:

1 increasing the collision radius of the particles; thus flocculation is self-enhancing as larger flocs are produced, also the presence of existing large particles, such as occurs in solids-contact flocculation, or floc-blanket clarifiers, will improve flocculation;
2 increasing the concentrations of particles present; thus flocculation is self-diminishing as particle numbers decrease due to aggregation; however, the provision of many new particles by precipitation from alum hydrolysis, for example, is advantageous; also the maintenance of a large number of flocs always to be present, as in solids-contact or floc-blankets is advantageous;
3 increasing the velocity gradient; however, there is a limit to the shear stress which flocs can withstand, so excessive gradients may cause floc break-up, particularly as the flocs grow in size; this can be overcome by decreasing the velocity gradient from an initially high value, when flocs are small, to lower values as the flocs grow: this is taper flocculation.

It must be stressed that equation 4.42 is a very simple form, because the aggregation of an i-particle with a j-particle creates a new particle (k), and the i- and j-particles disappear after aggregation. The new k-particle can itself interact with other i-, j- and k-particles, with appropriate concentrations and collision radii. The rate of change of aggregates of type $k(=i+j)$ is given by a two-term equation consisting of their appearance due to i+j collisions, and their disappearance due to collisions with other particles,

$$\mathrm{d}N_k/\mathrm{d}t = \frac{1}{2}\sum_{\substack{i=1\\ j=k-i}}^{i=k-1}\frac{4}{3}N_iN_j(\mathrm{d}u/\mathrm{d}z)R_{ij}^3 - N_k\sum_{i=1}^{\infty}\frac{4}{3}N_i(\mathrm{d}u/\mathrm{d}z)R_{ik}^3 \tag{4.43}$$

The derivation of equation 4.43 is given in Ives[5]. It can be seen that it sums all the possible collisions from the original ($i = 1$) particles up to an aggregate of infinite size. This upper limit is obviously impossible as it assumes an infinite supply of 1-particles, but more importantly it ignores the limit on floc size imposed by the disintegration of large flocs as a result of the shear stress provided by the velocity gradient. Therefore, equation 4.43 can be elaborated further with an upper limit aggregate size (p); it can also be written to replace the collision radii R_{ij} and R_{ik} by terms which include the radius of the original particles r_1 and the particle labels i, j and k.

Some simplifications are possible if the initial suspension is monodisperse at $t = 0$. Then $k = 1, N_k = N_o$ (original number concentration), and the initial rate of disappearance of 1-particles is:

$$-\mathrm{d}N_1/\mathrm{d}t = \frac{16}{3}(\mathrm{d}u/\mathrm{d}z)r_1^3 N_o^2 \tag{4.44}$$

At time t,

$$\sum_{k=1}^{p} N_k = N_t \quad \begin{matrix}\text{(the total number concentration} \\ \text{of all particles and aggregates)}\end{matrix}$$

$$-\mathrm{d}N_t/\mathrm{d}t = \frac{16}{3}(\mathrm{d}u/\mathrm{d}z)r_1^3 \sum_{k=1}^{p} N_k^2 k \tag{4.45}$$

If the rate of flocculation is slowed by an energy barrier (see chapter 4, Part I), or hydrodynamic effects between approaching particles, then the right-hand side of equation 4.45 is multiplied by a collision efficiency $\beta(\leq 1.0)$.

A fuller theoretical discussion of the orthokinetic flocculation rate equations is given in Ives[5]. Experimental tests of the kinetics of orthokinetic flocculation are described by Ives and Bhole[6,7] and Ives and Al Dibouni[2].

4.8.2 Variable velocity gradient (non-uniform shear field)

In most practical cases, the flow in flocculators is turbulent, fluctuating rapidly in both position and time. Where the flow may be laminar in tube flocculators or lamella separators or deep bed filters, the velocity gradients are not uniform but parabolic or quasi-parabolic in form.

The velocity gradient ($\mathrm{d}u/\mathrm{d}z$) is represented by an average value G, based on the power dissipated per unit liquid volume (P/V) by the non-uniform shear flow. Assuming that the liquid is Newtonian, the mean velocity gradient is given by:

$$G = \sqrt{\left(\frac{P}{V\mu}\right)} \tag{4.46}$$

where μ is the dynamic viscosity.

The derivation of equation (4.46) is based on the shear force on an element cube of liquid, causing torsional work which is evaluated as work/time = power. Consequently, the value of G assumes that all elemental cubes of liquid in the volume V are being sheared at the same rate (on average) and that G is also a time-averaged value[5].

The power P can be calculated in terms of the head lost in flow through a pipe, a tube module flocculator, lamella separators or fixed (deep bed) or fluidized bed flocculators, whether in laminar or turbulent flow. It can also be estimated for paddle flocculators and stirred beakers (jar test apparatus) on the basis of paddle drag, or torque on the drive shaft. Such practical cases are dealt with in section 4.10.

4.8.3 Transition from perikinetic to orthokinetic flocculation

The simple orthokinetic rate equation 4.42 has an analogous equation for perikinetic flocculation, due to Brownian-motion collisions of particles (see Part I of this chapter, which deduces the half life of particles from such flocculation). The perikinetic rate equation is:

$$^{\mathrm{p}}\left(\frac{\mathrm{d}N_{ij}}{\mathrm{d}t}\right) = 4\pi N_i N_j D_{ij} R_{ij} \tag{4.47}$$

where D_{ij} is the sum of the Stokes–Einstein diffusion coefficients for the i- and j-particles.

$$D_{ij} = \frac{2k_{\mathrm{B}}T}{3\pi\mu R_{ij}} \tag{4.48}$$

where

k_{B} is Boltzmann's constant (1.38×10^{-23} J K^{-1})
T is Kelvin temperature (K = °C + 273)
μ is dynamic viscosity of the liquid.

Combining equations 4.47 and 4.48:

$$^{\mathrm{p}}\left(\frac{\mathrm{d}N_{ij}}{\mathrm{d}t}\right) = \frac{8N_i N_j k_{\mathrm{B}}T}{3\mu} \tag{4.49}$$

The orthokinetic rate equation 4.42 is:

$$^{\mathrm{o}}\left(\frac{\mathrm{d}N_{ij}}{\mathrm{d}t}\right) = \frac{4N_i N_j G R_{ij}^3}{3} \tag{4.42}^*$$

$$\frac{^{\mathrm{o}}(\mathrm{d}N_{ij}/\mathrm{d}t)}{^{\mathrm{p}}(\mathrm{d}N_{ij}/\mathrm{d}t)} = \frac{\mu G R_{ij}^3}{2k_{\mathrm{B}}T} \tag{4.50}$$

Initially for a monodisperse suspension $i = j = 1$ and

$$R_{ij} = 2r_1$$

When the orthokinetic rate equals the perikinetic rate, their ratio is one:

$$r_1 = \left(\frac{k_B T}{4G\mu}\right)^{\frac{1}{3}} \tag{4.51}$$

At $25\,^{\circ}C, T = 298\text{K}$, $\mu = 0.895 \times 10^{-3}\text{kg m}^{-1}\,\text{s}^{-1}$

$$\left(\frac{k_B T}{4\mu}\right)^{\frac{1}{3}} = 1.05 \times 10^{-6}\text{m s}^{-\frac{1}{3}}$$

$$r_1 = 1.05 \times 10^{-6} G^{-\frac{1}{3}}\,\text{m}$$

$$= 1.05 G^{-\frac{1}{3}}\,\mu\text{m} \tag{4.52}$$

Equation 4.52 can be used to calculate the collision radii of particles when perikinetic and orthokinetic rates of flocculation are equal, and flocculation is in transition from Brownian-motion (diffusion) dominated kinetics to fluid-motion kinetics. For example:

G	s^{-1}	1	10	20	50	100
r_1	μm	1.05	0.5	0.4	0.3	0.23

So for most cases of fluid motion caused by stirring or baffled flow the perikinetic rate dominates for particles less than 1 μm diameter, and the orthokinetic rate dominates for particles larger than 1 μm. For example, at $G = 10\,\text{s}^{-1}$ when the particle radius has increased to 5 μm (diameter 10 μm) orthokinetic flocculation will proceed 1000 times faster than perikinetic (equation 4.50).

Even when the particles are completely destabilized, with no repulsion energy barrier, there is evidence[4] that orthokinetic collisions will be reduced by particles rolling around one another without aggregating. This will multiply the orthokinetic rate (equation 4.42) by a factor of less than one, which will make the sizes of particles undergoing equal effective rates of perikinetic and orthokinetic flocculation smaller than those listed above (which assumed that all collisions were permanent and effective).

4.8.4 Taper flocculation

As mentioned in section 4.8.1, the magnitude of the velocity gradient G is limited by the possibility of large flocs being broken by the shear stress. Both the nature of the material constituting the flocs and the conditions under which they were formed affect their shear strength. For example, flocs formed with polymers are usually stronger; those with hydroxide flocs are usually weak; flocs formed rapidly in intense velocity gradients are

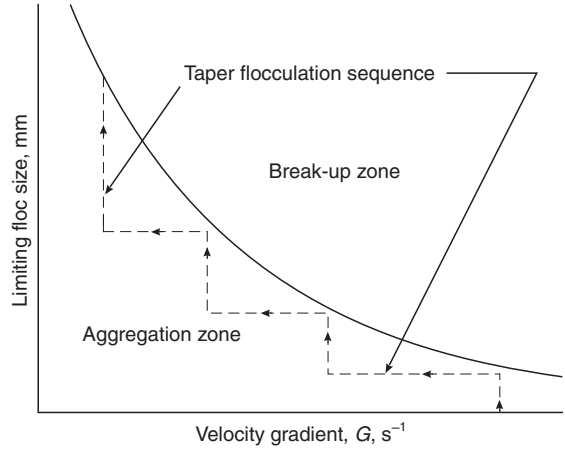

Figure 4.13 Aggregation/break-up diagram

usually more compact and, therefore, stronger than those formed in lower velocity gradients. As flocs become larger, they tend to become less dense and more susceptible to shear. Although studies have been made of floc break-up, no formal quantitative relationships are available because some flocs are broken by attrition of small particles and aggregates from their surfaces while others are sheared into two or more fragments of about equal sizes.

For aluminium or ferric hydroxide flocs, as formed in water treatment by paddle flocculators, the relationship illustrated schematically in *Figure 4.13* indicates the zones of aggregation and break-up. To maximize the rate of flocculation without break-up as the flocs grow in size, a flocculation scheme could follow the broken line in *Figure 4.13*. That starts at a high value of G when flocs are small; as they grow, they approach the break-up zone and G is therefore reduced allowing further growth in the aggregation zone. This progressive reduction in G to keep the flocculation rate as high as possible, but below the break-up zone, is called 'taper flocculation'. It is usually achieved in practice by passing the flocculating suspension through a series of rotating paddles, which are sequentially rotating more and more slowly, until the flocculated suspension containing large flocs passes into a settling chamber. Care has to be taken in transferring flocs from paddle to paddle and chamber to chamber as weirs, orifices etc. may produce local velocity gradients which would cause the flocs to break up.

4.8.5 Optimum flocculation conditions

The best flocculation conditions are those which rapidly form large separable flocs, leaving no residual primary particles or small aggregates. However, it

has already been shown that high rates of flocculation cannot be utilized if the velocity gradients are too high, thus causing floc break-up. So a balance has to be achieved between the velocity gradient G and the time of flocculation t, one compensating for the other.

In flow-through flocculation units (particularly paddle stirrers in series) where the concentration of suspended particles is low (typically 1000 p.p.m. v/v $= 10^{-3}$) the flocculation is characterized by the dimensionless product Gt (sometimes called the Camp number). Arising from observational data from waterworks in the USA, the optimum value of Gt is set between the limits 10^4 and 10^5 (see Camp[15]).

It has long been known (see Ives[5,12]) that this is an insufficient criterion to cover all cases of flocculation, particularly those of floc blanket clarification, and that integration of equation 4.45 yields a dimensionless group GtC, where C is the floc volume concentration. Consequently, the very low G values (typically $< 5\,s^{-1}$) in floc blanket clarifiers, are compensated by much higher C values (typically 0.1–0.2). It appears that the optimum GtC value lies between 100 and 500. This would agree with the value of $Gt = 10^5$ multiplied by $C = 10^{-3}$ ($GtC = 10^2$) for paddle-type flow-through flocculators.

4.9 Laboratory testing

4.9.1 Jar tests

The traditional form of laboratory testing of stirred flocculating suspensions is to use the jar test apparatus (*Figure 4.14*). This consists of a set of beakers (usually 4 to 6) which are simultaneously stirred by a paddle in each so that conditions in each beaker (jar) are identical. The beakers are normally tall-form 1 litre capacity containing 0.8 litre of suspension, but sometimes larger units are also used. Unfortunately, no standard design exists so the shapes of beakers may vary, and the paddle type and dimensions may include vertically slatted (picket fence) stirrers extending through the whole depth, propeller stirrers at the bottom of the liquid, or flat blades. In some cases, fixed baffles (stators) are included in the beakers. A typical flat-bladed design is shown in *Figure 4.15*. The stirring speeds are also not standard, but usually an initial high-speed mixing of about one minute is followed by 10–20 minutes of slow stirring. These variations of geometry and stirring conditions make comparisons difficult between different jar test apparatuses.

Comparative testing in the beakers of a particular jar test apparatus is, however, valid due to the identity of stirring conditions. So the effects of various doses of flocculating chemicals, of different pH conditions, and of different types of chemicals (e.g. indifferent electrolytes, aluminium or ferric salts, various polyelectrolytes) can be determined. Usually, an optimum is required and this relates to the formation by flocculation of a separable suspension.

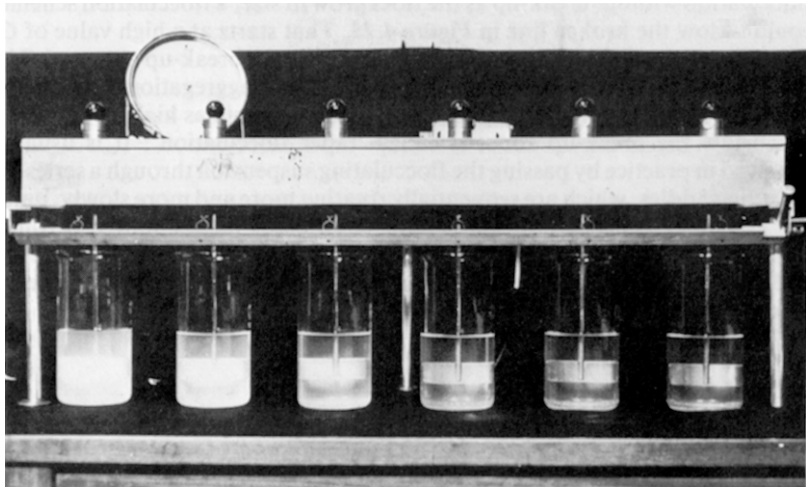

Figure 4.14 Jar test apparatus

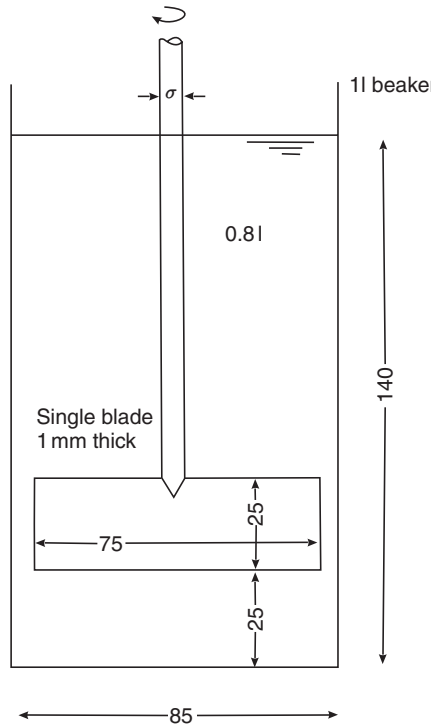

Figure 4.15 Typical jar test stirrer. All dimensions given in mm

Frequently, the first assessment is visual, looking for the appearance of visible flocs (which normally is greater than about 100 μm) and their growth to sizes of about 1 mm with clear liquid between. As flocculation is a prior step to some solid–liquid separation processes, an assessment is required of their settling, filtration or flotation behaviour.

Settling is usually assessed in the beaker, by stopping the stirring and allowing some period of quiescence and measuring the turbidity of the supernatant liquid. If this is by sampling at a known depth, after a known time, then it can be assumed that all flocs with settling velocity greater than the depth/time are removed from the supernatant liquid. By taking samples at a given depth at sequential times, in a manner similar to the Andreasen pipette method (see chapter 2) a settling velocity frequency distribution can be determined for the flocculated particles. Alternatively, the flocculated suspension could be transferred to a sedimentation balance, Coulter counter or some other measuring apparatus, but the act of transfer may affect the flocs, possibly breaking the larger ones. Such a settling velocity frequency distribution would guide the design of a subsequent settling stage after flocculation.

Filtration of flocculated suspensions can be assessed using the filterability test method described in chapter 11. Using the filterability number F against the product Gt an optimum flocculation can be determined for filtration through a sample of porous granular material as exemplified in *Figure 4.16*.

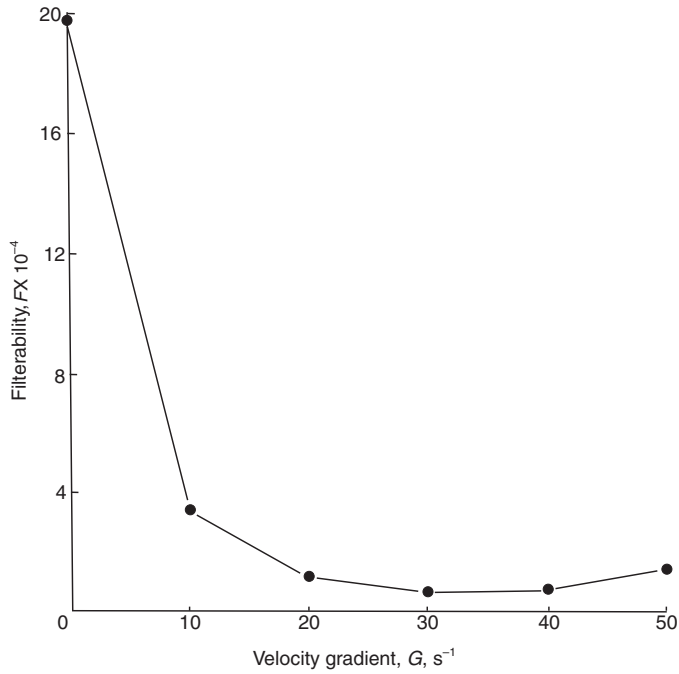

Figure 4.16 Effect of orthokinetic flocculation on filterability

A variant of the filterability test apparatus replaces the sample funnel (see *Figure 11.10*) with a paddle-stirred beaker to allow direct testing of the flocculated suspension without transfer from the jar test to the filterability apparatus.

Flotation of flocs by air bubbles can be tested by using jar test beakers which have a false bottom diffuser plate so that after flocculation by stirring, diffused air can be released through the suspension to form a floc froth scum on the surface. Such a modified jar test apparatus has been designed by the UK Water Research Centre. Similarly, if dissolved air flotation is of interest then compressed air can be released into the bottom of the beaker to float the flocculated particles. Obviously in flotation it is the clarity of the bottom liquid which is important and sampling near the bottom is required for turbidity or particle count measurements.

Comparisons of different jar test apparatuses can be made by estimating the mean velocity gradient (G value) using equation 4.46:

$$G = \sqrt{\left(\frac{P}{V\mu}\right)}$$

where

V is the volume of the stirred beaker
P is the power transferred from the stirrer to the suspension.

This power can be measured by using a sensitive torquemeter (0.01–0.2 N mm) on the stirrer drive shaft. Then $P = T_q\omega$, where T_q is the measured torque and ω the rotation speed in rad s^{-1}. *Figure 4.17* shows values of G measured in this way, against rotational speed for the paddle stirrer in *Figure 4.15*. This shows that for a stirrer speed of 40 rev min^{-1} the G value is 25 s^{-1}, which is typical of jar test apparatuses. With a typical flocculation time of about 15 min, the product $Gt = 2.25 \times 10^4$, which is within the range 10^4–10^5 quoted for paddle type flow-through flocculators in water treatment[15].

An alternative method of determining the power P is to calculate the drag force on the paddle blade and multiply by the velocity of the blade relative to the suspension.

$$P = \text{drag force} \times (v_p - v) \tag{4.53}$$

where $(v_p - v)$ is the paddle velocity minus the water velocity, giving the relative velocity.

$$\text{drag force} = C_D A_p \rho (v_p - v)^2/2 \tag{4.54}$$

where

C_D is the drag coefficient, which depends on blade geometry and rotational speed

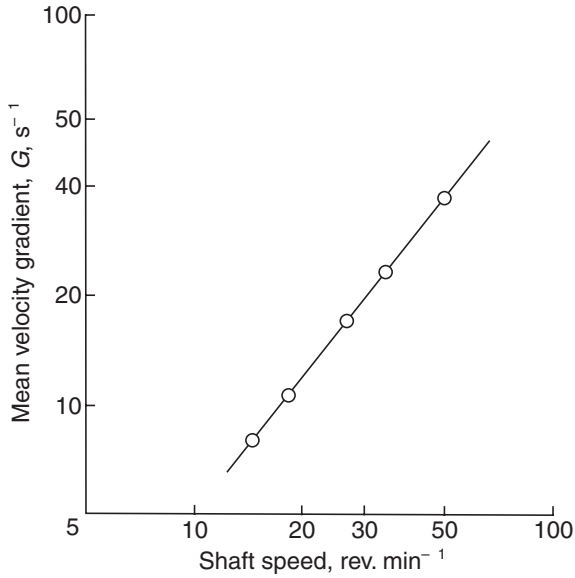

Figure 4.17 Velocity gradient produced by various shaft speeds in paddle flocculator of *Figure 4.15*

A_p is the projected area of the blade normal to the rotation direction
$\rho(v_p - v)^2/2$ is the Bernoulli dynamic pressure (the pressure energy equivalent of velocity energy).

It follows from equation 4.46 that G is given by

$$G = \sqrt{\left(\frac{C_D A_p \rho (v_p - v)^3}{2V\mu}\right)}$$

It is difficult to determine C_D and $(v_p - v)$ in a stirred beaker, but using special laboratory techniques Bhole[8] has determined for the stirrer geometry of *Figure 4.15* that C_D varies with G (and, therefore, with rotational velocity—*Figure 4.17*) as follows:

G	s^{-1}	10	20	30	40	50
C_D		1.81	1.20	1.13	1.02	0.94

and that $(v_p - v)$ was 0.52 times the blade tip velocity over this range of G values.

For example, taking the stirrer of *Figure 4.15*:

$$\text{velocity of blade tip at 40 rev min}^{-1} = \pi \times 75 \times 10^{-3} \times \tfrac{40}{60}\,\text{m s}^{-1}$$
$$\text{relative velocity}(v_p - v) = 0.52 \times \pi \times 75 \times 10^{-3} \times \tfrac{40}{60}\,\text{m s}^{-1}$$
$$= 0.0816\,\text{m s}^{-1}$$

drag coefficient at 40 rev min^{-1}, $C_D = 1.16$ by interpolation
projected area of blade, $A_p = 75\times10^{-3}\times25\times10^{-3}m^2$
density of liquid (water), $\rho = 10^3\,kg\ m^{-3}$
volume of liquid (0.8 litre), $V = 0.8 \times 10^{-3}\,m^3$
dynamic viscosity (20 °C), $\mu = 10^{-3}\,kg\ m^{-1}s^{-1}$

$$G = \sqrt{\left(\frac{1.16 \times 75 \times 25 \times 10^{-6} \times 10^3 \times 0.0816^3}{2 \times 0.8 \times 10^{-3} \times 10^{-3}}\right)} s^{-1}$$
$$= \sqrt{(738.6)} = 27\,s^{-1}$$

This agrees closely with the torquemeter value of 25 s^{-1}.

Assessment of flocculation in jar test apparatuses is useful in a comparative sense of finding the best chemical conditions, and showing that a separable floc can be formed under stirring conditions. The identification of the mean velocity gradient (G) is useful, but it cannot be assumed that conditions at full scale will be the same, even if the geometry of the beaker and stirrer were scaled up. Hydrodynamic conditions on the full scale are determined by the scale of the fluid motion and its spatial variation within the flocculator. Although a satisfactory G value may be determined in the jar test, the same average G value at full scale may lead to either better or poorer flocculation depending on the detailed geometry of the fluid motion, affected among other characteristics by the flow-through pattern in the full scale which is absent in the batch-type jar test.

4.9.2 Small-bore tubes

Bearing in mind the problem that scale-up is not meaningful from the jar test apparatus, an alternative test method is to avoid paddle stirrers (although they appear superficially like the full-scale paddle flocculators) and use small-bore tubes. These can be related to practice in the sense that they are flow-through devices, and their mean velocity gradients (G) can be easily measured or calculated.

Flow through small-bore tubes, of a few millimeters in diameter, is laminar and steady, not varying with time. The pressure drop along such a capillary can be measured manometrically, or calculated from Poiseuille's equation,

$$\Delta p = \frac{32\mu v L}{d^2} \tag{4.56}$$

The power dissipated along the tube, in laminar flow, is the weight of liquid per unit time ($\rho g Q$) multiplied by the loss of pressure head (H)

$$P = \rho g Q H \tag{4.57}$$

But

$$\rho g H = \Delta p$$

So

$$P = Q\Delta p = \frac{32Q\mu vL}{d^2} \tag{4.58}$$

The volume of liquid is the tube cross-sectional area (A) multiplied by the length (L).

$$\frac{P}{V} = \frac{32Q\mu vL}{AL\,d^2} \tag{4.59}$$

But

$$Q/A = v \quad \text{(mean velocity in the tube)}$$

$$\frac{P}{V} = \frac{32\mu v^2}{d^2} \tag{4.60}$$

The mean velocity gradient (G) is given by equation 4.46

$$G = \sqrt{\left(\frac{P}{V\mu}\right)} \tag{4.46}^*$$

$$G = \sqrt{\left(\frac{32v^2}{d^2}\right)} = 5.66\frac{v}{d} \tag{4.61}$$

If the flocculation criterion Gt is calculated, as a tube is a flow-through flocculator, with no retention of particles:

$$t\,(\text{mean residence time}) = \frac{AL}{Q} = \frac{L}{v} \tag{4.62}$$

$$Gt = 5.66\frac{L}{d} \tag{4.63}$$

This shows that the flocculation is dependent upon the tube geometry only, and independent of the flow rate, providing that G is within a reasonable range for aggregation without break-up.

There are refinements of the calculation of G and t to allow for the details of the paraboloid velocity distribution in a laminar flow tube. Among other aspects, this shows that particles which travel near the tube wall are subject to the highest velocity gradient, but the lowest velocity and hence the longest time. Therefore the local Gt near the tube wall is much higher than that near the centre of the tube. Such laboratory tube flocculators are usually coiled helically to make a more compact apparatus. The resultant curvature of the tube may induce a secondary circulation which is imposed on the primary laminar flow, therefore providing some lateral mixing of particles which would make the average values of G and t in equations 4.61 and 4.62 more realistic.

By taking certain values of G and t, it is possible to calculate the dimensions of laboratory tube flocculators. Assuming $G = 25\,\text{s}^{-1}$ and $Gt = 2.5 \times 10^4$ (values similar to the jar test—section 4.9.1), then $t = 10^3$ s. From equation 4.63

$$L = \frac{2.5 \times 10^4 d}{5.66}$$

Table 4.7

Tube bore *d*, mm	*Tube length* *L*, m	*Tube volume,* cm^3	*Flow rate,* $cm^3\ min^{-1}$
1	4.4	3.5	0.21
2	8.8	28.0	1.66
3	13.2	93.0	5.60
4	17.6	221.0	13.26
5	22.0	432.0	25.90

The dimensions flow and volumes of tubes from 1 to 5 mm bore, are as given in *Table 4.7*. The highest Reynolds' number occurs for the largest tube; for water at 20 °C, Re(max) = 110, i.e. well within the range of laminar flow.

The long tubes calculated above show the need to form them into helical coils in order to keep the apparatus compact. Such apparatuses have been used in several European countries but no published work has appeared up to 1981. Some references to microtube flocculation were made in 1979[9] but these were for specialized research and were below 0.1 mm in diameter.

It is claimed that small-bore tube flocculators have advantages over the conventional jar test because there is a rapid response to changes in chemical conditions and so optimum conditions can be established fairly quickly using quite small sample volumes, typically about 20% of the jar test requirements.

The full-scale analogue of tube flocculation is in flocculation in pipes, although the flow would be turbulent, not laminar; this is discussed later in section 4.10.3. It may also be considered that flocculation in inclined tube modules is similar, as these are often in laminar or transitional flow.

4.9.3 Couette apparatus

Couette flocculators consist of coaxial rotating cylinders, with an annular gap between the cylinders comprising the flocculating volume. These apparatuses provide a velocity gradient which is almost uniform, having a very slight non-linearity due to the curvature of the annular gap.

Several designs have evolved, many with horizontal axes (i.e. both ends closed) with the outer cylinder rotating and the inner cylinder fixed, which provides best hydrodynamic stability. Some horizontal-axis Couette flocculators are flow-through designs, even with a tapered gap to provide taper flocculation[6,7] However, horizontal-axis apparatuses suffer from end effects which cause secondary circulation, so only a limited central zone (about one quarter of the length) is in defined laminar flow.

Vertical-axis Couette flocculators, with a free liquid surface, have only a bottom-end effect. The design shown in *Figure 4.18* is 150 mm high, with an inner cylinder diameter of 27 mm and a 3 mm annular gap filled with 40 ml

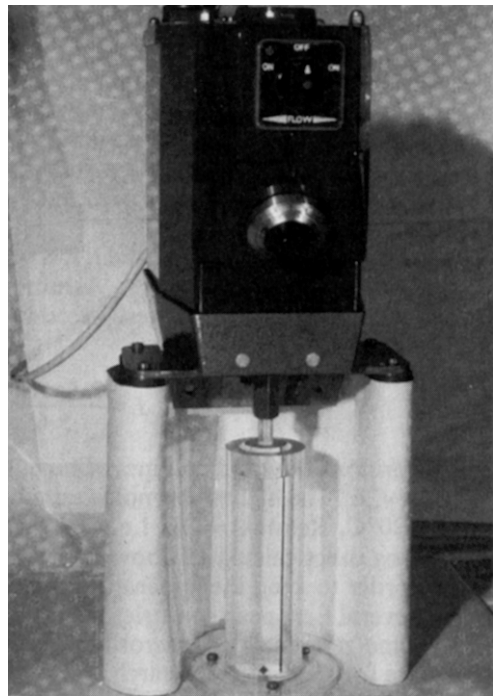

Figure 4.18 Couette flocculator

of liquid. For mechanical convenience the inner cylinder rotates, the outer being fixed, although this is slightly less hydrodynamically stable than the converse. The fluid motion in this apparatus has been fully analysed experimentally and theoretically by Elson[1], and the lower-end effect is confined to the bottom 6 mm depth; all the rest of the annular volume is in almost uniform shear, with a nearly linear velocity gradient. The design of such Couette flocculators is described in Ives[5] and flocculation data is given by Ives and Al Dibouni[2].

Couette flocculators are basic research apparatuses of flocculation kinetics, and can be used with particle counters (e.g. Coulter counter) as a standard for other laboratory flocculators which have ill-defined velocity gradients.

4.10 Practical flocculators

Flocculators used in practice can be classified into four groups:

1 *paddle:* revolving on horizontal or vertical axes, oscillating, vertically or pendulum-like, propeller or turbine blades;

2 *baffles:* fixed in channels or tanks providing either 'over-under' or 'round-the-end' motion,
labyrinth or honeycomb structures in modules for tanks or pipes (static mixers);
3 *pipes:* turbulent flow provides the power dissipation;
4 *particles:* fixed beds (filters),
fluidized beds (floc blanket, with possible solids recirculation), bubble swarms, differential settling.

Many, but not all, of these are reviewed and compared by Polasek[10].

4.10.1 Paddle flocculators

The power transferred from moving paddles to the liquid, for flocculation, is the drag force on the paddle multiplied by the distance moved per unit time (see section 4.9.1):

$$\text{power} = \text{force} \times \text{distance/time} = \text{force} \times \text{velocity}$$

$$\text{drag force} = C_D \rho (v_p - v)^2 A_p/2 \qquad (4.54)^*$$

where

$\rho v^2/2$ is the Bernoulli dynamic pressure
$(v_p - v)$ is the relative velocity of the liquid to the paddle blade, assumed to be about 0.8 paddle blade mean velocity, and
A_p is the projected area of the blades normal to motion.

$$\text{power} = C_D \rho (v_p - v)^3 A_p/2$$

Mean velocity gradient $G = \sqrt{(\text{power/volume} \times \text{viscosity})}$

$$G = \sqrt{\left(\frac{C_D \rho (v_p - v)^3 A_p}{2V\mu}\right)} \qquad (4.55)^*$$

The drag coefficient C_D depends on the length:width ratio of the paddle blade, at normal flocculator speeds:

length:width ratio	5	20	infinite
drag coefficient C_D	1.2	1.5	1.9

Example 4.1

Calculate the mean velocity gradient for the four-bladed paddle flocculator shown in *Figure 4.19*, in a tank containing 100 m^3 of water at 20 °C:

paddle length: width ratio $= 3/0.5 = 6$, therefore assume $C_D = 1.2$
water viscosity at 20°C $= 10^{-3}$ kg m^{-1} s^{-1}

paddle velocity $v_p = \dfrac{4\pi \times 2}{60}\,\mathrm{m\,s^{-1}}$ (mean)

relative velocity of water to paddle $(v_p - v) = 0.8\,v_p$

$$(v_p - v) = \frac{0.8 \times 4\pi \times 2}{60} = 0.33\,\mathrm{m\,s^{-1}}$$

mean velocity gradient G from equation 4.55:

$$G = \sqrt{\left(\frac{C_D \rho (v_p - v)^3 A_p}{2V\mu}\right)}$$
$$= \sqrt{\left(\frac{1.2 \times 10^3 \times 0.33^3 \times 4 \times 1.5}{2 \times 100 \times 10^{-3}}\right)}$$
$$= 36\,\mathrm{s^{-1}}$$

Generally, the G value should be between 20 and $75\,\mathrm{s^{-1}}$.

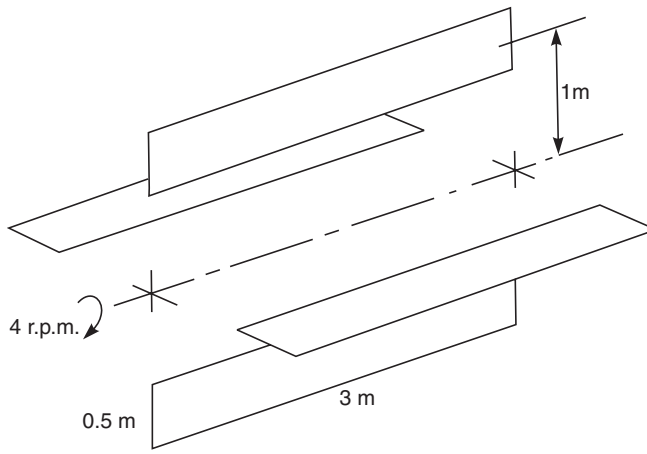

Figure 4.19 Four-blade paddle flocculator

Figure 4.20 shows typical arrangements of horizontal- and vertical-axis paddle flocculators. The axes should rotate in alternate directions along the tank, e.g. in *Figure 4.20* the first and third paddles rotate clockwise, but the second rotates anticlockwise. This rolls the liquid containing the flocs from paddle to paddle without excessive shear as the paddle blades pass each other. If taper flocculation is desired, each sequential axis will rotate more slowly. The choice between horizontal and vertical axes depends primarily on mechanical considerations, such as the power drive system and the maintenance of bearings and support frames.

Detention times for such flocculation tanks should be 1200–1800 s. For the example above, $G = 36\,\mathrm{s^{-1}}$ and, assuming $t = 1500\,\mathrm{s}$, the product

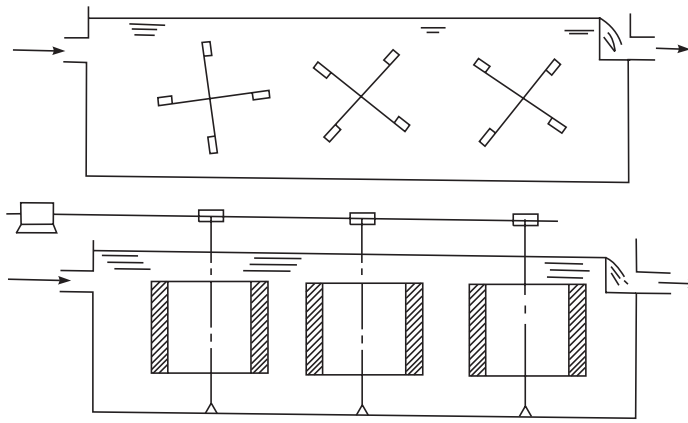

Figure 4.20 Paddle flocculators

$Gt = 5.4 \times 10^4$ which is within the optimum range $10^4 - 10^5$ for flow through flocculators with no solids retention.

The horizontal velocity (mean) of the liquid should be 0.25–0.4 m s^{-1}. Paddle tip velocities should not exceed 0.8 m s^{-1}, and the total paddle blade area should not be greater than 20% of the cross-sectional area of the tank, otherwise the liquid will roll with the blades without the desirable velocity gradient.

Oscillating or reciprocating paddle flocculators may be on shafts mounted vertically, which move vertically up and down in the direction of the shaft axis, or they may be on frames swinging to and fro in a pendulum-like motion. Both types impart a harmonic motion to the blades.

For the vertical agitator, the distance moved by the blades is the same for all and the relative velocity is expressed by the harmonic mean velocity; a drag coefficient of $C_D = 3.0$ has been suggested. With this information the velocity gradient is calculated from the power dissipated, using equation 4.55.

For the pendulum-type agitator (*Figure 4.21*, after Polasek[10]) the motion of the blades is through small arcs, increasing with distance down the pendular frame. To maintain a uniform intensity of agitation over the entire depth, it has been proposed that the blades should be distributed logarithmically along the frame depth as indicated in principle in *Figure 4.21*. Power can be calculated from the mean harmonic velocity and drag coefficient from paddle shape, summed for all the paddles. Further details are given by Polasek[10].

Propeller or turbine blade flocculators are difficult to assess from a theoretical standpoint as they vary greatly in form and efficiency. An example of successful taper flocculation using turbine agitators is described by Bernhardt and Schell[11], for the formation of ferric hydroxide flocs for phosphorus removal of the water supplying the Wahnbachtal reservoir. The practical approach to such propeller/turbine flocculators is to make torque

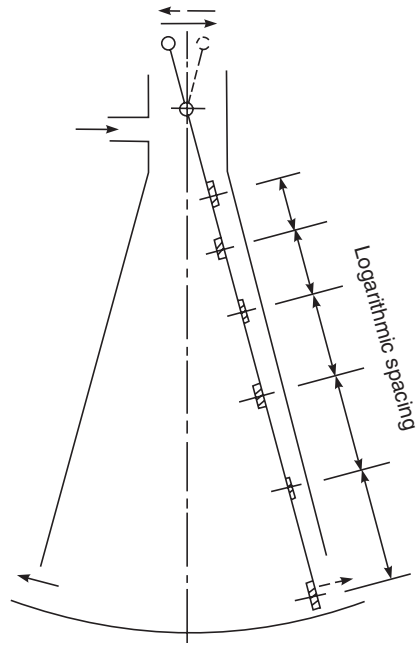

Figure 4.21 Pendulum flocculator

measurements on the shaft of a prototype in the liquid, using the relationship $P = T_q\omega$ (where T_q is torque and ω is angular velocity).

4.10.2 Baffle flocculators

The flows around baffles in a channel, whether 'over-under' or 'round-the-end', or through slatted baffles, or through labyrinths in channels or pipes, all dissipate energy as head loss, which per unit time gives the power. As in flow-through tubes (section 4.9.2) the power dissipated is the weight of liquid per unit time (ρgQ) multiplied by the head loss (H),

$$P = \rho gQH \qquad (4.57)^*$$

The head loss is greatest at each change of direction around a baffle H_B, and least in straight stretches of flow H_f. The direction-change head loss H_B is given by equation 4.64

$$H_B = nC_D \frac{v^2}{2g} \qquad (4.64)$$

where

n is the number of direction changes, and
v is the mean velocity (Q divided by cross-sectional area).

The drag coefficient C_D is about 3.0 for 180 degree changes in direction, and 2.0–2.5 for 90 degree changes.

The head loss along the straight channels is given by the Chezy equation 4.65,

$$H_f = \frac{Lv^2}{c^2 R} \tag{4.65}$$

where

c is the Chezy coefficient, and
R is the hydraulic radius of the channel.

The Chezy coefficient depends on the channel wall roughness and the hydraulic radius, and can be calculated from formulae in standard books on fluid mechanics. In practical terms H_f will be much less than H_B, so as a first approximation $H \triangleq H_B$.

Velocities in baffled channels are usually between 0.25 and 0.5 $m\,s^{-1}$, and retention time varies between 10 and 60 min. However, a disadvantage of baffled channels is that their performance varies with flow rate, whereas mechanical flocculators can be operated independently of flow rate.

Example 4.2

Calculate the number of baffles required in a round-the-end baffled channel under average conditions of water velocity, $v = 0.3\,m\,s^{-1}$, $t = 30$ min (1800 s) and Gt for flow-through flocculation $= 5 \times 10^4$:

$$G = \frac{5 \times 10^4}{1.8 \times 10^3} = 28\,s^{-1}$$

$$\text{volume of channel} = LA$$

From equations 4.46 and 4.57

$$G = \sqrt{\left(\frac{\rho g Q H}{LA\mu}\right)}$$

But $Q/A = v$ and $v/L = 1/t = 1/1800$ and, substituting equation 4.64 for H,

$$G = \sqrt{\left(\frac{\rho g n C_D v^2}{t\mu 2g}\right)}$$

$$n = \frac{2G^2\mu t}{\rho C_D \nu^2}$$

At 20°C, water viscosity $\mu = 10^{-3}\,kg\,m^{-1}\,s^{-1}$

$$n = \frac{2 \times 28^2 \times 10^{-3} \times 1800}{10^3 \times 3.0 \times 0.3^2}$$

$$= 10.45, \text{say } \textit{11 baffles}$$

For slatted baffles the head loss can be assessed using the flow past fixed blades where the relative velocity is the liquid flow-through velocity through the slat gaps, and the drag coefficient is given by the baffle geometry, as in section 4.10.1.

In labyrinth or honeycomb flocculators (static mixers) the head loss has to be measured experimentally with a prototype module in a test rig. Then equation 4.57 can be used to calculate the power dissipation and, hence, the mean velocity gradient G.

4.10.3 Pipe flocculators

The natural turbulence of flow through a pipe can create velocity gradients leading to flocculation. In the laboratory, small-bore tubes operate in laminar flow (section 4.9.2) with Reynolds' numbers less than 2000. In practical pipe flow the situation is turbulent and head loss is given by the Darcy–Weisbach equation 4.66.

$$H = \frac{4fL}{d} \times \frac{v^2}{2g} \tag{4.66}$$

where f is the pipe friction factor, which depends on the pipe roughness and Reynolds' number, and is usually given in graphical form in standard books on fluid mechanics.

The mean velocity gradient is calculated from equations 4.46 and 4.57

$$G = \sqrt{\left(\frac{\rho g Q H}{V \mu}\right)} \tag{4.67}$$

The pipe volume is LA, and the criterion $Gt = 10^4 - 10^5$ for flow-through flocculators is used.

Such pipe flocculators tend to create rather high velocity gradients at practical flow rates and need to be very long to give the required detention times. Therefore it may be useful to utilize an existing pipe as a flocculator, but it is not economic to build one for the purpose, as a concrete channel with baffles would be more compact and cost less.

Example 4.3

Calculate the length of 600 mm diameter pipe required to produce a Gt value of 5×10^4 at a water flow of 20 M1 d^{-1}:

friction factor $f = 0.005$
water temperature 10 °C
kinematic viscosity $\mu/\rho = 1.31 \times 10^{-6}$ $m^2\,s^{-1}$

From equation 4.67

$$G = \sqrt{\left(\frac{\rho g Q H}{L A \mu}\right)} = \sqrt{\left(\frac{\rho g v H}{L \mu}\right)}$$

$$v = \frac{Q}{A} = \frac{20 \times 10^3 \times 4}{3600 \times 24 \times \pi \times 0.6^2} = 0.82 \text{ m s}^{-1}$$

$$\frac{H}{L} = \frac{4f}{d}\frac{v^2}{2g} = \frac{4 \times 0.005 \times 0.82^2}{0.6 \times 2g} = \frac{0.011}{g}$$

$$G = \sqrt{\left(\frac{\rho g \times 0.82 \times 0.011}{\mu g}\right)} = \sqrt{\left(\frac{0.82 \times 0.011}{1.31 \times 10^{-6}}\right)} = 83 \text{ s}^{-1}$$

$$t = \frac{5 \times 10^4}{83} = 0.6 \times 10^3 \text{ s}$$

$$L = vt = 0.82 \times 0.6 \times 10^3 = 492 \text{ m , say } 500 \text{ m}$$

4.10.4 Particle flocculators

With the exception of sedimentation where differential settling velocities of flocs create relative motion, hence orthokinetic flocculation, particle flocculators rely on the liquid drag past the particles to create the velocity gradients.

4.10.4.1 Fixed bed (deep bed filters)

In the case of fixed bed (deep bed granular filters) flocculators the power is dissipated as laminar flow through granular media, with local velocity gradients in the pores formed by quasi-parabolic velocity distributions. The system is analogous to small-bore tubes (section 4.9.2) bearing in mind the capillary model concept of the Kozeny–Carman equation 4.68 for head loss through a fixed bed,

$$\frac{H}{L} = \frac{5\mu v(1-\varepsilon)^2}{\rho g \varepsilon^3}\left(\frac{6}{D}\right)^2 \tag{4.68}$$

where

ε is the porosity of the fixed bed (pore volume/total volume), and
D is the grain diameter of the particles of the fixed bed.

Combining equations 4.46 and 4.57 to give the mean velocity gradient, and substituting for the liquid volume in the pores $V = \varepsilon AL$

$$G = \sqrt{\left(\frac{\rho g Q H}{\varepsilon A L \mu}\right)} \tag{4.69}$$

Substituting for H/L from equation 4.68 and noting that $v = Q/A$

$$G = \sqrt{\left(\frac{180\,v^2(1-\varepsilon)^2}{\varepsilon^4 D^2}\right)} = \frac{13.4\,v(1-\varepsilon)}{\varepsilon^2 D} \tag{4.70}$$

The residence time t is the pore volume εAL divided by the volumetric flow rate Q,

$$t = \frac{\varepsilon AL}{Q} = \frac{\varepsilon L}{v} \tag{4.71}$$

The product Gt, being a criterion of flocculation for flow-through flocculators, is given by the product of equations 4.70 and 4.71

$$Gt = \frac{13.4(1-\varepsilon)L}{\varepsilon D} \tag{4.72}$$

Consequently, flocculation is dependent on the geometry of the fixed bed, and not on the flow rate.

Example 4.4

Calculate the value of Gt for a fixed bed, being a sand water filter, where the grain size $D = 0.5$ mm, porosity is 0.4 and thickness $L = 600$ mm:

$$Gt = \frac{13.4(1-0.4)0.6}{0.4 \times 0.5 \times 10^{-3}} = 2.4 \times 10^4$$

that is within the range 10^4–10^5.

The value of G requires the flow rate. For normal rapid sand filtration $v = 5\,\mathrm{m\,h^{-1}} = 5/3600\,\mathrm{m\ s^{-1}}$,

$$G = \frac{13.4v(1-\varepsilon)}{\varepsilon^2 D} = \frac{13.4 \times 5 \times (1-0.4)}{3600 \times 0.4^2 \times 0.5 \times 10^{-3}}$$
$$= 140\,\mathrm{s^{-1}}$$

This is a high value, so large flocs do not form, which is suitable as they would clog the small filter pores. Since filtration velocities may be used up to 15 m $\mathrm{h^{-1}}$ in water and waste water treatment practice, even higher G values may be experienced.

Such fixed bed flocculation is normally accompanied by simultaneous filtration of the flocs which are formed. This causes clogging and so the accumulated flocs must be flushed away periodically (typically, every day) by backwash fluidization, as in normal deep bed filtration practice.

Flocculation prior to deep bed filtration is normally used, either in a previous flocculator and settling (or flotation) tank, or by direct flocculation in the filter chamber above the filter media. Flocculation within the fixed bed is sometimes called contact flocculation, or flocculating filtration.

In studying flocculation in such fixed beds (and also for fluidized beds) it is difficult to follow the kinetics of flocculation, or even to study the reduction

in the numbers of primary particles, due to the removal of so many flocs by deposition on the fixed bed grains (filter effect). However, as the kinetics of removal of particles by filtration is first-order with respect to particle concentration (see chapter 11), but the kinetics of flocculation are second-order (equation 4.44), it is possible to separate the two effects by making observations at different inlet particle concentrations.

4.10.4.2 Fluidized bed (floc blanket clarifiers)

In the case of fluidized bed flocculators the power dissipated is the energy of drag past the fluidized bed particles per unit time. This occurs in the floc blanket clarifier where the previously formed floc particles comprise the fluidized bed. For a fluidized bed the drag force past the floc particles is equal to their weight in the liquid.

For such flocculator-clarifiers the hydraulic flow must be steady and maintain a steady fluidization of the existing floc particles; the incoming flocculating particles must aggregate to a size equal to the existing flocs or, more likely, be collected on them; and there must be a balance between the incoming solids and the withdrawal of excess floc to maintain a steady state.

The steady fluidization requires that the upward flow velocity v ($= Q/A$ where A is the tank plan area) be equal to the hindered settling velocity of the fluidized bed v_h:

$$v = v_h = v_s(1 - C)^{4.5} \tag{4.73}$$

where the hindered settling is expressed in terms of the single particle settling velocity (v_s, often Stokes' velocity) and the fluidized particle volume/volume concentration (C) in the liquid; equation 4.73 is the well-known Richardson—Zaki relationship (see chapter 5). Typically, C is maintained between 0.1 and 0.2 vol./vol., and the upflow velocity is about $2\,\mathrm{m\,h^{-1}} = 0.55\,\mathrm{mm\,s^{-1}}$.

From equation 4.73, taking $C = 0.15$,

$$0.55 = v_s(1 - 0.15)^{4.5}$$

from which $v_s = 1.14\,\mathrm{mm\ s^{-1}}$.

Using Stokes' law:

$$v_s = \frac{g(\rho_s - \rho)D^2}{18\mu} \tag{4.74}$$

diameter of flocs

$$D = \sqrt{\left(\frac{18\mu v_s}{g(\rho_s - \rho)}\right)}$$

In floc blanket clarifiers the density of the existing flocs is about $1005\,\mathrm{kg\,m^{-3}}$, and at 20 °C viscosity $\mu = 10^{-3}\mathrm{kg\,m^{-1}\,s^{-1}}$,

$$D = \sqrt{\left(\frac{18 \times 10^{-3} \times 1.14 \times 10^{-3}}{9.81(1005 - 1000)}\right)} \text{ m}$$
$$= 0.65 \times 10^{-3} \text{m} = 650\,\mu\text{m}$$

In constant plan (flat-bottom) clarifiers the upflow velocity should be uniform at all levels and the floc blanket (fluidized bed) should have a uniform concentration and uniform particle size. In expanding upflow clarifiers (conical, or hopper-bottom) the lower levels should have greater upflow velocities and, therefore, lower floc volume concentrations or particles. In practice, such expanding upflow is highly unstable and massive vertical eddies cause recirculation, with almost uniform concentrations and particle sizes throughout the fluidized bed. A definite zone of separation forms at the surface with a clean water zone above it, relatively free from primary particles and flocs.

The kinetics of flocculation in a fluidized bed are described by the equations in section 4.8. The simplified Smoluchowski equation 4.42 can be modified by the special bimodal distribution of the fluidized bed (floc blanket) particles:

$$\frac{dN_{ij}}{dt} = \frac{4}{3} N_i N_j G R_{ij}^3 \qquad (4.42)^*$$

The incoming primary particles $i = 1$ are very small ($< 1\mu$m), and it is the reduction of these particles N_1 which is important. The existing particles j are large (100−1000 μm) and form the fluidized floc particles. In steady state $N_j =$ constant, and the size of the aggregated particles $R_{ij} \triangleq R_j$ as the addition of primary particles scarcely increases their radii. Equation 4.42 therefore becomes:

$$\frac{dN_{ij}}{dt} = -\frac{dN_1}{dt} = \frac{4}{3} N_1 N_j G R_j^3 \qquad (4.75)$$

The floc volume concentration, in the fluidized bed, is the number of j-particles per unit volume (N_j) multiplied by the volume of one j-particle

$$C = N_j \frac{4}{3} \pi R_j^3 \qquad (4.76)$$

So the rate of disappearance of primary particles is

$$-\frac{dN_1}{dt} = \frac{GCN_1}{\pi} \qquad (4.77)$$

Integrating from $t = 0, N_1 = N_0$ to $t = t, N_1 = N_t$:

$$\frac{N_t}{N_0} = \exp\left(-\frac{GCt}{\pi}\right) \qquad (4.78)$$

So the kinetics of fluidized bed flocculation predicts an exponential decline in the number of primary particles as the liquid passes through the fluidized bed

(residence time t). This has been confirmed in experimental laboratory models using 1 μm polystyrene latex suspension destabilized in water, flocculated by passage through a fluidized bed of PVC/PVA co-polymer spheres 125–150 μm in diameter. These experiments, at University College London, have also confirmed that the flocculation is second-order with respect to concentration (equation 4.42) and removal of particles in the fluidized bed is first-order with concentration (filter effect—see chapter 11).

The mean velocity gradient is calculated from the power dissipated as drag past the fluidized bed particles. This exceeds by far any power dissipated in inlet turbulence or flow conditions (Ives[12]):

drag force = weight (fluidized bed equilibrium)
weight $= g(\rho_s - \rho)CAL$

where

A is the plan area of the tank (assumed constant), and
L is the depth of the fluidized bed.

$$\text{power} = \text{drag force} \times \text{velocity} = g(\rho_s - \rho)CAL\frac{Q}{A}$$

$$\frac{\text{power}}{\text{volume}} = \frac{P}{V} = \frac{g(\rho_s - \rho)CAL}{AL} \times \frac{Q}{A} = g(\rho_s - \rho)Cv \tag{4.79}$$

From equation 4.46

$$G = \sqrt{\left(\frac{P}{V\mu}\right)} = \sqrt{\left(\frac{g(\rho_s - \rho)Cv}{\mu}\right)} \tag{4.80}$$

Using the previous values for equations 4.73 and 4.74

$$C = 0.15, v = 0.55\,\text{mm}\,\text{s}^{-1}, \rho_s = 1005\,\text{kg}\,\text{m}^{-3}, \mu = 10^{-3}\,\text{kg}\,\text{m}^{-1}\text{s}^{-1}$$

$$G = \sqrt{\left(\frac{9.81 \times (1005 - 1000) \times 0.15 \times 0.55 \times 10^{-3}}{10^{-3}}\right)}$$

$$= 2\,\text{s}^{-1} \quad \text{(it is normally} < 5\,\text{s}^{-1}\ \text{in floc blanket clarifiers)}$$

This is a very low value compared with conventional paddle flocculators ($G = 20{-}75\,\text{s}^{-1}$). The mean residence time in practical fluidized bed flocculators (t) is usually 20–30 min (1200–1800 s). So the product $Gt = (0.24$ to $0.36) \times 10^4$. This is less than the range for flow-through flocculators with no solids retention ($10^4{-}10^5$). But the low value of Gt is compensated by the high value of solids concentration C, which results from the criterion GCt of the theory (equation 4.78). Taking typical values:

$$GCt = 2 \times 0.15 \times 1500 = 450$$

Starting with the assumption that in a flow-through paddle flocculator all the primary particles are identical ($i = j = 1$) equation 4.44 can be integrated

to a form similar to equation 4.48 but with a different numerical constant ($4/\pi$) because the appearance of a *k*-particle is accompanied by the disappearance of two *i*-particles (similar to equation 4.43). However, the term *GCt* appears relevant even for flow-through paddle flocculators. In water treatment a typical coagulant dose would be 50 mg l^{-1} as $Al_2(SO_4)_318H_2O$, being 4.05 mg l^{-1} as Al ion. It has been estimated by Hudson[13] that 1 g of Al ion produces 240 ml of floc particles. Therefore, floc volume concentration is:

$$\begin{aligned} C &= 4.05 \times 10^{-3} \times 240 \text{ ml } l^{-1} \\ &= 4.05 \times 240 \times 10^{-6} \text{ vol/vol} \\ &= 972 \times 10^{-6} \triangleq 10^{-3} \text{ vol/vol} \end{aligned}$$

Therefore

$$GCt = 10^{-3} \times 10^5 = 100 \text{ when } Gt = 10^5$$

It seems, therefore, that the values of *GCt* are comparable even in very different types of flocculation systems, such as the floc blanket and the flow-through paddle flocculators.

The balance of incoming and outgoing solids to maintain a steady volume fluidized bed is readily calculated from the volumetric concentrations of the incoming suspension and the fluidized bed. Solids are removed by withdrawing excess fluidized bed material (e.g. floc blanket) over a slurry weir or into a concentrator cone at the surface of the fluidized bed (zone of separation into the clear liquid zone). In the examples calculated above:

incoming solids from 50 mg l^{-1} aluminium sulphate

$$C_i = 10^{-3} \text{vol/vol}$$

outgoing solids (so-called sludge bleed) of floc blanket

$$C_o = 0.15 \text{ vol/vol}$$

Therefore ratio of sludge bleed suspension flow (q) to inflow (Q) is C_o/C_i because solids flux balance

$$C_i q = C_o Q$$

$$q = \frac{C_o Q}{C_i} = \frac{10^{-3} Q}{0.15} = 0.007 Q$$

Therefore sludge bleed flow rate $= 0.7\%\ Q$.

For high alum doses the percentage increases proportionately. Because of inefficient slurry weirs or cones, some clear liquid may also be withdrawn, increasing q to values up to $3\%\ Q$. This is a high value, leading to excess of sludge to be disposed. Values of 5% or more are normally unacceptable.

This discussion and calculations of fluidized bed flocculators are based on a parallel-sided tank. Hopper (inverted pyramid) and conical shapes are quite common and the values of *GCt*, and fluidized bed stability, involve

integrations throughout the fluidized bed depth (Ives[12]). In water treatment practice there is a growing interest in the development of flat-bottom, parallel-sided floc blanket clarifiers.

Solids recirculation with pumps or impellers takes advantage of the increase in the concentration term (C) in the criterion GCt, to enhance flocculation. There are many designs and these, together with normal floc blanket tanks, are presented by Sontheimer in Ives[5]. Also some discussion of such flocculators and the methods of model testing are described by Stevenson in Purchas[14].

4.10.4.3 Bubble flocculation

Bubbles rising through a suspension create velocity gradients due to their motion. These velocity gradients could be used for flocculation in principle, but early assessments of bubble flocculation indicated that the diffusers which existed at that time created bubbles that were too large to be effective (Camp[15]).

With the advent of flotation as a useful treatment process in water and waste water treatment, made possible by the creation of finer bubbles by dissolved air precipitation, and electrolysis, the concept of bubble flocculation can be reconsidered. In the flotation process in water treatment, flocculation takes place prior to bubble flotation, usually by mechanical (paddle) flocculator with a coagulant salt (such as alum). It seems possible that the flocculation and flotation processes could be combined with the bubbles providing the flocculating power.

As for other particle flocculators, the power is derived from the drag force on the rising bubbles. Small bubbles will rise in a laminar regime (Stokes).

Stokes' drag force per bubble = force = $3\pi\mu v_s D$

power per bubble = force × velocity = $3\pi\mu v_s^2 D$

Stokes' law $v_s = \dfrac{g(\rho_s - \rho)D^2}{18\mu}$ (rising velocity of bubble)

Assume density of air in bubble is negligible (1.2 kg m^{-3}) and that no hindered rising or mass lift will occur, then

$v_s = \dfrac{g\rho D^2}{18\mu}$ (negative sign is dropped as v is opposite vectorially to g)

$$\text{power per bubble} = \frac{\pi g^2 \rho^2 D^5}{108\mu} \tag{4.81}$$

From equation 4.46

$$G = \sqrt{\left(\frac{P}{V\mu}\right)} \tag{4.46}^*$$

$$\frac{P}{V} = \frac{\text{power}}{\text{volume}} = \frac{\text{power}}{\text{bubble}} \times \frac{\text{bubbles}}{\text{volume}}$$

$$= \frac{\text{power}}{\text{bubble}} \times \frac{\text{air volume}}{\text{volume}} \times \frac{1}{\text{1bubble vol}}$$

$$= \frac{\pi g^2 \rho^2 D^5}{108\mu} \times \frac{V_A}{V} \times \frac{6}{\pi D^3}$$

$$\frac{P}{V} = \frac{g^2 \rho^2 D^2 V_A}{18\mu V} \tag{4.82}$$

$$G = 0.236 \frac{g\rho D}{\mu} \sqrt{\left(\frac{V_A}{V}\right)} \tag{4.83}$$

where V_A/V = volume of air supplied per unit tank volume.

In dissolved air flotation bubbles are formed as microbubbles which grow with the release of pressure to values typically of 0.1–0.5 mm. The air is dissolved in recycled water, being about 10% of the flow, with values of 5–7 g air m^{-3}. This amounts to a free air volume per unit water volume (V_A/V) of about 5×10^{-4}.

Taking $D = 0.1$ mm and $\mu = 10^{-3}\,\text{kg}\,\text{m}^{-1}\,\text{s}^{-1}(20\,^\circ\text{C})$ for water, from equation 4.83:

$$G = \frac{0.236 \times 9.81 \times 10^3 \times 0.1 \times 10^{-3}}{10^{-3}} \sqrt{(5 \times 10^{-4})}$$

$$G = 5\,\text{s}^{-1}$$

If $D = 0.5$ mm

$$G = 25\,\text{s}^{-1}$$

Consequently, if the bubbles can be kept fine enough, useful G values can be generated. The use of bubble flocculators is still in the experimental stage, but there are indications that they may be applicable in practice.

4.10.4.4 Differential settling

Natural suspensions may flocculate, or previously flocculated suspensions may flocculate further, if the particles or flocs are settling at different velocities. Faster settling particles may collide with slower settling particles leading to aggregation if they are destabilized. The aggregates will then settle faster due to their increased mass, and possibly experience further collisions and aggregations.

The orthokinetic definition sketch of *Figure 4.12* will still apply, with relative velocity u replaced by the differential settling velocity $(v_i - v_j)$ in the direction of gravity (represented by the x-direction). The flux of i-particles through the cylinder radius R_{ij} $(= r_i + r_j)$, centred on a j-particle, is

$$N_i \frac{dV}{dt} = N_i \pi (r_i + r_j)^2 (v_i - v_j) \tag{4.84}$$

As there are N_j j-particles present, the collision rate is

$$N_i N_j \frac{dV}{dt} = \frac{dN_{ij}}{dt} = N_i N_j \pi (r_i + r_j)^2 (v_i - v_j) \tag{4.85}$$

Assuming that the particles settle according to Stokes' law, and that $\rho_i = \rho_j = \rho_s$ (constant particle density):

$$v_i - v_j = \frac{2g}{9} \frac{(\rho_s - \rho)}{\mu} (r_i^2 - r_j^2) \tag{4.86}$$

Noting that $(r_i^2 - r_j^2) = (r_i + r_j)(r_i - r_j)$

$$\frac{dN_{ij}}{dt} = N_i N_j \frac{2\pi g}{9\mu} (\rho_s - \rho)(r_i + r_j)^3 (r_i - r_j) \tag{4.87}$$

Equation 4.87 can be developed further to allow for the creation of k-particles and their possible collisions with i- and j-particles, and so on. This is set out by Ives[5].

The equations cannot be treated exactly like other orthokinetic equations because of the limitation $i \neq j$. If $i = j$ there would be no differential settlement and, therefore, no collisions and aggregation. Similarly, it cannot be applied to an initially monodisperse suspension because all particles would settle at the same rate. If the suspension were subject initially to significant perikinetic (Brownian diffusion) flocculation then it would become heterodisperse and flocculation by differential settling would follow.

If a sample of suspension to be settled is available it is not difficult to determine whether flocculation by differential settling will occur. An apparatus similar in principle to the Andreasen pipette method (chapter 2) is used, but with sampling at more than one depth, such as the settling tube with multiple sampling ports shown in *Figure 4.22*. Samples are taken at the various depths h_1, h_2, h_3 etc., below the surface level of the suspension, at

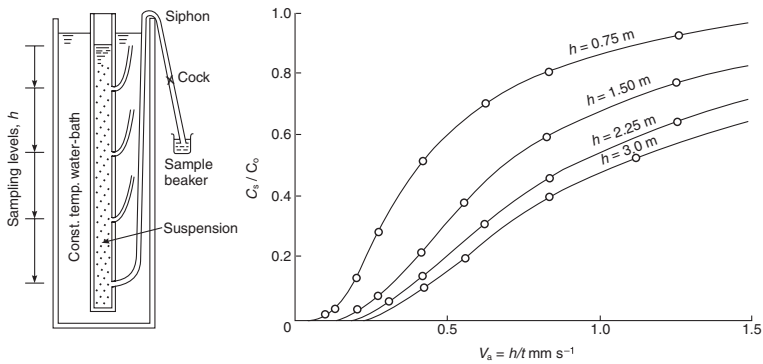

Figure 4.22 Multi-port settling tube and settling data (flocculating suspension)

Table 4.8 Settling analysis data

$h_1 = 750$ mm *times*(s)	*= 0*	*600*	*900*	*1200*	*1800*	*2700*	*3600*	*5400*	*7200*
h_1/t(mm s^{-1})	=	1.25	0.83	0.63	0.42	0.28	0.21	0.14	0.10
C_s(g m^{-3})	= 86	80	70	61	44	24	12	3	1.3
100 C_s/C_o	= 100	93	81	70.5	51.5	28	13.5	3	1.5
$h_2 = 1500$ mm	=	2.50	1.67	1.25	0.83	0.56	0.42	0.28	0.21
h_2/t(mm s^{-1})									
C_s(g m^{-3})	= 86	83	74	67	52	33	19	7	3
100 C_s/C_o	= 100	96	86	77.5	60	38	22	8	3
$h_3 = 2250$ mm	=	3.75	2.50	1.90	1.25	0.83	0.63	0.42	0.31
h_3/t(mm s^{-1})									
C_s(g m^{-3})	= 86	84	76	70	56	40	27	12	5
100 C_s/C_o	= 100	98	88.5	81	65	46.5	31	13.5	6
$h_4 = 3000$ mm	=	5.00	3.33	2.50	1.67	1.12	0.83	0.56	0.42
$h_4 t$(mm s^{-1})									
C_s(g m^{-3})	= 86	85	77	71	59	46	34	17	8
100 C_s/C_o	= 100	99	89.5	83	69	53	40	20	9.5

successive time intervals t. These samples are analysed for suspended solids concentration C_s, and reported as a fraction of the original concentration C_o. Such data are given in *Table 4.8* and plotted in *Figure 4.22*.

If these values all lay on one single curve of 100 C_s/C_o against h/t, the suspension would be discrete with particles retaining their settling velocities at all depths. As the values for different depths give different curves on *Figure 4.22*, the particles are flocculating as they settle, thus having increasing settling velocities at increasing depths.

Note that the settling velocity h/t is only an apparent settling velocity (ν_a) because the particles have been growing in size due to flocculation, and accelerating during their descent through h and time t. So the true instantaneous settling velocity (ν_s) is a function of h:

$$t = \int_0^h \frac{\mathrm{d}h}{\nu_s} \tag{4.88}$$

$$\nu_a = \frac{h}{t} = h \Big/ \int_0^h \frac{\mathrm{d}h}{\nu_s}$$

$$\nu_a \int_0^h \frac{\mathrm{d}h}{\nu_s} = h \tag{4.89}$$

Differentiating with respect to h,

$$\frac{\mathrm{d}}{\mathrm{d}h}\left(v_\mathrm{a}\int_0^h \frac{\mathrm{d}h}{v_\mathrm{s}}\right) = 1 \tag{4.90}$$

$$\frac{v_\mathrm{a}}{v_\mathrm{s}} + \frac{\mathrm{d}v_\mathrm{a}}{\mathrm{d}h}\int_0^h \frac{\mathrm{d}h}{v_\mathrm{s}} = 1$$

$$\frac{v_\mathrm{a}}{v_\mathrm{s}} + \frac{\mathrm{d}v_\mathrm{a}}{\mathrm{d}h}\frac{h}{v_\mathrm{a}} = 1$$

$$v_\mathrm{s} = \frac{v_\mathrm{a}}{1 - \left(\frac{\mathrm{d}v_\mathrm{a}}{\mathrm{d}h} \times \frac{h}{v_\mathrm{a}}\right)} \tag{4.91}$$

So it is possible to calculate the true settling velocities of the particles from their apparent settling velocities. This, however, is rarely required and *Figure 4.22* gives sufficient information for the design of a settling tank, providing that the observations in the settling tube cover the full range of depth expected in the tank.

4.11 Current developments

Compared with the rapid development of new synthetic organic polymer flocculants, the developments in orthokinetic flocculations will be slower, as quite substantial hardware is usually involved. Certain trends which are apparent now may be developed further, or become more widely adopted.

4.11.1 Tubular flocculators

Tube settler modules are commonplace in settling tanks, but their basic function is to increase the total plan area for settlement, as required by settling tank theory. However, these tube modules also act as orthokinetic flocculators, mainly in laminar flow, with Reynolds' numbers of about 500.

In pipes at higher Reynolds' numbers, ranging from 2000 to 25 000, and therefore in turbulent flow, Döll[16] has demonstrated the mixing and flocculation conditions in laboratory systems. These employed silica particle suspensions, flocculated with three different cationic polymers, and the turbulent root mean square velocity gradient (G) characterized the influence of flow rate on reaction rate. In West Berlin, a practical pipe flocculator has been used prior to the entry of treated waste water into a sedimentation tank, based on the concepts set out in section 4.10.3, with the pipe set out in a snake-like pattern on the ground surface.

4.11.2 Fixed beds

The use of deep bed filters as flocculators is quite well established; some were developed in the 1950s as 'contact clarifiers' (USSR). If the suspended solids loading is light (e.g. below 150 mg l^{-1}) they may function without undue rapid clogging; but if the filtration effect dominates, the advantages of flocculating filtration may be lost.

At the other extreme, the static mixer, comprising labyrinth baffles in a tubular module, can only provide flocculation with no retention.

There is a possibility of a development between these two, with a packed bed providing flocculation with a non-clogging retention. An example of this is the 'Banks' pebble bed clarifier, where sewage that has been previously biologically treated flows upwards through a fixed bed of gravel (pebbles). The resulting flocculation produces biological flocs which settle back loosely on top of the pebble bed, not impeding the flow. The accumulated flocs can be periodically flushed away from the top surface.

4.11.3 Fluidized beds

Floc blanket clarification uses the flocs themselves to form the fluidized bed, to enhance flocculation. In laboratory models a particulate suspension (such as polymer spherical beads) may be used to form the fluidized bed. In any case, the upflow rate is limited by the settling velocity of the fluidized suspension. This is affected linearly by the density of the suspension particles, and greater upflows (therefore more production per unit plan area of tank) can be passed through more dense particle suspensions.

Advantage has been taken of this effect in fluidized bed flocculators in practice, which use 'micro-sand' on which flocculation takes place. This development, which was pioneered in Hungary, now appears as the 'Cyclofloc' process. The sand is coated (activated) with an alginate flocculant, and incoming suspensions of flocculent aluminium or ferric salts are flocculated by the fluidized bed and retained on the sand. A continuous discharge of some floc-coated sand, recycles it through an external washing process which separates the floc and the sand. The cleaned sand is continuously fed into the tank inflow to sustain a steady-state process.

Further development of this concept of solid particle nuclei for fluidized bed flocculation has been described by Sibony[17].

There are also processes developing in which the particles are ion-exchangers, charged with Al^{3+} ions which exchange with Ca^{2+} in hard waters. The released aluminium hydrolyses to form alum floc, which can be retained on the particles in a fluidized bed. Such particles can be withdrawn, washed clean, and recharged with Al^{3+}.

The combination of a paddle flocculator within a fluidized bed produces much denser flocs by the turbulent eddies which provide pressure gradients on the flocs, squeezing out their interstitial water. The resultant particles are

dense, with a layered onion-like structure. The high density enables high upflow rates through such modified floc blanket clarifiers[18].

References

1. Elson, T. P., 'Velocity profiles of concentric flow between coaxial, rotating cylinders with a stationary low boundary'. *Chem. Eng. Sci.*, **34**, 373–377 (1979)
2. Ives, K. J. and Al Dibouni, M., 'Orthokinetic flocculation of latex microspheres'. *Chem. Eng. Sci.*, **34**, 983–991 (1979)
3. Arp, P. A., and Mason, S. G., 'Orthokinetic collisions of hard spheres in simple shear flow'. *Can. J. Chem.*, **54**, 3769 (1976)
4. van de Ven, T. G. and Mason, S. G., 'The microrheology of colloidal suspensions. VII. Orthokinetic doublet formation of spheres'. *Colloid and Polymer Sci.*, **255**, 468–479 (1977)
5. Ives, K. J., *The Scientific Basis of Flocculation*, Sijthoff and Noordhoff, Alphen aan den Rijn, Netherlands (1978)
6. Ives, K. J. and Bhole, A. G., 'Study of flowthrough Couette flocculators. I. Design for uniform and tapered flocculation'. *Wat. Res.*, **9**, 1085–1092 (1975)
7. Ives, K. J. and Bhole, A. G., 'Study of flowthrough Couette flocculators. II. Laboratory study of flocculation kinetics'. *Wat. Res.*, **11**, 209–215 (1977)
8. Bhole, A. G., 'Measuring the velocity of water in a paddle flocculator'. *J. Amer. Wat. Wks. Ass.*, **72**, 109–115 (1980)
9. Vadas, E. B., Goldsmith, H. L. and Mason, S. G., 'The microrheology of colloidal dispersions. 1. The microtube technique'. *J. Coll. Interfac. Sci.*, **43**, 630–648 (1973)
10. Polasek, P., 'The significance of mean velocity gradient and its calculation in devices for water treatment'. *Water S. A.*, **5**, 196–207 (1979)
11. Bernhardt, H. and Schell, H., 'The technical concept of phosphorus elimination at the Wahnbach estuary using floc-filtration (Wahnbach system)' [in German]. *Wasser u. Abwass Forsch.*, **12** (3/4), 123–133 (1979)
12. Ives, K. J., 'Theory of operation of sludge blanket clarifiers'. *Proc. Inst. Civ. Engrs*, **39**, 243–260 (1968)
13. Hudson, H. E., 'Physical aspects of flocculation'. *J. Amer. Wat. Wks. Ass.*, **57**, 885–892 (1965)
14. Purchas, D. B., *Solid/Liquid Separation Equipment Scale-up*, Uplands Press, Croydon (1977)
15. Camp, T. R., 'Flocculation and flocculation basins'. *Trans. Am. Soc. Civ. Engrs*, **120**, 1–16 (1955)
16. Döll, B., 'Particle destabilization in turbulent pipe flow', *Proc. 14th IAWPRC Biennial International Conference* (Brighton, 1988), Book 2, pp. 435–442, IAWPRC, London (1988)
17. Sibony, J., 'Clarification with microsand seeding. A state of the art', *Water Res.*, **15**, 1281–1290 (1981)
18. Ide, T. and Kataoka, K., 'A technical innovation in sludge blanket clarifiers'. *Proc. Second World Filtration Congress (London)*, pp. 377–385, Filtration Society, Uplands Press, Croydon (1979)

5 Gravity clarification and thickening

L. Svarovsky

FPS Institute, England and University of Pardubice, Czech Republic

This chapter is devoted entirely to separation produced by particle settling due to gravitational forces. Buoyancy occurs in gravitational systems and the deciding factor for particle settling to take place is the difference between the density of the solids and that of the suspending liquid. The existence of the density difference is therefore a necessary pre-requisite in sedimentation.

Gravitational settling of particles in liquids is an age-old process which can be used for a variety of purposes[1]. For example, it is used for the classification of solids, washing, particle size measurement or mass transfer, and in solvent extraction. The majority of applications of gravity sedimentation, however, are in solid–liquid separation duty. The object here is to remove the solids from the liquid either because the solids and/or the liquid are valuable or because the two phases have to be separated before disposal.

The obvious advantage of gravity settling is its low cost. This is primarily due to the fact that, on a planet such as ours, the acceleration field is readily provided and all one has to do is provide a space (a vessel), some residence time and some pumping power to deliver the suspension into the vessel (or take the products of separation out of the vessel). One equally obvious disadvantage is that the acceleration field is relatively weak. It works well and the vessels are not excessively big for fast-settling slurries, i.e. for particles coarser than, say, 30 or 40 microns for most minerals, for example. If, however, the particle size is fine and/or the density difference is low, the residence times and vessel dimensions required for efficient separation become excessive and uneconomic. All is not lost, though, because one can still use pre-treatment to artificially increase the particle size and transform the slurry into a fast-settling one. For solid particles, coagulation or flocculation provide such an option (see chapter 4) and for immiscible liquid mixtures, coalescence may be promoted.

Descriptions and discussions of gravity sedimentation in textbooks (and this one is no exception) are usually dominated by water treatment and mineral processing applications. One must not lose sight, however, of the many chemical, pharmaceutical, nuclear, petrochemical or petroleum applications where gravity settling is used to resolve emulsions or to separate other liquid–liquid dispersions. As the density difference in such cases is nearly always low, the benefits of coalescence are usually sought. The present book, as per its title, is concerned primarily with solid–liquid systems and a reader interested in separation of liquid–liquid dispersions is referred to an excellent review of such applications (and of electrostatic coalescence) [2].

When the primary purpose is to produce the solids in a highly concentrated slurry then the process is called thickening. If the purpose is to clarify the liquid, the process is called clarification. The feed concentration to a thickener is usually higher than that to a clarifier. Some thickeners, if correctly designed and operated, can accomplish both clarification and thickening in one stage.

The available sedimentation equipment can also be divided into batch operated settling tanks and continuously operated units. The first group is ignored here because of the simplicity and much diminished use, particularly recently. There is still a role for batch settling tanks, however, where relatively small quantities of liquids are to be treated, for example in lubrication oil cleaning and reclamation. Furthermore, batch settling as repeated decantation is an effective and well-predictable particle classification process for small quantities of products. The bulk of the processing by sedimentation, however, is in continuously operated units and those are reviewed in the following.

5.1 Clarifiers

The conventional one-pass clarifier uses horizontal flow in circular or rectangular vessels. The usual design, shown schematically in *Figure 5.1*, has a rectangular basin with feed at one end and overflow at the other. An orthokinetic, paddle-type flocculator for pre-flocculation of the feed often forms an integral part of the clarifier. The settled solids are raked to a discharge trench by paddles or blades which are driven by a chain mechanism, or by a travelling bridge from above the water surface. Some square basin clarifiers use circular raking mechanisms (with the solids discharge point in the centre) but they have to incorporate supplementary rake arms that reach into the corners of the square basin.

In circular basin clarifiers, the feed is usually through a centrally located feed well and the overflow is into a trough around the periphery of the basin. The bottom slopes gently to the solids discharge point in the centre and the solids are pushed down the slope by a number of motor-driven scraper blades which revolve slowly around a vertical centre shaft. This design closely

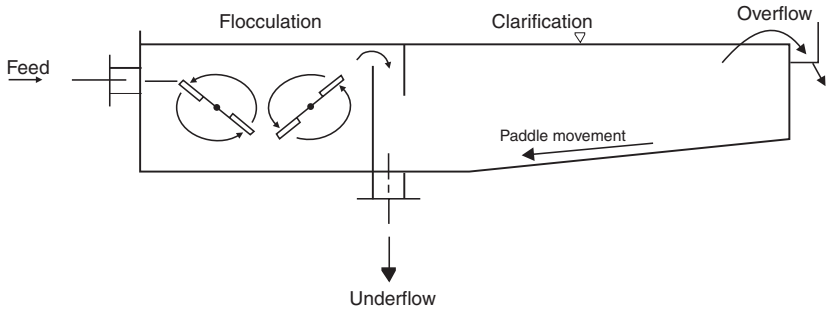

Figure 5.1 Rectangular basin clarifier

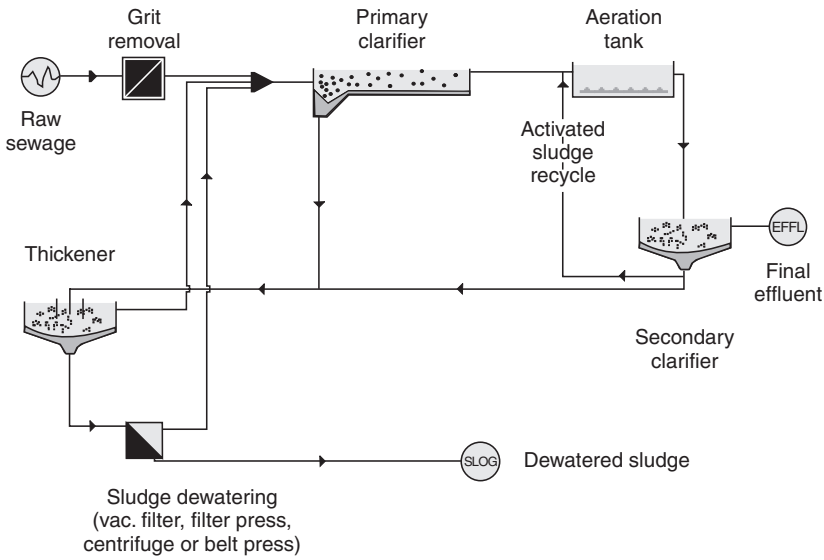

Figure 5.2 Schematic diagram of a sewage treatment plant (drawn with STOAT, Version 3, courtesy of WRc plc, Swindon)

resembles the conventional thickener described in the following section. The circular clarifiers can be stacked up in vertical multi-tray arrangements in order to save space. This is found in juice clarification applications, for example. Generally, the conventional clarifiers described above can be started and stopped without difficulty.

The largest user of gravity clarifiers is the water industry. *Figure 5.2* shows a schematic flow sheet of a typical sewage treatment plant where two stages

can be seen to consist of clarifiers: primary and secondary clarifiers. Sewage is a highly turbid liquid, consisting of a dilute complex mixture of mineral and organic matter in many forms, including:

1 coarse and fine solid particles floating and in suspension,
2 substances in true solution, and
3 very finely divided colloidal substances somewhere between the above two categories.

The object of modern methods of sewage treatment is to convert the unstable sewage into a stable effluent suitable for discharge to the local watercourse. The object is not, as is sometimes imagined, to produce an effluent of the quality of drinking water nor, necessarily, of the water in the receiving watercourse. In this treatment an offensive sludge is produced which must also be disposed of.

As can be seen from the schematic flow sheet, on arrival to the works the raw sewage passes first through some simple bar screens which remove the very coarse grit, plastic bags and other large objects. The first process of purification is the primary gravity clarifier of a design similar to that in *Figure 5.1*. After the settlement, the overflow still contains non-settleable polluting matter. This liquor is subjected to biological processes of aerobic oxidation and conversion of the remaining impurities to a settleable form. This can be done in two alternative pieces of equipment: biological ('slow', 'percolating', 'trickling') filters or activated sludge tanks. The latter method is becoming more popular and is shown in *Figure 5.1*.

An activated sludge tank is an aeration tank where a certain minimum solids concentration (required for the activation of the sludge) is maintained by an underflow recycle from the secondary clarifier which follows. The overflow from the secondary clarifier may be clean enough to be discharged into the local river as final effluent. The underflow then joins that from the primary clarifier and they both undergo thickening in a conventional thickener (see the following section, *Figure 5.9*). The underflow sludge may be further treated by anaerobic digestion and then further dewatered in a variety of alternative ways usually involving filtration. The dewatered sludge may then be incinerated, sold as a fertilizer or disposed of at sea. Both the filtrate and the thickener overflow are usually recycled into the plant feed as shown.

5.1.1 Design and scale-up of conventional one-pass clarifiers

The design overflow rate (flow rate per unit area of liquid surface) in conventional one-pass clarifiers is usually from 1 to 3 m /hour, depending on the degree of flocculation. Only clarifiers used with non-flocculating suspensions of low solids concentration can be modelled from first principles. The theory is identical with that for laminar plug flow in settling chambers for

cleaning gases [3] and, although clearly oversimplified, it is useful in making the best possible estimates of performance for non-flocculating systems. The grade efficiency curve $G(x)$ is given by

$$G(x) = u_g A/Q \tag{5.1}$$

where u_g is the terminal settling velocity of a particle of size x as determined from equation 18.10, Q is the feed flow rate which is often taken as approximately equal to the overflow rate, and A is the plan area of the basin. The above equation was derived assuming laminar plug flow in the tank and no end effects.

Note that equation 18.10 in chapter 18 essentially applies to settling at low particle concentrations (below 0.5% by volume) in Newtonian liquids, which have a constant viscosity. In principle, it can be also used in non-Newtonian fluids where viscosity μ then becomes the apparent viscosity but, depending on the type of the non-Newtonian behaviour (= model), its determination may require an iterative procedure. Not only is such behaviour shear-dependent (i.e. the apparent viscosity depends on how fast is the particle settling) but it may also be time-dependent and the model may contain a zero shear viscosity as a parameter. Ref. 4 reviews the state of the art to 1993 and research is still in progress, for example, on particle settling in the Carreau model fluids (e.g. polymeric liquids)[5].

Theoretically, the basin area A is the only design parameter affecting the theoretical separational performance, irrespective of the shape or depth of the pool. This is shown schematically in *Figure 5.3* which shows two vessels of

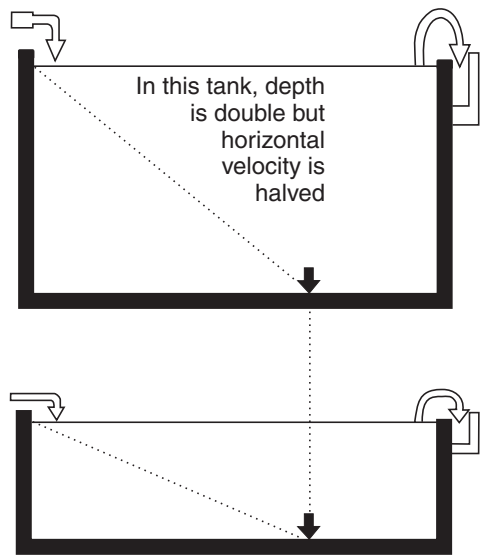

Figure 5.3 The vessel depth has no effect on the efficiency of a simple clarifier

the same plan area but one has one-half of the depth of the other. The same size particle is shown to enter both vessels at one end and it reaches the bottom at the same spot in both vessels. This is because, although the particle has a twice-as-long distance to settle in the deeper vessel, the flow velocity dragging it along horizontally is half, thereby cancelling the effect of the settling depth.

Equation 5.1 can be expressed in terms of conventional dimensionless groups as[1]

$$G(x) = Stk \cdot Fr \tag{5.2}$$

if Stokes' law is assumed for the particle settling velocity. The Stokes' number Stk is defined, for a Newtonian liquid, as

$$Stk = x^2 \cdot (\rho_s - \rho) \cdot Q/(18 \cdot \mu \cdot A \cdot H) \tag{5.3}$$

and Froude number Fr

$$Fr = H \cdot g \cdot A^2/Q^2 \tag{5.4}$$

where H is a characteristic dimension of the pool, e.g. its height, which in equation 5.2 cancels anyway, $(\rho_s - \rho)$ is the particle–fluid density difference, μ is the liquid viscosity and g is the acceleration due to gravity.

Equation 5.1 gives the model for a simple specific overflow-rate scale-up for the case of particulate clarification in Newtonian liquids where no flocculation takes place during settling (either the suspension is completely non-flocculant or the flocculation process is completed before the feed enters the basin). For the same performance, the flow rate is proportional to area or, from another point of view, the design area is proportional to the feed flow rate. As it is very difficult to measure the grade efficiency curve of a gravity clarifier (due to the long residence times involved during which the feed must remain constant) it is more practical simply to measure the specific overflow rate Q/A which gives satisfactory overflow clarity. This can be done in a pilot test or, more cheaply, in laboratory batch settling tests using the so-called short-tube procedure [6]. The sample is allowed to settle in and is decanted from a measuring cylinder to determine the overflow rate that gives satisfactory clarity. When the tests also include optimization of flocculant and its dosing, the procedure (and the equipment for it) is known as the 'jar test'[6].

If the clarification is not entirely 'particulate', i.e. when flocculation takes place during settling, the overflow clarity depends not only on the overflow rate but also on the detention time. The scale-up under such conditions is based on the long tube procedure[6]. This test is conducted in a vertical tube which is as long as the expected depth of the clarifier, under the ideal assumption that a vertical element of the suspension passing through the clarifier maintains its shape as it moves across the basin—see *Figure 5.4* for a schematic diagram.

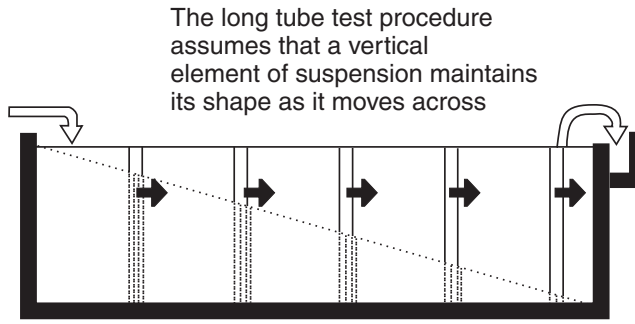

Figure 5.4 Schematic diagram of the long tube test (adapted from ref. 6)

Sometimes the effect of the detention time is so strong that the overflow rate can be ignored and the scale-up is based on the so-called second order test procedure (as the flocculation process usually follows a second order reaction model[6]). The required detention time is determined by testing the residual solids concentrations in the supernatant under the conditions of mild shear.

As a final note on the design of gravity clarifiers, specific guidance can be found in the literature for applications in the water industry, for example on the secondary clarifiers[7] such as the one in *Figure 5.2*.

5.1.2 Other types of clarifiers

As was pointed out above, when particulate clarification predominates, the most important design parameter is the pool area. The capacity per unit area can be substantially increased by using the Swedish invention called the Lamella clarifier/thickener[8] shown schematically in *Figure 5.5*, as manufactured for example by SALA or DENVER. It has a number of inclined plates stacked vertically, closely together. The flocculated feed enters the stack from the side feed box. The flow is upward between the plates while the solids settle out onto the plate surfaces and slide down into the sludge hopper underneath where the sludge is consolidated by vibration or raking. More even distribution of the flow through the plates is assisted by flow distribution orifices placed in the overflow exit.

The theoretical settling area is the sum of the horizontal projected areas of the individual plates but in practice, due to the various inefficiencies involved, only about 50% of this total area is usually effective. When treating sticky sludges the whole lamella pack can be vibrated (intermittently or continuously) to assist the sliding motion of the solids down the plates. In some designs the plates are corrugated instead of being flat, or they are replaced by tube bundles. In the latter case, the clarifier is called a 'tube settler' as manufactured, for example, by Wheelabrator (60° tube settlers). The tubes

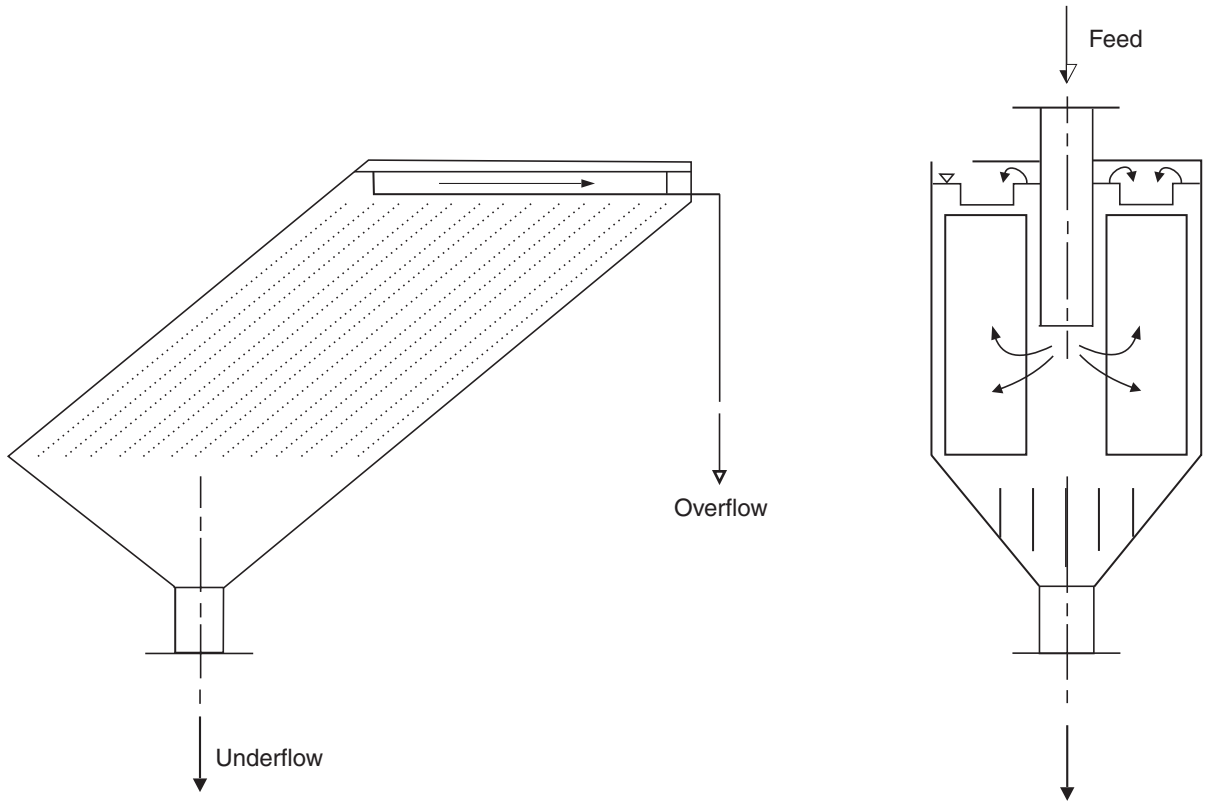

Figure 5.5 Lamella clarifier (may be also used as a thickener)

might be square, U-shaped or of other cross-section, typically 50 mm × 50 mm and about 1 m long.

The presence of an upper inclined surface in a shallow batch settling system is claimed to increase the settling rate of the particles due to the constant rearrangement necessary to keep the vertical concentration gradients level[9]. The phenomenon was observed and studied since 1920 but the enhancement has not been experimentally as high as predicted theoretically. In continuous settling systems and tube settlers in particular such rearrangement merely leads to a distinct flow pattern in the tubes, with clean liquid rising up through the tubes and settling solids falling to the settling surface. The saltation layer of sludge that forms at the bottom of each channel moves down the tubes (due to its greater weight) and a continuous counter-current flow is established. This merely speeds up the removal of the settled solids down the tubes and the overall theoretical settling capacity is no more than what corresponds to the projected plan area of all the tubes added together. In practice, as pointed out above, not all of this area is effective anyway.

The lamella plate and inclined tube principles have been used both in clarification and thickening since the early 1960s. Examples of applications include the treatment of coal, gas scrubber effluents, fly ash and leach solutions, or in battery manufacture. In coal concentration the typical overflow rates are from 1.7 to 2.9 m / hour.

An interesting combination of the Lamella sedimentation principle with an up-flow deep bed filter is known as the Rozka filter[10] shown schematically in *Figure 5.6*. This is in fact a filter-assisted clarifier sometimes used in water

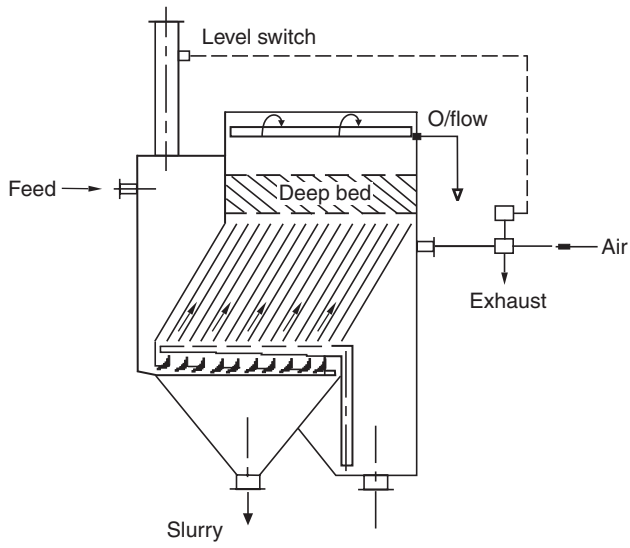

Figure 5.6 Rozka filter/thickener[9]

treatment. It allows higher overflow rates (typically from 3 to 7 m/hour) because it has an integral deep bed filter to treat the overflow which, due to the higher flow rate, might be cloudy. This is not an entirely new idea, as shallow layers of pea gravel or wedge-wire, suitably supported above a settler, have previously been used to improve the clarity of the overflow. In this design the bed is made of polystyrene spheres 1 to 2.5 mm in diameter and it floats on the overflow side of the tube settler. A screen above the bed keeps the bed in place and prevents it escaping with the overflow.

The feed suspension, treated with a flocculant, enters via the coagulation chamber and a distributor into the tube settler. There is a regeneration chamber alongside the settler and this is normally filled with air. When the pressure drop across the settler and the deep bed reaches a pre-set level, the level switch in the feed stand pipe triggers off the air exhaust valve which lets the air out of the regeneration chamber. The chamber quickly fills with water, thus lowering the water column in the settler and the bed, and the resulting back-flow cleans them both. The wash water is then slowly displaced from the regeneration chamber (as this is refilled with compressed air) back into the settler. The feed is not interrupted during this short regeneration cycle and the wash water is treated by the unit. Sizes from 1 to 12 square metres are available and examples of application include treatment of waste waters from paper and steel mills or from galvanizing processes, and pretreatment of surface water before ion exchange or reverse osmosis.

One last note about the lamella principle is to mention its enhancement with a high voltage electrostatic field. Generally, the enhancement of sedimentation velocities in non-aqueous suspensions by electrophoresis has been well exploited recently in solvent extraction[2]. Jayaswal *et al.*[11] have combined the lamella principle with electrophoresis and applied the system successfully to colloidal suspensions modelling those in the production of synthetic fuels from coal, oil shale and tar sands.

An interesting modification of a conventional, circular vessel clarifier specifically designed for treatment of waste water at sewage works has been described[12]. This involves installation of a horizontal annulus of a twin polyester membrane of a relatively large pore size (1.8 mm) next to the overflow launder around the periphery of the tank. This is essentially a crude filter placed in series with the settling tank. It is claimed that the flow lines converge on passage through the pores in the lower membrane, and the suspended solids agglomerate. The flocs then adhere to the membrane and produce a mat which filters out the fines. Larger sections of the mat fall away by gravity to the bottom of the tank. This system is supposed to allow loading of the conventional clarifiers up to or beyond their design capacity and protect against hydraulic overloading during storm conditions or a sudden deterioration in the feed sedimentation qualities. Hopefully, some operating data will emerge to allow technical evaluation of this interesting combination for separation principles.

There is another group of relatively newer clarifier designs which incorporate some vertical flow and combine gravity with inertial clarification, flocculation and solids recirculation. Some also use pulsed flow of liquid. Such units often achieve higher overflow rates and are referred to as 'rapid settling' or 'high rate' clarifiers. Flocculation is accelerated by external (or internal) recirculation of the settled solids into the feed. This leads to collection of fine particles by their interception with other solids. Fine sand may be added to induce separation by differential sedimentation (whereby fast-settling particles collide with the slow-settling ones), and this in some cases increases the overflow rates to as much as 8 m/hour.

Design and operation of recirculation systems can be complicated, however. Such problems are avoided by using a sludge blanket clarifier, in which the feed enters below a blanket of accumulated and heavily flocculated solids. The blanket is fluidized by the up-flowing feed and the feed solids are trapped in it. The solids content of the blanket increases continuously and a bleed stream is taken off to maintain the mass balance.

Sludge blanket clarifiers are available in flat bottom, trough bottom and hopper bottom types. The hopper bottom, vertical flow clarifier shown in *Figure 5.7* can achieve rates from 1 to 6 m/hour in waste water applications. It is 3 or 4 metres deep, with a 60 degrees square or circular hopper tank, and the feed is introduced via a downward pointing inlet, situated at the bottom of the tank. The flocculated feed suspension is clarified by its passage through the sludge blanket and it then overflows into decanting troughs that are usually one to 1.5 metres above the blanket. The blanket can be continuously bled off through a submerged weir-type regulator and then thickened in a conical concentrator, or the clarifier can be periodically shut down to allow settlement bleeding.

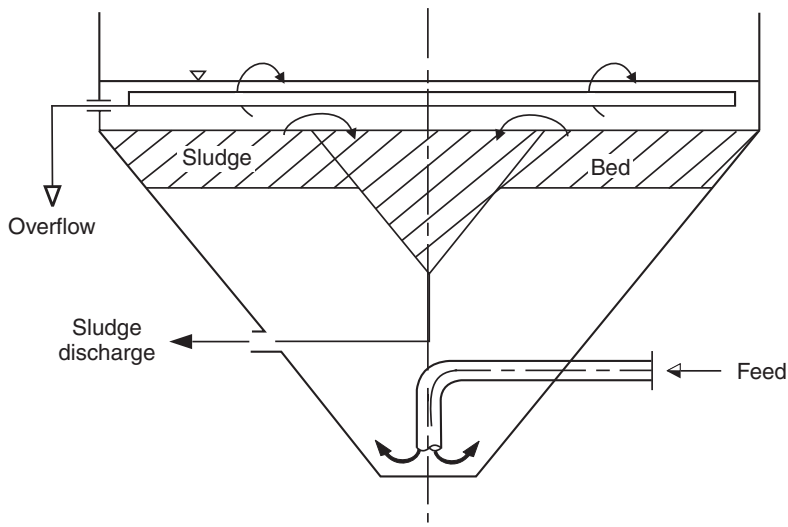

Figure 5.7 Hopper bottom vertical flow clarifier

The sludge blanket clarifiers are difficult to start up until the first blanket is established, and the large-scale units require major excavation due to their substantial depth. The available sizes range from 0.6 m × 0.6 m to 50 m × 50 m. Precipitation and crystallization can be carried out in similar hopper-shaped units, at higher overflow rates up to 80 m / hour or more.

The design of the sludge blanket clarifiers is usually based on the 'jar test' and a simple measurement of the blanket expansion and settling rate[6]. Different versions of the jar test exist but it consists essentially of a bank of stirred beakers which are used as flocculators to optimize the flocculant dosage for maximum solids settling rate. Visual floc size evaluation is also possible. A simple device has been developed for settling, clarification and filtration experiments necessary for the determination of the empirical constants in a new model of separation in sludge blanket clarifiers[13]. Alcan have developed a continuous settling analyser (as opposed to a batch settling experiment in a jar test) known as the Dynafloc[14], which is claimed to have overcome the frequent overdosing as a result of using the conventional jar test.

A combination of gravity settling and slow cyclonic action was first patented in 1983[15] and has since been available commercially. It is known as the hydrodynamic or 'gravity-and-vortex-induced' separator and used for the excess storm water treatment or for the separation of grits and sands from raw sewage and other liquids.

The principle of the new separator shown schematically in *Figure 5.8* is gravity settling in a circular vessel, from a slow vortex flow induced by a tangential feed. The bottom of the vessel is conical, with a large included angle, from which the settled solids are swept towards the central underflow discharge. The radially inward flow at the bottom responsible for the sweeping action is often referred to as the 'tea cup effect'. This is caused by rotating eddies that form in cyclonic flows in vessels with wide included angles or flat bottoms (such as in a tea cup having just been stirred where the settled tea leaves can be seen to move towards the centre of rotation).

The vessel design features a Chinese hat-like conical core stopper above the underflow sump, which is there to prevent the vortex reaching the latter and re-entraining the settled solids. The core stopper is also believed to stabilize and locate the vortex flow in the vessel.

The overflow from the vessel is through a wide cylindrical insert through the lid (similar to a vortex finder in a hydrocyclone[16]) and an optional provision can be made for collecting any floatables in a float trap.

Units are available in stainless steel or protected mild steel, often prefabricated, up to 12.5 m in diameter, capable of processing up to 5 m^3/s or more depending on the separation efficiency required. When the separator is used for classification of granular solids, smaller diameter units are used, up to 4 m in diameter, separating nearly all particles coarser than about 150 microns.

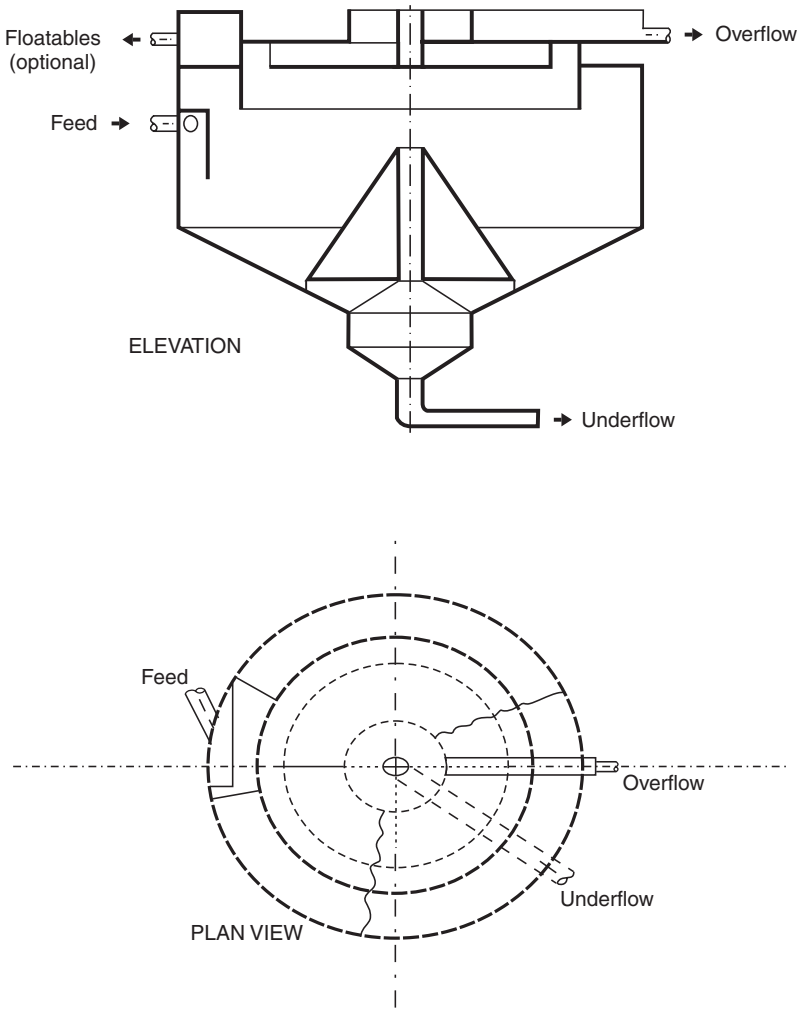

Figure 5.8 A schematic diagram of the gravity-and-vortex-induced separator (courtesy of Hydro Research & Development Ltd)

5.2 Thickeners

The most common thickener is the circular basin type shown in *Figure 5.9*. The flocculant-treated feed slurry enters through the central feed well which disperses the feed gently into the thickener. The feed suspension falls until it reaches a height where its density matches the density of the surrounding suspension and it spreads at that level. Solids concentration increases in the downward direction and this gives stability to the thickening process. The overflow is collected in a trough around the periphery of the basin. Raking mechanisms, slowly turning around the centre column, promote solids

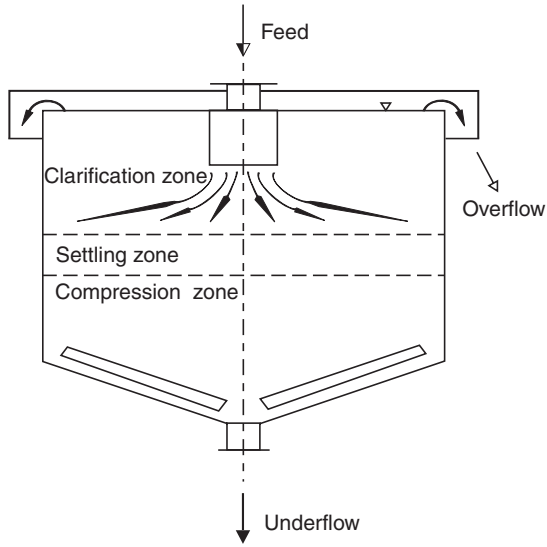

Figure 5.9 Circular basin thickener

consolidation in the compression zone and aid solids discharge through the bottom central opening.

Three layers of different settling regimes can be found in an operating thickener: a clarification layer, a zone settling layer (see chapter 18, Part I for explanation of zone settling) and a compression layer. The feed is often in the zone settling regime by the time it enters the thickener, due to the addition of flocculating agents. In that case, there is no theoretical need for a clarification layer because there is little chance for particles to escape through the interface between the zone settling layer and the supernatant clean liquid. In practice, however, the clarification layer is provided as a buffer for fluctuations in the feed and the interface level.

The most important design dimensions of a thickener are the pool area and the depth. The pool area is chosen as the largest of the three layer requirements. In most cases, only the zone settling and compression layer requirements need be considered. When the clarity of the overflow is critical, however, the clarification layer may need the largest area. As to the pool depth, only the compression layer has a real depth demand because the concentration of the solids in the underflow is largely determined by the detention time (as well as by the static pressure sometimes). The thickness of the other two layers is determined by practical considerations only.

5.2.1 Design and scale-up of gravity thickeners

The design and scale-up of conventional gravity thickeners is usually based upon batch settling tests on suspensions in the zone settling regime as

discussed in chapter 18. The assumptions behind this conventional method are as follows:

1 The settling velocity is only a function of slurry concentration.
2 The feed slurry is in the zone settling regime.
3 The largest area demand is in the zone settling layer.
4 Laboratory batch settling data are representative of the conditions inside a continuously operating thickener.

The critical settling flux, the knowledge of which is essential for the evaluation of the zone settling layer area demand of the thickener, is determined either by the Coe and Clevenger method or the simpler Talmage and Fitch procedure[6]. The former consists of a series of settling tests in a measuring cylinder where the initial settling rates of a visible interface in the suspension are measured at different initial solids concentrations. The Talmage and Fitch procedure simplifies the tests because it requires only one test at any concentration providing it is in the zone settling regime. Theoretically, the two methods should give an identical critical settling flux (and therefore identical pool areas) but this is not so in practice. Usually, the Coe and Clevenger method leads to underdesign of the thickener area whilst the Talmage and Fitch procedure tends to overdesign.

Either of the methods produces an experimental curve of the settling velocity u as a function of the slurry concentration c. From this data, settling flux $G_s(c)$ (= mass mass flow of the solids per unit thickener area, $kg \cdot m^{-2} s^{-1}$) is calculated using the following simple equation:

$$G_s(c) = c \cdot u(c) \tag{5.5}$$

$G_s(c)$ usually has a shape similar to that shown in *Figure 5.10* and only needs to be determined for concentrations between the feed and the underflow. Another measurement that is needed is an estimate of the achievable under-

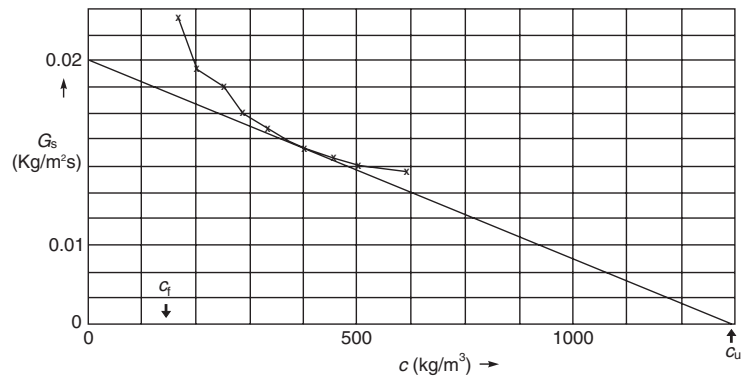

Figure 5.10 A settling flux plot for the data in Example 5.3, showing the determination of the critical flux G_c

flow concentration c_u and this is determined from simple time detention tests[6]. Using $G_s(c)$ and c_u, Coe and Clevenger derived an equation for the calculation of the total flux (being the sum of the settling flux and the transport flux) and showed that the critical flux is the minimum on the total flux curve between the feed and underflow concentrations. This minimum represents a layer inside an operating thickener, somewhere between the feed and the underflow, which can take the least solids through it. If the feed rate is greater than this critical flux, this layer will expand and lead to solids overflow.

The critical flux determination as proposed by Coe and Clevenger is no longer used because it is unnecessarily cumbersome. Yoshioka and Hotta[17] proposed a simpler method which does not require plotting (or repeated replotting) of the total flux curve. It uses the settling flux curve directly (see *Figure 5.10*) by drawing a tangent to the underneath of the curve, starting from the (estimated) underflow concentration on the *x*-axis. Note that all the points on the curve between the feed and underflow must lie above this tangent. The value of the critical flux G_c is where the straight line bisects the *y*-axis. The design area of the thickener A is then calculated as a simple mass balance, which assumes a complete separation of all solids into the underflow:

$$G_c \cdot A = Q \cdot c_f \tag{5.6}$$

See example 5.3 (page 186) for a calculation based on actual experimental results.

With highly flocculant slurries like waste water sludges and similar materials, the area demand of the compression layer may exceed that of the zone settling layer, and the compression zone also has a depth demand. No laboratory tests for this had existed until Kos[18] described a 'multiple-batch-upflow test' for compression zone evaluation. This is by no means standard yet, however, and its reliability remains to be seen in the future. Sludge compressibility testing can be speeded up by using a slow, 'long arm' bottle centrifuge. As always, pilot or large-scale tests, if properly conducted and evaluated, yield the best test data for thickener design.

5.2.2 Applications, construction and types of gravity thickeners

Most of the applications of gravity thickeners are in mineral and coal processing, and in waste water treatment. Typical examples include thickening of alumina red mud, alumina hydrate, coal and tailings, copper middlings and concentrate, magnesium hydroxide, china clay, phosphate or potash slimes, pulp mill wastes, gas washing effluents, and also in hydrometallurgical installations for the separation of dissolved components from leached residues in countercurrent washing configurations in the production of copper, uranium, aluminium and precious metals.

The conventional, circular basin thickeners are constructed of steel up to about 25 m in diameter or concrete up to 200 m in diameter. The floor is

usually sloped towards the underflow discharge in the centre, although some flat bottomed units are also in operation. The largest thickeners might have their bottom simply excavated out of earth. The raking mechanisms used in all units turn slowly around the centre column, thus aiding solids discharge and consolidation in the compression layer. The smaller units might be covered for the conservation of heat or to prevent freezing-up of the thickener in colder parts of the world.

The centre drive mechanism and the feed launder are usually supported by a walkway which extends across one half, or the whole diameter of the basin. If the drive mechanism and the rakes are supported by a truss across the diameter of the thickener, such units are referred to as bridge machines. Bridge thickeners usually do not exceed 25 to 45 m in diameter. Larger diameter thickeners have the drive mechanisms supported by a central column or pier, and the rakes are driven and supported by a drive cage. The discharge of the sediment is into an annular trench around the column.

Larger still, caisson thickeners have the central column large enough to accommodate the discharge pumps in the bottom of the column. The discharge pipework passes through the column and along the access walkway above the basin. The caisson thickeners can be built to very large diamaters of up to 200 m, often with earth bottom.

The thickeners described above use fixed connections to drive the rake arms. Another possibility is to drag the arms by cables or chains suspended from a drive boom which is rigidly connected to the drive mechanism. The rake arms are connected to the bottom of the central column by a special arm hinge which allows both horizontal and vertical movement of the rakes. This means that the rakes are lifted automatically if the torque becomes excessive. The drive arm can be below the liquid level or, if scaling is a problem, it can be above the basin.

The last common configuration of the conventional thickener is the traction thickener. The movement of the rake mechanism is provided here by a single long arm, pivoted round the centre column and driven by a drive trolley which travels on a peripheral rail around the basin. Such units exist from 60 to 130 m in diameter.

The thickeners described so far in metallurgical and mineral processing applications handle solids fluxes (mass flow rates per unit area) from 0.010 to 0.025 kg/m^2. Better understanding of the working and application of flocculating agents has led to the development of new, high capacity thickeners, which are capable of handling much higher solids fluxes of up to 0.2 or even 0.4 kg/m^2.

In the USA several companies market more efficient and compact thickeners, fully equipped with instrumentation and sensing devices. Some claims are made for improved equipment design but the higher thickening rates are mostly due to better use and control of flocculant addition. One example is the Dorr–Oliver Hi-rate Thickening System which uses a Fitch feed well (ref. 19, *Figure 5.24*). This is a new type of feed well consisting of three horizontal

shelves inside a cylinder. The feed is split into two streams, fed tangentially into the well in such a way that they impinge on each other. The dilute flocculant is added into the zone of shear, between the upper and lower feed shelves, where it mixes uniformly with the feed.

Two American thickener designs are based on feeding the slurry under the settling solids interface in a way similar to the sludge blanket clarifiers described in the previous section. They also have other features, all designed to accelerate the flocculation and increase the capacity.

The Eimco Hi-Capacity thickener introduces the feed from the top, through a hollow shaft which incorporates flocculant addition and a mixing device. The feed is then directed under the established sludge line which partially submerges a set of inclined settling plates. The settled solids are raked by a conventional mechanism at the bottom of the basin.

The principle of another high capacity unit, the Enviro-Clear thickener, is shown in *Figure 5.11*. The flocculated feed enters vertically from the bottom and is directed horizontally at a controlled velocity into the sludge blanket by an impingement plate. A number of other arrangements are offered: the feed can, for example, enter from the top, through a central well surrounding the drive shaft. A side glass allows visual observation of the sludge line. Available sizes range from 4 to 18 m diameter, with typical overflow rates from 2.5 to 14 m / hour. The applications include sugar production, mineral processing and the paper industry.

Another alternative in the manufacturers' efforts to increase the capacity per unit area is stacking up thickeners in vertical arrangements. Such units are known as multiple compartment or tray thickeners and consist of two or more conventional compartments up to 35 m in diameter. Each compartment has a set of raking arms operating from a rotating central shaft common to the whole

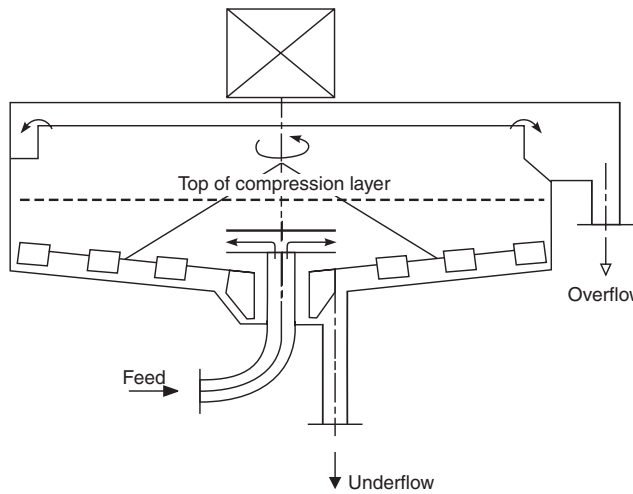

Figure 5.11 Enviro-Clear thickener

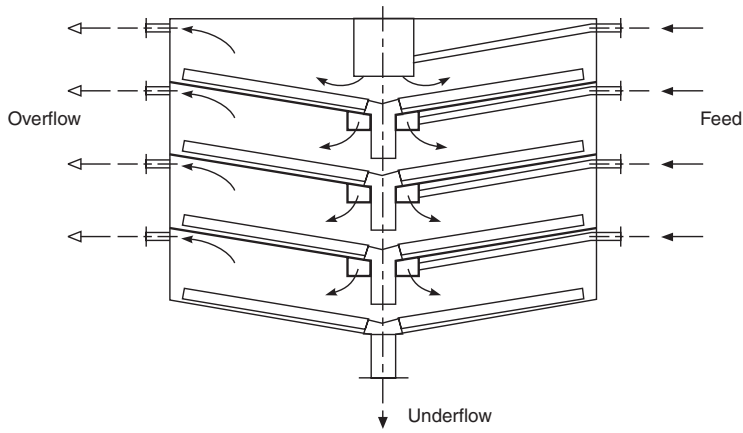

Figure 5.12 Tray thickener

stack. The compartments can be used either in series or in parallel. *Figure 5.12* shows an example of the parallel arrangement where each compartment has separate feed and overflow lines. It has to be said, however, that in some applications the tray thickeners do not perform well and have been replaced by deep vessels (by just taking out the innards of an installed tray thickener).

The Lamella thickener/clarifier also comes into this category but it has already been described in the previous section on clarifiers.

Another interesting development is that of high compression thickeners which are a lot deeper than the conventional ones and, consequently, are capable of producing more concentrated underflows. One such system is the deep cone thickener developed by the National Coal Board (now British Coal) in the UK [20]. This is based on a deep cone vessel and has been used for the treatment of coal and metallurgical ores since the early 1900s. As can be seen in the schematic diagram in *Figure 5.13* the vessel is equipped with a slow turning stirring mechanism (about 2 revs per minute) which enhances flocculation in the upper part, and acts as a rake in the lower section. The unit is used for densification of froth flotation tailings at overflow rates from 6.5 to 10 m / hour, with the final discharge moisture content from 25 to 35% by weight.

There are other commercial deep cone thickeners available and they are particularly suitable, as is the NCB unit, where the ultimate underflow density is increased by the large static head above the discharge point, e.g. with flocculated clays or other minerals, or waterworks sludges. This may be combined with better application of flocculation and with the use of mechanical 'pickets' to 'work' the compacting slurry to produce a 'high density thickener' for red mud thickening [21]. Another such example is the Supaflo High Compression Thickener [22] which uses a compression zone thickness about double that found in conventional thickeners. Bottom slopes are steepened to assist the transport of settled solids to the discharge, and the raking power is increased.

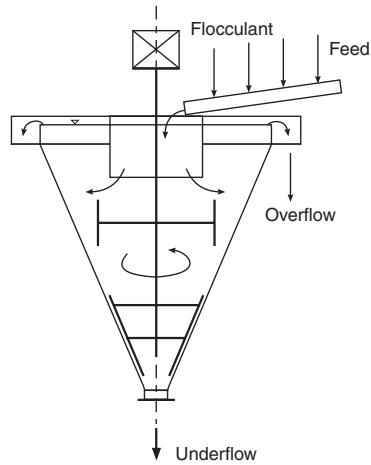

Figure 5.13 Deep cone thickener

An unraked version of the deep cone thickener was developed for the thickening of red mud (insoluble residue from caustic digestion of bauxite in the Bayer process) in a counter-current decantation system[23,24,25]. The deep cone units (the last two in a nine-stage system), while smaller in diameter for the same solids throughput, were able to produce thicker underflows than the remaining seven conventional, raked thickeners[24]. This greater thickening achieved in the deep cone units translates into fewer stages needed for the same washing and thus represents a further space saving.

Example 5.1 Clarifier cut size prediction

Check the ideal cut size of a settling tank used to remove silt from river water, the water being used as make-up water for the cooling system of a conventional coal-fired power station. The plan area of the tank is 1052 m^2, the water feed flow rate is 0.693 m^3/s, the density of the silt is 2600 kg/m^3, the density of water is 1000 kg/m^3 and viscosity is 0.001 Ns/m^2.

Solution 5.1

Equations 5.2 to 5.4 combined give the following relationship and the result for the cut size (i.e. when $G(x_{50} = 0.5)$:

$$x_{50} = \sqrt{\frac{18\mu Q}{2(\rho_s - \rho)gA}} = \sqrt{\frac{18^*0.001^*0.693}{2^*1600^*9.81^*1052}} = 19.4^*10^{-6}\text{m}$$

Note that the above is an example from industrial practice. The actual cut size obtained from subsequent measurements was much lower (about 4 microns as opposed to 19.4 microns) and this was a sure indication of flocculation taking place in or before the settling tank.

Example 5.2 Preliminary design of a settling vessel

Estimate the area of a gravity settler to achieve the cut size of 25 microns under the following conditions:

Liquid feed flow rate	$Q = 0.5\,\mathrm{m^3/s}$
Liquid density	$\rho = 1000\,\mathrm{kg/m^3}$
Solid density	$\rho_s = 2600\,\mathrm{kg/m^3}$
Liquid viscosity	$\mu = 0.001\,\mathrm{Ns/m^2}$
Feed concentration	$c =$ less than 0.5% v/v

Solution 5.2

For feed concentrations less than 0.5% v/v and particle size of 25 microns, Stokes' law in equation 5.3 can be assumed. As $G(x_{50}) = 0.5$, equations 5.2 to 5.4 combined give the area $A = 458.7\,\mathrm{m^2}$.

Example 5.3 Thickener design

Calculate the minimum area and the diameter of a thickener with a circular basin to treat $0.2\,\mathrm{m^3/s}$ of a slurry of concentration of $150\,\mathrm{kg/m^3}$. A value of $1200\,\mathrm{kg/m^3}$ for the underflow concentration was measured from a detention time test and the results of batch settling tests are as follows:

Concentration c ($\mathrm{kg/m^3}$)	*Settling velocity u(c)* (μm/s)
167	138.9
200	97.2
250	72.2
286	56.0
333	44.4
400	33.3
455	27.8
500	24.2
590	19.8

Solution 5.3

Firstly, settling flux G_s has to be calculated for every value of c in the table of measured data using equation 5.5:

Concentration c (kg/m^3)	*Settling velocity u* (microns/s)	*Settling flux* $G^s(c)$ (kg/m^2·s)
167	138.9	0.0232
200	97.2	0.0194
250	72.2	0.0181
286	56	0.0160
333	44.4	0.0148
400	33.3	0.0133
455	27.8	0.0126
500	24.2	0.0121

$G_s(c)$ is then plotted against c (see *Figure 5.10*) and a tangent is drawn to the curve, starting from the point corresponding to $c_u = 1200\,\text{kg/m}^3$ on the x-axis. Note that all the points on the curve between the feed and underflow must lie above this tangent.

The intercept on the y-axis determines the critical flux, which in this case is $0.02\,\text{kg/(m}^2\,.\,\text{s)}$. Assuming complete separation, equation 5.6 gives the thickener area $A = 1500\,\text{m}^2$, from which the diameter works out as $D = 43.7\,\text{m}$.

Further problems with answers

1 Calculate the minimum area and the diameter of a thickener with a circular basin to treat $0.2\,\text{m}^3/\text{s}$ of a slurry which contains $20\,\mu\text{m}$ particles of silica (density $2600\,\text{kg/m}^3$) suspended in water (density $1000\,\text{kg/m}^3$ and viscosity $0.001\,\text{Ns/m}^2$) at a concentration of $650\,\text{kg/m}^3$. Assume that the slurry cannot be tested and do your calculations on the basis of the Richardson and Zaki equation (equations 18.12 and 18.15 combined), i.e. $u/u_g = \varepsilon^{4.7}$ (notation as in chapter 18). Take the underflow concentration as $1560\,\text{kg/m}^3$ and also calculate the underflow volumetric flow rate assuming total separation of all solids. **Ans.** $1326.5\,\text{m}^2$, $41.1\,\text{m}$, $0.083\,\text{m}^3/\text{s}$.

2 Calculate the minimum area and diameter of a thickener with a circular basin to treat $0.1\,\text{m}^3/\text{s}$ of a slurry of solids concentration of $150\,\text{kg/m}^3$. The results of batch settling tests are as follows:

Concentration c (kg/m^3)	*Settling velocity u* (microns/s)
100	148.00
200	91.00
300	55.33
400	33.25
500	21.40
600	14.50

Table (*Contd.*)

Concentration c (kg/m^3)	*Settling velocity u* (microns/s)
700	10.29
800	7.38
900	5.56
1000	4.20
1100	3.27

A value of 1290 kg/m^3 for the underflow concentration was selected from a detention time test. Also estimate the underflow volumetric flow rate assuming total separation of all solids present in the feed. **Ans.** 974 m^2, 35.2 m, 0.0116 m^3/s.

Note: This problem was set by L. Svarovsky and used in a third year examination in chemical engineering at the University of Bradford in 1977.

References

1. Svarovsky, L., 'Sedimentation', *Kirk-Othmer Encyclopedia of Chemical Technology*, 4th edn, Volume 21, John Wiley & Sons, New York, ISBN 0–471–52690–8, 667–685 (1997)
2. Bailes, P. J., Freestone, D. and Sams, G. W., 'Pulsed DC fields for electrostatic coalescence of water-in-oil emulsions', *The Chemical Engineer*, 23 October, 34–39 (1997)
3. Svarovsky, L., *Solid-Gas Separation*, Elsevier, Amsterdam (1981)
4. Chabra, R. P., *Bubbles, Drops and Particles in Non-Newtonian Fluids*, CRC Press, Boca Raton, Fl. (1993)
5. Machac, I., Siska, B. and Machacova, L., 'Terminal falling velocity of spherical particles moving through a Carreau model fluid', *Chem. Eng. Proc*., accepted for publication in early 2000
6. Fitch, E. B. and Stevenson, D. G., *Gravity Separation Equipment, in Solid–Liquid Separation Equipment Scale-Up*, (Ed.) by D. B. Purchas, Uplands Press, London, 81–153 (1977)
7. Albertson, O. E., 'Design procedures for industrial secondary clarifiers', Paper B2.5, AFS Seminar and Expo, System Approach to Separation and Filtration Process Equipment, Chicago, Illinois USA, May 3–6, 1993, paper published in *Advances in Filtration and Separation Technology*, Vol. 7, American Filtration Society, Kingwood, Texas, April, 198–203 (1993)
8. Wenk, S. E., 'The Lamella gravity settler; theory, design and experience', Paper B2.6, AFS Seminar and Expo, System Approach to Separation and Filtration Process Equipment, Chicago, Illinois USA, May 3–6, 1993, in *Advances in Filtration and Separation Technology*, Vol. 7, American Filtration Society, Kingwood, Texas, April, 204–207 (1993)
9. Rushton, A., Ward, A. S. and Holdich, R. G., *Solid–Liquid Filtration and Separation Technology*, VCH, Weinheim (1996)

10. Rozkydalek, J. and Tesarik, I., 'Upflow filtration through a buoyant filter bed', undated paper SS9, 20–23, Technical University of Brno, Faculty of Civil Engineering, 637 00 Brno, Czech Republic, also CS Patent 141 652
11. Jayaswal, U. K., Gidaspow, D. and Wasan, D. T., 'Continuous separation of fine particles in nonaqueous media in a lamella electrosettler', *Separations Technology,* Vol. 1, Butterworth-Heinemann, 3–17 (1990)
12. Thorndahl, U. and Molyneux, B., 'Improvement of sludge sedimentation by installation of upward flow clarifiers', *Filtration & Separation*, September, 747–748 (1995)
13. Lin, J. L., *Ind. Engng. Chem. Process Des. Dev*., **20**, 3, July, 456–459 (1981)
14. 'Dynafloc, settling analyser by Alcan', Alcan International Limited, 188 Sherbrooke Street W., Montreal, Quebec, Canada H3A 3G2 (undated)
15. Smisson, B., *A Separator*, UK Patent GB 2 082 941 B, published 6 July, 1983
16. Svarovsky, L., *Hydrocyclones*, Holt Rinehart & Winston, London (1984)
17. Yoshioka, N., Hotta, Y., Tanaka, S., Naito, S. and Tongami, S., 'Continuous thickening of homogeneous slurries', *Chemical Engineering*, Tokyo, **21**, 66–74 (1957)
18. Kos, P., 'Theory of gravity thickening of flocculant suspensions and a new method of thickener sizing', *Proceedings of the Second World Filtration Congress 1979*, Olympia, London, Sept. 18–20, Filtration Society, 595–603 (1979)
19. Osborne, D. G., 'Gravity thickening', Chapter 5 in *Solid–Liquid Separation*, 3rd edn, (Ed.) L. Svarovsky, Butterworths, London, 132–201 (1990)
20. Abbott, J., 'Control systems and operational features of the deep cone thickener', *Filtration & Separation*, July/August, 376–393 (1979)
21. Marunczyn, M. and Laros, T. J., 'Bauxite residue disposal at Alcoa of Australia using the Hi-Density thickener', Paper B2.2, AFS Seminar and Expo, System Approach to Separation and Filtration Process Equipment, Chicago, Illinois USA, May 3–6, 1993, paper published in *Advances in Filtration and Separation Technology*, Vol. 7, American Filtration Society, Kingwood, Texas, April, 180–188 (1993)
22. Green, D., 'High compression thickeners are gaining wider acceptance in minerals processing', *Filtration & Separation*, November/December, 947 (1995)
23. Chandler, J. L., 'Dewatering by deep thickeners without rakes', *Filtration & Separation*, March/April, 104–106 (1983)
24. Chandler, J. L., 'Deep thickeners in countercurrent washing', IChemE Symposium on Solids/Liquids Separation Practice, Leeds, April 2–5, 177–182 (1984)
25. Paradis, R. D., 'Application of Alcan's deep thickener technology for thickening and clarifying', Paper B2.1, AFS Seminar and Expo, System Approach to Separation and Filtration Process Equipment, Chicago, Illinois USA, May 3–6, 1993, paper published in *Advances in Filtration and Separation Technology*, Vol. 7, American Filtration Society, Kingwood, Texas, April, 175–179 (1993)

Further reading

Bustos, M. C. and Concha, F., 'Settling velocities of particulate systems 10. A numerical method for solving Kynch sedimentation processes', *Int. J. Mineral Processing*, **Vol. 57**, No. 3, September, (1999)

Emmett, R. C., 'Selection and sizing of sedimentation–based equipment'. *In* (A. L. Mular and M. A. Anderson., Eds), *Design and Installation of Concentration and Dewatering Circuits,* Chap. 7, Soc. Mining Engineers, SME AIME,(1986)

Freitas, K. A., Fernandes, A. L., Barozzo, M. A. S. and Damasceno, J. J. R., 'Performance evaluation of a continuous thickener with filtering bottom', Proceedings Volume II, World Filtration Congress 8, European Federation of Chemical Engineering Event No. 607, organised by The Filtration Society and Elsevier Science, The Brighton Centre, Brighton, UK, 3–7 April 2000, 957–960 (2000)

Handley, J., 'Sedimentation: an introduction to solids flux theory', *Water Pollut. Control,* Paper 5, 230–240 (1974)

Keane, J. M., 'Sedimentation: theory, equipment and methods', *World Mining,* **Nov**., (1979)

King, D. L., 'Thickeners'. *In* (A. L. Mular and R. B. Bhappu, Eds) Chap. 27, pp. 541–577, Soc. Mining Engineers, SME AIME, (1980)

Leung, W. W. F., 'Flow in inclined plate settler', Proceedings Volume II, World Filtration Congress 8, European Federation of Chemical Engineering Event No. 607, organised by The Filtration Society and Elsevier Science, The Brighton Centre, Brighton, UK, 3–7 April 2000, 953–956 (2000)

Richardson, J. F. and Zaki, W. N., 'Sedimentation and fluidisation', *Trans. Inst. Chem. Eng.,* **32**, 35 (1954)

Ruiz, M. I., Arouca, F. O., Murata, V. V. and Damasceno, J. J. R., 'The use of gamma rays attenuation technique in the characterisation and mathematical modelling of batch sedimentation', Proceedings Volume I, World Filtration Congress 8, European Federation of Chemical Engineering Event No. 607, organised by The Filtration Society and Elsevier Science, The Brighton Centre, Brighton, UK, 3–7 April 2000, 407–410 (2000)

Savage, P., 'NCB refines waste dumping', *Coal Age,* **May**, 184–188 (1980)

Tiller, F.M. and Li, W., 'Catscan study of sedimentation', Proceedings Volume II, World Filtration Congress 8, European Federation of Chemical Engineering Event No. 607, organised by The Filtration Society and Elsevier Science, The Brighton Centre, Brighton, UK, 3–7 April 2000, 945–948 (2000)

6 Hydrocyclones

L. Svarovsky

FPS Institute, England and University of Pardubice, Czech Republic

Nomenclature

c	Feed solids concentration (fraction by volume)
c_o	Solids concentration in the overflow (by volume)
c_u	Solids concentration in the underflow (by volume)
Cy	Characteristic cyclone number
D	Hydrocyclone body diameter
D_i	Inlet equivalent diameter (by area)
D_o	Overflow diameter
D_u	Underflow diameter
E_T	Total mass recovery
E'_T	Reduced total recovery defined as $E'_\mathrm{T} = [E_\mathrm{T} - R_\mathrm{f}]/(1 - E_\mathrm{T})$
Eu	Euler number
$G(x)$	Grade efficiency (efficiency of separation for particle size x)
$G'(x)$	Reduced grade efficiency defined as $G'(x) = [G(x) - R_\mathrm{f}]/(1 - R_\mathrm{f})$
l	Vortex finder length
K	Constant
L	Overall length of hydrocyclone body
n	Exponent
n_p	Exponent
N	Number of hydrocyclones in parallel
m	Constant
p	Constant
Q	Suspension feed flow rate in each hydrocyclone
Q_T	Total suspension feed flow rate
r	Radius or constant
R_f	Underflow-to-throughput ratio (flow ratio)
Re	Reynolds number
Stk_{50}	Stokes' number
Stk'_{50}	Reduced Stokes' number (based on x'_{50})
Ss	Geometric standard deviation of $G'(x)$
T	Residence time
v_a	Axial velocity

v	Characteristic velocity
v_t	Tangential velocity
v_r	Radial velocity
x	Particle size
x_g	Solids mass median size
x_{50}	Cut size (particle size at $G'(x) = 50\%$)
x'_{50}	Reduced cut size (at reduced grade efficiency $G'(x) = 50\%$)
Δp	Static pressure drop
ϵ	Turbulent viscosity
λ	Dimensionless parameter
μ	Liquid viscosity
ρ	Liquid density
ρ_s	Solids density

6.1 Introduction and description

Cyclones have found wide application in various fields of technology, such as gas cleaning, burning, spraying, atomizing, powder classification etc. They are also used for solid–liquid separation; the cyclones specially designed for liquids are referred to as hydrocyclones, hydraulic cyclones or hydroclones. The basic separation principle employed in cyclones is centrifugal sedimentation, i.e. the suspended particles are subjected to centrifugal acceleration, which makes them separate from the fluid. Unlike centrifuges (which use the very same principle), cyclones have no moving parts and the necessary vortex motion is performed by the fluid itself.

Figure 6.1 shows a cross-section of a hydrocyclone of conventional design. It consists of a cylindrical section joined to a conical portion. The suspension of particles in a liquid is injected tangentially through the inlet opening in

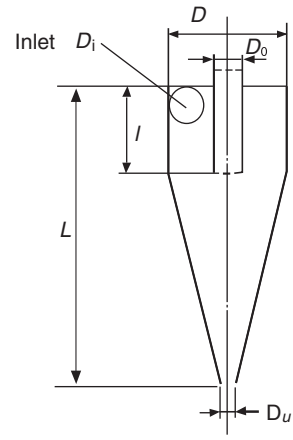

Figure 6.1 Schematic diagram of a typical hydrocyclone

the upper part of the cylindrical section and, as a result of the tangential entry, a strong swirling motion is developed within the cyclone. A portion of the liquid containing the fine fraction of particles is discharged through a cylindrical tube fixed in the centre of the top and projecting some distance into the cyclone; the outlet tube is called the overflow pipe or vortex finder. The remaining liquid and the coarse fraction of the material leave through a circular opening at the apex of the cone, called the underflow orifice.

As with all separation principles involving particle dynamics, a knowledge of the flow pattern in the hydrocyclone is essential for understanding its function and subsequently for the optimum design and evaluation of the particle trajectories, which in turn allow prediction of the separation efficiency. A short account of the flow pattern within typical hydrocyclones and the known or probable behaviour of solid particles in the flow is given in the following section. This is done for the case of low viscosity liquids under conditions in which the particles cause little or no interference to the flow patterns (i.e. for low solid concentrations).

The operating characteristics, optimum design criteria and applications of hydrocyclones are dealt with in the remaining sections.

6.2 Liquid flow patterns

The flow pattern in a hydrocyclone has circular symmetry, with the exception of the region in and just around the tangential inlet duct. The velocity of flow at any point within the cyclone can be resolved into three components: the tangential velocity v_t, the radial velocity v_r and the vertical or axial velocity v_a, and these can be investigated separately.

From the experimental data in the literature, values obtained by Kelsall[1] are shown in *Figures 6.2, 6.3* and *6.4*; they were obtained with an optical device which did not interfere with the flow. In spite of their limitations, because of the special conditions of measurement and the cyclone dimensions, these data have formed the basis of some theoretical correlations devised to account for cyclone performance.

6.2.1 Tangential velocity

At levels below the rim of the vortex finder, the tangential velocity v_t increases considerably with decreasing radius down to a given radius, which is smaller than the exit radius of the vortex finder (see *Figure 6.2*). This can be described by the relationship

$$v_t r^n = \text{constant} \quad (\text{where } n \text{ is normally } 0.6 \leqslant n \leqslant 0.9) \tag{6.1}$$

As the radius is further increased, the tangential velocity decreases and is proportional to r, this relationship holds until the cylindrical air column (which normally forms in a hydrocyclone discharging at atmospheric

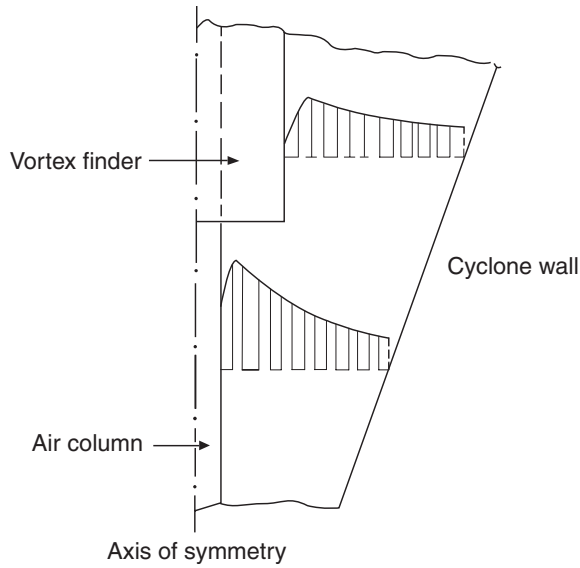

Figure 6.2 Tangential velocity distribution in a hydrocyclone

pressure) is reached. At levels above the rim of the vortex finder, the break in the rise of v_t occurs at a larger radius as can be seen in *Figure 6.2*. Apart from this phenomenon and the wall effects, v_t is independent of the vertical position so that envelopes of constant tangential velocity are cylinders coaxial with the cyclone.

6.2.2 Axial velocity

As can be seen from *Figure 6.3*, there is a strong downward flow along the outer walls of both the cylindrical and conical portions. This flow is essential for cyclone operation since it removes the particles that have been separated into the underflow orifice; it is for this reason that it is not essential to build cyclones with the apex pointing downwards and the cyclone efficiency is only very little influenced by its position relative to the gravity field.

The downward current is partially counterbalanced by an upward flow in the core region, depending on the underflow-to-throughput ratio. There is a well defined locus of zero vertical velocities (LZVV) which follows the profile of the cyclone.

Above the rim of the vortex finder, the largest downward velocities again occur near the cyclone wall. At radii between the cyclone wall and the vortex finder, the axial velocity becomes upward. Around the vortex finder strong downward flow may be observed. This is due to wall-induced flow which runs inward along the top of the cyclone.

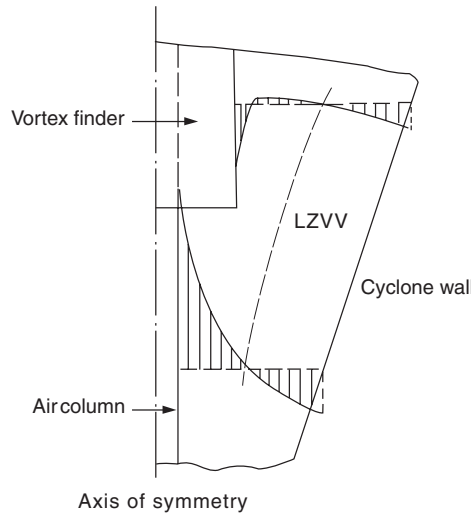

Figure 6.3 Vertical (axial) velocity distribution in a hydrocyclone. LZVV, the locus of zero vertical velocity

6.2.3 Radial velocity

The radial velocity components are normally much smaller than the other two components and, as such, they are difficult to measure accurately. As can be seen from *Figure 6.4*, the radial velocity is inward and its magnitude decreases with decreasing radius. The radial position of zero radial velocity is not known.

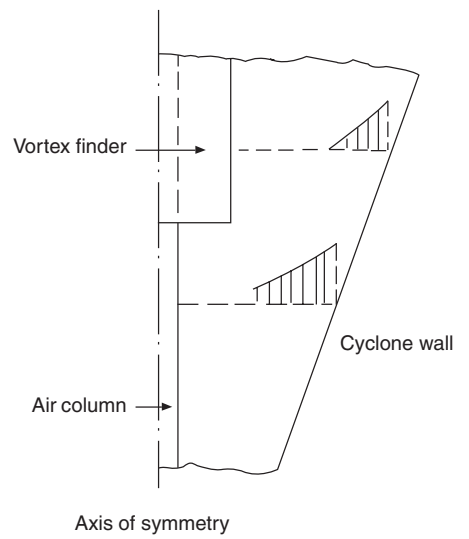

Figure 6.4 Radial velocity distribution in a hydrocyclone

At levels above the rim of the vortex finder, there may be outward recirculatory flows, and near the flat top of the cyclone there are strong inward radial velocities directed towards the root of the vortex finder, thus causing the above mentioned short circuit flow down the outside wall of the vortex finder.

It should be pointed out here that this short account of velocity profiles in a hydrocyclone is only qualitative; the flow patterns are highly complex even for water with a low specific gravity and viscosity, and it may be incorrect to assume that precisely similar profiles occur in cyclones with a considerably different geometry or with liquids of high viscosity.

6.3 Motion of suspended particles

Several authors have attempted to calculate particle trajectories in the cyclone and to derive formulae at least for the equiprobable size x_{50} if not for the whole grade efficiency curve. Some of these theories are discussed in section 6.6; certain observations are given here and refer to the probable behaviour of solid particles in sufficiently dilute suspensions.

When the solid particles enter near the cylindrical wall they can be dispersed radially inwards because of the intensive turbulent mixing in the feed sections. There is, however, very little information about the behaviour of the liquid in the cylindrical section: this portion of the cyclone is usually treated as a preliminary separating zone and the main separations are thought to be performed in the conical section.

As was suggested by Kelsall, any particles present in the downward flows near the conical wall (see *Figure 6.3*), can move radially inwards only if the liquid moves inwards. It is, therefore, obvious that if a fraction R_f of the feed liquid goes into the underflow, then the same fraction R_f of all particles, independent of their settling rate, must also go with the liquid, together with the particles separated from the remaining fraction of the liquid $1-R_f$ leaving in the underflow. This is an important phenomenon peculiar to hydrocyclones and, consequently, a correction has to be made in evaluation of the true grade efficiency curve—see section 3.4.

A particle at any point within the flow in a hydrocyclone is basically subjected to two forces: one from both the external and internal fields of acceleration (gravity and centrifugal forces) and the other from the drag exerted on the particle by the flow. The gravity effect is normally neglected in hydrocylones, so that only centrifugal and drag forces are taken into account. The movement of a particle in both the tangential and vertical (axial) directions is unopposed by any forces, so that its velocity components in those directions can be taken to be equal to the corresponding flow velocity components v_t and v_a. Since the centrifugal force acts in the radial direction, it prevents the particle following the inward radial flow—see *Figure 6.4*—and the particle is subjected to 'centrifugal elutriation'. If the centrifugal force

acting on a particle exceeds the drag, the particle moves radially outwards and, if the drag is greater, the particle is carried inwards.

Since the drag force and the centrifugal force are determined by the values of v_r and v_t respectively (for a given particle), the relative values of v_r and v_t at all positions within the separation zone are decisive for the overall performance of the cyclone.

Our aim in developing the theory of the separation in hydrocyclones is to have a model that describes the process so closely that any need for test work is obviated. This is an enormous task, however, because the process is extremely complex.

Consider the complexity of the flow patterns with clean liquid (see later in this section) before we even put any particles in the flow! As our knowledge of particle–particle interaction and of particle presence on swirling, turbulent flow is still inadequate for this application, there is really no such model in existence yet. Most theories, including the most up-to-date analytical and / or numerical flow simulations, only apply to dilute systems which are rare in industry.

The problem is that a hydrocyclone may be presented with a whole range of feed slurries: from nearly clean liquids to concentrations of solids of up to 30 or 40% by volume, and from very coarse, fast settling slurries to colloidal, slow settling ones.

Let us consider the following two extreme cases:

1 if the feed is very coarse, the particles will settle readily on entry into a ribbon of solids on the wall, swirling into the underflow (this can be observed in transparent cyclones), and the main bulk of the flow inside will be essentially clean liquid;
2 if the feed is very fine, say sub-micron in size, the centrifugal field inside will be insufficient to cause any separation and the concentration anywhere in the cyclone will be essentially the same as in the feed.

Clearly, most real cases will be somewhere in between, when the particle concentration varies with position throughout the cyclone body anywhere between that of the clean liquid and the underflow concentration. Accordingly, the suspension density and apparent viscosity will vary, and different feed solids particle size distributions will result in different spatial distributions of these two variables.

Both the pressure drop and the separation efficiency (as all the other performance criteria we may be interested in) depend strongly on the cumulative effect of the density and viscosity distributions within the cyclone flow and the precise knowledge of these distributions (for any distribution of particle size in the feed) is essential for any model to work. To predict these spatial distributions, together with the complex effects of underflow orifice crowding, internal flow eddies and turbulence, short circuit flow, turbulent pick-up of solids from the boundary layer, non-Newtonian behaviour of

concentrated slurries etc., is an enormous task, in my view still well beyond our capabilities today.

It is not surprising, therefore, that research workers and scientists searching for the ultimate model have had to make assumptions of one kind or another in order to circumvent this problem. Many will claim, however, universal validity of their model and some, like mathematicians for example, even suggest that we may no longer need actual tests because their computer simulation does the same job and much more cheaply!

6.4 Pressure distribution within the flow, static pressure drop

Due to the vortex flow in the hydrocyclone, the static pressure in the flow increases radially outward. This 'centrifugal static head' is primarily determined by the distribution of both, the tangential fluid velocities and the suspension densities, within the flow and it constitutes the major contribution to the total pressure loss across an operating hydrocyclone.

It follows, therefore, that tangential velocity distributions at low solids concentrations can be estimated from simple measurements of radial static pressure. This was the idea behind the early studies of tangential velocity distributions in clean liquid flow. Driessen[2] was the first to derive an expression relating the tangential velocity, v_t, to the radial pressure distribution by assuming the radial velocity component negligible in relation to the tangential component, so that

$$v_t^2/r = \mathrm{d}p/(\rho \cdot \mathrm{d}r) \tag{6.2}$$

This relationship was then used to calculate the tangential velocities from static pressure measurements in different places within hydrocyclones run with clean liquids. Driessen[2] and many others following him thus deduced the general expression for tangential velocity profiles in the outer vortex given previously in equation 6.1, where n is an empirical exponent, usually from 0.6 to 0.9. Note that for a free vortex in inviscid flow $n = 1$, while in a forced vortex (solid body rotation) $n = -1$.

It is a common misconception that the pressure loss in the hydrocyclone is due to friction; the friction component actually plays a minor part and the centrifugal head dominates. This can be demonstrated in analogy with the static head under gravity—see *Figure 6.5*. If the feed point to a gravity tank is at the bottom of the vessel, as indicated in the figure, the static head has to be overcome in order to pump in fluid and overflow it at the top. In a working hydrocyclone, as shown in the lower part of *Figure 6.5*, the spin of the fluid causes increasing pressure radially outwards and, because the inlet is in the region of high pressure and the overflow at a point of low pressure, the static head must again be overcome in order to pump in additional fluid.

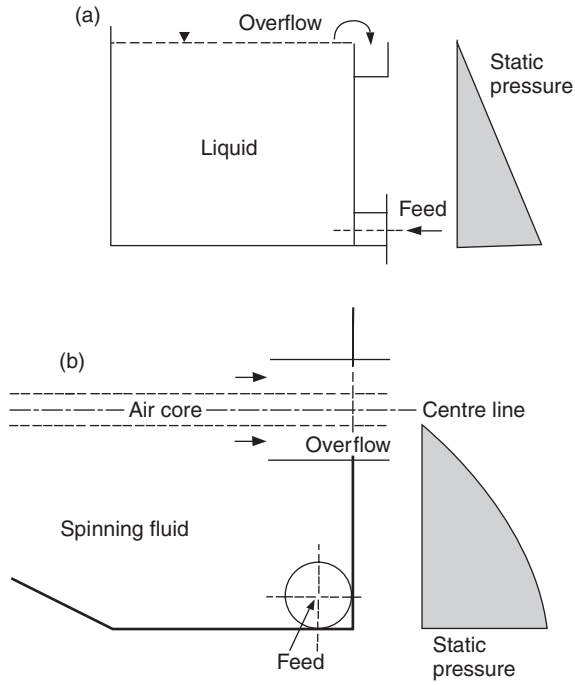

Figure 6.5 The analogy between the static head in a gravity tank (a) and the centrifugal head in a hydrocyclone (b) (note that the hydrocyclone is shown with its axis horizontal)

When describing the pressure loss in an operating hydrocyclone, it is common practice to relate pressure drop and flow rate in the same way as for any other flow devices, using a dimensionless pressure loss coefficient. This is defined later in this chapter (equation 6.9) as the Euler number, Eu, and, for the reasons indicated above, it must not be seen as an equivalent of the friction factor in pipes because it has very little to do with friction.

6.5 Hydrocyclone function, design and merits

The separation efficiency of a hydrocyclone has a character of probability. This is to do with the probability of the position of the different particles in the entrance to the cyclone, their chances of separation into the boundary layer flow and the general probability character of turbulent flow. Coarse particles are always more likely to be separated than fine particles. Effectively, the hydrocyclone processes the feed solids by an efficiency curve called 'grade efficiency', which is a percentage increasing with particle size (see chapter 3 for more details about grade efficiency). *Figure 6.6* shows the process schematically; the solids in the feed enter the cyclone and are

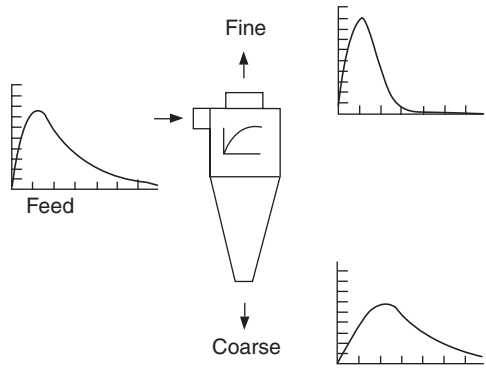

Figure 6.6 A schematic diagram of the results of the classification process in a hydrocyclone

processed by the grade efficiency curve. There are two products of the separation: the coarse product (i.e. the solids in the underflow) and the fine product (i.e. the solids in the overflow). Every hydrocyclone is therefore primarily a classifier, although we may use it as a separator by setting the cut size as low as possible to recover as much of the solids as possible into the 'coarse product'. Chapter 3 describes the classification process in more detail.

6.5.1 The effect of cyclone proportions

There has been a lot published about the relative proportions of the cyclone dimensions and their effect on separation efficiency and pressure drop. A user need not be concerned with this aspect except for two observations. Firstly, there is a rule by which every measure which increases resistance to flow improves solids recovery, and vice versa. This applies to all proportions of the cyclone body, within certain reasonable limits, except for the length of the cyclone. Thus for example, a cyclone with relatively small inlet and outlet openings is expected to give higher mass recovery but will offer higher resistance to flow and therefore have lower capacity. Several 'optimum' or recommended designs have been published and, as these have been well tested and enough is known about their performance, they may be adopted if needed.

Secondly, one dimension of a cyclone should be made variable and that is the underflow orifice diameter. Correct adjustment of this dimension is vital for the best operation of the cyclone because the optimum size of the opening cannot be predicted reliably. It is for this reason that the underflow orifice diameter is often regarded as an operating (rather than design) variable. The orifice diameter is best adjusted after start-up of the plant and also during operation whenever some operating conditions change or when the orifice itself gradually wears out.

6.5.2 The effect of operating variables

There is a whole host of operating conditions that affect the performance of hydrocyclones. Perhaps the most important are the operating pressure drop and the feed concentration. With increasing pressure drop the efficiency of separation increases but the law of diminishing returns applies. There is little point in increasing the pressure beyond 5 or 6 bar, the typical operating pressures for larger cyclones being between 1 and 2 bar. With increasing feed concentration the efficiency of separation rapidly falls off and hydrocyclones are therefore operated with dilute feeds whenever high total mass recoveries are sought.

6.5.3 Typical sizes and performance ranges

The diameters of individual cyclones range from 10 mm to 2.5 m, cut sizes for most solids range from 2 to 250 μm (for the definition of the cut size consult chapter 3), flow rates (capacities) of single units range from 0.1 to 7200 m^3 h^{-1}. The operating pressure drops vary from 0.34 to 6 bar, with smaller units usually operated at higher pressures than the large ones. The underflow solids concentrations that can be achieved with hydrocyclones rarely exceed 45 or 50% by volume, depending on the size and design of the unit, operating conditions and the nature of the solids being separated.

In order to make full use of the advantages of the hydrocyclone it is often best to use multiple units, connected either in series or in parallel. In clarification duties for example, the parallel connections allow the more efficient, smaller diameter units to be used to treat high flow rates. The series connections on the other hand, are used to improve overall recoveries in clarification, to produce thicker underflows and clearer overflows simultaneously, to wash solids or to sharpen the classification or sorting.

6.5.4 Merits and disadvantages

The relative merits of hydrocyclones can be summarized as follows:

1 they are extremely versatile in application in that they can be used to clarify liquids, concentrate slurries, classify solids, wash solids, separate two immiscible liquids, degas liquids or sort solids according to density or shape;
2 they are simple, cheap to purchase, install, and run, and require little in the way of maintenance and support structures;
3 they are small relative to other separators, thus saving space and also giving low residence times, which gives them an advantage in terms of the speed of control over the sedimentation classifiers for example;
4 the existence of high shear forces in the flow is an advantage in classification of solids because it breaks any agglomerates, and also in the treatment of thixotropic and Bingham plastic slurries.

The disadvantages of hydrocyclones may be listed as follows:

1 they are somewhat inflexible once installed and operated, giving low turn-down ratios due to the strong dependence of their separation performance on flow rate and feed concentration; they are also inflexible due to their general sensitivity to instabilities in feed flow rate and solids concentration;
2 there are limitations on their separation performance in terms of the sharpness of cut, the range of operating cut size, dewatering performance or the clarification power; some of these characteristics may be improved in multistage arrangements, but at additional costs of power and investment;
3 they are susceptible to abrasion but steps can be taken to reduce abrasive effects;
4 the existence of shear may sometimes turn into a disadvantage because flocculation cannot be used to enhance the separation as in the case of gravity thickeners (as most flocs do not survive the shear).

6.5.5 Two basic design types

The conventional, cono-cylindrical hydrocyclone with a single, tangential entry comes in two basic shapes, depending on the included angle of the cone—see *Figure 6.7*. The narrow-angle design, with angles of up to about 25°, is used more widely than the wide-angle design with angles being anywhere from 25° to 180°. The cone angle has a fundamental effect on the existence of circulating flows in the cone: at narrow angles such flows are suppressed and this makes the cyclone efficient for separation of fine particles. Such cyclones are then used whenever the required cut size is relatively low such as in clarification applications, in thickening and in classification of fine materials.

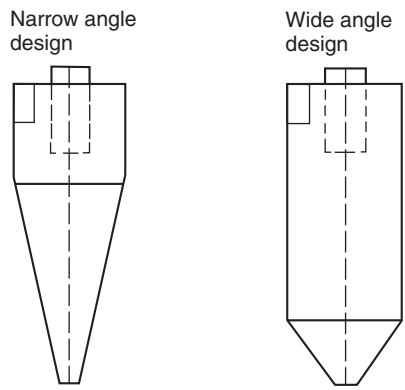

Figure 6.7 The two conventional hydrocyclone designs

The washing action of the circulating flows in cyclones with wide angles, however, is beneficial in the following cases:

1 in classification, the sharpness of cut is improved (bearing in mind, however, that the wide-angle cyclones are able to achieve only relatively coarse cuts);
2 the cut size of wide-angle cyclones may be as high as 400 μm or more, i.e. appreciably higher than is possible with the narrow-angle designs;
3 the circulating flows in wide-angle designs act like circulating fluidized beds and can sort materials according to particle density or particle shape; the best known application here is that of 'water only' cyclones in sorting minerals by density.

6.5.6 Categories of applications

Applications of hydrocyclones in industry fall into eight broad categories of two-phase separation with the liquid being the suspending medium:

1 liquid clarification;
2 slurry thickening;
3 solids washing;
4 solids classification by particle size;
5 solids sorting according to density or particle shape;
6 particle size measurement (off-line or on-line);
7 degassing of liquids;
8 separation of two immiscible liquids (the dispersed phase may be either lighter or heavier than the continuous phase).

Recent developments in the last category show that hydrocyclones can separate oil from water, dewater light oils and produce highly concentrated samples of a lighter dispersed phase.

Each application listed above has its particular requirements and goals, and it calls for changes in the design and operation of the cyclone to make the cyclone most suitable for each case. It is therefore necessary when discussing the design and operation of hydrocyclones to refer to the above-mentioned categories of application. In principle, however, any hydrocyclone separates particles (solids, droplets or gas bubbles) of the dispersed phase from the liquid (continuous phase) on the basis of the density difference between the phases, and the separation depends heavily on particle size (or on particle density if the system is not homogeneous).

Particle size which separates at 50% efficiency is referred to as the 'cut size' and is commonly used to characterize the performance of a hydrocyclone. This may be understood to be the aperture size of an ideal screen which would give similar recovery as the cyclone: smaller cut size leads to higher recovery. In the first three categories of use listed above, the aim is to

set the cut size sufficiently low to obtain high solids recovery. In classification and sorting applications, however, sharpness of cut is another important factor in assessing the hydrocyclone performance as it controls the amount of misplaced material in the two products.

6.6 Theories of separation

Before giving a short review of the current theories I warn the reader to view any theory or model with an open mind and only as an aid to our efforts in hydrocyclone design and modelling, and not as a complete solution or a substitute for real test results.

A vast amount of work has been published concerned with modelling the flow and the separation process in a hydrocyclone. The different approaches to the problem can be classified into seven categories (*Figure 6.8*) as follows.

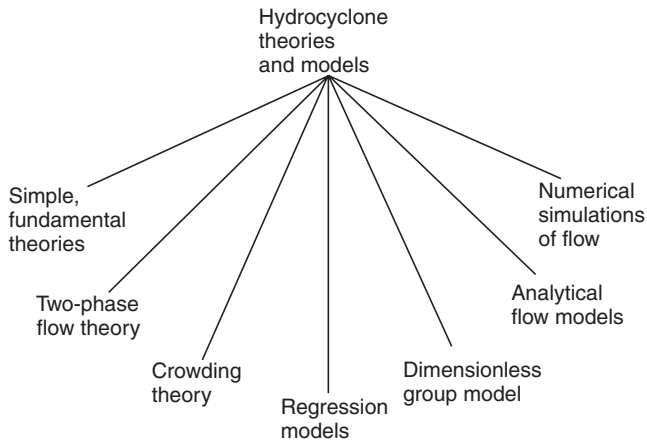

Figure 6.8 Hydrocyclone theories and models

1 Simple, fundamental theories which take no or little account of the effect of the flow ratio (or the size of the underflow orifice), of the feed concentration and of the feed size distribution. The influence of some cyclone dimensions on the cyclone performance is included.
2 A more sophisticated, two-phase flow theory which includes the effects of feed concentration and the mean particle size in the feed.
3 The crowding theory which explains the strong effect of the size of the underflow orifice on cyclone performance in some cases.
4 The all-embracing empirical models, based mostly on regression analysis of the measured data, applicable only to the specific systems tested (e.g. copper ore in Krebs cyclones etc.).
5 The chemical engineering approach based on dimensionless groups, combining 1, 2, 3 and 4 above.

6 The analytical mathematical models of the flow patterns inside the hydrocyclone and of the particle trajectories, including the boundary layer flow, the short circuit flow and the internal eddies but at low feed concentrations only.
7 The numerical simulations of fluid flows assuming axial symmetry within the main flow. Low feed concentrations are again often assumed and particle trajectories can be studied.

A short account of the above categories of theories is given in the following; a full review may be found in Svarovsky[3].

6.6.1 The simple, fundamental theories

Each theory in this category offers a relatively simple correlation for the static pressure drop and the cut size of a hydrocyclone described by a few (but often not all) dimensions. The theories fall into two main groups: the equilibrium orbit theory and the residence time theory.

6.6.1.1 The equilibrium orbit theory

The equilibrium orbit theory is based on the concept of the equilibrium radius, originally proposed by Driessen[4] and Criner[5]. According to this concept, particles of a given size attain an equilibrium radial orbit position in the cyclone where their terminal settling velocity is equal to the radial velocity of the liquid. Particles are therefore 'elutriated' by the inward radial flow according to the balance of the centrifugal and drag forces, and Stokes' law is usually assumed.

The fine particles reach equilibrium on small radii where the flow is moving upwards (and into the overflow), while the coarse particles will stay on large radii, in the downward flow, and finish in the underflow. The dividing line (or better, the surface) is the locus of zero vertical velocity (LZVV). The particle size, the equilibrium radius of which is coincident with LZVV must then be the cut size, x_{50}, which has an equal chance of reporting to either underflow or overflow. Detailed knowledge is required of the inward radial velocities which determine the drag force, as well as of the tangential velocities which cause the centrifugal force. Most authors assume some simplified shape for LZVV and then work out the average radial velocity through the surface. Most also assume Stokes' law but some consider a more general relationship for the drag coefficient. A detailed review of the different approaches is given by Bradley[6] and, more recently, by Svarovsky[3].

Probably the best known and most credible approach to the equilibrium orbit theory is that due to Bradley and Pulling[7]. This is based on the discovery of the 'mantle' by the same authors, i.e. an area in the region immediately below the vortex finder where there is no inward radial velocity. Consequently, the authors only used a conical surface below the mantle, as shown

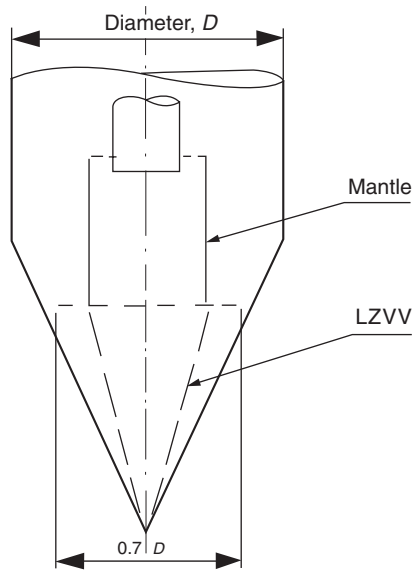

Figure 6.9 The conical surface and the mantle according to Bradley and Pulling[7]

in *Figure 6.9* in the derivation of an expression for the cut size. The theoretically obtained constants were slightly adjusted by comparison with experimental results with a 38 mm diameter cyclone.

The equilibrium orbit theory in all its various forms suggested by various authors, can be criticized on the grounds that it takes no account of the residence time of the particles in the cyclone. Not all particles may be able to attain equilibrium orbits within their residence time. The theory also takes no account of turbulence as it might affect particle separation. Despite the above disadvantages, many of the various forms of the equilibrium orbit theory (as reviewed more fully by Svarovsky[3]) give reasonable predictions of cyclone performance at low feed solids concentrations, particularly if used under similar conditions and with similar cyclone designs and sizes as in the original work of their respective proposers.

6.6.1.2 The residence-time theory

The residence-time theory assumes non-equilibrium conditions and considers whether a particle will reach the cyclone wall in the residence time available. Rietema[8] first proposed this theory and assumed homogeneous distribution of all particles across the inlet. The cut size will then be the size of the particle which, if entering precisely in the centre of the inlet pipe will just reach the wall in residence time T. In mathematical terms, this means that the particle radial settling velocity integrated with time should therefore be equal to half

the inlet diameter. Rietema proposed a 'characteristic cyclone number', Cy, and suggested that it should be as small as possible considering the variables in it.

A series of large-scale experiments[8] with a hydrocyclone 76 mm in diameter of variable proportions yielded a minimum value of Cy = 3.5 for a set of proportions which has since become one of the recommended 'standard' designs (refer to a later section for further discussion). Recent experimental investigations at Bradford University[9] carried out with three sizes of Rietema's optimum design (22, 44 and 88 mm in diameter) at 1% volume feed concentration have reproduced Rietema's results, but only with very dilute underflows: values of Cy about twice as large have been found under more practical operating conditions.

Rietema's theory does not take into account the radial fluid flow, it neglects any effects of inertia, it takes no account of hindered settling at higher concentrations and it assumes any influence of turbulence to be negligible. A more recent version of the residence-time theory, the so-called 'bulk model' due to Holland-Batt[10], does take into account the radial fluid flow. He simply used the hold-up time of the liquid in the cyclone (flow rate per cyclone volume) as the residence time, average radial fluid velocity (flow rate per wall area of the cyclone) and a general continuity equation for two-dimensional flow to derive an expression for the cut size.

The original equation for the cut size does not include the important effects of the inlet and vortex finder diameters. Holland-Batt suggested[10] that their omission '... will be compensated to some extent by specification of the pressure drop and volumetric capacity of the hydrocyclone as input variables', but it still represents a serious omission. Holland-Batt did not suggest any pressure drop–flow rate relationship to be used in conjunction with the above theory. One important contribution made by Holland-Batt was his introduction of hindered settling. He simply adopted a hindrance factor from gravity-hindered settling theory and multiplied it by the radial particle settling velocity. Strangely, the effect of the underflow-to-throughput ratio was not included. Holland-Batt also modified his 'bulk model' for the case when non-spherical particles are not characterized by the equivalent Stokes' diameter, and a shape factor must therefore be used. He also considered the case of particle motion outside the Stokes' region.

Another theoretical approach to cut size prediction that can be classified as another version of the residence-time theory is that of Trawinski[11]. In direct analogy with gravity settling Trawinski used Stokes' law, an effective clarification area and an average acceleration in a hydrocyclone to derive an expression for the cut size. The same author also proposed[11] a rather simplistic correlation for the pressure drop–flow rate relationship.

There has also been a Russian theoretical development that can be loosely classified as a version of the residence time theory[12,13]. This is primarily concerned with overall separation of solids into the overflow and underflow and is based on a stochastic theory of separation processes. Stokes' law is

used in describing resistance to particle motion but, curiously, angular velocity is employed to characterize the spin flow in the cyclone and not the tangential velocity as is more usual. The separation in either of the outgoing streams is expressed as an integral of radial gradients in the probability density with dimensionless particle residence time and it is shown to tend to a limiting value for a given set of operating conditions and feed material. The theory requires the knowledge of a coefficient described as 'intensity of random effects' and this can be found from experiments. Kutepov *et al.*[12] gave an empirical correlation for this, as obtained from a series of tests, expressed as a function of the cyclone design and inlet velocity. The prediction of efficiency using this theory is not particularly good: predicted overall penetrations of 9% and 3.5% in two different examples given by Kutepov *et al.*[12] were measured experimentally as 11% and 5% respectively. As the Russian theory does not use the concept of grade efficiency or cut size, it does not lend itself easily to direct comparison with other theories.

The residence-time theory, despite its very different approach and assumptions, often leads to correlations of very similar form to those from the equilibrium orbit theory. Either of the two theories will work better for the respective geometries to which they were 'tailored' and applied by their authors[3].

6.6.2 The turbulent two-phase flow theory

The effect of turbulence on the separation in hydrocyclones has been of concern to researchers ever since the early work of Driessen[4]. One aspect of interest is how turbulence modifies the tangential velocity profiles, i.e. its effect on the exponent n in the exponential equation for the tangential velocity in equation 2.2. Rietema[14] made a detailed investigation into this problem and estimated the turbulent viscosity with the aid of the tangential velocity profiles measured by Kelsall[1]. This was done using a dimensionless parameter λ:

$$\lambda = v_r \cdot v/\epsilon \tag{6.3}$$

where v_r is the radial velocity in the cyclone, r is the radius of the cyclone and ϵ is the turbulent viscosity.

A more rigorous viscous turbulent model of single-phase flow, based on a Prandtl mixing length theory was published by Bloor and Ingham[15]. Like Rietema, these authors obtained theoretical velocity profiles, but they used variable radial velocity profiles calculated from a simple mathematical theory. The turbulent viscosity was then related to the rate of strain in the main flow and the distribution of eddy viscosity with radial distance at various levels in the cyclone was derived.

Most recently, Duggins and Frith[16] have challenged the concept of isotropic eddy viscosity and showed that not only does the eddy viscosity vary

with position in the cyclone but its value is different in two mutually perpendicular directions and the ratio of the two values is not constant. They proposed a new method for calculating velocities where the eddy viscosity for the axial and radial momentum equations is calculated from the conventional turbulent model (*k–e* model) and the viscosity for the tangential momentum equation from a mixing length expression. This method, therefore, allows for anisotropy of turbulence in the swirling flow.

Schubert and Neesse[17] have recently proposed a separation model based on turbulent two-phase flow. They assumed a homogeneous, stationary turbulence field, with particles moving under Stokes' law. They also assumed that the particles are smaller than the smallest eddies and that their concentration is 'sufficiently low'. According to Schubert and Neesse particle transport consists of sedimentation flux superimposed on the turbulent diffusion flux. For mathematical convenience, they also assumed the centrifugal force field to be homogeneous. Schubert and Neesse derived two general models for turbulent cross-flow classification: depending on the way the underflow and overflow streams are removed, they distinguished between the suspension partition model where the flow is divided between the overflow and underflow without any change in total cross-section, and the suspension tapping model where the discharge streams are 'tapped' from the main flow through small outlet openings. The latter model was then applied to the separation in a cyclone, with the resulting equation for the cut size. This correlation takes no account of the spread of the feed distribution but it is the first one reported here which allows for the effect of the feed solids on the separation in a hydrocyclone, with turbulence damping effect increasing with increasing fineness of the solids.

The theory of Schubert and Neesse points to small cone angle and curved feed inlets for clarification duties where high mass recoveries are required. The authors compared the above correlation with many published experimental results and found the correspondence better for umbrella (or spray) discharge. No flow rate-pressure drop relationship was proposed.

The latest contribution from Neesse and Schubert[18] is concerned with the case of higher solids concentrations where the underflow orifice may restrict the free discharge of the solids. They propose the existence of a limit in the solids loading and propose an empirical correlation for the discharge capacity of the underflow orifice. This brings their work into the realms of the crowding theory considered below.

6.6.3 Crowding theory

This theory was first suggested by Fahlstrom[19] who proposed that the cut size is primarily a function of the capacity of the underflow orifice and of the particle size analysis of the feed. He argued that the crowding effect, or hindered discharge through the apex, can swamp the primary interaction to the extent that the cut size can be estimated from the mass recovery to the underflow.

Fahlstrom quoted the discharge capacity to be from 1.5 to 3t cm^{-2} h^{-1} in grinding circuits, but this depends on the absolute size of the underflow orifice and it is not realistic for small cyclones. In any case, any crowding effect must surely depend on the physical proximity of the solid particles and this depends on volume rather than mass. Fahlstrom's crowding theory seems feasible in principle but his original justification is false. He attributed the differences between the analytical cut size and the equiprobable size to the crowding effect. Furthermore, he found the difference to be a function of particle size. This difference is now known to be due to the non-ideal shape of the grade efficiency curve and it exists whether or not underflow crowding takes place.

A much more scientific proof of the crowding theory has recently emerged from some mathematical modelling work by Bloor *et al.*[20]. This is a hydrodynamic model of the flow both in the cyclone body and in the boundary layer (the cyclone design is that of Kelsall[1]), but it makes no predictions of conditions at underflow because it breaks down at the vertex. The model assumes inviscid flow in the main body and viscous flow in the boundary layer. It allows plots of particle trajectories, assuming their homogeneous distribution on entry to the cyclone cone.

Using a correlation for the slurry viscosity as a function of particle concentration and using concentration averaged across the boundary layer, Bloor *et al.*[20,21] then modelled the flow in the boundary layer and this represents the most interesting part of their work, later also published by Laverack[22]. The model allows plots to be made of particle concentrations, volume fluxes and layer thickness along the boundary layer. This in turn allows the effect of increased feed concentration on the conditions in the boundary layer to be studied: the increase was found to thicken the layer as well as to increase the flux, and the underflow would have to be increased to accommodate this. Furthermore, the authors found that the conditions at the cut-off point were decisive. The technique cannot deal with a double structured boundary layer near the vortex.

Unlike the theories reviewed in the previous sections, the model by Bloor *et al.* does not lead to any simple correlations for the cut size or the grade efficiency curve, but it is the first time that any direct proof of the crowding theory is given. On the basis of an actual set of conditions studied, the authors give a quantitative example: if a cyclone operates satisfactorily at 5% solids concentration and this is increased to 15%, the underflow rate must be increased by a factor of 1.6 in order to prevent overcrowding and possible blocking of the underflow orifice.

Another theoretical development, originating from Freiberg and also reported in the previous section[17], has recently been adapted to include the crowding of the underflow orifice[18]. An empirical equation for the discharge capacity of the underflow orifice is proposed.

In conclusion to this section on the crowding theory, this theory is certain to be valid in principle. Anyone involved in hydrocyclone testing will have

observed the strong influence of underflow orifice control on the cut size. The question is how to describe the effect quantitatively: ultimately, the effect may be simply related to the underflow concentration by volume, in conjunction perhaps with the absolute size of the orifice and the size distribution of the feed. Further development of this theory is expected.

6.6.4 Comparison of the simple theories reviewed so far

Direct comparison of the different theories is not really fair because the respective authors always tailored their theory to a set of experimental results which were never sufficiently comprehensive or general to allow them to include the effect of all design variables. Rietema's residence-time theory, for example, does not really offer a correlation for any design other than the 'optimum design' of his own obtained by optimization from his tests.

It can be concluded that none of the simple theories give a completely general correlation that can be applied to any combination of the relative cyclone proportions. The vast majority of them, however, show that for a family of geometrically similar cyclones, there is a dimensionless group (we shall call it the 'cyclone number') which should be a constant. This constant can be obtained from experiment, rather than from the correlations given by the various theories, and this approach leads to much more reliable performance prediction. This is the approach adopted in the chemical engineering model for hydrocyclone scale-up.

Design variables are not the only ones to affect the cyclone number. While the effects of pressure, flow rate, viscosity and the densities of the fluid and particles are included, the strong influence of the feed concentration and of underflow orifice control are not. Most of the theories only apply to low solids concentrations, some (Holland-Batt, Schubert and Neesse) offer a correction for hindered settling and others consider to some extent the effect of the underflow-to-throughput ratio (Bradley) or the limited capacity of the underflow orifice (Schubert and Neesse). Once again, the effect of solids concentration for the purpose of scale-up is best described by dimensionless correlations derived from pilot tests and this is shown in some detail later.

At higher concentrations, the size distribution of the feed solids, and perhaps particle shape too, also affect the cyclone performance (because the spatial distributions of suspension viscosity and density within the hydrocyclone depend on what is being fed to it). Only the turbulence theory of Schubert and Neesse[17], and the Russian stochastic approach[12,13] include the effect of the average particle size of the feed solids.

As was pointed out at the beginning of this section, there are several other models available for predicting cyclone performance, but those were obtained from curve-fitting exercises and, as such, do not represent a true physical model of the separation process in hydrocyclones. These models are reported in the next section.

6.6.5 The regression models

This is the group of so-called mathematical models which are in fact based almost entirely on regression analysis of test data. They are concerned with the two main performance characteristics of hydrocyclones, the capacity (or pressure drop) and the separation efficiency in the form of the cut size. These two aspects are dealt with separately here.

The presence of higher concentrations of particles in the flow modifies the velocity profiles in the cyclone and increases capacity. Some authors take the view that the effect is the same as of higher liquid viscosity and density, and recommend the use of the apparent suspension viscosity of the feed slurry and density of the slurry rather than that of the suspending liquid. While this approach oversimplifies the real process in the cyclone, the increase in cyclone capacity with concentration is small anyway and the errors may be acceptable (in practice, clean liquid data are often used regardless of concentration and the capacity may then be adjusted in plant by throttling or by other means).

The effect of really high feed concentrations on hydrocyclone capacity, in concentration of minerals, was studied by Lynch and co-workers[23–26] and also by Plitt[27]. Hundreds of experiments were carried out with various cyclone designs and operating conditions, leading to empirical 'models' suitable for mathematical modelling of closed circuit mineral grinding circuits or similar applications. Unfortunately, only aqueous systems were used and the authors did not seek conclusions in dimensionless form. The resulting equations are purely empirical and dimensionally inconsistent, requiring empirical constants with a dimension, and specified units to be used for each variable. There is little point in reproducing their equations in this report and the reader is referred to either the original references or the book[3].

The correlations for the pressure drop–flow rate relationship change from paper to paper in the publications by Lynch and co-workers[23–26] depending on the test system. Cyclones of 500 mm diameter were tested with silica and copper ore at concentrations of 15–65% by weight, whilst in another series of experiments[24,25], cyclones from 100 to 380 mm in diameter were tested with limestone at concentrations of 15–70% by weight. Finally, another series of tests[26] at concentrations of limestone from 40 to 70% by weight are reported.

The correlations usually take the following form:

$$Q = KD_{\mathrm{o}}^{n} \cdot D_{\mathrm{i}}^{m} \cdot D_{\mathrm{u}}^{p} \cdot (\Delta p)^{r} \tag{6.4}$$

where K, n, m, p and r are all empirical constants having specific values for each system tested. Some correlations also include a concentration term.

Plitt[27] took the data of Lynch and Rao[23] and added his own, with smaller cyclones up to 150 mm diameter tested with silica flour, and used the data, 297 individual tests in total, to derive by regression analysis yet another correlation for the pressure drop–flow rate relationship, not dissimilar to the above equation.

The formulae proposed by Lynch *et al.* and Plitt have been applied to other cyclone sizes and slurries (see, for example, Aplyng *et al.*[28]), and neither model was found to be entirely successful: it was necessary to change the constants to fit the predicted results to the experimental data.

The variety of equations given by Lynch and co-workers for different studies is in itself indicative of this problem. As the equations are not based on any physical model of the actual process and represent merely a curve-fitting exercise, it is only to be expected that they cannot be used for reliable predictions unless the constants used are measured for each system under consideration.

As to the effects of operating variables like pressure drop and the solids concentration on the cut size, most authors agree that it is an exponential relationship. The work of Lynch quoted above resulted in several correlations while Plitt[27] suggested another.

The above-mentioned correlations are subject to the same criticism as the pressure drop–flow rate correlations discussed previously. They were obtained by curve-fitting a set of experimental data and do not represent a real model of the separation process. In situations where materials different to those used in the original tests are being handled, it is necessary to obtain a new set of constants to make the correlations fit the test data.

A further note must be added here about the grade efficiency curve. All the above-quoted correlations use the cut size as the representative of the separation efficiency. The full grade-efficiency curve is the best way to characterize the separation efficiency because only if this is known can an accurate estimate of the total mass recoveries be made. The conventional way round this problem in practice is to make a prediction of the operating cut size and then generate the full grade-efficiency curve by using a generalized grade-efficiency curve which is plotted against a dimensionless size x/x_{50}. Such generalized functions were reviewed by Bradley[6], but since then more detailed studies have been made of this such as the work by Lynch and Rao, and a full review can be found in a later book by Svarovsky[3].

One of the functions successfully fitted to the reduced grade-efficiency curve is the log–normal law (consult chapter 2 for the definition of log–normal law). Gibson[29] tested small-diameter Mozley hydrocyclones (25 and 50 mm diameter) with china clay at concentrations up to 35% by weight, and found geometric standard deviations from 1.77 to 2.0, depending on the size of the vortex finder. Larger vortex finders yielded lower standard deviations, thus giving sharper classification.

On the basis of the available experimental evidence it can be concluded that for a given cyclone design and low feed solids concentrations (say below 1% by volume) the shape of the reduced grade-efficiency curve is reasonably constant. At higher solids concentrations, it becomes dependent on the feed material and experimental measurement may be necessary. Alternatively, with smaller diameter cyclones, the log–normal law with a measured geometric standard deviation may also be used. Knowledge of the cut size is of course necessary in any of these cases to obtain the full curve.

6.6.6 The dimensionless group model

The model developed and tested at Bradford recently[9, 30, 31] is an example of a chemical engineering approach to the design and scale-up of single or multiple cyclone installations. It is based on fundamental theory combined with dimensional analysis to produce the necessary correlations, and, in keeping with the usual practice in chemical engineering, the required constants are derived from tests rather than from theory.

The procedure centres around the three dimensionless equations 6.5 to 6.7 (below) which fully describe the function of a hydrocyclone within its operational limits. If a given cut size and underflow concentration are specified, simultaneous solution of the three equations yields the cyclone diameter, the number of cyclones to be used in parallel and the size of the underflow orifice which, in turn, gives the required performance and capacity (under the given pressure drop). If the operating pressure drop is not specified, several design options are obtained and the final design is selected either from some operating constraints or from economic optimization. In such optimization, the operating pressure drop can be traded off, for the same cyclone, against the flow ratio. The geometrical similarity normally concerns all internal dimensions of the individual cyclones except the size of the underflow orifice which is regarded as an operational variable.

In the model presented here, all design proportions were according to Rietema's optimum design as per *Table 6.1*. The model was tested with two materials: chalk of density 2780 kg m^{-3} and alumina hydrate of density 2420 kg m^{-3}. The suspending liquid used in the hydrocyclone tests was water with 0.1% Calgon as dispersing agent. The feed solids concentration was varied from 1 to 10% by volume.

Table 6.1 Two well-known hydrocyclone geometries and respective performance constants (narrow-angle designs)

Cyclone type	D_i/D	D_o/D	D_u/D	*1/D*	*L/D*	*Cone angle degrees*	$Stk_{50} \cdot Eu$	*K*	n_p
Rietema[8]	0.28	0.34	0.20	0.4	5	20	0.0611	316	0.134
Bradley[7]	0.133	0.20	0.07	0.33	6.85	9	0.1111	446.5	0.323

The correlations derived in the previous study[9] were as follows:

$$\mathrm{Stk}'_{50}\,\mathrm{Eu} = 0.0474\,[\ln(1/R_f)]^{0.742}\exp(8.96c) \tag{6.5}$$

$$\mathrm{Eu} = 371.5\mathrm{Re}^{0.116}\exp(-2.12c) \tag{6.6}$$

$$R_f = 1218\,(D_u/D)^{4.75}\mathrm{Eu}^{-0.30} \tag{6.7}$$

where the various dimensionless groups are defined as follows.

The Reynolds number, Re, to define the flow:

$$\mathrm{Re} = vD\,\rho/\mu \tag{6.8}$$

The Euler number is a pressure loss factor based on the static pressure drop across the cyclone:

$$\mathrm{Eu} = \Delta p/(\rho v^2/2) \tag{6.9}$$

Stk_{50} is the Stokes number (for cut size x_{50}):

$$\mathrm{Stk}_{50} = x_{50}^2(\rho_\mathrm{s} - \rho)\,v/(18\mu D) \tag{6.10}$$

where ρ_s and ρ are the densities of the solids and of the liquid respectively, μ is liquid viscosity and D is the cyclone diameter. If the reduced cut size x'_{50} is used in the above equation in place of x_{50}, the reduced Stokes number Stk'_{50} is obtained (for definitions of the parameters see the Nomenclature given at the beginning of this chapter).

All the above equations use the superficial velocity in the cyclone body as the characteristic velocity, i.e.

$$v = 4Q/(\pi D^2) \tag{6.11}$$

Equations 6.5 to 6.11 allow reliable cyclone design and scale-up at moderate concentrations up to about 10% by volume. If the full data on the operation and performance of a hydrocyclone are known then the dimensionless groups necessary for scale-up may be calculated directly from equations 6.8 to 6.10. Conversely, the knowledge of the scale-up constants as given in equations 6.5 to 6.7 may be used to predict the performance of a hydrocyclone of a given design or the design of a hydrocyclone installation to meet a particular performance requirement.

Looking at equations 6.5 to 6.7, one can make some interesting observations. Firstly, the resistance coefficient, Eu, in equation 6.6 is not affected by the size of the underflow orifice D_u/D (or by the flow ratio R_f). Secondly, something that every hydrocyclone operator will know well, the flow ratio R_f is very strongly affected by the setting of the underflow orifice D_u/D.

Equations 6.5 to 6.7 primarily represent the test results of the study published previously but, unlike some other models in the literature, they are based on a physical model of hydrocyclone operation and particle behaviour and, as such, have a much better chance of success when applied to conditions outside those tested. Another research project at Bradford is directed at the effects of solids concentrations greater than 10% when many practical slurries show non-Newtonian behaviour.

6.6.6.1 Examples of design choices

Equations 6.5 to 6.7 (with the dimensionless group definitions in equations 6.8 to 6.11) represent a full model necessary for hydrocyclone design or scale-up. Since its development, we have used the model for the design and

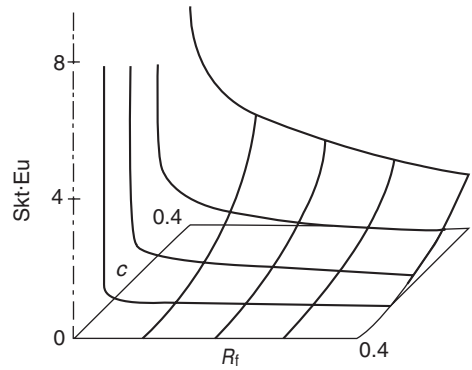

Figure 6.10 Graphical representation of equation 6.5

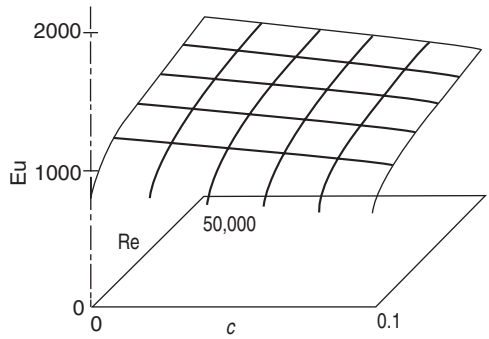

Figure 6.11 Graphical representation of equation 6.6

optimization of industrial hydrocyclone systems. The model can be easily programmed and used on a microcomputer, and thus provides valuable insight into the effects of any of the variables involved. *Figures 6.10* to *6.12* show three-dimensional representations of the three relationships.

In order to demonstrate the usefulness of the model, it was used to provide operating alternatives for an existing hydrocyclone of internal diameter $D = 88$ mm, Rietema's proportions and operated with chalk in water at feed solids concentrations up to 10% by volume. *Figure 6.13* gives the plot of the operating conditions if the overflow clarity is to be constant (reduced cut size of 10.6 μm). As can be seen from this plot, at any given feed concentration, the choice is between low pressure drops at high flow ratios, R_f, and high pressure drops at low flow ratios. The operating pressure drop can, therefore, be traded off against the concentration of solids in the underflow. A lower pressure drop (i.e. specific energy) requires greater amounts of water to be accepted with the solids, and vice versa. Depending on the particle size of the feed solids and the cost of further dewatering of the solids in underflow, the two running costs of pressure drop and of dewatering of the solids in the

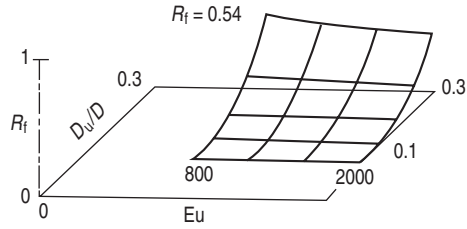

Figure 6.12 Graphical representation of equation 6.7

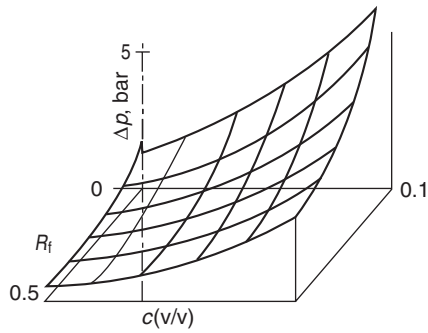

Figure 6.13 Plot of operating variables for a particular cyclone operated to give constant overflow clarity. $D = 88$ mm, chalk in water, $x'_{50} = 10.6$ μm, Rietema's design

underflow can be weighed against each other and the operating conditions optimized accordingly.

The scale-up model based on dimensionless groups simplifies hydrocyclone design and allows the designer to select the best compromise between hydrocyclone performance and the design and operating conditions likely to achieve it. The model is particularly suitable for computer simulations where many different alternatives can be computed and the interaction of the hydrocyclone with other plant items can be described for overall optimization—see the example later in this section. As to which particular alternative is adopted depends on the pressure drop which is available or suitable. If this is not determined by some other consideration, optimization of the total cost of the system (running costs and capital charges) may lead to the best design; Gerrard and Liddle[32] have proposed a procedure designed for precisely this choice.

6.6.7 Analytical flow models

The analytical flow models are based on mathematical solutions of the basic flow mechanics. Reference has already been made to the work of Bloor and Ingham[20–22] who have pursued this direction for many years. Their model assumes inviscid flow in the main body of the flow and is capable of

producing particle trajectories for efficiency calculations. It also considers flows in the top boundary layer, the side boundary layers and around the air core. They found that if the flow is assumed to be irrotational (i.e. having no vorticity) then unreasonable results are obtained.

In developing their model, Bloor and Ingham[15] first assumed the fluid to enter the hydrocyclone with uniform momentum and used the form of vorticity distribution determined by the Polhausen method. Bloor[33] has recently shown that the momentum cannot be distributed uniformly in the entering fluid and that the secondary motions produced from realistic entry conditions are of sufficient strength to generate the required levels of vorticity in the cyclone.

Bloor and Ingham published a whole series of papers when developing their main body flow model. At one stage[20] they introduced the effect of the leakage of particles to the overflow through the boundary layer under the top cover, calculated grade efficiency curves and found them to be in broad agreement with Kelsall's experiments[1]. The same authors also investigated the central region of solid-body rotation, which incorporates the air core, by employing a viscous turbulent model based on a Prandtl mixing length theory[15] as was discussed above.

A more recent development by Concha *et al.*[44] makes use of the analytical model by Bloor and Ingham to predict the classification performance of the conventional hydrocyclone. They divide the flow inside a hydrocyclone into six zones and use previously derived or measured velocity profiles and air core correlations. The zones are linked by boundary conditions and resulting classification predictions are validated with experimental tests using copper ore and quartz on three different industrial hydrocyclones.

Moraes *et al.*[40] modified the model by Bloor and Ingham to allow its application to the deoiling cyclone developed by Thew and co-workers in the early 1980s[41]. Their development permits new analytical solution for any split ratios and allows evaluation of operational performance of deoiling cyclones. Efficiency predictions, however, require additional experimental studies to take into account factors not considered in the analytical model. No account is made of the turbulent shear stress and/or turbulence unisotropy in the flow. As Small *et al.* have shown using CFD (Computational Fluid Dynamics) techniques[43], anisotropic turbulence effects have to be taken into account, particularly in the inlet region which contains zones of high turbulence intensity that have high influence on droplet breakup.

Lately, the analytical flow models have been largely abandoned in favour of numerical simulations.

6.6.8 Numerical simulations of the flow

Instead of solving the equations of flow analytically, the methods of computational fluid mechanics can be used to develop numerical simulations of the flow. There are now in existence several commercial general fluid flow

computer software packages which can be used for mapping the streamlines of the flow inside a hydrocyclone.

Numerical calculations of the complete flowfield, using axially symmetric flow models and solving the full viscous equations of motion, have been carried out by Boyson, Ayers and Swithenbank[36] and by Rhodes, Pericleous and Drake[37]. These simulations are suitable for assessing parameters in design optimization provided they are based on realistic boundary conditions and a comprehensive flow model. Bloor, Ingham and Ferguson have also[38] produced a numerical simulation for viscous flow in a hydrocyclone but at unrealistically low Reynolds numbers. Unlike the others they did not, however, ignore the three-dimensional character of the flow around the entry point and used three different models to simulate the entry flow.

The most interesting development in this area to date is that of Rajamani and Milin[39]. Their model caters for high feed concentrations and allows iterative computation to account for the gradual variation in particle concentration from the central region towards the walls in a hydrocyclone. The assumptions in their model are fairly conventional (particle–fluid coupling is absent, flow is axisymmetric, a modified Prandtl mixing-length model is used for turbulence). The crowding effect at the underflow orifice is accounted for by simply making a particle to circumvent a computational cell which is already filled with 50% v/v of solids.

Interestingly, Rajamani and Milin[39] found no need to iterate for feed concentrations up to 20% by weight where clean water velocity profiles were used and the separation results compared well with experiments (limestone in water, in a 75 mm hydrocyclone). This is due to the fast dilution process taking place in the flow as pointed out in section 1.4. Only for concentrations above 20% by weight the authors needed to iterate the computations: the first iteration of particle trajectories is done with the values of water viscosity and density, from which particle concentrations (and slurry viscosities and densities) are computed at each point. For this the authors use computed particle trajectories and assume that the concentration is proportional to particle residence time in each computational cell.

This new set of slurry local properties is then used to recalculate particle concentrations, and the process is iteratively repeated until the system converges, i.e. the predicted fluid velocities are consistent with the particle concentrations at all points. A further development of this model by Rajamani and co-workers[42] uses STP (Stochastic Transport of Particles) to predict the particle concentration gradients inside a hydrocyclone. This involves tracking particle clouds rather than individual particles and it makes the computing algorithm, still iterative, more efficient and faster.

The comparison of the Rajamani model with experiments is very good, done via grade efficiency curves in refs. 39 and 42. One paradox in this is that the grade efficiency concept is only useful if grade efficiency is independent of the particle size distribution in the feed. If, as seems to be true at high concentrations, this independence is no longer valid and we have to resort to

an iterative numerical procedure for each different size distribution in the feed, then the grade efficiency concept becomes less relevant in such cases.

I believe the iterative numerical simulation is the way to go in modelling and, although further tuning and scrutiny is clearly needed, it is the only method capable of good predictions at high solids concentrations, particularly when the overall recovery of solids to underflow is not very high. The current disadvantage of long computing times is sure to disappear gradually as time passes and the computers become even faster.

6.6.9 Conclusions on models

Numerical flow simulation models attract a lot of attention at the moment and undoubtedly hold the key to the future. I think, however, that both the regression and the dimensionless group models will still hold their own and continue to do so even when the numerical simulations become accurate and fast enough for practical use. The dimensionless group model (see ref. 45 for the latest development) in particular has great advantages in its ease of computation and incorporation into large plant scale-up and optimization software, and also in its value for teaching of hydrocyclone scale-up to chemical engineers. The regression model, on the other hand, has been widely embraced in mineral processing and is very likely to continue to be used and further developed.

The numerical simulations are cheaper and more flexible for individual hydrocyclone design than any of the other models or a full experimental investigation. They are, however, no substitute for experimental tests as yet, particularly for high solids concentrations when particle–particle interactions and possible non-Newtonian effects are at play. When considering a new geometry for a hydrocyclone, a numerical simulation of the flow is very useful.

Finally, even with the arrival of increasingly more realistic numerical simulation models, I do not expect any dramatic changes in either the conventional hydrocyclone geometry or in the way we scale it up. It is more a question of fine tuning.

6.7 Hydrocyclone selection and scale-up

6.7.1 General Strategy

The very first consideration in the process of hydrocyclone selection and sizing is the choice of narrow-angle or wide-angle designs. The choice is made according to the application: wide-angle designs are only beneficial in the cases of classification duties (and when the cut sizes are to be larger than about 50 μm) and of sorting by particle shape or density. For the other possible applications, namely in clarification, thickening and

classification of fine particles, narrow-angle designs are the only choice. The remainder of this section is, therefore, devoted entirely to narrow-angle designs and the reader is referred to Svarovsky[3] for further reading on wide-angle types.

There are two somewhat different schools of thought with regard to hydrocyclone geometry. Most manufacturers, due to commercial considerations, produce only a limited range of cyclone diameters and, in order to be able to cover a full range of flow rates and cut sizes, each cyclone size can be altered in design proportions to vary its performance. In marketing their units, manufacturers emphasize that their cyclones are always designed specifically for each application, almost custom-built, and that this is the only way to obtain an optimum design. Such an approach requires reliable quantitative know-how as to the effect of design variables and, as the equipment user normally does not have this information, he or she has to seek assistance from the supplier. The claim of custom-building is true of course, but it is a case of assembly from the range of standard parts as a commercial necessity rather than a scientific virtue.

An alternative approach open to users or suppliers who are in a position to build a hydrocyclone of any diameter, is to use geometrically similar families of cyclones of 'standard' design. All the cyclone proportions are related to body diameter and the only design variable is then the cyclone size. This simplifies the cyclone selection remarkably and makes it accessible to people who do not necessarily have access to reliable scale-up information on the effects of cyclone proportions. The above-mentioned cyclone designs are either geometries obtained by careful optimization by scientists like Rietema[8] or Bradley and Pulling[7] or simply any practical or commercial cyclone geometries that have been well tested and can therefore be reliably scaled-up. *Table 6.1* lists two such cyclone geometries and the test data (see *Figure 6.1* for cyclone dimensions and section 6.6.6 for definitions of the dimensionless groups in *Table 6.1*), others can be found elsewhere[3]. Hydrocyclones designed in this way have a better chance of being close to an optimum design than do those selected from only a few sizes and assembled from kits to suit a particular application. Commercial considerations force most manufacturers to follow the latter route, but many also adopt geometric similarity in their range, thus combining the two approaches.

The approach used in this chapter is based on families of geometrically similar cyclones so that all design variables are omitted from the scale-up correlations (except the size of the underflow orifice which should be variable and is considered here to be an operating variable).

The significance of the dimensionless groups and constants in *Table 6.1* will be explained in the following section. When faced with the problem of selecting the most suitable hydrocyclone or set of hydrocyclones for a particular task, one can consult manufacturers' literature and consider one size from their range. A preliminary selection is usually based on capacity and the separation performance is then checked using additional information

available from the manufacturer or using a model or theory. The following section considers this route.

The simple theories or simplified charts from manufacturers are usually satisfactory for a preliminary selection; when more detailed and reliable predictions of performance are required a model or theory must be used which includes the effects of feed solids concentration and of the underflow orifice setting. The choice is then narrowed to the empirical models or the semi-empirical scale-up using dimensionless groups because the other theories reviewed in section 6.6 are not yet useful for this.

As discussed in section 6.6.5, there have been some attempts to construct empirical 'models' based on large-scale tests, most notably those of Lynch and Rao[25] and Plitt[27] which include both design and operating variables in the correlations. The models are based on linear-regression analysis and are merely an analytical representation of tests with specific slurries on a range of cyclone sizes and designs. The apparent all-embracing nature of Plitt's and Lynch's equations is deceptive: the constants must usually be recalibrated for any particular slurry and hydrocyclone because the original correlations do not take into account all the effects which are important at high concentrations, like particle shape or surface properties. Should Plitt's or Lynch's correlations be used for hydrocyclone design, one would have to choose a particular set of design proportions to be used in the correlations, thus effectively choosing a hydrocyclone design and, when doing so, one may just as well use a known and well-tested design together with a simpler model, and test the effects of material properties at higher concentrations on a small cyclone of the same family. The correlations of Plitt and Lynch are very useful, however, for qualitative illustrations of the effect of changes of any particular variable.

It is, therefore, considered more appropriate in this book to use the 'chemical engineering' approach of dimensionless groups and their semi-empirical relationships, as given in section 6.6.6.

6.7.2 Preliminary design charts

As a very preliminary step in the process of hydrocyclone selection, the low concentration performance data is often used even when the actual feed concentrations are higher than 1% v/v. In clarification duties, however, this data would be correct for final design providing that high flow ratios are to be used.

At low solids concentrations of below 1 or 2% by volume, the flow pattern in hydrocyclones is unaffected by the presence of particles, and particle–particle interaction is negligible. The volume of the particles that separate into the underflow is small and the underflow-to-throughput ratio, R_f, is usually assumed to have no effect on the cut size, x_{50}, except for the effect of flow splitting which can be easily accounted for by using the reduced efficiency concept (section 3.4.1). Dimensional analysis coupled with the conclusion of most of the simple theories of separation in hydrocyclones

(see section 6.6.1, and Svarovsky[3] and Bradley[6] for full reviews) give two relationships between three dimensionless groups:

$$\mathrm{Stk}_{50} \cdot \mathrm{Eu} = \text{constant} \tag{6.12}$$

and

$$\mathrm{Eu} = K \cdot (\mathrm{Re})^{n_p} \tag{6.13}$$

where K and n_p are empirical constants for a family of geometrically similar cyclones; the dimensionless groups in the above equation have all been defined in section 6.6.6. *Table 6.1* gives the constants for two well-known and tested cyclone geometries. Our own test work[30] with Rietema's geometry confirmed the validity of the constants derived in the original work[8], but only for high R_f ratios, i.e. those greater than about 23%; at lower ratios the separation performance becomes worse than predicted.

Other geometries give other values of the constants in the above equations; the group $\mathrm{Stk}_{50} \cdot \mathrm{Eu}$ varies from 0.06 to 0.33 for most cyclones, and the exponent n_p is usually between 0 and 0.4. The constants may be computed from full experimental test data or, conversely, knowledge of the constants allows the prediction of performance (or design to match a required performance) of a hydrocyclone of a given size and geometry. Design charts can be constructed for a particular geometry to aid size selection or establish limits in performance. *Figure 6.14* gives an example of such a design chart for Rietema's geometry specified in *Table 6.1.*

Similar design charts exist for some commercial cyclones, but as only a limited range of cyclone sizes are available from a given manufacturer, such charts are not continuous but merely show areas of cut size/capacity covered by the range of cyclone diameters.

The selection chart in *Figure 6.14* is very simple to use: a hydrocyclone is selected on the basis of the required capacity and available pressure drop. If the reduced cut size is too high then the flow rate is divided by 2, 3, 4 etc., and the procedure repeated with the lower value of Q until the cyclones (to be used in parallel) become small enough to give the required value of reduced cut size. The chart shows that reduced cut sizes down to almost 2 μm should be possible with 10 mm hydrocyclones. This has recently been confirmed in another investigation[37], but the units had to be run at high underflow dilutions.

6.7.3 Design options

The conventional hydrocyclone design procedures have been based on a rather simplistic view of the hydrocyclone function: the cyclone size is selected from the capacity and available pressure drop requirements, with the cut size not being a free choice but fixed by the former two requirements (reduction in cut size can only be achieved by using a greater number of smaller cyclones in parallel). This approach ignores completely the effect of the underflow orifice size on the cut size, and also on the solids concentration in the underflow. The procedure based on the model in section 6.6.6 centres

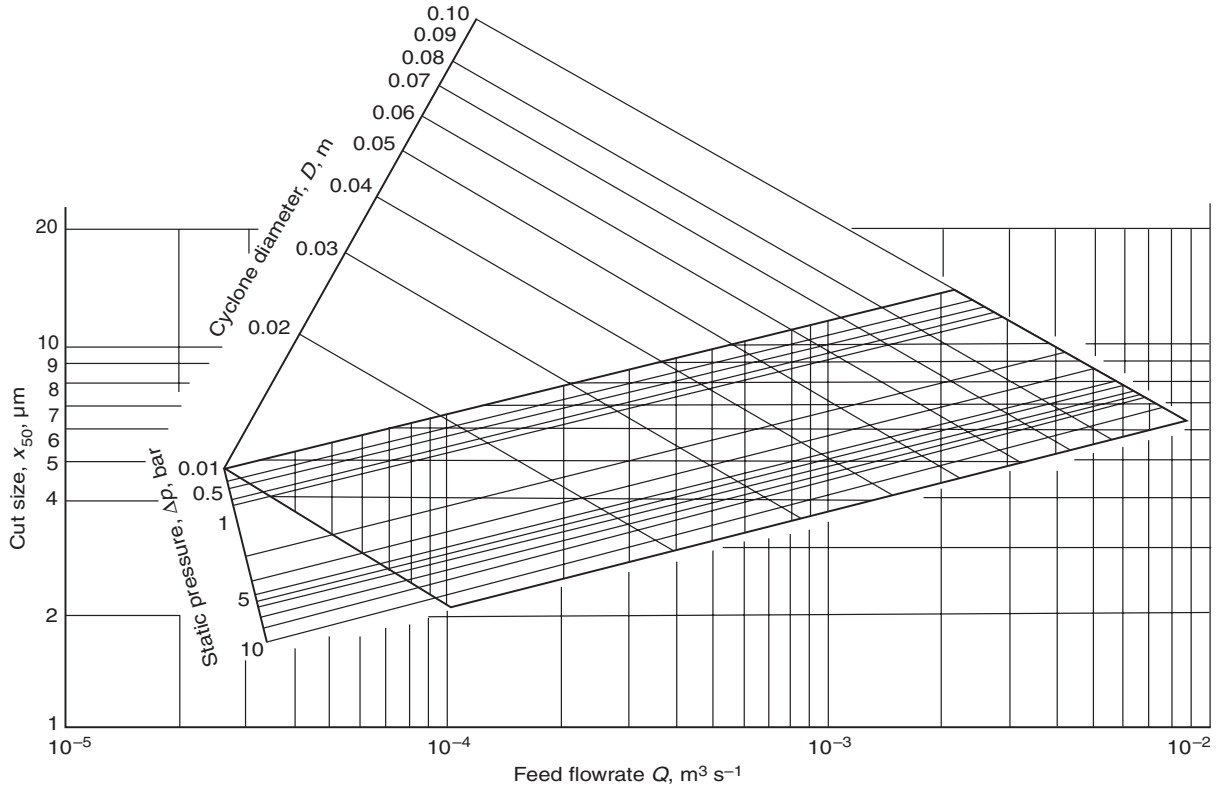

Figure 6.14 Hydroclone clarification performance as a function of body diameter, *D*, for Rietema's optimum separation design at high underflow dilutions and low feed concentrations, for quartz of density 2600 kg m^{-3} water, at ambient temperature (20°C)

around the three dimensionless equations 6.5, 6.6 and 6.7 which fully describe the function of a hydrocyclone within its operational limits. If a given cut size and underflow concentration are specified, simultaneous solution of the three equations will yield the cyclone diameter, the number of cyclones to be used in parallel and the size of the underflow orifice which will produce the required capacity (under the given pressure drop) and performance. If the operating pressure drop is not specified, several design options are obtained and the final design is selected either from some operating constraints or from economic optimization, see the example below.

It should be pointed out here that the scale-up procedure described here is specifically designed for separation or classification of fine particles. These are the particles predominantly used in the chemical industry and the approach, using dimensionless groups, is in common with the treatment of other unit operations in chemical engineering. The geometrical similarity concerns all internal dimensions of the individual cyclones except the size of the underflow orifice which is regarded here as an operational variable.

Another point worth making concerns the fluid density and viscosity used in this model. Some people believe that, at high solids concentrations, one should use the apparent viscosity of the suspension and the actual density of the feed suspension. This is an unrealistic approach for the following reasons. At the relatively moderate concentrations for which the model was designed (0–10% by volume), fine particles are surrounded by the suspending fluid and the drag on them depends on the viscosity of the fluid. Furthermore, the critical zone which determines whether or not a particle will separate is not in the entry but further down stream in the cyclone body, where the flow is depleted of the coarser, easily separated solids, and the concentration there is much less than that in the feed.

A similar case may be made for the use of density: in Stokes' law, the buoyancy of particles in the separation zone must be taken into account. The fine particles displace the continuous phase and hence it is the density of the liquid that is used in the model. In any case, the suspension density in the zone is not known but is likely to be much less than that of the feed. The second use of fluid density is in the resistance coefficient, Eu. The density to be used there depends on how we define the Euler number; the dynamic pressure in the denominator (equation 6.9) is simply a yardstick against which we measure the pressure loss through a cyclone. We have used the clean liquid density in the dynamic pressure; alternatively, the feed suspension density may be used. It is immaterial which of the two densities is used (they are both equally unrealistic) provided the case is clearly defined: conversion from one to the other is a simple matter.

Example 6.1 Hydrocyclone selection, Rietema's geometry

The design procedure described here is best carried out with a computer programme. The example below is calculated with one such commercially

available program[38]. The program sizes a hydrocyclone, or a number of units in parallel, for a given duty. The first problem to be solved is to establish the task required from the cyclone and relate it to the reduced cut size which can then be used by the program. In order to facilitate relatively easy conversion of performance data such as total recovery, overflow concentration and all the reduced values, both the size distribution of the feed solids and the reduced grade-efficiency of the hydrocyclone are assumed to follow the log–normal law. The data input needed for running the program, therefore, includes the median size and the geometric standard deviation of the feed solids, and the geometric standard deviation of the reduced grade-efficiency curve.

The program first converts the task given, via three different input options, into the operating cut size required. The three options are for classification, clarification or thickening duties. It then calculates, from the given operating conditions and the required cut size, the design options available (number of cyclones in parallel, their diameter and the operating pressure drop necessary) and allows the user to choose a suitable set. If the task specified leads to unreasonable design options, the user may select to go back and change the task. If one of the design options is selected as acceptable, the final design proportions of the hydrocyclones may also be obtained. A print option allows the printing of the final table of results.

The operating conditions used in this example are listed in *Table 6.2*. As can be seen, the same performance may be obtained either with fewer, larger cyclones operated at high pressures or with more smaller units at lower pressure drops. The designer must select from the options which is the most

Table 6.2 Summary of the operating conditions used in example 6.1

Feed flow rate, Q	0.005 $m^3\ s^{-1}$
Liquid viscosity μ	0.001 Ns m^{-2}
Liquid density ρ	1000 kg m^{-3}
Solids density ρ_s	2600 kg m^{-3}
Solids concentration, c	0.05 v/v
Solids median	20 μm
Geometric standard deviation of the feed solids size distribution	3
Geometric standard deviation of the reduced grade efficiency curve of the cyclone	2
Performance criteria	
Total coarse recovery by mass, E_T	70.92%
Total reduced mass recovery, E_T	67.69%
Actual cut size, x_{50}	10 μm
Reduced cut size, x'_{50}	11 μm
Overflow concentration, c_o	0.0162 v/v
Underflow concentration, c_u	0.3546 v/v
Flow ratio, R_f	0.1

Design options to meet the above performance

No. of cyclones in parallel	*Diameter, D,* m	*Pressure drop,* bar
1	0.1089	7.4620
2	0.0849	4.7819
3	0.0735	3.6860
4	0.0063	3.0645
5	0.0612	2.6555
6	0.0573	2.3622
7	0.0542	2.1396
8	0.0517	1.9638
9	0.0496	1.8208
10	0.0477	1.7017
11	0.0461	1.6007
12	0.0447	1.5138

appropriate or most economical; if, for example, two hydrocyclones are selected to be used in parallel, then the operating pressure will be 4.7819 bar and the cyclone diameter $D = 0.0849$ m. All the other dimensions may be calculated from the proportions given in *Table 6.1* (except for D_u which is determined from equation 6.7), i.e. $L = 0.4247$ m, $D_i = 0.0238$ m, $D_u = 0.0184$ m, $D_o = 0.0289$ m and $l = 0.0380$ m.

Finally, the whole of the above example can, of course, be calculated manually from the equations in section 6.6.6, but a computer program allows a faster computation of the alternatives and a better appreciation of the effect of the different variables on the final design solution.

6.7.4 Multiple cyclones in series

Series connections of separators are a common way of improving the performance of single units. In the case of hydrocyclones, due to their low capital and running costs, multiple series arrangements are quite frequently used. As to which particular layout and arrangement should be used depends on the actual application in question.

If clarification of the liquid is the ultimate purpose and it cannot be achieved in a single-pass arrangement, several stages in series in the direction of the overflow may be considered, such as the arrangement shown in *Figure 6.15*. Alternatively, a multiple-pass arrangement may be considered, such as that shown schematically in *Figure 6.16*; hydrocyclones are particularly suited for this. An additional benefit from this arrangement is that it dilutes the feed for the cyclone which improves the cyclone efficiency.

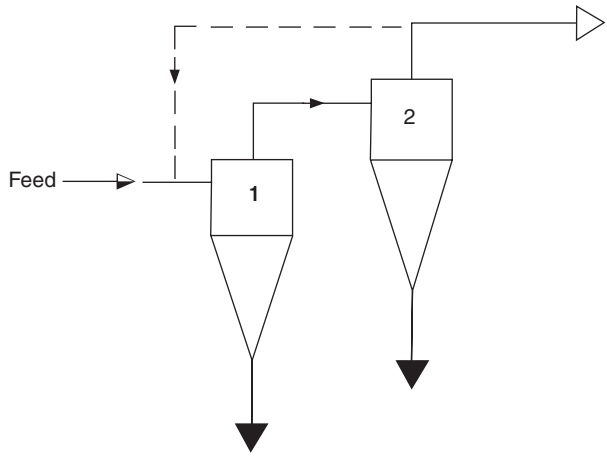

Figure 6.15 Two hydrocyclones in series for clarification, with a possible partial recycle

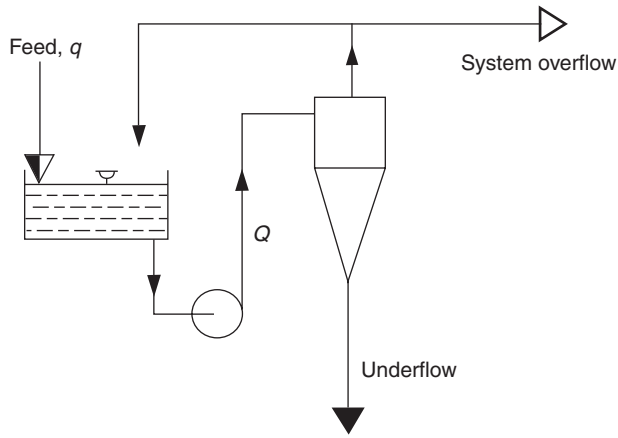

Figure 6.16 A multiple-pass arrangement for clarification

In thickening duties, if the required degree of thickening cannot be achieved with one cyclone, two or more in series may be used, this time in the direction of the underflow—see *Figure 6.17*. The overflow from the second or subsequent stages may be partially recycled back to the feed of the first stage.

If both thickening and clarification are required simultaneously, a two- or three-stage arrangement is required where some cyclones are used as thickeners and others as clarifiers. *Figures 6.18* and *6.19* show examples of such arrangements, depending on whether one or two thickening cyclones are needed (i.e. depending on the concentration of the feed: if the feed is very

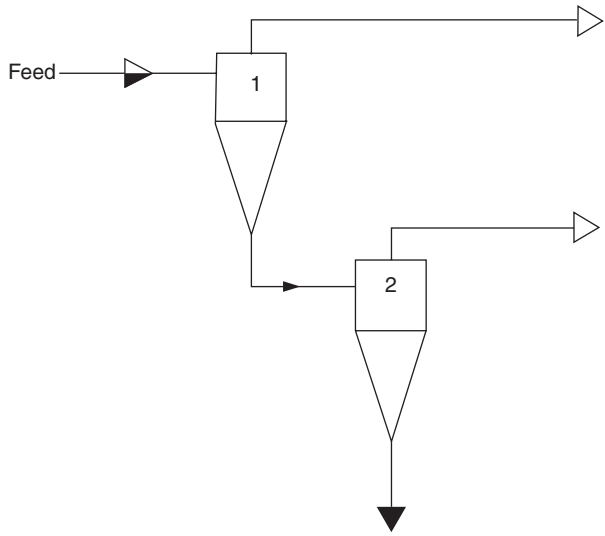

Figure 6.17 Two hydrocyclones in series for thickening

dilute, two thickeners will be needed). Whether a hydrocyclone is used as a thickener or as a clarifier is shown in *Figures 6.18* and *6.19* by the nature of the underflow stream: rope discharge indicates a thickening duty whilst a spray discharge is for clarification.

In one arrangement, shown schematically in *Figure 6.18* as an example, the thickener is in the first stage, followed by one (or more) clarification stage,

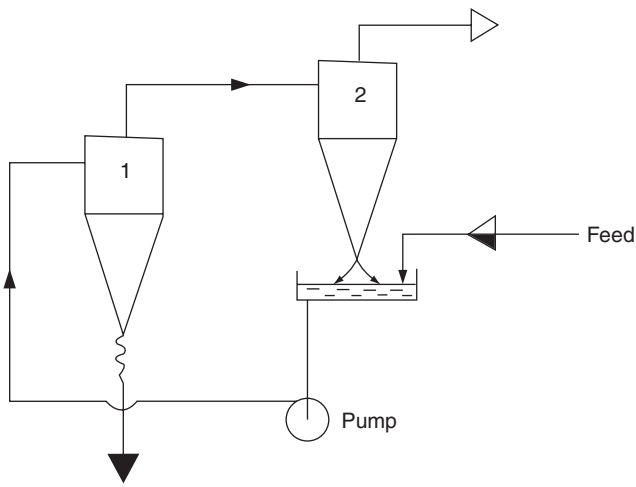

Figure 6.18 Two hydrocyclones in series with a second-stage underflow recycle, for simultaneous thickening and clarification

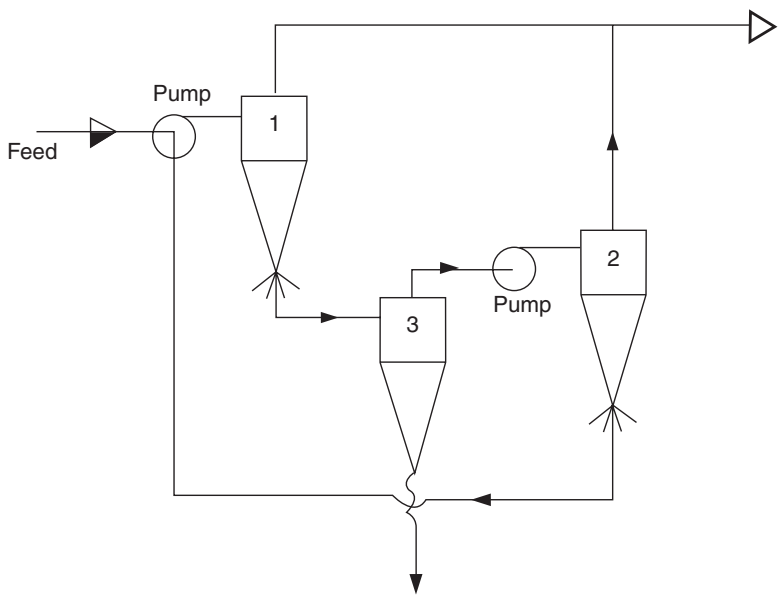

Figure 6.19 A three-stage arrangement for clarification and thickening of dilute feeds

the underflow from which is returned to the feed. The overall recovery of the whole plant is better than the recovery of any of the individual cyclones used. The recycle should be more dilute than the feed, so that the feed to the thickening cyclone is diluted, because divergent performance of the plant could result otherwise. If the feed is very dilute (less than say 1%) and the thickening cyclone might not produce sufficiently thick underflow in one stage, another arrangement may be used (*Figure 6.19*) where the first stage is clarification, with the thickener treating the underflow of the first stage. Another clarifier is then used to clean the overflow from the thickener. Such a plant is relatively small and achieves good thickening, but the recovery is not as good as in the arrangement shown in *Figure 6.18*.

In classification duties, hydrocyclones give a relatively poor sharpness of cut in one pass and, consequently, in order to minimize the amount of misplaced material, the classification may be done in two or more stages. *Figure 6.20* shows how the classification can be sharpened by using another stage on both the overflow and the underflow. If the cut size of all three cyclones is the same, the process will cut at the same particle size as the front cyclone but the grade efficiency will be significantly steeper. Typically, a sharpness index (x_{75}/x_{25}) of 2.4 for a single cyclone can be reduced to 1.6 using this arrangement. Note from *Figure 6.20* that if the underflow from the previous stages is to be classified further, it must be diluted in order to obtain good sharpness of cut and the required cut size.

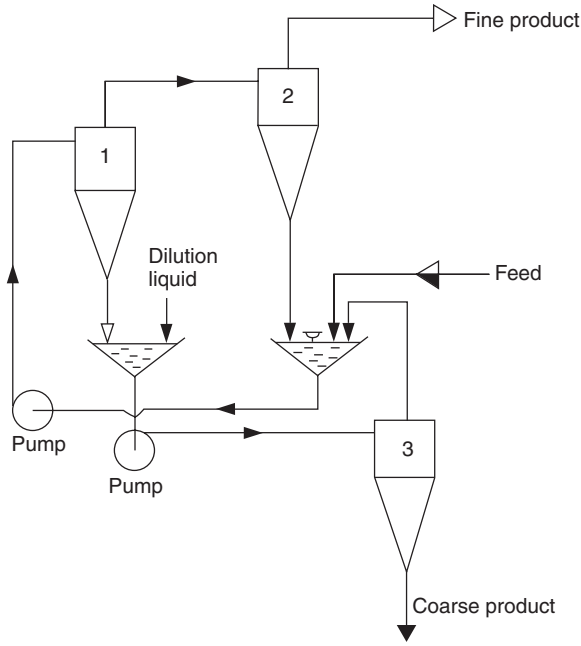

Figure 6.20 A reclassification arrangement designed to sharpen the cut

Finally, multiple-series arrangements are also extensively used in countercurrent washing of solids. The reader is referred to chapter 15 for the description and design of the washing trains used for this purpose.

6.8 Design variations, other design features

The conventional hydrocyclone has been subjected to considerable development to improve its characteristics. A selection of various design features is given below.

In the pulp and paper industry, water is often added in the underflow 'rejects' chamber to reduce losses of fibre with the rejected granular dirt. Similarly, the sharpness of cut in the classification of granular solids can be improved by injecting clean liquid into the flow near the apex of the cone. The liquid displaces the slime fraction that would normally end up in the underflow; commercial systems exist for this (e.g. Krebs Engineer's Cyclowash). The quantity of liquid added is usually equal to or greater than the underflow rate without liquid injection. The benefits of this depend on the cost of clean liquid needed for the injection: reclassification may be a cheaper alternative.

Another way to sharpen the classification is to operate the cyclone upside down so that the solids are separated into a container above the cyclone and

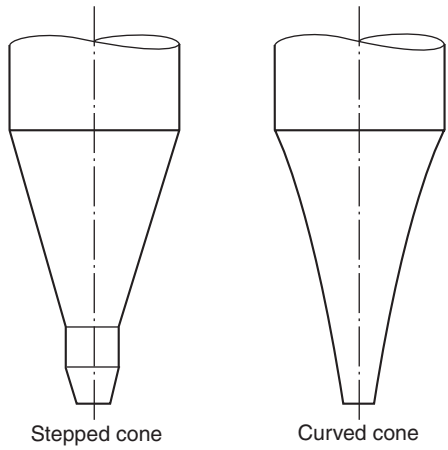

Figure 6.21 The curved cone and the stepped cone as alternative cone shapes

subsequently fall back into the cyclone to be washed again. In this way, the container contents recirculate until the fines entrained first time around are disentrained to go to the overflow. A multistage operation using cyclones of different cut size at each stage can then separate the feed into several closely sized fractions depending on the number of cyclones used.

If magnetic particles like finely divided magnetite are to be recovered with hydrocyclones, the recovery may be enhanced with an external magnetic field suitably shaped so as to produce a radial field perpendicular to the cyclone axis. A commercial 'magnetic cyclone' is based on this principle.

Some hydrocyclones used in the pulp and paper industry use cones which steepen gradually towards the lower end, as shown in *Figure 6.21*, This steepening reduces the centrifugal force which presses the separated particles onto the wall and it is supposed to reduce the abrasion in the lower part of the cone. An alternative to a curved cone may be a stepped cone, also shown in *Figure 6.21*, which is found to be particularly beneficial in gas cyclones where it reduces re-entrainment.

The cleaning efficiency and the blocking characteristics of cyclones applied to pulps (saw dust, newsprint, sulphite, etc.) can be improved by using spiral cones. These have a single or double spiral cast into the cone, with two sides inclined at a negative angle which represents no or negligible extra cost with plastic cones. However, there is no improvement for granular solids.

6.8.1 The underflow orifice design and control

When operating a hydrocyclone with a free underflow orifice discharging into atmospheric pressure, the discharging slurry can be observed to have different shapes depending on the feed size distribution, separation efficiency

and the size of the underflow orifice. At relatively low underflow concentrations, the discharge has an 'umbrella' or spray-type shape because the outgoing slurry is still spinning quickly. Under such conditions, the air core inside the cyclone is vented to the atmosphere through the centre of the umbrella discharge. When more solids report to the underflow, because of an increase in the feed concentration, in the separation efficiency or because of a decrease in the orifice size, the boundary layer flow carrying the particles into the underflow joins in the middle and the underflow comes out as 'rope' discharge, no longer spinning out in a spray. The underflow orifice becomes overloaded and significant quantities of solids will start overflowing, resulting in loss of efficiency. On further throttling of the underflow orifice the discharge becomes 'lazy', in the form of a snake, and there is an acute danger of blocking (in fact blocking sometimes occurs before this stage is reached).

The simplest way to operate a hydrocyclone is to open both the underflow and overflow to the atmosphere because this ensures correct hydraulic balance between the two outlets, independent of what happens downstream of either of the outlets. Virtually all test data available on different cyclone designs, as well as theoretical or empirical formulae for performance characteristics, are for such conditions of equal back pressure on both discharge streams.

If for some reason the cyclone discharge must be against back pressure, it may still be worthwhile to maintain the balance between the underflow and overflow. In some applications such as when two or more cyclones are used in series, the back pressure may not be the same on both outlets (in the case of the liquid–liquid separation cyclones for example), and this is quite acceptable provided that the pressures are maintained in the same ratio because this has a profound effect on the flow split in the cyclone and the operating cut size.

Underflow rate can be controlled by back pressure with a valve downstream but this is generally not recommended for individual, small-diameter cyclones because in such cases the throttling valve itself is likely to block. It is, however, the only option for multiple assemblies of small-diameter cyclones because the underflow opening of the individual units cannot be reduced below a certain size for the increased danger of blocking. In any case, it is not feasible with a multi-unit arrangement to change the underflow orifices of the constituent cyclones as the cyclones are numerous and often cast in blocks of steel or plastic, and are, therefore, inaccessible anyway.

Only small-diameter or specialized hydrocyclones have a fixed underflow orifice, but most commercial units are supplied with a variable one. This is because the optimum size of the opening cannot be reliably predicted and the correct adjustment of it is vital for the best operation of the cyclone. The size of the underflow orifice affects directly the underflow-to-throughput ratio, the underflow concentration and the cut size. The underflow orifice is best adjusted after start-up of the plant and during operation whenever any operating conditions change. Several possible designs are available for this adjustment: replaceable nozzles, mechanically adjustable openings, pneumatically or hydraulically controlled orifices, or even self-adjusting devices

which maintain a constant underflow density or concentration. Whatever the method of controlling the size of the underflow opening, the orifice should always be kept circular because the underflow slurry is still rotating when it comes out and blocking would be more likely with an orifice of any other shape.

It is also important to mention here that a hydrocyclone by no means necessarily requires continuous underflow: it can just as well be operated with a closed 'grit pot' under the discharge orifice and this can then be intermittently discharged by a manually or automatically operated purge valve. The separation efficiency with a grit pot is always lower than with continuous underflow (in other words the use of the grit pot coarsens the separation) but this can often be offset by using a multiple-pass system. The grit pot improves the sharpness of cut, due to the exchange of liquid between the pot and the cyclone, and the accompanied washing effect (with no net flow in either direction).

6.8.2 Types and shapes of inlet

Another important design feature is the method of introducing the feed slurry to the hydrocyclone. A single tangential inlet is most common: there is little advantage in using multiple entry which would complicate the design of the manifolding. One commercial design of multicyclone systems for separating organic matter from seawater or other classification duties, however, features multiple entry (3–6 inlets evenly distributed around the periphery) and an annular overflow orifice. A dual inlet is used in one of the designs developed for liquid–liquid separation duties.

The shape of the cross-section of the inlet is another design variable. It might be circular or rectangular (with the longer side parallel with the cyclone axis), the latter being slightly better because, for the same flow area, it brings the particles a little closer to the wall on entry. Rectangular inlets do not represent a manufacturing complication because nowadays most cyclones are cast.

The form of the entry along the flow and the shape of the top cover are probably more important to the cyclone performance than the cross-sectional shape of the inlet, and these parameters are subject to many proprietary variations. At least one manufacturer uses an involute entry where, instead of a simple tangential inlet, the feed enters via a spiral. This is supposed to minimize the intersecting angle between the incoming feed and the already rotating fluid inside the cyclone, and thus reduce turbulence and energy requirements. This is bound to have some effect on separation efficiency but whether the gain is significant enough to justify the design complication remains to be seen. Other manufacturers reduce the turbulence on entry by making the top cover in the shape of a helix so that the tangentially introduced feed does not impinge on the flow inside and it also gets some downward momentum. Helical inlets are also known to increase abrasion resistance of gas cyclones but no direct evidence exists for hydrocyclones.

The turn-down ratio and/or the cut size of a hydrocyclone can be altered by changing the size of the inlet. Some small-diameter cyclones are available

with replaceable cylindrical sections which are cast together with the vortex finder and inlet section, and two or more alternative inlet sizes may be used. Another alternative is to use inserts in the inlet or shrouds which can be set without disassembly of the inlet section. Our own development work at Bradford University has produced a piston-like inlet control device which allows inlet size to be changed without interrupting the flow, but this would probably prove too expensive to be produced commercially.

6.8.3 Size and shape of the vortex finder, pressure recovery

The inside diameter of the vortex finder is also often used to control the capacity and cut size. This is done by using the above-mentioned replaceable cyclone tops or by inserting different sized nozzles into the vortex finder. The shape of the vortex finder is not subject to much variation; the only significant feature is the occasional use of skirts or discs at the bottom edge to counter the short circuit flow down the outside of the vortex finder. This is relatively rare, however, as the benefit is doubtful and possibly not worthwhile in view of the manufacturing or casting complications.

Cylindrical overflow boxes are sometimes used, with a tangential off-take, on top of some larger cyclones. This is supposed to recover some of the energy of the spinning overflow but, once again, the actual benefit is small in view of the total pressure drops involved in hydrocyclones. Such pressure recovery devices are much more common and beneficial with gas cyclones where the operating pressure drops are about 100 times lower than those normally used with hydrocyclones.

6.8.4 Multicyclone arrangements

Both theory and practice show that smaller diameter hydrocyclones give for the same pressure drop better separation efficiency. In clarification duties or when classifications at low cut sizes are required, banks of small-diameter hydrocyclones are used in parallel to treat high flow rates. This may be done either by manifolding several single cyclones in parallel or, when a large number of really small units is to be used, by enclosing the cyclones in a single housing, with common discharge chambers. Such multicyclone units may themselves be manifolded in parallel in multiple arrangements, or they might be stackable to produce compact columns capable of treating very high flow rates.

The available arrangements can be divided into four basic types (as shown schematically in *Figure 6.22*), with small variations within each type. The first two types, (a) and (b), are linear arrangements while the other two, (c) and (d), are circular. Circular arrangements lend themselves much better to an even distribution of the feed because each unit can have an identical length of piping between it and the centrally positioned header.

Arrangement (c) in *Figure 6.22* is probably most common for manifolding a multiplicity of single cyclones together. It is sometimes referred to as the

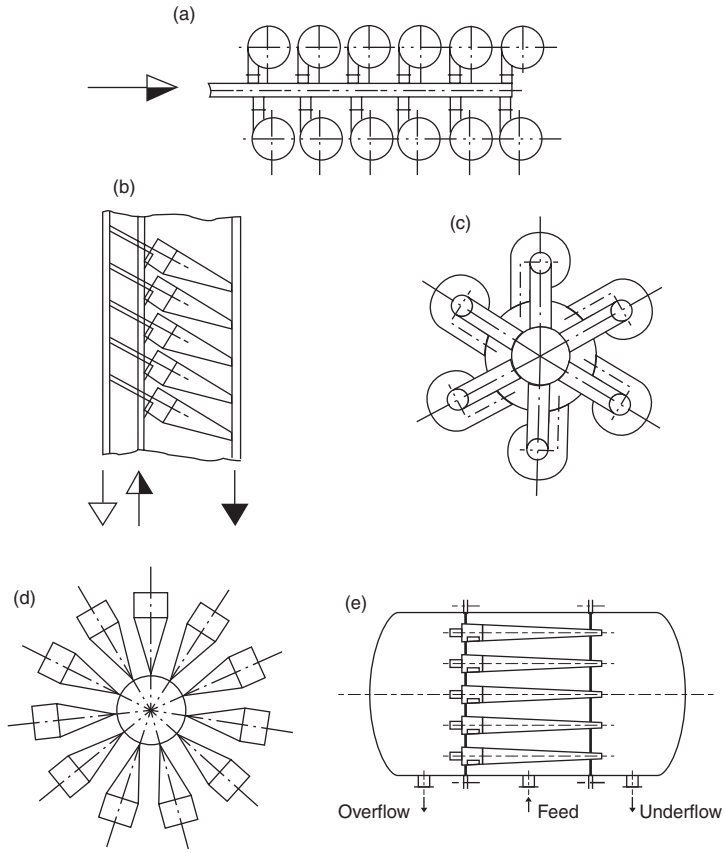

Figure 6.22 Types of multiple hydrocyclone arrangements. (a) Plan view (b) Elevation (c) Plan view (d) Plan view (e) Cross-section

'spider arrangement' due to the shape of the necessary pipework, particularly the sweeping 180° turns of the overflow pipes from each unit to the central well. Like in the horizontal linear arrangement, the cyclones here are also in vertical positions or slightly inclined. The underflow discharge may be arranged to discharge freely into a common launder around the central feed well and the operator is therefore able to see the discharges of the individual units and spot any blockages.

The vertical circular arrangement is also highly suitable for use in the compact multiple cyclone units which in this case take the shape of circular boxes, often stackable. The cyclones are either mounted inside as individual units, using simple clamping systems, or cast into plastic or metal, often together with a prestrainer and the associated ducting.

A relatively new development having taken place since 1984 (when Vol. 1 of *Hydrocyclones* was published) is in high technology applications such as in

the petroleum and chemical industries. As the particle size and density are usually low, such applications inevitably require small diameter units and a lot of them operated in parallel in order to treat the high flow rates involved. The idea of compact multiple cyclone units which are mounted inside circular or rectangular boxes is not new but in the novel, high technology applications they have been better engineered. It is now common to see hydrocyclones made in high grades of stainless steel, mounted in between tube sheets in pressure vessels as shown schematically in *Figure 6.22*(e).

The two tube sheets devide the vessel into three separate compartments:

1 the feed space into which the feed is pumped under pressure and distributes itself into the individual cyclone's feed orifices which open into this space, and
2 the overflow and underflow compartments, into which the cyclones discharge their respective overflows and underflows. Please note that *Figure 6.22*(e) is merely a schematic representation and that in practice these compartments are usually made as small as possible to minimize both the liquid hold-up and the danger of particle settling in such spaces.

In order to facilitate replacement and/or cleaning of the individual units, the cyclones are sealed into the tubesheets with rubber gaskets and secured with bolts so that they can be individually removed if necessary. A further variation of this design is possible in using four tubesheets and two sets of hydrocyclones, with either the underflows or the overflows opening into a common space inside the vessel.

In the case of really small cyclones (e.g. 10 mm diameter units), these are sometimes cast into disks and such disks are stacked into columns. Such systems resemble other chemical engineering columns for mass transfer or cartridge systems for filtration. One problem common to all compact multiple hydrocyclone systems is with the operator's inability to see any blockages. He or she must then diagnose any such difficulties from other operating performance such as an increase in pressure drop. Having detected a blockage problem, the only remedy available is to replace the unit or the whole column and clean it off-line.

6.9 Applications

Applications of hydrocyclones in industry fall into several broad categories: clarification, thickening (or both simultaneously), classification, washing, sorting, liquid–liquid separation, liquid degassing and particle size measurement. Here, we shall concentrate on the first three categories, and for examples of the other categories the reader is referred to Svarovsky[3].

6.9.1 Clarification

The aim of clarification is to produce clear overflow, which is the same as maximizing the mass recovery of solids from the feed. The feed liquid has only small amounts of solids and it is the clarification of the liquid which is of primary interest, not the concentration of the solids in the underflow.

The operating variables for clarification are: dilute feed, relatively open underflow orifice (i.e. dilute underflow, typically below 12% of solids by volume but the less the better), and high pressure drop. The design variables are: small-diameter, narrow-angle cyclones (there is a limit in the body diameter here due to the liability to blocking) nested in parallel in multi-cyclone arrangements, high efficiency design (i.e. small inlet and overflow orifices, etc.). In single-pass installations, hydrocyclones can give minimum cut sizes of around 2 μm but this can be further improved by using multiple-pass or recirculating systems.
Applications of hydrocyclones in clarification include, for example:

1 recovery of catalysts in the oil and chemical industries;
2 separation of sand from sugar cane juice;
3 removal of scale particles from the jet water and cooling water of the rollers in steel rolling plants;
4 separation of corrosion products in circulating systems in the nuclear power industry;
5 removal of solids (steel or metal swarf) from metal working coolants, cutting fluids or circulating washwater in the engineering industry;
6 clean-up of washwater in washing machines for motor parts;
7 removal of silt from well water;
8 clean-up of water from gas scrubbers for recycling;
9 clean-up of water in car wash systems;
10 precleaning of primary sewage sludge (1–2% solids);
11 removal of sand, scale and other organic or inorganic particles to protect heat exchangers, boilers, glands and seals;
12 recovery of salts from saline solutions;
13 cleaning of washwater for potato processing;
14 cleaning of washwater in coal or ore processing plants;
15 degritting of milk of lime;
16 clarification of seed oil;
17 removal of drill chips from drill mud;
18 primary treatment of wool scour effluent, or removal of any other fine particles from aqueous or non-aqueous suspensions.

6.9.2 Thickening

Thickening means concentrating the solids present in a suspension into a smaller amount of fluid; the goal is to produce high concentration of solids in

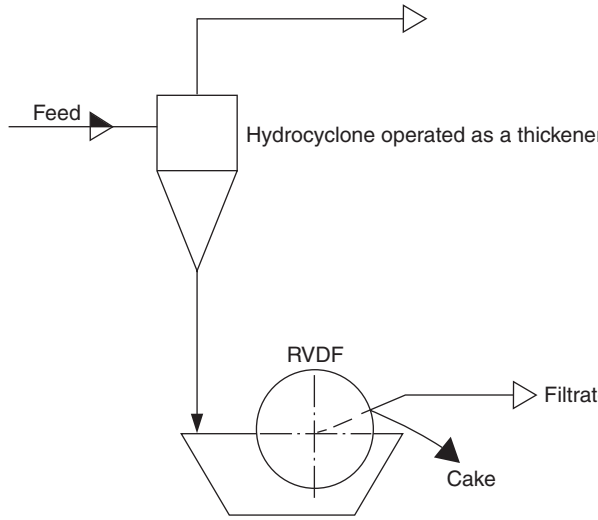

Figure 6.23 Prethickening of feed to a vacuum filter with a hydrocyclone

the underflow and any loss of solids to the overflow is undesirable but of secondary importance. The feed solids concentrations in thickening applications are usually higher than in clarification duties.

If hydrocyclones are to be used to produce thick underflows (i.e. to dewater the solids), the total mass recovery of the feed solids must be sacrificed because throttling the underflow orifice inevitably leads to some loss of solids to the overflow. A hydrocyclone as a single unit cannot therefore be used for both clarification and thickening at the same time. The underflow concentrations that can be achieved with hydrocyclones may be as high as 50% by volume with some materials. Thus, for example, the AKW cyclone, 125 mm in diameter, can give 45% by volume with chalk. In this thickening performance hydrocyclones compare favourably with gravity thickeners and hydrocyclone systems are sometimes used to replace the much larger and more expensive gravity thickeners.

The limiting factor in how far the underflow orifice can be closed is the danger of blocking. In terms of design variables, there is no particular need for small cyclone diameters; smaller units are, in any case, more liable to block. Normally, narrow-angle cyclones are used. A variable underflow orifice is very useful here.

The following is a list of some reported applications of hydrocyclones in thickening of slurries:

1 thickening of the waste product from flue-gas desulphurization systems where cyclones are used to replace the more costly gravity thickeners;
2 dewatering of mine back-fill;

3 dewatering of silt in dredging operations;
4 densification of the recovered and cleaned medium in medium recovery plants in dense medium separation.

Apart from many existing applications in mineral processing, there are also actual and potential applications for hydrocyclones in the chemical industry, like recovery and concentration of ammonium chloride crystals or sodium bicarbonate.

A typical example of a hydrocyclone as a thickener is in prethickening of feed to vacuum filters, screens or dewatering centrifuges (*Figure 6.23*). Unless the feed is coarse, however, the overflow from the hydrocyclone used as a thickener must be clarified further (if it is required clean). The hydrocyclones are also used for preconcentration of slurries before decanting centrifuges as it improves overflow clarity. This may not affect the centrifuge capacity, however, because the limiting factor in dewatering duties is usually the mass flow rate of solids.

6.9.3 Classification of solids according to size

This application of hydrocyclones is for solid–solid separation by particle size. As the grade efficiency of a cyclone increases with particle size, it can be used to split the feed solids into fine and coarse fractions. This may be a process requirement, by which coarse and fine solids are separated to follow different routes in the plant, such as for example in closed-circuit wet grinding where the oversize particles are returned to the mill for further grinding (*Figure 6.24*). There are other possible grinding arrangements than that shown in *Figure 6.24*: open circuit, or open/closed (double function or two-stage), also

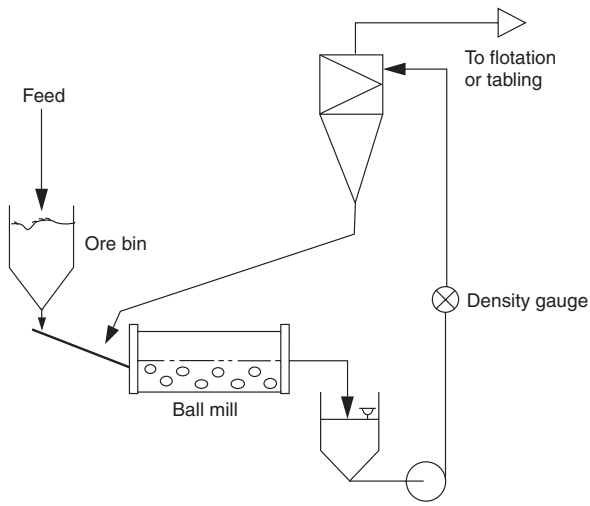

Figure 6.24 A hydrocyclone classifier in closed-circuit grinding

with a post-desliming or post-refining stage. In this type of application, hydrocyclones are most frequently used either to remove coarse particles from the product (in a degritting or 'refining' operation) or to remove fine particles from the product (in a desliming or 'washing' operation). In other applications, the feed material may simply be split in half into two commercially useful products of narrow size distribution. Hydrocyclones are, therefore, used to engineer the size distribution of products or intermediates.

The requirement in classification is to be able to set the cut size to a predetermined value dictated by the application, and to achieve a good sharpness of cut (this requires a steep grade-efficiency curve). As pointed out previously, wide cone angles improve the sharpness of cut. There is a problem, however, in achieving low cut sizes with such cyclones. Consequently, when classifying at low or moderate cut sizes, say up to 50 μm, narrow-angle cyclones are still used to achieve those cuts. With increasing cut size, larger angles are used until at over 250 μm, such coarse cuts can in fact only be achieved with wide-angle or flat-bottomed cyclones. Liquid injection into the cone or an upside-down operation are also sometimes used to sharpen the cut.

Hydrocyclones are also used as classifiers simply to improve the performance of other filtration or separation equipment. A good example is in applications where the cyclone separates the feed into coarse and fine particles, and the coarse material is fed onto the horizontal belt filter first, as a precoat, with fines to follow (see *Figure 6.25*). This will, if the cut point of the cyclone is set correctly, give good filtrate clarity and extend the usefulness of vacuum filters to finer feeds without necessarily adversely affecting the moisture content of the cake.

Some further examples of hydrocyclones in a classification duty are:

1 desliming of minerals prior to flotation which leads to less reagent to be used and easier flotation;
2 desliming prior to leaching leading to higher extraction coefficients, desliming prior to filtration equipment to reduce the cake resistance to flow;
3 degritting of drilling muds;

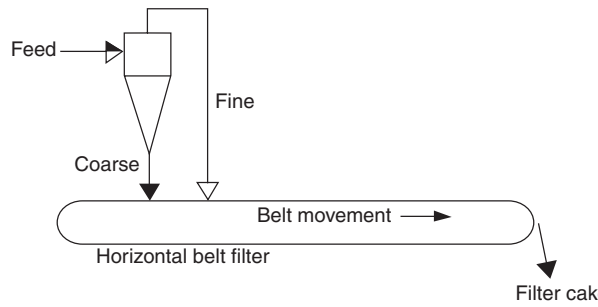

Figure 6.25 Precoating of a horizontal vacuum belt filter with hydrocyclone underflow

4 separation of clay from barytes in drilling muds for control of specific gravity;
5 degritting of underground waters prior to pumps;
6 classification of 'raw' cement slurries before rotary kilns performed at high solids concentrations (to reduce thermal load on the kilns) as the high shear forces in the cyclone overcome the yield stress of the slurry which normally behaves as a Bingham plastic;
7 removal of impurities and unground particles from chalk;
8 desliming of phosphate rock;
9 classification of iron ore into coarse fraction (sinter feed) and fine fraction (pellet feed);
10 sizing of sand into fractions;
11 recovery of filter aid;
12 beneficiation of china clay (kaolinite).

6.10 Conclusions

There are several recognizable trends and avenues in the future development and application of hydrocyclones; the recent international conferences on the subject have served as a good indicator in this respect. The following is a list of the author's main conclusions, and it necessarily represents a personal view.

Major changes in the conventional cyclone design for solid–liquid separation are unlikely, but many refinements will be made, based on the development of gradually more realistic flow models. Such models already give qualitative assistance in design decisions and provide the reasons why the previously empirically determined optimum geometries are better than others. In particular, the real value of the various pressure recovery devices will be established and other power-saving measures pursued (like the possibly beneficial effect of vorticity in the inlets of the second and further stages in multiple-stage systems). There will be, however, more changes in the geometry of cyclones for other phase separations where droplet or bubble break-up have to be minimized.

A better understanding of the performance characteristics of hydrocyclones, whether from fundamental or empirical work, will allow the best to be made of the advantages of hydrocyclones. In particular, combinations of hydrocyclones in series will continue to make it possible to overcome the inherent limits on the performance of a single hydrocyclone, and the design of such systems will be optimized.

Development is particularly expected to continue in liquid–liquid and liquid–gas separations, both in hardware and in the operating experience or performance.

It is the opinion of the author that hydrocyclones are undergoing a transformation from low to medium or high technology and that this process will continue well into the next century.

A further problem with answers

Determine the diameter and the minimum number of hydrocyclones to be operated in parallel to clarify a suspension of the following properties:

Liquid vicosity $\mu = 0.001\,\text{Ns/m}^2$
Liquid density $\rho = 1000\,\text{kg/m}^3$
Solids density $\rho_s = 2600\,\text{kg/m}^3$
Flow rate $Q = 0.01\,\text{m}^3/\text{s}$
Pressure drop $\Delta p = 100\,000\,\text{Pa}$
Feed concentration: very low, below 0.1% v/v

Bradley's design is to be used (see the design proportions in *Table 6.1*). The following relationships apply for scale-up:

$$\text{Stk}_{50} \cdot \text{Eu} = 0.1111$$
$$\text{Eu} = 446.5\text{Re}^{0.323}$$

where Stk_{50}, Eu and Re are based on cyclone diameter and the superficial velocity in the cyclone body as defined in equations 6.9 to 6.11. Assume that the cut size of 10 μm is needed for satisfactory clarification of the feed suspension. Also assume that, for this case of clarification at very low feed solids concentration, the required flow ratio R_f is to be very small and its effect on efficiency can therefore be neglected.

Answer

7 cyclones are to be used in parallel, 114 mm in diameter each.

References

1. Kelsall, D. F., 'A study of the motion of solid particles in a hydraulic cyclone', *Trans. Inst. Chem. Eng.*, **30**, 87–104 (1952)
2. Driessen, M. G., *Trans. Am. Inst. Min. (Metall.) Eng.*, **177**, 240 (1948)
3. Svarovsky, L., *Hydrocyclones*, Holt, Rinehart and Winston, London (1984)
4. Driessen, M. G., *Rev. Ind. Mining*, **Special Issue 4**, 449–461 (1951)
5. Criner, H. E., '*The Vortex Thickener*', Int. Conf. on Coal Preparation, Paris (1950)
6. Bradley, D. *The Hydrocyclone*, Pergamon Press, London (1965)
7. Bradley, D. and Pulling, D. J., 'Flow patterns in the hydraulic cyclone and their interpretation in terms of performance', *Trans. Inst. Chem. Eng.*, **37**, 34–45 (1959)
8. Rietema, K., 'Performance and design of hydrocyclones, Parts I to IV', *Chem. Eng. Sci.* **15**, 298–325 (1961)
9. de Andrade Medronho, R., 'Scale-up of hydrocyclones at low concentrations', Ph.D. Thesis, University of Bradford, 1984
10. Holland-Batt, A. B., 'A bulk model for separation in hydrocyclones', *Trans. Inst Min. Metall. (Sect. C: Min. Process Extr. Metall.)*, **91**, (1982)
11. Trawinski, H. F., *Filtration and Separation*, **6**, (1969)
12. Kutepov, A. M., *et al.*, 'Calculation of separation efficiencies in hydrocyclones', *Izv. Vuzov, Chim. Chim. Technol.*, **XX**, 144–145 (1977)

13. Kutepov, A. M., 'Study and calculation of the separation efficiency of hydrocyclones', *Zh. Prikl. Khim.*, **51**, 614–619 (1978)
14. Rietema, K., 'The mechanism of the separation of finely dispersed solids in cyclones'. In K. Rietema and C. G. Verver (Eds), '*Cyclones in Industry*', Chap. 4, Elsevier, Amsterdam (1961)
15. Bloor, M. I. G. and Ingham, D. B., *Trans. Ind. Chem. Eng.*, **53**, 1 (1975)
16. Duggins, R. K. and Frith, P. C. W., 'Turbulence effects in hydrocyclones', *3rd International Conference on Hydrocyclones* (Oxford, 1987), Paper D1, Elsevier Applied Science Publishers, Barking (1987)
17. Schubert, H. and Neesse, T., A hydrocyclone separation model in consideration of the turbulent multi-phase flow', *Proc. Int. Conf. on Hydrocyclones* (Cambridge, 1980), Paper 3, pp. 23–36, BHRA Fluid Engineering, Cranfield (1980)
18. Neesse, T. and Schubert, H., 'Die Trennkorngrosse des Hydrozyklones bei Dunnstrom – und Dicht–stromtrennungen', *First European Symposium on Particle Classification in Gases and Liquids*, Nuremberg (1984)
19. Fahlstrom, P. H., 'Discussion', *Proc. Int. Min. Processing Congress 1960*, pp. 632–643, Inst. Mining and Metallurgy (1960)
20. Bloor, M. I. G., Ingham, D. B. and Laverack, S. D., 'An analysis of boundary layer effects in a hydrocyclone', *Proc. Int. Conf. on Hydrocyclones* (Cambridge, 1980), Paper 5, pp. 49–62, BHRA Fluid Engineering, Cranfield (1980)
21. Bloor, M. I. G. and Ingham, D. B., 'Theoretical analysis of the conical cyclone', *First European Conf. on Mixing and Centrifugal Separation* (Cambridge, 1974), Paper E6, BHRA Fluid Engineering, Cranfield (1974)
22. Laverack, S. D., *Trans. Ind. Chem. Eng.*, **58**, 33 (1980)
23. Lynch, A. J. and Rao, T. C., *Ind. J. Technol.*, **6**, 106–114 (1968)
24. Lynch, A. J., Rao, T. C. and Prisbrey, K. A., *Int. J. Min. Proc.*, **1**, 173–181 (1974)
25. Lynch, A. J. and Rao, T. C., 'Modelling and scale-up of hydrocyclone classifiers', *11th Int. Mineral Processing Congress* (Cagliari, 1975), Paper 9, pp. 9–25, Instituto di Arte Mineraria (1975)
26. Rao, T. C., Nageswararao, K. and Lynch, A. J., *Int. J. Min. Proc.*, **3**, 357–363 (1976)
27. Plitt, L. R., 'A mathematical model of the hydrocyclone classifier', *CIM Bull.*, **December**, 114–122 (1976)
28. Aplyng, A. C., Montaldo, D. and Young, P. A., 'Hydrocyclone models in an ore-grinding context', *Int. Conf. Hydrocyclones* (Cambridge, 1980), Paper 9, pp. 113–125, BHRA Fluid Engineering, Cranfield (1980)
29. Gibson, K., 'Large scale tests on sedimenting centrifuges and hydrocyclones for mathematical modelling of efficiency', in *Proc. Symp. Solid–Liquid Separation Practice* (Leeds, 1979), pp. 1–10, Yorkshire Branch of the Institute of Chemical Engineers, Leeds (1979)
30. Medronho, R. A. and Svarovsky, L., 'Tests to verify hydrocyclone scale-up procedure', *2nd Int. Conf. on Hydrocyclones* (Bath, 1984), Paper A1, pp. 1–14 (1984)
31. Svarovsky, L., 'Selection of hydrocyclone design and operation using dimensionless groups', *BHRA 3rd Int. Conf. on Hydrocyclones* (Oxford, 1987), Paper A1, Elsevier Applied Science Publishers, Barking (1987)
32. Gerrard, A. M. and Liddle, C. J., 'Numerical optimization of multiple hydrocyclone systems', *Chem. Eng.*, **February**, 107–109 (1978)
33. Bloor, M. I. G., 'On axially symmetric flow models for hydrocyclones', *BHRA 3rd Int. Conf. on Hydrocyclones* (Oxford, 1987), Paper D2, Elsevier Applied Science Publishers, Barking (1987)

34. Boyson, F., Ayers, W. H. and Swithenbank, J., 'A fundamental mathematical modelling approach to cyclone design', *Trans. Ind. Chem. Eng.*, **60**, 222–236 (1982)
35. Rhodes, N., Pericleous, K. A. and Drake, S. N., 'The prediction of hydrocyclone performance with a mathematical model', *BHRA 3rd Int. Conf. on Hydrocyclones* (Oxford, 1987), Paper B3, Elsevier Applied Science Publishers, Barking (1987)
36. Bloor, M. I. G., Ingham, D. B. and Ferguson, J. W. J., 'A viscous model for flow in the hydrocyclone', *Session I, Solid–Liquid Separation Practice III, 397th Event of the European Federation of Chemical Engineering* (Bradford, 1989)
37. Svarovsky, L., 'Evaluation of small diameter hydrocyclones', *Inst. Chem. Eng. Symp. on Solid/Liquids Separation Practice and the Influence of New Techniques* (Leeds, 1984), Paper 24, pp. 193–205, Institute of Chemical Engineers, Yorkshire Branch (1984)
38. Hydrocyclone Design, Catalogue of In-Company Short Courses, Books and Particle Technology Software, FPS, The Lares, Maple Avenue, Cooden, Bexhill-on-Sea, TN39 4ST, 2000
39. Rajamani, R. K. and Milin, L., 'Fluid flow model of the hydrocyclone for concentrated slurry classification', in L. Svarovsky and M. T. Thew (Eds), *Hydrocyclones, Analysis and Applications*, Kluwer Academic Publishers, Dordrecht, 95–108 (1992)
40. Moraes, C. A. C., Hackenberg, C. M., Russo, C. and Medronho, R. A., 'Theoretical analysis of oily water hydrocyclones', in D. Claxton, L. Svarovsky and M. T. Thew (Eds), *Hydrocyclones '96*, MEP, London, 383–398 (1996)
41. Colman, D. A., Thew, M. T. and Lloyd, D. D., 'The concept of hydrocyclones for separating light dispersions and a comparison of field data with laboratory work', 2nd International Conference on Hydrocyclones, (1984)
42. Devulapalli, B. and Rajamani, R. K., 'A comprehensive CFD model for particle-size classification in industrial hydrocyclones', in D. Claxton, L. Svarovsky and M. T. Thew (Eds), *Hydrocyclones '96*, MEP, London, 83–98 (1996)
43. Small, D. M., Fitt, A. D. and Thew, M. T., 'The influence of swirl and turbulence anisotropy on CFD modelling for hydrocyclones', in D. Claxton, L. Svarovsky and M. T. Thew (Eds), *Hydrocyclones '96*, MEP, London, 49–61 (1996)
44. Concha, F., Barrientos, A., Munoz, L., Bustamante, O. and Castro, O., 'A phenomenological model of a hydrocyclone', in D. Claxton, L. Svarovsky and M. T. Thew (Eds), *Hydrocyclones '96*, MEP, London, 63–82 (1996)
45. Castilho, L. R. and Medronho, R. A., 'A simple procedure for design and performance prediction of Bradley and Rietema hydrocyclones', *Minerals Engineering*, **Vol. 13**, No. 2, February (2000)

Bibliography

Seven new papers on hydrocyclones in Proceedings Volume I/II, World Filtration Congress 8, European Federation of Chemical Engineering Event No. 607, organised by The Filtration Society and Elsevier Science, The Brighton Centre, Brighton, UK, 3–7 April 2000 (2000)

Sixteen papers on hydrocyclones in Proceedings, Vortex Separation, 5th International Conference on Cyclone Technologies, organised by BHR Group, Warwick, UK, 31 May–2 June 2000 (2000)

7

Separation by centrifugal sedimentation

L. Svarovsky

FPS Institute, England and University of Pardubice, Czech Republic

Nomenclature

g	Gravity acceleration
G or $G(x)$	Grade efficiency curve
G_1	Grade efficiency curve of a single centrifuge
K	Constant
K_1	Constant
K_2	Constant
L	Length of the bowl
Q	Flow rate
r	Radius
r_1	Radius of the liquid surface
r_3	Inner radius of the bowl
t	Time
v	Liquid velocity
x	Particle size
x_{50}	Cut size of a centrifuge
X_{50}	Cut size of the whole separation plant
y	Variable
z	Position in the axial direction
$\Delta\rho$	Density difference between the solids and the liquid
μ	Liquid viscosity
Σ	Sigma factor
σ_g	Geometric standard deviation
ω	Angular speed

7.1 Introduction

Centrifugal sedimentation is based on a density difference between solids and liquids (or between two liquid phases); the particles are subjected to

centrifugal forces which make them move radially through the liquid either outwards or inwards, depending on whether they are heavier or lighter than the liquid. Centrifugation may thus be regarded as an extension of gravity sedimentation to finer particle sizes and it can also separate emulsions which are normally stable in the gravity field.

A sedimenting centrifuge consists of an imperforate bowl into which a suspension is fed and rotated at high speed. The liquid is removed through a skimming tube or over a weir while the solids either remain in the bowl or are intermittently or continuously discharged from the bowl.

Five main types of industrial sedimenting centrifuges may be distinguished according to the design of the bowl and of the solids discharge mechanism. *Figure 7.1* shows a schematic classification of the equipment; the mode of discharge and operation is quoted for each type of equipment.

A general analysis, which forms a basis for predictions of performance, for a simple form of tubular centrifuge is given, followed by a detailed technical discussion of each available type of equipment and its particular design features, operation characteristics, performance and typical applications. Finally some notes and a guide to equipment selection are given.

7.2 Theoretical performance predictions

If a particle of mass m is rotating with an angular velocity ω at a radius r from its centre of rotation it is acted upon by a centrifugal force $mr\omega^2$ in the radial direction. In sedimenting centrifuges the centrifugal acceleration $r\omega^2$ is very much larger than the acceleration due to gravity g (so gravity forces are neglected) and the ratio of $r\omega^2/g$ is used as a measure of the separating power of the machine. The centrifugal force is large enough to overcome the Brownian diffusion forces, which in gravity sedimentation hinder or prevent settling of very fine particles. As the separation efficiency is mainly affected by the behaviour of the smallest particles in the system, and as the fine particles moving in liquids have low Reynolds numbers (in the region of viscous resistance), it is common to assume, in describing particle motion in rotating liquids, that Stokes' law holds. It should be borne in mind therefore that the following analysis only applies to slowly moving fine particles with Re less than say 0.2 and that the resistance to motion of the larger particles would be in the transient or even Newton's law region (but that in any case all such particles would be separated with 100% efficiency anyway)—see chapter 1, section 1.2.2.

There are many other assumptions made in the following analysis (these are stated where they are introduced) but despite their often obvious over-simplicity the final results give a reasonable estimate of equipment performance. The analysis is made for a simple tubular centrifuge but the same approach, with slight modifications, may be used for other types of sedimenting centrifuges. An attempt is first made to derive the whole grade efficiency

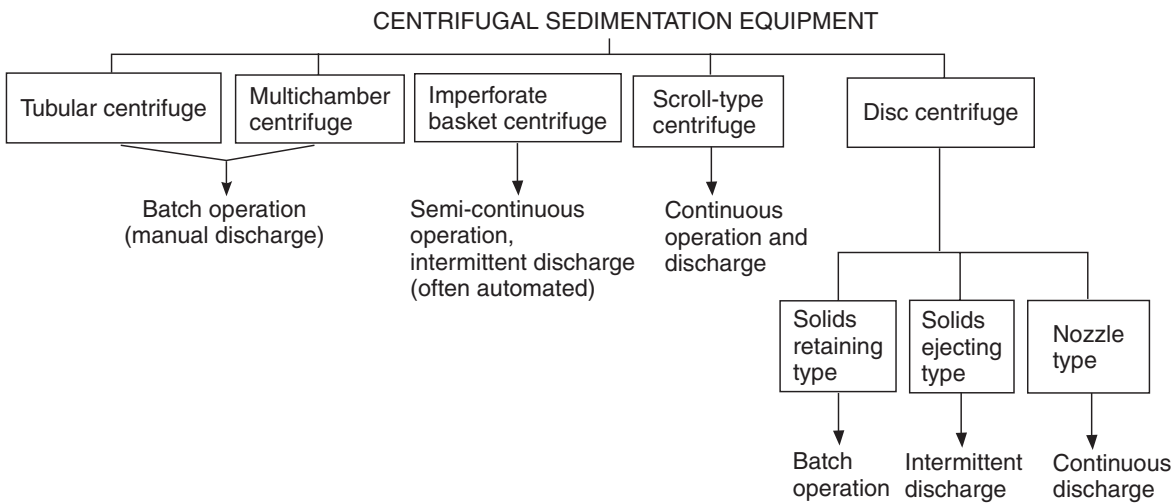

Figure 7.1 Classification of centrifugal sedimentation equipment

curve, which gives the only complete description of equipment separation efficiency (see chapter 3, 'Efficiency of Separation'), and the widely used Sigma concept, which gives an estimate of the cut size x_{50} only, is then derived as a special case.

7.2.1 Grade efficiency function for a simple tubular centrifuge

A simple tubular centrifuge consists of a vertical tube with a large length-to-diameter ratio which rotates at high speed about its vertical axis. The liquid is introduced at the bottom—see *Figure 7.2*—and the flow is essentially axial except in areas immediately adjacent to the inlet and the outlet. The radius of the liquid surface r_1 is determined by the radius of the outlet, which functions as an overflow dam or a weir.

At the bottom of the tube, the particles that enter with the liquid are assumed to be homogeneously distributed in the annulus between the radius r_1 and the inner surface of the tube r_3. The suspension enters through a set of fixed quadrant plates which ensure that its angular velocity soon becomes identical with that of the cylinder. As the particles move upward with the liquid they are subjected to high centrifugal forces and follow trajectories (relative to the cylinder) similar to those shown in *Figure 7.2*.

The velocity of a particle (relative to the centrifugal bowl) at a point at a vertical distance z and radius r may be resolved into two components; one perpendicular to and the other parallel to the axis of rotation of the bowl (radial and axial velocity components).

If the input concentration of the solids is sufficiently low for any interaction between particles to be neglected, the magnitude of the radial velocity can be

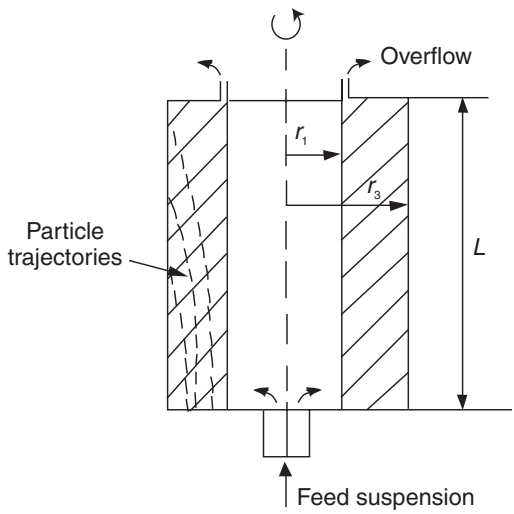

Figure 7.2 Schematic diagram of a simple tubular centrifuge

approximated by a modified version of Stokes' law for falling bodies (see chapter 1, section 1.2.2.2):

$$\frac{\mathrm{d}r}{\mathrm{d}t} = \frac{\Delta\rho x^2 r\omega^2}{18\mu} \tag{7.1}$$

where r is the radial position of a particle of size x, t is the time interval during which this particle is subjected to the centrifugal acceleration, $\Delta\rho$ is the solid–liquid density difference and μ is the viscosity of the liquid.

The assumption inherent in equation 7.1 is that as particles move from smaller radii to larger radii and are continuously accelerated, their instantaneous velocity on any point along their trajectory is equal to the terminal settling velocity corresponding to the centrifugal acceleration $r\omega^2$ at the appropriate radius r. In other words, equation 7.1 is derived from a simple balance between the drag force and the centrifugal force with the inertial force neglected.

The axial velocity may be approximated by the velocity of the liquid at the point (r, z) so that

$$\frac{\mathrm{d}z}{\mathrm{d}t} = v(r, z) \tag{7.2}$$

This of course assumes that there is no slip between the particles and the liquid flow in the axial direction.

If the end effects are neglected, the liquid velocity profile is only a function of the radius r. Schachman[1] derived an equation for the velocity profile $v(r)$ for the case of liquid flow in a concentric shell of fluid as follows

$$\frac{\mathrm{d}z}{\mathrm{d}t} = \frac{QK_1}{\pi\left(r_3^2 - r_1^2\right)}\left(r_1^2 \ln\frac{r}{2} + \frac{r_3^2 - r^2}{2}\right) \tag{7.3}$$

where K_1 is a bowl constant

$$K_1 = \frac{r_3^2 - r_1^2}{\frac{3}{4}r_1^4 + \frac{1}{4}r_3^4 - r_1^2 r_3^2 - r_1^4 \ln\left(r_1/r_3\right)}$$

and Q is the volumetric flow rate of the liquid.

Particle trajectories may be found using equations 7.1 and 7.3 thus leading to the theoretical limit of separation and the grade efficiency—see Bradley[2] and equation 7.21 in section 7.3.1.

The method of grade efficiency derivation will be demonstrated using a much simpler model in which the velocity profile in the liquid shell is assumed to be uniform, as in the so-called 'plug flow':

$$\frac{\mathrm{d}z}{\mathrm{d}t} = \frac{Q}{\pi\left(r_3^2 - r_1^2\right)} \tag{7.4}$$

The ratio of equations 7.1 and 7.4, when integrated between the limits $r = r_3$ at $z = L$ and $r = r_1$ at $z = 0$, determines the smallest radius at which the sedimentation of a particle size x may begin in order that it may just reach the

cylinder wall after covering the full length L of the separation zone (an approach commonly employed in the theory of settling tanks and settling chambers).

The radius r is then implicitly expressed as

$$\ln(r_3/r) = \frac{Kx^2 L\pi\left(r_3^2 - r_1^2\right)}{Q} \tag{7.5a}$$

where K is a sedimentation constant defined as

$$K = \frac{\Delta\rho\omega^2}{18\mu} \tag{7.5b}$$

The first parameter that can be derived from equation 7.5a is the limit of separation, i.e. the maximum particle size that would ever get a chance of escaping with the overflow; this size is obtained from the limiting particle trajectory which starts at radius r_1 at $z = 0$, i.e. $r = r_1$ in equation 7.5a thus giving

$$x_{\max} = \left(\frac{Q\ln(r_3/r_1)}{K\pi L\left(r_3^2 - r_1^2\right)}\right)^{1/2} \tag{7.6}$$

The value of the grade efficiency for a particle size x is the fraction contained in an annulus between radii r and r_3 where r is, as previously stated, the smallest radius at which the sedimentation of a particle size x may start at $z = 0$ in order that it may just reach the wall of the cylinder at $z = L$. The grade efficiency is therefore

$$G(x) = \frac{r_3^2 - r^2}{r_3^2 - r_1^2} \tag{7.7}$$

where r is determined from equation 7.5a.

$$r = r_3 \exp\left(-K\frac{L\pi\left(r_3^2 - r_1^2\right)}{Q}x^2\right) \tag{7.8}$$

Equations 7.6, 7.7 and 7.8 combined give the final formula for the grade efficiency function as

$$G(x) = \frac{r_3^2}{r_3^2 - r_1^2}\left[1 - \exp\left(-2KK_2x^2\right)\right] \tag{7.9a}$$

or

$$G(x) = \frac{1 - \exp\left(-2KK_2x^2\right)}{1 - \exp\left(-2KK_2x_{\max}^2\right)} \quad \text{for } 0 \le x \le x_{\max} \tag{7.9b}$$

and

$$G(x) = 1 \quad \text{for } x > x_{\max}$$

where K_2 is constant for a particular centrifuge geometry and volumetric flow rate and is equal to the residence time of the liquid because

$$K_2 = \frac{L\pi\left(r_3^2 - r_1^2\right)}{Q} = \frac{V}{Q} \tag{7.10}$$

where V is the effective volumetric capacity of the bowl.

Equation 7.9 gives the typical S-shaped grade efficiency curve (see *Figure 7.3*); the limit of separation $x_{\max}$ that appears in equation 7.9b may be determined from equation 7.6.

The method shown above is typical for the grade efficiency derivation for most of the following centrifugal equipment. It must however be emphasized that the theoretical efficiency functions are only as good as the assumptions made in their derivation.

An important parameter that can be derived from equation 7.7 (or 7.9) is the size corresponding to 50% on the grade efficiency curve, i.e. the equiprobable size or 'cut size' x_{50} (see chapter 3, 'Efficiency of Separation'). The corresponding radius r_{50} is the one that splits the annulus between r_1 and r_3 into equal areas hence

$$r_3^2 - r_{50}^2 = r_{50}^2 - r_1^2 \tag{7.11}$$

The cut size x_{50} can either be calculated from equation 7.9 by putting $G(x_{50}) = 0.5$ or by substitution of r_{50} from equation 7.11 into equation 7.5 thus

$$x_{50}^2 = \left(\frac{Q}{2\pi LK}\right)\left[\ln\left(\frac{2r_3^2}{r_3^2 + r_1^2}\right)\right]\left(\frac{1}{r_3^2 - r_1^2}\right) \tag{7.12a}$$

or, in terms of the liquid residence time K_2

$$x_{50}^2 = \frac{1}{2K\,K_2}\ln\left(\frac{2r_3^2}{r_3^2 + r_1^2}\right) \tag{7.12b}$$

An example of the comparison between the theoretical and practical grade efficiencies of a tubular centrifuge is given in section 7.3.1.

7.2.2 The sigma concept

The so-called Sigma concept has been widely used in the field of centrifugal sedimentation ever since its first development by Ambler[3] in 1952. It is a simplified relation between the machine performance in terms of x_{50}, total volumetric flow rate Q and an index of the centrifuge size Σ. The cut size x_{50} is represented by its terminal settling velocity v_g in the given liquid under gravity so that from Stokes' law (using equation 7.5b for the definition of K)

$$v_g = \frac{x_{50}^2 \Delta\rho g}{18\mu} = x_{50}^2\, K \frac{g}{\omega^2} \tag{7.13}$$

Equation 7.12a may thus be rewritten as

$$Q = 2v_g\left(\frac{\omega^2}{g}\right)\pi L\frac{r_3^2 - r_1^2}{\ln\frac{2r_3^2}{r_3^2+r_1^2}} \tag{7.14}$$

or

$$Q = 2v_g\Sigma \tag{7.15}$$

where

$$\Sigma = \frac{\omega^2}{g}\pi L\frac{r_3^2 - r_1^2}{\ln\frac{2r_3^2}{r_3^2+r_1^2}} \tag{7.16}$$

As equation 7.16 is rather cumbersome for routine calculations, an alternative expression may be used, based on an approximation of the logarithmic function

$$\ln y \simeq 2\frac{y-1}{y+1}$$

(taking the first term in a series) so that in equation 7.16

$$\ln\frac{2r_3^2}{r_3^2 + r_1^2} \simeq \frac{r_3^2 - r_1^2}{\frac{3}{2}r_3^2 + \frac{1}{2}r_1^2}$$

and equation 7.16 itself becomes

$$\Sigma \simeq \frac{\omega^2}{g}\pi L\left(\frac{3}{2}r_3^2 + \frac{1}{2}r_1^2\right) \tag{7.17}$$

This is an approximation for which Ambler[4] claims a maximum error of 4%.

Equation 7.15 is the basic expression of the Sigma concept. It gives an estimate of the flow rate above which particles of size x_{50} will largely be unsedimented and below which they will mostly be separated. Σ is a constant containing factors pertaining only to the centrifuge; it is often called the theoretical capacity factor; it has the dimension of an area and it allows comparison between the performances of geometrically and hydrodynamically similar centrifuges operating on the same feed material. Theoretically, Σ represents the area of a settling tank capable of the same separational performance in the gravitational field; this is of course a false comparison because it ignores Brownian diffusion, convection currents and other effects which could mean that such a settling tank may hardly perform as well as the centrifuge, if at all. Equation 7.17 represents the Σ factor for a tubular centrifuge, similar expressions can be derived for other types of sedimenting centrifuges and these are given in the appropriate sections in the following. Extensive work on Σ comparisons in the past two decades, mostly made by equipment manufacturers, has shown that while experimental results differ from calculated values when different types of centrifuges are being

considered, the scale up between centrifuges of the same type is fairly reliable; this is based on a simple application of equation 7.15

$$\frac{Q_1}{\Sigma_1} = \frac{Q_2}{\Sigma_2} \tag{7.18}$$

if x_{50} is to remain constant.

Despite some attempts[5] to extend the application of equation 7.18 to 'cross-type' scale up between different centrifuge configurations via the use of the efficiency factors μ_i using

$$\frac{Q_1}{\mu_1\Sigma_1} = \frac{Q_2}{\mu_2\Sigma_2} \tag{7.19}$$

where μ_i are relative efficiencies of different types, this has not found much response in practice. In fact it is difficult to find the actual values of these efficiencies in the literature except from the paper by Morris[5] (tubular bowl, 90%; imperforate basket, 75%; scroll type, 60% and disc type, 45%). Equipment manufacturers claim that this cross-type scale up is not reliable in practice unless many more factors than just the Sigma values are considered (see the discussion in Woolcock[6], p. 180).

Example 7.1 Use of the sigma theory

A low-concentration suspension of clay (density 2640 kg m^{-3}) in water with a viscosity of 0.001 Ns m^{-2} and density 1000 kg m^{-3} is to be separated by centrifugal sedimentation. Pilot runs on a laboratory tubular bowl centrifuge operating at 20 000 rev. min^{-1} indicate that satisfactory overflow clarity is obtained at a throughput of 8×10^{-6}m^3 s^{-1}.

The centrifuge bowl is 0.2 m long, has an internal radius of $r_3 = 0.0220$ m and the radius of the liquid surface $r_1 = 0.0110$ m. If the separation is to be carried out in the plant using a tubular centrifuge 0.734 m long with an internal radius of 0.0521 m and $r_3 - r_1 = 0.0295$ m, operating at 15 000 rev. min^{-1} with the same overflow clarity, what production flow rate could be expected? Also determine the effective cut size.

Using equation 7.17

$$\Sigma_1 = \left(\frac{\pi\, 20\,000}{30}\right)^2 \frac{\pi\, 0.2}{9.81}\left[\frac{3}{2}(0.022)^2 + \frac{1}{2}(0.011)^2\right] = 221\ \text{m}^2$$

$$\Sigma_2 = \left(\frac{\pi\, 15\,000}{30}\right)^2 \frac{\pi\, 0.734}{9.81}\left[\frac{3}{2}(0.0521)^2 + \frac{1}{2}(0.0226)^2\right] = 2510\ \text{m}^2$$

hence from equation 7.18

$$Q_2 = \frac{\Sigma_2}{\Sigma_1} Q_1 = \left(\frac{2510}{221}\right) 8 \times 10^{-6} = 9.08 \times 10^{-5}\ \text{m}^3\ \text{s}^{-1}$$

The terminal settling velocity of the cut size under gravity is, from equation 7.15

$$v_g = \frac{Q_1}{2\Sigma_1}\left(=\frac{Q_2}{2\Sigma_2}\right) = \frac{8\times10^{-6}}{2\times221} = 1.81\times10^{-8}\,\mathrm{m\,s^{-1}}$$

hence the cut size is, from equation 7.13

$$x_{50} = \left(\frac{18\mu v_g}{\Delta\rho g}\right)^{1/2} = \left(\frac{18\times0.001\times1.81\times10^{-8}}{1640\times9.81}\right)^{1/2} = 1.42\times10^{-7}\mathrm{m}$$
$$= 0.142\,\mu\mathrm{m}$$

There have been a few attempts to modify the Σ theory since its conception by Ambler. The most important improvements have been concerned with the introduction of more realistic flow patterns in different types of centrifuges, with account taken of end effects (Frampton[7] used $0.5L$ as the effective bowl length), with the introduction of particle shape factors etc.

Although experimental values of Σ can be obtained from the test data via the grade efficiency curve (from which x_{50} is determined—see chapter 3, 'Efficiency of Separation'), industrialists[8] prefer to measure the fraction of solids unsedimented $(1 - E_T)$ and plot this against the ratio of the measured flow rate and the calculated Σ value (which can be varied by changing the speed of rotation). This curve, which often comes out as a straight line on log–probability paper, is naturally a function of the size distribution of the feed but can be used to find the ratio of Q/Σ for acceptable efficiency with the given feed material. Extrapolation of the data over the linear parts of the graph can be made with caution.

There is however one major shortcoming of the Sigma concept: the cut size is insufficient as a criterion of separation efficiency because different total efficiencies can be obtained at a given cut size, if the size distribution of the feed particles differs. Murkes[9] recognized this but suggested a method which assumes a certain form of the feed distribution function, thus introducing an unnecessary limitation.

Zeitsch[10] recently pointed out and analysed the effect of the exchange of momentum between the feed entering a rotating bowl and the charge already in the bowl on the effective acceleration within the bowl. The feed slows down the rotation of the fluid in the bowl, and the lag between the bowl speed and that of the liquid surface in the bowl ranges in practice between 3 and 10%. Zeitsch concluded that the effect of the feed rate on separation efficiency is significant and derived a correction factor by which the nominal bowl speed has to be corrected to obtain the true effective centrifugal acceleration to which the particles in the flow are subjected.

The only way to describe fully the performance of a sedimenting centrifuge is by the grade efficiency curve; knowledge of this curve allows accurate and reliable (subject to the operation characteristics, the state of dispersion of solids and other variables remaining constant) predictions of total efficiencies

with different feed solids. It appears that, rather than to keep modifying the Sigma concept to make it more flexible and complete, we should employ the grade efficiency concept; this of course requires many tests, together with deeper theoretical considerations. Research projects are in progress to fill this gap; some results of recently reported work[11] are included in the appropriate sections in the following account of equipment.

7.3 Equipment

7.3.1 Tubular centrifuge

The principle of operation of a tubular centrifuge was described in section 7.2.1 together with a derivation of the theoretical grade efficiency curve based on certain assumptions. One of these assumptions is that the amount of sedimented solids in the bowl is negligible throughout the operating cycle. In practice, however, these devices have to be stopped and cleaned (most often manually) when the solids content in the bowl reaches a certain level. During the operation period, a cake (or heel) of solids is gradually building up in the bowl, thus reducing the area available to flow. This in turn reduces the residence time of the liquid in the bowl and the efficiency of separation gradually drops. Reduction in efficiency reflects itself in increasing solids content in the overflow which can be monitored, for example by turbidity measurements. In order to avoid the necessity for excessively frequent cleaning, tubular centrifuges are usually used with suspensions which contain less than 1% v/v of solids, i.e. for liquid clarification. For continuous operation two centrifuges are used alternately, one running while the other is being cleaned.

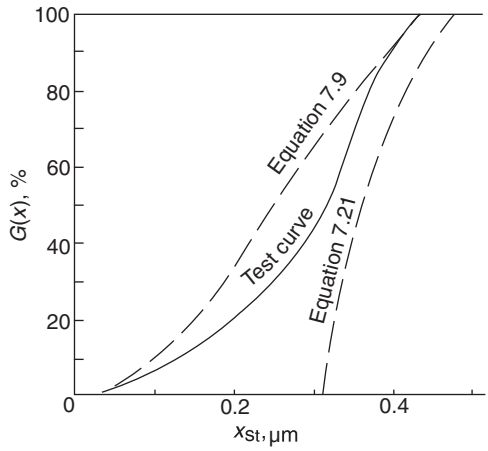

Figure 7.3 Example of an experimental grade efficiency curve for a tubular centrifuge in comparison with theoretical predictions

If no test data are available, use can be made of equation 7.9 to predict roughly the order of the cut size and the grade efficiency curve. Because of end effects, non-uniform velocity distributions etc., the predicted curve is always better than what can be expected in practice. *Figure 7.3* gives an example from a series of tests with the Sharples Supercentrifuge (standard 8RY separator: $r_3 = 2.223\,\text{cm}$, $r_1 = 1.071\,\text{cm}, L = 19.6\,\text{cm}$) operated at 8000 rev. min^{-1} and a flow rate $Q = 7.57 \times 10^{-6}\,\text{m}^3\,\text{s}^{-1}$ with a suspension of 0.5% v/v of very fine TiO_2 ($\rho = 4000\,\text{kg}\,\text{m}^{-3}$) in water at 23°C.

The experimental grade efficiency given in *Figure 7.3* was evaluated from size distributions of the feed and the overflow suspensions (measured by the Ladal X-ray Centrifugal Sedimentometer[12]), and from the total efficiency obtained by simple gravimetric concentration measurements (see chapter 3, 'Efficiency of Separation' for the method). *Figure 7.3* also gives the predicted curve from equation 7.9 ($K = 1.2 \times 10^{11}\text{m}^{-2}\,\text{s}^{-1}, K_2 = 30.87\,\text{s}$) which in this case becomes

$$G(x) = 1.302[1 - \exp(-7.41 \times 10^{12}x^2)]$$

(in SI units).

Another theoretical curve may be obtained using the model by Bradley[2] who assumed the velocity distribution in equation 7.3 and used an approximation, specific to the Sharples Supercentrifuge 8RY, of the form

$$\frac{x^2K}{Q} = 4.1 \times 10^{-3}r^{-1.2} \tag{7.20}$$

Substitution of r from equation 7.20 into equation 7.7 gives

$$G(x) = \frac{r_3^2 - 1.05 \times 10^{-4}(Q/x^2K)^{5/3}}{r_3^2 - r_1^2} \tag{7.21}$$

which becomes, for our example

$$G(x) = 1.302(1 - 0.986 \times 10^{-15}x^{-10/3})$$

and this is also plotted in *Figure 7.3*.

As can be seen from the graph, Bradley's model gives conservative predictions of efficiency, mainly because he applied the approximation in equation 7.20, which was originally fitted to data obtained at radii between 1 and 2 cm, to radii up to $r_3 = 2.223\,\text{cm}$ where large discrepancies occur; this leads to underestimates of separation efficiency. Bradley's model is still useful because it gives a lower estimate of efficiency, the actual grade efficiency curves are usually found to lie between those predicted by equations 7.9 and 7.21.

Tubular centrifuges are available in both laboratory and industrial versions. The former can reach 50 000 rev. min^{-1} with flow rates between 0 and $0.1\,\text{m}^3\,\text{h}^{-1}$ (driven by an electric motor or by an air/steam turbine) whilst the latter reach 15 000 rev. min^{-1} and flow rates in the range of 0.4 to $4\,\text{m}^3\,\text{h}^{-1}$ (driven by an electric motor). Tubular centrifuges are the most efficient of all

industrial sedimenting centrifuges because of their high speed and relatively thin settling zone; they are therefore used for the separation of very fine solids whose settling velocities are in the range 5×10^{-8} to 5×10^{-7} m s^{-1}. The laboratory models, namely the widely used Sharples Supercentrifuge, have also been used for particle size measurement[2] and the classification of solids.

7.3.2 Imperforate basket centrifuge

This is an adaptation of the standard basket centrifuge used for centrifugal filtration made by replacing the bowl with an imperforate one.

The resulting arrangement is very similar to the tubular centrifuge in *Figure 7.2* but the length-to-diameter ratio is much smaller—usually about 0.6 compared to 4–8 for the tubular centrifuges. Subsequently the mathematical model used for the tubular centrifuge can be applied to the imperforate basket centrifuge as well, but the end effects become more significant here. The efficiency of separation is generally lower because of the relatively short clarification length of the bowl compared with the zone disturbed by feeding and it varies widely with different methods of feeding.

The basket centrifuges are usually operated with a vertical axis of rotation (see *Figure 7.4*) (except for the peeler centrifuges which usually have a horizontal axis), the feed is normally introduced near the bottom of the bowl, the solids separate at the bowl wall and the clarified liquid overflows the lip of the 'ring dam' at the top and is discharged continuously. At the end of an operating cycle, usually triggered by a cake thickness detection device, the supernatant liquid that remains on top of the cake may be first skimmed off to produce a drier cake on discharge. The mode of solids discharge depends on the type of solids handled; soft and plastic solids are skimmed at full speed

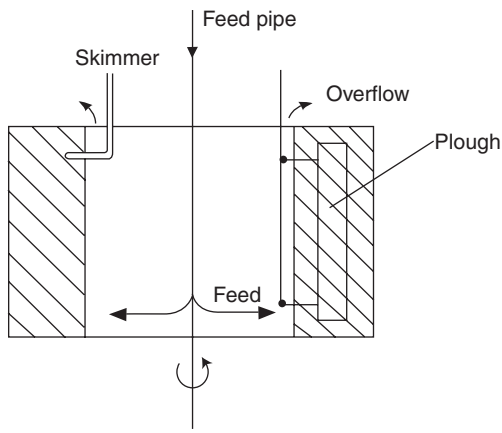

Figure 7.4 Schematic diagram of an imperforate basket bowl in cross-section

and coarse and fibrous solids are removed at slower speeds by a ploughing knife; the cake drops through the open bottom of the bowl. Sometimes, for example in nuclear fuel processing applications, the cake is re-slurried by a liquid fed through a set of nozzles and flows out through the bottom of the bowl at a slow speed. The Donaldson Hydro-Clean Centrifuge uses a novel way of re-slurrying by the stirring action of the blades of a rotor; the rotor blades reach into the suspension inside the bowl and, during the normal operation, drive the freely suspended bowl via the resistance of the liquid. When the discharge operation is initiated, the bowl is simply stopped by a brake while the rotor blades continue to rotate. The cake is re-slurried in the residual supernatant liquid and is then discharged through the bottom of the bowl.

Several workers[13,14] have observed that, contrary to the common assumption that there is a regular stream of liquid through the whole cross-section available to flow within the bowl, the incoming liquid tends to flow within a thin layer near the surface of the liquid whilst the bulk of the liquid is essentially stagnant. As this is clearly detrimental to the separation efficiency, because it shortens the residence time of the liquid in the bowl, some manufacturers build in special baffles which are designed to stop the surface flow and make the liquid flow nearer to the bowl wall.

The solid content is usually low (3–5% by weight) in basket centrifuges, again to prevent frequent cleaning. Speeds of rotation range from 450 to 3500 rev. min^{-1} with typical flow rates of between 6 and 10 $m^3 h^{-1}$. Typical applications include the dewatering of sludges[6] and the recovery of solids from a waste stream.

An interesting modification of the basket centrifuge is the triple bowl unit reported by Riesberg and Dudrey[15], and manufactured by Donaldson Co. Inc. as the Liqua Pac Centrifuge. As can be seen from *Figure 7.5* it consists of

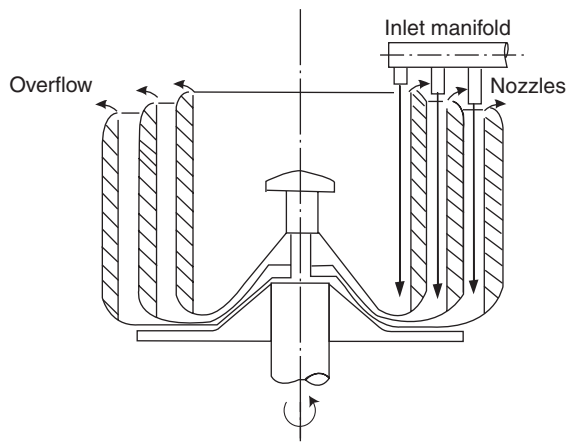

Figure 7.5 Schematic diagram of a triple bowl centrifuge[15]

three bowls of different diameters mounted in one unit. The suspension comes in through an inlet manifold which divides it into three separate streams and directs each stream into a different bowl. There are then three independent and parallel flows each discharging separately and bypassing the other two bowls. This makes a more efficient use of the space available within the bowl and, as it increases the residence time of the liquid in the bowl, a lower rotational speed (650 rev. min^{-1}) can be used for the same efficiency (this produces a number of advantages in design and operation). As in the multi-chamber centrifuge discussed in the next section, the solids holding capacity is also increased. The triple bowl centrifuge has been successfully applied to cleaning metal-working coolants[15].

7.3.3 Multi-chamber centrifuge

This type of centrifuge utilizes a closed bowl which is sub-divided into a number of concentric vertical cylindrical compartments through which the suspension flows in series—see *Figure 7.6*. The suspension is made to pass through zones of progressively higher acceleration and this results in a classification effect, with the coarsest fraction being deposited in the inner chamber and finest fraction in the outermost chamber. Another advantage is the large solids holding capacity; in a large machine this may be up to as much as 751($= 7.5 \times 10^{-2}\ m^3$).

Westfalia Separator AG make models with either a six-chamber bowl (five cylindrical inserts), or a two-chamber bowl (one cylindrical insert), which also incorporates a centripetal pump on the discharge side of the bowl (this converts the kinetic energy of the liquid on discharge into pressure). The Broadbent–Hopkinson centrifuge is a two-chamber type specially designed for reclaiming cutting-oil from grinding machines.

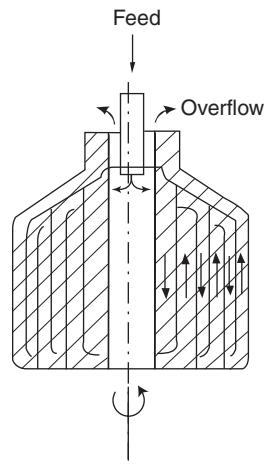

Figure 7.6 Schematic diagram of a multi-chamber bowl in cross-section

The efficiency of the multi-chamber centrifuges is high because of the long residence time of the liquor in the unit. A mathematical model similar to that used for the tubular centrifuge can be applied to the multi-chamber centrifuge provided that satisfactory assumptions and modifications are made.

The cleaning of multi-chamber centrifuges is more difficult and takes longer than for the tubular type. The manual discharge generally limits this type of machine to suspensions containing less than 4–5% solids by volume.

Available speeds range between 4500 and 8500 rev. min^{-1}, flow rates from 2.5 to 10 $m^3 h^{-1}$ and bowl diameters from 335 to 615 mm. Multi-chamber centrifuges, apart from the separation of grinding swarf from cutting oils already mentioned, are mainly used for the clarification of beer, wine, fruit juice and varnishes.

7.3.4 Scroll-type centrifuge

A characteristic feature of the scroll-type (often called 'decanter' type) continuous conveyor discharge centrifuge is the horizontal conical or conocylindrical bowl, with a length-to-diameter ratio of about 1.5 to 3.5, containing a screw conveyor that rotates in the same direction but at a slightly higher or lower speed (the difference being 5 to 100 rev. min^{-1} with respect to the bowl). The centrifugal fields are lower than in other centrifugal equipment; speeds range from 1600 to 6000 rev. min^{-1}. The operating principle is shown in *Figure 7.7*. The slurry enters through an axial tube at the center of the rotor, passes through openings in the screw conveyor and is thrown to the rotor wall. Deposited solids are moved by a helical screw conveyor up a sloping 'beach' out of the liquid and discharged at a radius smaller than that of the liquid discharge. The liquid level is maintained by ports adjustable to the desired overflow radius.

For the conical conveyor type centrifuge the Sigma value can be calculated as[8] (see *Figure 7.7* for dimensions)

$$\Sigma = \frac{\omega^2}{g} \pi L \frac{r_3^2 + 3r_3 r_1 + 4r_1^2}{4} \tag{7.22}$$

where L is the length of the liquid layer or 'pond' measured at the liquid surface.

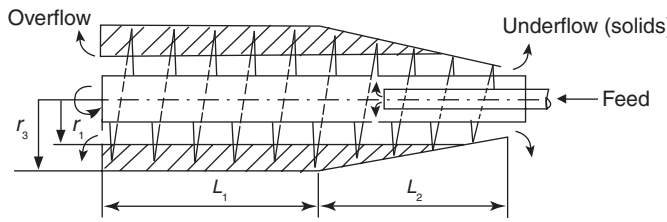

Figure 7.7 Schematic diagram of a scroll-type centrifuge bowl in cross-section (conocylindrical bowl)

For the conocylindrical conveyor-type centrifuge the Sigma value is usually assumed to be the sum of the values for a true cylindrical section of length L_1 given by equation 7.17 and for a conical section of length L_2 thus (see *Figure 7.7*)

$$\Sigma = \frac{\omega^2}{g}\pi\left[L_1\left(\frac{3}{2}r_3^2 + \frac{1}{2}r_1^2\right) + L_2\left(\frac{r_3^2 + 3r_3r_1 + 4r_1^2}{4}\right)\right] \tag{7.23}$$

This is of course a theoretical formula; two correction factors are usually applied in practice. Ambler[4] recommends that 6% should be deducted from this theoretical value of Sigma to allow for the finite volume of the conveyor flights in the suspension (this reduces the residence time). In addition to the volume of the conveyor flights, the sedimented solids which are being conveyed through the rotor also displace their own volume of liquid; Ambler[4] suggested a reduction factor of 0.62 for a conical conveyor type and 0.67 for a conocylindrical type to account for this effect.

Particles of settling velocities of the order of 1.5×10^{-6} to about 15×10^{-6} m s^{-1} are handled at medium to large flow rates (typical throughputs range from about 0.4 to 60 m^3 h^{-1}, depending on the machine and the application). When operating as a clarifier, this type of centrifuge recovers medium and coarse particles from feeds at high or low solids concentration 2–50% v/v. As a classifier, the flow rates are higher than for clarification. Particles smaller than 2 μm are normally not collected.

Gibson[11] has published some interesting results of tests with a scroll-type centrifuge, which show the cut size as a function of the feed rate and feed solids concentration—see *Figure 7.8*.

Polyelectrolytes are widely used for the flocculation of slurries to be separated in the scroll-type centrifuges; the point of addition varies depending on the type of polyelectrolyte and the type of slurry. Anionic polyelectrolytes

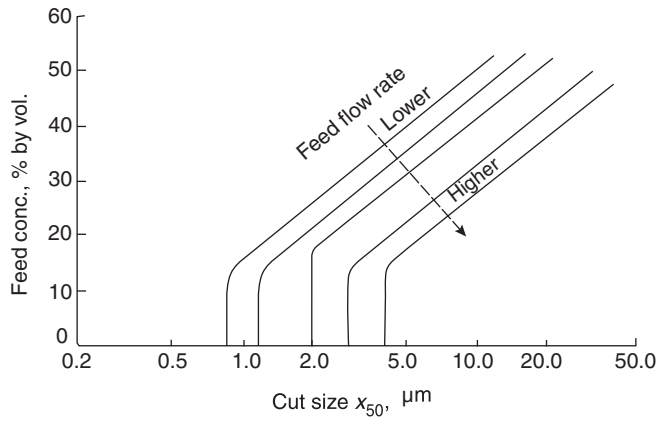

Figure 7.8 Effect of feed concentration and flow rate on cut size x_{50} for scroll-type centrifuge

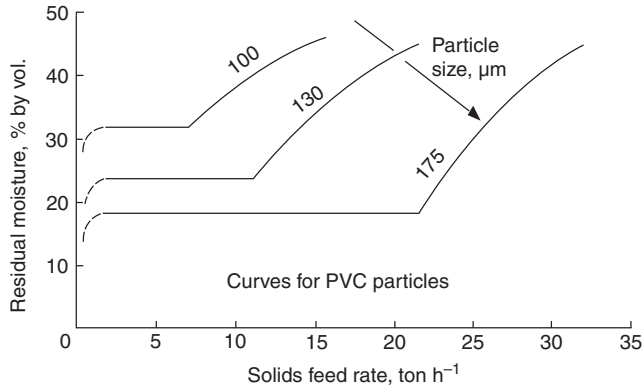

Figure 7.9 Scroll-type centrifuge dewatering performance declines at a critical feed rate

are usually dosed upstream of the centrifuge whilst cationics, which react faster, are usually added to the slurry within the centrifuge.

In design, considerable variations occur in the contour of the centrifuge shell, the flight angle and pitch, beach angle and length, conveyor speed and feed position. An alternative to the liquid overflow open outlet is a paring tube for skimming off the liquid. The most common position of the axis of rotation is horizontal but Pennwalt for example have introduced a large vertical machine (model P6000) specifically designed for higher temperatures and pressures.

The scroll-type centrifuge has found a wide variety of industrial applications; as a clarifier for example, it is used to recover crystals and polymers. Most recently it has been used widely in the UK for the dewatering of both municipal and industrial sludges[16]. Stahl[17] has successfully applied the centrifuge to the dewatering of coarse solids, namely PVC particles with a median size between 100 and 190 μm. Some of his results are shown in *Figure 7.9*.

Efficient washing and dewatering may be achieved with the Broadbent Screen Bowl centrifuge, which is in fact an end-to-end combination of a solid bowl scroll-type centrifuge with a cylindrical scroll-screen-type centrifuge (the scroll is common to both), see *Figure 7.10* for a schematic diagram of the principle. A similar machine is available from Humboldt Wedag.

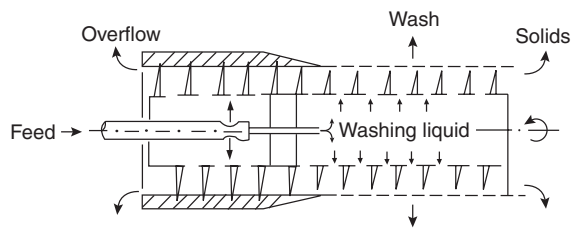

Figure 7.10 Schematic diagram of a solid/screen bowl scroll centrifuge

Another major area of application of the scroll-type centrifuge is in the classification of solids such as kaolin coating clay, TiO_2 etc.

7.3.5 Disc centrifuge

This type of centrifuge contains a stack of conical discs, as shown in *Figure 7.11*. The feed is introduced through the centre, passes underneath the disc stack and into the space between the stack and the wall of the bowl while both the stack and the bowl are rotating at a speed ω. The liquid then flows in thin layers between the discs, radially inwards, towards the outlet, which is an annulus at the top centre. Particles settle on the lower surface of the upper of the two discs which form each 'disc channel'. The settling motion of the particles is the first, usually decisive, stage of the separation process. The second stage is the downward–outward sliding motion of the particles on the disc surface towards the disc periphery and their subsequent impingement on the wall of the bowl.

The basic idea here of increasing the settling capacity by using a number of layers in parallel is the same as the Lamella principle[18] in gravity sedimentation.

Murray[19] considered possible improvements in the separation efficiency of disc centrifuges by reversing the liquid flow through the disc stack but found no advantage in using this method in practice.

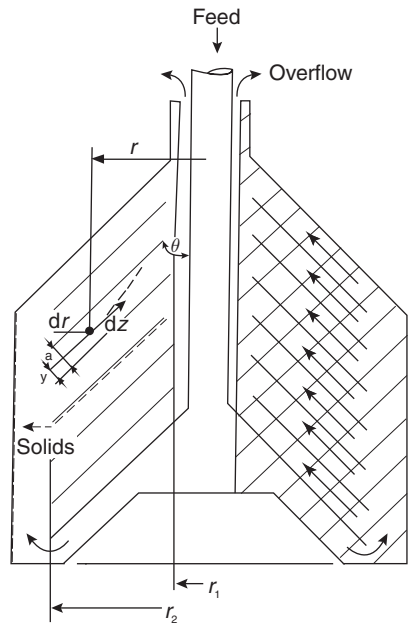

Figure 7.11 Schematic diagram of a disc centrifuge bowl in cross-section

The motion of a particle between two adjacent conical discs is shown schematically in *Figure 7.11*. The flow of the suspension is assumed to be divided equally between the spaces formed by the discs, so that the flow rate in each disc channel is equal to Q/n where Q is the throughput and n is the number of channels. The flow is also assumed to be in a radial plane (i.e. having the same angular velocity as the stack) and directed parallel to the surface of the discs. Under these conditions, the velocity of a particle of size x at radius r from the axis of rotation can be resolved into two components: the radial velocity $\mathrm{d}r/\mathrm{d}t$, which can be approximated by Stokes' law in equation 7.1, and the velocity in the direction of flow z: $\mathrm{d}z/\mathrm{d}t$, which can be approximated by the velocity of the liquid at that point (if a plug flow is assumed)

$$\frac{\mathrm{d}z}{\mathrm{d}t} = \frac{Q}{2\pi nra} \tag{7.24}$$

where a is the perpendicular clearance between the adjacent discs.

Since also

$$\frac{\mathrm{d}y}{\mathrm{d}t} = \frac{\mathrm{d}r}{\mathrm{d}t}\cos\theta \tag{7.25}$$

where θ is half the included angle of the discs and the y axis is perpendicular to the z axis, equation 7.1, 7.24 and 7.25 combined give (with K as defined in equation 7.5b)

$$\frac{\mathrm{d}y}{\mathrm{d}z} = Kx^2r^2\frac{2\pi na}{Q}\cos\theta \tag{7.26}$$

thus

$$\frac{\mathrm{d}y}{\mathrm{d}r} = -Kx^2r^2\frac{2\pi na}{Q}\cot\theta \tag{7.27}$$

since

$$\frac{\mathrm{d}z}{\mathrm{d}t} = -\frac{\mathrm{d}r}{\mathrm{d}t\sin\theta} \tag{7.28}$$

Equation 7.27, if integrated between the limits $y = y_1$ at $r = r_2$ and $y = a$ at $r = r_1$ determines the distance y_1 from the bottom plate at which sedimentation of a particle size x may start in order that it may just reach the top disc after covering the full length of the space between the discs, i.e.

$$a - y_1 = Kx^2\frac{2\pi na}{3Q}\cot\theta\left(r_2^3 - r_1^3\right) \tag{7.29}$$

For the limit of separation this integration is done between $y = 0$ at $r = r_2$ and $y = a$ at $r = r_1$, leading to

$$a = Kx_{\max}^2\frac{2\pi na}{3Q}\cot\theta\left(r_2^3 - r_1^3\right) \tag{7.30}$$

The grade efficiency can now be determined if we assume a homogeneous concentration of particles at the entry to the separation zone at r_2 because

$$G(x) = \frac{a - y}{a} \tag{7.31}$$

which becomes (if equation 7.29 is substituted for $a - y$ and equation 7.30 for a)

$$G(x) = \frac{x^2}{x_{\max}^2} \quad \text{for } x \leq x_{\max} \tag{7.32}$$

and

$$G(x) = 1 \quad \text{for } x > x_{\max}$$

where $x_{\max}$ is, from equation 7.30

$$x_{\max} = \frac{3Q}{2\pi n K \cot\theta\left(r_2^3 - r_1^3\right)} \tag{7.33}$$

Equations 7.32 and 7.33 fully describe the theoretical grade efficiency curve which, as can be seen, is independent of the spacing between the discs but depends on the number of discs n. Equation 7.32 is a simple parabola and the cut size x_{50} can be determined from equation 7.32 since $G(x_{50}) = 0.5$ hence

$$x_{50} = x_{\max}\sqrt{0.5} = 0.707 x_{\max} \tag{7.34}$$

The Sigma factor for a disc centrifuge becomes

$$\Sigma = \frac{\omega^2}{g}\frac{2}{3}\pi n\left(r_2^3 - r_1^3\right)\cot\theta \tag{7.35}$$

(from equations 7.13, 7.15, 7.34 and 7.33).

Fitch[20] subjected this theoretical estimate of separation efficiency (equation 7.32) to a detailed investigation and tests, and found in practice considerably lower efficiencies than predicted. He found that this was not a result of the non-uniformity of the radial flow pattern between the discs because most disc centrifuges have radial spacing ribs which block tangential flow and cause the flow pattern to be fairly uniform except for variations close to the disc surfaces. Fitch found both theoretically[20] and more recently by taking photographs of the actual flow patterns in a disc centrifuge[21], that vortices exist in the disc sectors bounded by spacing ribs along the axis of rotation and these are the major cause of the deviations from theory.

The disc centrifuges are operated at speeds up to 12 000 rev. min^{-1} depending on the bowl diameter, which is typically 150 mm to 1 m. Flow rates of up to 100 $\text{m}^3\,\text{h}^{-1}$ are obtained on easy separations; the range of theoretical settling velocities handled is 8×10^{-8} m s^{-1} at solids concentrations below 15%. Bowls normally have approximately equal height and diameter for optimum capacities, and the angle of the cones is sufficiently large for the

deposited particles to slide on their surfaces—usually between 35 and 50 degrees. The primary process modifications to the disc centrifuge design concern the method of solids discharge. These modifications are discussed below.

7.3.5.1 Solids retaining type

The simplest disc centrifuge bowl (*Figure 7.11*) is designed with a non-perforated bowl wall parallel to the axis of rotation. In order to avoid frequent manual cleaning, this type is used with low solids concentrations (less than 1% by volume). Cleaning is sometimes facilitated by using disposable paper liners. Typical dirt-holding capacity is 5 to 20 l. The most frequent application is the separation of cream from milk; applications are generally restricted to safe liquids because toxic materials may be a source of hazard during the manual cleaning.

7.3.5.2 Nozzle type

Continuous discharge of the solids as a slurry is possible with the nozzle-type disc centrifuges. The shape of the bowl is modified so that the sludge space has a conical section as shown in *Figure 7.12* thus providing a good storage volume and also giving a good flow profile for the ejected sludge. The walls of the bowl slope towards a peripheral zone containing a number of evenly spaced orifices. The number and size of these orifices, commonly called nozzles, are optimized in order to avoid build up of the cake or pluggage and to obtain a reasonably concentrated sludge. The number of nozzles ranges from 12 to 24, the size from 0.75 to 2 mm and the under flow-to-through-put

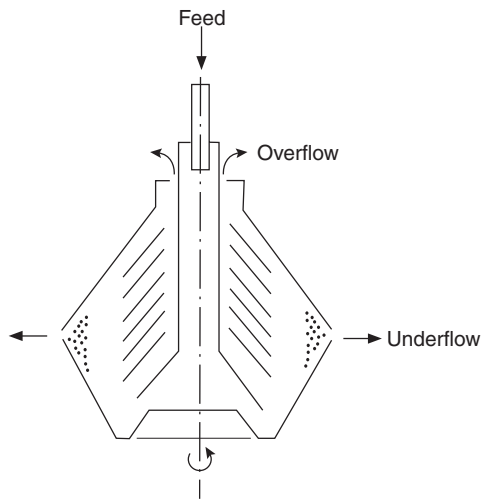

Figure 7.12 Schematic diagram of a nozzle-type disc centrifuge

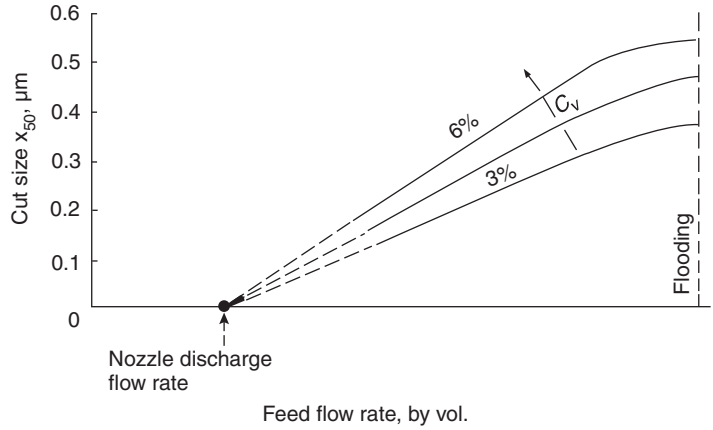

Figure 7.13 Dependence of cut size x_{50} on feed concentration and flow rate for nozzle-discharge disc centrifuge

ratio is normally between 5 and 50%. The underflow flow rate is determined almost solely by the size and number of nozzles used. Similarly to hydrocyclones, the appreciable underflow flow rate in the nozzle-type disc centrifuges increases the proportion of the 'dead flux' of particles going in to the underflow and thus obscures the evaluation of the net separation effect. The concept of 'reduced' efficiency is applicable here, as described in chapter 3, 'Efficiency of Separation', section 3.4.

A recently concluded series of large-scale tests[11] in the UK revealed a dependence of cut size on feed concentration and volumetric feed rate (*Figure 7.13*). The feed rate is bound by two limiting values: a minimum equal to the nozzle discharge rate (when no overflow occurs) and a maximum equal to the rate at which the centrifuge is flooded. The increase in cut size with increasing feed concentration is attributed to hindered settling.

There are several variations of the design such as the recirculation of part of the solids discharge, nozzles at reduced rotor diameter, a facility for washing before discharge, internal nozzles and a paring tube for pressurized solids discharge and others.

Important applications include kaolin clay dewatering, tar dehydration and clarification of wet process phosphoric acid.

7.3.5.3 Solids ejecting type

Intermittent solids ejection is achieved with the solids ejecting type of disc centrifuge (*Figure 7.14*). A number of peripheral ports, which are closed with valves, are provided and these are controlled either by a timer or by a self-triggering device that operates automatically depending on the cake depth. Sliding annular ring scales may also be used; these open wide slots around the

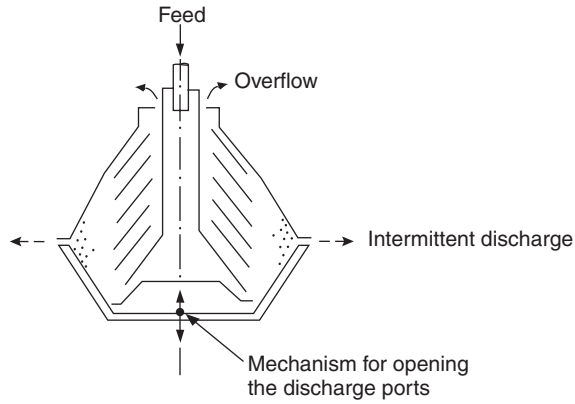

Figure 7.14 Schematic diagram of the solids ejecting type disc centrifuge

periphery and handle considerably coarser and stiffer solids than the orifice ports could handle. The solids ejecting type is used where there is a medium concentration of solids, such as 2–6%, so that neither continuous discharge nor batch operation would be optimum. It is also useful for solids which break down or de-aggregate under the shear forces of nozzle discharge. A better concentration of solids which are slow to compact is also achieved. Depending on the length of time the rotor remains open, either total discharge (of the entire contents of the bowl) or partial discharge (solids only) may be obtained.

Applications for this type of centrifuge include the clarification of various juices and food extracts, and the purification of marine fuels.

7.4 Factors affecting the choice of centrifugal equipment

The engineer who is faced with the selection of centrifugal sedimentation equipment can first consult a guide similar to the one published by Lavanchy *et al.*[22], which is presented in *Figure 7.15* in a modified, metric version, and gives the limiting flow rates and settling capabilities of various types of equipment. The equipment can be located in *Figure 7.15* in its normal operating (region of greatest utility) on the basis of nominal effluent flow rates (normal flows for good and economical clarification in standard applications) and the applicable equiprobable particle sizes or the actual Q/Σ values. Conversion to physical conditions other than those given ($\Delta\rho = 1\,\mathrm{g\,cm^{-3}}$ and $\mu = 1\,\mathrm{cP}$) can be carried out by converting the particle size using equation 3.12 in chapter 3. Note that a theoretical performance curve of a settling tank of unit area is also included in *Figure 7.15* for comparison.

The selection made using this guide may be narrowed by other material characteristics and process requirements. These include the solids content of

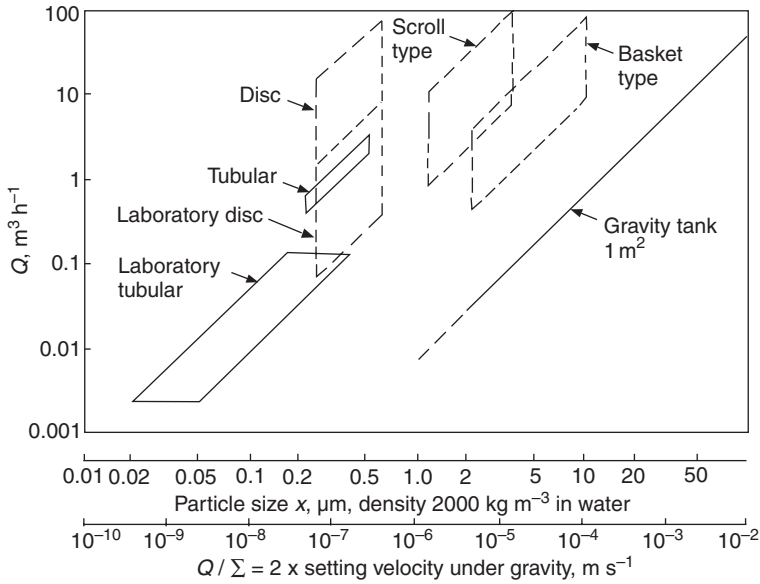

Figure 7.15 Performance of various centrifugal sedimentation equipment

the feed, the nature of the solids (sticky, fibrous or otherwise difficult), the nature of the liquid (corrosive or sensitive to contact with air), explosion hazards, and also the necessity of continuous, intermittent or batch operation. If all these factors are known, the information on each type of equipment selected has to be consulted and a compromise made by choosing the equipment which satisfies all demands to a tolerable degree.

7.4.1 Centrifuges in series or in parallel

When more than one sedimenting centrifuge is to be used in order to improve separation efficiency, the question arises whether it is better to use the units in parallel or in series. Both arrangements are beneficial to the overall recovery of the whole plant: the parallel arrangement increases the residence time which improves the separation, whilst the series arrangement (in the direction of the overflow) benefits the recovery by giving the particles that escaped the process in the first stage another chance to separate.

Let us take an example of two identical sedimenting centrifuges in a clarification duty, such as may be the case on board ships for cleaning fuel or lubricating oil. The question is whether the centrifuges would be best connected in parallel or in series. The general argument is made below for any type of sedimenting centrifuge, but when performance figures need be inserted a specific case of the disc-type centrifuge is used as an example and the conclusion then applies to that type only.

7.4.1.1 The series arrangement

The grade efficiency, G, of a series arrangement of two identical centrifuges, each having the same grade efficiency G_1, is according to chapter 3, equation 3.51

$$G = 2G_1 - G_1^2 \tag{7.36}$$

The series arrangement moves the grade-efficiency curve to the left, to a lower cut size and to higher values of $G(x)$.

In terms of the cut size, its value for the whole plant, X_{50}, is always less than that of the individual centrifuge, x_{50}, but how much less? This depends on the shape of the grade-efficiency curve: if G_1 is log-normal, for example, the improvement depends on the geometric standard deviation of the curve. *Table 7.1* gives three calculated examples. The lower the value of the multiplier in *Table 7.1*, the lower will be the cut size and the higher the resulting recovery of the plant; less steep grade-efficiency curves are clearly favoured in the series arrangements.

Table 7.1 The improvement in the cut size in series connection

Geometric standard deviation of $G_1(X)$, σ_g	*The cut size of the whole plant, X_{50}, μm*
3	$0.53\,x_{50}$
2	$0.68\,x_{50}$
1.75	$0.73\,x_{50}$

7.4.1.2 The parallel arrangement

If the two centrifuges are arranged in parallel, each one takes one half of the total flow, Q, and the performance is compared with that of one centrifuge taking the whole of the flow. In terms of cut size, the Sigma theory (see section 7.2.2) can be used to write for the same machine (same Σ value):

$$\frac{x_{50}}{\sqrt{Q}} = \frac{X_{50}}{\sqrt{Q/2}} \tag{7.37}$$

because, for otherwise the same conditions, the cut size of a sedimenting centrifuge is proportional to the square root of the feed flow rate. Equation 7.37 leads to

$$X_{50} = 0.707x_{50} \tag{7.38}$$

If this result is compared with the values in *Table 7.1*, the conclusion depends critically on the shape of G_1, the dividing line being at $\sigma_g = 1.85$ for a log–normal G_1 (the series arrangement being better for larger values of σ_g). As σ_g

Table 7.2 Measured performance of some disc centrifuges

Centrifuge model	*Ref.*	σ_g
Alfa-Laval QX 412	11	
1.6 mm nozzles		2.35
2 mm nozzles		2.61
Alfa-Laval LAPX 202	23	
(solids-ejecting)		2.14

is very unlikely to be less than 1.85 for sedimenting centrifuges, it seems that the series arrangement is better.

Taking a specific example of disc centrifuges, some test results published in the literature are listed in *Table 7.2*. These data confirm the conclusion that for disc centrifuges the series arrangement gives better recovery than does the parallel one.

7.5 Recent developments

In addition to the now more-or-less standard features and designs of the sedimenting centrifuges described in section 7.3, there have been many refinements and improvements added to the existing technology over the past decade or so. The most important ones are briefly reviewed here, with references given for further details and reading.

In their applications, sedimenting centrifuges are still spreading. They have advanced well into biotechnology and pharmaceutical industries, where sanitary versions equipped with CIP (clean-in-place) and SIP (steam-in-place) capabilities are now available[30,31]. It is interesting to see that this range now also includes a new version of the laboratory tubular centrifuge[30]. This to my knowledge is the most recent competitor to the Sharples Super-centrifuge which has been around since the 1930s.

The Powerfuge[31] is something of a hybrid of an imperforate basket centrifuge and a disc centrifuge: it has four or five compartments (depending on the model) along the axis of the bowl, separated from each other by shallow radial partitions (internal 'baffle rings'), see *Figure 7.16*. In the pilot model shown in the figure (used for scale-up tests), the feed is introduced through a stationary tube into a low shear acceleration zone at the bottom of a titanium bowl. The clarified liquid passes through the bowl, across the compartments and over the weir at the top. The solids form a heel in each compartment until the available volume has been filled. The bowl is then stopped, the remaining liquid is drained and the bowl is disassembled for manual cleaning. In larger models, an automatic pivoting scraper removes the

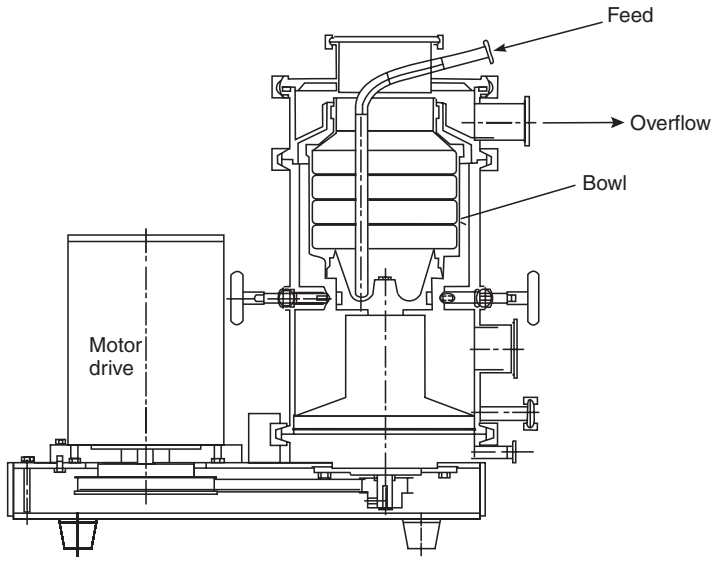

Figure 7.16 A schematic diagram of the Powerfuge Pilot (courtesy of Carr Separations Inc.)

solids from the bowl at a lower speed. Speeds producing up to 20 000 g/s are used and six models are available with capacities from 20 to 9000 litres/hour. The high speeds allow difficult separations from high viscosity slurries and/or in low density differentials. Applications include cell harvesting, inclusion body recovery and cell debris clarification in biotechnology, plasma fractionation, precipitate capture and vaccines in pharmaceuticals, and catalyst recovery, pigments, dyes and toners in the chemical industry. Recently, the Powerfuge has also shown to be useful in sub-micron classification and recovery, see section 7.5.3.

At the other end of the application scale, the conventional decanter centrifuge is now also used in and made specifically for processing of drilling mud ('mud technology')[32].

7.5.1 The scroll-type centrifuge

The most usual design of the scroll centrifuge is the one in which the solids and the liquid move in a countercurrent fashion in the bowl, with the feed point being well away from the liquid discharge point (refer to section 7.3.4). A relatively recent, co-current design offers certain advantages, mostly because it requires lower speeds for the same separation duty. The feed point is close to the liquid discharge end of the bowl but the slurry cannot bypass the process; it moves with the solids towards the beach until it reaches a point when it overflows into the scroll and then it moves back to the liquid discharge end, not interfering with the flow of the solids.

A co-current design is obviously a little more complex than a counter-current one, because it requires a running seal to prevent the incoming feed from passing directly into the overflow, but it may well be worthwhile in applications where lower speeds are desirable, e.g. when there is a danger of the solids sliding down the beach at high speed. An alternative to the liquid overflow open outlet is a paring tube for skimming off the liquid.

The conventional, countercurrent decanters, if applied to very fine slurries, can suffer from problems of discharge of the solids. The separated sludge can flow back, countercurrent to the movement of the scroll conveyor; the flow may be through the clearance between the conveyor blades and the inner surface of the bowl and also along the helical canal formed by the conveyor blades and the cone. This highly undesirable phenomenon may cause variations in the solids discharge rate, with the accompanying fluctuations in the torque, poor centrate clarity and poor overall performance of the machine. Karolis and Stahl[24] studied the effect with the view of developing a model and proposing design and operating measures to counter the problems. The project has led to the development of grooved inner walls of decanters which reduce backflow problems[25].

Another important recent development is that of a slender decanter centrifuge[26]. Through a novel way of supporting the bowl, the centrifuge can be made much longer relative to its diameter than was previously possible. Both manufacturing costs and energy consumption are claimed to be reduced with the slender decanter as compared with the conventional short and thick unit of the same separating capacity. The G force for a given length of the decanter can also be increased. Further reductions in energy consumption can be achieved due to a design which allows a very small liquid surface radius for a given decanter diameter.

The industrial use of the scroll-type centrifuge has been growing, particularly in coal preparation[27] and in other mineral-processing applications where, in order to reduce abrasion, the internal walls are coated with a ceramic lining. Another major area of growing application of the scroll-type centrifuge is in the dewatering of municipal and industrial sludges[28].

7.5.2 The disc centrifuge

There are now several variations of the design of the nozzle-type bowl including the following features:

1 recirculation of a part of the solids discharge;
2 nozzles at reduced rotor diameter;
3 a facility for washing before discharge;
4 internal nozzles and a paring tube for pressurized solids discharge.

The solids recirculation system offered in the Merco Centrifuge, for example, takes part of the slurry discharged through the nozzles back into

the bowl and reintroduces it close to the nozzles. This allows control of the underflow solids concentration without the need to change nozzles or use very small nozzles which are susceptible to blocking. Furthermore, washing liquid can be added to the recycled stream, thus allowing some co-current washing. The Merco Centrifuge is available with capacities of up to 230 $m^3 h^{-1}$.

A relatively recent newcomer in this category of disc centrifuges is the Roto-Filter pump. This pump clarifies and pumps at the same time. The 400 mm diameter rotor has one flat disc in it and the suspension enters centrally, as in a centrifugal pump; it goes round the outside of the disc and back to the centre where it is collected by a stationary pipe. The solids discharge through nozzles situated on the periphery of the disc, as in the nozzle-type centrifuge described previously, except that the nozzles (1.5 mm diameter) face tangentially rather than radially. Only two or four nozzles are provided, making this centrifuge suitable for clarification only. The effective cut size is large by centrifuge standards, 10 μm or more for sand in water. This is because the residence time of the solids in the bowl is short, with some elutriation also taking place. Flow rates of 27 $m^3 h^{-1}$ and delivery pressures of 6.7–27 bar can be achieved. The bowl speed is 3550 rev. min^{-1}. The use of this machine can only be justified if pumping is necessary and relatively coarse separation is acceptable. Otherwise, any conventional centrifuge will achieve much finer cuts.

7.5.3 Centrifuges for wet classification of superfine solids

Classification of very fine solids in sedimenting centrifuges is, of course, nothing new. It has been done almost ever since Gustav de Laval first patented a continuous centrifugal separator for separating cream from milk in 1878. The sedimenting centrifuge is generally suitable for classification because the separation process is highly particle size-dependent, characterized by the grade efficiency curve (refer to section 3.2.2). One problem with this duty is that the sharpness of cut achieved by sedimenting centrifuges is not particularly good. An extensive study carried out at ECC International[11], for example, showed that the disc centrifuges gave the geometric standard deviation (σ_g) of the reduced grade efficiency curve from 2.35 to 2.61 (see *Table 7.2*) whilst hydrocyclones gave from 1.8 to 2 (i.e. sharper cuts), with the same test materials. Furthermore, many air classifiers specially built for such duty usually give even sharper cuts, with σ_g as low as 1.5.

Generally, when sedimenting centrifuges were used for classification in the past, no attempt was made to modify the design to make it produce a sharper cut. Reclassification in another stage, as a remedy generally available, has not been widely used because of the high costs involved (with the much cheaper hydrocyclones multi-stage classification is practised frequently). One relatively recent exception is the Merco centrifuge (see a mention in section 7.5.2) where the washing facility through the recycling of liquid into the bowl can be used to sharpen the cut.

As the trend in industry is towards finer particles, the need to classify at superfine (micron or submicron) cut sizes is gradually increasing. Air classifiers can produce such fine cuts but they have to be specially designed for such duty. And with some materials, dry classification is not an option. Consequently, some attempts have been reported recently to do the same in wet classification and to design special centrifuges capable of micron or submicron cuts at relatively high feed concentrations. Such attempts have to remove one or both of the major causes of poor sharpness of cut: overcrowding of the classification zone and non-uniform conditions for different particles during their passage through the machine. This may be done by switching from a co-current separation principle (as employed in most sedimenting centrifuges) to a counterflow one, more suited for classification.

Stein[33] at Hosokawa Alpine AG has developed, in the range of their wet classifier mills ('Hydroplex Wet Processing Systems'), the Hydroplex Wet Classifier. This centrifuge can produce sharp cuts from 2 to 20 microns with solids concentrations up to 30% w/w.

Another development was sponsored by Fryma-Maschinenbau GmbH, BASF and Westfalia Separator AG[34]. This centrifuge was designed to produce fine product which has no particles above a preselected size (e.g. 4 microns) present and in that it succeeded. However, it did that at a cost of extremely low fine product yield: less than 1% of solids was recovered as fine product yet there was 20% present in the feed! The machine run with the split ratio R_f (see section 3.4.1 for the definition) 70.8% which led to the coarse recovery of 99.2%. The particle size distributions presented in the paper did not allow grade efficiency evaluation because they were not in mass balance.

The relatively new arrival, the Powerfuge by Carr Separations Inc. described in section 7.5, has also proved to be suitable for classification of superfine solids. An interesting study on the flow and its effects on classification in the Powerfuge has recently been published by Kessler and Kremer[35]. They followed on some earlier flow visualization studies in imperforate basket centrifuges that concluded that the flow in these machines was quite distinct from plug flow and instead assumed the form of a boundary layer on the pool surface[36,37]. At the 1999 AFS Technical Conference, Beiser *et al.* presented results of a study of residence time distribution (RTD) in a decanter centrifuge[38]. They concluded that the flow was best modelled by CSTRs in series or plug flow with axial dispersion.

In their new study, Kessler and Kremer[35] used a tracer method to measure the residence time distribution (RTD) within the bowl of a high-speed Pilot Powerfuge. Two variations in bowl geometry were studied. The nature of flow in the Powerfuge was shown to be dependent upon bowl speed, flow rate, bowl geometry and temperature distribution between the bowl and feed liquid. The effects of the different flow regimes on size classification of particulate suspensions were evaluated by classifying polyvinyl acetate suspensions of particle size distribution between 0.1 and 10 μm. Particle size distributions of feed and centrate samples were measured using a Coulter LS

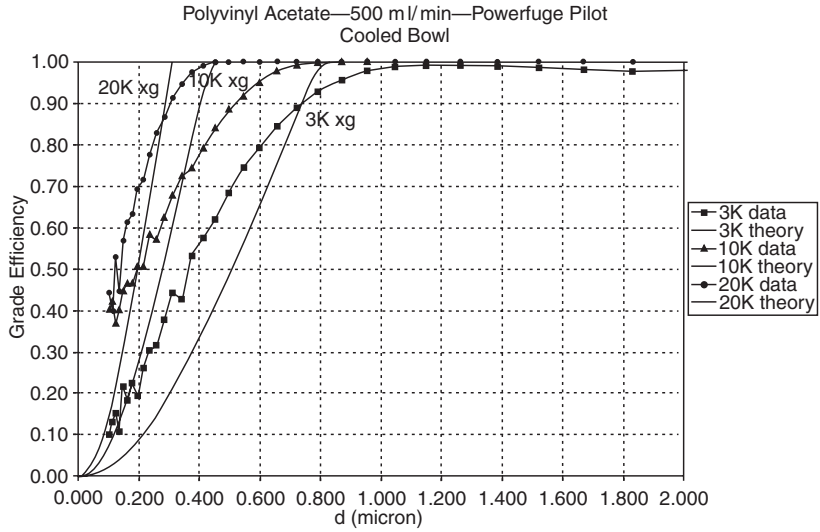

Figure 7.17 Classification performance of the Powerfuge Pilot with a cooled bowl.

230 laser diffraction particle size analyser. In addition to the operating conditions listed above with respect to RTD measurements, concentration of the feed suspension was also varied during the classification study. Classification results were expressed in the form of grade efficiency curves and correlated with operating conditions, as well as the flow regimes defined by RTD measurements.

Figures 7.17 and *7.18* show grade efficiency curves for the cooled- and heated-bowl operating conditions at 500 ml/min and three bowl speeds. Included on these graphs are a family of theoretical curves based on equation 7.9a which predicts grade efficiency based on the assumption of plug flow in a tubular centrifuge. For the 20 000 g runs, there is little difference in the classification result between the heated and cooled condition and good agreement is seen with the prediction of equation 7.9a in both cases. At 10 000 g the cooled condition gives increased sharpness of cut, as seen from the slope of the grade efficiency curve. This result corresponds to an RTD curve[35] tending more toward boundary layer flow for the cooled condition. For the 3000 g runs, the classification result is markedly different between heating and cooling, with the cooled condition yielding a cut that matches reasonably well with the theoretical curve. The heated condition at 3000 g gives a cut higher in particle size than predicted and not at all sharp at the upper end of the curve. Referring to the RTD curves in ref. 35, it seems that the tendency to boundary layer flow in the cooled condition is important to obtain good classification at lower bowl speeds, e.g. 3000 g. However, at 20 000 g the temperature effects appear unimportant.

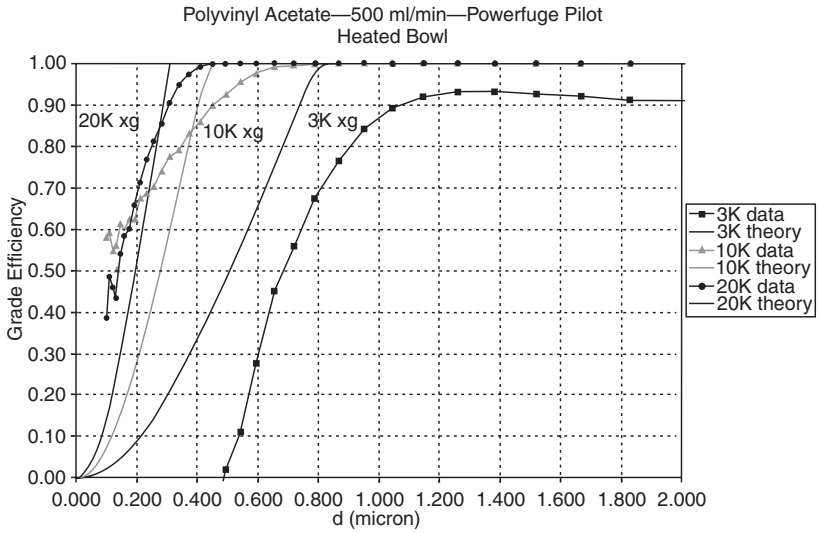

Figure 7.18 Classification performance of the Powerfuge Pilot with a heated bowl

From the results of RTD studies[35] it can be concluded that small changes in bowl temperatures above or below the feed temperature have a significant effect on flow patterns in the bowl. This result supports the hypothesis that thermally induced density gradients lead to mixing currents. In addition to temperature, flow patterns are affected by feed flow rate and bowl speed. Separation efficiency and classification studies show that the various flow patterns produced under different operating conditions affect separation performance in both types of separations studied. This fact leads to the conclusion that flow patterns must be better understood and controlled in order to optimize classification of superfine solids.

As the use of superfine solids in industry increases, further development of the centrifuges for wet classification of such solids is likely to continue in the future.

7.5.4 Safety

Before leaving the subject of sedimenting centrifuges it is important to mention safety. As with other machines with parts rotating at high speeds, the necessary safety precautions must be observed. The enclosure must be designed to withstand possible disc failure and vibration switches are usually provided to give warning of excessive vibration due to bowl imbalance. When dealing with flammable solvents and vapours, extra precautions must be taken to prevent explosion: these include inert gas (nitrogen or carbon dioxide) blanketing, explosion suppression devices (which eject suppressant during

explosion) and the elimination of possible sources of ignition. Hermetically sealed decanters, for example, have been designed for this purpose[29].

References

1. Schachman, H. K., *J. Colloid Phys. Chem.* **52**, 1034–1045 (1948)
2. Bradley, D., *Chem. & Proc. Eng.* November & December, 1–8 (1962)
3. Ambler, C. M., *Chem. Eng. Progress*, **48**, 150–158 (1952)
4. Ambler, C. M., *J. Biochem. & Microbiol. Tech. & Eng.*, **1**, 185–205 (1959)
5. Morris, B. G., *Brit. Chem. Eng.*, **11**, 347 (1966)
6. Woolcock, R. J., *Filtration and Separation*, **12**, 174–180 (1975)
7. Frampton, G. A., *Chem. & Proc. Eng.*, **44,** 402 (1963)
8. Purchas, D. B., *Industrial Filtration of Liquids*, 2nd edn, Leonard Hill Books, London (1971)
9. Murkes, J., *Brit. Chem. Eng.*, **14**, 636–641 (1969)
10. Zeitsch, K., 'Effect of the feed rate on the active acceleration of overflow centrifuges', *Trans. I. Chem. E.*, **56**, 281 (1978)
11. Gibson, K., 'Large scale tests on sedimenting centrifuges and hydrocyclones for mathematical modelling of efficiency', pp. 1–10. In *Proc. Symp. on Solid-Liquid Separation Practice*, Yorkshire Branch of the I. Chem. E., Leeds, 27–29 March (1979)
12. Allen, T. and Svarovsky, L., *Powder Technol.*, **10**, 23–28 (1974)
13. Bass, E., *Periodica Politechnica Eng. Machinen u. Burwesen, Budapest*, **4**, 1 (1960)
14. Reuter, H., *Chem. Ing. Tech.*, **39**, 311, 548 (1967)
15. Riesberg, K. D. and Dudrey, D. J., *Filtration Engineering*, May/June (1972)
16. Ford, J., 'The sludge dewatering centrifuge', *I. Chem. E. Symp. Series No. 41*, QI–Q14 (1975)
17. Stahl, W., *Personal Communication*, Krauss-Maffei A. G., München, West Germany (1975)
18. '*The Sala Lamella Thickener*', SALA Information SIM 374, Sala International, Sweden
19. Murray, K. R., *1st European Conf. on Mixing and Centrifugal Separation*, Paper F4, BHRA Fluid Engineering (1974)
20. Fitch, B., 'Separating power of disc centrifuges', *55th Int. Meeting of A.I. Chem. E.*, Preprint 11a (1965)
21. Willus, C. A. and Fitch, B., *Chem. Eng. Progress*, **69**, 73–74 (1973)
22. Lavanchy, A. C., Keith, F. W. and Beams, J. W., 'Centrifugal separation'. In Kirk, R. E. and Othmer, D. F., *Encyclopedia of Chemical Technology*, 2nd edn, vol **4**, Wiley Interscience, London, 710–758 (1964)
23. Allen, T. and Baudet, M. G., *Powder Technol.*, **18**, 131–138 (1977)
24. Karolis, A. and Stahl, W., 'Discharge of pasty material from decanter centrifuges', *Inst. Chem. Eng. Symp. on Solid/Liquids Separation Practice and the Influence of New Techniques* (Leeds, 1984), Paper 6.
25. Stahl, W. and Langeloh, T., 'Improvement of clarification in decanting centrifuges', *Ger. Chem. Eng.* **7**, 72–84 (1984)
26. Madsen, N. F., 'Slender decanter centrifuges', *Conference on Solid–Liquid Practice III, 397th Event of the EFCE* (Bradford, 1989), Inst. Chem. Eng. Symp. Ser. No. 113 (1989)

27. Osborne, D. G., 'Coal fines dewatering', *Trans. Soc. Mining Eng. AIME*, **276**, 1843–1849 (1982)
28. Spinosa, L. and Eikum, A., 'Dewatering of municipal sludges'. In L'Hermite, P. and Ott, H. (Eds), *Proc. 2nd European Symp. on the Characterization, Treatment and Use of Sewage Sludge* (Vienna, 1980), D. Reidel, Dordrecht (1980)
29. Jaeger, E. A., 'Hermetically sealed solid bowl decanter—a part of solvent chemistry', *Inst. Chem. Eng. Symp. on Solid–Liquid Separation Practice and the Influence of New Techniques* (Leeds, 1984), Paper 5
30. 'Alfa Laval Separation Ltd', *The Chemical Engineer*, 26 September, 15 (1996)
31. Powerfuge, Carr Separations Inc., 10 Forge Park, Franklin, MA 02038, USA
32. HS 3000 Centrifuge, Pigott Shaft Drilling Ltd, PO Box 63, Preston, PR4 0BT
33. Stein, J., 'Nassaufbereitungstechnik: Besonders fein mahlen und klassieren', *Verfahrenstechnik*, **31**, No. 3, 30–34 (1997)
34. Bickert, G., Stahl, W. and Bartsch, R., 'Wet classifying in the superfine range by reverse current flow centrifugal elutriation', Filtech Conference, Karlsruhe, 19–21 October, 1993, paper published in the Proceedings, Vol. 2, by the Filtration Society, Horsham, 53–61 (1993)
35. Kessler, S. and Kremer, I., 'Flow and its Effects on Classification in Process Centrifuges', presented at the American Filtration and Separations Society Annual Technical Conference, Myrtle Beach, SC, March, 14–17 (2000)
36. Bass, E., *Periodica Polytechn.*, **4**, 41 (1960)
37. Reuter, H., 'Strömungen und Sedimentation in der Uberlaufzentrifuge', *Chemie-Ing.-Techn.*, **39** 311 (1967)
38. Beiser, M., Frost, S. and Stahl, W., 'Investigations on the Residence Time Distribution of the Fluid in a Decanter Centrifuge', presented at AFS Annual Technical Conference, Boston, April, (1999)

Bibliography

Leung, W. F. and Shapiro, A. H., 'Dewatering of fine-particle slurries using a compound-beach decanter with cake-flow control', Proceedings Volume I, World Filtration Congress 8, European Federation of Chemical Engineering Event No. 607, organised by The Filtration Society and Elsevier Science, The Brighton Centre, Brighton, UK, 3–7 April 2000, 271–274 (2000)

Stahl, W., Stiborsky, M., Beiser, M., Ettmaye, A. and Frost, S., 'A summary of the academic research on decanting centrifuges', Proceedings Volume I, World Filtration Congress 8, European Federation of Chemical Engineering Event No. 607, organised by The Filtration Society and Elsevier Science, The Brighton Centre, Brighton, UK, 3–7 April 2000, 267–270 (2000)

8

Filter media, filter rating

Lawrence G. Loff

Tetko Inc., Briarcliff Manor, New York, USA

8.1 Introduction

The primary goal of this chapter is to gain a better understanding of filter media and filter ratings. Our definition of filtration will be in reference to liquids and will be the process whereby solids are separated from a liquid by passage through a permeable medium. Particles larger than the passages through the medium are retained, while the liquid (filtrate) passes through. Smaller particles may or may not be retained, depending upon the complexity of the channels through which the filtrate must pass.

The filter medium is installed in the filter over a stationary structure and provides adequate porosity capable of passing liquid through, while retaining solids. The medium is characterized by its filtration properties of permeability and retention. Filtration will not take place without the medium and the overall performance of the filtration system depends directly upon the properties and its interaction with the influent.

Filter media can be natural, synthetic or glass, woven or non-woven cloth: paper, ceramic, cellulosic or synthetic membrane, or, in some cases, woven, etched or sintered metal, depending upon the requirements and/or allowable cost.

Most filtration techniques require the use of a filter medium. The medium can be considered as the heart of the filtration device or machine. It is important to choose a suitable material of construction and to specify correctly the filter medium according to the properties and characteristics of the material to be filtered. The manner of application and attention to maintenance during the use are additional factors of importance. Failure to consider carefully each of these factors relative to each filtration application, will reduce the efficiency of separation and the operational performance achieved.

Prior to discussing any specific types of filter media, I wish to give a small representation of various types of filtration equipment or hardware, which is the vehicle in which the medium operates.

Various types of filtration equipment or hardware employ one of four main classes of driving force: gravity, vacuum, pressure or centrifugal force. The choice of which type of equipment to use in a specific application depends upon many widely differing factors, which will not be detailed in this chapter.

Gravity is simple, and has zero direct running cost. However, the equipment is usually bulky and fairly coarse solids will still contain an appreciable amount of liquid after separation. This may lead to unfavorable capital and running costs overall.

Gravity filters depend upon atmospheric pressure to force the solids through the medium. The slurry is fed into the top of the filter and through the medium, with the clear filtrate emerging from the underdrain. Sand filters, travelling belt filters and rotary drum gravity filters are found in this group.

In vacuum filters, vacuum can be easily produced either by the suction of an ordinary liquid pump or by a gas displacement device, such as a rotary vacuum pump or steam ejector. Depending upon the device, the effect is to find a driving force of up to about 12 p.s.i. (0.81 bar), which in many instances is sufficient to give vastly improved rates of filtration with all except the finest solids.

The vacuum is created behind the filter medium, which causes the atmospheric pressure in front of the filter medium to drive the slurry through the medium, filtering out suspended solids in the process. Types of vacuum filters include: belt, horizontal pan, vertical disc, and drum varieties.

The third type of driving force is pressure. Pressure filters produce a greater output per unit area, so enabling smaller equipment to fit easily into the process circuit, and making the handling of volatile liquids easier. However, it is sometimes difficult for continuous discharge of solids, such as cake. The feed slurry is introduced into the filter under pressure and forced through the filter medium. There are two basic designs used in pressure filtration: plate-type filter presses, whereby a series of plates utilize a filter medium between them; and casing-enclosed pressure filters, which consist of filter medium-covered elements enclosed in a pressure tank.

Another type of pressure filter utilizes two belts which move in the same direction. These belts are normally on top of each other and for a certain distance they share the same rollers with the sludge travelling in between the two belts. These rollers decrease in diameter as the belt travels, and thus the sludge is subjected to a tremendous shear force as it goes over the roller. This assists in the dewatering and filtration process.

Centrifugal driving force takes in two types of separators: cyclones and centrifuges. Cyclones have simple, compact construction with low running costs. However, separating efficiency falls off rapidly for particles below about 10 μm, and solids are discharged as a slurry. Centrifuges give higher separating efficiency even for very fine particles. Discharge of solids is either in cake or slurry form, although with very fine particles continuous discharge is only possible as a slurry. High throughputs are achieved relative to the size

of a centrifuge so, hopefully, justifying the high capital cost of this piece of equipment.

The liquid is passed under centrifugal force through a filter medium or perforated plate. Filtration occurs as the liquid passes through the interstices of the solid particles that have built up on the medium surface. Depending upon the degree of separation desired, filter media can be a filter fabric of twilled weave, dutch weave or plain weave in either stainless steel or synthetic fibre.

8.2 Filter media—general

Just as there are vast numbers of different types of filters, the same holds true for filter media, on which the filters are so dependent. I will present as many types of media as feasible, and will concentrate on those that are most commonly used.

An important question on filter media is to ask how fine a degree of filtration it will give. There are three groups of considerations which are raised when attempting to define the degree of fineness of filtration that can be achieved with a given medium. The first is the structure of the medium; the second is the mechanism by which filtration occurs, which is dependent upon the medium and the fluid–particle system to be handled; and the third group is the method of measurement used.

Structural considerations are only relevant for solid media in rigid or semi-rigid form such as porous metals, fabrics, screens or layers of powders (precoats). Filtering characteristics are greatly affected by the size and shape of the holes, as well as by their path through the medium (i.e. straight or tortuous), and whether they vary in size and shape through the depth of the medium. Also, the number of holes per unit area, and their uniformity, affect filtering.

Obvious uniformity is found in simple form with plain-weave metal cloth of light gauge wire. As the gauge of the wire becomes heavier and the weave is changed to a twilled or Dutch-type weave, we have a more elaborate medium that is generally used for filtration. The nature of the holes is more complex and more difficult to recognize with the unaided eye. Woven fabrics become more complicated due to the flexible nature of yarns, and therefore it is more difficult to try to define the size of the hole in a woven fabric. The same is true for media with random structure, such as felts, paper, fibrous and porous material.

The main types of mechanism by which filtration occurs are surface and depth. These are also referred to as classifications of filter media. Other classifications are rigid versus flexible, loose versus integral, and permanent versus disposable media.

An example of surface filtration would be a straining process with wire cloth, wherein all of the solids larger than the media openings are deposited

on the cloth surface, while the smaller particles pass through. Depth filtration utilizes the thickness of the medium as well as its surface, primarily to trap particles within the interstices of their internal structure as the fluid travels a tortuous path through the medium. Porous media, felt or the wound type of filter cartridge, are examples of depth media.

Cake filtration occurs after surface filtration where a cake acts as the filter medium. In some instances the cake formed has a lower permeability than the filter medium and thus becomes the limiting factor in the filtration cycle.

The last factor, when attempting to define the degree of fineness of filtration achieved with a given medium, is the method of measurement used. The three criteria by which the performance of a medium is judged revolve around:

1 the measured data of how small a particle it can stop;
2 the permeability (the ability of the medium to allow flow);
3 the relationship between build-up of dirt in the medium and the rate of increase of resistance to flow.

These three criteria are discussed in section 8.9.

8.3 Cartridge filters

Cartridge filters are one of the most widely used types and have the advantage of being simple, with minimal installation cost. Areas of common use for cartridges are in the automobile and aerospace industries for protection of hydraulic and lubricating systems. They are also used in electroplating for filtration of solutions, as well as in the beverage manufacturing field and in chemical processing. Cartridges have had many improvements in manufacturing and pore size control. Some media used in making cartridges, such as porous ceramics, sintered metals, felts and papers, are dealt with separately as we proceed. However, there are certain media that are used only for cartridges because of their physical form. These media are wound cartridge and bonded cartridge, which are discussed with depth filters in the following. There are three basic types of cartridge filters: edge, surface and depth.

The edge filter is of a solid fabrication structure wherein the medium consists of the edges of a stack of specially formed washers or thin discs mounted on a central perforated core (shaft), and held under compression so as to form a continuous cylindrical outer surface. Each washer has grooves or scallops cut into it, such that very fine and carefully controlled gaps occur between the adjacent washers. The gaps are usually sized from 5 μm upwards. Filtration takes place by flow of liquid inward through the narrow gaps between adjacent discs. The filter is essentially a strainer in that particles are stopped on the outside surface. The discs are usually metal but they can be nylon, polypropylene or paper.

Another filter medium in the same category is that of elements made by winding a wire on a cylindrical support. The wire can be round or wedge shaped. Wedge-shaped wire gives wider apertures on one face than the others of adjacent wires wound edgeways on to the perforated support. The micron retention range for the edge filters can range from 1 μm for the paper disc type, from 25 μm for the wire wound, and upwards of 50 μm for the metal disc type. Edge filters can also be cleaned by a back-flushing on paper disc-type or scraping on wire wound or metal disc types. Their cleanability could make them more economical than less expensive media.

The depth cartridge filter holds to the meaning of depth filtration whereby the particles are primarily trapped within the interstices of the internal structure. The two main types of depth cartridges are bonded and wound. Both types offer a simple, compact disposable unit with a high dirt-holding capacity able to remove solid particles from liquids, down to about 1 μm. They have a small surface area but it can be increased by cutting grooves on the outer surface, which also increases life by delaying plugging.

Bonded cartridges are composed of fine, loose fibres of wool, cotton, cellulose, glass and various synthetic materials built into a thick-walled tube by a filtration technique wherein the fibres are formed wet. After drying, the tube is impregnated with resin and cured, forming a light, very porous rigid structure with good dirt-holding capacity. These cartridges are inexpensive because they are self-supporting and do not generally have a central support core. Dirt holding is improved by changing the density of the medium. Bonded cartridges are not cleanable.

Wound cartridges consist of spun stable fibres of wool, cotton, glass and various synthetic products. The fibres can be brushed to raise the nap after each layer is formed, wound on a hollow perforated core until the desired cartridge thickness is achieved. The nap forms the filtering medium by varying the closeness of the winding from the central to the outside layer. The porosity of the medium is determined by control of winding pitch, tension, fibre length and other characteristics. Wound cartridges are similar to bonded filters in that they are inexpensive with large dirt-holding capacity; also, they cannot be cleaned.

In going now to surface filtration cartridges, we find the most widely used media are in thin, sheet-form of cellulose paper or resin-treated paper. They are normally corrugated or pleated to increase useful filter life and filter surface area (e.g. automobile air filters). A single compact cartridge can have up to 2.8 m^2 of surface area. The retention range of this type of cartridge is from 0.5 to 50 μm. Woven materials, primarily woven wire, are also used for this type of cartridge. The bulk of the filtration takes place on the surface but some depth filtration is also involved.

In general, and in summary, cartridge filters have an integral cylindrical configuration made with disposable or cleanable filter media and utilize either plastic or metal structural hardware. Appropriate housings form the filter assembly and for large flows, multiple cartridges are installed in a pressure

vessel. Such materials as cotton, wool, rayon, cellulose, fibreglass, polypropylene, acrylics, nylon, asbestos, cellulose esters, fluorinated hydrocarbon polymers and ceramics are commonly employed in the manufacture of disposable cartridge filters. Porous media for cleanable or re-usable cartridges typically employ such materials as stainless steel, monel, ceramics and fluorinated hydrocarbon polymers, as well as exotic metal alloys.

8.4 Rigid porous media

Ceramics and stoneware have good resistance to chemical attack and high temperature. Stoneware is made from certain types of clay rich in silica and is more a sub-class of ceramics, but all ceramics are made from powdered solids by a process that involves kiln temperatures of 1400 °C.

The ceramic elements are made in many shapes and sizes in various grades, which correspond to different average pore sizes. One disadvantage is that they are often fragile. However, their fragility is off-set by their low cost and high resistance to corrosion, as well as the wide range of porosities available when compared with available alternatives. Pore sizes can range from 2500 down to 1 μm. Ceramics are widely used in gas filtration, and in separating dust and liquid droplets from gases.

Sintered metals can be produced either from powdered metals or from woven wire. Various mesh-size powders are sintered in a controlled atmosphere at temperatures slightly below their melting point, causing a strong metal-to-metal fusion forming a tortuous path (depth) for filtration, approximately 1.6 mm (1/16 in) thick. Many different metals, such as bronze, various stainless steels and Inconel, can be used. Cutting, bending and welding of sheets into parts is also possible. The cost is usually high but can be off-set by the media's ability to be cleaned for re-use by back-flushing or chemical cleaning.

The woven wire-type, sintered media can be made either with a single layer or several layers of woven wire sintered with the powder. By controlling the particle size of the powder or the wire gauge and weave of the woven metal, the porosity of the sintered product can be made with precision from 400 to under 1 μm.

Keeping our discussion to the different types of porous media, we should not forget to include porous plastics. The range of porous plastics and the shapes (forms) in which they are available, are still growing. A variety of materials such as nylon, polyester polyurethane, polyethylene and fluorocarbon, among others, have gained in popularity. Pore sizes can vary from large holes down to under 1 μm, produced by sintering and foaming techniques. Nucleopore medium, which is a form of porous plastic, is produced by a radiation technique on polycarbonate and polyester which can yield uniform holes in the range 1–10 μm at will. Laser technology is also used to produce membranes of uniform openings at under 1 μm.

The Nuclepore membrane is a thin film of about 6–10 μm thick, containing very fine pores ranging from 0.015 to 14.0 μm of polycarbonate and polyester materials. Membranes of mixed esters of cellulose or PTFE can range between 100 and 200 μm thick with pore sizes of 0.1–5 μm. This medium has found wide use in water filtration, cell culture, and serum filtration among others. Membranes are formed from dissolving the raw material in a mixture of two solvents leading to an evaporation to form the porous structure. Some are formed around woven monofilament fabrics or paper for reinforcement. Their main use has been for liquid and gas filtration where high standards of resolution are needed, such as in water desalination by reverse osmosis or separation by ultra-filtration (separation of colloid substances such as clays or pigments, and relatively high-molecular weight materials as polymers or protein separated from liquids in which they are suspended). For a wide diversity of applications membrane is available in materials other than those mentioned above. Examples are PVDF, polypropelene, nylon, acrylic co-polymer plus others which may be standard or special.

There are two general types of membrane, symmetrical and asymmetrical. Both sides of a symmetrical membrane are the same, therefore, either side can be used in filtration. Symmetrical membranes have very uniform pores, such as a Nuclepore membrane. The sides of the asymmetrical membrane, unlike the symmetrical membrane, are very different. One side has very small openings that branch out through the membrane to form a very large opening on the other side; the performance of the filtration depends upon which side is used. This membrane has a tendency to load up with solids.

8.5 Non-woven media

Although this section is particularly about non-woven media, much of what we have discussed earlier has, in fact, been non-woven. In this sense of the term, ‘non-wovens’ are loose assemblages of fibres arranged in short form and physically bonded with a bonding system. They are lighter and thinner than felts with higher permeability, lower retention and greater strength than paper media. In direct contrast to this, I find a paper manufacturer describing his paper-making process for filter paper in the same manner. From studying what both sources are presenting, I believe it to be a matter of how one wishes to interpret ‘non-woven’. Purchas (1967) classifies felts, papers, sheets and mats, among other similar media, all in the category of non-woven—so will I. They all basically have random pore structures.

Felts, also known as ‘non-woven fabrics’, have been used for many years for filtration, but they were formerly made from wool. Once synthetic materials were used in the manufacture of felts, they became very widely accepted and used for many filtration applications. In fact, the word ‘filter’ is derived from the mediaeval Latin word *filtrum*, which means felt. Felts are now made from a wide range of materials such as olefin, nylon, polyester

acrylic and fluorocarbon fibres. These fibres are arranged at random, in mass, with or without a resinous bonding agent (or heat or chemical bond), and are formed into compacted pads which control the thickness of the fibre as well as the porosity and density of the medium. They have fibrous finishes but can be calendered in order to smooth this out.

Felts have many applications in chemical, electrolytic, biological, thermal, cryogenic and foodstuff fields, for gas and liquid filtration. They can be used for filter presses, moulded filter elements, and fabricated cartridges where felt would be formed with the pleated woven wire. Felts can also be used as a drum cover or filter belt for rotary vacuum filters and in the manufacture of filter bags. Synthetic felts also show an excellent particle retention, freedom from blinding (plugging) and resistance to fungus and corrosion. They have dimensional stability and maintain their clean-cut edges in addition to being easy to sew for fabrication. Felts also make efficient gaskets, preventing side leakage between elements on filter press applications. They provide ease of cleaning with hosing or backwashing, which helps to reduce down-time.

An item that we all see throughout our daily lives but do not realize that it is, in one of its forms, a filter medium, is paper. It is a very widely used medium, made by dispersing fibres into a suspension in water. This suspension is then filtered into a mat form, which is compressed and dried. By varying the process, different porosities are achieved. The size of the fibre is important. Cellulose fibres are relatively coarse while glass is finer. Cellulose-based papers have poorer retentive power and are widely used in industrial liquid filtration applications because of lower cost and good mechanical properties. Glass is typically used in laboratory applications.

Both glass and cellulose papers can be impregnated with bonding agents such as melamine, resin and neoprene to increase strength and to modify filtration characteristics. Silicon is also used to give water repellancy for coalescer and separation applications. A very popular end-use for filter paper is for pleated cartridges in automotive and industrial applications where the micron range is from 0.5 to 500 μm. Filter paper is also used on plate and frame presses and pressure leaf presses. Because of its weakness, paper is usually supported by perforated metal, woven wire or synthetic cloth.

Glass fibre paper has workable temperatures up to 500 °C, which will exceed that of cellulose paper, membrane and porous plastic materials. This brings glass into competition with asbestos and metallic media. Glass fibre is known for good retention and high flow rates. In the same respect as paper, we have filter sheets and mats which are distinguished as slightly different due to characteristics of thickness that classify them as depth media, whereas paper is primarily a surface medium. Sheets are basically made from asbestos mixed with cellulose for a binder or diatomaceous earth for increased permeability. Other materials such as carbon, lime, synthetic powders, etc. are also used. One face of the filter sheet is usually harder than the other. The harder side is intended for use on the outlet side to prevent fibre loss in the filtrate. Other treatments are also available depending upon the end-use application.

Before describing woven filter media further, it should be noted that there are many filter media available which cannot be detailed in this chapter. The following are some not previously mentioned and they are presented here only in name in order to indicate the vast variety available. Filter sheets are available, formed from diatomaceous earth rather than asbestos. Loose fibre filter media, made from asbestos, cellulose and glass wool, are other types of material available. There are a wide variety of loose particles available as filter media, including precoats, sand or body aids. Body aids are additives to the liquid to be filtered. Lastly, perforated sheets in both synthetic materials and metals are used but have restrictions because hole sizes are generally no smaller than 50 μm. They are commonly used as support or back-up for finer media, or alone as strainers or roughing filters.

8.6 Woven wire

Woven media can be called woven wire, woven fabric, wire mesh, wire cloth etc. Precision woven wire cloth is a versatile, wear-resistant filter medium which has been widely used for many years and is available in a large variety of weaves made from many metals. The most frequently used metal is stainless steel, in either type 304 or type 316. The basic difference between the two types is the addition of molybdenum to the type 316 for increased corrosion resistance. Both are otherwise 18–8 alloys, i.e. 18% chromium and 8% nickel. Actually type 304 is 18–20% chromium and type 316 is 16–18% chromium.

Woven wire can be made very fine with small wire diameters spaced very close, yielding as many as 635 openings per lineal inch with wires as small as 0.0008 in (0.02 mm) and aperture size of 20 μm. However, this combination, which is woven in a twill square weave of over two wires and under two in each direction, gives a very delicate material for filtering on a large scale. The answer to this situation lies in the weaving of a Dutch weave material, wherein there are a greater number of fine wires in the weft, or width, of the material and a smaller number of heavier wires in the warp, or length. Over one and under one gives a plain Dutch and to achieve a denser cloth the weft wires cross over two warp wires at a time in a staggered arrangement called a ‘twilled Dutch’. Both materials are very strong and can be woven with retention down to 1 μm on a twill Dutch and down to 8 μm on a plain Dutch (duplex-twin warp). We will see more details on these weaves a little further on.

Woven wire lends itself easily to fabrication of pressure filter leaves and filter baskets. It is easily applied to filter drums. It is resistant to blinding and is easily cleaned. Stretching or shrinking is non-existent. It usually costs more than non-metallic media, but usually has a long life which helps to off-set the cost along with the other factors above.

Another use for woven wire is for cleanable cartridge filters with nominal ratings from 300 to 1 μm. Although the use of metal media is expensive, the cartridge can be chemically cleaned and re-used. The aircraft and aerospace industries have been big users of these types of elements.

There are several available weaves of woven wire. Some of these weaves lead the product to be called woven fabric. The basic types of weaves of wire cloth, which are woven for filtration purposes, are plain, twilled, plain Dutch, twilled Dutch, plain reverse Dutch, duplex (twin warp) plain Dutch, Betamesh and braided (basket of multibraid)—see *Figure 8.1*.

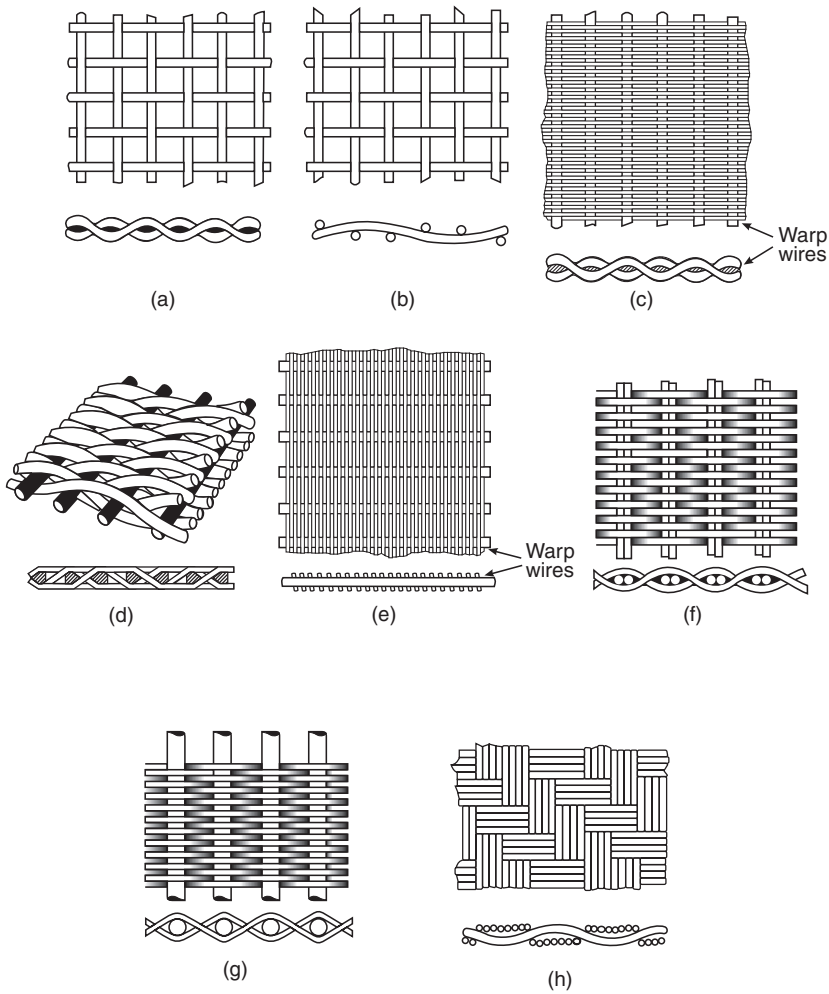

Figure 8.1 Different types of weaves. (a) Plain square weave. (b) Plain twilled weave. (c) Plain Dutch weave. (d) Twilled Dutch weave. (e) Reverse Dutch weave. (f) Duplex (twin warp) plain Dutch weave. (g) Betamesh Dutch weave. (h) Basket (braided or multibraid) weave

As mentioned above, a plain weave has each shute or fill wire passing alternately over and under each warp wire. Square or rectangular openings are available. Openings are 'straight through', thus permitting filtrate to pass through the cloth in a perpendicular path. The width of the opening is limited by the wire diameter and the number of wires per lineal inch. Finer meshes with smaller openings are lacking in physical strength.

Twilled weave (plain twill), also has straight through openings. Each shute or fill wire alternately crosses over two and under two warp wires, forming a diagonal pattern. Larger wires can be used for a given mesh size yielding proportionally smaller openings and greater physical strength. For example, if a 0.0055 in (0.14 mm) square opening is required for a particular application, it could be obtained with plain square weave, 100 mesh with 0.0045 in (0.11 mm) wire diameter; or in the twilled weave, 80 mesh with 0.007 in (0.18 mm) wire diameter, which is a stronger fabric; stronger yet is 60 mesh 0.010 in (0.25 mm) wire diameter with 0.0057 in (0.14 mm) openings. Each of the two latter specifications would have longer service life and good wear resistance, but at the expense of a smaller percentage of open area or slower flow rates through the woven wire.

When the twilled weave is woven with multiple wires in both warp and shute, it results in a strong, dense fabric known as braided, basket or multi-braid weave. The mesh openings are irregular because the multiple shute wires have a tendency to twist around each other.

In plain Dutch weave, the warp wires are generally larger than the shute or fill wires, and are spread far enough apart so that each shute wire passes alternately over one and under one warp wire and is positioned tightly against the adjacent shute wire. This yields relatively small openings with high strength. There are no straight through openings; they are similar to a triangle in shape and twist through the material on an angle. These materials are mainly rated by particle retention in microns because opening sizes and percentage of open area are difficult to determine. A popular plain Dutch weave is 24×110 mesh with 0.010×0.015 in (0.25×0.38 mm) wire diameters.

Duplex (twin warp) plain Dutch weave is a stronger weave than conventional plain Dutch weave with the same micron rating. Although similar to a plain Dutch weave, it has two small-diameter warp wires in place of one large warp wire. This arrangement gives an even stronger material than plain Dutch weave and smaller openings can be achieved. The openings are triangular shaped and twist through the material on an angle, as described for the plain Dutch weave. Duplex weave is rated by particle retention, in microns, as are all the Dutch weaves. Filter ratings generally range from 65 to 8 μm.

With a twilled Dutch weave the mesh count of the warp wires is much lower than that of the shute. The shute wires pass over two and under two wires in both directions. They are pushed together such that one shute wire is on top of the next one, which is directly under the warp wire. This yields

twice as many shute wires for the same wire diameter as in the plain Dutch weave. This is a very strong and dense weave, through which it is almost impossible to see light on a perpendicular projection. Mesh counts range from 20×250 with 100 μm retention to 510×3600 with less than 1 μm retention.

Reverse Dutch weave is a weave where the arrangement of the warp and shute wires is reversed as compared with the plain Dutch or twilled Dutch weave. The greater number of wires closely woven together are found in the warp, and the shute wires have the larger diameter. This yields a very strong material with high rates of flow as compared with twilled Dutch weave with the same micron rating. It has characteristics of good cleanability and resistance to blinding. Mesh counts range from 140×40 with approximately 100 μm retention to 850×155 with 10 μm retention.

The last weave to be mentioned at this point is betamesh Dutch weave. Betamesh is similar to a plain Dutch weave with superior performance characteristics. A larger portion of solids is retained on the surface of the material than with other Dutch weaves. This results in a higher contaminant tolerance and excellent back-flushing properties. Betamesh has more open area and consequently allows higher flow rates than do the other Dutch weaves. The ratio of warp-to-shute wire sizes and the spacing of warp wires have been carefully established to yield precise equilateral triangular openings. Their uniform 60° angles are set during weaving, so that internal flow passages of the fabric will always be larger than the surface openings; flow rate is thus improved, and blinding reduced. The surface slots are narrower than the inner triangular openings. Thus, particles are retained on the medium surface before they can plug the inner passages. Betamesh Dutch weave is available in the retention range 81–10 μm.

8.7 Woven fabrics

Woven fabrics are made with natural and synthetic fibres. In some cases there is similarity with woven wire in the fabric construction or job capability. Many synthetics are woven in order to replace as many woven wire applications as possible and/or to replace a similar competing fabric in natural or synthetic fibre itself.

Woven fabrics are made from three different forms of yarn. One is the spun staple yarn, which is made by twisting short lengths of natural or synthetic fibre into a continuous strand; it has good particle retention because of its hairy filaments, and offers excellent gasketing properties. Next are monofilament yarns, which are made of a single continuous filament of synthetic fibre. They allow minimum blinding, good cleaning and excellent cake discharge characteristics. Lastly, multifilament yarns are made by twisting two or more continuous monofilament threads together. They have the greatest tensile strength of any yarn and allow better cake discharge than spun yarns. Cloths

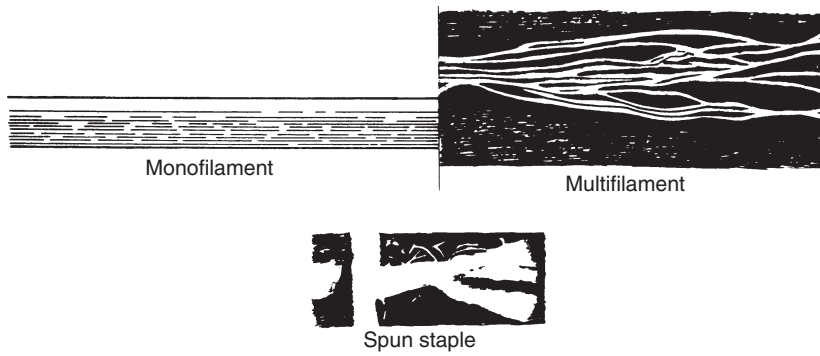

Figure 8.2 Effect of yarn. (Courtesy of Purchas, 1967)

woven with multifilament or spun fibre are called 'multifilament fabrics' while materials woven with monofilament fibre are known as 'monofilament fabrics'—see *Figure 8.2* and *Table 8.1*.

Table 8.1 Effect* of type of yarn on cloth performance (from Purchas, 1967)

Maximum filtrate clarity	*Minimum resistance to flow*	*Minimum moisture in cake*	*Easiest cake discharge*	*Maximum cloth life*	*Least tendency to blind*
Staple	Monofil	Monofil	Monofil	Staple	Monofil
Multifil	Multifil	Multifil	Multifil	Multifil	Multifil
Monofil	Staple	Staple	Staple	Monofil	Staple

* In decreasing order of preference.

Filter fabrics are mainly woven in four common weaves: plain, twill, plain reverse Dutch and satin. The first three are overlaps from wire cloth weaves but may have slightly different characteristics when put into the framework of woven non-metallic cloth. The weaves will not be detailed again here. The fourth weave is the satin weave where the shute (or warp) fibre passes over several warp (or shute) fibres, then under one in an alternating pattern. *Figure 8.3* shows an over three–under one pattern for the satin weave (three shaft satin); see also *Table 8.2*.

The woven fabric can be supplied either off-loom (greigh goods) or subjected to a finishing process. The two most common to the filtration industry are heat treatment and calendering. Heat treatment is applied to synthetic cloth in order to stabilize the fabrics and make them more suitable at elevated temperatures. Calendering uses high-pressure, hot rollers whereby

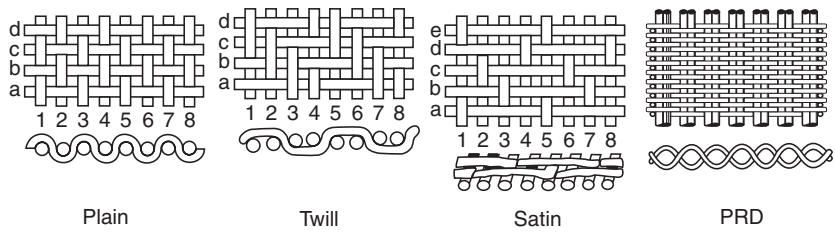

Figure 8.3 Basic weaves

Table 8.2 Effect* of weave pattern on cloth performance (based on a 40 μm nominal retention fabric of each weave)

Maximum filtrate clarity†	*Minimum resistance to flow*	*Minimum moisture in cake*	*Easiest cake discharge*‡	*Maximum cloth life*§	*Least tendency to blind*
Satin	Plain	Plain	Satin	Satin	Plain
Twill	PRD	PRD	Twill	Twill	PRD
PRD	Twill	Twill	Plain	PRD	Twill
Plain	Satin	Satin	PRD	Plain	Satin

* In decreasing order of preference.
† If cake is formed then clarity would be the same.
‡ Depends on the texture of the cake (i.e. for sticky cake the order is reversed).
§ Can depend on the type of equipment.

the fabric runs between the rollers, which cause the cloth surface to have a smooth polish that improves cake discharge and helps keep the cloth clean while in service.

Filter fabrics are commonly woven from such synthetic fibres as nylon, polyester, polypropylene and occasionally polyethylene. Other thermoplastics can be, or may have been woven, but are not commonly available. Each fibre type has specific characteristics in relation to chemical, thermal and mechanical properties that singles it out as the best candidate for use on the specific application. *Table 8.3* summarizes the use of common fibres.

Even though fibres of the above synthetic materials can be woven multifilament or monofilament, there is a trend towards the use of monofilament filter fabrics. This is so mainly because in years past it was very difficult to weave monofilaments in the fine, low-micron retention areas. Today, monofilament filter fabrics can be woven twilled down to 6 μm and plain reverse Dutch down to 14 μm. Further finishing (shrinking and calendering) can bring the particle removal rating down to the 1 μm area.

Table 8.3 Physical properties of fibres

	Softening point, °C	*Estimated safe temperature, °C*	*Specific gravity*	*Moisture regain %*, 70°F (21.1°C), 65% r.h.*	*Wet breaking tenacity**, g density^{-1}*	*Wet breaking elongation†, %*	*Resistance to wear*
Acetate	204–229	99	1.32	6.3–6.5	0.8–1.0	35–50	Fair
Acrylic	NA	143	1.17	1.5	1.8–3.0	34–60	Good
Fluorocarbon	275	204	2.10	0	0.5	52	Fair
Glass (multifilament)	732–877	302	2.50	0	6.7	5.3–5.7	Poor
Modacrylic	NA	77	1.35	2.5	1.5–2.4	45.65	
Nomex	—	218	1.38	—	4.1	14	Excellent
Nylon (6 or 6.6)	170–235	116	1.14	2.8–5.0	3.7–6.2	20–47	Excellent
Nylon 12	155–170	90	1.01	0.8	—	—	Excellent
Polyester	220–240	149	1.38	0.4	3.2–4.2	21–35	Excellent
Polyethylene							
Low density	107–113	71	0.92	0	1–3	20–80	Fair
High density	116–102	102	0.95	0	3.5–7	10–45	Fair
Polypropylene	141–149	121	0.91	0.01–0.1	3.5–5.0	14–30	Fair
PVDF	143–149	141	1.78	<0.1	—	—	Good
Rayon	NA	99	1.54	11	0.95–1.1	24–28	Poor
Saran	—	77	1.70	0.1–1.0	1.5	15–30	Fair

NA—Not applicable to these fibres.

* That percentage by weight of moisture gained by an oven-dried textile product in a standard atmosphere of 70°F (21.1°C) with 65% relative humidity.

** The stress at which a fibre breaks.

† The increase in length or deformation of a fibre as a result of stretching as a percentage of the original length.

‡ Difficult to ignite. Does not propagate flame. Does not melt. Decomposes at 499°C.

8.8 Material selection

A very important, if not the most important, part of the filtration process is the proper selection of a filter fabric. When selecting a fabric, one must first look at the material from which it is made and take into account that material's chemical, heat and abrasion resistance with regard to the product to be filtered. The next consideration is the fabric weave and how this affects filtrate clarity, blinding characteristics and cake release properties. Multifilaments can yield clearer filtrates but have a greater tendency towards blinding than monofilaments. Where fine solids must be handled and a clear filtrate is required, one of the high-twist multifilament yarn, twilled-type weaves frequently provides the best compromise between clarity and blinding tendencies. This is not to say that some of the very fine monofilament calendered fabrics would not be a good choice. Assumptions are not the proper way to make a fabric selection. Bench scale and/or actual testing on the filter is what should be done. We will discuss this aspect of selection further on.

In many cases, the filter fabric selection is based on a compromise rather than on locating the Utopian material that will do everything required at an economical price. The user of the medium must decide whether he is primarily interested in the filter rate or clarity, and whether the initial price of the material or life is important.

It is important to note that suppliers of filter media can make qualified recommendations based on experience, but no one can guarantee the performance of a filter fabric for an end-use until it is actually applied to the equipment for the application (proven). When selecting a filter fabric, a supplier looks for certain characteristics of the filtration problem in detail. Basic questions should be asked to narrow the choice down fairly accurately. Important points would be the filter type and size, temperature of the product being filtered, pH of the product being filtered, physical characteristics of the product (i.e. crystalline or granular), distribution of particle size and the current problem with existing media (blinding or mechanical failure). These, along with other questions about the wash cycle, should be answered to help achieve the best possible material to replace an existing medium and to obtain greater productivity for the filtration equipment. Just because a piece of equipment arrives at the plant with a certain material on it does not necessarily mean that it is the best material for the job. The operator should always be on the look-out for a 'better' medium based on the results he obtains from his existing media. *Table 8.4* shows a typical questionnaire for fabric selection.

The three methods for testing filter media are laboratory tests, pilot plant and full-scale tests. The laboratory tests usually consist of a Buchner funnel, in which the filter medium is placed in the mouth of the funnel and a sample of the slurry is poured on top of the medium. The slurry is then drawn through the medium and such factors as filtrate clarity and time can be checked. Laboratory tests are quick and economical, but often deceptive. The pilot

Table 8.4 Questionnaire for fabric selection

Make of filter ..... Type and size .....

Filter operating data:

1. Minimum and maximum pressure employed .....
2. Temperature at which solution to be filtered is maintained .....
3. Kind and concentration if liquid is acid, and pH value if known .....
4. Nature and percentage if liquid is alkaline or caustic, and pH value if known .....
5. Chemical composition or nature and density of liquid .....
6. Chemical composition or nature and specific gravity of solids .....
7. Physical characteristics of solids—i.e., crystalline, granular, slimy, colloidal, etc .....
8. Retained on mesh 40 80 100 150 200 300 400 +500
   Percentage .... % ..... % ..... % ..... % ..... % ..... % ..... % ..... %
9. Maximum particle size that can be permitted to pass through filter .....
10. Relative proportion by weight of solids to liquid. .....
11. Is cake difficult to discharge? .....
12. Is a filter aid used? If so, state kind .....
13. Would there be any advantage to increasing the acidity or causticity of the solution as now fed to your filters? If so, what would be the desired acid or caustic content? .....

Present type of filter medium .....

Average operating period of present filter medium:

1. Average total time it remains in place .....
2. Average total operating time obtained (if filter is not operated on a 24 hour daily basis) .....

Reason for removing present filter medium:

1. Mechanical failure ☐
2. Chemical corrosion ☐
3. Medium becomes blinded ☐

Remarks. State any special conditions not specified that are present in your process and that you feel affect the filter medium you are now using:

Source: 'Filter Media', *Chemical Engineering*, 1963 (Oct. 14).

plant, or small operating filter, is an improvement over the laboratory process as it gives results that are more likely to be reproduced in production.

The most reliable method of test as well as the most expensive, is to conduct a full production test. However, when testing, it is far better to test the entire filter—for example, a full press load of cloths on a plate and frame press, rather than one or two cloths, as these cloths might be doing the work of the others in the press, yielding no specific indication as to their actual capacity. The same situation applies to the disc filter where each sector of an entire disc should be covered, or even on the drum of a caulked-in fabric where the entire drum should be covered.

From the above, it is clear that the operator has many cloth selection factors to consider in order to obtain optimum performance. Often the only way is by trial and error, guided by broad general principles. Once the optimum cloth is found, the following benefits are obtained: a clean filtrate with no loss of solids by bleeding, an economic filtration time (production rate), an easily discharged filter cake, no deterioration of the medium by sudden or gradual blinding and an adequate cloth life.

8.9 Filter rating

There are many questions which centre around testing and rating methods of filter fabrics. Manufacturers generally do not use identical rating methods by following any one established test procedure. No universal standard seems to be followed. Any successful effort to standardize test methods lies in the distant future. However, current rating methods make it difficult for uniform procurement as well as causing frustration to the user in selecting the optimum medium. Suppliers make qualified recommendations based on their own experience but cannot really guarantee the performance of a filter medium for a given end-use until it has been thoroughly tested and found satisfactory.

Some common filter rating characteristics that are considered prior to testing the media are as follows: nominal filter rating in microns, absolute filter rating in microns, bubble point (inches water gauge) and air permeability. The nominal and absolute filter ratings can be determined by computations through the bubble point test. Other considerations that are not often used are: mesh count per inch, fibre diameter, cloth thickness, weight of material, tensile strength and water permeability.

Nominal ratings are intended to describe an average pore size for filtration performance. This would give a reading as to what size particles, in general, the cloth will retain. The absolute rating is intended to measure the largest single pore rather than an average pore. There are several tests to determine nominal and average pore size but a frequently used test is the bubble-point test described in the next paragraph. Other tests (see Cole, 1975), which are not detailed here, include filtration efficiency and bead transmission.

Bubble-point tests are, as already mentioned, frequently used to estimate pore sizes and distributions. The tests consist of immersing the test specimen in a wetting liquid and then displacing the liquid from the pore structure with gas or air pressure. The first bubble through is a measure of the largest pore or absolute rating of the specimen. These tests are reproducible but do not give much information about the general pore structure.

Mean flow ratings, sometimes called 'boil-all-over bubble points', attempt to indicate a defined average pore size which can be more meaningful than the 'average' pore size alone. Once the first bubble appears as the largest pore, or absolute rating, the air pressure is slowly increased. The filter will then, fairly suddenly, 'boil all over'. At this point we have the mean flow rating. We can directly associate mean flow rating and nominal rating as the same in this regard, as the key objective is the average pore size. However, they are distinguished as different, depending on which test method is used. For example, flow permeability test for nominal rating and bubble-point test for mean flow rating.

The last factor presented here to rate filter media, is that of air permeability. This is the measurement of a filter medium's ability to pass air. Air permeability is stated in CFM, the number of cubic feet of air that could pass through a square foot of medium per minute at a given pressure rating to determine air flow. The standard equipment used for this rating in the USA is the Frazier differential pressure air permeability machine. The air permeability test is based on Frazier method number 5450, equivalent to Federal Test Method Standard number 191 and ASTM D737-75(80). The test pressure is 0.01806 p.s.i. and the inches of water column is 0.5 in.

8.10 Summary

It should be remembered that the filter medium is the keystone of any filtration system, and for the filter to give an optimum performance the medium used must be the best one available for the purpose. We should be aware that by changing the filter medium, a user can perhaps significantly alter the economics of his process.

The users of filter media continue to benefit from new developments in materials technology. Manufacturers respond to the challenges of various applications by making continued improvements in the quality of more traditional materials, in addition to the new products they may offer. Many monofilament filter fabrics were virtually unavailable ten years ago. New fabrics are continually being added, and those already available are refined by calendering, shrinking, etc., to meet new applications or to improve performance for existing applications.

One main advantage that filter media users have is that there are several qualified suppliers, who are willing to work with users on potential applications. It is a two-way street. Suppliers need users to test, analyse and report back, while users need suppliers to make these materials available by working

with the user to pin-point the best possible material. Confide in your supplier—it will help improve your operation.

Bibliography

Bosley, R., 'Vacuum filtration equipment innovations', *Filtration and Separation*, March/Apr., 138 (1974)

Cole, F. W., 'Filter ratings—an alternative to "black art"', *Filtration and Separation*, Jan./Feb., 17 (1975)

Corte, H., 'Why can paper be used as a filter medium?', *Filtration and Separation*, Jan./Feb., 42 (1980)

Dean, J. H., 'Nonwoven west-laid filter media', *Filtration and Separation*, Nov./Dec., 669 (1972)

Dickey, G. and Bryden, C., *Theory and Practice of Filtration*, Reinhold Publishing, New York (1946)

Deitrich, H. and Gurtler, H. C., 'A new textile for high temperature filtration of dust and gases', *Filtration and Separation*, July/Aug., 403 (1974)

Dyson, N. W., 'Cartridge filtration for processing edible oils', *Filtration and Separation*, March/Apr., 167 (1979)

Early, S. R. and Amsler, N., 'Gradient structure media for liquid filtration applications', Proceedings Volume I, World Filtration Congress 8, European Federation of Chemical Engineering Event No. 607, organised by The Filtration Society and Elsevier Science, The Brighton Centre, Brighton, UK, 3–7 April 2000, 71–74 (2000)

Franks, E. H., *Tetko Training Manual* (1972)

French, R. C., 'Filter media', *Chem. Eng.*, Oct. 14 (1963)

Gale, R. S., 'Control of sludge filter operation', *Filtration and Separation*, Jan./Feb., 76 (1975)

Goeminne, H., de Bruyne, R., Roos, J. and Aernoudt, E., 'The geometrical and filtration characteristics of metal-fibre filters—a comparative study', *Filtration and Separation*, July/Aug., 351 (1974)

Hutto, F. B., 'What the filter man should know about filter aid filtration', *Filtration and Separation*, March/Apr., 164 (1975)

Jensen, K. E., 'Concepts of fabric filtration for air pollution control', *Filtration and Separation*, May/June, 254 (1969)

Johnson, P. R., 'Submicron filtration with cartridges', *Filtration and Separation*, July/Aug., 352 (1975)

Lloyd, P. J. and Ward, W. S., 'Filtration applications of particle characterization', *Filtration and Separation*, May/June, 246 (1975)

Lydon, R. P. 'New composite filter media', *Filtration + Separation*, 26–28 (June 2000)

Makarevich, A. V. and Pinchuk, L. S., 'Fibrous polymer composite filtering materials', Proceedings Volume I, World Filtration Congress 8, European Federation of Chemical Engineering Event No. 607, organised by The Filtration Society and Elsevier Science, The Brighton Centre, Brighton, UK, 3–7 April 2000, 83–86 (2000)

Muller, H. R and Maurer, Ch., 'New filter media', Proceedings Volume I, World Filtration Congress 8, European Federation of Chemical Engineering Event No. 607, organised by The Filtration Society and Elsevier Science, The Brighton Centre, Brighton, UK, 3–7 April 2000, 95–98 (2000)

Nickolaus, N., 'What, when and why of cartridge filters', *Filtration and Separation*, March/Apr., 155
Penderson, G. C., 'Fluid flow through monofilament fabrics', *Filtration and Separation*, Nov./Dec., 586 (1974)
Pointon, C. W. and Giles, J. W., 'Industrial screening filters with special reference to cartridge filters', *Filtration and Separation*, May/June, 259 (1974)
Purchas, D. B., *Industrial Filtration of Liquids*, CRC Press, Cleveland (1967)
Purchas, D. B., 'Art, science and filter media—I', *Filtration and Separation*, May/June, 253 (1980)
Purdy, A. T., 'The structural mechanics of needlefelt filter media', *Filtration and Separation*, March/Apr., 134 (1980)
Redmon, O. C., 'Improvements in filters and separators for jet fuel', *Filtration and Separation*, May/June, 241 (1969)
Rushton, Albert and Griffiths, P. V. R., 'Role of the cloth in filtration', *Filtration and Separation*, Jan./Feb., 81 (1972)
Rushton, Albert and Rushton, Alan, 'Size and concentration effects in filter cloth pore bridging', *Filtration and Separation*, May/June, 274 (1972)
Rushton, A., Ward, A. S. and Holdich, R. G. Chapter 4 in *Solid–Liquid Filtration and Separation Technology*. VCH, Weinheim (1996).
Schweitzer, P. A. (Ed.), *Handbook of Separation Technology for Chemical Engineers, Part 4*, McGraw-Hill, New York (1979)
Shoemaker, W., 'Filtration fundamentals, filter media, filter rating', *Filtration Symposium* (1974)
Shoemaker, W., 'The spectrum of filter media', *Filtration and Separation*, Jan./Feb., 62 (1975)
Shoemaker, W., 'The industrial filtration market for non-wovens', *Filtration and Separation*, May/June, 252 (1979)
Snow, C., 'Toward improving standards in nonwoven filter media', *Filtration Engineering*, Sept./Oct., 23 (1974)
Squires, B. J., 'Fabric filter plants for cleaning gases from non-ferrous metal furnaces', *Filtration and Separation*, May/June, 277 (1974)
Suttle, H. K., 'The proportions and properties of particles', *Filtration and Separation*, May/June, 272 (1972)
Tarala, F. E., 'The particle size war', *Filtration Engineering*, May/June, 7 (1973)
'Tenth Magdeburg Conference', *Filtration and Separation*, Jan./Feb., 28 (1973)
Tetko Catalog, No. 1000, Tetko Inc. (1974)
Tetko Betamesh Brochure, Tetko Inc. (1981)
Tetko Catalog, No. 3000 WC, Tetko Inc. (1985)
Tetko Catalog, No. 3000 S, Tetko Inc. (1986)
Thomas, C. M., 'Filter media for filter pressing applications', *Filtration and Separation*, Nov./Dec., 629 (1975)
Ward, A. S., 'Filter media development and innovation', *Filtration and Separation*, Jan./Feb., 61 (1973)
Wrotnowski, A. C., 'Felt filter media', *Filtration and Separation*, Sept./Oct., 426 (1968)

9 Filtration fundamentals

L. Svarovsky

FPS Institute, England and University of Pardubice, Czech Republic

Nomenclature

a	Constant
a_1	Constant
A	Face area of a filter
b	Constant
b_1	Constant
c	Solids concentration in the feed
f	Submergence or filtration time/cycle time
K	Permeability of a packed bed
K_o	Kozeny constant
L	Cake thickness
L_f	Final cake thickness
m	Mass of wet cake/mass of dry cake
n	Exponent
Q	Volumetric flow rate
Q_1	Flow rate at the start of a constant pressure period
R	Medium resistance
R_c	Cake resistance
S_o	Volume-specific surface of the bed
t	Time
t_c	Cycle time
t_s	Time at the start of a constant pressure period
v	Superficial velocity in a packed bed
V	Filtrate volume collected
V_f	Final volume of filtrate per frame
V_s	Filtrate volume at the start of a constant pressure period
w	Mass of cake deposited per unit area
α	Specific cake resistance
α_{av}	Average specific cake resistance
α_o	Cake resistance per unit pressure drop
Δp	Static pressure drop
Δp_c	Pressure drop of the cake

Δp_m Pressure drop of the medium
ε Voidage of a packed bed
μ Liquid viscosity
ρ Liquid density
ρ_s Solid (particle) density

9.1 Introduction

Filtration may be defined as the separation of solids from liquids by passing a suspension through a permeable medium which retains the particles. A filtration system can be shown schematically as in *Figure 9.1*.

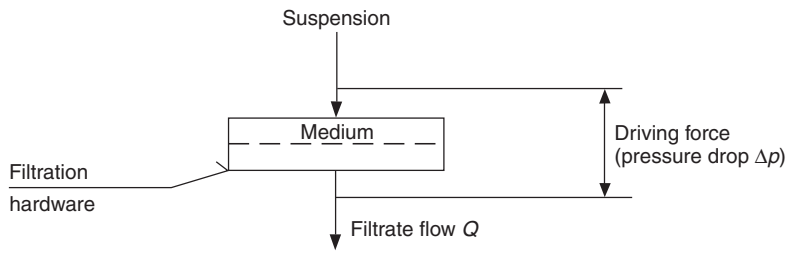

Figure 9.1 Schematic diagram of a filtration system

In order to obtain fluid flow through the filter medium, a pressure drop Δp has to be applied across the medium; it is immaterial from the fundamental point of view how this pressure drop is achieved but there are four types of driving force:

gravity,
vacuum,
pressure,
centrifugal.

Before introducing the basic filtration relationships it is worthwhile examining the actual process of particle removal.

There are basically two types of filtration used in practice: the so-called *surface filters* are used for *cake filtration* in which the solids are deposited in the form of a cake on the up-stream side of a relatively thin filter medium, while *depth filters* are used for *deep bed filtration* in which particle deposition takes place inside the medium and cake deposition on the surface is undesirable.

In a surface filter, the filter medium has a relatively low initial pressure drop and, as can be seen in *Figure 9.2*, particles of the same size as, or larger than, the openings wedge into the openings and create smaller passages which remove even smaller particles from the fluid. A filter cake is thus formed, which in turn functions as a medium for the filtration of subsequent input suspension. In order to prevent blinding of the medium, filter aids are used as

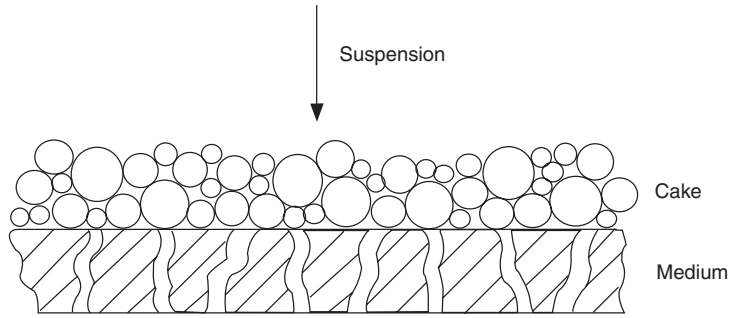

Figure 9.2 Mechanism of cake filtration

a precoat which forms an initial layer on the medium. Some penetration of fine solids into the precoat or the medium itself is often inevitable.

Surface filters are usually used for suspensions with higher concentrations of solids, say above 1% by volume, because of the blinding of the medium (or of the precoat) that occurs in the filtration of dilute suspensions. This can, however, sometimes be avoided by an artificial increase of the input concentration, in particular by adding a filter aid as a 'body feed'; as filter aids are very porous their presence in the cake improves permeability and often makes cake filtration of dilute and generally difficult slurries possible.

Note that the model described above and shown in *Figure 9.2* is that of conventional batch cake filtration where both the particles and the liquid approach the medium at an angle of 90° and no attempt is made to disturb the cake or prevent its formation. There is an alternative, which Tiller and Cheng[1] call 'delayed cake filtration', when the cake is prevented from forming or kept thin by hydraulic or mechanical means; the solids are thus continuously stirred back into the suspension, which gradually thickens. The effective particle motion is then parallel to the medium while the liquid approaches the medium at an angle. Continuous filter thickeners based on this principle are available; Tiller and Cheng[1] have demonstrated that appreciably higher filtration rates and lower cake porosities can be obtained by using mechanical agitators and have proposed a mathematical model for the delayed cake filtration process. A similar mechanism is used in the so-called by-pass centrifugal filtration where particles are removed from the medium by centrifugal forces while the liquid flows through it; this is further discussed in chapter 14 'Centrifugal Filtration'. Chapter 11 reviews the methods available for limiting cake growth.

In a depth filter—*Figure 9.3*—the particles are smaller than the medium openings and hence they proceed through relatively long and tortuous pores where they are collected by a number of mechanisms (gravity, diffusion and inertia) and attach to the medium by molecular and electrostatic forces.

The initial pressure drop across the depth filter is generally higher than that across a surface filter of comparable efficiency but the build-up of pressure

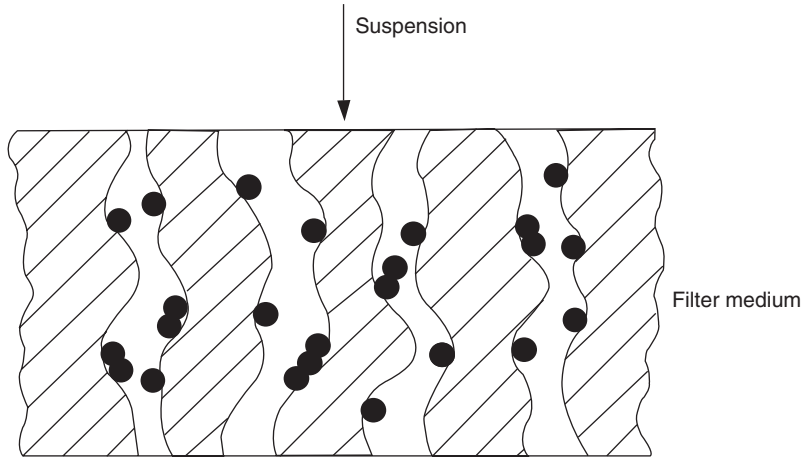

Figure 9.3 Mechanism of deep bed filtration

drop as particles are collected is more gradual for a depth filter. Depth filters are commonly used for clarification, i.e. for the separation of fine particles from very dilute suspensions, say less than 0.1% by volume.

Although the above classification of filtration into cake and deep bed filtration is clear cut in most cases, in some instances, such as with some cartridge filters, it may be difficult to decide which of the two is the governing process.

Of the two types of filtration, cake filtration has the wider application, particularly in the chemical industry (because of the higher concentrations used) and the following discussion will, on the whole, be concerned with cake filtration and surface filters. Deep bed filtration is discussed further in chapter 1.

As with other separation equipment, the main characteristics of filters are the flow rate–pressure drop relationships and other performance characteristics such as the separation efficiency. In filtration however, these relationships are more complex as there are many variables and factors (cake thickness, mass of cake per unit area, specific cake resistance etc.) which greatly influence the process.

9.2 Flow rate–pressure drop relationships

9.2.1 Clean medium

At the beginning of batch cake filtration, the whole pressure drop available (i.e. the driving force) is across the medium itself since as yet no cake is formed. As the pores in the medium are normally small and the rate of flow of filtrate is low, laminar flow conditions are almost invariably obtained.

Darcy's basic filtration equation relating the flow rate Q of a filtrate of viscosity μ through a bed of thickness L and face area A to the driving pressure Δp is

$$Q = K\frac{A\Delta p}{\mu L} \tag{9.1}$$

where K is a constant referred to as the permeability of the bed. Equation 9.1 is often written in the form

$$Q = \frac{A\Delta p}{\mu R} \tag{9.2}$$

where R is called the medium resistance (and is equal to L/K, the medium thickness divided by the permeability of the bed).

If the suspension were a clean liquid, all the parameters in equations 9.1 and 9.2 would be constant, resulting in a constant flow rate for a constant pressure drop and the cumulative filtrate volume would increase linearly with time, as shown in *Figure 9.4*.

In batch filtration, however, where the suspension contains particles, a cake starts to build up on the surface of the filter so that, gradually, a greater proportion of the available pressure drop is taken up by the cake itself. This results in an effective increase in the bed resistance thus leading to a gradual drop in the flow rate Q. The cumulative filtrate volume therefore slows down with time as shown in *Figure 9.4*.

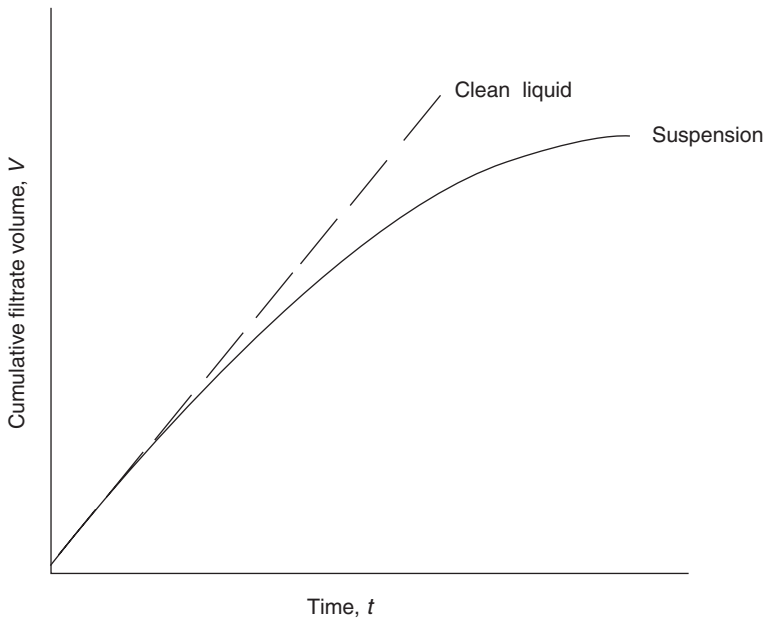

Figure 9.4 Plot of cumulative filtrate volume against time

9.2.2 Medium with a cake forming on its face

As explained in the previous section, the filtrate flow rate at constant driving pressure becomes a function of time because the liquid is presented with two resistance in series, one of which, the medium resistance R may be assumed constant and the other, the cake resistance R_c increases with time.

Equation 9.2 then becomes:

$$Q = \frac{A\Delta p}{\mu(R + R_c)} \tag{9.3}$$

In practice, however, the assumption made above that the medium resistance is constant is rarely true because some penetration and blocking of the medium inevitably occurs when particles impinge on the medium.

As the resistance of the cake may be assumed to be directly proportional to the amount of cake deposited (only true for incompressible cakes) it follows that

$$R_c = \alpha w \tag{9.4}$$

where w is the mass of cake deposited per unit area (in $\mathrm{kg\,m^{-2}}$ in SI units) and α is the specific cake resistance (in $\mathrm{m\,kg^{-1}}$ in SI).

Substitution of equation 9.4 for R_c in equation 9.3 gives

$$Q = \frac{\Delta pA}{\alpha\mu w + \mu R} \tag{9.5}$$

Equation 9.5 relates the flow rate Q to the pressure drop Δp, the mass of cake deposited w and other parameters, some of which can, in certain circumstances, be assumed to be constant. These parameters are discussed briefly.

9.2.2.1 Pressure drop

The pressure drop Δp may be constant or variable with time depending on the characteristics of the pump used or on the driving force applied. If it varies with time the function $\Delta p = f(t)$ is usually known.

9.2.2.2 Face area of the filter medium

The face area of the medium A is usually constant, but with a few exceptions such as in the case of equipment with an appreciable cake build-up on a tubular medium or a rotary drum.

9.2.2.3 Liquid viscosity

The liquid viscosity μ is constant provided that the temperature remains constant during the filtration cycle and that the liquid is Newtonian.

9.2.2.4 Specific cake resistance

The specific cake resistance α should be constant for incompressible cakes but it may change with time as a result of possible flow consolidation of the cake and also, in the case of variable rate filtration, because of variable approach velocity.

Most cakes, however, are compressible and their specific resistance changes with the pressure drop across the cake Δp_c. In such cases, an average specific cake resistance α_{av} should replace α in equation 9.5 α_{av} can be determined from

$$\frac{1}{\alpha_{av}} = \frac{1}{\Delta p_c} \int_0^{\Delta p_c} \frac{d(\Delta p_c)}{\alpha} \tag{9.6}$$

if the function $\alpha = f(\Delta p_c)$ is known from pilot filtration tests, bomb filter tests or from the use of a compressibility cell (which often provides useful data despite the fact that it replaces hydraulic pressure by mechanical pressure applied to the cake by a piston).

An experimental empirical relationship can sometimes be used over a limited pressure range[2]

$$\alpha = \alpha_0 (\Delta p_c)^n \tag{9.7}$$

where α_0 is the resistance at unit applied pressure drop and n is a compressibility index (equal to zero for incompressible substances) obtained from experiments.

Using equation 9.7, the average cake resistance α_{av} can be shown to be (from equation 9.6)

$$\alpha_{av} = (1 - n)\alpha_0 (\Delta p_c)^n \tag{9.8}$$

9.2.2.5 Mass of cake deposited per unit area

The mass of cake deposited per unit area w is a function of time in batch filtration processes. It can be related to the cumulative volume of filtrate V filtered in time t by

$$wA = cV \tag{9.9}$$

where c is the concentration of solids in the suspension (mass per unit volume of the filtrate, in kg m^{-3}). This makes no allowance for the solids that are in the liquid retained by the cake (see section 9.7) but in most cases this is negligible.

9.2.2.6 Medium resistance

The medium resistance R should normally be constant but it may vary with time as a result of some penetration of solids into the medium and sometimes it may also change with applied pressure because of the compression of fibres in the medium.

As the overall pressure drop across an installed filter includes losses not only in the medium but also in the associated piping and in the inlet and outlet

ports, it is convenient in practice to include all these extra resistances in the value of the medium resistance R.

9.3 Filtration operations—basic equations, incompressible cakes

The general filtration equation, equation 9.5, after substitution of $w(t)$ from equation 9.9, becomes

$$Q = \frac{\Delta pA}{\alpha\mu c(V/A) + \mu R} \tag{9.10}$$

As the total flow volume is an integral function of the flow rate

$$Q = \frac{\mathrm{d}V}{\mathrm{d}t} \tag{9.11}$$

Equation 9.10 can be rewritten in reciprocal form (thus giving time per unit flow), which is more convenient for further treatment

$$\frac{\mathrm{d}t}{\mathrm{d}V} = \alpha\mu c\frac{V}{A^2\Delta p} + \frac{\mu R}{A\Delta p} \tag{9.12}$$

It is useful for the mathematical simplicity of the final equations to define two constants a_1 and b_1:

$$a_1 = \alpha\mu c \tag{9.13}$$

this is a constant (if α, μ and c are constants) relating the properties of the feed suspension and of the suspended solids;

$$b_1 = \mu R \tag{9.14}$$

is a 'cloth–filtrate' constant.

Equation 9.12 then becomes

$$\frac{\mathrm{d}t}{\mathrm{d}V} = a_1\frac{V}{A^2\Delta p} + b_1\frac{1}{A\Delta p} \tag{9.15}$$

9.3.1 Constant pressure filtration

If Δp is constant, equation 9.15 can be integrated

$$\int_0^A \mathrm{d}t = \frac{a_1}{A^2\Delta p}\int_0^V V\mathrm{d}V + \frac{b_1}{A\Delta p}\int_0^V \mathrm{d}V \tag{9.16}$$

giving

$$t = a_1\frac{V^2}{2A^2\Delta p} + b_1\frac{V}{A\Delta p} \tag{9.17}$$

Using equation 9.17 either t or V can be calculated from the value of the other variable provided all the constants are known.

For experimental determination of α and R, equation 9.17 is often put in the form

$$\frac{t}{V} = aV + b \tag{9.18}$$

where

$$a = \frac{a_1}{2A^2\Delta p} \quad \text{and} \quad b = \frac{b_1}{A\Delta p}$$

which gives a straight line if t/V is plotted against V—see *Figure 9.5*. The use of equation 9.18 and the plot in *Figure 9.5* are, of course, limited to those cases when it is possible to apply the given pressure drop right from the commencement of the filtration.

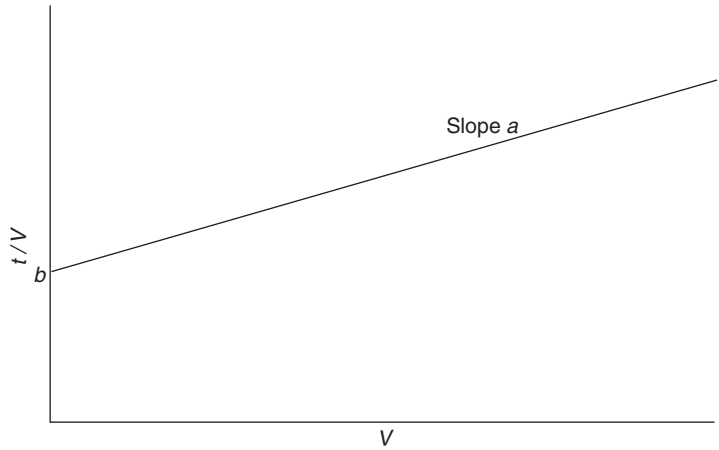

Figure 9.5 Plot of $t/V = f(V)$ for constant pressure filtration and incompressible cakes

Often high initial flow rates through a clean medium have to be avoided in order to prevent the penetration of solids through the clean medium, which would cause contamination of the filtrate, and also to ensure an even deposition of the cake.

It is therefore necessary in such cases to precede the constant pressure period with a period in which the applied pressure drop is gradually increased from a low value (this may be a nearly constant rate period).

The governing equation from which α and R may be evaluated, is then obtained by integrating equation 9.16 starting from a point t_s,V_s at the beginning of the truly constant pressure period; the resulting equation is

$$\frac{t - t_s}{V - V_s} = \frac{\alpha\mu c}{2A^2\Delta p}(V + V_s) + \frac{\mu R}{A\Delta p} \tag{9.19}$$

The actual procedure for the evaluation of results is best explained in an example.

Example 9.1 Evaluation of specific cake resistance α and medium resistance R from pilot scale tests

Filtration tests were carried out with a plate and frame filter press (for details of the construction of the press see chapter 12, section 12.2.1) under the following conditions:

solids:	$\rho_s = 2710\,\mathrm{kg\,m^{-3}}$
liquid:	water at 20°C, $\mu = 0.001\,\mathrm{Ns\,m^{-2}}$
suspension:	concentration $c = 10\,\mathrm{kg\,m^{-3}}$
filter:	plate and frame press, 1 frame, dimensions 430 × 430 × 30 mm (the actual cake thickness can be larger by 5 mm because of a recess in the plates).

The data obtained during the filtration experiment are shown in *Table 9.1*; the initial stages of filtration were controlled manually before constant pressure

Table 9.1 Data from filtration experiment, example 9.1

$10^{-5}\Delta p$, N m^{-2}	t, s	V, m^3	$\frac{t-t_s}{V-V_s}$ (*calculated*), s m^{-3}
0.4	447	0.04	12 458
0.5	851	0.07	12 326
0.7	1262	0.10	12 120
0.8	1516	0.13	12 765
1.1	1886	0.16	12 857
1.3	2167	0.19	13 809
1.3	2552	0.22	14 175
1.3	2909	0.25	15 540
1.5	3381	0.28	15 250
1.5	3686	0.30	—
1.5	4043	0.32	17 850
1.5	4398	0.34	17 800
1.5	4793	0.36	18 450
1.5	5190	0.38	18 800
1.5	5652	0.40	19 660
1.5	6117	0.42	20 258
1.5	6610	0.44	20 886
1.5	7100	0.46	21 337
1.5	7608	0.48	21 789
1.5	8136	0.50	22 250
1.5	8680	0.52	22 700
1.5	9256	0.54	23 208

The frame was full of cake at $V = 0.56\,\mathrm{m^3}$.
The value of $0.30\,\mathrm{m^3}$ corresponding to 3686 s was chosen as a starting point for constant pressure operation, i.e. $V_s = 0.3\,\mathrm{m^3}$, $t_s = 3686\,\mathrm{s}$

filtration at $150\,000\,\mathrm{N\,m^{-2}}$ was carried out. Determine the specific cake resistance α and the medium resistance R for this test.

Solution

Equation 9.19 can be used to evaluate the constants a and b:

$$\frac{t - t_s}{V - V_s} = a(V + V_s) + b$$

$(t - t_s)/(V - V_s)$ is plotted against V—as in *Figure 9.6*—and the slope (a) and the intercept on the vertical axis ($b + aV_s$) of the best straight line drawn through the part of the graph that corresponds to constant pressure operation, i.e. for $V \geqslant V_s$ (i.e. $0.3\,\mathrm{m^3}$) are measured.

The slope obtained is

$$a = 26\,219\,\mathrm{s\,m^{-6}}$$

and the intercept is

$$b + aV_s = 9030\,\mathrm{s\,m^{-3}}$$

from which

$$b = 9030 - 26\,219 \times 0.3 = 1164.3\,\mathrm{s\,m^{-3}}$$

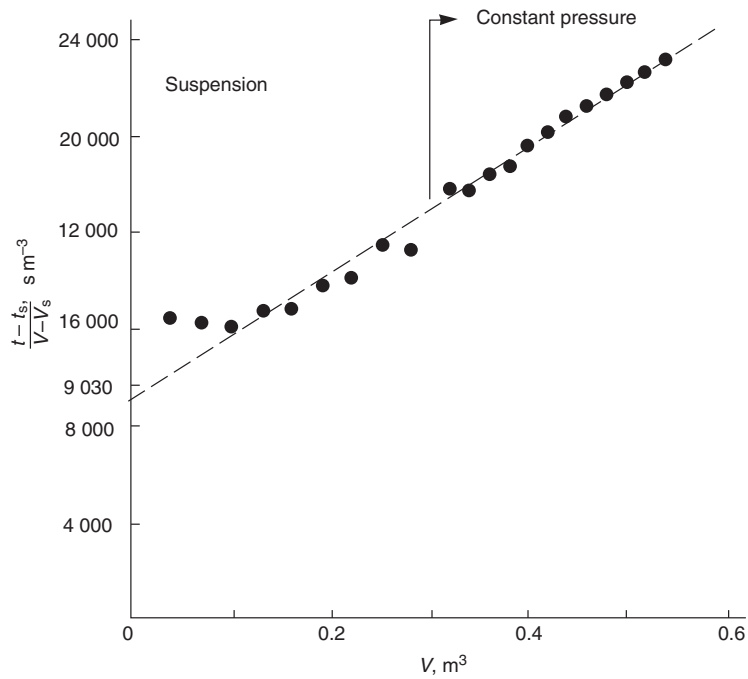

Figure 9.6 Plot of t/V for example 9.1

From the definition of the constants a and b (equations 9.13, 9.14 and 9.18)

$$a = \frac{\alpha\mu c}{2A^2\Delta p} \qquad b = \frac{\mu R}{A\Delta p}$$

from which α and R can be calculated, using $A = 0.43 \times 0.43 \times 2 = 0.37\,\text{m}^2$ and $c = 10\,\text{kg}$ per cubic metre of suspension $= 10/(1 - 0.00369) = 10.037\,\text{kg}$ per cubic metre of filtrate (as the volume occupied by 10 kg of solids is $10/2710 = 0.00369\,\text{m}^3$)

$$\alpha = \frac{2A^2\Delta pa}{\mu c} = \frac{2 \times 0.13675 \times 1.5 \times 10^5 \times 2.6219 \times 10^4}{0.001 \times 10.037}$$
$$= 1.069 \times 10^{11}\,\text{m kg}^{-1}$$

and

$$R = \frac{A\Delta pb}{\mu} = \frac{0.37 \times 1.5 \times 10^5 \times 1164.3}{0.001}$$
$$= 6.4619 \times 10^{10}\,\text{m}^{-1}$$

9.3.2 Constant rate filtration

If the flow rate Q is kept constant and the pressure Δp varied, equation 9.10 becomes

$$Q = \frac{\Delta p(t)A}{\alpha\mu c[V(t)/A] + \mu R} \tag{9.20}$$

where V is simply

$$V = Qt \tag{9.21}$$

thus

$$\Delta p = \alpha\mu c\frac{Q^2}{A^2}t + \mu R\frac{Q}{A} \tag{9.22}$$

which, using the definitions of a_1 and b_1 from equations 9.13 and 9.14, becomes

$$\Delta p = a_1 v^2 t + b_1 v \tag{9.23}$$

where v is the approach velocity of the filtrate

$$v = \frac{Q}{A} \tag{9.24}$$

this is of course constant for constant rate filtration. A plot of Δp against t as in *Figure 9.7*, will, from equation 9.23, be a straight line.

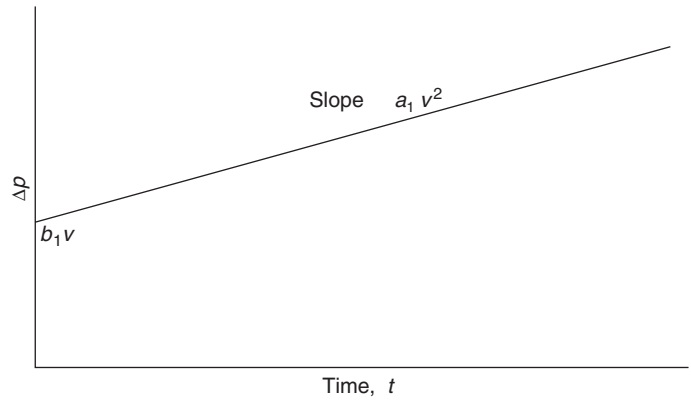

Figure 9.7 Plot of $\Delta p = f(t)$ for constant rate filtration, incompressible cake

9.3.3 Constant rate followed by constant pressure operation

In many cases, for example a plate and frame or a leaf press operated with the suspension supplied from a centrifugal pump, the early stages of filtration are conducted at a nearly constant rate. As the cake becomes thicker and offers more resistance to the flow, the pressure developed by the pump becomes a limiting factor and the filtration proceeds at a nearly constant pressure. For such a combined operation, the plot of Δp against time is as shown in *Figure 9.8*. The equations are (see equation 9.23)

$$\left.\begin{aligned} &\Delta p = a_1 v^2 t + b_1 v \qquad \text{for } t < t_s \\ \text{and} \qquad &\\ &\Delta p = \Delta p_s = \text{constant} \quad \text{for } t \geqslant t_s \end{aligned}\right\} \tag{9.25}$$

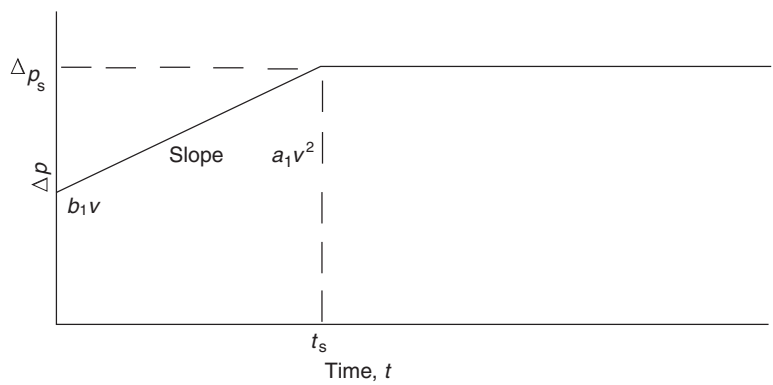

Figure 9.8 Plot of $\Delta p = f(t)$ for constant rate followed by constant pressure operation (incompressible cakes)

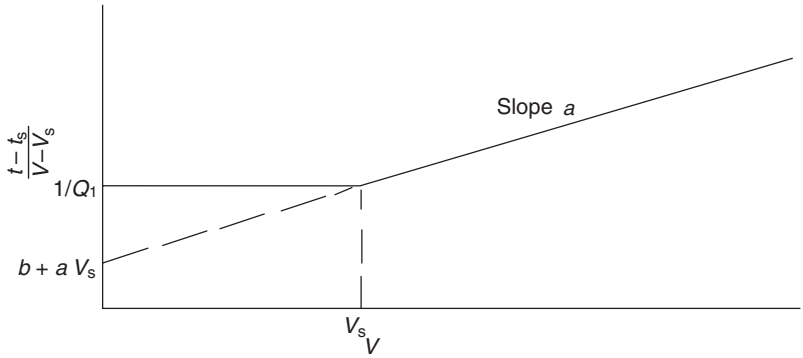

Figure 9.9 Plot of $t/V = f(V)$ for constant rate followed by constant pressure operation

The plot of $t/V = f(V)$ will be as shown in *Figure 9.9*.

The equations are (see equation 9.21)

$$V = Q_1 t \qquad \text{for } V \leqslant V_s \tag{9.26}$$

and

$$\frac{t - t_s}{V - V_s} = a(V + V_s) + b \qquad \text{for } V > V_s$$

(this is the same as equation 9.19 derived by integration of equation 9.15, and is similar to equation 9.18) where Q_1 is the flow rate in the initial constant rate operation. V_s and t_s are related by

$$V_s = Q_1 t_s \tag{9.27}$$

Example 9.2

A filtration experiment is carried out on a single cloth of area $0.02\,m^2$ to which a slurry is fed at a constant rate, yielding $4 \times 10^{-5}\,m^3 s^{-1}$ of filtrate. Readings taken during the test show that after 100 s the pressure is $4 \times 10^4\,N\,m^{-2}$ and after 500 s the pressure is $1.2 \times 10^5\,N\,m^{-2}$.

The same filter cloth material is to be used in a plate and frame filter press, each frame having dimensions $0.5\,m \times 0.5\,m \times 0.08\,m$, to filter the same slurry. The flow rate of slurry per unit area of cloth during the initial constant rate period is to be the same as that used in the preliminary experiment and the constant rate period is to be followed by constant pressure operation once the pressure reaches $8 \times 10^4\,N\,m^{-2}$. If the volume of cake formed per unit volume of filtrate, v is 0.02, calculate the time required to fill the frame.

1. Constant rate period

The filtrate approach velocity for the constant rate period is

$$v = \frac{Q_1}{A} = \frac{4 \times 10^{-5}}{0.02} = 2 \times 10^{-3}\ \mathrm{m\,s^{-1}}$$

which is the same for both the experimental and the filter press.

As two experimental values of Δp and t are known, the two constants a_1 and b_1 can be determined by substituting the values of Δp and v in equation 9.23:

$$4 \times 10^4 = a_1 \times 4 \times 10^{-6} \times 100 + b_1 \times 2 \times 10^{-3}$$
$$12 \times 10^4 = a_1 \times 4 \times 10^{-6} \times 500 + b_1 \times 2 \times 10^{-3}$$

giving

$$a_1 = 5 \times 10^7$$

and

$$b_1 = 10^7$$

so that $\Delta p = 200t + 2 \times 10^4$ (this is applicable to both the experiment and the filter press) from which t_s can be determined because from the experimental data $\Delta p_s = 8 \times 10^4$, therefore

$$8 \times 10^4 = 200t_s + 2 \times 10^4$$

thus

$$t_s = 300\ \mathrm{s}.$$

A graph of $\Delta p (= f(t))$ against t can now be drawn (*Figure 9.10*). The cumulative volume V_s passed through one frame in 300 s can be calculated from equation 9.26

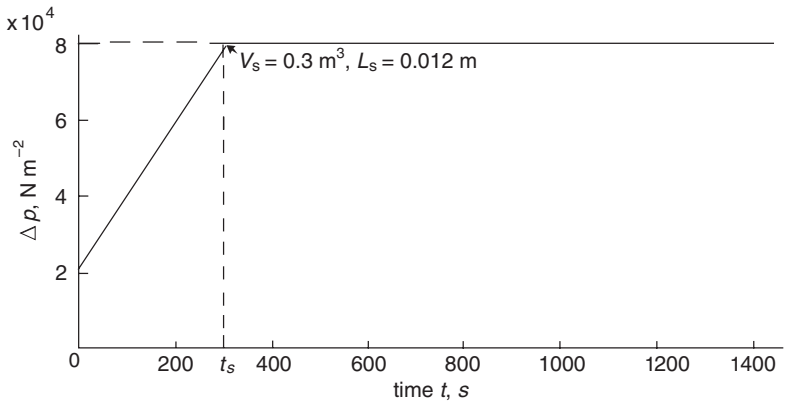

Figure 9.10 Plot of $\Delta p = f(t)$ for example 9.2

$$V_s = Q_1 t_s = vAt_s = 2 \times 10^{-3} \times 0.5 \times 300$$
$$= 0.3 \text{ m}^3$$

and the resulting thickness L_s of cake is

$$L_s = v\frac{V_s}{A} = 0.02 \times \frac{0.3}{0.5} = 0.012 \text{ m}$$

2. Constant pressure period

The final (total) volume of filtrate per frame V_f at the end of the whole combined filtration operation can be determined from the final cake thickness L_f, which is 0.04:

$$V_f = \frac{L_f A}{v} = \frac{0.04 \times 0.5}{0.02} = 1 \text{ m}^3$$

The time required to fill the frame (which is the total time of the combined operation) can be determined from equation 9.19

$$t_f = t_s + \frac{a_1}{2A^2\Delta p_s}(V_f^2 - V_s^2) + \frac{b_1}{A\Delta p_s}(V_f - V_s)$$
$$= 300 + \frac{5 \times 10^7}{2 \times 0.25 \times 8 \times 10^4} \times (1^2 - 0.3^2) + \frac{10^7}{0.50 \times 8 \times 10^4}(1 - 0.3)$$
$$= 300 + 1137.5 + 175 = 1612.5 \text{ s}$$

Note that it can be shown that this result is independent of the filtration area.

Compare this value of 1612.5 s with the time in which 1 m^3 of filtrate would be filtered at all-constant rate operation

$$t = \frac{V}{Q} = \frac{V}{vA} = \frac{1}{2 \times 10^{-3} \times 0.5} = 1000 \text{ s}$$

The plot of *t/v* against *V* for this operation is shown in *Figure 9.11*.

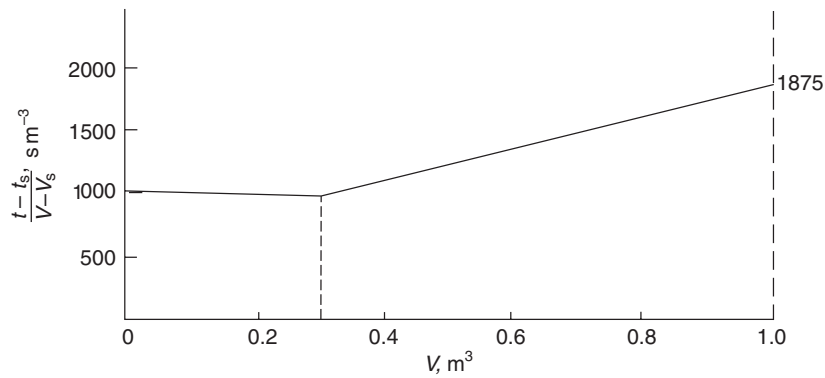

Figure 9.11 Plot of $(t - t_s)/(V - V_s)$ as a function of V for example 9.2

9.3.4 Variable pressure–variable rate operation

If a centrifugal pump is used, its flow rate–pressure drop relationship may follow the curve shown in *Figure 9.12*.

Equation 9.10 can be written as

$$V = \frac{A}{\alpha\mu c}\left(\frac{\Delta pA}{Q} - \mu R\right) \tag{9.28}$$

where Δp and Q are related by the pump characteristics.

The time necessary for the filtration of a volume V of filtrate can be calculated by integration of the reciprocal rate $1/Q$ as a function of V since

$$\mathrm{d}t = \frac{\mathrm{d}V}{Q}$$

hence

$$t = \int_0^v \frac{\mathrm{d}V}{Q} \tag{9.29}$$

The actual method of calculation is best explained by giving a worked example.

Example 9.3

Determine the time necessary for the filtration of 50 m^3 of the same slurry as in example 9.1 in a plate-and-frame filter press with 25 frames of dimensions $1 \times 1 \times 0.035$ m. Use the test data for cake resistance and medium resistance (the same cloth is used) obtained in example 9.1. The pump characteristic is shown in *Figure 9.12*.

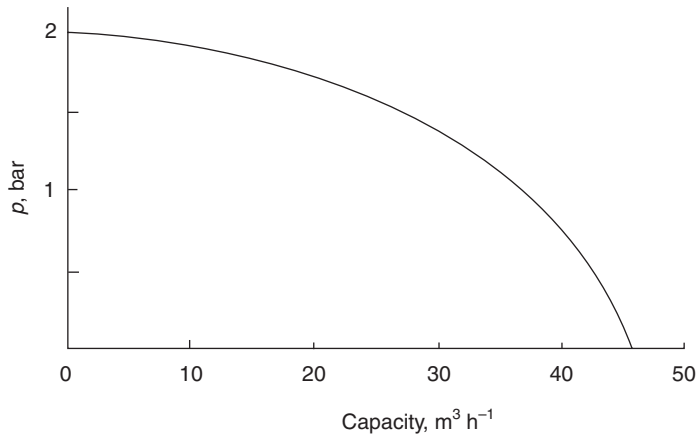

Figure 9.12 Pump characteristics

Data:

cake resistance,	$\alpha = 1.069 \times 10^{11}$ m kg^{-1}
medium resistance,	$R = 6.462 \times 10^{10}$ m^{-1}
viscosity,	$\mu = 0.001$ Ns m^{-2}
concentration,	$c = 10.037$ kg m^{-3}
filtration area,	$A = 1 \times 1 \times 2 \times 25 = 50$ m^2

Solution

Equation 9.28 is used to find $V = f(Q)$ as follows:

$$V = \frac{50}{1.069 \times 10^{11} \times 10^{-3} \times 10.037}\left(\frac{\Delta p}{Q}50 - 10^{-3} \times 6.462 \times 10^{10}\right)$$

$$V = 2.32 \times 10^{-6}\left(\frac{\Delta p}{Q} - 1.2924 \times 10^{6}\right)$$

Using the data from *Figure 9.12, V* can be calculated as a function of Q; a summary of the results is given in *Table 9.2*. To obtain the total filtration

Table 9.2

Q, m^3 h^{-1}	$\Delta p \times 10^{-5}$, N m^{-2}	V, m^3	$1/Q$, s m^{-3}
45	0.2	0.7	80
40	0.75	12.71	90
35	1.15	24.44	103
30	1.4	35.98	120
25	1.6	50.46	144
20	1.75	69.48	180
15	1.8	97.23	240

time, equation 9.29 must be integrated up to, in this case, $V = 50$ m^3; this can be done graphically from a plot of $1/Q$ against V (*Figure 9.13*). Graphical integration gives a value of 1.463 h (1 h 27 min 47 s).

A check also has to be made as to whether there is enough cake-holding capacity available.

The filtration tests in example 9.1 showed the volume of cake formed per unit volume of suspension is

$$\frac{0.43 \times 0.43 \times 0.035}{0.56} = 0.01156\,\text{m}^3$$

The actual volume available in one frame is

$$1 \times 1 \times 0.035 = 0.035\,\text{m}^3$$

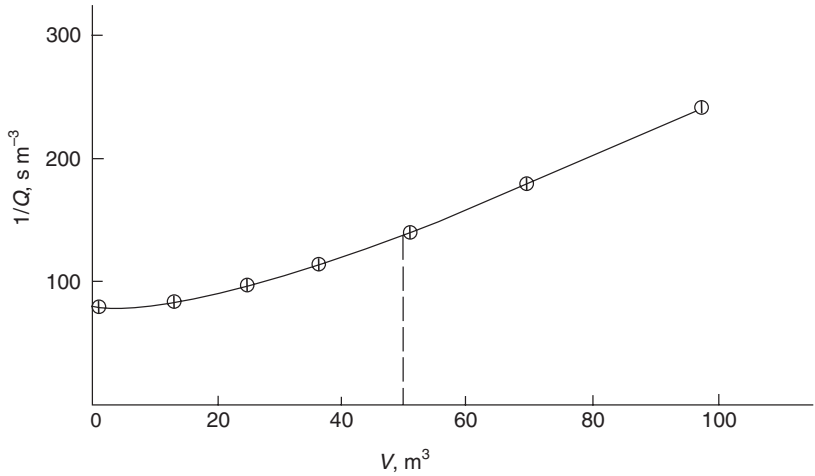

Figure 9.13 Plot of $1/Q = (V)$ for example 9.3

i.e. the maximum volume of suspension that can be filtered in one period is:

$$V_{\max} = \frac{0.035 \times 25}{0.01156} = 75.69 \text{ m}^3$$

which is greater than the $50\,\text{m}^3$ given in the example, and therefore the cakeholding capacity is sufficient.

9.4 Filtration operations—basic equations, compressible cakes

The compressibility of cakes, i.e. the increasing resistance of cakes with pressure, can be tested in various ways. As was briefly mentioned in section 9.2.2, one way of testing the relationship $\alpha = f(\Delta p_c)$ is in the compression–permeability cell. The solids compression is created by the mechanical action of the piston—an obvious assumption made is that hydraulic pressure can be simulated by mechanical compression.

Another method is to use pilot test data from constant pressure operations carried out at different pressures. This yields a family of lines on a plot of t/V against V (*Figure 9.5*) with varying slopes, from which the cake resistances α can be determined.

Jahreis[3] has suggested a procedure in which a single test run can be used for obtaining such data. The pressure is stepped up from one operating pressure to another, without interrupting the flow, and at each pressure step measurement of the cumulative volume of filtrate is started from zero again. Purchas[4] suggests an alternative plot of $\Delta p/Q = f(V)$ which makes the slope independent of pressure and yields a series of lines which diverge if the cake is incompressible.

An obvious way of dealing with compressible cakes is to use the concept of average cake resistance α_{av} as defined in equation 9.6. This is of course only possible if the final pressure is known, otherwise a solution can only be obtained by a series of iterative calculations.

If, however, an analytical relationship such as equation 9.7 is applicable, usually over a limited range of pressure drops, the function $\alpha = f(\Delta p)$ can be employed directly as shown in the following.

For an analytical solution of the filtration of compressible cakes which satisfy equation 9.7, pressure drops across the medium Δp_m and across the cake Δp_c have to be treated separately.

Let

$$\Delta p = \Delta p_c + \Delta p_m \tag{9.30}$$

$$\Delta p_m = \frac{\mu R Q}{A} \tag{9.31}$$

and

$$\Delta p_c = \frac{\alpha_{av} \mu c V Q}{A^2} \tag{9.32}$$

If equation 9.8 is substituted into equation 9.32

$$\Delta p_c = (1 - n)\alpha_0 \Delta p_c^n \frac{\mu c V Q}{A^2}$$

from which

$$\frac{\mu c V Q}{A^2} = \frac{(\Delta p_c)^{1-n}}{(1 - n)\alpha_0} \tag{9.33}$$

This is the basic equation from which the special cases can be derived.

9.4.1 Constant pressure filtration

This operation is of course unaffected by compressibility and, consequently, the governing relationships remain the same as in section 9.31 (where α is now the specific cake resistance corresponding to the given pressure).

9.4.2 Constant rate filtration

Substituting

$$V = Qt$$

from equation 9.20 into equation 9.33 gives

$$(\Delta p_c)^{1-n} = \alpha_0 (1 - n) \mu c \frac{Q^2}{A^2} t \tag{9.34}$$

A plot of log Δp_c against log t should give a straight line. The pressure drop across the medium is constant and given by equation 9.31.

9.4.3 Variable pressure—variable rate operation

This is a complicated case in which Δp_c, Δp_m, V, Q and t are all variable. Equation 9.33 can be written in the form (using equation 9.30):

$$V = \left(\frac{A^2}{(1-n)\alpha_0 \mu c}\right)\left(\frac{(\Delta p - \Delta p_m)^{1-n}}{Q}\right) \tag{9.35}$$

where Δp and Q are related by pump characteristics (as in section 9.3.4) and Δp_m is given by equation 9.31.

Equation 9.35 can then be treated in a similar manner to equation 9.28 in section 9.3.4; the time of filtration can again be calculated from equation 9.29.

Example 9.4

As in example 9.3, determine the time necessary for the filtration of 50 m^3 of the same slurry in the same filter but assuming a compressible filter cake with cake resistance α following the law

$$\alpha = 6.1094 \times 10^9 (\Delta p_c)^{0.24}$$

The medium resistance is constant and equal to (as in example 9.3) $R = 6.462 \times 10^{10}$ m^{-1}.

Use the same pump characteristics as in example 9.3.

Solution

Equation 9.35 is used to find V as a function of Q:

$$V = \left(\frac{2500}{0.76 \times 6.1094 \times 10^9 \times 10^{-3} \times 10.037}\right)\left(\frac{(\Delta p - \Delta p_m)^{0.76}}{Q}\right), \text{ m}^3$$

A summary of the values for V, Q and Δp are given in *Table 9.3*. Note that pressure drops across the medium have been calculated from equation 9.31

$$\Delta p_m = \frac{10^{-3} \times 6.462 \times 10^{10} \times Q}{50}, \text{ N m}^{-2}$$

Table 9.3

Q, $m^3\ h^{-1}$	$\Delta p \times 10^{-5}$ $N\,m^{-2}$	$\Delta p_m \times 10^{-5}$ $N\,m^{-2}$	V, m^3	$1/Q$, $s\,m^{-3}$
45	0.2	0.1616	2.3	80
40	0.75	0.1436	20.8	90
35	1.15	0.1257	35.4	103
30	1.4	0.1077	49.2	120
25	1.6	0.0898	66.5	144

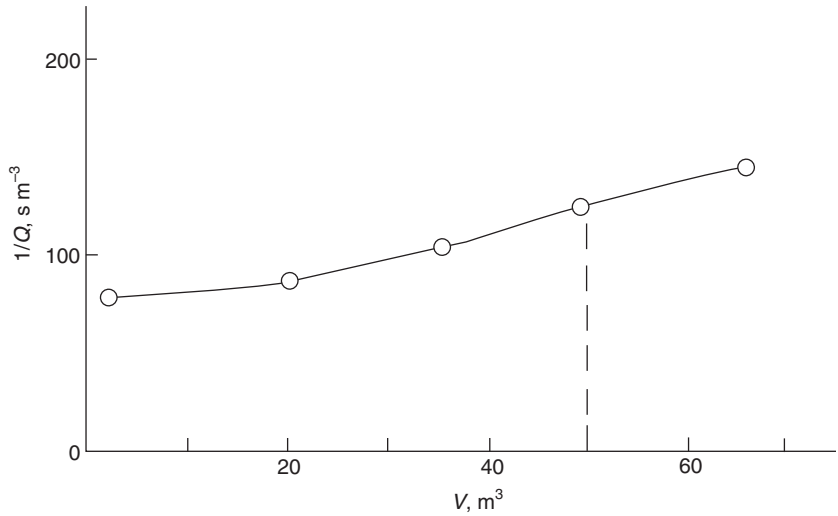

Figure 9.14 Plot of $1/Q = f(V)$ for example 9.4

A plot of $1/Q$ against V is drawn (*Figure 9.14*) and the time required for the filtration is obtained by integration of the area under the curve up to $50\,m^3$ (from equation 9.29), giving

$$t = 4750\text{ s} = 1.3194\text{ h}$$
$$= 1\text{ h }19\text{ min }10\text{ s}$$

9.5 Relationship between specific cake resistance, porosity and specific surface

Considering the flow of clean liquid through a packed bed, Kozeny[5] assumed that the pore space of a packed bed of powder could be regarded as equivalent to a bundle of parallel capillaries with a common equivalent radius, and with a cross-sectional shape representative of the average shape of the pore cross-section. Using Poiseuille's law for the flow of fluids through capillary tubes, Kozeny[5] and later Carman[6] were able to relate the permeability to the porosity, the specific surface and the density of the powder in the bed.

Using the Kozeny–Carman equation it can be shown that the specific cake resistance is equal to

$$\alpha = \left(\frac{K_0 S_0^2}{\rho_s}\right)\left(\frac{(1-\varepsilon)}{\varepsilon^3}\right) \tag{9.36}$$

where K_0 is the so-called Kozeny constant which approximates to a value of 5 in the lower porosity ranges; it generally depends on particle size, shape and the porosity. S_0 is the specific surface of the particles making up the bed,

$$S_0 = \frac{\text{surface area of solids}}{\text{volume of solids}}$$

ρ_s is the density of solids and ε is the porosity defined as

$$\varepsilon = \frac{\text{volume of voids}}{\text{volume of cake}}$$

Equation 9.36 combined with equation 9.5, indicates the high sensitivity of the pressure drop to the cake porosity and to the specific surface. Unfortunately, the importance of equation 9.36 in filtration is limited, despite its frequent quotations and derivations in textbooks. Although it has been found to work reasonably well for incompressible cakes over narrow porosity ranges, it cannot be used for compressible cakes and its most valuable use is for illustration of basic principles. For its derivation from the capillary model, the reader can consult either the original works by Kozeny[5] and Carman[6] or other texts, e.g. by Tiller[2].

9.6 Cake moisture correction—mass balance

In some cases, particularly in the filtration of highly concentrated suspensions, when working out the mass of dry cake from filtrate volume collected a cake moisture correction has to be applied, which accounts for the presence of moisture in the cake. The relationship that replaces equation 9.9 in such cases is obtained from solids concentration c (kg m^{-3}) in the original suspension and from the moisture content of the cake

$$m = \frac{\text{mass of wet cake}}{\text{mass of dry cake}}$$

(kg/kg) via the mass balance:

$$\text{mass of dry cake} = \text{volume of filtrate collected} \times \frac{\text{mass of solids}}{\text{volume of filtrate}} + \text{volume of filtrate in cake} \times \frac{\text{mass of solids}}{\text{volume of filtrate}}$$

hence

$$Aw = V\left(\frac{c\rho_s}{\rho_s - c}\right) + \left(\frac{m-1}{\rho}\right)wA\left(\frac{c\rho_s}{\rho_s - c}\right) \tag{9.37}$$

which gives

$$w = \frac{V}{A}\left(\frac{1}{c} - \frac{1}{\rho_s} - \frac{m-1}{\rho}\right)^{-1} \tag{9.38}$$

Comparison of equations 9.9 and 9.38 may be used to define a 'corrected' concentration $c_{\text{corrected}}$, i.e.

$$c_{\text{corrected}} = \left(\frac{1}{c} - \frac{1}{\rho_s} - \frac{m-1}{\rho}\right)^{-1} \tag{9.39}$$

which takes into account the presence of moisture in the cake. Clearly, for low values of c when $\rho_s \gg c$ and $\rho \gg c$:

$$c_{\text{corrected}} = c$$

Example 9.5

A suspension of incompressible solids at a concentration of $300\,\text{kg}\,\text{m}^{-3}$ of slurry is to be filtered at constant pressure drop. Estimate the filtration area necessary to produce $50\,\text{kg}\,\text{h}^{-1}$ of dry solids.

Data:

pressure drop,	$\Delta p = 10^5$ N m^{-2} (1 bar)
cake moisture content,	$m = 1.2$
cake specific resistance,	$\alpha = 10^{11}$ m kg^{-1}
medium resistance,	$R = 6.5 \times 10^{10}$ m^{-1}
liquid density,	$\rho_l = 1000$ kg m^{-3}
solids density,	$\rho_s = 2600$ kg m^{-3}
liquid viscosity,	$\mu = 0.001$ N s m^{-2}

Solution

The corrected solids concentration (equation 9.39)

$$c_{\text{corrected}} = \left(\frac{1}{300} - \frac{1}{2600} - \frac{0.2}{1000}\right)^{-1}$$
$$= 363.8 \text{ kg m}^3$$

hence the volume of filtrate required to produce 50 kg of solids (equation 9.38) is

$$V = \frac{wA}{c_{\text{corrected}}} = \frac{50}{363.8} = 0.1374\,\text{m}^3$$

Substituting $\Delta p = 10^5$, $V = 0.1374$ and $t = 3600$ s in equation 9.17 gives:

$$A^2 - 0.0248A - 0.954 = 0$$

i.e.

$$A = 0.99 \text{ m}^2$$

9.7 Further development of filtration theory

The filtration theory presented here is only very basic and the assumptions on which it is built are often too simplistic. This so-called classical filtration

theory has been under considerable criticism from many research workers recently. A brief account of the main points is given in the following.

Starting with the medium resistance, R, which can be determined from the intercept in constant pressure filtration (section 9.3.1), this is subject to great uncertainty and in practice often comes out either unrealistically small or even negative. Tiller *et al.*[7] have pointed out that the plots of t/V against V have marked curvature at the start of the filtration experiment and this can easily be missed. They defined the intercept values as 'false medium resistance' and showed that a 'good' value of medium resistance is obtained only if the ordinate of the first experimental point ($1/Q$) is close to the intercept value.

Another, even more troublesome variable is the specific cake resistance, α, and the concept of using an average value α_{av}. Even in a constant pressure experiment, the pressure varies through the depth of the cake and subsequently the porosity and cake resistance vary also. The average value of α_{av} defined by equation 9.6 is an average of the values of the effective cake resistances obtained from a series of constant-pressure experiments, which in turn are averages of the point values within the cake. The underlying assumption of the conventional theory is that the point and average values of α are functions of applied pressure only. In practice the porosity, and therefore the cake resistance also, depend on time (due to time consolidation of the cake), filtration velocity and solids concentration. Rushton *et al.*[8] have shown, for example, the effects of velocity and concentration on specific cake resistance of several inorganic materials. They found that the values of α in a constant-pressure experiment go through a maximum with increasing concentration. For concentrations above that corresponding to the maximum, resistance decreases exponentially with concentration and this is attributed to shorter cake formation times at those concentrations and the resulting open cake structures. At concentrations below the maximum α, the lower cake resistance is attributed to higher initial fluid velocities which are also likely to produce open cake structures. Rushton *et al.*[8] also found that the maximum α itself increases exponentially with pressure.

It is now certain that the only truly rigorous approach to filtration theory is by using point values of α within the cake itself and those can only be obtained from studies of flow and local porosities in practical cakes. This is inevitably very complicated and beyond the scope of this book. The reader is referred to the already mentioned review by Tiller *et al.*[7] and to a theoretical paper by Wakeman[9].

The conventional filtration theory has been challenged by Willis *et al.*[10] (as an example of the many published) who have applied a two-phase theory to filtration and explained the deviations from parabolic behaviour in the initial stages of the filtration process. This new theory incorporates the medium as an integral part of the process and shows that it is the interaction of the cake particles with the medium which in fact controls the filterability. The authors define a cake-septum permeability which then appears in the slope of the conventional plots (*Figures 9.5* and *9.7*) instead of the cake resistance. This

theory is not yet accepted by the engineering community, probably because it merely represents a new way of interpreting test data rather than a new method of sizing or scaling filters.

9.8 The benefits of pre-thickening

The feed solids concentration has a profound effect on the performance of any cake filtration equipment. It affects the capacity and the cake resistance, as well as the penetration of the solids into the cloth (which influences filtrate clarity and medium resistance). Thicker feeds lead to improved performance of most filters through higher capacity and lower cake resistance.

The effect on solids yield can be easily demonstrated using the following equation derived in appendix I of Svarovsky[11] (neglecting medium resistance):

$$Y = \left(\frac{2\Delta pfc}{\alpha\mu t_c}\right)^{\frac{1}{2}} \tag{9.40}$$

where Δp is the pressure drop, c is the feed solids concentration, α is the specific cake resistance, μ is the liquid viscosity, Y is the solids yield (dry cake production in kg m^{-2} s^{-1}), f is the ratio of filtration to cycle time and t_c is the cycle time. For the same cycle time (i.e. the same speed), if the concentration is increased by a factor of four, production capacity is doubled. In other words, filtration area can be halved for the same capacity.

For given operating conditions and submergence, the dry cake production rate increases with the speed of rotation (see equation 9.40) and the limiting factor is usually the minimum cake thickness which can still be successfully discharged by the method used in the filter. Equation 9.41 (also derived by Svarovsky[11]) shows the dependence of the solids yield on cake thickness:

$$Y = \frac{2\Delta pfc}{\alpha\mu L(1-\epsilon)\rho_s} \tag{9.41}$$

where L is the cake thickness, ρ_s is the solids density and ε is the cake porosity. It can be seen that for constant cake thickness, doubling the feed concentration doubles the yield. This is the secret of the success of the so-called high duty vacuum drum filters which, by using a unique cake discharge method, allow very thin cakes to be discharged and can therefore be operated at very high speeds up to 25 rev. min^{-1}.

For those filters which allow variations in cake formation time within a fixed cycle time (such as the horizontal vacuum belt filter, for example), the advantage of pre-thickening is that for thicker feeds the cake formation time can be shortened, thus giving more time for dewatering, washing or other cake-processing operations. On the other hand, it can be shown (see Svarovsky[11] or section 12.2.1.3) that in an optimum cycle time, at

constant-pressure operation and where medium resistance is low compared with cake resistance, the cake-formation time should be equal to the time the filter is 'out of service' for cake dewatering, washing or discharge. This result of course takes no account of any optimum operating conditions for minimum moisture content of the cake produced. In any case, this theoretical result may be outside the operational range governed by the design of a particular continuous filter: for example, design limitations on submergence in vacuum drum filters prevents the application of the above optimum condition. It can, however, be applied to any batch filters.

One additional benefit of pre-thickening not taken into account in the above analysis is the reduction in cake resistance which it causes. If the feed concentration is low, there is a general tendency of particles to pack together more tightly, thus leading to higher specific resistances. If, however, many particles approach the filter medium at the same time, they may bridge over the pores; this reduces penetration into the cloth or the cake underneath and more permeable cakes are thus formed. This effect of concentration is particularly pronounced with irregularly shaped particles. A possible explanation of the variation in the specific resistance is in terms of the time available for the particles to orientate themselves in the growing cake. At higher concentrations, but with the same approach velocities, less time (referred to as particle relaxation time) is available for a stable cake to form and a low resistance results.

An example of the concentration effect on the specific cake resistance is given by Svarovsky and Walker[12] who reported results of some experiments with a laboratory horizontal vacuum belt filter. In spite of the operational difficulties in keeping conditions constant, the effect of feed concentration on specific cake resistance was so strong that it swamped all other effects. *Figure 9.15* shows this in a log–log plot and the measured values correlate quite well in a straight line. The function fitted, for the aluminium hydroxide tested, was in the following form:

$$\alpha = 13.47 \times 10^{10}\, c^{-0.8031} \tag{9.42}$$

where α is in $\mathrm{m\,kg^{-1}}$ and c is in $\mathrm{g\,l^{-1}}$ ($\mathrm{kg\,m^{-3}}$) from 5 to $580\,\mathrm{g\,l^{-1}}$.

The form of the above equation is in keeping with a similar study by Rushton *et al.*[8] who used a pressure filter to test a range of inorganic materials (calcium carbonate, silicate and sulphate, and two grades of magnesium carbonate) at constant pressure and obtained a range of values for the numerical constant in equation 9.42 from 9.14 to 37 800, and the exponent from -0.08 to -1.92, with feed concentrations ranging from 5 to $190\,\mathrm{kg\,m^{-3}}$ ($\mathrm{g\,l^{-1}}$). Unlike Rushton *et al.*, however, we did not find a maximum on the curve of specific cake resistance versus feed concentration.

The physical reason for the higher feed concentrations to reduce the specific cake resistance has been the subject of a computer modelling project. The model used was similar to that of hard spheres used in molecular studies[13]. The determining factor in the formation of local voids and higher

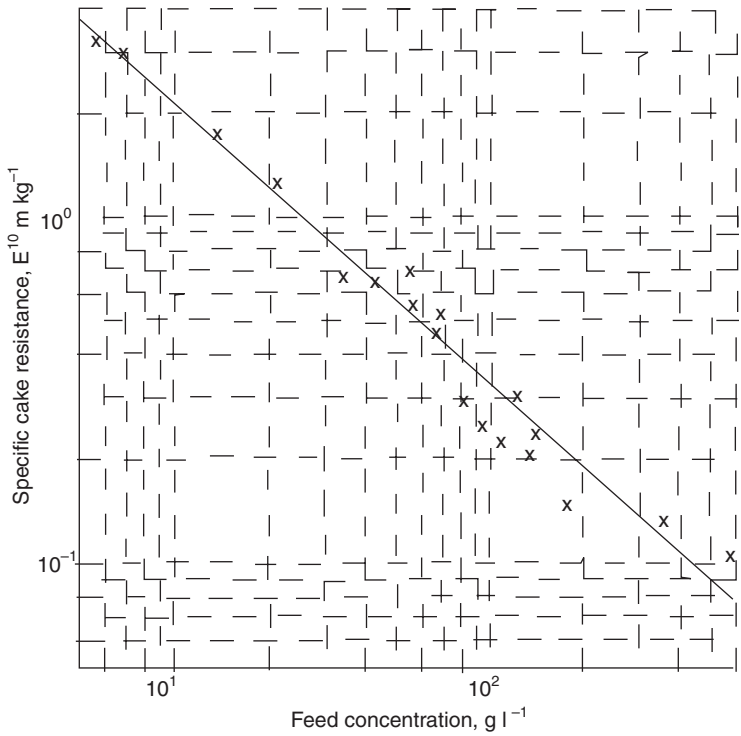

Figure 9.15 A plot of the specific cake resistance against the feed solids concentration for aluminium hydrate[12]

porosity in cakes was found to be the time available for particle relaxation when particles hit the top of the cake. At high concentrations, each particle just deposited on the cake is locked into position by other particles in its vicinity before it has time to roll and fill the open crevices in cake (which it is allowed to do at lower concentrations). Thus, at high concentrations, the cake formed is more open and, consequently, it has more voids within it. This has been proved experimentally as well as in a modelling exercise by Walker[15,16]. Another part of the same project was concerned with precoating a belt filter with the underflow from a hydrocyclone and studying the properties of such highly stratified cakes against the predictions by Zeitsch[14], see section 13.10.2 for a discussion of this.

As to how such pre-thickening can be done, there are mainly two options. Gravity thickening is one option, especially applicable to fast settling slurries. A hydrocyclone (or several units in parallel) as shown in *Figure 6.23* is another good and relatively cheap possibility. The main advantage here is that the particle size ranges that vacuum filtration can handle broadly coincide with those for which hydrocyclones are also suitable. Even filters can be designed to limit or to completely eliminate

cake formation and, therefore, be used in this thickening duty as 'thickening filters' (see chapter 11).

9.9 Filtration of non-Newtonian liquids

Given the importance of non-Newtonian fluids in chemical engineering generally, it is surprising how relatively little attention the filtration of such liquids has attracted in the scientific literature. Even today, many filtration textbooks do not even mention the problem. It was not until the late 1960s[17] that the first workable filtration equations were developed for the basic, incompressible, time-independent power-law fluids. The constant pressure and constant rate filtration relationships developed by Kozicki *et al.*[17] were verified experimentally using slurries of calcium carbonate in water and dilute carboxylmethyl cellulose solutions.

More recently[18], Machač and Crha reviewed the progress to date and showed the importance of the correct values of the constants of the power law model, n and K, in the evaluation of filtration experiments with power law fluids. This is because these constants appear in the governing filtration equations. For example, for constant pressure filtration and when the medium resistance can be neglected, the governing equation for a power law fluid characterized by constants n and K (i.e. when shear stress τ and rate of shear γ are related as $\tau = K\gamma^n$) is

$$\left(\frac{V}{A}\right)^{\frac{n+1}{n}} = \frac{n+1}{n}\left(\frac{\Delta p}{K\gamma' c}\right)^{1/n} t \tag{9.43}$$

where γ' is an average value of a generalized cake resistance for a non-Newtonian liquid, which is best determined experimentally.

Machač and Crha developed plots which, like in Newtonian liquid filtration, have to be linear. The cake and medium resistances are then determined from the slope and the intercept, as is usual in filtration. The problem here is that, in filtration at constant pressure, the filtration velocity may vary widely and this requires the parameters K and n also to apply in a wide interval of the corresponding rate of shear. The way to relate the shear rates to filtration velocities is via the following equation:

$$\gamma \cong \frac{3n+1}{4n} * \frac{18u(1-\varepsilon)}{x_{\mathrm{av}}\varepsilon^2} \tag{9.44}$$

where ε is porosity, x_{av} is a mean particle size (effective equivalent diameter) and u is filtration velocity $u = Q/A$. Equation 9.44 is then used to determine the limits within which the rheological constants n and K have to apply but they rarely do over such a wide range. If they do not, the above-mentioned linearity is not obtained. If it is not possible to achieve the linearity even by altering the value of index n, the authors conclude that the basic equations

derived cannot be used and much more complex filtration theory has to be used[18].

As the use of non-Newtonian fluids in industry (such as in plastics and synthetic fibre manufacture, in polymer processing, in enhanced oil recovery, in biochemistry and biotechnology, and in petrochemicals) is increasing, the interest and research in filtration of such fluids are also growing. Such research is closely linked to further work on the fundamentals of flow through packed beds for non-Newtonian fluids, such as, for example, the recent work of Machač and co-workers on purely viscous[19] and viscoelastic[20] fluids. In future editions of this book or any other in this subject I expect more prominence given to the filtration of non-Newtonian liquids.

Example 9.6

A recessed plate filter with a recess of 5 mm is to be filled with cake in 13 minutes. The cake volume is 2.5% that of the corresponding filtrate, and for the system in question:

$$c = 10 \text{ kg/m}^3,\ \mu = 0.001 \text{ Ns/m}^2,\ \alpha = 92 \times 10^{10} \text{ m/kg}$$

The pump characteristics may be represented by (shown graphically in *Figure 9.16*):

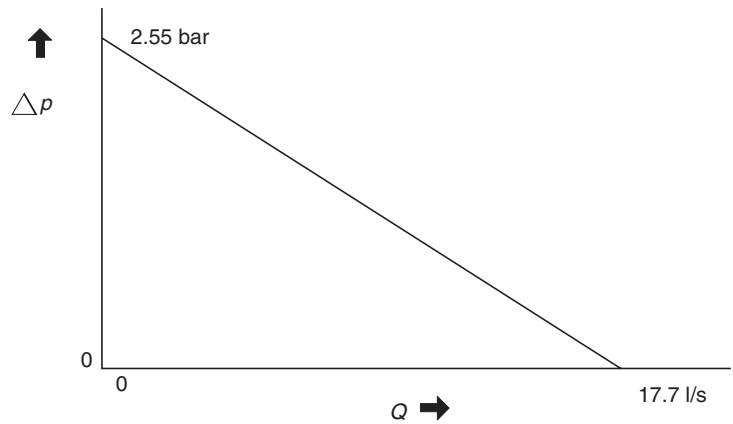

Figure 9.16 The pump characteristics for example 9.6

$$\Delta p = 255 \times 10^3 - 1.44 \times 10^7 Q$$
$$\text{for } 0 \leq Q \leq 0.01771$$
$$\text{where } \Delta p = \text{pressure drop (Pa)}$$
$$Q = \text{filtration rate } (\text{m}^3/\text{s})$$

If the resistance of the associated pipework and of the filter medium is assumed to be negligible:

(a) estimate the filtration area needed,
(b) find the intitial and final filtration rates, and the overall dry cake production capacity (in kg per minute) if the down time is also 13 minutes.

Solution

If the medium resistance is neglected:

$$\text{i.e.} \quad \Delta p = 92 \times 10^{10} \times 0.001 \times 10 \times QV/A^2$$
$$= 0.92 \times 10^{10} QV/A^2$$

If this is assumed equal to the pressure developed by the pump,

$$\Delta p = 255 \times 10^3 - 1.44 \times 10^7 Q$$
$$\text{i.e.} \quad Q = f(A,V)$$

But we also have $Q = dV/dt$, i.e. $t = \int \frac{dV}{Q}$

$$\text{where} \quad 1/Q = \frac{0.92 \times 10^{10}}{255 \times 10^3} \cdot \frac{V}{A^2} + \frac{1.44 \times 10^7}{255 \times 10^3}$$
$$= \frac{36078V}{A^2} + 56.47$$

$$\text{i.e} \quad t_{\max} = 13 \times 60 = 780 = \int_0^{V_{\max}} \left[\frac{36078V}{A^2} + 56.47\right] dV \qquad \text{(i)}$$

Now, filtrate volume to fill 5 mm recess, $V_{\max}$, is given by:

$$V_{\max} = (1/0.025)\ 0.005A = 0.2A\ \text{m}^3$$

$$\therefore \text{ from equation (i), } 780 = \left|\frac{36078V^2}{2A^2} + 56.47V\right|_0^{0.2A}$$

$$\text{i.e.} \quad 780 = \frac{36078 \times 0.04A^2}{2 \times A^2} + 56.47 \times 0.2A$$

$$\text{or} \quad 780 = 721.56 + 11.29A$$

$$\text{hence} \quad A = \mathbf{5.17}\ \text{m}^2$$

Also, suspension volume per cycle $= V_{\max} = 0.2 \times 5.17 = 1.034\ \text{m}^3$ and mass of dry cake per cycle $= 1.034 \times 10 = \mathbf{10.34}$ kg

Also, from the pump characteristic equation,

$$\text{i.e.} \quad \Delta p = 255 \times 10^3 - 1.44 \times 10^7 Q$$

Initial filtration rate given by $\Delta p = 0$,

$$\text{i.e.} \quad Q = (255 \times 10^3)/(1.44 \times 10^7) = 0.0177\ \text{m}^3/\text{s or } \mathbf{17.7}, \mathbf{\text{litre/s}}$$

Final filtration rate given by:

$$1/Q = \frac{36\,078V}{A^2} + 56.47 \quad \text{for } V = V_{\max} = 0.2A \text{ with } A = 5.17 \text{ m}^2$$

$$\text{i.e.} \quad 1/Q = (36\,078 \times 0.2)/5.17 + 56.47 = 1452$$

$\therefore\ Q = 0.000689 \text{ m}^3/\text{s}$ or **0.7 litre/s**

Finally, *average dry cake production rate* is given as:

(mass of dry cake/cycle)/(cycle time)

$$\text{i.e.} \quad 10.34/26 = 0.397 \cong 0.4 \text{ kg/min}$$

References

1. Tiller, F. M. and Cheng, K. S., 'Delayed cake filtration', *Filtration and Separation*, **14**(1), 13–18 (1977)
2. Tiller, F. M., *Filtration and Separation*, **12**, 386 (1975)
3. Jahreis, C. A., *Filtration and Separation*, **2**(4), 308 (1965)
4. Purchas, D. B., *Industrial Filtration of Liquids*, 2nd Edition, Leonard Hill Books, London (1971)
5. Kozeny, J., *Ber. Wien. Akad.*, **136a**, 271 (1927)
6. Carman, P. C., *Trans. Inst. Chem. Eng.*, **15**, 150 (1937)
7. Tiller, F. M., Crump, J. C. and Ville, F., 'Filtration theory in its historical perspective, a revised approach with surprises', *The Second World Filtration Congress 1979*, Filtration Society, London (1979)
8. Rushton, A., Hosseini, M. and Hassan, I., 'The effects of velocity and concentration on filter cake resistance', pp. 78–91, *Proc. Symp. on Solid–liquid Separation Practice*, Leeds, UK, Yorkshire Branch of the I. Chem. E., 27–29 March (1978)
9. Wakeman, R. J., 'A numerical integration of the differential equations describing the formation of and flow in compressible filter cakes', *Trans. I. Chem. E.*, **56**, 258–265 (1978)
10. Willis, M. S., Bridges, W. G. and Collins, R. M., 'The initial stages of filtration and deviations from parabolic behaviour', *Filtech Conference 1981*, pp. 167–176, Filtration Society, London (1981)
11. Svarovsky, L., '*Solid–Liquid Separation Processes and Technology*,' Elsevier, Amsterdam (1985)
12. Svarovsky, L. and Walker, A. J., 'The effect of feed thickening on the performance of a horizontal vacuum belt filter', *1st World Congress Particle Technology, 331 Event of EFCE, Part IV*, NMA mbH, Nuernburg (1986)
13. Woodcock, L. V., 'Glass transition in the hard-sphere model and Kauzmann's paradox', *Ann. NY Acad. Sci.*
14. Zeitsch, K., Eine neue Theorie fuer die Permeabilitaet eines durch sedimentation enstandenen Filterkuchens, *Tech. Mitt. Krupp Forsch.-Ber.*, **42**, 71–76 (1984)
15. Svarovsky, L. and Walker, A. J., 'Development of a Computer Model for Predicting the Filtration Characteristics of a Suspension', Refereed Papers, *Filtration and Separation*, January/February, 57–65 (1994)

16. Walker, A. J., 'The effect of particle size, and its distribution within a filter cake, on cake filtration', a PhD Thesis, University of Bradford (1992)
17. Kozicki, W., Tiu, C. and Rao, A. R. K., 'Filtration of non-Newtonian fluids', *The Canadian Journal of Chemical Engineering*, **Vol. 46**, October, 313–321 (1968)
18. Machač, I. and Crha, B., '*Koláčová filtrace z nenewtonské kapaliny*', *Chem. Prům.*, **38**, 621 (1988)
19. Machač, I., Cakl, J., Comiti, J. and Sabiri, N. E., 'Flow of non-Newtonian fluids through fixed beds of particles: comparison of two models', *Chemical Engineering and Processing*, **37**, 169–176 (1998)
20. Cakl, J. and Machač, I., 'Pressure drop in the flow of viscoelastic fluids through fixed beds of particles', *Collect. Czech. Chem. Commun.*, **Vol. 60**, 1124–1139 (1995)

Bibliography

Friedmann, T. E., Windhab, E. J. and Mayer, G., 'Flow of non-newtonian fluids through compressible porous media in centrifugal filtration', Proceedings Volume I, World Filtration Congress 8, European Federation of Chemical Engineering Event No. 607, organised by The Filtration Society and Elsevier Science, The Brighton Centre, Brighton, UK, 3–7 April 2000, 37–40 (2000)

Oja, M. and Martin, H., 'Filter cake compression: modelling the consolidation period', Proceedings Volume I, World Filtration Congress 8, European Federation of Chemical Engineering Event No. 607, organised by The Filtration Society and Elsevier Science, The Brighton Centre, Brighton, UK, 3–7 April 2000, 53–56 (2000)

Reichmann, B. and Tomas, J., 'Expression dynamics of finest particle suspensions', *Filtration + Separation*, 45–49 (June 2000)

Reymann, S., Koenders, M. A. and Wakeman, R. J., 'Critical modelling parameters in the dead-end filtration process', Proceedings Volume I, World Filtration Congress 8, European Federation of Chemical Engineering Event No. 607, organised by The Filtration Society and Elsevier Science, The Brighton Centre, Brighton, UK, 3–7 April 2000, 25–28 (2000)

10 Cake washing

L. Svarovsky

FPS Institute, England and University of Pardubice, Czech Republic

10.1 Introduction, methods of washing solids

Solid–liquid separation often has to be followed by washing of the separated solids in order to:

1 Remove the last traces of the mother liquor from which the solids have just been separated and which is chemically unacceptable in the product solids or has some undesirable constituents such as dissolved species (e.g. salts) or ultrafine insoluble material.
2 Recover the last traces of the mother liquor (or a dissolved/insoluble constituent) from the solids because it is a valuable product.
3 Clean the solids before disposal, for environmental reasons.

This chapter can be started with a statement identical to that found in chapter 15 because it is equally valid here: 'The ever-increasing demands on product purity and environmental acceptability of waste materials, accompanied by gradual reduction in the quality of raw materials, make washing of solids a frequent and often inevitable choice in process engineering.' The difference here is that, whilst chapter 15 is concerned with countercurrent (as opposed to co-current) washing as a way of interconnecting the stages in a multi-stage washing operation, this chapter is about one of three methods of carrying out the washing in each stage. These methods are:

1 Washing by displacement in cakes (= cake washing).
2 Washing by reslurrying of filter cakes or sediments.
3 Washing by successive dilution.

Any of the above can, of course, be single-stage or multi-stage and, for the latter, co-current or countercurrent. Methods 2 and 3 are similar in that both are based on diluting the solids in the wash liquid except that method 2 starts with a solid mass (filter cake or sediment) and method 3 starts with the solids

still in suspension. Their use and design is relatively simple because they are performed by mixing and refiltration, and the dilution ratios effectively control the washing efficiency (allowing of course for mass transfer where applicable). These two methods are not dealt with separately in this book but method 1, cake washing, requires special attention due to its potentially high washing efficiency and low wash liquid requirement relative to the other two methods in the above list. Another advantage is that it can be carried out *in situ* on an existing filter, with no or little additional equipment.

For coarse, non-porous solids, a quick cake wash by displacement (i.e. whilst the cake is still resting on the filter medium) may be sufficient, performed on thick cakes (for good distribution of the wash). Many different types of filter are suitable for this, other than some vacuum filters with vertical filtration surfaces where the distribution of wash might be difficult. Just about the only things that might prevent a good wash are cake cracking (less likely with coarse solids) and possible holes in the filter medium which will lead to craters forming in the cake during the cake formation and the subsequent preferential passage of the wash liquid through any such craters. Good housekeeping will prevent such problems.

For fine and/or porous solids, longer residence times are needed, the cake permeability is poorer and cake cracking is more likely. (Note that the reduced cake permeability leads to longer residence times to a large extent automatically but if this is not enough, even longer times may be achieved using the 'stop-start' washing.) It is here where the challenge lies and where good design is necessary to optimize the process or even just make it work before resorting to the inevitably less efficient alternative of washing by reslurrying the cake and repeated filtration. Prediction of wash rates, wash times and solute concentration is needed in the design calculations. The following short account of cake washing is focused somewhat more on the washing of fine solids.

10.2 Principle of cake washing, the washing curve

Cake washing can be and is performed on any type of filter, be it pressure, vacuum or centrifugal, as long the wash can be distributed well over the cake surface and the washings can be separated from the filtrate (the latter only if it is necessary for the process). *Figure 10.1* shows cake washing schematically, as a batch process capable of being performed on any scale including that with a laboratory Buchner funnel. The figure also defines some variables used later in this chapter.

As can be seen from *Figure 10.1*, the cake formed by filtration, which may or may not have been dewatered after its formation, is washed by the passage of the wash liquid which is distributed over the cake surface. The wash is usually driven through the cake by the same driving force as the one used for the filtration itself, so, effectively, the wash liquid is filtered through the cake.

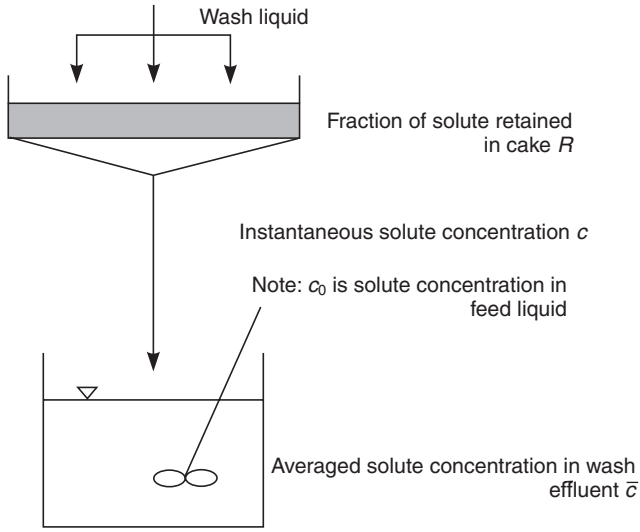

Figure 10.1 Schematic diagram showing some variables during cake washing

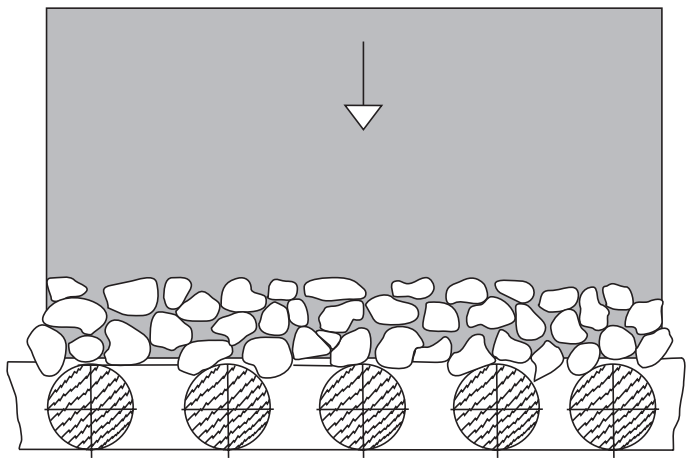

Figure 10.2 Cake washing by displacement

The intention is to drive the mother liquor from the pores in the cake in plug flow, thereby displacing it with the wash liquid as shown schematically in *Figure 10.2*. This is only possible in those pores open to the flow, holding what is called 'free liquid', although some longitudinal mixing inevitably takes place at the interface. The mother liquid held between particles and within them is removed by much slower processes of diffusion and mixing, which often become the rate-determining stages.

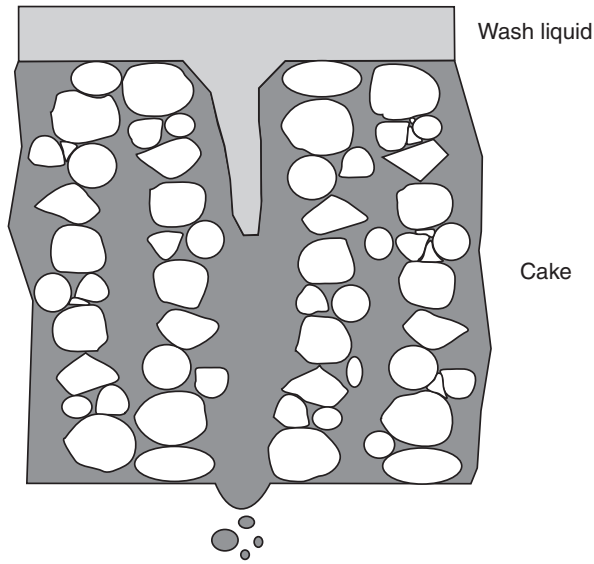

Figure 10.3 Section of cake with mother liquor coming off, before breakthrough

If true plug flow through the cake were possible, only the equivalent of one void volume within the cake, of the wash liquid, would be needed to displace all of the mother liquor from the cake. In a real case, the pores in the cake are not uniform, the structure is unisotropic and longitudinal mixing with diffusion takes place. As shown in *Figure 10.3*, a short period of displacement might take place initially, before the first amount of wash liquid breaks through the largest pores (giving least resistance to flow). Consequently, if the instantaneous concentration of solute in the liquid just coming off the cake is plotted against time or wash volume such as in *Figure 10.4*, there may be a short plateau before the values start dropping. The ideal plug flow curve stays flat, as shown, until the void volume in the cake is displaced by the wash liquid and it then drops to zero. The plug flow displacement is the ideal washing model giving maximum efficiency at a minimum wash requirement. *Figure 10.4* is called a washing curve where the y-axis is the normalized solute concentration in the wash effluent and the x-axis represents the number of filter cake void volumes of wash liquid used (this is also a time axis if the washing is at constant rate).

The washing curve in *Figure 10.4* must not be confused with the plot of the fraction of solute retained inside the cake R plotted against the wash ratio T, shown in *Figure 10.5*. This is of somewhat higher practical use than the washing curve because it relates directly to the quality of the cake and it never has a plateau in it, of course. Washing curves are, however, usually somewhat easier to measure and/or predict. Using mass balance, the R curve can be calculated from the washing curve by integration.

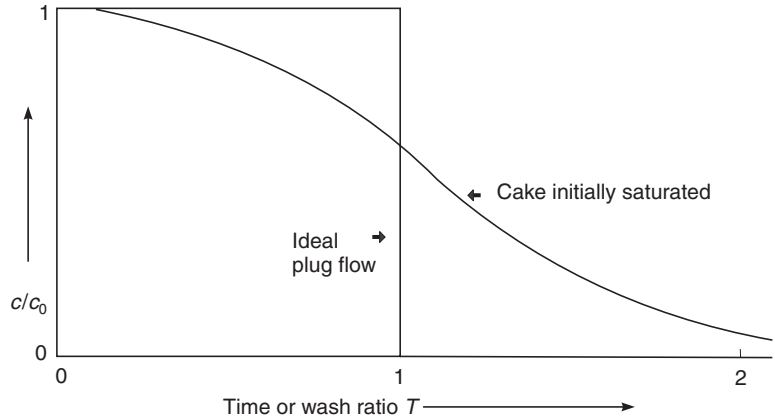

Figure 10.4 A typical washing curve for a cake initially saturated, also showing one for ideal plug flow

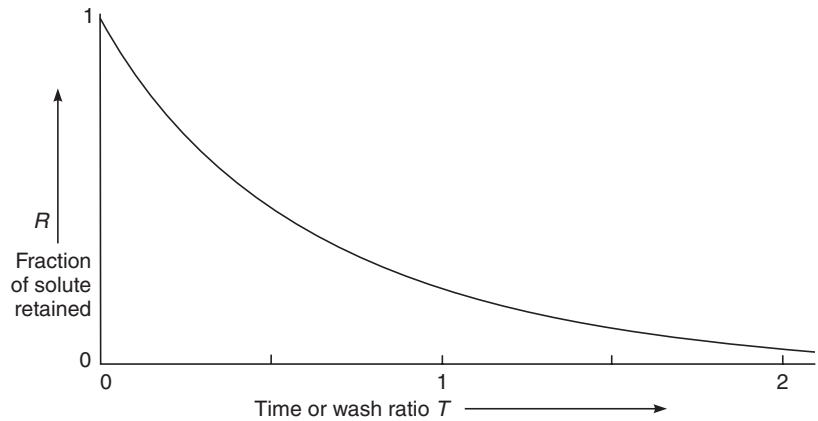

Figure 10.5 The plot of the fraction of solute retained in cake shows no plateau

The shape of the washing curve depends on many variables (as shown later) and one important one is the amount of dewatering done on the cake before washing. *Figure 10.6* shows a case when no dewatering is done, i.e. the cake is full (saturated) of the mother liquor to start with. If the cake is well dewatered, the curve is much lower because much less mother liquor needs to be removed. Partially dewatered cakes would result in curves in between these two.

Clearly, prior knowledge or prediction of the washing curve (or of the R curve) is crucial in the design of the washing operation. It can either be measured experimentally or predicted using theoretical models. As always

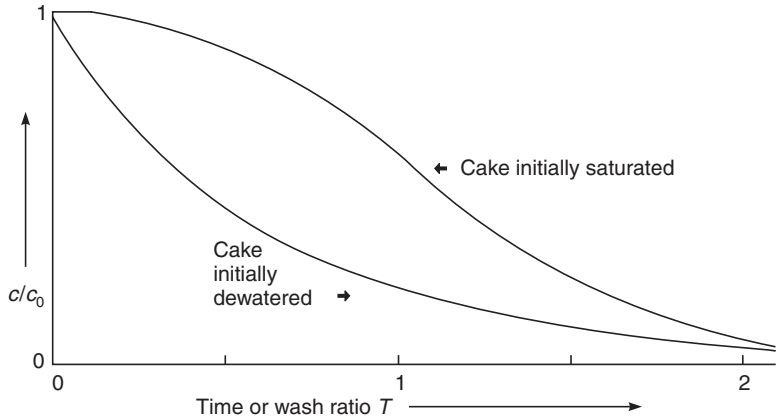

Figure 10.6 Comparison of typical washing curves with saturated and dewatered cakes

in chemical engineering, any tested data is always superior to using predictive models, providing any such tests (be it pilot or laboratory scale) are carried out under the same conditions as those prevailing in the large-scale operation. It might be useful to give a list here of the conditions and variables that are known to affect the washing curves and which have to be kept the same in testing, if at all possible:

1 Flow rate of wash liquid through the cake, usually expressed as the interstitial velocity u (flow rate per unit open area of the cake). The expected wash rates need to be known anyway, in their own right, for the washing process design. Predictions are relatively simple if the wash liquid properties are not too different from those of the mother liquor and if the specific cake resistance (and the medium resistance if not negligible) is known. Measurement of wash rate on an actual cake and medium is relatively simple (Buchner funnel, vacuum leaf, pressure leaf, pressure cell, pilot-scale or full-size filter, etc.).
2 Mother liquor and wash liquid properties such as viscosity, density (both affected by temperature). If non-Newtonian, full rheology should be known. Also solids concentration in the feed before filtration.
3 Solute to solvent diffusivity—see section 10.5.
4 Porosity, structure, initial saturation and homogeneity of the filtration cake, uniformity of its thickness. This depends on many things such as the solids properties making up the cake (particle size distribution, particle shape, particle porosity, specific surface area), the history and direction (with respect to gravity) of the cake formation, degree of dewatering prior to washing, cake pre-compression (if used for smoothing over cracks, for example), etc. When obtaining experimental washing curves,

it is necessary to keep the above cake properties constant and the same as expected to prevail on the large-scale filter. It follows, therefore, that the cake formation in the tests has to follow closely that on the actual filter, it has to use the same solids/liquid system, at the same feed concentration.

5 Washing inefficiencies such as run-off, cake cracking, channelling, bypassing, splashing, frothing, leakage, local blinding of (or holes in) the cloth, furrows in the cake surface which direct the wash liquid flow, wash liquid maldistribution or even inadequate supply of wash liquid.

10.3 Is it always best to dewater before cake washing?

Figure 10.6 indicates that dewatering before washing, for the same wash ratios, leads to better washing. For high wash ratios, however, as needed with fine or porous solids, the difference is much less dramatic than at low ratios. In practice, however, cakes made of fine solids often crack on dewatering by displacement because the air introduced into the cake causes high capillary stresses within the cake. Cake cracking, when it happens, is disastrous in cake washing because, unless the cracks are smoothed over by remedial action of squeezing or rolling over the cake, the wash water flows preferentially through the cracks and thereby by-passes the cake. Cake cracking can be avoided by starting the wash with a fully saturated cake. Therefore, by sacrificing some washing efficiency (or by having to use a little more wash liquid for the same efficiency) one can avoid cake cracking problems altogether.

When cake cracking does not occur or its effects can be neutralized, dewatering before washing is beneficial.

10.4 How much wash liquid is needed?

Depending on the desired reduction of the solute or mother liquor in the cake, the wash ratio required can be read off the R curve directly. This multiplied by the void volume in the cake gives the wash liquid volume needed. One, therefore, needs either the R curve or the washing curve applicable. Note that using mass balance, the R curve can be calculated from the washing curve by integration. Experimental values are superior but, if unavailable, some predictive models exist for this.

The simplest, semi-empirical approach is that of Choudhury and Dahlstrom who studied cake washing of relatively coarse materials on continuous vacuum filters[1]. If E is the washing efficiency defined as the fraction of solute recovered to the filtrate at wash ratio equal to one (i.e. $E = 1 - R$ $(n = 1)$) then the rest of the R curve can be approximated as

$$R(n) = (1 - E)^n \tag{10.1}$$

where R is the mass fraction of the original soluble material remaining in the cake after washing and n is the wash ratio. Choudhury and Dahlstrom found good agreement with experiment for a wash ratio less than 2.1 and experimental values of efficiency from 35 to 86%.

Equation 10.1 is useful for rough estimates of wash liquid requirements for relatively fast washing cakes where no more than $n = 2.1$ is needed. It requires one experimental value of R at $n = 1$. See section 10.6 for an example.

For wash ratios greater than 2.1, more sophisticated models that account for the effects of diffusion have to be used and those predict washing curves as per the next section.

10.5 Can the washing curve be predicted?

Yes it can be estimated from theory if the right data are available but the results are subject to simplifying assumptions, which do not hold in practice. Experimental, direct determinations are always more reliable if carried out under correct conditions.

There has been a great deal of work done in order to describe and model the cake washing process theoretically and an excellent review can be found in ref. 2. Marecek and Novotny[3], for example, divided the washing curve into three regions: an initial displacement region of constant c/c_o, followed by an ideal mixing region where c/c_o decays exponentially and another region, at low concentrations, where diffusion prevails and which is described by another exponential decay. This division is rather artificial, however, as all three processes take place in all three parts of the washing curve with only their dominance shifting somewhat between the parts. The current state of thinking is to regard the whole washing curve as one and the so-called dispersion model is favoured by the scientific community at the moment.

For reasons of clarity in demonstrating the use, a simplified version of the model is shown here, as used by Hermia and Rahier, for example[4]. This is applicable to washing fully saturated cakes containing non-porous solids, at relatively high washing rates, i.e. with more porous cakes and/or at higher applied pressures (high Pe_c see later). For the full model which is more complex mathematically but applied in much the same way, see ref. 2.

The dispersion model takes into account diffusion. In modelling, the Peclet number Pe is used as a ratio of the convective transport to diffusive transport. Here we can define two different Peclet numbers: one for the overall flow in the cake Pe_c and another, Pe_p, for the flow in the vicinity of a particle of an average size x_{av}, characterizing the particles in the cake. The definitions are as follows:

Cake Peclet number is

$$Pe_c = uL/D_L \tag{10.2}$$

where u is the average interstitial wash velocity (flow rate Q per unit free area of the cake, i.e. $u = Q/(\varepsilon \cdot A)$ where ε is cake porosity and A is the surface area of the cake), L is cake thickness and D_L is the axial dispersion coefficient for the solute/solvent system in the cake. This definition of Peclet number indicates the level of dispersion in the cake. When it approaches zero, the bed behaves like a perfect mixing vessel. The perfect plug flow (displacement) would be characterized by $Pe_c \rightarrow \infty$.

Particle Peclet number is

$$Pe_p = ux_{av}/D \tag{10.3}$$

where D is the molecular diffusion coefficient for the solute/solvent system and x_{av} is an average particle size, usually taken as the surface/volume diameter.

As may be expected, Pe_c depends on Pe_p and this was studied by many workers. Wakeman and Attwood[5], for example, found the following relationship for relatively thin cakes (up to 10 cm) of fine particles:

$$D_L/D = 0.707 + 55.5Pe_p^{0.96} \tag{10.4}$$

The first term represents the effect of molecular diffusion and that dominates up to about $Pe_p = 0.005$ whilst the second term, for convective dispersion, dominates for higher Pe_p numbers.

The dispersion model derived from theory gives the following predictive equation for the washing curves, for fully saturated cakes washed at relatively high rates[4]

$$\frac{c}{c_o} = 0.5\left[1 + \text{erf}\left(\frac{1-n}{2n^{1/2}}Pe_c^{1/2}\right)\right] \tag{10.5}$$

where the erf function is defined as

$$\text{erf}(z) = \frac{2}{\sqrt{\pi}}\int_0^{z_0} e^{-t^2}dt \tag{10.6}$$

and this can be computed numerically or determined from tables.

10.6 An example of a cake washing calculation

Estimate the time and rate of washing of an initially saturated cake formed at constant pressure of 5 bar on a batch pilot pressure filter of filtration area equal to 0.5 m^2. Washing is to be done at the same pressure as filtration, the washing efficiency was determined experimentally at 77%, the required solute reduction in the cake is 95% and the wash liquid is pure water. The mother liquor is an aqueous solution of salt and other constants are as follows:

molecular diffusion coefficient for the salt in water	$D = 1.5 \times 10^{-9}\ \mathrm{m^2/s}$
specific cake resistance	$\alpha = 1.07 \times 10^{11}\ \mathrm{m/kg}$
cake porosity	$\varepsilon = 0.24$
medium resistance	$R_\mathrm{m} = 6.5 \times 10^{10}\ \mathrm{l/m}$
feed solids concentration	$c_\mathrm{s} = 105.2\ \mathrm{kg/m^3}$
solids density (solids are non-porous)	$\rho_\mathrm{s} = 2600\ \mathrm{kg/m^3}$
water density	$\rho = 1000\ \mathrm{kg/m^3}$
water viscosity	$\mu = 0.001\ \mathrm{Ns/m^2}$
volume of suspension filtered to form the cake	$V_\mathrm{s} = 0.028\ \mathrm{m^3}$

Solution

1 Try the simple approach by Choudhury and Dahlstrom[1] in equation 10.1 which for $E = 0.77$ and $R = 1 - 0.95$ gives $n = \ln(0.05)/\ln(0.23) = \mathbf{2.0}$. This is within the applicability of this simple approach and $n = 2$ is, therefore, our first estimate of the wash ratio needed.

2 Equation 10.5 can be used to predict the washing curve but the washing rate has to be determined first, from the cake and medium resistance, using the general filtration equation 9.5 for $\Delta p = 5$ bar. As the mother liquor and the washing liquid have the same properties, the washing rate is equal to the final rate of filtration when the cake has been formed (i.e. after $0.028\ \mathrm{m^3}$ of the feed suspension has been filtered). The sequence of the calculations is as follows:

mass of solids in cake: (assuming total solids removal)	$0.028 \times 105.2 = 2.95\ \mathrm{kg}$
volume of solids in cake:	$2.95/2600 = 1.13 \times 10^{-3}\ \mathrm{m^3}$
volume of voids in cake:	$1.13 \times 10^{-3} \times (0.24/0.76) = 0.36 \times 10^{-3}\ \mathrm{m^3}$
total volume of cake:	$(0.36 + 1.13) \times 10^{-3} = 1.49 \times 10^{-3}\ \mathrm{m^3}$
cake thickness for area $A = 0.5\ \mathrm{m^2}$	$1.49 \times 10^{-3}/0.5 = 2.98 \times 10^{-3}\ \mathrm{m}$

final filtration rate (= flow rate of wash liquid):

$$Q = \frac{5 \times 10^5 \times 0.5}{0.001 \times (1.07 \times 10^{11} \times 2.95/0.5 + 6.5 \times 10^{10})} = 3.60 \times 10^{-4}\ \mathrm{m^3/s}$$

average interstitial wash velocity $u = 3.60 \times 10^{-4}/(0.24 \times 0.5) = 3.00 \times 10^{-3}\ \mathrm{m/s}$

mean particle size (from equation 9.36 and assuming spherical particles for which $S_\mathrm{o} = 6/x_\mathrm{av}$)

$$x_\mathrm{av} = \left[\frac{180(1 - 0.24)}{1.07 \times 10^{11} \times 2600 \times (0.24)^3}\right]^{0.5} = 5.96 \times 10^{-6}\ \mathrm{m}$$

(note that the result at 6 microns seems very fine but this is the surface/volume diameter which is the arithmetic mean of a distribution by surface and that is always finer than by mass)

particle Peclet number Pe_p (equation 10.3)	$3.00 \times 10^{-3} \times 5.96 \times 10^{-6}/1.5 \times 10^{-9} = \mathbf{11.9}$
axial dispersion coefficient D_L	$1.5 \times 10^{-9}(0.707 + 55.5 \times (11.9)^{0.96}) = \mathbf{8.99 \times 10^{-7} m^2/s}$
cake Peclet number Pe_c (equation 10.2)	$3.00 \times 10^{-3} \times 2.98 \times 10^{-3}/8.99 \times 10^{-7} = \mathbf{9.93}$

and this now allows calculations of the cake washing curve with equation 10.5, giving the following table of results, also plotted in the graph below.

wash ratio n	0.25	0.50	0.75	1.00	1.50	2.00	2.50	3.00
c/c_0	1.000	0.942	0.738	0.500	0.183	0.058	0.017	0.005

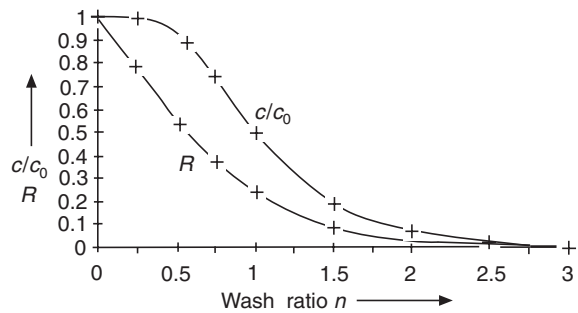

Figure 10.7 The washing curve and the *R* curve predicted in the example in section 10.6

(Note that the simplified model used here requires a high Pe_c and this is reasonably satisfied with the value of 9.93 here. Also note that the simplified model always comes up with $c/c_0 = 50\%$ at $n = 1$ for all values of Pe_c. The full model would in this case give a somewhat lower value at $n = 1$ (about 45%) but the effect on the rest of the washing curve would be small).

Using mass balance, the fraction of solute remaining in the cake R can now be calculated by integration, following equation 10.7:

$$R(n) = 1 - \frac{\int_o^n \left(\frac{c}{c_0}\right) \mathrm{d}n}{\int_0^\infty \left(\frac{c}{c_0}\right) \mathrm{d}n} \tag{10.7}$$

Figure 10.7 also gives the fraction of solute remaining in cake R as computed with equation 10.7 from the washing curve. In the present example, wash ratio n corresponding to $R = 0.05$ is sought and the result is about $n = 1.75$. The total theoretical amount of wash liquid needed is, therefore, the void volume times the wash ratio $0.36 \times 10^{-3} \times 1.75 = 0.63 \times 10^{-3}\,\mathrm{m}^3$ whilst the washing time is $0.63 \times 10^{-3}/3.60 \times 10^{-4} = 1.75\,\mathrm{s}$.

If the value of $n = 2$ is taken from the semi-empirical approach[1] under the first paragraph of the above solution, both the wash liquid required and the washing time would increase proportionately. As the washing efficiency predicted by theory (see *Figure 10.7*) of $E = 76.9\%$ is close to the experimental value given, the simple approach by Choudhury and Dahlstrom[1] gives in this case a somewhat more pessimistic result than the full dispersion model.

Final remarks: Wakeman and Attwood[5] published pre-calculated graphs of washing curves c/c_0 and fractions retained R as functions of $\mathrm{Pe_c}$ but these are unnecessary nowadays, given the ease of computing using packages such as spreadsheets (e.g. in the above example) for the full calculation. Even the erf function is now widely available in spreadsheets such as Excel, for example.

The above example of predictive cake washing might create false feelings of security. The theory it is based on makes such a predictive calculation very much an academic exercise, based on many simplifying assumptions, dubious data, not enough experimental verification and not including practical, efficiency-reducing effects such as run-off, splashing and cake cratering/cracking. One of the important data required is the molecular diffusivity, which is difficult enough to find even for idealized, clean solvent/solute systems. If this diffusivity needs to be tested in order to enable a predictive calculation, it may be argued that, given the many limitations of the available theory, it is much better to test the washing process directly. As the nature of the cake is so important to the washing that follows, such testing has to be done in conjunction with testing and controlling the cake formation process itself, on the same filter medium and at identical operating conditions as expected in the large-scale process.

10.7 Cake washing on continuous filters

Figure 10.1 represents batch washing. The average solute concentration in wash effluent at any time (or wash ratio) can be calculated from the washing curve using the following equation (if washing with a clean wash liquid):

$$\frac{\bar{c}}{c_0} = \frac{1}{n}\int_0^n \frac{c}{c_0}\,\mathrm{d}n \tag{10.8}$$

and this very same equation also applies to the output washings from the washing zone of a continuous filter, where n is now a fixed value (if the conditions in the washing zone are steady state). The value of n is determined

from the rate of the washings coming off the washing zone to the rate of passage of the void volume in the cake through the same zone. When doing laboratory batch tests to obtain washing characteristics for continuous filters, therefore, it is advantageous to measure time-averaged values of solute concentration directly rather than the instantaneous concentrations as the liquid emerges from the cake, as shown in *Figure 10.1*. An even better alternative, in the experience of the author, is to use a continuous pilot filter where any such experiments have a much closer relevance and where operating experience can also be gained at the same time.

Continuous filters, particularly the vacuum variety, often suffer from maldistribution and run-off of the washing liquid, and the wash liquid demand is sometimes dominated by such inefficiencies. Wakeman[6] reported an experimental study of these effects on drum filters and, in spite of some inevitable data scatter, found interesting relationships, correlated these with batch leaf tests and proposed calculation methods to predict the effects from leaf test data.

10.8 Practical considerations

Some practical observations, to a large extent borne out by theory (equation 10.6), are that:

1 Thicker cakes can be washed more effectively but thinner cakes are required for high cake production capacity. A compromise has to be struck in practice unless one or the other operation has a clear priority.
2 For cake thickness less than about 30 mm, the thickness has a major influence on washing.
3 For cake thickness less than about 20 mm, both the thickness and the pressure drop are important.

When a filter press is employed, however, it has been shown[4] that cake thickness has an insignificant effect on washing efficiency. As a result, Hermia[4] has argued that, contrary to common belief, simple washing in filter presses has a similar washing efficiency to thorough washing which, performed on cakes twice in thickness than simple washing, suffers from four times slower washing rates. Bottom feeds are reported to reduce the detrimental effects of particle settling inside the frames on cake homogeneity and the subsequent washing problems. Hermia also recommends gentle pre-compression of filter cakes, with rubber membranes fitted in some filter presses, which improves cake homogeneity and closes any cracks.

Whether the estimates of wash liquid requirements are based on experimental or predicted washing curves, these are for the washing operation only and do not include the amounts needed to fill pipework, feed vessels (if any), pumps and receivers. A suitable allowance has to be made.

Further allowances have to be made for any of the following effects that have an effect on washing characteristics of cakes: uneven cake thickness and structure, cracking, channelling, bypassing, splashing, frothing, leakage, local blinding of (or holes in) the cloth, furrows in the cake surface which direct the wash liquid flow, wash liquid maldistribution or even inadequate supply of wash liquid.

References

1. Choudhury, A. P. R. and Dahlstrom, D. A., *AIChE J*., 433 (1957)
2. Marecek, J. and Novotny, P., 'Optimising the performance of leaf filters', *Filtration & Separation*, January/February, 34–40 (1980)
3. Rushton, A., Ward, A. S. and Holdich, R. G., *Solid–Liquid Filtration and Separation Technology*, VCH, Weinheim (1996)
4. Hermia, J. and Rahier, G., 'Designing a new wort filter, underlying theoretical principles', *Filtration & Separation*, November/December, 421 (1990)
5. Wakeman, R. J. and Attwood, G. J., *Filtration & Separation*, **25**, 272 (1988)
6. Wakeman, R. J., 'Washing thin and nonuniform filter cakes: effects of wash liquor maldistribution', *Filtration & Separation*, March, 185–190 (1998)

Bibliography

Gucbilmez, Y., Tosun, I. and Yilmaz, L., 'Analysis of mass transfer for washing of unsaturated filter cakes', Proceedings Volume I, World Filtration Congress 8, European Federation of Chemical Engineering Event No. 607, organised by The Filtration Society and Elsevier Science, The Brighton Centre, Brighton, UK, 3–7 April 2000, 307–310 (2000)

Hartmann, K. and Kiselev, V., 'Novel technology for intensive washing, drying and sterilisation of filter cakes', Proceedings Volume I, World Filtration Congress 8, European Federation of Chemical Engineering Event No. 607, organised by The Filtration Society and Elsevier Science, The Brighton Centre, Brighton, UK, 3–7 April 2000, 284–287 (2000)

Lihong, S., Qiuyu, Z., Huayu, Q. and Rongchang, N., 'Filter cake washing process mathematics-physics', Proceedings Volume I, World Filtration Congress 8, European Federation of Chemical Engineering Event No. 607, organised by The Filtration Society and Elsevier Science, The Brighton Centre, Brighton, UK, 3–7 April 2000, 311–314 (2000)

Linden, M., Norrgard., G., Forsell, T., Allenius, H. and Ekberg, B., 'Cake washing performance of the Ceramec filter—from laboratory to full scale', Proceedings Volume II, World Filtration Congress 8, European Federation of Chemical Engineering Event No. 607, organised by The Filtration Society and Elsevier Science, The Brighton Centre, Brighton, UK, 3–7 April 2000, 1137 (2000)

Salmela, N. and Oja, M., 'The effect of starch compressibility of different starches on starch washing and dewatering', Proceedings Volume I, World Filtration Congress 8, European Federation of Chemical Engineering Event No. 607, organised by The Filtration Society and Elsevier Science, The Brighton Centre, Brighton, UK, 3–7 April 2000, 288–291 (2000)

11 Methods for limiting cake growth

L. Svarovsky

FPS Institute, England and University of Pardubice, Czech Republic

11.1 Introduction

This is an area of solid–liquid separation which has enjoyed considerable interest recently, although the basic concept is an old one. In conventional cake filtration, a cake is allowed to form on the filter medium and this gradually increases resistance to flow, leading to increasing time or pressure requirement for filtration of a given volume of slurry.

The flow rate of the liquid through the medium can be maintained high if no, or little, cake is allowed to form on the medium. Most of the methods used for such limitation of cake growth lead to mere thickening of the slurry. The cake can be prevented from forming by hydraulic or mechanical means and such operation can be carried out over either a part or the whole of the filtration cycle. The methods for limiting cake growth vary in the extent of their commercial exploitation; their general classification is as follows:

1 removal of cake by mass forces (gravity or centrifugal) or electrophoretic forces tangential to or away from the filter medium;
2 mechanical removal of the cake by brushes, liquid jets or scrapers;
3 dislodging of the cake by intermittent reverse flow;
4 prevention of cake deposition by vibration;
5 cross-flow filtration by moving the slurry tangentially to the filter medium so that the cake is continuously sheared off.

The above-listed methods are briefly described in the following, with particular reference to known commercial exploitation whenever applicable. As most of the concepts are relatively new, a greater use of references than usual is made to enable the reader to follow up any topic of interest.

11.2 Removal of cake by mass forces

This is a method of limiting cake growth through the action of gravity, centrifugal or electrophoretic forces, which act on the particles either tangentially to, or away from, the filter medium. *Figure 11.1* shows the method schematically on a gravity 'side filter' which has a vertical filter medium. The filtrate flow is essentially horizontal and this results in a horizontal drag force on the particles. Additionally, the particles are subjected to a gravity force pulling them down. This effect takes place both in the main body of the suspension where it leads to gravity settling and in the cake that forms on the face of the medium. Whether or not the particles deposited on the medium will fall off depends on the relative magnitude of the forces and the angle of friction between the particles and the filter medium. In the case of a gravity system, if the filter were to be operated continuously, this would only work with relatively coarse particles with a high mass-to-surface ratio. It is quite practicable, though, in an intermittent system where the cake is first formed in a conventional way and the feed is then stopped to allow gravity removal of the cake. Henry *et al.*[1] described and studied a similar system of pressure filtration of 2.5–5 μm particles (in the neutralized acid mine drainage water) in vertical hoses where a pressure shock associated with relaxing the pressure in the hose was used to aid cake removal.

While a system similar to that shown in *Figure 11.1* may be impractical under gravity, it is used in a centrifugal field as the 'bypass filtration'. Zeitsch[2] describes the side filter centrifuge, which combines the conventional centrifugal filtration on the cylindrical basket with filtration through the sides, as sometimes incorporated in peeler centrifuges. He laid down the theoretical basis of the side filtration process and showed that the side filters reduce the filtration time to less than 35% of the normal value. To take the concept a step further, Zeitsch also described and patented[3] a planetary filter centrifuge, which has two or more baskets rotating about their own axes and both

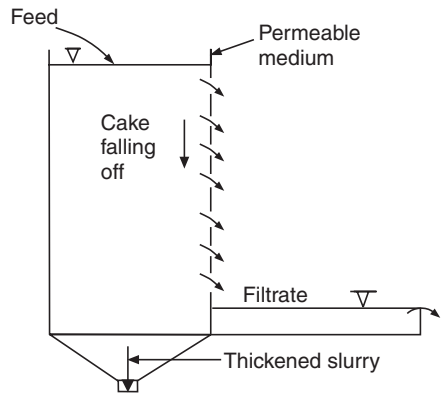

Figure 11.1 A gravity side filter

spinning on arms around a parallel central axis. This arrangement, under certain operating conditions, gives rise to centrifugal forces on the particles which keep a portion of the medium free of particles and thus allow the filtrate to bypass the cake. While this is certainly an attractive concept it remains to be seen whether it will find wider application in practice. Another method of keeping particles away from the filtration medium is by using electrophoretic forces in 'electrokinetic filtration'[4]. This is achieved by application of a d.c. voltage between two electrodes, one on either side of the filter medium. The electrical charge on the upstream electrode is opposite to that carried on the surface of the particles (zeta potential). The rate of cake formation is reduced by electrophoresis and at the same time the rate of permeation is increased by electro-osmosis occurring inside the filter cake. The theoretical basis of electrokinetic filtration has been studied and examined experimentally in Japan[4]; for a given electric field strength E the filtrate volume V is related to electric power consumption W_p by an empirical equation[4]:

$$V = a \cdot W_p^n \tag{11.1}$$

where a and n are experimental constants. There is an optimum field strength because cake resistance decreases and electric power consumption increases with increasing E.

11.3 Mechanical cake removal

This is a method by which the cake is prevented from forming by the mechanical action of brushes, scrapers or liquid jets. Tiller[5] showed theoretically that the capacity of a drum or belt filter can be increased by using brushes to keep the cake off a portion of the available filtration surface, with the remaining portion used for normal filtration of the thickened slurry. The reduction in filter area available for cake formation need not lead to reduction in solids handling capacity because the thicker slurry would give faster cake build-up. This method has not caught on in practice, with the exception of the scraping action of the turbine rotors used in the American version of the dynamic filter (see section 11.6).

11.4 Dislodging of cake by reverse flow

This is a method limiting cake thickness by intermittent back-flushing of the filter medium, as reported by Muira[6] and Brociner[7], for example. Conventional vacuum or pressure filters can be used with some modifications for the effects of the forces of the back-flush. Thus filtering through thin cakes in short cycles can be used.

One commercial application of this principle is the Ebclear filter (Applied Products Corp.), shown schematicallly in *Figure 11.2*. This consists of a

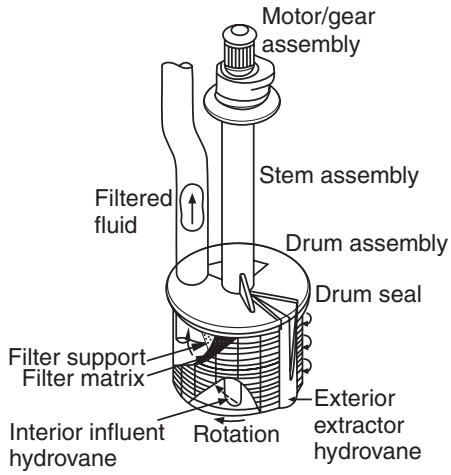

Figure 11.2 Ebclear filter (Courtesy of Applied Products Corp.)

rotating filter basket under vacuum, with particle deposition on the outside surface. The filtration flow is also assisted by interior fixed vanes, and periodic cake removal is accomplished through the hydrodynamic action of an external fixed vane which momentarily reverses the flow. The dislodged cake flies off due to the centrifugal acceleration of more than 20 g. Units up to 5 $m^3\,h^{-1}$ are available and can be simply dipped into an existing tank or a pond.

11.5 Prevention of cake deposition by vibration

Vibration is another means of preventing formation of a dense filter cake. An example of a commercial application of this principle is the tubular pressure filter reported elsewhere[8]. It consists of elements of three 38 mm (1.5 in) diameter tubes enclosed in a cylindrical housing, with the elements being pneumatically vibrated. The high-frequency, low-amplitude vibration leads to slurry agitation, cuts premature blinding and helps the dislodging of the solids during backwash which is used to follow the filtration cycle. The filter is designed for pressures up to 10 bar and flow rates up to 1.3 $m^3\,h^{-1}$, its applications include filtration of paper-coatings, colloidal gels and ceramic slips.

Sawyer[9] has patented a similar pressure filter, also tubular, in which the filter blanket in the form of a membrane is constantly cleaned by a sonic sinusoidal wave. This is induced by a transducer which is affixed to the tubular wall at an antinodal point and which causes cavitation and continuous cake removal within the annular filtration chamber. This invention is specifically related to the membrane process of filtration, such as ultra-filtration reported in the following section.

11.6 Cross-flow filtration

This is another, and certainly the most popular, method of limiting cake growth in which high relative velocities of the suspension with respect to the filter medium, and parallel with it, are induced (*Figure 11.3*). The slurry forces in the flow close to the medium continuously remove a part or the whole of the cake and mix it with the remaining suspension. As more and more of the filtrate is removed from the slurry, the latter gradually thickens and may become thixotropic. Surprisingly, a higher solids content in the final slurry can sometimes be obtained than with the conventional pressure filters (by as much as 10 or 20%). Kaspar *et al.*[10] suggested a range of velocity gradients from 70 to 500 s^{-1} which, depending on the suspension properties, are necessary to prevent cake formation and to keep the thickening slurry in a fluid state.

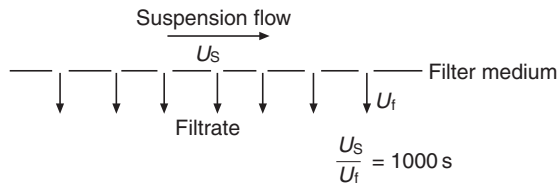

Figure 11.3 Principle of cross-flow filtration

Depending on how the relative velocity of the fluid and the filter medium is achieved there are two basic methods of cross-flow filtration: by using rotating elements (which may or may not carry the filter medium) in a stationary vessel, or by pumping the slurry through pipes made of permeable medium.

11.6.1 Cross-flow filtration with rotating elements

The first literature reference to this principle is in a patent by Morton[11]. His was a cylindrical rotating filter element mounted in a cylindrical pressure vessel, and the suspension was pumped into the annulus between the rotor and the stator. This is just one possible arrangement; the British Patent Specification by Kaspar *et al.*[10], first filed in 1964, covers virtually all possible arrangements in this category. *Figure 11.4* gives an example of one principle of a 'dynamic' filter, which comprises a pressure vessel filter with a hollow shaft and a hollow filter leaf attached to the shaft. The slurry is continuously fed at a constant rate into the vessel via the inlet; the filtrate passes through the rotating filter medium and out through the hollow shaft while the thickened slurry is discharged via a control valve that is used to maintain optimum slurry concentration.

As can be seen from the principle in *Figure 11.4*, the cake removal by fluid shear is aided by spinning off the cake under the centrifugal action. Kaspar

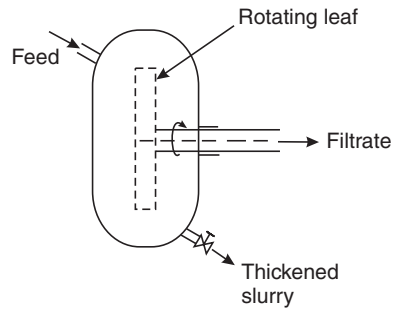

Figure 11.4 Kaspar's dynamic filter

et al.[10] also described alternative arrangements with stationary filtration media and rotating discs to create the shear effects, rotating cylindrical elements, etc. and also showed how such filters can be used for cake washing.

Since its conception by Kaspar *et al.* there have been several published reports of developments of the dynamic filter. Most European designs (*Figure 11.5*) pass the slurry through a series of stages which have both stationary and rotating filter surfaces. Such filters have been found, for the same moisture content of the final slurry, to be 5–25 times more productive[12] (in terms of mass of dry cake per unit area and time) than filter presses; in several cases the moisture content with the dynamic filter was lower and the productivity was 5–10 times greater than with a filter press. The maximum productivity was achieved with peripheral disc speeds of 2.8–4.5 m s^{-1}.

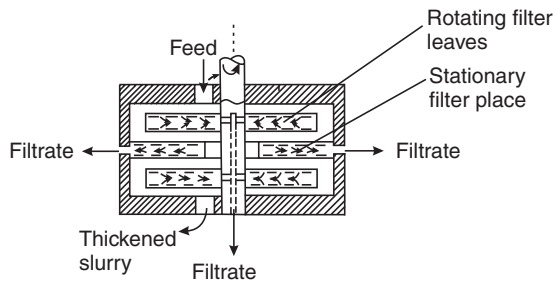

Figure 11.5 European dynamic filter (only two stages shown)

The so-called 'axial filter', developed in the Oak Ridge National Laboratory[13], is remarkably similar to Morton's and Kaspar's dynamic filter in that the filter leaf is in the tubular form and the outer shell is also cylindrical. An ultra-filtration module based on this principle has also been described more recently[14]. Unlike the European dynamic filters referred to in the previous paragraph, however, this filter is not suitable for scale-up because it poorly utilizes the available space. The Escher–Wyss pressure filter described[15] (identical copy of this paper also appeared subsequently in *Filtration and Separation*[15]) takes the idea of axial filtration a step further: in

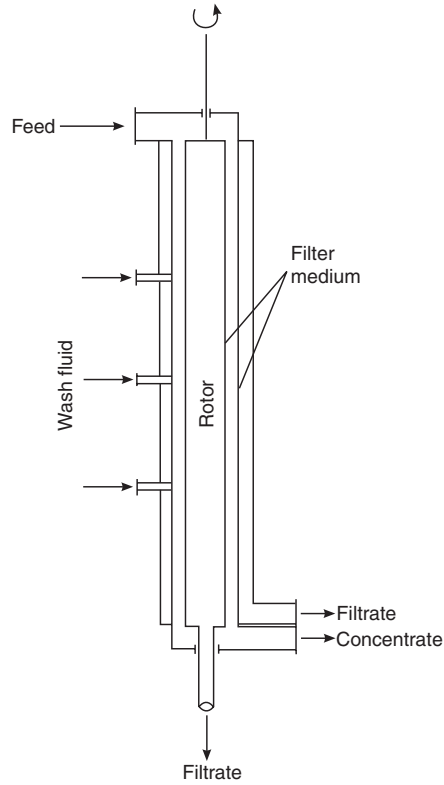

Figure 11.6 Escher–Wyss filter

addition to the cylindrical rotating filter surface, it also provides a stationary outer cylindrical filter surface (*Figure 11.6*) so that the suspension passes through a narrow annulus between the two, and filters through both cylinders. Strategically placed washwater entry points allow continuous and efficient washing (equivalent to reslurrying) if needed. This filter is particularly suitable for intrinsically viscous, plastic or thixotopric slurries.

There are several general disadvantages that apply to all dynamic filters with rotating filter elements. The filter medium is subjected to a centrifugal force and this imposes special requirements on its fastening and stretch resistance. The filtrate is collected into a rotating element radially inwards, i.e. against the centrifugal force, and discharged through the central hollow shaft—this reduces filtering velocities and makes the filter relatively complicated. Finally, any solids that may penetrate through the medium can accumulate inside the rotating element due to centrifugal settling.

These disadvantages can be avoided by replacing the rotating filter elements by solid elements, so as to prevent or reduce cake formation.

The American version of the dynamic filter, known as the 'Artisan continuous filter' (*Figure 11.7*), uses turbine-type elements as rotors and

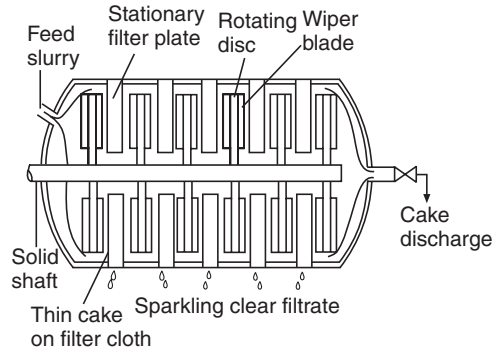

Figure 11.7 Artisan continuous filter (Courtesy of Artisan Industries Inc.)

filtration medium only on the stationary surfaces. This arrangement gives less filtration area per volume of the pressure vessel (productivities up to 5 times those with conventional machines are claimed) but provides a better control of cake thickness. At low speeds the cake thickness is governed by the clearance between the scraper and the filter medium on the stationary plate while at higher speeds part of the cake is swept away and a thin layer remains to act as the actual medium. Tiller *et al.*[16–18] published results of their work with this type of filter, producing cakes with 1 mm thickness using 3 mm clearance. They found that the cake formed on the medium was generally stable, thus giving high filtration rates over long period of time. The precoat-type cake did not blind with time and there was generally no evidence of size selectivity of the process (with the exception of conventional filter aids, which are preferentially picked up by the rotating fluid). This was attributed to inertial bypassing of the cake by larger particles and re-entrainment of the smaller ones. Good control of the agitator speed and operating pressure was recommended in order to maintain a balance between the overall filtration and the slurry flow rates, so that the critical mud concentration and excessive torque are avoided.

The energy going into the agitation converts into heat and thus the extruded cake may be quite hot, 50–80 °C. This makes the final product adaptable to drying. Little information exists about power requirements but in a discussion following one paper (reference 18, p. 598) a favourable comparison with a solid bowl centrifuge, used with the same calcium carbonate slurry, is quoted.

Murkes[19] has reported tests with the same 'American' dynamic filter, except that he eliminated cake formation altogether by spinning the discs faster. No visible abrasion of the medium was observed while the filtration velocities could be maintained high even at relatively low pressures, below 5 bar. Murkes showed clearly the effect of speed and number of rotor vanes on filtration velocities and specific energy input. His results show, for any number of rotor vanes, an increase in specific energy input (kWh per m^3 of filtrate) with rotor speed; this increase can be minimized by optimization of

the number of vanes, but not eliminated. This does not justify the use of higher speeds in terms of running costs but a saving can be made in capital expenditure because a smaller filter can be used for the same capacity.

11.6.2 Cross-flow filtration in porous tubes

This is a method of limiting cake growth by pumping the slurry through porous tubes at high velocities, so that the ratio of the axial flow velocity to filtration velocity through the tube walls is of the order of thousands. This is in direct analogy with the now well-established process of ultra-filtration applicable to much finer solids, which itself borders with reverse osmosis on the molecular level. It is therefore appropriate to review briefly the latter and then to follow on with ultra-filtration and, finally, with the relatively recently explored cross-flow filtration in porous tubes.

11.6.2.1 Analogy with reverse osmosis

The reverse osmosis process, also known as 'hyperfiltration', is based on the passage of solvent molecules through a dense membrane from a concentrated solution to a dilute one. As this process is opposed by osmotic pressure, the pressure drop across the membrane must be higher to overcome it. *Figure 11.8* shows how simple the process is in principle. The solution is pumped over a membrane held on a permeable support and it is split into the solvent (permeate) and concentrate streams.

The osmotic pressure which has to be overcome depends on the concentration of the solution and on the nature of the solutes. As the osmotic pressure increases with concentration, the rate of permeation of the solvent diminishes as the concentrate thickens and it is not economically viable to aim at above a certain concentration[20] (5% for NaCl and 30% for a sugar solution, for example). The usual operating pressures are 40–50 bar giving solvent flux anywhere between 2 and 40 $l\,m^{-2}\,h^{-1}$, depending on the solution and the membrane used. Most membranes are made of cellulose acetate or its close relatives and they usually allow a limited solute passage in order to obtain reasonable permeate flow rates.

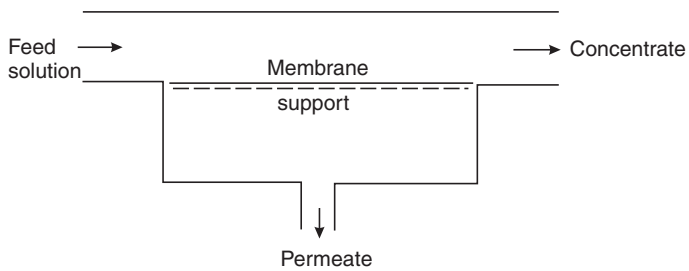

Figure 11.8 Principle of reverse osmosis

Although known for over two decades, reverse osmosis has only been accepted commercially in the last ten years, mainly due to the development in membrane technology. It is now used on a large scale in portable water treatment, for desalination of sea water, for concentration of sulphite-spent liquor and generally as a pre-concentration step before evaporation or thermal processing. There is a wide energy margin in favour of reverse osmosis as compared with evaporation[20] but the final concentrations economically achievable are limited. The types of equipment used are the same as in ultra-filtration that follows.

11.6.2.2 Ultra-filtration

There is no distinct limit between reverse osmosis and ultra-filtration but the latter employs lower pressures of no more than 10 bar (seldom above 6 bar) and more open membranes for separation of large molecules and ultra-fine, sub-micron solids. Henry[21] tried to make a clear distinction between ultra-filtration and cross-flow filtration by defining the former as retention of only dissolved species from solutions (as opposed to retention of particulate material from suspensions) but this has not caught on in practice, mainly because of the fact that dissolved and undissolved (ultra-fine) solids are often separated together. Thus, ultra-filtration is used for example for the concentration of proteins from low-cost dairy byproducts, or in the separation of emulsified oil and suspended solids from waste waters. In such processes a cake or a layer of gel would form on the membrane and reduce the filtration rates if it were not for the cross-flow characteristics of most designs, in which the suspension flows at high speed across the membrane surface and prevents cake build-up.

The original reverse osmosis and ultra-filtration system was based on traditional plate and frame filter designs, in which modules were made up of spaces and membrane-covered plates mounted in a sandwich fashion, pressed together. *Figure 11.9* gives a schematic diagram of such a module by DDS, which is probably the only major company still using this design.

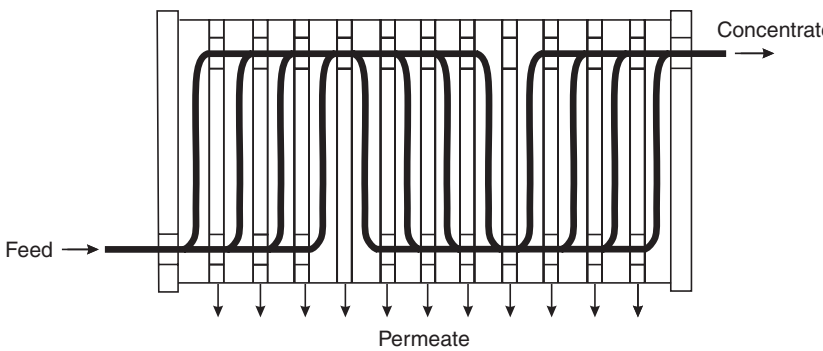

Figure 11.9 The DDS ultra-filtration module—internal flow

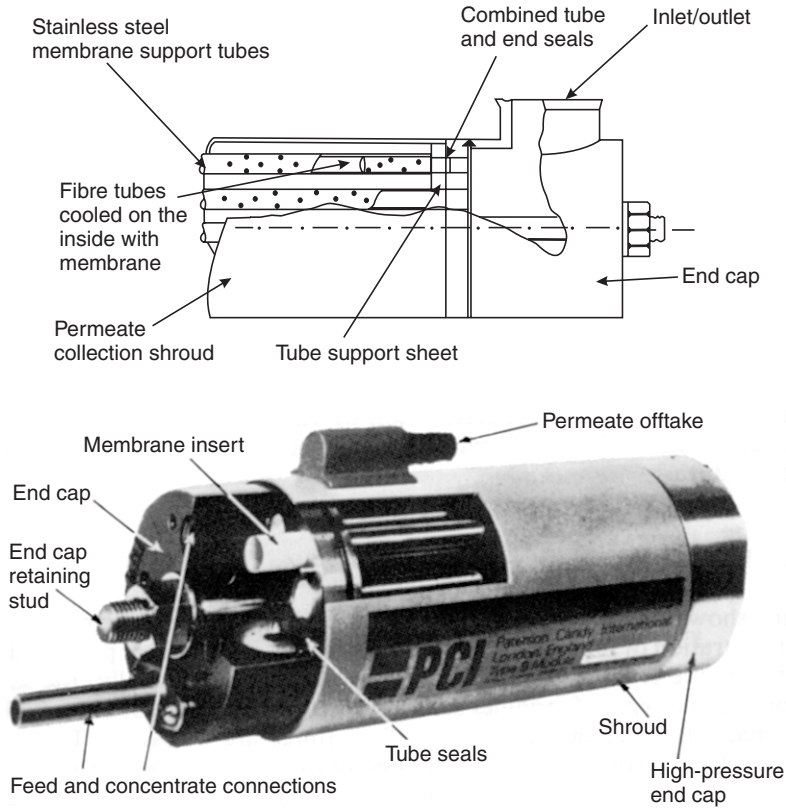

Figure 11.10 Tubular ultra-filtration module (Courtesy of Miller)

This has been largely superseded by the tubular, hollow fibre, spiral and leaf-type systems.

The simplest configuration is the tubular system, shown schematically in *Figure 11.10*. It usually consists of stainless steel membrane support tubes with porous glass fibre backing tubes inside. The very frail membranes are coated on to the inside of the fibre tubes, and several of the complete tubes are connected in parallel in modules which resemble, both internally and externally, a long and thin single-pass shell and tube heat-exchanger. The tubes are commonly 13–26 mm in diameter, easy to clean physically and chemically, and are simple to remove. However, the modules occupy a large area and the liquid hold-up in them is high.

The hollow fibre systems are based on very small-bore tubes cemented at both ends in a wide plastic tube, which also serves as a receiver for the filtrate. A large membrane area can be packed into a small volume, and the liquid hold-up is also reduced. The main disadvantages of the hollow fibres are in their susceptibility to blocking due to the small internal diameters, and difficulties with cleaning.

The spiral and leaf systems both use two rectangular sheets of membrane placed one on top of the other, separated by a porous sheet and sealed together on three sides. In the spiral systems, the fourth sides are separately sealed along a length of a tube which forms a header to receive the permeate from the membranes. With spacers laid on top of the two membranes, the whole sandwich is rolled around the header tube to form a spiral which is sealed into a tubular housing, and the liquid is pumped from one end to the other across the membrane surfaces. In the leaf systems, the double-sheet leaves are attached to a square section metal header common to several leaves so that a whole section resembles a comb. The feed passes along several such sections in series through the teeth of the comb. Both the spiral and the leaf systems have a high surface-to-volume ratio but they can create problems with abrasive materials, are difficult to clean and susceptible to blocking, particularly where the feed contains fibrous matter.

Whatever system is used, high fluid velocities over the membranes must be used. This, coupled with the small rate of permeation through the membrane, makes it impracticable to use a one-pass arrangement and, consequently, the fluid must be recirculated. This is done either on a batch or on a continuous 'feed and bleed' basis. The latter, continuous operation often incorporates two or more 'feed and bleed ' stages with the concentration increasing from the first stage to the last.

In application, ultra-filtration is mostly applied to effluent treatment but the major advantage is using ultra-filtration for recovery of a valuable component which is difficult to recover by other means. Thus details of applications have been published[22] on recovery of electrophoretic paint, protein extraction from cheese whey or from skimmed milk, pre-concentration of starch and enzymes, textile de-sizing, latex concentration, recovery of oil from oil–water emulsions or waste machining and metal-rolling emulsions, recovery of lanolin from wool-scouring effluent, recovery of lignosulphonates from spent sulphite liquor in pulping mills, and concentration of impurities in alkaline cleaning-bath effluents. Ultra-filtration is also used for concentration of viruses. The process of ultra-filtration is still undergoing rapid development and it is certain to have a healthy future.

11.6.2.3 Filtration in porous pipes, cross-flow microfiltration

Having shown the principles of ultra-filtration it is now simple to extend the idea to filtration of more conventional suspensions with coarser particle size, and this is the cross-flow filtration in porous pipes. Essentially, the same equipment and types of modules as in ultra-filtration can be used but thicker flow channels or greater-diameter hollow fibres are necessary. It seems, however, that porous pipe systems represent the most practicable approach here. Zhevnovatyi[23] was first to report the use of porous tubes for cross-flow filtration, in his case for separation of hydrated alumina and red bauxite. Dahlheimer *et al.*[24] published an investigation on concentration of kaolin clay

with woven fibre hoses, and Krauss[25] reported on sewage filtration in permeate hose pipes with the addition of activated carbon. The latest investigation is that of Rushton *et al.*[26], who studied the effect of filtrate velocity on the slurry velocity required for particle transport and examined the separation of particles with porous stainless steel tubes.

If cross-flow filtration in porous tubes is carried out at constant pressure, the permeate flux drops, initially approaching steady state, which ideally would result in a constant rate at which cake deposition and stripping are equal and the resistance of the precoat layer is unchanged. In practice, however, the rate decreases slowly with time and back-flushing[26] or even chemical treatment[27] must be used for clearing the pipes.

The most important parameter in designing the porous tube filtration systems is the ratio of filtrate velocity to pumping velocity because the latter determines the shear rates at the wall and these, in turn, control the rate of cake stripping. In contrast to reverse osmosis and ultra-filtration of large molecules, the permeate flux here is much less dependent on the concentration in the pipe flow and thus higher final slurry concentrations can be achieved.

Theoretical investigations at low permeate fluxes[21] predict the permeate flux to increase exponentially with shear rate

$$J \sim \gamma^m \tag{11.2}$$

The shear rate γ for circular pipes in Newtonian fluids is:

$$\gamma = \frac{8u}{d} \tag{11.3}$$

where u is the average piping velocity and d is the diameter of the pipe. This shows that if the pipe diameter is reduced, a given shear rate or permeate flux can be achieved at lower flow velocity.

Rushton *et al.*[26] derived empirical equations relating the slurry velocity u_s to the permeation velocity u_f in the form:

$$u_s = a + bu_f \tag{11.4}$$

for $MgCO_3$ where constants a and b depend on particle size.

The possibility of using conventional precoating techniques in cross-flow filtration in tubes has also been suggested[26]. With respect to the filtration velocity, Krauss[25] suggested that tubular filtration systems should obtain filtration velocities in excess of $4.72 \times 10^{-5}\ \mathrm{m\,s^{-1}}$ to be economically viable.

A very interesting development of a tubular filter press as a variation of the cross-flow filter took place in the Chemical Engineering Department of the University of Natal in around 1990[28,29]. A prototype of this filter was first constructed and operated at Umgeni Water's Hill Water Treatment Plant near Pietermaritzburg. The filter was later available in Britain from Crossflow Microfiltration Ltd (as 'Exxflow'), further prototypes were tested by Yorkshire Water and an installation made at a new plant at Harrogate, North Yorkshire. The filter consists of several arrays of horizontal tubes hung in

parallel, rather like tubular curtains. The tubes are woven to support membranes coated on the inside of the tubes. Waste-water sludge is pumped under pressure into the tubes at one end while the other end is closed. Filtration takes place in the tubes, partly in cross-flow, leaving the sludge as a solid layer coating inside. The filtered water collects in a tray beneath the tubes.

After the filtration cycle has ended, valves are open at both ends of the tubes and rollers move up and down, squeezing the tubes and breaking the sludge layer on the inside. The dewatered sludge fragments are flushed out of the tube with some of the filtered water, to be collected on a screen. The main problems identified with this filter were tube blockages and low cake recoveries, depending of course on the material filtered. The cleaning systems range from simple stopping of the feed pump (and subsequent flexing of the tubes), internal ball cleaning, water or air jet, roller cleaning with or without reverse flow flushing, to chemical cleaning. Besides the above-mentioned waste-water treatment, applications also include groundwater filtration, removal of selenium from irrigation drainage water, pulp and paper applications, and pre-treatment for reverse osmosis in bleach, biological and textile dyehouse effluents.

The last decade of the twentieth century has generally seen accelerated development in the area of cross-flow membrane microfiltration, as can be seen in a selection of research topics in the Bibliography. This is now a generally accepted term for a separation process for the removal of dispersed matters in sizes ranging from 0.05 to 10 μm from a liquid stream by forcing the liquid through a porous membrane.

Cross-flow microfiltration of dispersions is encountered in a wide variety of engineering applications, such as solid–liquid separation, water purification, and drilling operations. The selection of literature references in the Bibliography is broadly classified into five themes (this is inevitably somewhat biased by the author's interests):

1 A large portion of the recent work is concerned with characterization and testing of membranes for scale-up and selection, as well as with visualization of cake formation. This is particularly strong in the area of ceramic membranes.
2 Studies of process characteristics such as fouling and flux decline, cake properties, concentration polarization and performance with non-Newtonian slurries represent another area of fast development. The non-Newtonian slurries, which exhibit complex rheological behaviour, arise in various industrial applications such as paints, coatings, and joint treatment compounds.
3 There is also a large body of papers which can be characterized as concerned with intensification of the microfiltration process. These are mostly concerned with remedies for fouling, with flux enhancement or reduction of concentration polarization (e.g. by changes in the membrane surface characteristics, by pre-treatment of the feed, by feed flow management, cyclonic flow fields or by using fluidized beds).

4 Separation of biological materials (cells) is another area of fast development and this is at its strongest in clarification of beer (removal or recovery of yeast).
5 Last but not least, there is the mathematical modelling. Models based on the theory of fouling phenomena and concentration polarization, and hydrodynamic models have been developed to predict the steady state permeate flux of cross-flow microfiltration. These models can be loosely categorized as being either based on the film theory or the cake theory. The former is based on convection of matter towards the membrane and diffusion of the retained species back into the cross-flow, possibly incorporating lift forces, and the latter applies Darcy's law to relate filtration rate to average pressure difference between inside the filter and the permeate line. However, these theories do not necessarily consider the influence of all of the operating conditions and their interactions, including temperature, cross-flow velocity, pressure drop, particle size, particle concentration in the dispersion, pH, and electrolyte concentration. For any model to be realistic, it must also be able to show the effects of the dispersion viscosity and particle–particle interactions. In particular, the cross-flow microfiltration behaviour of non-Newtonian dispersions under constant tangential feed and constant inlet pressure conditions is not predicted well by these models and more research in this area is needed.

11.6.3 Conclusion

In conclusion to cross-flow filtration as a unit operation, it is probably the most exciting development in solid–liquid separation yet to be fully explored. Its advantages are in high filtration rates due to minimized particle deposition on the medium without a strong effect of particle size on performance, and in the absence of chemical additives or filter aids in the products.

References

1. Henry, J. D. Jr, Lui, A. P. and Kuo, C. H., 'A dual functional solid–liquid separation process based on filtration and settling, *A.I.Ch.E.*, **22,** 433–441 (1976)
2. Zeitsch, K., 'Centrifugal filtration', ch. 14 in *Solid–Liquid Separation*, ed. by L. Svarovsky, Butterworths, London (1977)
3. Zeitsch, K., Dos. No. 2357 775, Deutsches Patentamt, München
4. Yukawa, H., *et al.*, 'Studies of electrically enhanced sedimentation, filtration and dewatering process', in *Progress in Filtration and Separation*, ed. by R. J. Wakeman, pp. 83–112, Elsevier, Amsterdam (1979)
5. Tiller, F. M., 'Improving filtration rates through delayed cake formation', *29th Res. Conf. Filtration and Separation*, Nagoya, Japan, Soc. Chem. Engrs (Japan) pp. 150–153 (1972)
6. Muira, M., 'Water filtration with the reversible flow filter', *Filtration and Separation*, **4**, 551–554, 556 (1967)

7. Brociner, R. E., 'An improved vacuum leaf thickener for china clay slurries', *Filtration and Separation*, **9**, 562–565 (1972)
8. Ronningen–Petter Div., Dover Corp., *Chem. Eng.*, **80**(6), Mar. 19 (1973)
9. Sawyer, H. T., 'Dynamic self-cleaning filter for liquids', US Patent No. 4158 629, June 19 (1979)
10. Kaspar, J., Soudek, J. and Gutwirth, K., 'Improvements in or relating to a method and apparatus for dynamic filtration of slurries', British Patent No. 10577 015
11. Morton, C. D., 'Method of filtering', US Patent No. 1762 560, June 10 (1930)
12. Malinovskaya, T. A. and Kobrinsky, I. A., 'The separation of finely divided suspensions in a dynamic filter', *Mechanical Liquid Separation (9th Symp.)*, Magdeburg, Oct., pp. 47–51 (1971)
13. Irizarry, M. M. and Anthony, D. B., Ornt-Mit-129, Oak Ridge National Laboratory, 28 April (1971)
14. Hallström, B. and Lopez-Leiva, M., 'Description of a rotating ultra-filtration-module', *Desalination*, **24,** 273–279 (1978); also in: 'Membranes: desalination and waste water treatment', *Proc. 13th Annual Desalination Conf.*, Jerusalem, 8–12 Jan. (NRD 8/78) (1978)
15. Tobler, W., 'Dynamic filtration—the engineering concept of the Escher–Wyss pressure filter, *Escher-Wyss News*, 2/1978–1/1979, pp. 21–23; also in: *Filtration and Separation,* **16**, 630–632 (1979)
16. Tiller, F. M. and Cheng, K. S., 'Delayed cake filtration', *Filtration and Separation*, **14**, 13–18 (1977)
17. Bagdasarian, A., Tiller, F. M. and Donovan, J., 'High-pressure, thin-cake, staged-filtration', *Filtration and Separation*, **14**, 455–460 (1977)
18. Bagdasarian, A. and Tiller, F. M., 'Operational features of staged pressure, thin cake filters', *Filtration and Separation*, **15**, 594–598 (1978)
19. Murkes, J., 'Cake-free filtration in a rotary, high shear filter', *The Second World Filtration Congress*, Filtration Society, London (1979)
20. Pepper, D., 'Reverse osmosis for preconcentration', *The Chemical Engineer*, **339**, 916–918 (1978)
21. Henry, J. D., Jr, 'Cross-flow filtration in recent development', in *Separation Science*, **11**, ed. by N. N. Li, Chemical Rubber Co., Cleveland, Ohio (1972)
22. Bailey, P. A., 'Ultrafiltration—the current state of the art', *Filtration Separation*, **14**, 213–219 (1977)
23. Zhevnovatyi, A. I., 'The thickening of suspensions without cake formation', *Intl J. Chem. Eng.*, **4**, 124 (1964)
24. Dahlheimer, J. A., Thomas, D. G. and Krauss, K. A., 'Application of woven fiber hoses to hyperfiltration of salts and cross-flow filtration of suspended solids', *I.E.C. Proc. Des. Dev.*, **9**, (1970)
25. Krauss, K. A., *Eng. Bull, Purdue University*, **145**, 1059 (1974)
26. Rushton, A., Hosseini, M. and Rushton, A., 'Shear effects in cake formation mechanisms', pp. 149–158. In *Proc. Symp. on Solid–Liquid Separation Practice*, Yorkshire Branch of the I. Chem. E., Leeds, 27–29 March (1979)
27. Zhevnovatyi, A. I., *Zhurnal Prikladnoi Khimii*, **48**, 334 (1973)
28. Joseph, J. B., 'Crossflow microfiltration—a treatment process for potable and waste waters', Paper presented to the Northern Group of the Institution of Water and Environmental Management at Thornaby-on-Tees, 7 December 1988
29. Rencken, G. E., 'Performance studies of the Tubular Filter Press', PhD Thesis, Faculty of Engineering, University of Natal, South Africa (1992)

Bibliography

(a) Characterization and testing of membranes

Cardrew, P. and Byrne, M., 'Scale-up of cross-flow filters: Reducing the risks', *Filtration & Separation*, June, 493–498 (1995)

Mikulášek, P. and Dolecek, P., 'Characterisation of Ceramic Tubular Membranes by Active Pore Size Distribution', *Sep. Sci. Technol*., **29**, 1183 (1994)

Mikulášek, P., Dolecek, P., Rambousek, V., Cakl, J. and Šedá, H., 'Testing of Microfiltration Ceramic Membranes', *Ceramics—Silikáty*, **38**(2), 99 (1994)

Mikulášek, P., Dolecek, P., Šedá, H. and Cakl, J., 'Alumina Ceramic Microfiltration Membranes: Preparation, Characterisation and Some Properties', *Dev. Chem. Eng. Miner. Process*, **2**, 115 (1994)

Wakeman, R. J., 'Visualisation of cake formation in crossflow microfiltration', *Trans. IChemE*., **72A**, 530 (1994)

(b) Process characteristics

Belfort, G., Davis, R. H. and Zydney, A. L., 'The behaviour of suspensions and macromolecular solutions in crossflow microfiltration', *J. Membr. Sci*., **96**, 1 (1994)

Cakl, J. and Mikulášek, P., 'Flux and Fouling in the Cross-flow Ceramic Membrane Microfiltration of Polymeric Colloids', *Sep. Sci. Technol*., **30**, 3663 (1995)

Cakl, J., Šír, J., Medvedíková, L. and Blaha, A., 'Demineralisation of Protein Hydrolysates from Enzymatic Hydrolysis of Leather Shavings Using Membrane Diafiltration', *Sep. Sci. Technol*., **33**, 1271 (1998)

Datta, S. and Gaddis, J. L., 'Dynamic and rheology of fouling cakes formed during ultrafiltration', *Sep. Sci. Technol*., **32**, 327 (1997)

Holdich, R. G., Cumming, I. W. and Ismail, B., 'The variation of crossflow filtration rate with wall shear stress and the effect of deposit thickness', *Trans. IChem*., **73A**, 20 (1995)

Marchant, J. Q. and Wakeman, R. J., 'Crossflow microfiltration of concentrated titania suspensions', *Proc. IChemE Jubilee Research Event*, **Vol. 2**, 1061, Nottingham (1997)

Mikulášek, P., Wakeman, R. J. and Marchant, J. Q., 'Crossflow Microfiltration of Shear-Thinning Aqueous Titanium Dioxide Dispersions', *Chem. Eng. J*., **69**, 53 (1998)

Rautenbach, R. and Schock, G., 'Ultrafiltration of macromolecular solutions and cross-flow microfiltration of colloidal suspensions. A contribution to permeate flux calculations', *J. Membr. Sci*., **30**, 231 (1988)

Rushton, A. and Matsis, V. M., 'Studies of constant rate filtration in dead-end and crossflow modes', *Filtration & Separation*, September/October, 643–646 (1994)

Schulz, G. and Ripperger, S., 'Concentration polarisation in cross-flow microfiltration', *J. Membr. Sci*., **40**, 173 (1989)

Tarleton, E. S. and Wakeman, R. J., 'Understanding flux decline in crossflow microfiltration: Part II—Effects of process parameters', *Trans. IChemE*., **72A**, 431 (1994)

Vassilieff, C. S., Momtchilova, I. G. and Krustev, R. A., 'Cross-flow microfiltration of kaolinite-in-water dispersions', *Colloids Surf*., **A92**, 231 (1994)

Xu-Jiang, Y., Dodds, J. and Leclerc, D., 'Cake characteristics in cross-flow and dead-end microfiltration', *Filtration & Separation*, September, 795–798 (1995)

(c) Methods of process intensification

Dolecek, P. and Cakl, J., 'Permeate Flow in Hexagonal 19-Channel Inorganic Membrane under Filtration and Backflush Operating Modes', *Membr. Sci*., **149**, 171 (1998)

Dolecek, P. and Cakl, J., 'The effect of multichannel membrane geometry on permeate flow in filtration and backflush operational modes', The 25th Conference of the Slovak Society of Chemical Engineering, Jasná, Demänovská dolina, Slovakia, 25–29 May 1998, published in the proceedings (CD ROM by INTERCOMP Services s.r.o. Bratislava)

Dolecek, P., Mikulášek, P. and Belfort, G., 'The Performance of a Rotating Filter. 1. Theoretical Analysis of the Flow in an Annulus with Rotating Inner Porous Wall', *J. Membr. Sci*., **99**, 241 (1995)

Holdich, R. G. and Zhang, G. M., 'Crossflow microfiltration incorporating rotational fluid flow', *Trans IchemE*, **Vol. 70**, Part A, September, 527–536 (1992)

Hsieh, H. P., 'Inorganic membranes', *J. Membrane Sci*., **39**, 221–241 (1988)

Mikulášek, P., 'Methods to Reduce Concentration Polarization and Fouling in Membrane Filtration', *Collect. Czech. Chem. Commun*., **59**, 737 (1994)

Mikulášek, P., 'Microfiltration of non-Newtonian dispersions', The 25th Conference of the Slovak Society of Chemical Engineering, Jasná, Demänovská dolina, Slovakia, 25–29 May 1998, published in the proceedings (CD ROM by INTERCOMP Services s.r.o. Bratislava)

Mikulášek, P. and Cakl, J., 'Flux Enhancement Methods in Cross-Flow Microfiltration of Dispersions', *Chem. Biochem. Eng. Q*., **11**, 193 (1997)

Mikulášek, P. and Dolecek, P., 'Use of a Rotating Filter to Enhance Membrane Filtration Performance of Latex Dispersions', *Sep. Sci. Technol*., **29**, 1943 (1994)

Mikulášek, P. and Hrdý, J., 'Permeate Flux Enhancement Using a Fluidized Bed in Microfiltration with Ceramic Membranes', *Chem. Biochem. Eng. Q*., **13**, 133 (1999)

(d) Microfiltration of beer

Burrell, K., Kotzian, R. and O'Sullivan P., 'Progress in the crossflow microfiltration of beer', *BDI*, **25**, 22 (1994)

Girr, M. and Bartels, H., 'One year of crossflow yeast filtration', *Brauwelt*, **131**, 46 (1991)

Howell, J. A., Field, R. W. and Wu, D., 'Yeast cell microfiltration: Flux enhancement in baffled and pulsatile flow systems', *J. Membrane Sci*., **80**, 59 (1993)

Kiefer, J. and Gans, U., 'Overview of the different yeast/beer separation technologies', Proceedings of the Institute of Brewing (Australia and New Zealand Section), 24th Scientific Convention (1996)

Leeder, G. and Girr, M., 'Cross-flow microfiltration for processing brewery tank bottoms, *MBAA Technical Quarterly*, **31**, 58 (1994)

Lojkine, M. H., Field, R. W. and Howell, J. A., 'Crossflow microfiltration of cell suspensions: A review of models with emphasis on particle size effects', *Trans. IChem. E*, **70**, 150 (1992)

Potgieter, D., Parsotam, R. and Perry, M., 'Extract recovery from surplus yeast', *MBAA Technical Quarterly*, **33**, 110 (1994)

Schlenker, R., 'Beer recovery from spent yeast by Schenk TFF system', *BDI*, **25**, 26 (1994)

Stopka, J., Schlosser, Š., Dömény, Z., Šmogrovièová, D. and Búziková, Ž., 'Microfiltration of yeast suspensions of saccharomyces uvarum', The 25th Conference of the Slovak Society of Chemical Engineering, Jasná, Demänovská dolina, Slovakia, 25–29 May, 1998, published in the proceedings (CD ROM by INTERCOMP Services s.r.o. Bratislava)

Walla, G. E., 'Yeast beer recovery with crossflow microfiltration', Proceedings of the Institute of Brewing (Australia and New Zealand Section), 23rd Scientific Convention (1994)

(e) General and modelling

Asaadi, M. and White, D. A. 'A model for determining the steady state flux of inorganic microfiltration membranes', *Chem. Eng. J.*, **48**, 11 (1992)

Davis, R. H. 'Modelling of fouling of crossflow microfiltration membranes', *Sep. Purif. Methods*, **21**, 75 (1992)

Davis, R. H. 'Theory for crossflow microfiltration', *Membrane Handbook*, W. S. Winston Ho and K. K. Sirkar (Eds), Van Nostrand Reinhold, New York, NY, 480–505 (1992)

Fane, A. G. 'New insights from non-invasive observations of membrane processes', Proceedings Volume I, World Filtration Congress 8, European Federation of Chemical Engineering Event No. 607, organised by The Filtration Society and Elsevier Science, The Brighton Centre, Brighton, UK, 3–7 April 2000, 11–17 (2000)

Litvai, E., Kulik, P. and Parti, M., 'The effect of roughness and turbulence on the concentration polarisation', Proceedings Volume I, World Filtration Congress 8, European Federation of Chemical Engineering Event No. 607, organised by The Filtration Society and Elsevier Science, The Brighton Centre, Brighton, UK, 3–7 April 2000, 191–194 (2000)

Madec, A., Buisson, H. and Aim, R. B., 'Aeration to enhance membrane critical flux', Proceedings Volume I, World Filtration Congress 8, European Federation of Chemical Engineering Event No. 607, organised by The Filtration Society and Elsevier Science, The Brighton Centre, Brighton, UK, 3–7 April 2000, 199–202

Romero, C. A. and Davis, R. H. 'Global model of crossflow microfiltration based on hydrodynamic particle diffusion', *J. Membr. Sci.*, **39**, 157 (1988)

Romero, C. A. and Davis, R. H. 'Transient model of crossflow microfiltration', *Chem. Eng. Sci.*, **45**, 13 (1990)

Threlfall, D., 'Ceramic membrane microfiltration in the treatment of domestic sewage –pretreatment to reverse osmosis', Proceedings Volume I, World Filtration Congress 8, European Federation of Chemical Engineering Event No. 607, organised by The Filtration Society and Elsevier Science, The Brighton Centre, Brighton, UK, 3–7 April 2000,111–114 (2000)

Van Gauwbergen, D. and Bayens, J., 'Hydrodynamic study of membrane modules using the mesh step approach', Proceedings Volume I, World Filtration Congress 8, European Federation of Chemical Engineering Event No. 607, organised by The Filtration Society and Elsevier Science, The Brighton Centre, Brighton, UK, 3–7 April 2000, 183–186 (2000)

Ventakatamaran, C., and Gupta, K., 'Revealing the pore characteristics of membranes', *Filtration + Separation*, 20–23 (July/August 2000)

Winston Ho, W. S. and Sirkar, K. K. (Eds), *Membrane Handbook*, Van Nostrand Reinhold, New York, NY (1992)

12

Pressure filtration
Part I—Batch pressure filtration

L. Svarovsky

FPS Institute, England and University of Pardubice, Czech Republic

12.1 Introduction

The driving force for filtration in pressure filters is usually the liquid pressure developed by pumping or by the force of gas pressure in the suspension feed vessel. Alternatively, or in addition, the liquid may be squeezed through and out of the cake by the mechanical action of an inflatable membrane, a piston or a porous medium pressed on top of the cake. Pressure filtration is, therefore, defined here as any means of surface filtration where the liquid is driven through the medium by either hydraulic or mechanical pressure, greater than atmospheric. The solids are deposited on top of the filter medium (as in all surface filters), with the possible exception of some cartridge filters which also use a certain amount of depth filtration. In this chapter, the suspension is assumed to approach the medium at 90° and this excludes the so-called dynamic filter/thickeners or cross-flow filters (also driven by pressure) which are dealt with in a separate chapter (11).

Most conventional pressure filters are batch-wise in operation, i.e. the whole of the filter medium surface in each unit is going through a cyclic process of cake formation (possibly preceded by coating with filter aid, followed by cake washing or dewatering and, finally, cake removal). This leads to discontinuous solids discharge from the filter, usually taking place during that part of the cycle when the filter is taken off pressure and opens to atmosphere (some do not have to open but the solids discharge is still occasional). The batch pressure filters are dealt with in part I of this chapter.

There have been some relatively recent developments of continuous pressure filters, of both the hydraulic and squeezing variety. The different parts of the filtration surface in these units at any point in time are undergoing different stages of the filtration and dewatering cycle, with one part continuously discharging the cake. The cake and filtrate production is continuous,

therefore, with all the associated advantages of continuous or large-scale production processes. The continuous pressure filters are dealt with in part II of this chapter. Both parts of this chapter start with a brief fundamental introduction.

12.2 Batch pressure filtration

12.2.1 The case for pressure filtration in general

High pressure drops have a two-fold effect: on capacity and on displacement dewatering which often follows. It is best to consider these two effects separately.

12.2.1.1 The filtration part of the cycle

The most important feature of the pressure filters which use hydraulic pressure to drive the process is that they can generate a pressure drop across the medium of more than 1 bar, which is the theoretical limit of vacuum filters. Whilst the use of a high pressure drop is often advantageous, leading to higher outputs, drier cakes or greater clarity of the overflow, this is not necessarily the case. For compressible cakes, an increase in pressure drop leads to a decrease in permeability of the cake and hence to a lower filtration rate relative to a given pressure drop. This reduction in permeability due to cake consolidation or collapse may be so large that it may nullify or even overtake the advantage of using high pressures in the first place and there is then no reason for using the generally more expensive pressure filtration hardware. Whilst a simple liquid pump may be cheaper than the vacuum pump needed with vacuum filters, if air-displacement dewatering is to follow filtration in pressure filters, an air compressor must be used and this is expensive.

The fundamental case for pressure filters may be made using the following equation for dry cake production capacity, Y (kg m^{-2} s^{-1}), derived from Darcy's law when the filter medium resistance is neglected (for the full derivation see appendix I in Svarovsky[1]):

$$Y = \left[\frac{2\,\Delta p\, f c}{\alpha \mu t_c}\right]^{1/2} \tag{12.1}$$

where Δp is the pressure drop, c is the feed solids concentration, α is the specific cake resistance, μ is the liquid viscosity, Y is the solids yield (dry cake production in kg m^{-2} s^{-1}), f is the ratio of filtration to cycle time, and t_c is the cycle time. For the same cycle time (i.e. same speed), if the pressure drop is increased by a factor of four, production capacity is doubled. In other words, filtration area can be halved for the same capacity but only if α is constant. If α increases with pressure drop and depending on how fast it

increases, the increased pressure drop may not give much more capacity and, in some extreme cases, it may actually cause capacity reductions.

For most industrial inorganic solids such as minerals, etc., the increase in α with Δp is not too large and thus, if the material to be filtered is too fine for vacuum filtration, pressure filtration may be advantageous and will give better rates.

Pressure filters can treat feed concentrations of up to and in excess of 10% solids by weight and having large proportions of difficult-to-handle fine particles. Typically[1], slurries in which 10% of the solid particles are larger than 10 μm may require pressure filtration, but increasing the proportion of particles larger than 10 μm may make vacuum filtration possible. The range of typical filtration velocities in pressure filters is 0.025–5 $\mathrm{m\,h^{-1}}$ and of dry solids rates is 25–250 $\mathrm{kg\,m^{-2}\,h^{-1}}$. The use of pressure filters may also, in some cases (such as in filtration of coal flotation concentrates), eliminate the need for flocculation.

Simulation, modelling and sizing of batch pressure filters has recently been described by Tarleton[19,20].

12.2.1.2 The dewatering part of the cycle

The key to the understanding of the dewatering process by air displacement is the capillary pressure diagram. *Figure 12.1* shows an example typical for a fine coal suspension; there is a minimum moisture content which cannot be removed by air displacement at any pressure, called irreducible saturation (about 12% in this case). There is also a threshold pressure (about 0.13 bar in this case) which must be exceeded in order that air may enter the filter cake.

The capillary retention forces in the pores of the filter cake are primarily affected by the size and size range of the particles forming the cake, and by the way the particles have been deposited when the cake was formed. There is

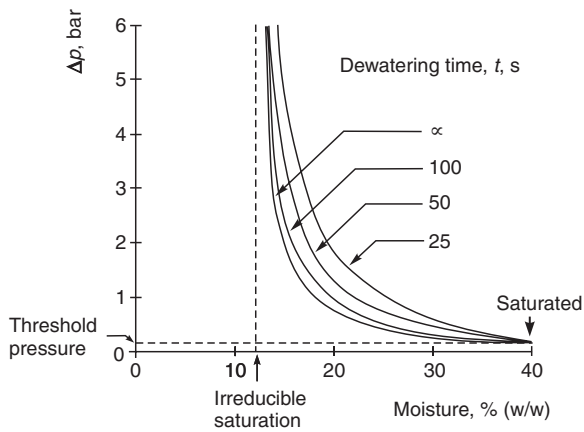

Figure 12.1 A capillary-pressure diagram for fine coal

no fundamental relation to allow the prediction of cake permeability but, for the sake of the order-of-magnitude estimates, the pore size in the cake may be taken loosely as though it were a cylinder which would just pass between three touching, monosized spheres. If d is the diameter of the spherical particles, the cylinder radius would be 0.0825 d. Using this simple argument and the surface tension of water at 20°C of 0.07275 N m^{-2}, the capillary pressure of 1 bar would correspond to $d = 17.6$ μm.

Bearing in mind that although most cakes consist of poly-disperse, non-spherical particle systems that are theoretically capable of producing more closely-packed deposits, the practical cakes usually have large voids and are much more loosely packed due to the lack of sufficient particle relaxation time available at the time of cake deposition (see a further discussion of this phenomenon in chapter 9) the above-derived value of 17.6 μm probably becomes nearer the often-quoted 10 μm limit when pressure air dewatering becomes necessary.

The lowest curve in *Figure 12.1* gives the moisture content at different pressure drops which can be achieved given infinite time of dewatering. The dewatering kinetics, are such, however, that many such curves can be measured and drawn, depending on the time available for dewatering. Although, strictly speaking, *Figure 12.1* or any such diagram only applies to one cake thickness, Bott *et al.*[2] have recently shown that, given a suitable filter cloth and a sufficiently high pressure differential, the filter speed (of a continuous pressure filter) can be increased nearly up to the speeds giving the minimum practicable cake thickness without any increases in moisture content. A capillary-pressure diagram, such as the one in *Figure 12.1*, obtained for a given cake thickness can, therefore, also be used for thinner cakes.

Figure 12.2 shows clearly that the same moisture content of the produced cake can be obtained in shorter dewatering times if higher pressures are used.

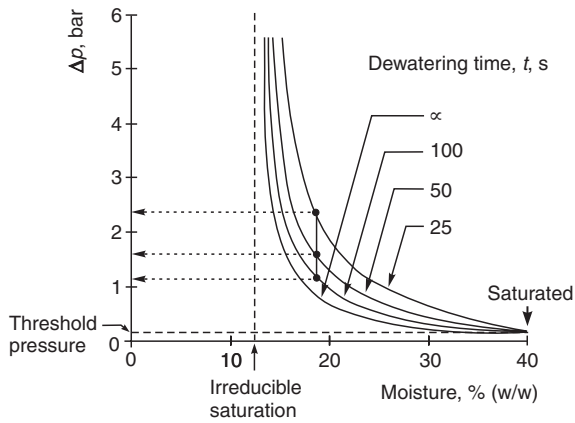

Figure 12.2 Diagram to show that higher pressure allows shorter dewatering times

If a path of constant dewatering time is taken, on the other hand, moisture content is reduced at higher pressures, with a parallel increase in cake production capacity. This is a clear and indisputable advantage of pressure filtration of reasonably incompressible solids like coal and other minerals: it has been substantiated by experiments by many workers, including Bott *et al.*[2] and workers in Bradford[3].

12.2.1.3 Optimization of cycle times

In batch filters, one of the important decisions to be made is how much time is to be allocated to the different operations such as filtration, displacement dewatering, cake washing and cake discharge (which may involve opening the pressure vessel). All of this will have to happen within a cycle time, t_c, which itself is not fixed. However, some of the times involved, such as the cake discharge time, may be defined. The question we want to answer here is how much time is to be given to the filtration part of the cycle relative to the other operations. Are we to run the filtration for a long time, thus forming a thick cake, with the inevitable consequence of rapidly diminishing filtration rates towards the end, or should we stop the filtration earlier whilst the rate is still reasonably high?

If all the non-filtration operations are grouped together into a 'downtime', t_d, and this is assumed to be fixed and known, we can derive an optimum filtration time, t_{opt}, in relation to t_d by optimizing the average dry cake production obtained from the cycle. The full derivation may be found in appendix II of Svarovsky[1] and only the final result is given below.

For constant-pressure filtration and where the medium resistance, R, and the specific cake resistance, α, are constant, the following equation applies:

$$t_{opt} = t_d \left[1 + \sqrt{\frac{2\mu R}{\alpha c \, \Delta p \, t_d}} \right] \tag{12.2}$$

where Δp and c are the operating pressure drop and the feed solids concentration respectively.

When the medium resistance, R, is small compared with the specific cake resistance, α, the second term in the above equation becomes negligible and the optimum filtration time, t_{opt}, becomes equal to the down time, t_d. For any other situation t_{opt} is always greater than t_d.

It follows, therefore, that the filtration time should always be set to be at least equal to the sum of the other, non-filtration periods involved in the cycle.

12.2.1.4 Cake squeezing

The compressibility of many industrial filtration cakes, an unwanted phenomenon in filtration by hydraulic pressure, may be turned into an advantage by considering mechanical squeezing of the pre-formed cake as an alternative or additional dewatering method. The fact that a cake has a reasonable or high

porosity does not necessarily mean that the liquid within it can be easily removed. Some of the liquid can, however, be removed simply by altering the cake structure by mechanical compression. In fact, the more compressible materials are often also less permeable. It is, therefore, the very cakes which consolidate under hydraulic pressure and render such filtration (and subsequent displacement dewatering) difficult that are the best candidates for mechanical squeezing, sometimes referred to as 'expression'. Compressibility of cakes can often be promoted by addition of flocculation agents and, indeed, some available hardware such as the belt presses almost entirely depend on chemical pre-treatment of slurries. There is very little that can be done using fundamental theory. The compressibility and permeability of practical filtration cakes, which affect the choice of equipment for dewatering, must be tested experimentally and this is best done in a compression filtration cell[4,5].

The specific volume of a cake, v, after compression is usually related to the applied pressure, p, in a way similar to that used in soil mechanics[6].

$$v = v_o - \lambda \ln p \tag{12.3}$$

where v_o is the value of v corresponding to unit pressure p and λ is a characteristic of the material and may sometimes itself depend on p.

Carleton[7], who has studied the economics of using the relatively expensive compression filters, states that if the volume of the cake is not reduced by at least 2% when the applied pressure is doubled, then it is unlikely that a compression filter can be justified.

The values of v in the above equation are the equilibrium values after an infinite pressing time. There are kinetics involved here too in that the deformation of the cake due to a mechanical stress is not instantaneous but dampened by the necessary permeation of the liquid out of the cake. Baluais *et al.*[5] considered a rheological model for this in analogy with the action of a shock absorber in parallel with one spring and in series with another.

Those pressure filters which use the squeezing of the cake are, on the whole, expensive and their use can be justified only if the energy savings are large enough. The squeezing process itself may extend the down-time of the filtration cycle and a full economical analysis is needed[7] to optimize the choice of equipment and the operating conditions. It should be borne in mind, however, that compared with thermal drying, cake compression requires about 25 times less energy.

There are other positive features of cake squeezing in that it often improves cake release, it closes any cracks and tightens the cake, thus making any subsequent cake washing more effective.

Excluding variable-chamber presses, which rely on mechanical squeezing of the cake and which will be dealt with in a separate section, pressure filters may be grouped into two categories, plate-and-frame filter presses and pressure vessels containing filter elements. The latter group also includes the cartridge filters but these have their own section in the following.

12.2.2 Filter presses

In the conventional plate-and-frame press (*Figure 12.3*), a sequence of perforated, square or rectangular plates alternating with hollow frames is mounted on suitable supports and pressed together with hydraulic or screw-driven rams. The plates are covered with a filter cloth and the cloth also forms the sealing gasket. The slurry is pumped into the frames and the filtrate is drained from the plates.

The drainage surfaces are usually made in the form of raised cylinders, square-shaped pyramids or parallel grooves in materials such as stainless steel, cast iron, rubber or resin-coated metal, polypropylene, rubber or wood. Designs are available with every conceivable combination of inlet and outlet location: top feed, centre feed, bottom feed, corner feed and side feed, with a similar profusion of possible positions of discharge points, each combination having particular advantages, depending on whether washing is required and also on the application and the nature of the suspension.

Sometimes, the discharge is through a separate cock on each plate rather than through a common filtrate port and manifold. This allows observation of the filtrate from each plate and sampling from it, thus enabling the operator to spot cloth failure and to isolate the plate, or segregate the cloudy filtrate. The cocks discharge into open channels or enclosed pipe systems (the latter being fitted with a sight glass).

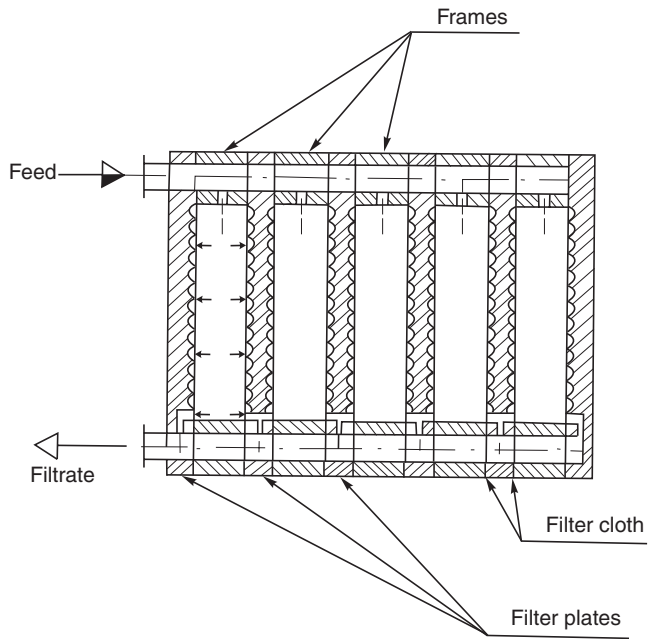

Figure 12.3 Scheme to show the principle of plate-and-frame presses

Both flush plates and recessed plates can be specified, the latter obviating the need for frames but being a little tougher on filter cloths due to the strain around the edges. Recessed plate presses are more suitable for automation, however, because of the difficulty of the automatic removal of residual cake from the frames in a plate-and-frame press. Recessed plates with no frames limit the chamber width to less than about 32 mm (to limit the strain on the cloth), whilst plate-and-frame presses allow this width to be more than 40 mm if necessary. Plate sizes range from 150 mm^2 to 2 m^2, giving filtration areas up to 200 m^2. The number of chambers varies up to 100, and exceptionally up to 200.

Plate-and-frame filters are the most versatile filters because their effective area can be varied simply by blanking off some of the plates. Cake-holding capacity can be altered by changing the frame thickness or by grouping several frames together. These filters are available in a variety of semi-automated or fully automated versions that feature mechanical leaf-moving devices, cake removal by vibration or by pulling the cloth when the press is open, etc. An operator usually has to be present, however, because it is not certain that each and every chamber will discharge its cake unaided every time. Should manual intervention be necessary, the operator has to be protected from injury by the leaf-moving mechanism, by a suitable safety photo-electric device.

Some attempts have been made to re-slurry the filter cake without having to open the filter press. However, a number of problems tend to crop up, such as for example, bending of the plates due to uneven cake deposition or cavitation, uneven dewatering and washing within the frames or plugging of the inlet ports.

There are two ways in which washing can be performed in filter presses: simple washing and thorough washing. In simple washing, the wash liquid is introduced either through the main feed port or through a separate port into each chamber, and the washing is therefore in the same direction as the filtration process that formed the cake. In thorough washing, the wash liquid enters through a separate port, behind the filter cloth on every other plate, thus passing through the whole thickness of the cake in the chamber. Washing is less efficient with recessed chamber presses than with flush plate frame presses, probably because of poorer distribution of the wash liquid. In either case the amount of wash liquid necessary tends to be high.

Filter media for plate-and-frame presses include various cloths, mats and paper. In the case of paper, this usually has to be provided with a backing cloth for support.

The typical operating pressure of filter presses is around 6 or 7 bar, although some manufacturers offer presses for up to 20 bar or higher. As the pressure builds up during filtration, it tends to force the plates apart and this may be offset by a pressure compensation facility offered with some large mechanized presses.

Full mechanization of filter presses began in the late 1950s and this was closely followed by addition of the mechanical expression (i.e. cake

squeezing) mechanism. Rubber or plastic membranes are sometimes fitted to compress the cake which is formed by conventional pressure filtration. The membranes normally rest on the plates and have grooves and openings in their surfaces for filtrate collection. The membranes are inflated at the end of the filtration cycle by air or, for pressures higher than 1000 kPa, by water or hydraulic fluid. The membranes should be designed to last up to or in excess of 10 000 pressings. The main advantage of using mechanical expression of cakes here is the additional dewatering usually achieved and also the ability to handle thin cakes. Another advantage is that the main filtration process can be done at lower pressures (so that a relatively cheap, centrifugal pump can be used) and the compression by the membrane then goes to higher pressures.

The automation of filter presses brought about several other advantages and developments. Plate-shifting mechanisms have been developed, allowing the cloths to be vibrated, filter-cloth washing (on both sides) has been incorporated to counteract clogging from the expression, and, most importantly, the down-times have been reduced with automation, thus increasing capacities.

One of the recent developments in this filter category is the vertical recessed plate automatic press shown schematically in *Figure 12.4*. While the conventional filter press usually has the plates hanging down and linked in a horizontal direction, this type has the plates in a horizontal plane and placed one upon another. This design offers semi-continuous operation, savings in floor space and easy cleaning of the cloth, but it allows only the lower face of each chamber to be used for filtration. The filter usually has an endless cloth,

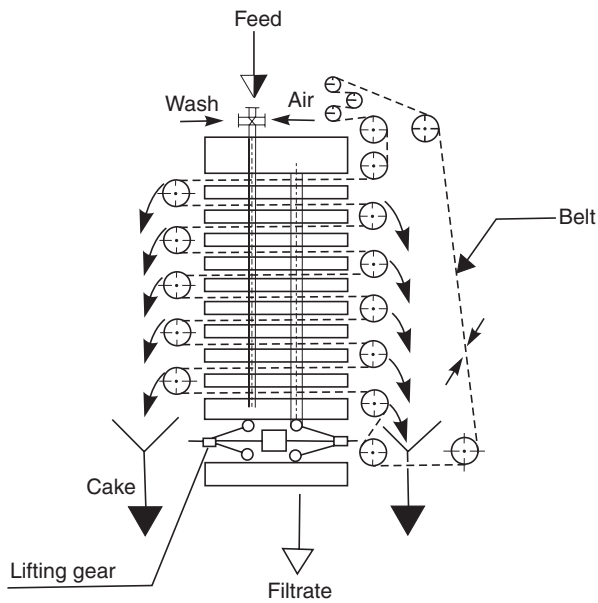

Figure 12.4 Scheme to show the vertical automatic filter press

travelling intermittently between the plates via rollers to peel off cakes. The disadvantage of this is, however, that if an endless cloth is damaged anywhere, the whole cloth has to be replaced, which is a difficult process. As the filter cloth zig-zags through the filter, the filtering direction is reversed each time and this tends to keep the cloth clean. Most of these filters incorporate membranes for mechanical expression, and cakes sometimes stick to the membranes and remain in the chamber after discharge. Some vertical filters are available with a separate cloth for each frame. The cloths may be disposable and such filters are designed to operate with or without filter aids.

As the height of the vertical press makes maintenance difficult, the number of the chambers is restricted, usually to 20, with a maximum of 40, with filter areas of up to $32\,m^2$.

The application of filter presses spans virtually all areas of the processing industries due to their versatility. Examples of use include the clarification of beer and juices or waste-water and activated sludge filtration in breweries, paper mills and petrochemical plants, the dewatering of fine minerals and lime mud separation and washing in the sugar industry. The filtration velocities are usually 0.025 to $1\,m\,s^{-1}$ and the dry solids handling capacities are less than $1000\,kg\,m^{-2}\,h^{-1}$, the higher values being more usual with the automatic presses due to their shorter down-times.

12.2.3 Pressure vessel filters

There are several designs of pressure vessel filters. They all consist of pressure vessels, housing a multitude of leaves or other elements which form the filtration surface and which are mounted either horizontally or vertically. With the horizontal leaves there is no danger of the cake falling off the cloth and they are most suitable where thorough washing is required, whereas with the vertical elements, a pressure drop must be maintained across the element to retain the cake. The disadvantage of the horizontal-leaf types is, however, that half the filtration area is lost because the underside of the leaf is not normally used for filtration (because of the danger of the cake falling off). Discharge of the cake may also be more difficult in this case.

The elements or leaves normally consist of a coarse stainless-steel mesh over which a fine (often metal) gauze or filter cloth is stretched and sealed at the edges. The leaves are in parallel, each connected to a header and, almost without exception, the filtration is from the outside inwards through the gauze. These filters are all essentially batch operated and most require the use of a filter aid for pre-coating, because cloudy filtrates and blinding would otherwise occur.

One operational problem with these filters is concerned with the disposal of the heel of unfiltered slurry which is still in the vessel at the end of the filtration period. This is particularly troublesome with the vertical-leaf filters because compressed air cannot be used to complete the filtration of this heel

(as the air would preferentially escape through the tops of the leaves as soon as they emerged from the suspension). It is common practice to install a separate filtering element at the bottom of the vessel as a 'scavenger filter' for the filtration of the residual slurry. During the scavenge filtration the main leaves are usually isolated so that compressed air is not lost through them.

12.2.3.1 Cylindrical element filters (Figure 12.5)

Cylindrical element filters, often referred to as 'candle filters', have cylindrical elements or sleeves mounted vertically and suspended from a header sheet, which divides the filter vessel into two separate compartments. The filtration takes place on the outside of the sleeves. The inlet is usually in the bottom section of the vessel and the filtrate outlet in the top section above the header sheet. A less usual design is to locate the filtrate outlet at the bottom of the elements and thus allow the top chamber to be opened for easy inspection of the elements during operation.

The tubes are generally 25–75 mm in diameter, and up to 2 m in length, made from metal or cloth-covered metal, and provide filtration areas of up to 100 m^2. Alternatively, the tubes can be made of stoneware, plastics, sintered

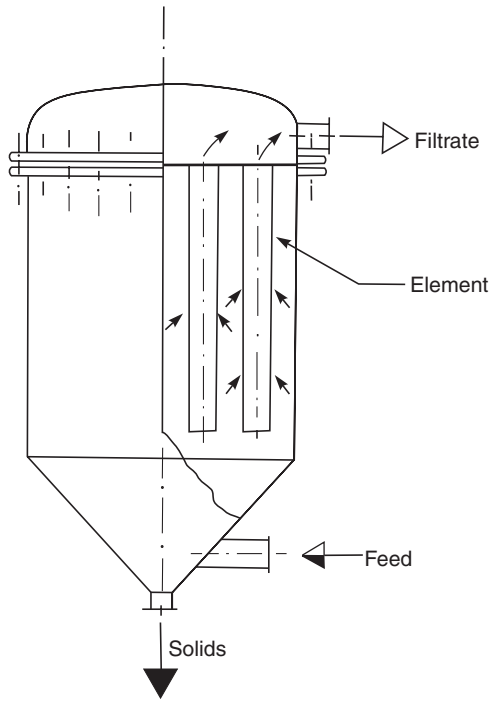

Figure 12.5 A cylindrical element (candle) pressure filter

metal or ceramics. The elements may be made deliberately flexible, sometimes filled with loose packing. Tank diameters of up to 1.5 m are available. Cake removal is performed by scraping with hydraulically operated scraper rings, by vibration or by turbulent flow 'bumping'. The mechanical strength of the tubular element makes it ideal for cleaning by the sudden application of reverse pressure. Physical expansion or 'flexing' of the tubular elements on application of the reverse flow aids cake discharge.

Cylindrical element filters find wider use where cake washing is not required. Their inherent advantage is that, as the cake grows on the tubular elements, the filtration area increases and the thickness of a given volume of cake is therefore less than it would be on a flat element. This is of course only of importance where a thick cake is being formed and the rate of increase in the pressure drop is less with tubular elements in such cases.

The pressure filter with tubular elements has also been used as a thickener, when the cake, backwashed by intermittent reverse flow, is redispersed by an agitator at the bottom of the vessel and discharged continuously as a slurry. In some cases the filter cake will build up to a critical thickness and then fall away without blow-back.

12.2.3.2 Vertical-tank, vertical-leaf filters (Figure 12.6)

These are the cheapest of the pressure leaf filters and have the lowest volume-to-area ratio. Their filtration areas are limited to less than 80 m^2. Large

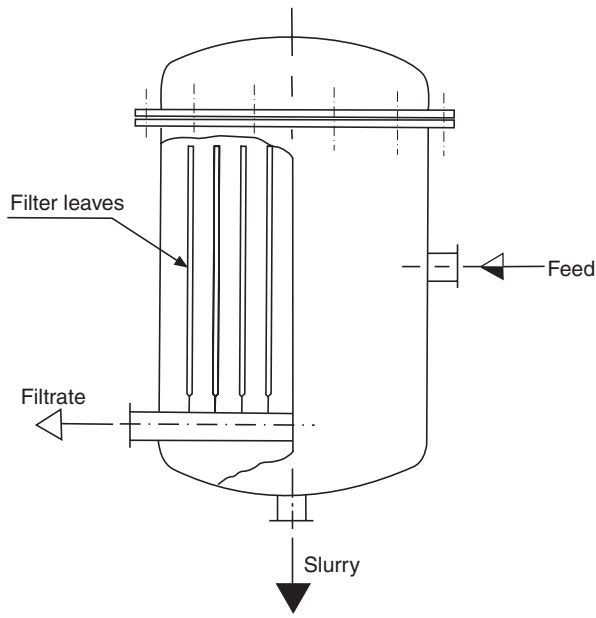

Figure 12.6 A vertical-tank, vertical-leaf filter

bottom outlets, fitted with rapid-opening doors, are used for dry cake discharge and smaller openings are used for slurry discharge. Wet discharge may be promoted by spray pipes, vibrators, reverse flow, bubble rings, scrapers etc., while dry discharge is usually caused by vibration. As all vertical leaf filters, these are not suited for cake washing.

In one somewhat different design, known as the Scheibler filter, the filter leaves take the form of bags, each suspended in a rectangular pressure vessel from a horizontal tube which acts as the filtrate outlet. The sides of the bag are prevented from meeting by looped chains which are attached at the tops of their loops to the horizontal tube and hang downwards. With this method of separating the cloth surfaces by chains the bags can be wide enough to hang in pleats and the filtering area can thus be as much as three times the area of the frames which are inside the bags. Filtration areas of up to $250\,m^2$ are available, applications being mostly in the chemical industry.

Special mention should also be made of the pressure version of the Moore filter developed in France for the sugar industry. The vertical cylindrical vessel, which houses a set of radially arranged leaves, is twice the height of the leaves, allowing the leaves to be raised, rotated and lowered into the different compartments in the bottom half of the vessel. Positive air pressure must be maintained throughout the operation to prevent cake fall-off and the cake is blown off the leaves by air blow-back.

12.2.3.3 Horizontal-vessel, vertical-leaf filters (Figure 12.7)

In a cylindrical vessel with its axis horizontal, the vertical leaves can be arranged either laterally or longitudinally. The latter arrangement is less common; such filters may be designed as vertical-vessel, vertical-leaf filters

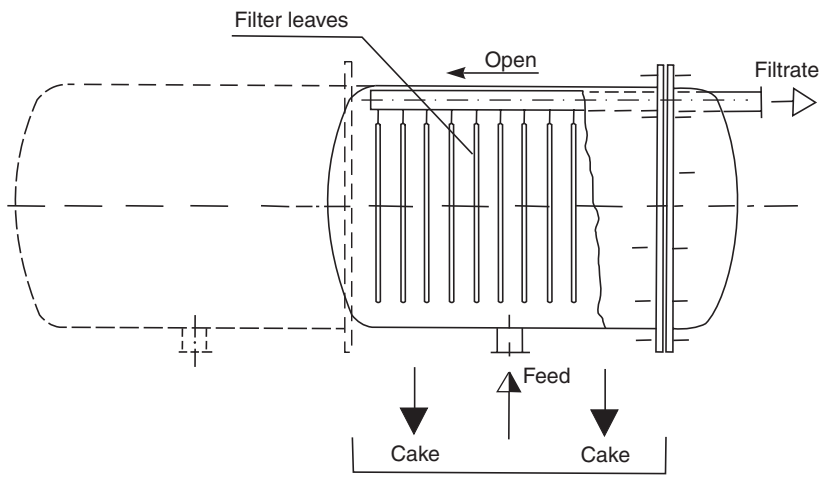

Figure 12.7 A horizontal-vessel, vertical-leaf filter

but mounted horizontally. Those designs are suitable for smaller duties and the leaves can be withdrawn individually through the opening end of the vessel.

Filtration areas of up to $120\,m^2$ are available with the second longitudinal arrangement, the Kelly leaf filter. This was probably the earliest pressure leaf filter and it has been used for the filtration of very viscous liquids such as glycerin and concentrated sugar solutions. The leaves, the height of which varies according to the space available at their location in the vessel, are attached to the removable circular front cover, each leaf having an outlet connection through this cover. The leaves together with the cover and outlet pipes are attached to a carriage which can be run into and out of the shell to facilitate cake discharge outside the vessel by air blow-back or rapping. This arrangement requires a considerable amount of floor space and to minimize this drawback the presses are often constructed in pairs on a single runway, with their opening ends facing each other. Thus, each filter can be opened in turn into the common space between them.

By far the greatest use of the horizontal-vessel filters is made of those types which have vertical leaves arranged laterally (i.e. in a plane perpendicular to the axis of symmetry of the vessel) because this design provides easy access to the leaves. Most of these filters open in a way similar to the Kelly filter, sometimes by moving the shell rather than the leaf assembly, so that the filtrate pipe can remain permanently connected; sometimes withdrawal of one leaf or a bundle of leaves at a time is possible. The leaves may be rectangular, circular or of some other shape, and may be designed to rotate during cake discharge. Sluicing by sprays is sometimes used for wet discharge, with or without rotation of the leaves. If the leaves are designed for rotation they are invariably circular and mounted on a central hollow shaft which serves as the filtrate outlet. Dry cake discharge may be carried out with rotating leaves by application of a scraper blade. If this is to be done without opening the vessel, then the bottom of the vessel must be shaped like a hopper, with a screw conveyor if necessary.

The original Vallez filter developed in the USA for the sugar industry, and the more modern developments of it, also rotate the leaves at about $1\,rev.\,min^{-1}$ during the filtration operation, in order to keep the solids in suspension and achieve a more uniform cake.

One significant departure from the standard end-opening design is known as the Sweetland filter, which has the cylindrical shell split in a horizontal plane into two parts, where the bottom half can be swung open for cake discharge. The upper half is rigidly supported and both the feed and the filtrate piping are fixed to it. The lower part is hinged to the upper along one side and is counterbalanced for easy opening. Cake discharge is either by sluicing or by dropping, assisted by some scraping. If much scraping has to be done, there is not much advantage in using this type of filter. As the leaves are stationary, the cake deposited on them may be uneven, with the greater mass of the cake being at the bottom of the leaves.

In general, the horizontal-vessel, vertical-leaf filters with the leaves arranged laterally can be designed up to filtration areas of 300 m^2. Cake washing is possible but it must be carried out with caution because there is a danger of the cake falling off.

Horizontal-vessel filters with vertical rotating elements have been under rapid development recently with the aim of making truly continuous pressure filters, particularly for the filtration of fine coal—see part II of this chapter.

12.2.3.4 Vertical-vessel, horizontal-leaf filters (Figure 12.8)

These filters, like all horizontal-leaf filters, are advantageous where the flow is intermittent or where thorough cake washing is required. Filtration areas are limited to about 45 m^2. Special mention must be made of the pressure version of the Nutsche filter which, strictly speaking, falls into this category. These are either simple pressurized filter boxes or more sophisticated agitated Nutsches, much the same in design as the enclosed agitated vacuum filters described in another section. These are extremely versatile, batch-operated filters, used in many industries, for example in agrochemistry, pharmaceuticals or dyestuff production.

An obvious method of increasing the filtration area in the vessel is to stack several plates on top of each other; the plates are operated in parallel. One

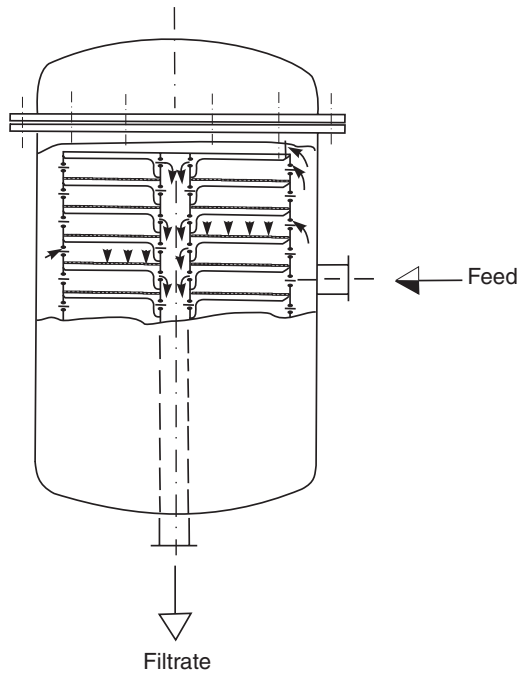

Figure 12.8 A vertical-vessel, horizontal-leaf filter

such design, known as the plate filter, uses circular plates and the stack can be removed as one assembly. This allows the stack to be replaced after the filtration period with another, clean stack, so that the filter can be put back into operation quickly. The filter consists of dimpled plates supporting perforated plates on which filter cloth or paper is placed. The space between the dimpled plates and the cloth is connected to the filtrate outlet, which is either into the hollow shaft or into the vessel, the other being used for the feed. When the feed is into the vessel, a scavenger plate may have to be fitted because the vessel will be full of unfiltered slurry at the end of the filtration period. This type of filter is available with filtration areas of up to 25 m^2 and gives cakes of up to 50 mm thick.

Centrifugal discharge filters form another group in this category. As the name suggests, the cake discharge is accomplished by rotating the stack of plates around the hollow shaft. The cake slides off the plates due to the centrifugal action; sometimes it is necessary to supplement this process by sluicing with a suitable liquid, in which case the discharge is wet. The filtrate leaves through the hollow shaft. These filters lend themselves to automation and, as opposed to manually operated leaf filters, they can be operated with short cycle times and very short down-times, which is very economical. Many different makes are available, with various ways of driving the shaft and locations of the electric motor as well as with other varying constructional details. The sizes available vary up to 65 m^2.

A helical version of the centrifugal discharge filter has recently been described by Patnaik[21]. The multiple circular filter plates are combined into a helix mounted on a central shaft and the filtrate collects into and flows through the helix and out through a bottom header. Discharge of the cake is accomplished by rotation of the helix by a bi-directional motor mounted to the central shaft. A system of scraper blades at the bottom of the helix forces the solids through a large opening. The helical filter comes optionally equipped with a dryer, where heat is transferred to the cake through heating coils in the helix.

Another available design allows discharge of the cake by vibration of the circular plates, which are then slightly conical, sloping downwards towards the outside of the plates. This design allows higher pressures to be used as no rotating seals are necessary.

12.2.3.5 Horizontal-vessel, horizontal-leaf filters (Figure 12.9)

These filters consist of a horizontal cyclindrical vessel with an opening at one end. A stack of rectangular horizontal trays is mounted inside the vessel; the trays can usually be withdrawn for cake discharge, either individually or as the whole assembly. The latter case requires a suitable carriage to be supplied. One alternative design allows the tray assembly to be rotated through 90° so that the cake can fall off into the bottom part, designed in the shape of a hopper and fitted with a screw conveyor.

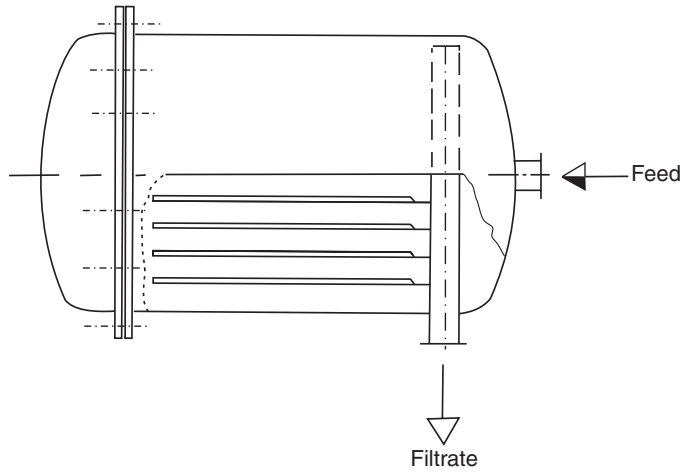

Figure 12.9 A horizontal-vessel, horizontal-leaf filter

The leaves are sometimes fitted with rims, thus forming trays and this is particularly useful for flooding the trays in washing operations. Scavenger leaves are often used. Filtration areas of up to 50 m^2 are available. Like all horizontal-leaf filters, they are particularly suitable when thorough washing is needed.

12.2.4 Cartridge filters (*Figure 12.10*)

This short review of pressure filters would not be complete without a mention of cartridge filters. These use easily replaceable, tubular cartridges made of paper, sintered metal, woven cloth, needle felts, activated carbon or various membranes of pore size down to 0.2 μm. Filtration normally takes place in the direction radially inwards, through the outer face of the element into the hollow core. Cartridge filtration is limited to liquid polishing or clarification, i.e. removing very small amounts of solids, in order to keep the frequency of cartridge replacements down. Typically, suspensions of less than 0.01% volume concentration of solids can be treated with cartridge filters and such filters are favoured in small-scale manufacturing applications.

Cartridge filters can be divided into depth and surface types, according to where most of the solids separate, although the precise demarcation line is sometimes difficult to draw. Probably the most common type of depth cartridge is the yarn-wound type which has a yarn wound around a central core in such a way that the openings closest to the core are smaller than those on the outside. The aim is to achieve depth filtration, which increases the solids-holding capacity of the cartridge. The yarn may be made of any fibrous material, ranging from cotton or glass fibre to the many man-made fibres like polyester, nylon or teflon. The spun staple fibres are brushed to raise the nap

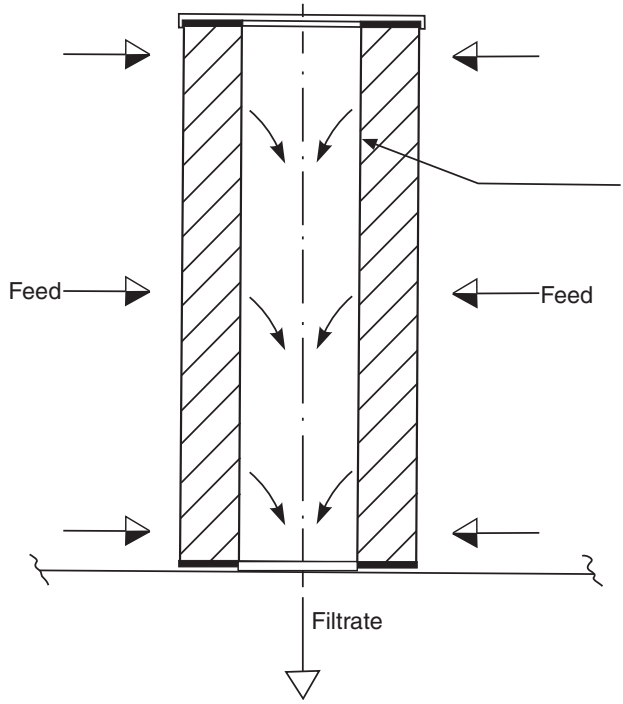

Figure 12.10 Scheme to show the principle of cartridge filters

and this makes the filter medium. The cores are made from polypropylene, phenolic resin, stainless steel or other metals or alloys. The nominal rating of this type of cartridge varies from 0.5 to 100 μm. Cartridges intended for higher viscosity liquids are often made of long, loose fibres, again either natural or synthetic, impregnated with phenolic resin. Such bonded cartridges are usually formed into the shape of a thick tube by a filtration technique and do not normally require a core because they are self-supporting. The porosity of the medium can be graded during the formation process, again to increase the solids-holding capacity. Bonded cartridges are available in somewhat coarser ratings of 10–75 μm.

Depth-type cartridges cannot be cleaned but have high solids-holding capacity, and are cheap and robust. Considerable standardization of the cartridge size throughout industry (approximately 25 cm long, 6.3–7.0 cm overall diameter and 2.5 cm internal diameter) allows testing of different cartridge makes and types in the same holder.

In the category of surface cartridges is another very common type, the pleated-paper construction, which allows large filtration areas to be packed into a small space. Oil filters in the automobile industry are of this type. The paper is impregnated, for strength, with epoxy or polyurethane resin. Any other medium in sheet form, similar to cellulose paper, such as wool,

polypropylene or glass may be used. The nominal rating varies between 0.5 and 50 μm. Pleating in the radial direction is most usual, but some cartridges have axial pleating, or have hollow discs of lenticular shape, in an effort to pack as much filtration surface into a given space as possible; up to 3 m^2 of surface in one cartridge is possible. The solids-holding capacity is low but some applications allow the prolonged build-up of solids on the surface, until the pleats are completely filled up.

Another type of cartridge is the edge filter, which contains a number of thin discs mounted on a central core and compressed together. The discs are usually made of metal, although paper or plastics are sometimes used. Filtration takes place on the surface of the cylinder, with the particles unable to pass between the discs. The main advantage of the edge-type filter is that it is cleanable, and this is done by reverse flow, ultrasonics or by scraping the outside surface of the cylinder with a mechanical scraper. Edge filters made from paper discs have been known to retain particles as fine as 1 μm but the metal variety retains solids larger than 50 μm or so.

Other designs of cartridges use active carbon, Fuller's earth, sintered metal or other specialized media.

The most important characteristics of cartridge filters are the filter rating, i.e. the largest spherical particle which will pass through the filter (usually, the 98% retention cut size is used), the relationship between the pressure drop and solids-holding capacity, and the maximum allowable pressure drop beyond which the cartridge will fail structurally. Both the retention and the solids-holding capacity depend on filtration velocity and this must be borne in mind when testing cartridges. Thermal or shock stresses sometimes lead to cracking of cartridges, with the subsequent loss of overflow clarity.

The housings of cartridge filters are simple pressure vessels designed for one cartridge or a number of cartridges in parallel, in multi-element filters. Some housings are designed to withstand pressures of up to 300 bar. Proper sealing of the elements is a necessary prerequisite of their efficient use. Frequent replacement of cartridges should be facilitated by quick-opening clamping fittings.

Cartridge filters are used to clean power fluids, lubrication oils, wines, fruit juices or pharmaceutical liquids. They are also used to protect other equipment, e.g. in reflux control systems or automatic valves. Low capital and installation costs, low maintenance costs, simplicity and compactness are the main advantages of cartridge filters. The running costs are high, particularly when disposable cartridges are used. It is most important, therefore, that a full economic analysis, based on reliable cartridge replacement frequency, is carried out before adopting a cartridge filtration system; the low cost of the basic hardware may be deceptive.

Evaluation and testing of cartridge filters has been the subject of several studies recently[22–25], with an independent European cartridge testing laboratory emerging at IFTS[22,24] and similar work at the Universities of Leeds and Sheffield[23,25].

12.2.5 Compression filters

In conventional cake filtration the liquid is expelled from the slurry by fluid pressure in a fixed-volume filtration chamber, while in mechanical compression this is achieved by reducing the volume of the retaining chamber. This compression of either a slurry or a cake (which might have been formed by conventional filtration) offers advantages to a wide variety of industries handling a variety of different materials. Such materials include highly compressible, sponge-like solids, very fine particles such as clays, fibrous pulps, gelatinous mixtures like starch residues or some pharmaceuticals, and flocculated waste-water sludges.

The compressibility of filter cakes is a nuisance from the point of view of filtration theory, but in practice it means that with increasing pressure cakes become more compact and therefore drier. The resistance to flow increases due to reduced porosities, however, and, with some materials such as paper-mill effluents higher pressures do not necessarily give increased flow rates. In cakes undergoing conventional pressure filtration, only the bottom layers closest to the medium are subjected to the highest compression forces, whereas the top layers are only subjected to light hydraulic forces and are not compacted so tightly. If a mechanical force is applied to the top of the filter cake, the distribution of pressure through the cake is more uniform, and drier cakes can thus be achieved than by using high pumping pressures of the feed suspension.

In the past decade or so, a number of new filters have appeared on the market, utilizing some form of mechanical compression of the filter cake, either after a conventional pressure filtration process or as a substitute for it. In most designs the compression is achieved by inflating a diaphragm which presses the slurry or the freshly formed filter cake towards the medium, thus squeezing an additional amount of liquid out of the cake—see *Figure 12.11*.

Other designs squeeze the cake between two permeable belts or between a screw conveyor of diminishing diameter (or pitch) and its permeable

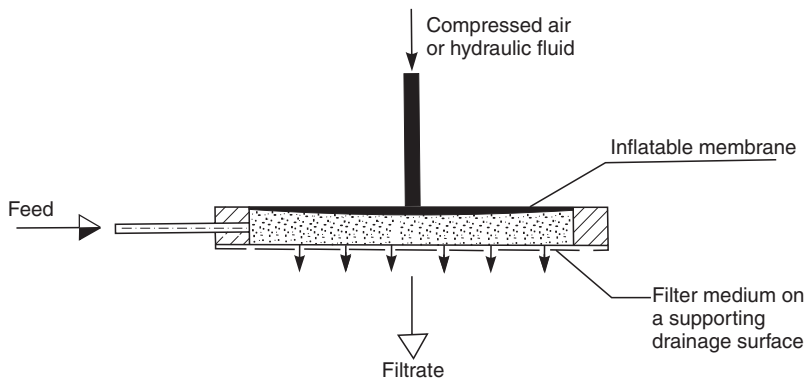

Figure 12.11 Scheme to show the variable-chamber principle

enclosure. The available filters which use mechanical compression can be classified into four principal categories:

1 membrane plate presses,
2 tube presses,
3 belt presses,
4 screw presses.

Only the first two are dealt with here as the others are continuous and are, therefore, included in part II of this chapter (section 12.3.5).

The advantages of using mechanical compression with compressible cakes are in the increased solid contents of the cakes (leading to reduced energy requirements if thermal drying has to follow, or to better handling properties), improved washing efficiencies, increased filtration rates and easier or automatic cake discharge. Invariably, however, the capital cost of such filters is higher than for conventional pressure filters.

12.2.5.1 Membrane plate presses

Membrane presses are closely related to the conventional plate-and-frame presses described in section 12.2.2. They consist of a recessed plate press in which the plates are covered with an inflatable diaphragm which has a drainage pattern moulded into its outside surface. The filter cloth is placed over the diaphragm as shown in *Figure 12.12*. During the first stage of filling the filter chambers with the slurry and conventional pressure filtration, the membrane is pushed against the plate body. When the chambers are full of cake, the feed is terminated and the membranes are inflated by pumping compressed air or hydraulic fluid in between the membranes and the plates, so that the cake in the chamber is compacted as the two membranes move towards one another. Washing of the cake may follow and can be carried out more effectively than in a normal press, because the cake is compacted to a more uniform density by squeezing. The resulting advantage is in the reduction of the washing time and washwater requirements. The squeeze pressures vary from 6 to 15 bar. Additional reductions of up to 25% in the moisture content over that obtained with conventional filter presses can be achieved. The membranes are usually made of a solvent-resistant rubber compound.

Another major advantage of the membrane plate is in its flexibility to cake thickness: thinner cakes can be handled easily without loss of dryness. Cake-release characteristics are also improved by deflating the membrane prior to cake discharge. Alternating arrangements have also been used in which the membrane plates and the normal recessed plates alternate, and this reduces the cost.

Retter[26] has recently described the use of the membrane filter press in the de-bottlenecking of titanium dioxide calcination and in filtration of sugar carbonation sludge.

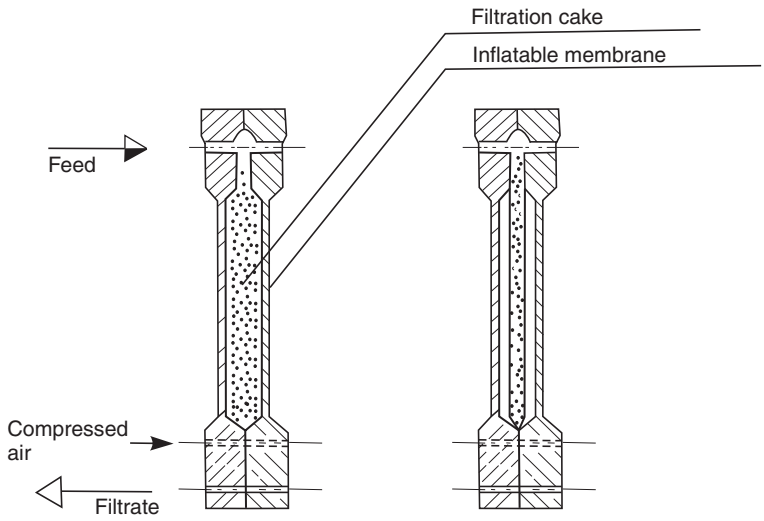

Figure 12.12 A recessed plate in a variable-chamber press

In the plate press filter the pneumatically operated membranes are replaced by flexible seals and by compression by a hydraulically powered ram. *Figure 12.13* depicts the compression stage after the cake has been formed in the chambers between the hollow circular frames carrying the filter medium and the flat rectangular discharge plates. The frames are sealed against the discharge plates by rubber rim seals which form the filtration chambers. As the rim seals are compressed by the hydraulic ram, the cake inside is squeezed. The filter is then opened, the cake adheres to the discharge plates and, as the plates are lowered and raised again, the cake is removed by

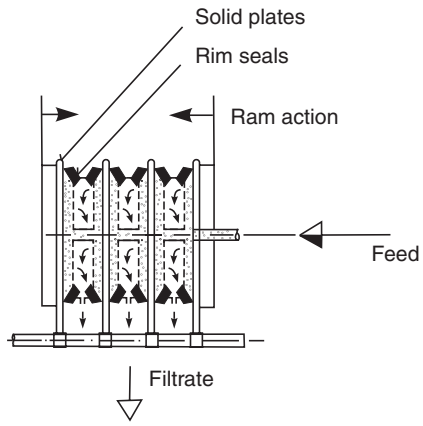

Figure 12.13 A plate-press filter

scrapers. The process is fully automated and filtration areas of up to 20 m^2 are available. No washing of the cake is possible.

A similar principle is used in the OMD leaf filter from Stella Meta Filters. This is a vertical-leaf filter with a rubber diaphragm suspended between the leaves. The cake which forms on the leaves eventually reaches the diaphragm at which point pump pressure is used to inflate the diaphragm and compress the cake. Cake discharge is by vibration.

Another variation of the same principle is the DDS vacuum pressure filter[8] which has a number of small discs mounted on a shaft which rotates discontinuously. The cake is formed on both sides of the discs when they are at the bottom position, i.e. dipped in the slurry. When the discs come out of the slurry and reach the top position, hydraulically driven pistons squeeze the cake and the extra liquid then drains from both sides of the cake. The cake is removed by blow-back with compressed air.

Cake compression by flexible membranes is also used in the new automated vertical presses that use one or two endless cloth belts, indexing between plates (as described in section 12.2.2). Filtration and compression take place with the press closed and the belt stationary, the press is then opened to allow movement of the belt for cake discharge over a discharge roller of a small diameter. This allows washing of the belt on both sides (see *Figure 12.4*). Cycle times are short (typically between 10 and 30 min) and the operation is fully automated. Sizes of up to 32 m^2 are available and the maximum cake thickness is 35 mm.

Washing and dewatering (by air displacement) of cakes are possible. Applications are in the treatment of minerals, in the sugar industry, and in the treatment of municipal sewage sludge and fillers like talc, clay, whiting etc.

12.2.5.2 Cylindrical presses

Another group of filters which utilize the variable-chamber principle are those with a cylindrical filter surface. There are two designs in this category, both of which originate from Britain.

The VC filter shown in *Figure 12.14a* consists of two concentric hollow cylinders mounted horizontally on a central shaft. The inner cylinder is perforated and carries the filter cloth, the outer cylinder is lined on the inside with an inflatable diaphragm. The slurry enters the annulus between the cylinders and conventional pressure filtration takes place, with the cake forming on the outer surface of the inner cylinder. The filtration can be stopped at any cake thickness or resistance, as required by the economics of the process, and hydraulic pressure is then applied to the diaphragm which compresses the cake.

As with other filters of this type, washing can be carried out by deflation of the diaphragm and introduction of washwater into the annulus. Re-inflation of the membrane then forces the wash liquor through the cake, thus displacing

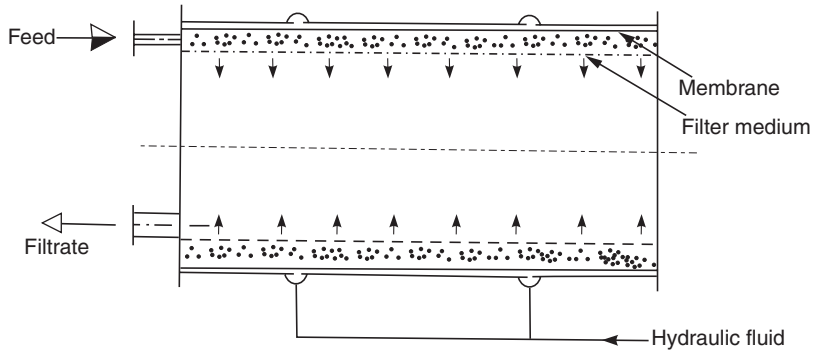

Figure 12.14a Scheme to show the principle of the VC filter

the mother liquor. At the end of the process, the inner cylinder is withdrawn from the outer shell and the cake is either discharged manually or blown off with compressed air. Sizes available range from small, mobile test units of 0.4 m^2 filtration area to large, fully automated machines of 6.1 m^2 filtration area. A choice of two alternative core sizes is offered, giving annuli of 6 or 2.8 cm available for the cake. The hydraulic pressure for operating the membrane goes up to 14 bar. Although originally developed for filtration of dyestuffs, the VC filter has been used successfully for the filtration of gypsum, china clay, cement, industrial effluents, metal oxides, coal washings, nuclear waste and other slurries.

The second filter in this category is the ECLP Tube Press, *Figure 12.14b*. This is smaller in diameter and, unlike the VC filter, it is operated in a vertical position. It uses compression only, both for filtration and for squeezing the cake. The space between the cylindrical rubber membrane and the cloth tube is first filled with slurry and the hydraulically operated membrane is used to drive the liquid through the cloth. It follows, therefore, that this filter is suitable for higher solids concentrations, usually in excess of 10% by weight, in order to obtain the minimum cake thickness necessary for efficient cake discharge of about 4 mm. At the end of the process, the central core is lowered by about 300 mm and the cake is removed by a blast of compressed air from the inside. The hydraulic operating pressures are higher than those of the VC filter at about 100 bar, the single tube area is from 0.9 to 3.5 m^2. Multiple tube assemblies have to be used to treat larger flows. Cake washing is possible but with some solids there is a danger of the cake falling off the inner core whilst the annulus is being filled with water.

The ECLP Tube Press was originally developed for the filtration of china clay[9] but it has been used since with many other slurries such as those in mining, TiO_2, cement, sewage sludge, etc. [27] The usual cycle time is about 4 min or more.

In conclusion, the method of mechanical compression of the cake is very attractive and can lead to very dry cakes. The compressibility of cakes can be

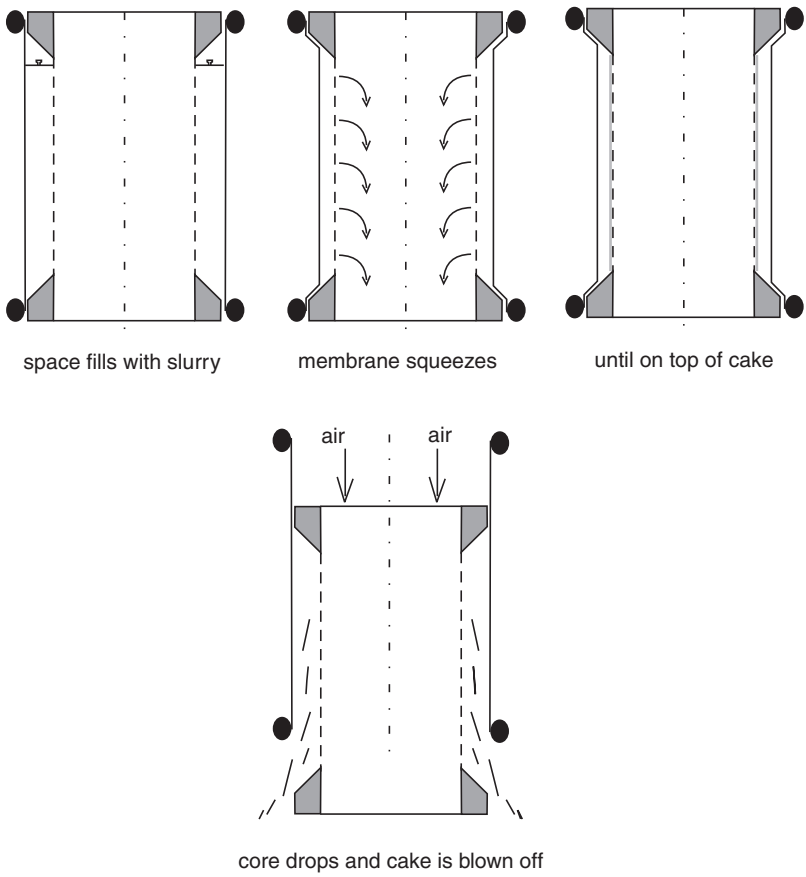

Figure 12.14b Schematic diagram of the function of the ECLP Tube Press

very easily tested and most manufacturers provide such tests. Whenever a rubber membrane is used for the compression, however, this inevitably increases the capital cost and thus variable-chamber filters tend to be more expensive than conventional filters of the same category.

Carleton[7] gives some useful advice on how to select the right type of cake squeezing filter for a given application and process requirements.

Pressure filtration
Part II—Continuous filtration

12.3 Continuous pressure filtration

12.3.1 The case for continuous pressure filtration

The following notes should be read in conjunction with section 12.2.1 where the general aspects of pressure filtration are discussed. This section only adds some notes specific to continuous pressure filtration.

The first advantage of any continuous filter is the absence of or reduction in down-times which means gains in capacity. Bearing in mind the effects of compressibility of cakes discussed in section 12.2.1.1, the effect of higher driving force on capacity can be seen in equation 12.1 which is derived for constant-pressure filtration from the well-known law of Darcy. The effect of resistance of the filter medium is neglected here and the cake is assumed to be incompressible.

If everything else remains constant, the equation can be rewritten in the form of equation 12.4, whereby the dry cake production capacity, Y, is proportional to the square root of the applied pressure drop, Δp, and to the square root of the speed of rotation, n:

$$Y = \text{constant} \cdot \sqrt{\Delta p\, n} \tag{12.4}$$

Note that the above equation is only valid for incompressible cakes, negligible medium resistance and constant submergence, f.

The increased pressure drop in pressure filtration clearly affects the capacity in two ways: it increases capacity directly through higher driving force, and it allows the speed of rotation, n, to be increased without increasing moisture contents (because higher pressures lead to better dewatering, as shown in section 12.2.1.2). Higher speeds (at constant feed concentrations) lead to thinner cakes, and the limiting condition is the minimum cake thickness that can still be successfully removed from the filter medium and discharged. Another practical limit is the air consumption in the dewatering period that follows filtration: thin cakes offer little resistance to air flow and air rates (and energy consumption) become excessive.

It seems, therefore, that continuous pressure filters should be built to run at high pressures and high speeds (see equation 12.4). There are, however, two additional considerations: the higher the design pressure, the more expensive

is the pressure vessel with its associated hardware, and thin cakes and high pressures lead to excessive air rates (and energy consumption). There must be compromise, therefore, between cake thickness and pressure: if high pressures are used, the cakes have to be thicker than for lower pressures. Different companies tackle this problem differently: KHD for example[10] limit themselves to moderate pressures (2.5 bar) and run their disc filter at high speed (up to 3 rev. min^{-1}). Amafilter, on the other hand[11], use a gauge pressure of 6 bar but run their disc filter more slowly (about 1 rev. min^{-1}) at higher submergence, which results in thicker cakes. As the equivalent speeds (taking into account different lengths of time provided for dewatering in their cycle) are in about the same ratio as the pressure drops used in the two machines, the cake production capacity with the same solid would probably be similar but the KDF filter is likely to have the edge on moisture content because it operates higher on the capillary pressure curve (*Figure 12.1*). Having a sophisticated computer-controlled system, it can also optimize the operating variables for maximum capacity, minimum moisture content, lowest energy consumption or any combination of these as required.

A continuous pressure filter may be defined as follows: it is a filter which operates at pressure drops greater than 1 bar and its operation does not need to be interrupted to discharge the cake. The cake discharge itself, however, does not have to be continuous. As there is little or no down-time involved, the dry solids rates can sometimes be as high as 1750 kg m^{-2} h^{-1} with continuous pressure filters.

Most of the continuous pressure filters available today[18] have their roots in vacuum-filtration technology. It is obvious that a rotary drum or rotary-disc vacuum filter can be adapted to pressure by enclosing it in a pressure cover but the disadvantages of this measure are equally obvious. The enclosure is a pressure vessel which is heavy and expensive, the progress of filtration cannot be watched and the removal of the cake from the vessel is the most difficult problem of the whole design. Other complications of this method are caused by the necessity of arranging for two or more differential pressures between the inside and outside of the filter, which requires a troublesome system of pressure-regulating valves. Despite these disadvantages, the advantages of high throughputs and low moisture contents in the filtration cakes have justified the recent and vigorous development of continuous pressure filters, and the trend is certain to continue in the future.

Horizontal- or vertical-vessel filters with vertical rotating elements in particular have been under rapid development recently with the aim of making truly continuous pressure filters, particularly, but not exclusively, for the filtration of fine coal. There are basically three categories of continuous pressure filters presently available: disc filters, drum filters and belt filters, the last category including both the hydraulic and compression varieties. For the purpose of this review, we shall also briefly consider some semi-continuous, indexing cloth filters and other types with intermittent movement of elements. Only those filters which discharge the solids in the

form of a semi-dry cake are considered here and the so-called filter-thickeners (which discharge the solids in a thick slurry) are, therefore, excluded; these are reviewed in chapter 11.

The advantages of continuous pressure filtration are clear and indisputable, particularly with slow-settling slurries and fairly incompressible cakes. Such filters are expensive, however, both to install and to run, and the most likely applications are either in large-scale processing of products that require thermal drying after the filtration stage (fine coal or cement slurries in the dry process) or in small-scale processing of high-value products, like in the pharmaceutical industry.

There are, obviously, many technical problems to be solved when developing a new commercial and viable filter; all are solvable and some of the recently developed and proven systems show this. However, the filtration hardware in itself is not enough: as the control of a continuous pressure filter is much more difficult than that of its equivalents in vacuum filtration, the necessary development may also include an automatic, computerized control system. This moves pressure filtration from low to medium or even high technology.

12.3.2 Disc filters

12.3.2.1 The McGaskell and Gaudfrin disc filters

One of the earliest machines in this category is the McGaskell rotary pressure filter[12] which is essentially a disc-type filter enclosed in a pressure vessel. Just like the vacuum rotary-disc filters, the rotating discs in this filter are each composed of several wedge-shaped elements connected to a rotary filter valve at the end of the shaft. This filter was originally designed for the filtration of waxes in the oil industry and was equipped for a gradual increase in pressure with cake build-up. This is said to have produced high filtrate clarity. Pressures of up to 7 bar have been used.

The slurry reservoir is divided into pockets or 'crenellations', which have spring-loaded scrapers. The scrapers press against the discs and direct the cake into the spaces between the pockets around the discs which lead to a chute connected to an inner casing in which is placed a worm gear. The worm conveys and compresses the cake, thus squeezing more liquid from it, through a filter cloth surround. The compressed cake forms a plug round a spring-loaded, tapered discharge valve, and the plug prevents leakage of gas. The cake can be washed but probably not very effectively.

This filter is reported in filtration literature[12] but whether or not it is available on the market at present is not known to the author; it is, however, included in this review for completeness and also to show that the idea of a pressure disc filter is by no means new.

Another disc-type pressure filter based on a similar principle is the Gaudfrin Disc Filter, originally designed for the sugar industry and available

in France since 1959. It is also similar in design to a vacuum disc filter but it is enclosed in a pressure vessel with a removable lid. The discs are 2.6 m in diameter and composed of 16 sectors. The cake discharge is by air blow-back, assisted by scrapers if necessary, into a chute where it may either be reslurried and pumped out of the vessel or, for pasty materials, it can be pumped away with a monopump without reslurrying. The Gaudfrin Disc Filter is designed for only relatively low pressures of 1 bar on average and it provides for cake washing which can be in two stages, in two separate compartments within the same vessel.

12.3.2.2 The KDF filter

A recently developed KDF filter (*Figure 12.15*) from Amafilter[11] is based on a similar principle to that of a disc filter. It was developed mainly for the treatment of mineral raw materials like coal flotation concentrates or cement slurries. It can produce a filter cake of low moisture content, at very high capacities of up to $1750\,kg\,m^{-2}\,h^{-1}$. The pressure gradient is produced by pressurized air above the slurry level which, besides providing the necessary driving force for the filtration, is also used for displacement dewatering of the cake.

Assemblies of small discs are rotated in a planetary movement around a central screw conveyor. The discs are mounted on six hollow axles and the axles revolve on overhanging bearings from the gearbox at one end of the vessel where they are driven, via a drive shaft, by an electric motor. The filtrate is collected from the discs via the hollow shafts and a filter valve into a large collecting pipe. The hollow shafts also collect the water and air from the dewatering process, in another part of the rotational cycle. The number of

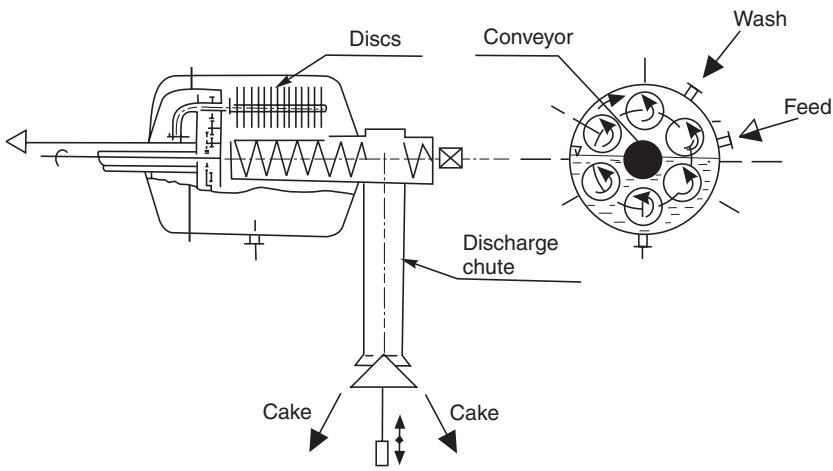

Figure 12.15 The KDF continuous-pressure filter

discs mounted on the shafts can be adjusted for different materials, depending on the required capacity and the cake thickness to be used. As the vessel is only about half-filled with slurry, the discs become coated with the cake when immersed, the cake is then dewatered when they emerge from the slurry and scraped or blown off (by reverse blow) into the central conveyor, which takes the cake to one end of the vessel. The planetary action and the slow movement of the discs through the feed slurry ensure exceptionally good homogeneity of the cake which is critically important for good dewatering characteristics; the typical speed of rotation of the planetary system of shafts is 0.8–1.0 rev. min^{-1}.

A screw conveyor was used for conveying the cake at first but this has been replaced with a chain-type conveyor in the filter marketed and sold recently. The first prototype used a tapered screw to form a plug before discharge into atmospheric pressure but this has now been replaced by compaction in a vertical pipe.

The cake discharge is initiated and stopped by two level indicators inside the vertical pipe. The cake is actually discharged using the pressure inside the vessel; a specially designed, hydraulically operated discharge valve momentarily opens and the cake 'shoots' out. The air pressure used for driving the slurry through the filter is 6 bar and filtration areas are available up to 120 m^2. Cake washing is possible but it has not been reported as actually being performed.

The KDF filter was first tested in prototype on a coal mine in northern Germany. It was installed in parallel with existing vacuum filters and it produced filter cakes consistently lower in moisture content by 5–7% than the vacuum filters. Two production models have now been installed and operated at a coal mine in Belgium. The filter is controlled by a specially developed computer system; this consists of two computers, one monitoring the function of the filter and all the detection devices installed, and the other controlling the filtration process. The system allows optimization of the performance, automatic start-up or shut-down and can be integrated into the control system of the whole coal-washing plant.

12.3.2.3 The KHD pressure filter

Another development of the disc filter has been reported more recently from KHD Humboldt Wedag AG[10]. A somewhat different system, probably a predecessor, was also patented by the same company[13]. The patented system[13] has stationary discs mounted inside a pressure vessel (horizontal vessel, vertical discs) which is mounted on rollers and can rotate slowly about its axis. A screw conveyor is mounted in the centre of rotation but this is stationary; it conveys the cake, which is blown-off the leaves when they pass above the screw, to one end of the vessel where it falls into a vertical chute. The cake-discharge system involves two linear slide valves which slide the cake through compartments which gradually depressurize it and move it out

of the vessel without any significant loss of pressure. The system relies entirely on the cake falling freely from one compartment to another, as the valves move across, and this may well be a rather unrealistic assumption, particularly with sticky cakes. This, combined with lots of sliding contact surfaces which are prone to abrasion and jamming, makes one wonder if the idea is practicable at all. There is another major disadvantage involved here in that there are two large running seals involved in the main body of the filter as the vessel rotates around a stationary central arrangement; this seal is another potential source of trouble. All in all, this version has, in my view, very little chance of commercial success and it seems to have been shelved in favour of a more conventional system of a stationary vessel as reported recently[10].

The newer version, actually built and tested with coal slurries in a pilot plant facility and also, most recently in production, with a 90 m^2 version, has the rotating discs and all the driving elements inside a stationary vessel. The discs, according to the manufacturer's literature, range from 1300 to 3000 mm in diameter, with up to 10 being housed in one vessel, giving filtration areas of up to 480 m^2. The cake discharge is through a rotary lock discharger which has cylindrical compartments rotating around a vertical axis. Once again, sliding surfaces are involved and the cake is assumed to be non-sticky so that it will fall out when the compartment opens to the atmosphere. The filtration area can be varied by changing the size and number of discs; no overall vessel dimensions or further details of the filter construction, other than those quoted above, are given.

The test results reported show the advantages of pressure filtration quite clearly: the dry-cake production capacity obtained with the test solids (coal suspensions) was raised by 60–70% by increasing the pressure drop from 0.6 bar to 2 bar. At the same time, the final moisture content of the cake reduced by as much as 5–7%. There is, obviously, a law of diminishing returns at play here, in that further increases in the operating pressure bring about less and less return in terms of capacity and moisture content.

The authors claim that, if the pressure '... is increased beyond 2 bar, the residual moisture content cannot be further reduced remarkably', but their own data does not seem to support this. The reduction continues at pressures beyond 2 bar, albeit at a lower rate, and, surely, statements on whether or not it is feasible to go to higher pressures should be supported by an economical analysis in which the cost of thermal drying is considered. The tests also show fairly predictable effects of particle size and cake thickness on dry-cake production capacity.

Another reason for keeping the operating pressure low is the air consumption: in order to obtain high capacities, the manufacturers designed the discs to spin fairly fast (up to 2 or 3 rev. min^{-1}) and this leads to thin cakes. Thin cakes, however, give little resistance to air flow and, consequently, the only way to keep this flow within economical limits is to reduce the air pressure in the vessel—see the previous discussion of this in section 12.3.1.

12.3.2.4 Krupp pressure disc filter

A recent arrival in amongst the continuous pressure filters is the Krupp filter[28]. This is another disc filter, operated at 6 bar, where the disc assembly is driven hydraulically from outside of the pressure vessel. The cake is discharged into an internal conveyor by a blast of compressed air and removed from the vessel through a two-stage lock installed in the vessel floor. Filtration areas range from 4 to 300 m^2 and a sophisticated automatic control and monitoring system involving a number of sensors and underwater cameras is used.

12.3.3 Drum filters

Another idea borrowed from vacuum filtration to produce a continuous pressure filter is the rotary-drum filter. This filter has the disadvantage that it makes relatively poor use of the space available in the pressure vessel and the filtration areas and capacities of such filters cannot possibly match those of the disc pressure filters. In spite of this disadvantage, however, the pressure drum filter has recently been extensively developed.

The drum is sometimes mounted in a vertical rather than a horizontal vessel. Once again the pressure is created by pumping compressed gas into the vessel. Sometimes, the intake of the compressor is connected to the filtrate side of the filter and the gas goes round in a closed circuit. The method used to discharge the cake continuously from the high pressure inside the vessel into the atmosphere is, once again, the real heart of the design. Variable pitch screws, star valves, alternating or serial decompression chambers, mono-pumps (for pasty and thixotropic cakes) and other similar devices have been tried with a varying degree of success, obviously depending very much on the properties of the cake. Another, rather obvious, alternative is the use of two storage vessels into which the cake is alternately discharged at the same pressure as in the filter, the pressure is later released and the cake is discharged from the vessel under atmospheric pressure.

12.3.3.1 The development at 'TU Karlsruhe'

Professor Stahl and his co-workers[2] at the University of Karlsruhe have worked in continuous filtration for many years and have developed a test unit of a small drum filter (total filter area of 0.7 m^2 with 30% submergence) housed in a large horizontal pressure vessel and, with it as a model, developed and tested several interesting concepts.

One such concept is the so-called hyperbar vacuum filtration. This is a combination of vacuum and pressure filtration in a pull–push arrangement, whereby a vacuum pump or a fan generates a vacuum downstream of the filter medium, whilst a compressor maintains higher-than-atmospheric pressure

upstream. If, for example, the vacuum produced is 0.8 bar (i.e. an absolute pressure of 0.2 bar) and the absolute pressure before the filter is 1.5 bar, a total pressure drop of 1.3 bar is created across the filter medium. This is clearly a new idea in principle, but in practice it requires three primary movers: a liquid pump to pump in the suspension, a vacuum pump to produce the vacuum and a compressor to supply the compressed air. The cost of having to provide, install and maintain one additional primary mover is probably the main reason why the idea of hyperbar vacuum filtration has not yet taken off: only Andritz in Austria offer a system commercially.

Apart from the hyperbar vacuum filtration, the work at Karlsruhe also includes fundamental investigations into cake filtration generally, pressure filtration of coal and ore suspensions, and studies of dewatering of cakes. As an alternative to the small drum filter, they have apparently also used a small belt filter in the same pressure vessel. Some commercial developments, like the KHD pressure filter, are reported to have originated from the work at Karlsruhe.

12.3.3.2 The TDF drum filter

The TDF drum filter was developed at Krauss Maffei and the product is a fairly conventional drum filter housed in a vertical pressure vessel. Some test data can be found in the company literature[14], obtained with the smallest model of only $0.75\,m^2$ filtration area; larger models have also been announced, ranging up to a filtration area of $46\,m^2$ but at this limit the vessels become very large. The operating pressures quoted are moderate (2.5–3.5 bar) and the drum speeds are fairly conventional (0.3–1.5 rev. min^{-1}). The range of dry-cake production quoted is 250 to $650\,kg\,m^{-2}\,h^{-1}$ for fine coal.

The cake is scraped-off with a conventional knife arrangement and is then conveyed in a screw conveyor to one end of the vessel where it enters the discharge system; there are apparently four design alternatives depending on the cake to be processed. A tapered rotary valve (with a horizontal axis), a pump (presumably a mono-pump), a rotary valve (vertical axis) with a blow-through, similar to the one used in pneumatic conveying, and a vertical pipe compactor similar in design to the Fuller-Kinyon pump in pneumatic conveying. It is not known to what extent these systems have been developed or whether they merely represent possibilities yet to be proven.

A plate-type filter has also been mentioned in the Krauss Maffei literature; the PDF filter which, instead of a drum, uses a paddle wheel (like in a paddle steamer) with radial, longitudinal plates covered with filter cloth and manifolded to the filter valve at one end of the vessel. This filter apparently used a horizontal pressure vessel and was built to have only 0.75 or $1.5\,m^2$ area and operated at 2.5 bar. A central screw conveyor collected the cake blown-off the plates and conveyed it to the discharge end of the vessel.

12.3.3.3 The BHS-Fest filter

A different approach to the use of a drum for pressure filtration is made in the BHS-Fest filter[15] (*Figure 12.16*). This permits a separate treatment of each filter section, in which the pressure may vary from vacuum to a positive pressure of several bar; pressure regulation is much less difficult than in the conventional enclosed drum-type pressure filter.

The BHS-Fest pressure filter has a rotating drum, also divided into sections but the separating strips project above the filter cloth and thus form cells. The drum is almost completely surrounded by an outer shell and the space between the shell and the drum is divided into a number of compartments.

The compartments are separated by seals under adjustable pressure. As the drum rotates, each cell on the drum passes successively through the series of compartments, thereby undergoing different processes such as cake formation, dewatering, cake washing or cake drying, and these can be carried out in several stages under different pressures or even under vacuum.

Cake discharge occurs at atmospheric pressure by the action of a roll or a scraper, assisted by blow-back. The cloth may be washed by a spray before the cycle starts again. Filtering areas range up to 8 m^2 and drum diameters up to 2 m. The necessity for large seals limits the operating pressure to less than 3 bar, typically. The cake thickness can be from 2 to 150 mm; depending on machine sizes and the speed of drum rotation is up to 2 rev. min^{-1} (usually 0.3–1 rev. min^{-1}). Applications occur in the manufacture of pharmaceuticals, dyestuffs, edible oils and various chemicals and minerals.

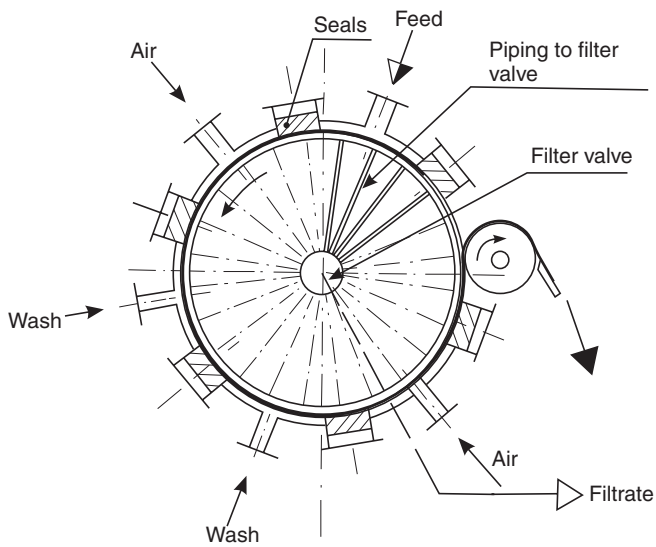

Figure 12.16 The BHS-Fest pressure filter

12.3.4 Horizontal belt pressure filters

As much as the vacuum horizontal belt filters have made a considerable impact in vacuum filtration, one would expect that the same principle may be used in pressure filtration, by enclosing the whole or part of the belt in a pressure vessel. This idea has to be seen as entirely separate from the so-called belt presses (section 12.3.5.1) which use the squeezing of cake by a second belt and do not use the pressure of the liquid or air to drive the filtrate through and out of the cake.

Horizontal belt filters have a great advantage in cake washing application due to their horizontal filtration surface. In the context of pressure filtration and the requirements of good dewatering, however, they have a major disadvantage because the cake is not very homogeneous; gravity settling on the belt and the inevitable problems of distribution of the feed suspension over the belt width give rise to particle stratification and non-homogeneous cakes.

It has already been mentioned in the previous section that a horizontal belt filter has been used in place of the small drum filter in the filtration studies at Karlsruhe[2]. In this case, the whole of the filter was placed in a large pressure vessel and there were, therefore, no moving parts passing through the filter shell. To the best of my knowledge, there is no commercial filter based on this principle; the utilization of the space inside the pressure vessel would be rather poor and the filtration areas very limited indeed.

Another possibility is to enclose only the working, top part of the horizontal belt in the pressure vessel and to pass the belt through the sides of the vessel. Inevitably, the operation has to be intermittent because the belt cannot be dragged over the support surface with the pressure on and, also, the entrance and exit ports for the belt must be sealed during operation to prevent excessive losses of air. The movement of the belt is intermittent, therefore, and is synchronized with decompression in the vessel. This means that the whole of the vessel volume must be depressurized in every cycle and this is wasteful; there is also the inevitable down-time involved but there are no problems with discharging the cake because this is done at atmospheric pressure. Strictly speaking, such filters do not fall in the scope of this review because the movement is not continuous, and they are only briefly reviewed in the following.

The idea is not new: the flat-bed pressure filter by Hydromation Engineering Co. Ltd[16], for example, is based on this principle. The pressure compartment consists of two halves, top and bottom. The bottom half is stationary whilst the top half can be raised to allow the belt and the cake pass out of the compartment and to be lowered onto the belt during the filtration and dewatering stages. The filter can be considered as a horizontal filter press with an indexing cloth; in comparison with a conventional filter press, however, this filter has a disadvantage in that it allows only the lower face of the chamber to be used for filtration.

A recent patent from KHD AG[17] describes the same idea except that the top half of the pressure compartment is not lifted but opens and closes little gates for the belt to pass through. This is another filter proposed for dewatering of fine coal in particular.

One relatively recent development in this filter category is the vertical recessed plate automatic press (shown schematically in *Figure 12.4*), also described in section 12.2.2. This filter has many filtration chambers placed vertically one upon another. It has an endless cloth belt, travelling intermittently between the plates via rollers to peel off the cake. As the filter cloth zig-zags through the filter, the filtering direction is reversed each time and this tends to keep the cloth clean. As it goes round, the filter belt can be washed on both sides as shown in *Figure 12.4*. The height of the vertical press makes maintenance difficult and the number of the chambers is, therefore, restricted, usually to 20, maximum 40, with filter areas of up to 32 m^2. Cycle times are short, typically between 10 and 30 mins, and the operation is fully automated. The maximum obtainable cake thickness is about 35 mm, washing and dewatering (by air displacement) of cakes is possible. Applications include the treatment of mineral slurries, sugar, sewage sludge, and fillers like talc, clay, whiting and similar. The filtration velocities are usually from 0.025 to 1 $m\,h^{-1}$ and dry solids handling capacities are up to 1000 $kg\,m^{-2}\,h^{-1}$ due to the short down-times involved.

12.3.5 Continuous compression filters

The variable-chamber principle applied to batch filtration, as described in section 12.2.5, can also be used continuously, in belt presses and screw presses.

12.3.5.1 Belt presses

The next category of continuous pressure filters is the belt filter press which usually combines gravity drainage with mechanical squeezing of the cake between two running belts. The first example is the Manor Tower Press, a Swiss invention, which is also available in the UK. A schematic diagram of the principle of this press is shown in *Figure 12.17*. Essentially it consists of two acutely angled vertically converging filter belts running together downwards. The shallow funnel formed between the belts (and the ends sealed by a special edge-sealing belt) is filled from the top with the slurry to be filtered and the slurry moves together with the driven belts down the vertical narrowing gap where filtration takes place. The hydrostatic pressure causes the solids to be deposited on the faces of the belts until the two cakes combine to form a continuous ribbon of filter cake which is squeezed in the closing gap at a pressure of 2.5 bar (gauge pressure) and discharged at the bottom. In order to protect the press against overload, the final gap at the bottom is automatically controlled so that the above-mentioned pressure is not exceeded.

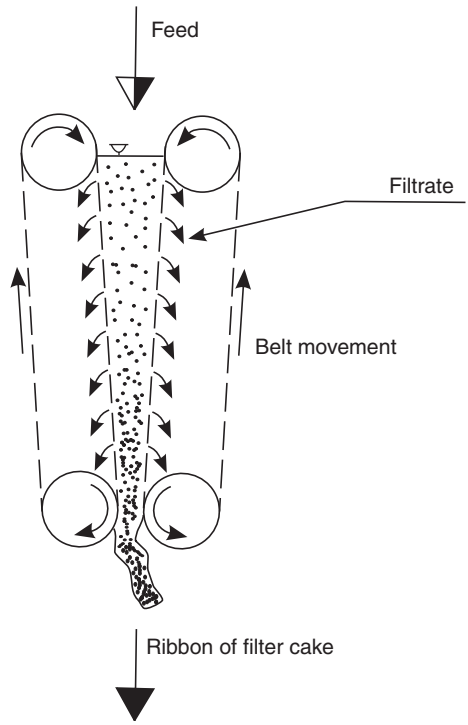

Figure 12.17 Scheme to show the principle of the Manor Tower press

Although originally designed for the continuous filtration of conditioned sewage sludges (as are most of the filter belt presses available), the Manor Tower Press is increasingly used for the treatment of paper mill sludge, coal or flocculated clay slurries.

There is a bewildering variety of horizontal filter presses, with probably more than 20 designs on the market; most of these were developed in the past three decades. They owe their existence to the availability of cationic polyelectrolytes which promote the release of water from organic sludges which is the area where belt-filter presses are most used. Some are therefore called sewage-sludge concentrators. As an example, the Unimat Belt Filter Press, which has most of the features characteristic of many belt presses, is shown in *Figure 12.18*. The flocculated feed is first introduced onto the horizontal drainage section where the free water is removed by gravity. Sometimes a system of ploughs may be employed to turn over the forming cake and allow any free water on the cake surface to drain through the belt mesh. The sludge is then sandwiched between the carrying belt and the cover belt and compression dewatering takes place; liberated water passes through the belts. The third zone ('shear zone') is designed to produce yet drier cake by shearing the cake by flexing it in opposite directions during passage

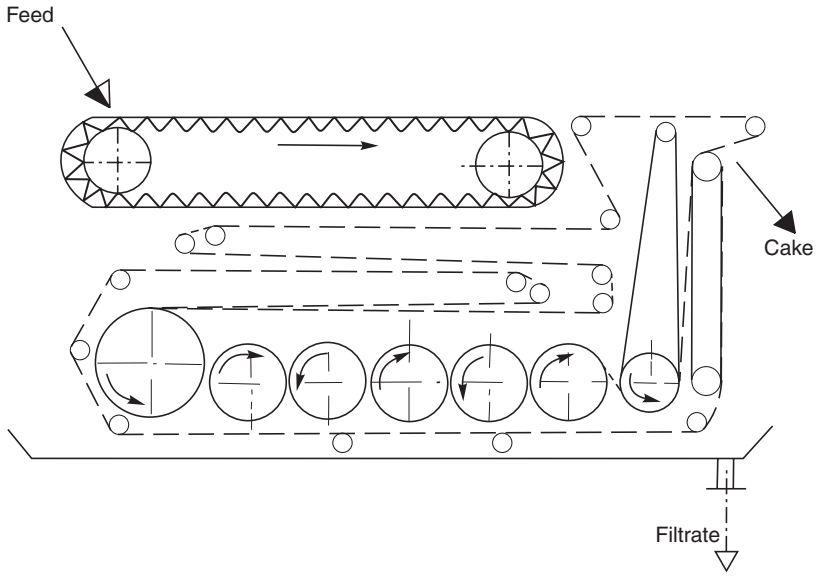

Figure 12.18 The Unimat belt filter press

through a train of rollers in a meander arrangement. In order to prevent the released water being absorbed back into the cake on the cake release, scrapers or wipers are sometimes installed to remove the water from the outside of the belts. Belt-filter presses are made up to a width of 2.5 m and produce a final solids concentration of the discharge sludge in the range 35–60%.

An early paper by Austin[29], reviewed the development of the belt press and its applications. More recently, Smollen and Kafaar have developed electro-osmotic dewatering as an enhancement for belt presses used for dewatering of sludges[30].

It should be added here that, apart from the specially designed belt presses described above, the compression principle is also utilized in some conventional vacuum drum or belt filters by the addition of compression rollers or belts. The benefit in terms of further dewatering in such cases is small, if indeed there is any advantage, because the compression time is short and the excluded liquid might be sponged back into the cake before it can be removed. Such devices probably have greater value in tackling cake-cracking problems.

12.3.5.2 Screw presses

Another way of achieving compression of the cake is by squeezing in a screw press—see *Figure 12.19*. This process is only suitable for the dewatering of rough organic materials, pastes, sludges or similar materials, because it does not include a filtration stage. The material is conveyed by a screw inside a

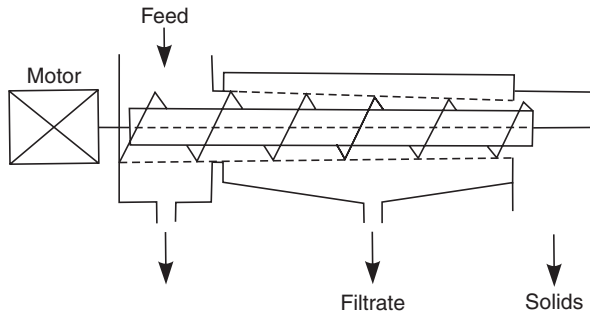

Figure 12.19 Scheme to show the principle of a screw press

perforated cage, and the available volume continuously diminishes. This can be done either by reducing the pitch of the screw in a cylindrical cage, or by reducing the diameter of the screw in which case the cage is conical, as shown in *Figure 12.19*. The cage is either perforated or constructed from longitudinal bars in a split casing. The solids discharge is controlled by a suitable throttling device which controls the operating pressure. Washing or dilution liquid can be injected at points along the length of the cage. The power requirements are high.

The Stord Twin Screw Press uses two counter-rotating, intermeshing screws in a perforated cage. The gradual reduction in the space between the screw flights and the strainer plates is achieved by a combination of reduction in the cage (and screw) diameter and of increase in the diameter of the hollow trunk of the screw body. Although more than one type of material can be handled in the same press, the press usually has to be adapted to different raw materials, according to their dewatering characteristics. Typical applications include dewatering of sugar-beet pulp, fish meal, distillers and brewers spent grains, starch residues, fruit, potato starch by-products, grass, maize, leaves and similar materials.

A Japanese firm, Kuri Chemical Engineers[31], has a vertical screw press, with the dewatered solids discharging at the bottom. A scraper part of the screw leaves a thin heel of cake which acts as a precoat, which is either formed directly from the process slurry or from a filter aid such as diatomite. The filtration screen (wedge wire screen of 25 μm aperture) is cleaned automatically by back-washing. The tests reported were with potassium chloride crystals in a solution of PVC in acetone, and with activated carbon in an aqueous solution of alanine. Particle size ranged from 1 to 100 μm.

References

1. Svarovsky, L., *Solid–Liquid Separation Processes and Technology, Vol. 5, Handbook of Power Technology*, Elsevier, Amsterdam (1985)

2. Bott, R., Anlauf, H. and Stahl, W., 'Continuous pressure filtration of very fine coal concentrates', *Aufbereitungstechnik*, **5**, 245–258 (1984)
3. Svarovsky, L., 'Pressure filtration of coal flotation concentrates', *Conference on Solid–Liquid Practice III, 397th Event of the EFCE* (Bradford, 29–31 March 1989), Institute of Chemical Engineers Symposium Series, London (1989)
4. Wakeman, R. J. 'The application of expression in variable volume filters', *J. Separ. Proc. Technol.*, **2**, 1–8 (1981)
5. Baluais, G., Rebouillat, S., Laclerc, D. and Dodds, J. A., 'Modelisation of compression dewatering and the application to filter design, I', *Chem. Eng. Symp. on Solid/Liquids Separation Practice and the Influence of New Techniques* (Leeds, 3–5 April 1984), Paper 3, pp. 32–41, Institute of Chemical Engineers, Yorkshire Branch (1984)
6. Carleton, A. J. and Moir, D. N., 'Optimisation of compression filters, I', *Chem. Eng. Symp. on Solid/Liquids Separation Practice and the Influence of New Techniques* (Leeds, 3–5 April 1984), Paper 2, pp. 19–31, Institute of Chemical Engineers, Yorkshire Branch (1984)
7. Carleton, A. J., 'Choosing a compression filter', *Chem. Eng.*, **April**, 20–23 (1985)
8. Johnsen, A. F., Madsen, R. F. and Nielsen, W. K., 'DDS-vacuum pressure filter', *2nd World Filtration Congress 1979*, pp. 163–171, Filtration Society, London (1979)
9. Gwilliam, R. D., 'The EEC tube filter press', *Filtr. Sep.*, **March/April**, 1–9 (1971)
10. Blankmeister, D. and Triebert, Th., 'Dewatering ultrafine coal slurries by means of pressure filtration', *Aufbereitungstechnik*, **1**, 1–5 (1986)
11. Dosoudil, M., 'The application of the continuous pressure filter to flotation concentrates', *Aufbereitungs-Technik, Jahrgang*, **25**, 259–265 (1984)
12. Mills, F. D., *Report on Filtration*, Imperial Chemical Industries (1957)
13. Heintges, S., German Patent DE 3316561 A1 (1984)
14. Krauss Maffei, Information, Trommeldruckfilter TDF
15. BHS Trenntechnik, Sonthofen, BHS-Fest-Filter
16. Purchas, D. B., *Solid/Liquid Separation Technology*, Uplands Press, Croydon (1981)
17. Heintges, S., US Patent 4,477,358 (1984)
18. Svarovsky, L., 'Recent developments in continuous pressure filtration', *Aufbereitungs-Technik*, **5**, 242–250 (1986)
19. Tarleton, E. S. and Wakeman, R. J., 'Simulation, modelling and sizing of pressure filters', *Filtration & Separation*, June, 393–397 (1994)
20. Tarleton, E. S., 'Predicting the performance of pressure filters', *Filtration & Separation*, April, 293–298 (1998)
21. Patnaik, T., 'The helical filter—the next generation in centrifugal discharge filtering equipment', *Filtration & Separation*, November/December, 929–937 (1995)
22. Jourdan, M.-F., Peuchot, C. and Hunt, T., 'New test method for evaluation of water cartridge filters', *Filtration & Separation*, July/August, 427–434 (1994)
23. Williams, C. J. and Edyvean, R. G. J., 'Testing cartridge filters in aqueous media: Interpreting the results—The pitfalls and problems. Part 1: Evaluating performance methods', *Filtration & Separation*, February, 157–161 (1995)
24. Peuchot, C., 'New standard designation for process cartridge filter efficiency', *Filtration & Separation*, April, 217–223 (1997)
25. Williams, C., 'The case for a new European standard designation for process cartridge filter efficiency?', *Filtration & Separation*, June, 459–462 (1997)

26. Retter, E., 'Membrane filter presses: an alternative to rotary vacuum filters', *Filtration & Separation*, June, 422–423 (1997)
27. Sullivan, S., 'The use of high filtration pressure in the dewatering of industrial mineral effluents for disposal to landfill', *Filtration & Separation*, May, 339–344 (1998)
28. 'Krupp Pressure Disc Filter—continuous filtration at pressures above atmosheric', Krupp Fordertechnik GmbH, Bulk Solids Handling, **Vol. 17**, No. 3, July/September, 437 (1997)
29. Austin, E. P., 'The filter belt press—application and design', *Filtration & Separation*, July/August, 320–330 (1978)
30. Smollen, M. and Kafaar, A., 'Development of electro-osmotic sludge dewatering technology', WRC Report No. 427/1/95, CSIR, Stellenbosch, January 1995, ISBN: 1 86845 163 1
31. 'Continuous filter press', Kuri Chemical Engineers, *The Chemical Engineer*, **11** October, 23 (1990)

Bibliography

Bunten, K., 'Membrane filter presses in the sugar industry' in Proceedings Volume II, World Filtration Congress 8, European Federation of Chemical Engineering Event No. 607, organised by The Filtration Society and Elsevier Science, The Brighton Centre, Brighton, UK, 3–7 April 2000, 910–913 (2000)

Jamsa-Jounela, S. L. and Oja, M. 'Modelling module of the intelligent control system for the variable volume pressure filter, *Filtration + Separation*, 39–49 (March 2000)

Krimitsas, N., Vorobiev., E. and Petryk, M., 'Continuous solid–liquid expression from cellular materials in screw presses: process analysis and modelling', Proceedings Volume II, World Filtration Congress 8, European Federation of Chemical Engineering Event No. 607, organised by The Filtration Society and Elsevier Science, The Brighton Centre, Brighton, UK, 3–7 April 2000, 763–766 (2000)

Kurita, Y. and Ito, Y., 'New developed fully automatic dehydrator, in Proceedings Volume II, World Filtration Congress 8, European Federation of Chemical Engineering Event No. 607, organised by The Filtration Society and Elsevier Science, The Brighton Centre, Brighton, UK, 3–7 April 2000, 906–909 (2000)

Sulong, M., Tan, R. C. W., and Aziz, R. A., 'Membrane filtration system for crude palm oil clarification' in Proceedings Volume II, World Filtration Congress 8, European Federation of Chemical Engineering Event No. 607, Organised by The Filtration Society and Elsevier Science, The Brighton Centre, Brighton, UK, 3–7 April 2000, 901 (2000)

13 Vacuum filtration

L. Svarovsky

FPS Institute, England and University of Pardubice, Czech Republic

In vacuum filters, the driving force for filtration results from the application of suction on the filtrate side of the medium. Although the theoretical pressure drop available for vacuum filtration is 100 kPa, in practice it is often limited to 70 or 80 kPa or even less.

In applications where the fraction of fine particles in the solids of the feed slurry is low, a simple and relatively cheap vacuum filter can yield cakes with moisture contents comparable to those discharged by pressure filters. Furthermore, this category includes the only truly continuous filters built in large sizes that can provide for washing, drying and other process requirements.

Vacuum filters are available in a variety of types, and are usually classified as either batch-operated or continuous. One important distinguishing feature is the position of the filtration area with respect to gravity. A number of vacuum filter types use a horizontal filtering surface with the cake forming on top. This arrangement offers the following advantages[1]:

1 Gravity settling can take place before the vacuum is applied. In many cases, this may prevent excessive blinding of the cloth due to action of a pre-coat formed by the coarser particles.
2 Heavy or coarse materials can be filtered because if they settle out from the feed they do so onto the filter surface.
3 Fine particle penetration through the medium can be tolerated because the initial filtrate can be recycled back onto the belt.
4 Top-feed filters are ideal for cake washing, cake dewatering and other process operations such as leaching.
5 A high degree of control can be exercised over cake formation. Allowances can be made for changed feeds and/or different cake quality requirements. This is particularly true of the horizontal belt vacuum filters. With these units the relative proportions of the belt allocated to filtration, washing, drying, etc., as well as the belt speed and vacuum quality, can be easily altered to suit process changes.

There are, however, two major drawbacks:

1 Such filters usually require large floor areas.
2 Their capital cost is high.

Saving in floor area as well as in installed cost can be made by using a filter with vertical or other non-horizontal filtration surfaces but at the cost of losing most if not all of the five advantages of horizontal filters listed above.

The following is a brief account of the most important and widely used vacuum filters.

13.1 Nutsche filter (*Figure 13.1*)

The Nutsche filter is simply an industrial-scale equivalent of the laboratory Buchner funnel. Nutsche filters consist of cylindrical or rectangular tanks divided into two compartments of roughly the same size, by a horizontal medium supported by a filter plate. Vacuum is applied to the lower compartment, into which the filtrate is collected. It is customary to use the term 'Nutsche' only for filters, which have sufficient capacity to hold the filtrate from one complete charge. The cake is removed manually or sometimes by reslurrying.

Depending on the chemical nature of the slurry to be filtered the materials of construction vary from wood, plastics, earthenware, steel, lead-lined steel, to brick-lined cast iron. These filters are particularly advantageous when it is

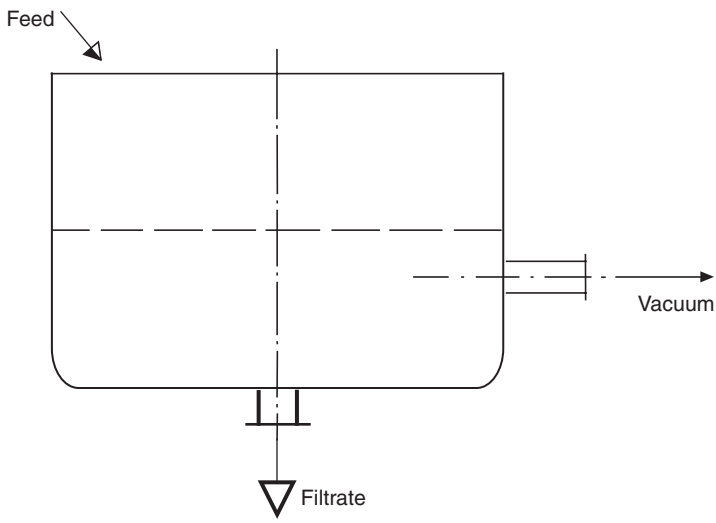

Figure 13.1 Nutsche filter

necessary to keep batches separate, and when extensive washing is required, although separation of wash from the mother liquor is difficult. Washing is carried out either by displacement or by reslurrying, the latter being more conveniently performed in the enclosed agitated Nutsches described separately. If cake cracking occurs, the cracks can be closed manually for the subsequent washing.

Nutsche filters are simple in design, but laborious in cake discharge. They are prone to high amounts of wear due to the digging-out operation. Being completely open, they are quite unsuited for dealing with inflammable or toxic materials. For such applications enclosed agitated Nutsche filters (see the following) are used. Throughputs are limited but the range of solids that can be filtered is very wide, ranging from easily filterable precipitates to dyestuffs, Beta salt, etc.

As an alternative to a classical Nutsche with a flat filtration surface, a rotary Nutsche ('RN Filter') has been developed by Pierson[2] and recently tested by Machac *et al*.[3] It is constructed as a drum with the bottom inner half used as filter area. The drum is placed on four wheels and a simple rope drive is used to rock it from side to side. This arrangement, if operated at optimum conditions, offers several advantages. As mentioned above, the flat Nutsche has a tendency to lead to cake cracking, which has a detrimental effect on washing and dewatering. In the semi-tubular bed of the rotary Nutsche, which is allowed to rock from side to side, a more uniform cake is formed and it has an ability to fill in the cracks as long as the cake maintains a degree of fluidity. Washing can take place after cake formation, during which the drum can be made to rock more vigorously, or even inverted, causing the cake to reslurry. If hot air is introduced, the RN filter can become a tumble dryer. For cake discharge, the drum is inverted and the cake is blown off with compressed air. The entire filter is enclosed.

Machac *et al*. have recently tested a pilot version of the RN filter with aqueous suspensions of diatomite, limestone and cellulose[3]. The results showed a dependence of filter performance and cake quality on the mode of filter drum rocking and the solids properties. In other words, the rocking mode has to be optimized for each material to be filtered and this optimization can only be done on an RN filter. At optimum rocking frequency, the filter cake quality was better than that for a static mode, and cake cracking was either eliminated or reduced.

13.2 Enclosed agitated vacuum filters (*Figure 13.2*)

These filters, often called 'mechanized Nutsches', are circular vessels provided with a cover, through which passes a shaft carrying a stirrer. The stirrer can sweep the whole area of the filter cake and it can be lowered or raised vertically as required. During the filtration process the stirrer is in the top position, if necessary in motion in order to prevent the formation of an

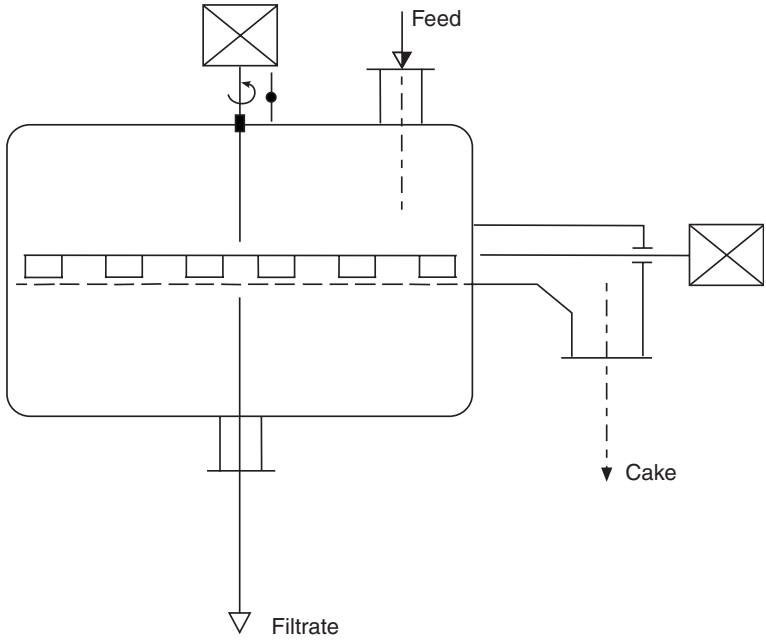

Figure 13.2 Enclosed agitated vacuum filter

unequal layer of cake with fast settling suspensions. The suspension is fed through a connecting piece in the cover. When filtration is completed, any cracks which might occur in the filter cake can be smoothed over by lowering the stirrer on top of the cake and 'pasting' over the cake to cover the cracks. The stirrer is rotated in the reverse direction for this operation and the pressing of the cake by the rotor blades might result in an additional dewatering, particularly with thixotropic cakes.

The filter cake can then be washed either by displacement or by reslurrying. Reslurrying is easily accomplished using the stirring action of the rotor blades when the rotor is lowered into the cake. The cake may also be dried *in situ* by the passage of hot air through it, or may be steam distilled for the recovery of solvent.

For discharge of the cake, a discharge door is provided at the edge and the cake is moved by the rotor towards the door, the stirrer blades being gradually lowered onto the surface so that a small depth of solids is scraped away. Alternatively, the cake may be reslurried and pumped away.

The enclosed agitated filters are especially useful when volatile solvents are in use, or when the solvent gives off toxic vapour or fumes. Another major advantage is that their operation does not require any manual labour. Control can be manual or automatic, usually by timers or by specific measurements of the product. Most filters are made of mild steel, with the surfaces exposed to attack protected by lead, tile or rubber lining, or by coating or spraying with

other substances as necessary. Filtration areas up to 10 sq. metres are available and the maximum cake thickness is one metre.

Applications are mainly in the chemical industry for the recovery of solvents.

The pressure version of the enclosed agitated filter is known as the Rosenmund filter; it uses a screw conveyor to convey the cake to a central cake discharge hole.

13.3 Vacuum leaf filter (*Figure 13.3*)

The vacuum leaf, or Moor filter, consists of a number of rectangular leaves manifolded together in parallel and connected to vacuum or to a compressed air supply by means of a flexible hose. Each leaf is composed of a light pervious metal backing, usually of coarse wire grid or expanded metal set in a light metal frame and covered on each surface with filter cloth or woven wire cloth. The leaves, which are carried by an overhead crane during the filtration sequence, are dipped successively into a feed slurry tank, where the filtration takes place, a holding tank, where washing occurs, and a cake-receiving container, where cake discharge is performed, usually by back-blowing with compressed air. An alternative arrangement is to move the tanks rather than the leaf assembly.

The operating cycle is seldom less than two hours and several sets of frames can be operated in rotation. The cake thickness should be more than 3 mm, 9 mm being a typical value. Sluicing of the cake with a jet of compressed air has been used to permit thinner cakes and shorter filtration times. The leaves are spaced sufficiently far apart that there is always clearance between the finished cakes.

A static leaf filter is used for cleaning machine tool coolants. These are used on the suction side of a pump circulating system, with the same pump employed for withdrawal of the filtrate as well as for back flushing the filter elements. Solids in this case are removed from the sump by a scraper conveyor.

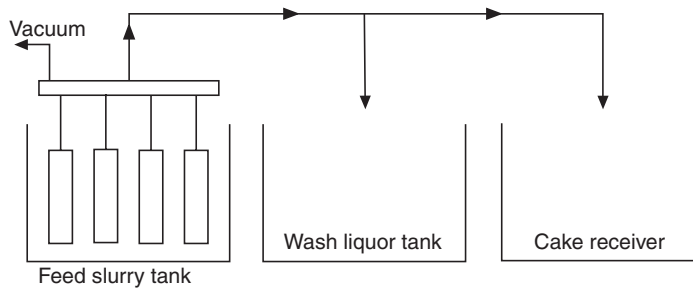

Figure 13.3 Vacuum leaf filter

Simple design, general flexibility, and good separation of the mother liquor and the wash are the important virtues of vacuum leaf filters. On the other hand, they are also labour intensive, require substantial floor space, and introduce the danger of the cake falling off during transport. Vacuum leaf filters are particularly useful when washing is important but the washing is difficult with very fine solids, such as occur in titanium dioxide manufacture.

13.4 Tipping pan filter (*Figure 13.4*)

This is in fact a Nutsche filter with a small filtrate chamber, in the form of a pan, which is built so that it can be tipped upside down to discharge the cake. A separate vessel is used to receive the filtrate and this allows segregation of the mother and wash liquor if necessary.

A variation on this type of filter is the double tipping pan filter, which is a semi-continuous type consisting of two rectangular pans fitted with a filter cloth and pivoted about a horizontal axis. Slurry is first fed onto one pan, which is turned over for cake discharge at the end of the cycle. The second pan is used for filtration while the first is being discharged.

In general, pan filters are selected for freely filtering solids and thick filter cakes. Cake washing can be introduced easily. Most applications are in the mining and metallurgical industries for small-scale batch filtration.

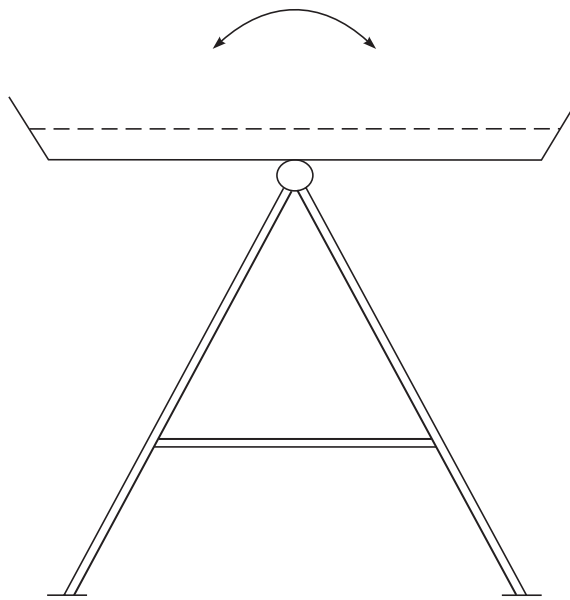

Figure 13.4 Tipping pan filter

13.5 Horizontal rotating pan filters (*Figure 13.5*)

Horizontal rotating pan filters represent a further development of the tipping pan filter, for continuous operation. They consist of a circular pan rotating around the central filter valve. The pan is divided into wedge-shaped sections covered with the filter medium. Vacuum is applied from below. Each section is provided with a drainage pipe, which connects to a rotary filter valve of the same type as in drum filters. This allows each section, as it rotates, to go through a series of operations such as filtration, dewatering, cake washing and discharge. Two basic designs exist, depending on the method of solids discharge.

The horizontal pan filter with scroll discharge incorporates a spiral scroll in a radial position just ahead of the feed zone. The scroll scrapes the cake off the medium. The need for a clearance between the scroll and the medium can cause incomplete cake discharge and consolidation of the remaining heel, due to the action of the scroll. This problem may be overcome by injection of compressed air in the reverse direction through the cloth under the feed zone or by sucking air through the cloth in the opposite direction, combined with cloth washing. Filtration areas range from 0.5 to 100 sq. metres.

One important variation of this type of filter is based on replacing the rigid outer wall necessary for containing the feed and the cake on the rotating table by an endless rubber belt. The belt is held under tension and rotates with the table. It is in contact with the table rim except for the sector where the discharge screw is positioned, where the belt is deflected away from the table

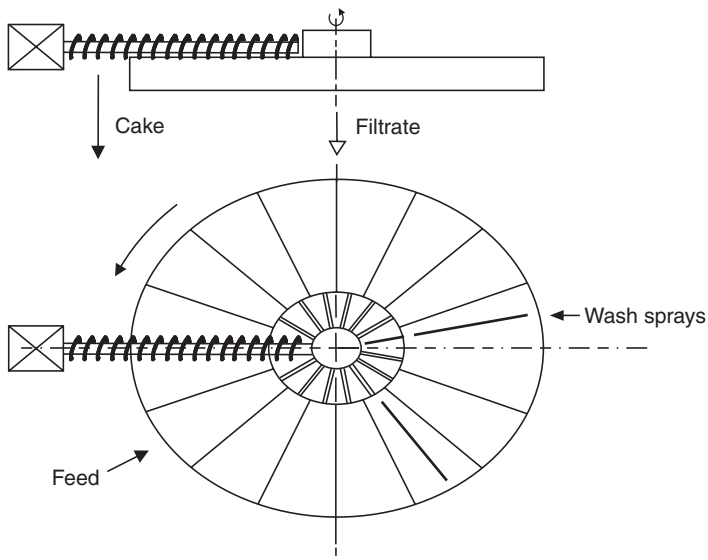

Figure 13.5 Horizontal rotating pan filter

to allow the solids to be pushed off the table. The cloth can also be washed in this section by high-pressure water sprays. This filter, recently developed in Belgium, is available in sizes up to 250 sq. metres, operated at speeds of 2 minutes per revolution and cake thicknesses are up to 200 mm.

In horizontal rotary tilting pan filters, the wedge-like compartments are arranged as independent pans. Each is connected to the centre valve by a swivel pipe joint that inverts the pan as it passes the discharge point. Air blowback is often used to assist the cake discharge. The units can also be adapted for cloth washing. Typical applications include filtration of gypsum from phosphoric acid and many mineral-processing uses. Areas from 15 to 250 sq. metres are available.

Of the two versions, the tilting pan is more expensive, requires more floor space and high maintenance. Its advantages are, however, in its excellent cake discharge and control of wash liquor, and in the fact that larger sizes are available.

13.6 Horizontal belt vacuum filters (*Figure 13.6*)

The horizontal belt vacuum filter is another development of the pan filter idea. A row of vacuum pans arranged along the path of an endless horizontal belt was the original patented design but that has been superseded by the horizontal belt vacuum filter, which resembles a belt conveyor in appearance. The top strand of the endless belt is used for filtration, cake washing and drying, while the bottom return is used for tracking and washing of the cloth. There is appreciable flexibility in the relative areas allocated to filtration, washing and drying. Hooded enclosures are available wherever necessary. Modular construction of many designs allows field assembly as well as future expansion if process requirements change.

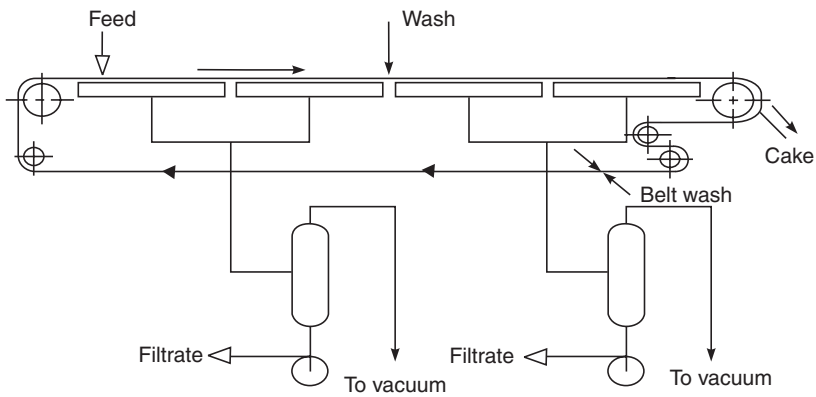

Figure 13.6 Horizontal belt vacuum filter

Horizontal belt filters are well suited to either fast or slowly draining solids, especially where washing requirements are critical. Multi-stage counter-current washing can be effectively carried out due to the sharp separation of filtrates available here. Horizontal belt vacuum filters are classified according to the method employed to support the filter medium.

One common design is typified by a rubber belt mounted in tension. The belt is grooved to provide drainage towards its centre. Covered with cloth, the belt has raised edges to contain the feed slurry, and it is dragged over stationary vacuum boxes located at the belt centre. Wear caused by friction between the belt and the vacuum chamber is reduced by using replaceable, secondary 'wear' belts made of a suitable material such as PTFE, Terylene, etc.

The rubber belt filters are available in large capacities with filtration areas up to 200 sq. metres or more. They can be run at very high belt speeds (up to 30 m per minute) when handling fast-filtering materials such as mineral slurries. The main disadvantages of rubber belt filters are the high replacement cost of the belts, the relatively low vacuum levels, and limitations on the type of rubber that can be used in the presence of certain solvents. The vacuum pumps are usually sized to give from 2 to 20 m per minute air velocity over the filtration area, at 160 torr, depending on the filterability of the solids. The solids capacity ranges from 10 to 500 kg of solids per sq. metre of filtration area per hour with cake thicknesses from 3 to 150 mm.

Another type of horizontal belt vacuum filter uses reciprocating vacuum trays mounted under a continuously travelling filter cloth. The trays move forward with the cloth as long as the vacuum is applied, and then return quickly to their original position after the vacuum is released. This overcomes the problem of friction between the belt and the trays because there is no relative movement between them while the vacuum is being applied. The mechanics of this filter are rather complex, and the equipment is expensive and requires intensive maintenance. A range of solvents can be used. Widths up to 2 m and areas up to 75 sq. metres are available. The cloth can be washed on both sides.

The indexing cloth machines are a further development along these lines. In these, the vacuum trays are stationary and the cloth is indexed by means of a reciprocating discharge roll. During the time the vacuum is applied, the cloth is stationary on the vacuum trays. When the vacuum is cut off and vented, the discharge roll advances rapidly, moving the cloth (and the cake with any suspension on it) forward, say by 500 mm. The cycle is then repeated, with the dwell time being adjustable according to the feed rate and any cake dewatering or washing requirements.

As with the reciprocating tray types, the cloth can be washed on both sides. The cake discharges by gravity at the end of the belt when it travels over the discharge roll. The major advantages of this filter are its simple design and low maintenance costs. It is also claimed to be about 30% cheaper in installed costs, mainly due to cheaper construction (can be made from plastics) and

because there is no need for heavy foundations. The main disadvantage is the difficulty of handling very fast filtering materials on a large scale. Areas up to 93 sq. metres are available.

Some designs of horizontal belt vacuum filter now incorporate a final compression stage for maximum mechanical dewatering. This is achieved by a press roll or a compression belt, which presses down on the cake formed in the preceding conventional filtration stage. Frothy cakes can be smoothed over by dragging a polythene sheet, placed in a strategic position, over the cake. In the cloth indexing version, the sheet is periodically sucked onto the surface of the cake, thereby compressing it and smoothing over any cracks or channels in the cake.

13.7 Rotary vacuum drum filters (*Figure 13.7*)

This is still the most popular vacuum filter today. There are many versions available and they all incorporate a drum which rotates slowly (1 to 10 minutes per revolution typically but see some exceptions later) about its horizontal axis and is partially submerged in a slurry reservoir. The perforated surface of the drum is divided into a number of longitudinal sections of about 20 mm in thickness. Each section is an individual vacuum chamber, connected through piping to the drum centre and out through a central outlet valve at one end of the drum. The drum surface is covered with a cloth filter medium and the filtration takes place as each section is submerged in the feed slurry. A rake type, slowly moving agitator is used to keep the solids in suspension in the slurry reservoir, without disturbing the cake formation. The agitator usually has a variable speed drive. Materials of construction of rotary drum filters include mild steel (sometimes rubber covered), stainless steel, nickel, tantalum or plastics.

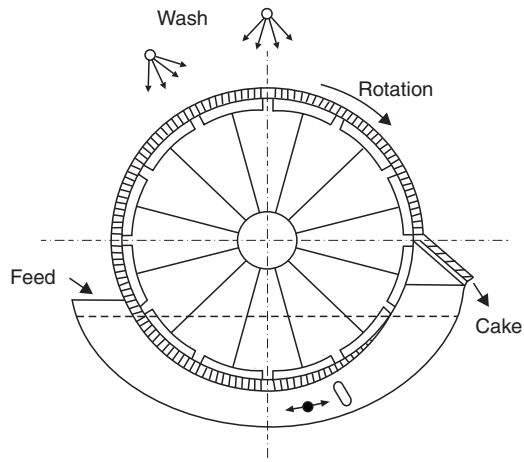

Figure 13.7 Rotary vacuum drum filter

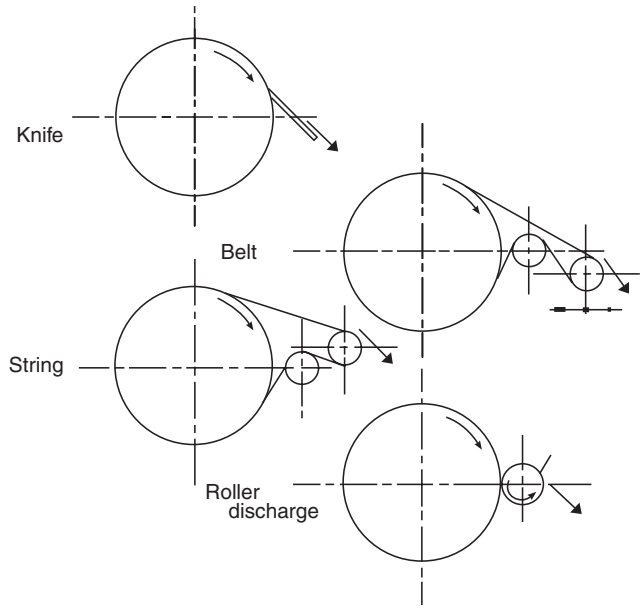

Figure 13.8 Types of discharge used in rotary drum vacuum filters

Filtration can be followed by dewatering, washing and drying. In some applications, compression rolls or belts are used to close possible cracks in the cake before washing or to further dewater the cake by mechanical compression. Final dryness of the cake can also be enhanced by fitting a steam hood. Several different systems of cake discharge are used (*Figure 13.8*), all of which can be assisted by air blowback: they include simple knife discharge, advancing knife discharge (with pre-coat filtration), belt or string discharge, and roller discharge.

The type of discharge selected depends upon the nature of the material being filtered. The scraper or knife discharge consists of a blade that removes the cake from the drum by direct contact with the filter cake. It is normally used for granular materials with cake thickness greater than about 6 mm. In order not to damage the filter cloth, a safety distance of 1 to 3 mm between the blade and the cloth must be observed. If the residual layer is made not of filter aid but of the product, then there might be danger of its blocking by fine particles and by successive consolidation by the scraper blade.

The string discharge arrangement uses a number of parallel strings (wire, chains or coil springs have also been used) tied completely around the filter at a pitch of 1 to 2 cm, passing over the discharge and return rolls. As the strings leave the drum before the discharge point, they lift the filter cake from the medium and discharge it at the discharge roll. This type of discharge is recommended for gelatinous or cohesive cakes. The coil spring discharge has been successfully applied to fibrous solids such as the waste from a pulp mill, or highly flocculated slurries such as in sewage treatment.

Another variation of the string discharge is the use of a thick plastic belt, which is perforated by conical openings. The drum is covered with filter cloth and the belt covers the cloth for the filtration and dewatering operations. The solids fill the perforations in the belt and then leave the drum with the belt to be discharged by air blow as pellets. This is a very effective way of palletizing coarse mineral ores.

The cloth belt discharge is based on taking the cloth endless belt off the drum in the same way as with the string discharge. The advantage here is the ease of washing both sides of the cloth before the cloth returns to the drum. The disadvantage is in the need for an additional control device for the guidance of the cloth.

Roll discharge systems use a roll, which rotates at a slightly greater peripheral speed than the cake and is in contact with the cake. The cake is transferred from the drum to the discharge roll by adhesion which, by giving the roll a rough surface or because of the presence of residual cake on the roll, is designed to be greater to the roll than to the drum. The cake is usually removed from the roll by a knife. This type of discharge is designed to discharge tacky cakes, which cannot be handled effectively by either of the previously described discharge designs. The cake thickness is small here, from 0.5 to 3 mm.

Multicompartment drum filters range in size from about 1 sq. metre to over 100 sq. metres; they are widely used in mineral and chemical processing, in the pulp and paper industry, and in sewage and waste materials treatment. Despite their uneven wash distribution and frequently high run-off (as the filter surface is not horizontal), many continue to be used as cake washing filters. Effective washing of the filter cloth can be done only with the belt discharge type, where the cloth leaves the drum for a brief period and can thus be washed on both sides.

As the feed suspension enters the drum from the bottom (in the most common bottom feed version), fast settling slurries are not suitable for most rotary drum filters. Nor are very fine slurries because of the inevitable penetration problems. Note the unfavourable stratification of particle size within the cake discussed in section 13.10.2 and shown in *Figure 13.15*. In units designed to use a pre-coat filter aid (rotary drum pre-coat filters), the drum can be evacuated over the full 360 degrees and fitted with an advancing knife system that continuously shaves off the deposited solids together with a thin layer of the pre-coat. The pre-coat has to be renewed periodically.

No internal piping and no conventional filter valve are needed with single cell drum filters (*Figure 13.9*) where the entire drum operates under vacuum. The cake discharge is effected by air blowback from an internal stationary ‘shoe’ mounted inside the drum at the point of discharge. There are very close tolerances between the inside surface of the drum and the shoe in order to minimize the leakage. The inside of the drum acts as a receiver for the separation of air and filtrate; conventional multicompartment drum filters require a separate external receiver. Washing is possible through nozzles on

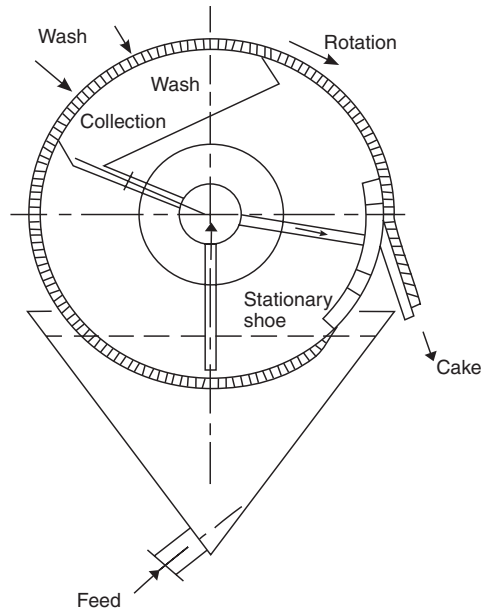

Figure 13.9 Single cell drum filter

top of the drum and the wash liquor is collected by an internal collection pan (see *Figure 13.9*). Two-stage countercurrent washing can apparently also be accomplished[4]. This type of filter (represented, for example, by the Humboldt–Bird High Duty or the Humboldt Wedag high efficiency filter) permits operation of the filter with thin cakes so that high drum speeds (up to 40 rpm) can be used and high capacities can be achieved. Sizes up to 20 sq. metres are available.

In most rotary drum filters, the submergence of the drum is usually about one-third of its circumference. Greater submergence is achieved in units equipped with submerged bearings, although this is inevitably more costly.

Another option available with rotary vacuum drum filters is full enclosure. This enables operation under nitrogen or other atmospheres, for reasons such as safety, prevention of vapour loss, etc. Enclosure may also be used to prevent contamination of the material being filtered or to confine the spray from washing nozzles. The rotary drum filter can also be enclosed in a pressure vessel and operated under pressure and this is the idea behind some simple pressure filters introduced in chapter 12.

The disadvantages of the bottom feed arrangement can be overcome by using top feed drum filters, which use the nearly horizontal surface on the top of the drum. The area available for filtration is small, however, and only a limited pool of slurry can be contained within the feed box and the rims at the edges of the drum for cake formation. These two factors severely limit the application of this filter to fast settling solids that dewater readily and to

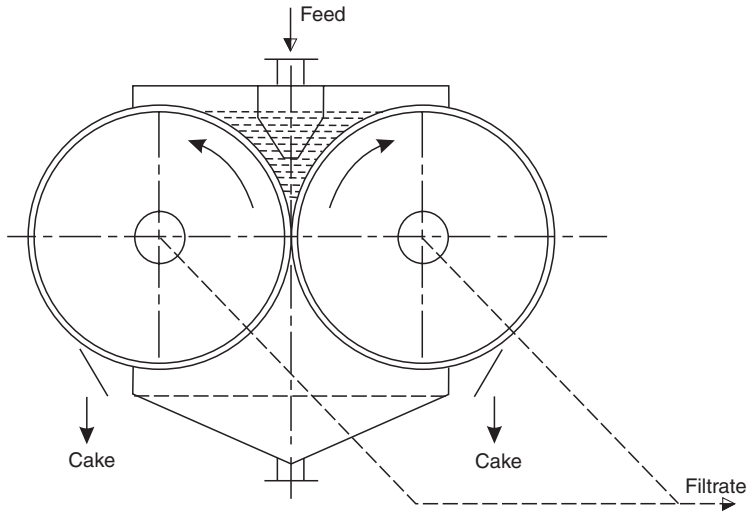

Figure 13.10 Dual drum filter

applications that require (and permit) pre-coating. These top feed arrangements are more common in the brewing industry. Drying is sometimes also carried out in top feed filters in totally enclosed systems.

A variation to the top feed drum filter is the dual drum filter (*Figure 13.10*) which uses two drums of the same size in contact with each other and rotating in opposite directions.

The feed enters into the V-shaped space formed on top of the two drums and the cake that starts forming initially contains coarser particles due to the settling which takes place in the feed zone. This is beneficial to the clarity of the filtrate because the coarser particles act as a pre-coat. From the point of view, however, of the final moisture content of the cake the stratification of the solids in the cake may lead to somewhat wetter cakes. The utilization of the area of the drums is poor, as there are dead spaces under the two drums. The main application of the dual drum filters is in dewatering of coarse mineral or coal suspensions at feed concentrations greater than about 200 kg per cubic metre.

An interesting but not widely used variation is the internal drum filter, which has the filtering surface on the inside of the drum. It has no slurry reservoir, as the feed is supplied to the inside of the drum. The filtrate piping is mounted externally at one end of the drum and it terminates in a conventional filter valve. Cake discharge is by a scraper and a chute. Filters of this type are suited to handling fast settling materials and are cheaper in installed costs than conventional drum filters. Cake washing is impractical, however, because it has to be done against gravity. There is also a danger of the cake falling off and cloth replacement is difficult. As the disadvantages of this filter tend to outweigh the advantages, this filter has been largely superseded by horizontal vacuum filters.

13.8 Rotary vacuum disc filters (*Figure 13.11*)

An alternative to the drum filter is the disc filter, which instead of one large drum uses a number of discs mounted vertically on a horizontal shaft and suspended in a slurry reservoir. This arrangement provides a much greater surface area for a given floor space, by as much as a factor of 4, but cake washing is more difficult and cloth washing virtually impossible. Not only is the cake surface vertical on a disc filter but also there are differing components of horizontal and vertical speeds everywhere on the disc. In spite of that, however, cake washing can still be done[5] by careful design of the wash spray system.

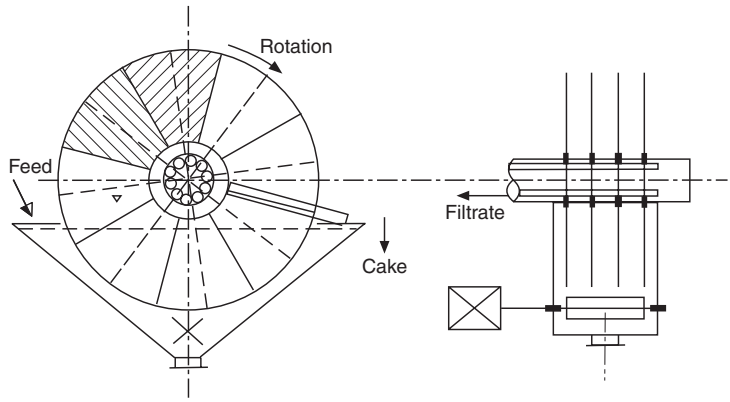

Figure 13.11 Rotary vacuum disc filter

As in the case of drum filters, each disc is divided into a number of separate segmental sectors (normally 12, sometimes more, up to 30 for increased filter capacity[6] that have suitable drainage and cloth support, and the sectors are connected to a filter valve similar to the type used in drum filters. Whereas with drum filters, the method of cake discharge can be chosen to suit the cake properties, in conventional disc filters the cake discharge is usually performed by a scraper blade with air blowback often used to assist the discharge, or sometimes by a tapered roll. High pressure sprays have also been used for cake discharge. Furthermore, the minimum cake thickness necessary for cake discharge is usually somewhat higher (10 mm) for disc filters[6] than for the drum filters (3 mm). Thin plastic cakes discharged by air blowback seem to be an exception to this.

It is necessary to operate disc filters at high submergence because a sector must be completely submerged during cake formation. There is also, however, a top limit to the liquid level to allow the scraper to discharge the cake under gravity. The higher submergence (40% or even higher, up to 55%) reduces the area available for dewatering. As with drum filters, the slurry reservoir has to be agitated to prevent settling. Rather than using one large vat

for all the discs, some designs provide individual low volume, closely fitting vats for each disc, thus avoiding the need for an agitator. If individual discs (or bunches of discs) have separate troughs, cake discharge chutes, filtrate receivers and also separate feed pipes, multi-stage countercurrent, reslurry washing can be carried out in one filter[5].

The speed of rotation is relatively high, from 20 to as much as 180 rpm. The disc size varies from 0.5 to 5.3 metres, with up to 20 discs assembled on one shaft, providing filtration areas up to 380 sq. metres. Disc vacuum filters are principally used in mining and metallurgical applications for handling large volumes of free-filtering materials. They have also been successfully operated with cement, starch, sugar, paper and pulp, and fly ash.

Whereas the conventional disc filters usually use a highly permeable cloth for the filter medium, there are some that use micro-porous membranes or ceramic filter plates. Liquids can still pass through such media, driven by the static pressure difference (be it at lower rates than through a more open filter cloth) but when air displacement dewatering follows, air cannot pass due to the high capillary pressure. This saves vacuum pump costs whilst still achieving good dewatering. In the case of the rigid ceramic medium (alumina based) the cake is scraped off and the plates are cleaned with ultrasound[7].

Total submergence is used in the vacuum disc filter thickener (*Figure 13.12*), in which case the cake discharge, by backwashing with filtrate, occurs as each sector passes through the lowest point of the slurry tank.

Finally, the rotary disc filter can also be enclosed in a pressure vessel and operated under pressure and this is the idea behind most of the continuous

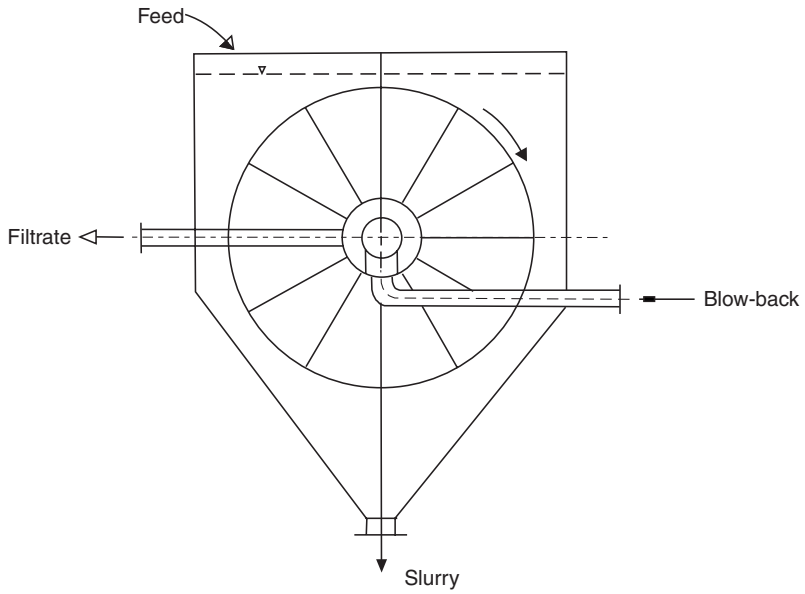

Figure 13.12 Vacuum disc filter thickener

pressure filters introduced in chapter 12. When a combination of vacuum and pressure is used, these are called 'hyperbaric filters' but the actual use of such hybrids is limited.

13.9 Selection of continuous vacuum filters

The batch types of vacuum filters (sections 13.1 to 13.4) are basically industrial versions of the Buchner funnel and, as such, there is not much between them in terms of their suitability for different types of slurries. This is due to their versatility thanks to the batch operation, and, consequently, their selection is simply done on the basis of their process suitability or convenience.

It is quite different with the continuous vacuum filters (sections 13.5 to 13.12) which have to be selected according to the filterability of the slurry. *Figure 13.13* shows a very useful selection diagram for continuous vacuum filters[8]. Cake thickness is plotted here against cake formation time, these values having been typically obtained from vacuum leaf tests (or pilot plant tests) done with a sample of the actual slurry. Four separate areas (A, B, C and D) are shown and the corresponding ranges of filtration velocities (m/h = m^3/m^2 h) and dry cake production rates (g/m^2 s) are given, together with lists of suitable filter types.

As can be seen from *Figure 13.13*, cake thicknesses below about 3 millimetres cannot be discharged with a knife or a scraper (area A). This area clearly represents a very difficult-to-filter slurry, which if fine and very dilute, may even require a rotary drum pre-coat filter (section 13.7). Areas B, C and D show the types of filters applicable to increasingly filterable slurries, with

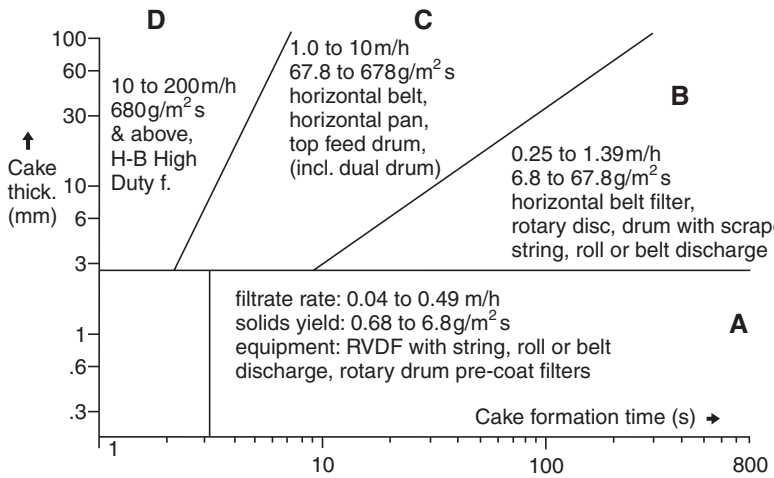

Figure 13.13 A selection diagram for continuous vacuum filters[8]

area D representing a fast-settling slurry that can be filtered at high speeds with high capacity vacuum filters such as the Humboldt–Bird High Duty filter (section 13.7).

13.10 Improvement of filter performance by physical pretreatment of the slurry

The general importance of pretreatment in all solid–liquid separation cannot be overemphasized. Such pretreatment can be chemical or physical. Chemical pretreatment consists mainly of coagulation and flocculation, and this is dealt with in chapter 4.

Physical pretreatment also has an important role to play not just to improve the performance of filters in general but in the case of vacuum filters it may even decide whether or not a vacuum filter can be used at all. Without such pre-treatment, a generally more expensive pressure filter may have to be used. Pretreatment may include crystallization, freezing, temperature adjustment, thermal treatment or ageing, but the three main methods used with vacuum filters are:

1 thickening of the feed slurry,
2 stratification of particle size in cakes by pre-classification,
3 addition of filter aids as pre-coat and/or body feed.

The above two alternatives are briefly discussed in the following, the filter aid addition is dealt with in some depth in chapter 1, section 1.1.2.

13.10.1 Feed thickening

It is sometimes jokingly said, with some justification, that there are three golden rules of cake filtration: thicken, thicken and thicken. That is because there are three good reasons to increase the feed concentration c (within limits determined by other operating conditions such as the need to pump the slurry or a poor pick-up on the filter) because it:

1 increases cake production capacity with $c^{1/2}$ as shown in equation 9.40,
2 reduces specific cake resistance α and that also increases cake production capacity (equation 9.40),
3 improves filtrate clarity and reduces cloth blinding at the very start of the filtration cycle (due to better bridging over the pores in the filter medium).

Reason 1 comes from mass balance and it is indisputable. For the same cake production capacity, the filter has less slurry to handle at higher feed concentrations and is, therefore, smaller[9].

Reason 2 has a large body of experimental evidence (e.g. *Figure 9.15* and other references reported in chapter 9) and the physical reason is that higher feed concentrations reduce the time available for particle relaxation when particles hit the top of the cake. Each particle just deposited on the cake is locked into position by other particles in its vicinity before it has time to roll and fill the open crevices in the cake. Thus, at high concentrations, the cake formed is more open and, consequently, it has more voids within it. This has been proved experimentally as well as in a modelling exercise by Walker[10,11].

Reason 3 has much less hard experimental evidence but is confirmed by operating experience. At low concentrations, the filtrate clarity at the beginning of the filtration cycle is poor, so much so that the first bit of filtrate has often to be recycled into the feed. This, however, is not helpful because it dilutes the feed, thereby making the problem worse.

As to how such pre-thickening can be done, there are mainly two options. Gravity thickening is one option, especially applicable to fast settling slurries. A hydrocyclone (or units several in parallel) as shown in *Figure 6.23* is another good and relatively cheap possibility. The main advantage here is that the particle size ranges that vacuum filtration can handle broadly coincide with those for which hydrocyclones are also suitable.

13.10.2 Pre-classification of the slurry in top-fed vacuum filters

With top-fed vacuum filters, this to some extent takes place naturally by gravity settling: the resulting cake is somewhat coarser at the bottom, nearer the filtrate medium. This size stratification is the right way up and beneficial to the filtration process. *Figure 13.14* shows this schematically for a horizontal belt filter.

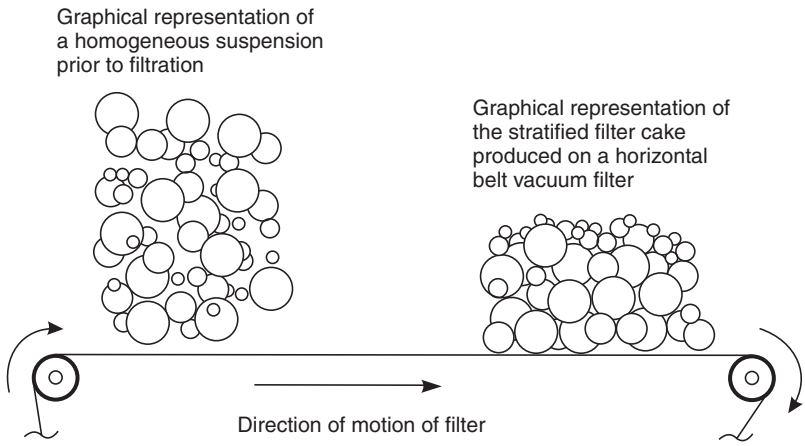

Figure 13.14 Particle size stratification on a horizontal belt vacuum filter due to gravity settling (picture adapted from ref. 12, Figure 1.1)

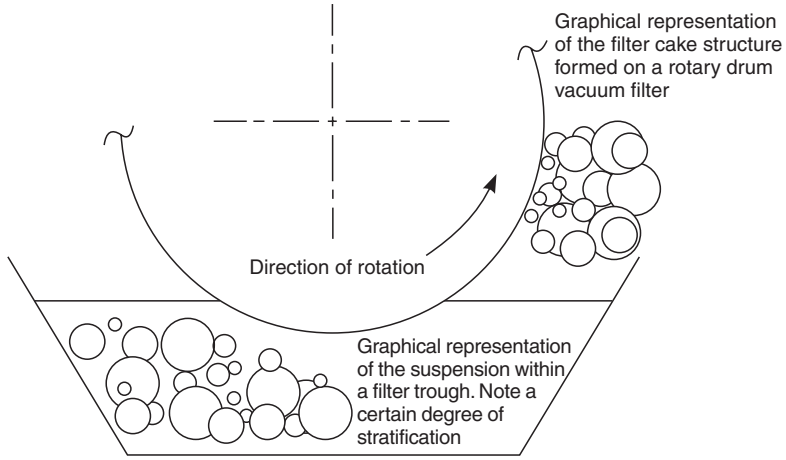

Figure 13.15 Schematic of cake formation on a rotary vacuum drum filter (picture adapted from ref. 12, Figure 1.2)

This is in contrast to what happens in bottom-fed filters, such as the rotary vacuum drum filter shown in *Figure 13.15*. Here, fine particles are sucked onto the medium first and the coarser ones settling away from it. The resulting distribution of particle size within the cake is undesirable, with the layers close to the medium being finer than the rest of the cake.

The desirable stratification in *Figure 13.14* can be enhanced by artificial classification of the slurry prior to feeding it onto the filter belt. *Figure 6.25* shows this schematically when a hydrocyclone with a relatively coarse cut size was used[12] to select a coarse fraction from the feed slurry. This fraction was fed to the filter first, thus forming a 'pre-coat', onto which the more dilute, fine fraction was fed through a washing weir. This works well but only if the cyclone cut size is correctly set. The system gives better filtrate clarity (particularly in the vacuum tray(s) under the feed section) and extends the applicability of the filter to finer feeds without necessarily adversely affecting the moisture content of the discharged cake. Note that this goes against the conventional wisdom, which advises perfectly homogeneous cakes for best moisture content.

Commercially, the above pre-classification cannot be supplied 'off the shelf' because it could do more harm than good unless the classifier (a hydrocyclone most likely) is carefully tuned and set to give the right cut size. This depends on the particle size distribution in the original feed and has to be optimized for each installation individually. The system is, therefore, more likely to be installed by equipment users than by filter suppliers.

Example 13.1: Sizing of a rotary drum vacuum filter

Find the diameter of a rotary drum filter rotating at 0.2 rev/min operated at 0.7 bar with a submergence of 30% and a length to diameter ratio of 1.5. A dry

cake production capacity of 1 kg/s is required for a suspension having the following characteristics:

Feed concentration	$c = 84.14\,\text{kg/m}^3$
Solids density	$\rho_s = 2600\,\text{kg/m}^3$
Liquid density	$\rho = 1000\,\text{kg/m}^3$
Liquid viscosity	$\mu = 0.001\,\text{Ns/m}^2$
Wet/dry cake mass ratio	$m = 1.45$
Specific cake resistance	$\alpha = 3.03 \times 10^7 \times (\Delta p)^{0.2}$

It may be assumed that the resistance of the medium is negligible but concentration c should be corrected for cake moisture content.

Solution 13.1

Correction of the slurry concentration for cake moisture (equation 9.39):

$$c_{\text{corrected}} = \left(\frac{1}{c} - \frac{1}{\rho_s} - \frac{m-1}{\rho}\right)^{-1}$$
$$= 90.5\,\text{kg/m}^3$$

$$\text{Specific cake resistance, } \alpha = 3.03 \times 10^7 \times (7 \times 10^4)^{0.2}$$
$$= 2.82 \times 10^8\,\text{m/kg}$$

(noting that, although the cake is compressible, the (average) specific resistance of the cake is constant for constant pressure operation)

There are two ways to solve this problem:

Method 1—by calculating the filtration rate and using the solution for constant pressure operation.

$$\text{For constant pressure operation (equation 9.17), } \frac{t}{V} = \frac{\alpha\mu c}{2A^2\Delta p} + \frac{\mu R}{A\Delta p}$$

Alternatively, neglecting the second term associated with the resistance of the filter media,

$$\frac{t}{V} = \frac{\alpha\mu c}{2A^2\Delta p}$$

On the basis of a single cycle, i.e. cycle time = 300 s
filtration time, $t = 0.3 \times 300 = 100\,\text{s}$
and filtrate volume $= 300 \times (1/90.5) = 3.31\,\text{m}^3$

$$\therefore A^2 = \frac{3.31^2 \times 2.82 \times 10^8 \times 0.001 \times 90.5}{2 \times 90 \times 0.7 \times 10^5}$$

$$\text{hence } A = 4.71\,\text{m}^2 = \pi d^2 \times 1.5$$
$$\therefore d = 1.0\,\text{m}$$

Method 2—by direct use of the equation for dry cake production capacity (equation 9.40)

$$\text{i.e. dry cake production, } Y, = \left[\frac{2\Delta pfc}{\alpha\mu t_c}\right]^{0.5} \text{kg/m}^2\,\text{s}$$

where $\Delta p = 70\,000\,\text{N/m}^2$

$\alpha = 2.82 \times 10^8\,\text{m/kg}$

$\mu = 0.001\,\text{Ns/m}^2$

$f = 0.3$

$c = 90.5\,\text{kg/m}^3$

and $t_c = 300\,\text{s}$

hence $Y = 0.212\,\text{kg/m}^2\,\text{s}$

i.e. for required dry cake production rate of 1 kg/s,

$$\text{total area of filter } = 1/Y = 1/0.212 = \mathbf{4.71\,m^2}$$

References

1. Svarovsky, L., 'Solid–Liquid Separation Processes and Technology', Volume 5 in the *Handbook of Powder Technology*, Elsevier, Amsterdam (1985)
2. Pierson, H. G. W., US Patent 5130021 (1992), also other patents: GB 2234188, J 2201098, DE 4022469
3. Machač, I., Cakl, J. and Siska, B., 'Filtration on a rotary nutsche', SSCHI 99 Conference, Hotel Jasna, Demanovska dolina, Slovakia, 24.5–28.5.1999, published in the *Proceedings by the Slovak Society of Chemical Engineers* (1999)
4. Buttner, R. and Langeloh, T., 'Current trends in filtration—Drum filter design, *The Chemical Engineer*, 9 April, 17–19 (1992)
5. Stahl, W., 'Cost/performance comparisons between disc and drum filters', *Filtration & Separation*, January/February, 38–40 (1978)
6. Wetzel, B., 'Disc filter performance improved by equipment re-design, "What's New in Liquid–Solid Separation"', Filtech 73, Olympia, London, September 25–27, proceedings by Filtration Society, 1–4 (1973)
7. Rantala, P., 'Capillary filtration technology—Non-polluting to nature', *Filtration & Separation*, March/April, 135–137 (1994)
8. Egee, P. Leonard, *Private Communication*, Komline-Sanderson Engineering Corporation, Peapack, New Jersey, published in the short course manual, *Separation of Solids from Liquids*, CfPA, East Brunswick, New Jersey, October 17–20 (1977)
9. Carleton, A. J. and Cousens, T. W., 'The performance of industrial vacuum filters', *Filtration & Separation*, March/April, 136–142 (1982)
10. Walker, A. J. and Svarovsky, L., 'Development of a computer model for predicting the filtration characteristics of a suspension', *Filtration & Separation*, January/February, 57–65 (1994)

11. Svarovsky, L. and Walker, A. J., 'The effect of feed thickening on the performance of a horizontal vacuum belt filter', 1st World Congress Particle Technology, 331st Event of EFCE, Part IV, NMA mbH, Nuremberg (1986)
12. Walker, A. J. 'The effect of particle size, and its distribution within a filter cake, on cake filtration', a PhD Thesis, University of Bradford (1992)

Bibliography

Pascoe, J. N. and Tarleton, E. S., 'The prediction of process scale vacuum filter cycles from laboratory scale tests', Proceedings Volume II, World Filtration Congress 8, European Federation of Chemical Engineering Event No. 607, organised by The Filtration Society and Elsevier Science, The Brighton Centre, Brighton, UK, 3–7 April 2000, 773–776 (2000)

14 Centrifugal filtration

L. Svarovsky

FPS Institute, England and University of Pardubice, Czech Republic

The driving force for filtration in centrifugal filters is due to centrifugal forces acting on the fluid. Such filters essentially consist of a rotating basket (see *Figure 14.1*) equipped with a filter medium. Similarly to other filters, centrifugal filtration does not require a density difference between the solids and the suspending liquid. If such density difference exists, however, then sedimentation takes place in the liquid head above the cake, at the start of the filtration cycle. This may lead to beneficial particle size stratification in the cake, with somewhat coarser particles being closer to the filter medium and acting as a pre-coat for the finer ones to follow.

Probably the most important difference between other types of filters and centrifugal filters is that in centrifuges, in addition to the pressure due to the centrifugal head due to the layer of the liquid on top of the cake, the liquid

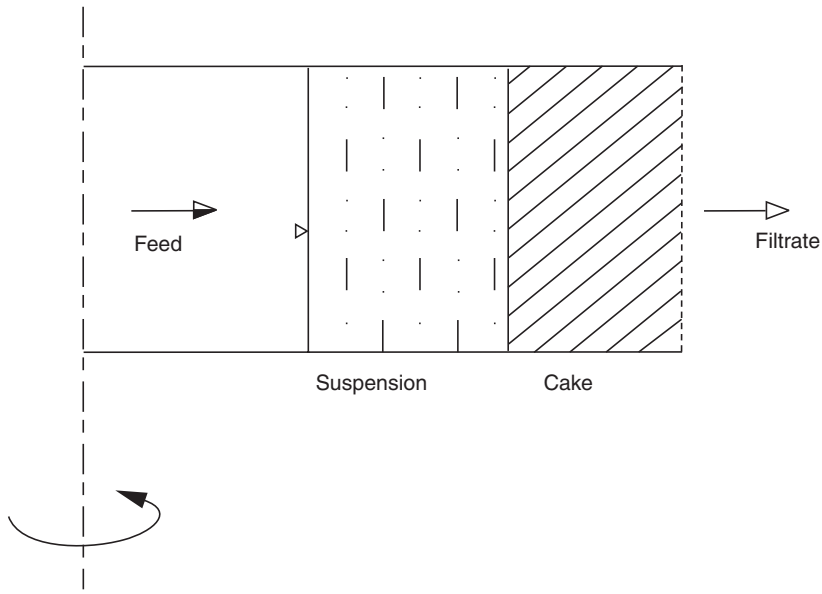

Figure 14.1 Schematic diagram of a centrifugal filter

flowing through the cake is also subjected to centrifugal forces which tend to pull it out of the cake. This makes filtering centrifuges excellent for dewatering applications. From the fundamental point of view, there are two important consequences of these additional dewatering forces. Firstly, Darcy's law and all of the theory based on it are incomplete because it does not take into account the effect of mass forces acting on the liquid within the cake and medium. Secondly, pressures below atmospheric can occur in the cake in the same way as it sometimes takes place in gravity fed deep bed filters. Zeitsch[1] modified the conventional filtration theory to make it applicable to centrifugal filters and gave a full account of the effects involved.

Due to their good performance and high cost, centrifuges in general are often referred to as the 'Rolls Royces' of solid–liquid separation. They all have parts rotating at high speeds and therefore require high engineering standards of manufacture, high maintenance costs and special foundations or suspensions to absorb vibrations. In return, they do well whether they are sedimenting or filtering centrifuges.

What distinguishes the filtering centrifuges from their close but fundamentally different relatives, the sedimenting centrifuges (the latter covered in chapter 7), is the particle size range they are applicable to. Their range of application is generally much coarser, from 10 microns to 10 mm (*Figure 14.2*) as opposed to the micron and sub-micron sizes for the sedimenting centrifuges. Of the sedimenting centrifuges, only the decanter centrifuge (see *Figure 14.2*) overlaps the coarse range of particle size where filtering centrifuges apply but that is merely in its dewatering applications where particle settling is not really the governing principle.

The applicable size range is particularly coarse for those filtering centrifuges that move the cake across the filter medium (the 'moving bed' type in *Figure 14.2*) because they are restricted to metal screens as filter media which, by their very nature, can only be coarse (typically 100 microns or more, unless assisted by high feed concentrations as shown in the figure). The medium has to be metal because no cloth can withstand the abrasion by a cake

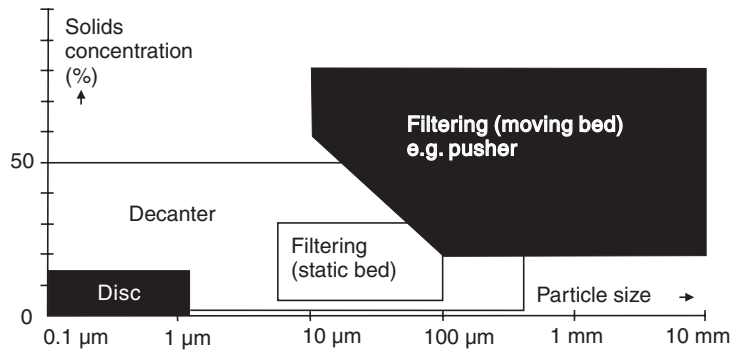

Figure 14.2 Range of application of different centrifuges (adapted from ref. 2)

pushed over its surface while held down by the centrifugal forces. The static bed, batch-operated centrifuges, however, can use cloth as the filtration medium and, therefore, be applied to somewhat finer suspensions while still not really competing with sedimenting centrifuges.

14.1 Perforate basket centrifuge

The simplest of the fixed bed centrifuges is the well-known perforate basket centrifuge (*Figure 14.3*). It has a vertical axis, a closed bottom and a lip or overflow dam at the top end. Some domestic machines of this type are in use for straining vegetable or fruit juices. In the industrial versions, the basket housing is often supported by a three-point suspension and because of this, the machine is sometimes called the 'three-column' centrifuge.

The basket centrifuge has found a wide range of applications in the filtration of slow draining products that require long feed, rinse and draining times, and for materials which are sensitive to crystal breakage or which require thorough washing. It can be applied to the finest suspensions of all filtering centrifuges because filter cloths may have a pore size approaching a few microns. The cloth is supported by a steel mesh.

The basket centrifuge exists in many different versions. The slurry is usually fed into the basket through a tangential pipe or a distributor cone, at a reduced speed. The feed rate and/or basket speed is adjusted so that the feed matches the filtration rate. The aim is for the slurry to cover the inside basket surface from top to bottom, thus forming an evenly distributed cake.

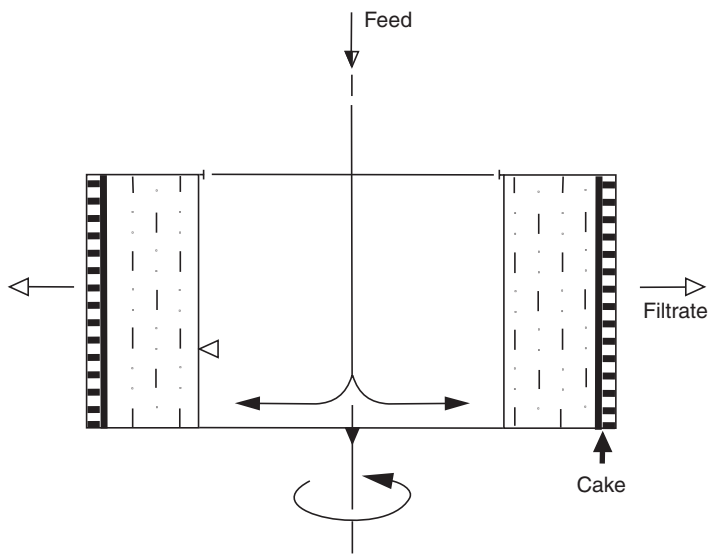

Figure 14.3 Perforate basket centrifuge

The cake, which deposits on the inside surface, may be discharged manually by digging it out in the top discharge machines, usually underdriven. Alternatively, some versions allow the cake discharge by pulling the cloth inside out from the centre (the axis of rotation can be horizontal (Heinkel) or vertical (Broadbent)). This method of cake discharge is particularly suitable for crystalline or thixotropic materials.

Alternatively, in the bottom discharge machines (these may be either under- or overdriven[3]), the cake can be ploughed out by a traversing scraper or 'plough', which moves into the cake after the basket slows down to a few revolutions per minute. This is gentle to crystalline solids, which may be prone to attrition. The plough directs the solids towards a discharge opening provided at the bottom of the basket, through which the cake simply falls out. The speed of the bowl varies during the cycle: filtration is done at moderate speed, dewatering at high speed and cake discharge by ploughing at low speed.

The cycle can be automated and controlled by timers. The frequent speed changes—see *Figure 14.4* can be wasteful in power but this can be alleviated by the use of inverter drives, which can regenerate the power during the braking part of the cycle. The frequent changes in speed also lead to dead times which limit the capacity. The plough cannot be allowed to reach too close to the cloth and, consequently, some residual cake ('heel') remains. This has to be removed after each cycle or at predetermined intervals. This is achieved either by the use of an air knife behind the plough or by a jet wash reslurry.

If cake washing is required, a static rose spray system is usually used for distributing the wash over the cake surface. Washing can be carried out at a reduced basket speed, while the basket is accelerating to full speed or at full speed only. The wash should be started before the cake is dewatered in order to prevent cake cracking, which would of course much reduce washing efficiency[3]. If the cake is evenly distributed within the basket, 'flood washing' can be carried out when the wash is introduced at a slightly higher rate than

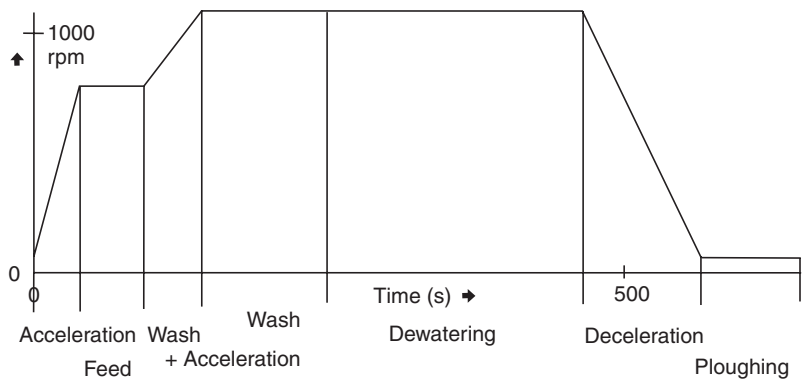

Figure 14.4 Speed changes in a typical basket centrifuge cycle (adapted from ref. 3)

can pass through the cake, so that a liquid layer forms on top of the cake. Alternatively, 'spray washing' at low feed rates requires minimum amounts of wash liquor and it is the only effective way of washing non-uniform cakes. In either case, mother liquor and wash liquors can be separated, if required, by means of a diverter valve on the filtrate outlet pipe.

The maximum speeds of basket centrifuges with cake discharge filter bag pullout or manual digging vary from 1200 to 2100 rpm (some have two-speed drives), and basket diameters are in the range from 500 to 1250 mm. A 1200 mm diameter, 750 mm long basket may handle as much as 200 kg of cake in one charge. Interlocks and inert gas blanketing may be used.

Basket centrifuges with plough discharge often have a hydraulic, variable speed drive, are of three-point support or overdriven construction (e.g. Broadbent or Mirlees) and their diameters vary from 260 to 1500 mm (filtration areas from 0.13 to 2.9 m^2). Applications of all types of basket centrifuges include separation of crystals (such as sugar where throughput rates up to 36 t/h have been reported[3]), nitro-cellulose, metal swarf or enamel frit, and lately also gypsum from gas desulphurization processes at coal-fired power stations[3].

14.2 Peeler centrifuge

The vertical axis of some basket centrifuges may cause some non-uniformity due to the effects of gravity, with the accompanying problems when cake washing is used. Such gravity effects can be eliminated by making the axis horizontal such as in the 'peeler' centrifuge shown in *Figure 14.5*. Another advantage is that it is designed to operate at constant speed so that the non-productive periods of acceleration and deceleration are eliminated. Cake discharge is effected at full speed, by means of a sturdy knife, which peels off the cake into a screw conveyor or a chute in the centre of the basket. This, however, can lead to considerable breakage of crystals. A narrow-bladed reciprocating knife is usually preferred because it causes less crystal damage and less severe glazing of the heel surface than a full-width blade, which would work faster.

The presence of the residual heel is not avoidable in either case, and it may be necessary to recondition it by suitable washes in order to restore its drainage properties. Some designs incorporate cake feeler/leveller mechanisms, which ensure that an even cake is formed.

One interesting improvement of the peeler principle is the addition of a rotating siphon in the form of an additional outer filtrate chamber. This retains the filtrate at a larger diameter than the basket diameter, therefore siphoning higher flow rate through the cloth than would otherwise be achieved. An adjustable siphon pipe controls the total pressure drop across the filter medium. Large increases in throughput are claimed due to the use of the rotating siphon. The additional chamber, however, increases the size of the

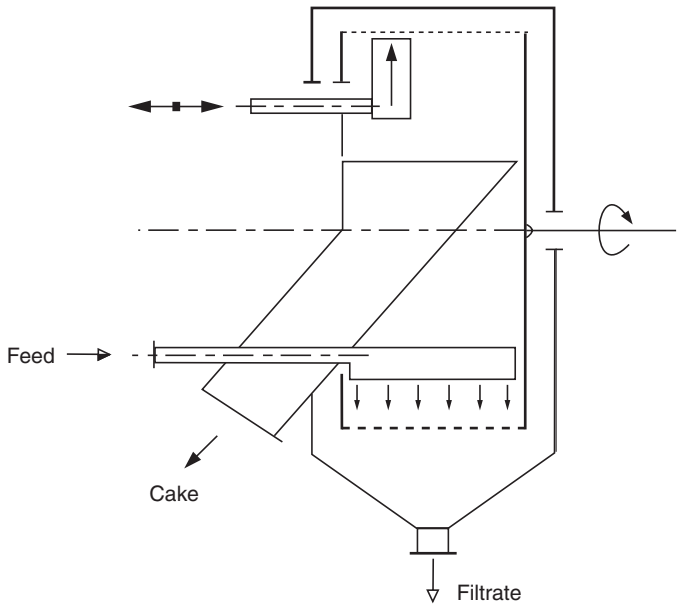

Figure 14.5 Peeler centrifuge

bowl and similar gains could be obtained by simply making the size of the conventional bowl as large as the one with the siphon. It is also not always desirable to lower the absolute pressure in the cake or the medium because cavitation may result due to the release of gas or liquid vapour.

The peeler centrifuge is attractive where filtration and dewatering times are short. The principal application is for high output duties with non-fragile crystalline materials giving reasonable drainage rates which require good washing and dewatering. Overhung or double-supported construction may be used (e.g. by Alfa-Laval or Krauss-Maffei), feed solids concentrations from 5 to 50% by weight. Basket diameters range from 250 to 2500 mm and speeds from 460 to 3800 rpm.

14.3 Conical basket centrifuge

The continuously fed, moving bed machines are available with conical or cylindrical screens. As can be seen in *Figure 14.6*, the conical screen centrifuges have a conical basket, rotating either on a vertical or horizontal axis, with the feed suspension fed towards the narrow end of the cone. If the cone angle is sufficiently large for the cake to overcome its friction on the screen (usually above 20 degrees), the centrifuge is self-discharging (e.g. Smith Mirrlees or Alfa-Laval). Such machines cannot handle dilute slurries and require high feed concentrations of the order of 50% by mass, as occurs in

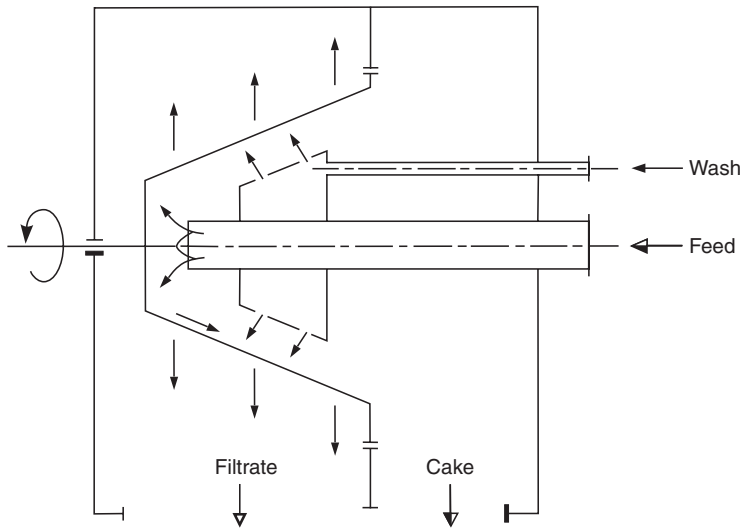

Figure 14.6 Conical basket centrifuge

coal dewatering, for example. Different products, however, require different cone angles. Unnecessarily large angles shorten the residence time of the solids on the screen surface and thus lead to poor dewatering. Heinkel have a resettable cone angle using a 'guide duct system'. Aperture size of the screen is from 125 to 250 microns, solids-handling capacities from 1 to 20 t/h, slurry flows from 1.2 to 36 m^3/h, bowl speeds from 2400 to 4300 rpm and bowl diameters from 225 to 610 mm.

The movement of the solids along the screen may be assisted by vibrating the basket either in the axial direction or in a 'tumbler centrifuge' in a tumbling action.

The axially oscillating machines use a cone angle of less than 20 degrees, can process from 20 to 300 t/h but the accelerations in the bowl only reach about 100 g. The bowl diameters are from 1000 to 1300 mm, feed concentrations from 20 to 75% by weight. The applications include dewatering of washed coal fines, washed tailings or sea salt.

The conical baskets tumble through an angle up to 5 degrees, and are used with relatively high feed concentrations, with bowl diameters from 540 to 1200 mm; they are used mainly for dewatering of coarse crystals.

A positive control of the solids on the screen is achieved with the scroll type conical screen centrifuge. Here the scroll moves slowly in relation to the bowl, conveying the solids along the bowl; variable speed differential drive allows good control of the solids movement. Crystal breakage is more severe here, however, due to the action of the scroll. Basket speeds vary from 900 to 3000 rpm, while the basket diameters range from 300 to 1000 mm. Washing is possible with all the conical screen centrifuges but it is not very efficient, giving poor separation of the mother liquor and the wash liquid.

14.4 Pusher centrifuge

The pusher type centrifuge has a cylindrical basket with its axis horizontal. The feed is introduced through a distribution cone at the closed end of the basket (*Figures 14.7* and *14.8*) and the cake is pushed along the basket by means of a reciprocating piston, which rotates, with the basket. The screen is made of self-cleaning trapezoidal bars of at least 100 microns in spacing, so that only particles larger than 100 microns can be efficiently separated by this machine. Each stroke of the piston stops just short of the discharge end of the basket, thus allowing a layer of the cake to act as a lip or a dam to effect the

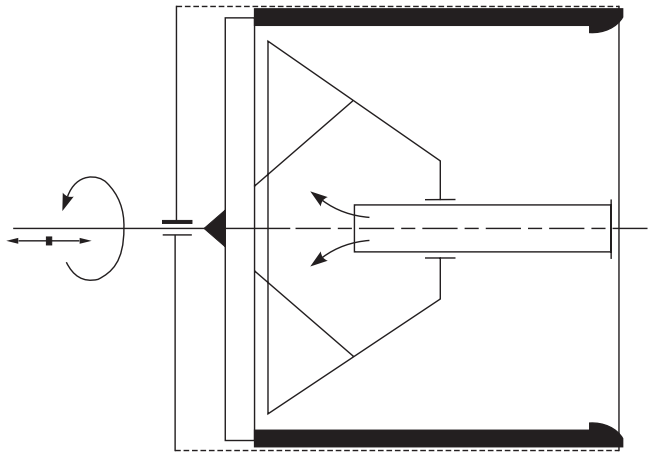

Figure 14.7 Pusher centrifuge in a backward stroke

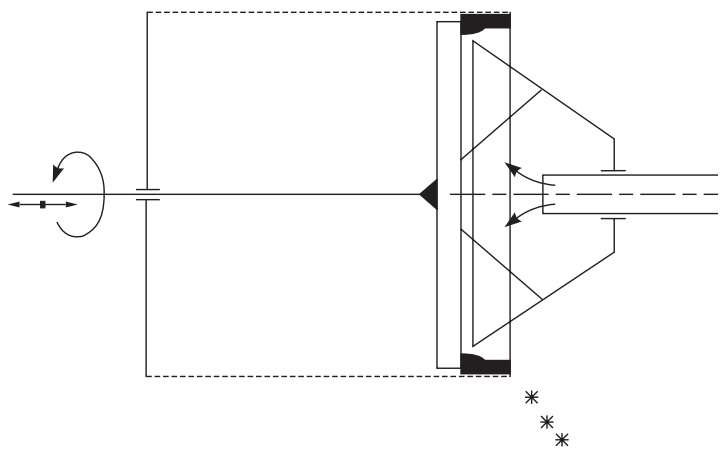

Figure 14.8 Pusher centrifuge in a forward stroke

axial retention of the feed suspension. If the feedstock is allowed to rise to a height exceeding this remnant cake thickness, the suspension will overflow at the discharge end and rapidly erode a deep furrow in the cake. This is highly undesirable and an 'overflow' limit therefore exists as an upper limit for the feed rate[1].

Pusher centrifuges can be made with multi-stage screens consisting of several steps of increasing diameter. This is advantageous for liquids of high viscosity, or where the cake is soft, plastic or of high frictional resistance to sliding. It also makes washing better, the washing liquid being introduced over the second stage screen. The transit of the solids over the step reorientates the particles.

Pusher centrifuges require high feed concentrations to enable the formation of a sufficiently rigid cake to transmit the thrust of the piston. The diameters vary from 150 to 1400 mm, the stroke frequency from 20 to 100 strokes per minute and the solids-handling capacities up to 40 tons per hour or more.

14.5 Scale-up and testing

The scale-up of filtration centrifuges is usually done on an area basis, based on small-scale tests. Buchner funnel type tests are not of much value here because the driving force for filtration is not only due to the static head but also due to the centrifugal forces on the liquid in the cake. Zeitsch[1] recognized this effect and described a test procedure with a specially designed filter beaker to measure the 'intrinsic permeability' of the cake. The cake is first formed (minimum cake thickness of 20 mm is recommended) and then clear filtrate (obtained by vacuum filtration or other methods) is filled into the beaker. The time required for the liquid to pass through the cake is measured by observation with a stroboscopic light. Following the notation in *Figure 14.9*, the intrinsic permeability $k\,(\mathrm{m^4\,N^{-1}\,s^{-1}})$ as defined by Zeitsch[3] can be derived from experimental measurements with a filter beaker as follows:

$$k = \frac{H_c}{\tau \cdot \rho \cdot g \cdot C} \ln\left(\frac{H_o}{H_c}\right) \tag{14.1}$$

where C is number of gs, H_c and H_o are distances defined in *Figure 14.9*, ρ is liquid density and τ is the time for the liquid level to fall to the cake surface.

The filter beaker can also be used for testing for moisture content in dewatering, which is a function of cake thickness, residence time and of gs in the centrifuge. When the permeability is high or when the effect of discharge peeler or plough on cake permeability is to be investigated, then a test filter basket is used. *Figure 14.9* gives a schematic diagram for such testing.

This may be a small-scale version of the ultimate large-scale centrifuge, using the actual suspension. Many manufacturers offer small laboratory models for such tests. An expression for intrinsic permeability similar to

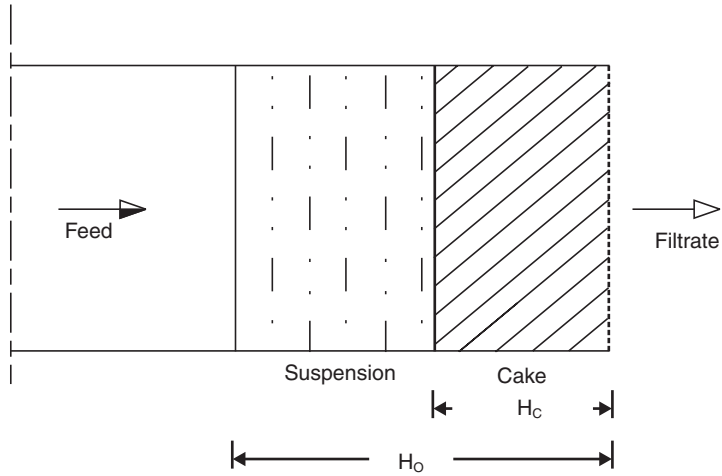

Figure 14.9 Intrinsic permeability testing

equation 14.1 is also available for the basket measurements[1], where the filtrate is fed to the basket continuously. The scale-up is reported to be most reliable if the basket diameter does not increase by a factor of more than 2.5 from the small scale.

Once the intrinsic permeability k has been determined, a rough selection of the most suitable centrifuge type can be made following the rules of thumb given below:

1 If k is above $20 \times 10^{-10}\,m^4\,N^{-1}\,s^{-1}$, the moving bed machines (usually pusher centrifuges) may be appropriate.
2 If k is between 10×10^{-10} and $20 \times 10^{-10}\,m^4\,N^{-1}\,s^{-1}$, peeler centrifuges may be selected.
3 If k is between 0.02×10^{-10} and $10 \times 10^{-10}\,m^4\,N^{-1}\,s^{-1}$, perforate basket centrifuges may be suitable.
4 If k is below $0.02 \times 10^{-10}\,m^4\,N^{-1}\,s^{-1}$, sedimenting centrifuges may be a better choice (providing there is a density difference between the solids and the liquid).

References

1. Zeitsch, K., 'Centrifugal filtration', Chapter 14 in *Solid–Liquid Separation*, 3rd edn, L. Svarovsky (Ed.), Butterworths, London, 476–532 (1990)
2. Punch, K., *Private communication*, Sulzer Bros (UK) Ltd and Escher Wyss Ltd, Farnborough, 14 July (1980)
3. Wright, J., 'Practical guide to the selection and operation of batch-type filtering basket centrifuges', *Filtration & Separation*, November, 647–653 (1993)

15 Countercurrent washing of solids

L. Svarovsky

FPS Institute, England and University of Pardubice, Czech Republic

15.1 Introduction

The ever-increasing demands on product purity and environmental acceptability of waste materials, accompanied by gradual reduction in the quality of raw materials, make washing of solids a frequent and often inevitable choice in process engineering. Industrial applications cannot afford the huge amounts of wash liquid required by co-current washing (such as used in domestic washing machines) when clean liquid is added before each washing stage.

Countercurrent washing offers a great saving on the quantity of wash liquid together with many other important advantages listed below. Consequently, its application in industry is spreading quickly. Even washing of filter cakes by displacement, where the wash liquid requirement in the co-current mode is not excessive, is in some cases performed countercurrently if the additional cost of equipment needed for the separate collection of filtrates can be justified.

The countercurrent arrangement is a special case of separator series connections in the underflow direction where overflow recycles are made to the feeds of the preceding stages. In this arrangement, as shown in *Figure 15.1*, the feed slurry and the wash liquid move through the separator series in the opposite directions. The wash liquid is gradually more contaminated with the mother liquor while the concentration of the mother liquor in the solids stream reduces. The solids leave the washing train as a slurry in the system underflow whilst most of the decanted wash liquid leaves through the system overflow.

Just like washing generally can be done by washing filter cakes *in situ* (whilst they are still on the filter medium), by reslurrying of filter cakes or sediments, or by successive dilutions of slurries, the same is done in countercurrent washing. Applications and examples exist in industry for all of the above three types.

The majority of countercurrent washing performed in industry is in a continuous process where all the flows are truly continuous. It can also be

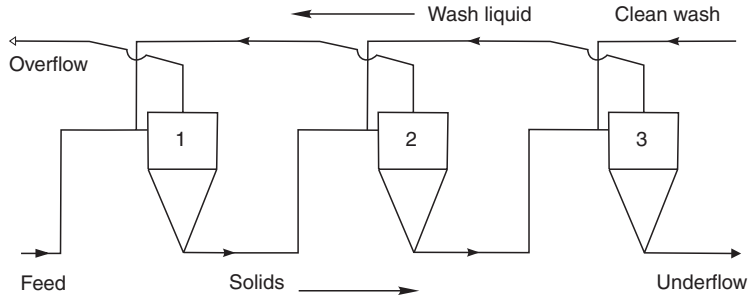

Figure 15.1 Schematic diagram of a countercurrent washing train—three stages are shown as an example but up to 12 or more stages may be used

done semi-continuously, however, which involves batch washings with batches of wash liquids saved from previous washing operations in later stages. White and Bashir[1] optimized such washing (by reslurry) of ion exchange flocs for the treatment of radioactive waste and describe a laboratory batch test procedure to obtain working data needed for specifying continuous processes. A similar laboratory batch test scheme was described by Komline-Sanderson Engineering Corporation[2] for the case of cake filtration and this is shown schematically in the appendix at the end of this chapter.

The rest of this chapter, however, is concerned with continuous countercurrent washing. The separators used may be sedimenting centrifuges, gravity thickeners or filters but the preferred choice is often hydrocyclones. The inherent advantages of hydrocyclones are compactness, small hold-up of liquid, high shear forces and turbulence in the flow, the latter two of which improve mass transfer and dispersion.

Washing is not the only application of the arrangement in *Figure 15.1*. It may be also used for thickening (often simultaneously with washing), solids recovery or classification. As with a single separator, the actual function of the arrangement in *Figure 15.1* depends on what it is designed and set to do. In other words, it depends on where the system cut size is set in relation to the particle size distribution of the feed solids.

In washing, thickening and recovery applications we try to set the cut size of the system below the finest particle size present in the feed, so that any loss of particles into the system overflow is minimized. When the system cut size cannot be set sufficiently low it may be necessary to use an additional separator on the system overflow to return the escaping solids back in the feed—refer to the case study on washing of wheat starch later in this chapter, for an example.

In classification, the system cut size is purposely set within the size distribution of the solids, depending where the cut needs to be made. The arrangement in *Figure 15.1* is capable of a significant improvement in the sharpness of cut compared with that of a single-stage separator and this is further discussed and documented in chapter 16.

What is the difference, if any, between countercurrent decantation and countercurrent washing? In the method of using successive dilutions and separations with overflow recycles shown in *Figure 15.1*, the two terms are synonymous. In actual applications, the term countercurrent decantation tends to be used when gravity thickeners are the system separators. The product is a solute in the wash liquid 'decanted' into the system overflow (for example, in the washing of red mud in the Bayer process of aluminium oxide refining where caustic is recovered from the red mud which is then discarded). The term countercurrent washing of solids implies that the solids are the products. In this chapter it will be used irrespective of the purpose of the washing process, which may be one of the following:

1 Actual washing of solids, for example removal of salts from the surface of or from within porous particles such as in washing of soda from hydrogel—see the case study later. A large application in this category is washing of paper pulps[3,4,5]. Washing of soils or sand is another example and it may be combined with solvent extraction. Generally, the solids may enter the washing train either dry (then suspended by the recycle stream returning from the second stage) or already suspended. One great advantage of countercurrent washing is that the contaminant is much more concentrated in the effluent stream (system overflow) than it would be in a co-current washing system.
2 Removal of solids from a solution which contains the product as a solute. The solids represent the contaminant or carry it adsorbed on the surface (e.g. heavy metals). The aim is to thicken the solids into the wash liquid, as free as possible of the solute (i.e. with a minimum loss of the product). The system overflow contains the solute at a concentration only a little lower than that in the system feed. The process essentially removes the solution from the solids in a similar way as a cake filtration process, except it can do this for fine, difficult-to-filter solids and without exposure to air or to any filter medium, in a completely enclosed pipework free of moving parts (except for the pumps). This process is gaining favour in the chemical industry and it can be driven by high pressure at the front of the washing train—see the next section.
3 Removal of a soft, semi-solid and light material from granular solids, such as the washing of starch where both the soluble and insoluble proteins (gluten) are removed into the overflow. Hydrocyclones are ideal separators for this application because of the high shear forces in the flow, which separate the semi-solid, sticky gluten from the granules of the starch particles. Since it is the gluten, which is the high value product in wheat starch washing, the countercurrent system concentrates it into the overflow, which is then further dewatered in subsequent processing.
4 Removal of superfine solids from coarser particles. This brings countercurrent washing into the realms of particle classification as considered in chapter 16. An example of this application is separation of the two sizes of

granules present in wheat starch from each other. The coarse fraction is used as stilting material in the production of carbonless copy paper.

15.2 The pumping arrangements

In the most common set-up a separate pump drives each stage (see *Figure 15.2*) and both the overflow and underflow are discharged at atmospheric pressure (see *Figure 15.3*). This may be accomplished by discharging into an open sump and using the sump for mixing the forward moving solid streams with the recycling overflows (as shown in *Figure 15.4*) or by simply plumbing the two streams together (*Figure 15.2*). The latter alternative is more dependent on careful hydraulic balancing of the system to obtain the design flow rates in all streams, and it is more difficult to take samples from but it offers a completely enclosed system such as used in starch washing.

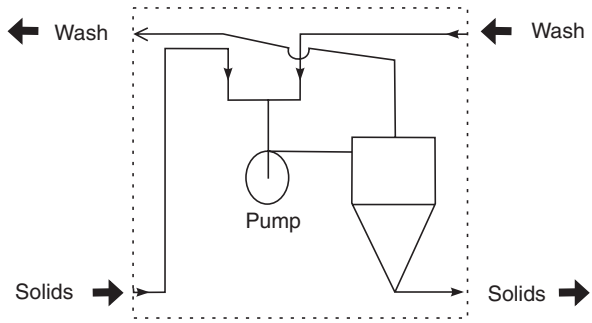

Figure 15.2 Each stage in *Figure 15.3* has a pump to drive it, and the forward passing solids stream is simply plumbed in together with the returning wash stream into the pump feed

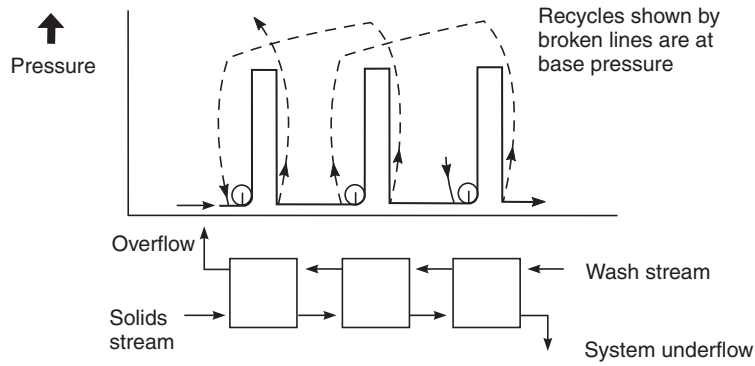

Figure 15.3 A system driven by intermediate pumps

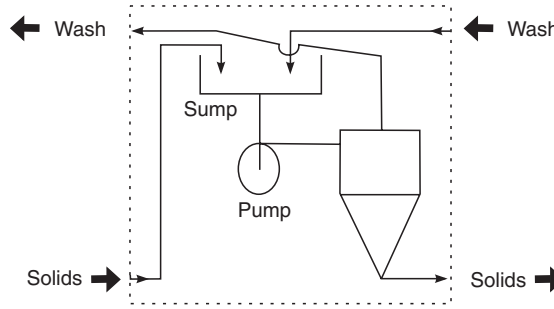

Figure 15.4 Each stage in *Figure 15.3* has a pump to drive it, and a sump is used here to mix the forward passing solids stream with the returning wash stream

The use of sumps in between stages, however, is more forgiving and allows increasing (and designing for) contact time between the solids and the liquid needed for mass transfer to take place. It also simplifies sampling the incoming flows, for flow rate, concentration or particle size determinations. Another way of increasing the residence time of the solids in each stage is by periodically switching the whole set-up to a recirculation mode in which all stages are isolated and recirculate their underflows and overflows back to their own feed sumps. This control over the residence time is particularly useful where a mass transfer process is involved, such as the diffusion of salts from the inside of very porous solids, or in solvent extraction.

In the countercurrent washing system with intermediate pumps shown in *Figure 15.3*, whether it uses sumps or just T-pieces to mix the streams together, the recycling overflows do not need pumping because the total pressure is atmospheric at both ends and only a small back pressure on the cyclone overflow is enough to drive the returning flow through the connecting pipework. With careful thinking at the design stage, it is also possible at start-up to fill the washing train from the back with wash liquid before allowing the feed in (therefore not exposing any of the incoming feed to air when such exposure is not desirable). This is also necessary when the solids come in dry or with little liquid and the recycling wash liquid is needed to suspend the solids. The usual way to start up a system where the solids come in already suspended is to simply commence feeding and pumping from the front and progressively start the pumps further down the train as the system fills up.

One possible alternative to the system of intermediate pumps is a system driven by high pressure at the front of the washing train (by a high-pressure pump, by hydrostatic pressure or by pressure from a reactor). This idea applied to an underflow series was first used by Povarov[6] and later by Kelsall *et al.*[7]. There are no pumps needed between the stages and each stage consumes its share of the total pressure drop across the whole series as shown in *Figure 15.5*. The recycling overflows, however, have to go back to the higher pressure levels of the preceding stages and this requires pumping.

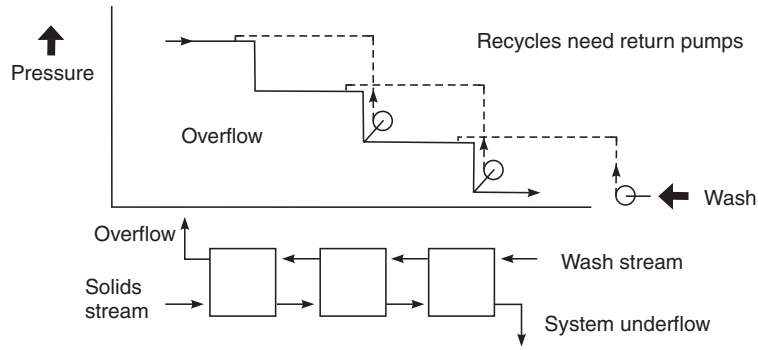

Figure 15.5 A system driven by feed pressure

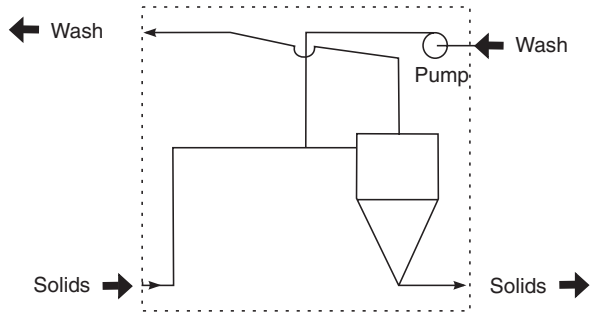

Figure 15.6 Each stage in *Figure 15.5* looks like this—there is no pump needed to drive the solids stream forward but a pump is now needed on the returning wash stream. There can be no open sumps used here but intermediate buffer vessels can provide the hold-up time if required

Thus, the intermediate pumps normally driving a washing system forward are now replaced by the same number of pumps (if the wash liquid feed requires one too) on the overflow recycling streams as shown in *Figures 15.5* and *15.6*. The advantage is that the pumps now handle much cleaner flows. If necessary, the pipework can be easily filled with the wash liquid from the back of the washing train at start-up, before allowing the feed in from the front.

15.3 Advantages and capabilities of a countercurrent washing system

The main advantage of the system over co-current washing is the low wash liquid requirement. The system is also capable of the following:

1 high efficiency of washing (depending on the number of stages and the flow ratios in the stages),

2 high recovery of solids (depending on the efficiency of particle removal in all stages but critically on the efficiency of the stages at the front of the train),
3 good thickening in the system underflow (when the highest concentration of solids is designed to be in the underflow of the last stage) limited only by the capability of a hydrocyclone in a thickening duty (45 to 50% by volume for most solids, for example 23 to 24 Baumé for wheat starch),
4 high concentration of solute in the system overflow, requiring much less evaporation to thicken it afterwards,
5 good sharpness of cut in classification depending on the number of stages and their split ratios—see chapter 16 for more details.

The advantages listed above apply to systems using virtually any separator but hydrocyclones offer additional merits. A totally enclosed system can be built preventing any exposure of personnel to the chemicals used, escape of vapours or exposure of the fluids to atmospheric air. Hydrocyclones are small, easy to insulate or trace-heat, contain little liquid hold-up, are relatively inexpensive and robust, respond fast to control and require simple supports. Also, the high shear in the flow ensures good separation/dispersion of individual particles and phases, and the high turbulence increases mass transfer coefficients. However, if greater residence times are required in the mixing, intermediate sumps or recirculating systems may have to be installed.

One slight disadvantage of countercurrent washing is that the demands for high washing efficiency and high solids recovery (for fine solids) are to some extent contradictory and careful design is necessary for optimum performance. Due to the use of recycles, the mass balance calculations for an optimum design are more complex than for other separation processes. With the assistance of computer software for the design of countercurrent washing systems, however, this obstacle has been largely removed.

Before laying down the main rules of washing train design, it is necessary to consider mass balance calculations. This is done separately for particles and for the dissolved species in the following two sections.

15.4 Mass balance calculations for the solids

If the solids to be washed are much coarser than the cut sizes in all stages of the washing train, complete separation in each stage may be assumed and the mass balance calculations become trivial (i.e. each underflow stream carries the same mass flow rate of the solids, equal to the feed rate, and all overflows are free of solids).

On the other hand, if some solids do escape because the stage cut size is not low enough, mass balance calculations may have to be performed when designing or troubleshooting the system. The difficulty is that, from the particle separation standpoint, not all stages have the same effect even when

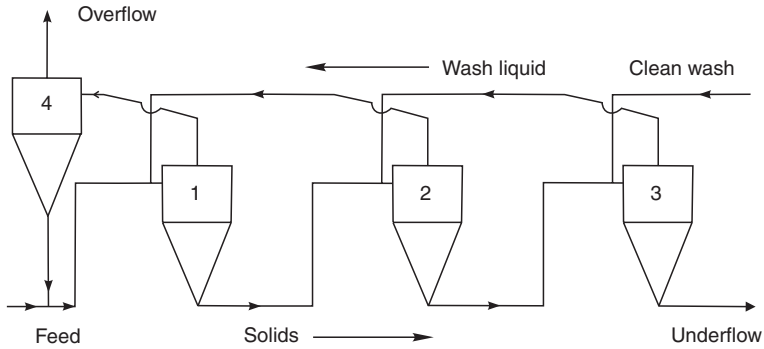

Figure 15.7 A three-stage washing train with an additional separator on system overflow

identical in design and operation. A close inspection of *Figure 15.1* reveals that while the stages further along the train are protected by the overflow recycles which return any escaping particles back into the train, the first stage does not have that protection. A certain proportion of predominantly fine particles (depending on the position of the system cut size relative to the particle size distribution of the feed solids) will end up in the overflow of the first stage (which is the system overflow) and be lost.

If this particle loss cannot be tolerated for whatever reason, either the washing train has to be suitably modified or, if that is not possible, an additional separator (or separator series) may be installed which may not necessarily be the same separator type. *Figure 15.7* shows a good example of the latter case in washing of wheat starch where even a 10 mm diameter cyclone operated at high pressure in the first stage cannot prevent particle loss due to the low particle density and the presence of some very fine particles. The additional separator No. 4 shown in *Figure 15.7* may be a sedimenting centrifuge (usually the disc type), a hydrocyclone, or an overflow series of hydrocyclones.

It is possible in some cases to overcome any particle loss problem by a more careful design of the washing train itself. The front units of the train and most importantly the first stage have to have a much lower cut size than the units further down the train where the repeated overflow recycles provide protection. If this cannot be achieved by increasing the operating pressure or by reducing the diameter of the cyclones used, another option is an increased R_f flow ratio. This will sacrifice some washing efficiency in the front stage (or a few front stages if the R_f ratio settings are 'tapered' from the front of the train). It is possible to compensate by using correspondingly lower values of R_f in the latter stages where high stage recovery is much less critical—see more about this in the section on washing train design.

As can be seen from the above, mass balance calculations for the solids are needed in all non-trivial cases of equipment design, modelling and

troubleshooting. Before the advent of computers, this was difficult due to a large number of streams and the many recycles employed in a typical washing train. One method still useful today is a short-cut method, which allows comparison of different systems, as follows.

15.4.1 A short-cut method for system particle separation efficiency calculations

If the concentrations and particle size distributions of the solids within the washing train itself do not have to be known then the train can be considered as a single separator and its efficiency can be calculated from that of the individual stages within it. The system efficiency thus obtained can then be used in simple one-pass predictions of particle losses to overflow and other overall separation performances of the train. This allows direct comparisons of alternative systems, as shown in the worked example below.

If the grade efficiency curves are known for all stages in a system, an equation for the grade efficiency of the whole system may be derived from mass balances around the arrangement. My book on hydrocyclones[8] gave, for the first time, such equations for many different series arrangements comprising no more than three stages. An even more comprehensive list of such equations may be found in chapter 16.

The following equation applies to the three-stage system in *Figure 15.1*, as an example (ref. 9, p. 538):

$$G(x) = \frac{G_1 G_2 G_3}{(1 - G_1 - G_2 + G_1 G_2 + G_2 G_3)} \tag{15.1}$$

where G_i is the grade efficiency of stage i for $i = 1$ to 3 and $G(x)$ is the grade efficiency of the whole arrangement.

Note that the same equation can be written for the system total recovery because the total recoveries in the individual units combine into the overall recovery of the whole train in exactly the same way as the grade efficiencies do.

If an additional separator (No. 4) is added on the system overflow, equation 15.1 now becomes

$$G(x) = \frac{G_1 G_2 G_3}{1 - G_1 - G_2 + G_1 G_2 + G_2 G_3 - G_4(1 - G_1 - G_2 + G_1 G_2 + G_2 G_3 - G_1 G_2 G_3)} \tag{15.2}$$

where G_i is the grade efficiency of stage i for $i = 1$ to 4.

15.4.1.1 Worked example 15.1

Compare the relative particle losses to overflow for a three-stage washing train with and without an additional separator (*Figures 15.7* and *15.1* respect-

Table 15.1 Grade efficiency data for worked example 15.1, *Figure 15.7*

x micron	*f(x) %/micron*	G_1 %	G_2 %	G_3 %	G_4 %
0.75	0.00	9.28	6.29	3.30	1.31
1.50	0.02	12.74	9.87	6.99	5.07
2.25	0.16	20.33	17.72	15.08	13.32
3.00	0.53	29.96	27.67	25.34	23.79
4.50	1.85	48.97	47.32	45.61	44.48
6.00	3.36	63.91	62.75	61.53	60.73
7.50	4.52	74.56	73.75	72.88	72.31
9.00	5.17	81.94	81.37	80.75	80.35
12.00	5.26	90.59	90.29	89.97	89.76
15.00	4.52	94.85	94.69	94.51	94.40
18.00	3.59	97.05	96.96	96.86	96.79
21.00	2.74	98.25	98.19	98.13	98.09
27.00	1.52	99.32	99.30	99.27	99.26
33.00	0.84	99.70	99.69	99.68	99.68
39.00	0.46	99.86	99.86	99.85	99.85
45.00	0.26	99.93	99.93	99.93	99.92
51.00	0.15	99.96	99.96	99.96	99.96
63.00	0.05	99.99	99.99	99.99	99.99
75.00	0.02	100.00	100.00	100.00	100.00

ively) installed on the overflow stream to minimize such losses. The grade efficiencies of all three stages (Nos 1 to 3) and of the extra separator (No. 4), and the particle size distribution in the feed, are given in *Table 15.1*.

15.4.1.2 Solution

Equations 15.1 and 15.2 can be used to compute the grade efficiency curves for each system in *Figures 15.1* and *15.7*. This calculation is best performed in a spreadsheet where each line in *Table 15.1* is processed by the two equations, yielding two additional columns. These are given in *Table 15.2* where the given values of particle size x and differential size distribution in the feed $f(x)$ are repeated in the first two columns.

As can be seen from the plots of the two grade efficiency curves in *Figure 15.8*, the additional separator increases the efficiency of the system significantly. In order to compare the relative losses to the overflow of the two systems, it is necessary to determine the overall system recoveries by integrating the product of $G(x) \cdot f(x)$ with x. This can be done either graphically or numerically to give 88.4% for the three-stage system in *Figure 15.1* and 95.8% for the four-stage system in *Figure 15.7*. The relative loss to

Table 15.2 The resulting grade efficiency curves for the two alternative systems in *Figures 15.1* and *15.7*

x micron	*f(x)* %/micron	*G(x)* 3-stage	*G(x)* 4-stage
0.75	0.00	0.02	0.02
1.50	0.02	0.11	0.12
2.25	0.16	0.80	0.92
3.00	0.53	3.64	4.73
4.50	1.85	21.81	33.44
6.00	3.36	47.40	69.65
7.50	4.52	66.32	87.67
9.00	5.17	77.95	94.73
12.00	5.26	89.58	98.82
15.00	4.52	94.56	99.68
18.00	3.59	96.96	99.90
21.00	2.74	98.22	99.97
27.00	1.52	99.32	99.99
33.00	0.84	99.70	100.00
39.00	0.46	99.86	100.00
45.00	0.26	99.93	100.00
51.00	0.15	99.96	100.00
63.00	0.05	99.99	100.00
75.00	0.02	100.00	100.00

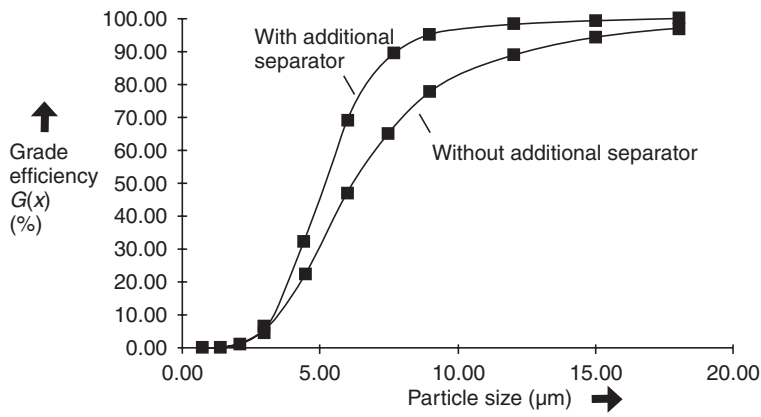

Figure 15.8 The plots of the two grade efficiency curves of *Table 15.2*

overflow is then the deficit from 100%, i.e. 11.6% and 4.2% respectively for the two systems.

15.4.2 A detailed mass balance for solids and liquids

The short-cut method described in the preceding section does not produce data on particle concentrations and flows in between stages. This information is needed for efficient equipment design. One common failure of washing trains is insufficient thickening in the system underflow. Full mass balance calculations often reveal that the thickest concentration occurs somewhere within the washing train instead of at the end thus providing a bottleneck preventing the best function of the system. This can be prevented by accurate mass balance calculations at the design stage—see the case study on wheat starch washing later, in section 15.7.

Manual calculations of detailed particle mass balances in washing trains are tedious and complicated. This is one area where computers come into their own. The available software ranges from large solid processing plant simulators such JKMetSim, SPEEDUP or METSIM to smaller but dedicated packages developed especially for separation applications by Alcan Chemicals Europe[10] or by Fine Particle Software (FPS)[11]. The latter offer more specialist features allowing direct comparisons between alternative separation and washing systems.

In order to demonstrate the level of detail that computer modelling can produce, Worked example 15.1 presented in the previous section is analysed in the following with the Computer Aided Design of Separator Networks developed and marketed by FPS[12]. This package has a user-friendly graphical interface which allows the drawing of any network first, using the usual tools such as separators, sumps, feed lines, clean liquid supplies, flow splitters and instrumentation for on-screen display of data on liquid flows, solids concentrations, particle size distributions in pipes and sumps as well as total and grade efficiencies, sharpness of cut and split ratios in separators.

One additional feature here, not shown in other packages, is the overall performance monitor which evaluates the performance of the whole separation plant (as if it were just one separator) to allow direct comparisons of alternative systems or set-ups. This package is designed for any separator arrangements in series or parallel, with or without recycles but it comes into its own particularly with countercurrent washing systems because these usually represent the most complicated arrangements in the separation business. Some washing trains come pre-drawn in a library of networks that comes with the package.

As soon as the network is drawn and connected, and when any feed items are specified, the program works out the mass balances (this involves iteration if re-cycles are used such as in a washing train) and this can be observed on screen if suitable instrumentation is strategically positioned within the schematic diagram of the network and connected to chosen items. Changes to input data (through an appropriate control panel) can be made at any time and the effect of any changes observed on screen or in a control panel. This system is excellent for specifying alternative systems for achieving a given task and for

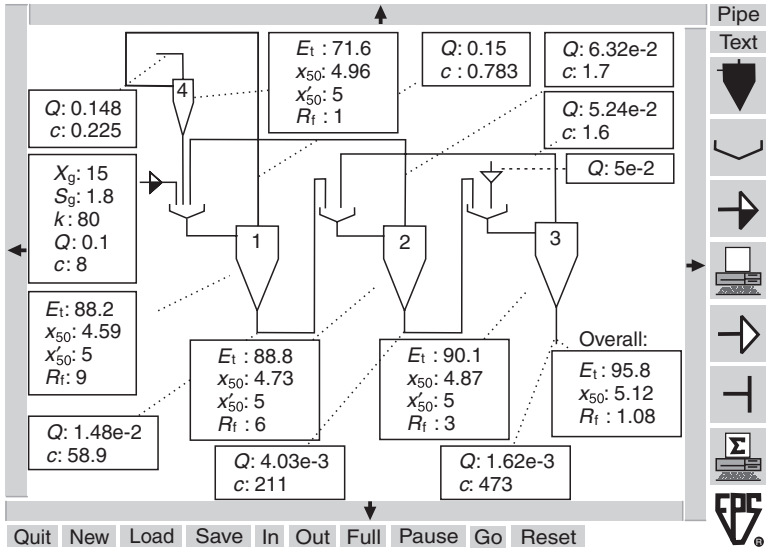

Figure 15.9 A three-stage countercurrent washing train with an additional separator on overflow (No. 4) drawn with the CAD of Separator Networks software, suitably furnished with displays

evaluation of optimum arrangements; when a final set-up is decided upon, the design data then becomes available for the sizing of separators, pumps, sumps and pipework.

Figure 15.9 shows the three-stage countercurrent washing train with an additional separator on overflow (stage 4) of the Worked example 15.1 drawn into the CAD with Separator Networks program, with some instrumentation strategically positioned around to monitor the most important variable in the arrangement. Each box displayed is capable of showing several alternative pages such as particle size distributions in the streams or other data. It was not possible to display data from every stream around the washing train to avoid too much clatter but a lot more can be displayed, say in the areas off the screen to which the view can be moved using the scroll bars, or by accessing the control panels of individual equipment.

Figure 15.10 shows the data in the control panel of the feed line from which it can be seen that, unlike manual calculations, the program allows the use of a much greater number of points on the feed size distribution or in the form of a three-parameter log–normal size distribution (the median, the geometric standard deviation and the maximum size). The overall performance monitor shown in *Figure 15.9*, displaying just the total efficiency, the cut size and the reduced cut size of the system, can also show the system grade efficiency curve as a graph (*Figure 15.11*) or a table (*Figure 15.12*), and the latter can be compared with the result of the manual calculation shown in the last column in *Table 15.2*.

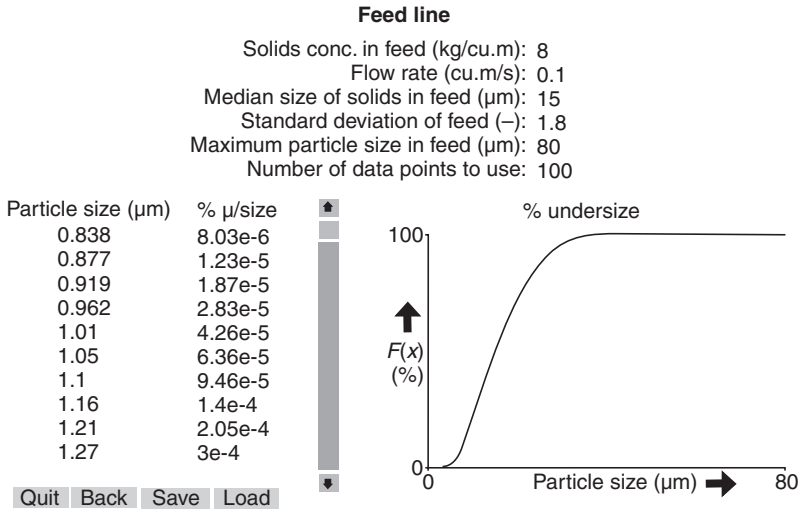

Figure 15.10 Display of the data in the control panel for the feed line of example in *Figure 15.9*

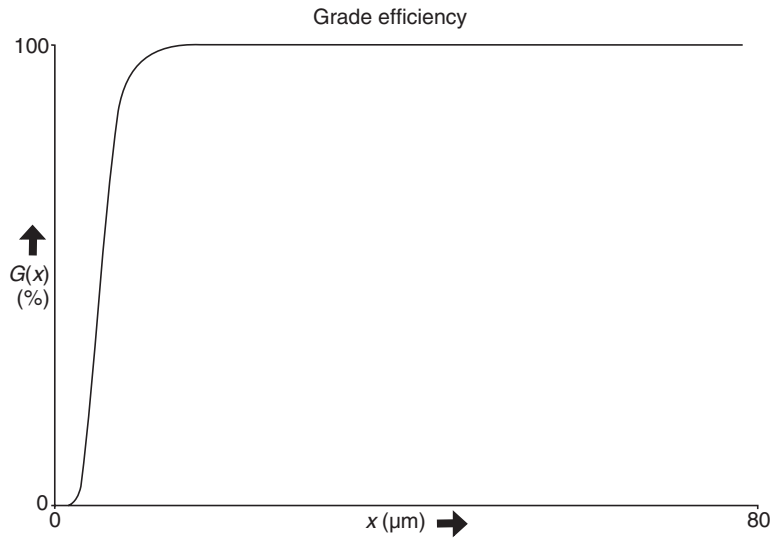

Figure 15.11 Example of the display of the overall grade efficiency curve of the whole system as shown by the overall performance monitor in the example of *Figure 15.9*

In conclusion, mass balance calculations for particles can be quite complex for countercurrent washing, unless the separation is (or can be assumed) complete in all stages. Preliminary calculations for system comparisons can

x (μm)	$G(x)$ (%)
3.74	15.2
3.92	18.9
4.1	23.2
4.3	28.1
4.5	33.4
4.71	39.2
4.93	45.2
5.17	51.3
5.41	57.3
5.67	63.1
5.93	68.4
6.21	73.3
6.5	77.6
6.81	81.4
7.13	84.7
7.47	87.4
7.82	89.8

Figure 15.12 Example of a part display of the detailed table of the overall grade efficiency of *Figure 15.11*

be done using the short-cut method but full mass balances for pump, pipework and separator sizing are best done with one of the few computer programs available for this on the market.

15.5 Washing efficiency calculations

Mass balance calculations for the soluble species to be washed off or from the solids are a lot easier than for particles because, assuming perfect mixing and mass transfer, the solubles are split in each stage in the same proportions as the liquid. Such calculations can be done by hand, as shown below, and some inexpensive software exists for this too[13].

Fitch showed a simple way of working out the algebraic solubles balance[14] which can also be used for the volumetric balance of the liquid flows. *Figure 15.13* shows rectangles representing the different stages, each containing a separator and its feed sump, and a pump. The critical information needed for easy calculation of a general case such as this is the ratio, in each stage, of the quantity of solubles carried in the feedback flow to that carried in the advancing flow. This ratio for perfect mixing in the tank and separator is equal to $1/S_i$ in each stage No. 'i', if S_i is the free liquid underflow/overflow split (in *Figure 15.13* this is set to 2 in all stages). The algebraic solubles balance can thus be calculated, starting at the final stage.

An unknown value x is assigned to the mass flow rate of the solubles in the outflow of washed solids from the final stage (the system underflow)—see *Figure 15.14*. This unknown x will carry through the system and appear as a factor in the solubles balance around all stages in the system. The difference

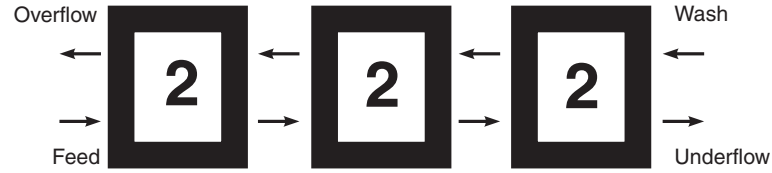

Figure 15.13 A schematic diagram displaying each stage as a box and its value of the overflow/underflow split

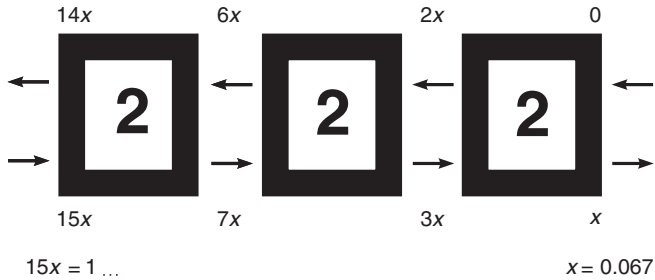

Figure 15.14 A schematic diagram depicting the manual method of mass balance calculations for the solute

between the advancing flow and the return flow between any two stages in the system therefore has to be equal to x. Taking the wash liquid introduced in the final stage to be clean and free of any mother liquor, the return flow from the last stage in *Figure 15.14* would have $2x$ of the solubles while the advancing flow, entering stage 3, would contain x more, i.e. $2x + x = 3x$. As this diagonal multiplication is taken all the way to the solids feed, the resulting expression at the solids feed ($15x$ in this case, see *Figure 15.14*) is then set equal to the actual mass flow rate of the solubles coming with the solids, and the unknown multiplier x is calculated. The now known x is used in calculating the mass flow rates of solubles in all other streams around the washing train.

Application of the above quoted method by Fitch[14] to the three-stage system in *Figure 15.13* yields the following equation for the overall loss of the solubles to the system underflow[9]:

$$x/M_s = \frac{1}{1 + (1/S_1) + [1/S_1 \cdot S_2)] + [1/S_1 \cdot S_2 \cdot S_3)]} \tag{15.3}$$

or in terms of the underflow–throughput ratios R_f (again as free liquid ratios):

$$x/M_s = \frac{R_{f1} \quad R_{f2} \quad R_{f3}}{[1 - (1 - R_{f3}) \cdot (R_{f1} + R_{f2})]} \tag{15.4}$$

where M_s is the mass flow rate of solubles in the solids feed.

If x/M_s represents the overall loss of solubles into the system underflow then $(1 - x/M_s)$ is the washing efficiency as the fraction of the feed solubles' mass rate removed into overflow.

Note that the amount of the wash liquid added to the circuit only affects the dilution of the solubles in the system underflow and overflow, and has no effect on the overall washing efficiency.

Another important overall performance parameter is the loss of wash liquid in the system underflow. This can be calculated from the mass balance for the wash liquid: Fitch's method shown in *Figure 15.15* yields the loss of wash liquid in the underflow (w) for the simple case where no wash liquid comes with the solids, as

$$w/W = \frac{1}{1 + 1/(S_1 \cdot S_2 \cdot S_3 + S_2 \cdot S_3 + S_3)} \tag{15.5}$$

where W is the wash liquid feed flow rate. As can be seen, this ratio only depends on the splits in each stage and increasing the wash liquid supply merely dilutes the underflow solids stream. Reducing the wash liquid supply may therefore thicken the system solids underflow stream but only if there is enough liquid to carry the solids through all of the other underflows in the train. In addition, as the underflows of any individual stages get thicker, the separation efficiency of the solids may be reduced, causing some solids to leave through the overflow of the stages affected. This is to do with the effect of underflow crowding on the separation efficiency of most separators, see details of this in chapter 5 for gravity thickeners, chapter 6 for hydrocyclones and chapter 7 for centrifuges.

In the limit, there is a minimum wash liquid flow required to carry the solids, and the wash liquid supply must not be reduced below this point because this would cause severe carry-over of solids into the overflow. For hydrocyclones, the maximum solids concentration in the underflow is of the order of 45 or 50% by volume and enough liquid has to be provided in all stages for the solids to be able to pass through to the system underflow.

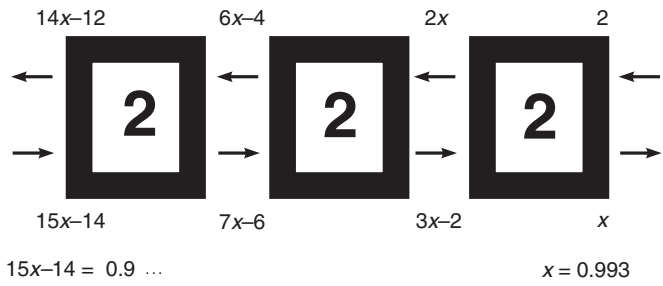

Figure 15.15 A schematic diagram depicting the manual method of working out volumetric balances

The mass balances of simple washing trains with clean wash liquid and with the solids entering the system being dry can be easily calculated manually using the above-described method proposed by Fitch[14]. If some wash liquid enters with the solids or if the wash liquid feed contains some solubles, the mass balance becomes a little more complicated and is best carried out with a computer. This involves simultaneous solution of several linear equations and allows interactive, 'what if' scenarios to be considered in a graphical environment. This is the principle behind the program distributed by Fine Particle Software[13]. The program has been used to study the countercurrent washing systems and make the conclusions presented here; it has also been used to compare the predicted performance with experimental tests in industrial systems such as washing hydrogel[15].

15.5.1 Examples of washing efficiency calculations

Table 15.3 sets out three cases of a three-stage countercurrent washing train in which the solids come in dry (no wash liquid with the solids feed) and the wash liquid comes in clean (no solubles in the wash liquid). All three cases are designed to give the same washing efficiency (from 1 g/s with the feed to 0.008 g/s in the system underflow) they all have the same minimum amount of liquid in any underflow along the train to carry the solids along (0.261 l/s), as indicated in *Table 15.3*.

The three cases are shown at this stage only as a demonstration of how a computerized mass balance calculation can be used to test a system and optimize it quickly. It also shows the effect of the values and order of the flow ratios on the wash liquid requirement and the position of the thickest underflow in the system.

Case 1: Note from *Table 15.3* that, for the case of the R_f ratios increasing along the train, the wash requirement is high and the system underflow is very dilute because the thickest underflow is in the first stage. As it happens, this case is also very bad for the separation of the solids, as shown previously. Case 1 therefore has to be rejected.

Case 2 of equal flow ratios is clearly good for wash requirement but the thickest underflow is still at the front of the train rather than at the end of it as is required in practice. It could be shown, however, that the point of thickest underflow may be moved to the back end of the train by adding some of the wash liquid with the solids rather than having it all come in at the end of the train.

Case 3 is best from the point of view of solids separation because the separator in the first stage, as the unit responsible for passing solids in the system overflow, operates with dilute underflow, i.e. high separation efficiency. The point of thickest underflow is firmly at the back end of the train and the wash liquid requirement is still low.

The conclusions drawn from the mass balances presented in *Table 15.3* are further discussed in the next section.

15.6 Washing train design recommendations

The countercurrent washing trains installed in industry often represent the most complex parts of the overall processes and are usually designed and

Table 15.3 Three cases of mass balance calculations for liquid flows and solubles mass rates for comparison. Note that all three cases have the same washing efficiency, marked*, and the point of thickest underflow, marked, has moved to the end of the train for case 3**

Case 1 (Worst)	*No. of stages*		*3*			
	Solids feed:					
	Flow rate of wash	(l/s)	0.000			
	Mass rate of solubles	(g/s)	1.000			
	Wash:					
	Flow rate of wash	(l/s)	**3.640** ← **high**			
	Mass rate of solubles	(g/s)	0.000			

Stage no:	R_f		*Input*		*Output*	
			Feed	*Feedback*	*Overflow*	*Underflow*
1.	0.100	Wash	0.000	2.613	2.352	**0.261****
		Solubles	1.000	0.103	0.992	0.110
2.	0.200	Wash	0.261	3.005	2.613	0.653
		Solubles	0.110	0.018	0.103	0.026
3.	0.300	Wash	0.653	3.640	3.005	1.288
		Solubles	0.026	0.000	0.018	**0.008***

Case 2 (Best for wash requirement)	*No. of stages*		*3*			
	Solids feed:					
	Flow rate of wash	(l/s)	0.000			
	Mass rate of solubles	(g/s)	1.000			
	Wash:					
	Flow rate of wash	(l/s)	**1.520** ← **low**			
	Mass rate of solubles	(g/s)	0.000			

Stage No.	R_f		*Input*		*Output*	
			Feed	*Feedback*	*Overflow*	*Underflow*
1.	0.180	Wash	0.000	1.450	1.189	**0.261****
		Solubles	1.000	0.209	0.992	0.218
2.	0.180	Wash	0.261	1.507	1.450	0.318
		Solubles	0.218	0.038	0.209	0.046
3	0.180	Wash	0.318	1.520	1.507	0.331
		Solubles	0.046	0.000	0.038	**0.008***

Case 3: (Best for solids separation) *No. of stages* *3*

Solids feed:
- Flow rate of wash (l/s) 0.000
- Mass rate of solubles (g/s) 1.000

Wash:
- Flow rate of wash (l/s) **2.110** ← **medium**
- Mass rate of solubles (g/s) 0.000

Stage No.	R_f		*Input*		*Output*	
			Feed	*Feedback*	*Overflow*	*Underflow*
1.	0.300	Wash	0.000	2.641	1.849	0.792
		Solubles	1.000	0.417	0.992	0.425
2.	0.160	Wash	0.792	2.352	2.641	0.503
		Solubles	0.425	0.072	0.417	0.079
3.	0.100	Wash	0.503	2.110	2.352	**0.261****
		Solubles	0.079	0.000	0.072	**0.008***

operated at conditions far from optimum. Experimenting with and optimizing such systems is difficult, particularly where there are no inter-stage sumps used and samples of the intermediate streams cannot easily be taken. It is, therefore, advantageous to use a computer model to find out how such systems work and how they respond to operational or design changes.

The following recommendations may be drawn from the mass balance calculations performed on different possible scenarios encountered in industry. Consulting experience with several working systems in industry confirms the conclusions.

15.6.1 Washing efficiency

The washing efficiency of a countercurrent washing train is primarily determined by the values and order of the flow ratios R_f used in the train, and by the number of stages employed. It is not affected by the supply rate of wash liquid, irrespective of whether the liquid comes in with the solids or through the wash liquid feed at the end of the train. The wash liquid supply only determines the dilution of the solids in the underflows in the different stages and overall.

15.6.2 Wash liquid requirement

The wash liquid requirement of an existing washing train designed for a given washing efficiency and maximum underflow solids concentration anywhere in the train is also determined by the values and order of the flow ratios R_f and by the number of stages employed. Fewer stages require lower R_f ratios and greater wash liquid supplies if they are to achieve the same washing efficiency and are to operate at the same maximum underflow solids concentration.

15.6.3 Setting of the flow ratios

It is clear from equation 15.2 that the washing efficiency is maximized by minimizing the flow ratios in all stages. The solubles/wash system cannot, however, be considered in isolation. The transport of the solids along the washing train and the solids separation efficiencies in the individual stages and overall also have to be taken into account. The problem is, therefore, one of optimization of a three-component separation system.

In order to be able to optimize the system, we have to know how the flow ratio affects the separation of the solids. In the case of hydrocyclones, the effect of the ratio is two-fold: increasing R_f leads to improvements to separation efficiency through the contribution of 'dead flux' and a further improvement is caused by the reduction in the crowding of the underflow orifice. Both of the effects can be described analytically for certain hydrocyclone geometries and the above-mentioned optimization is therefore possible, using the entropy index[16] as a general criterion for the optimization.

Often, the flow ratios are set the same in all stages either because the solids are easy to separate (and hence there is no reason for them to be set different) or for some engineering reasons such as in the case study reported in ref. 15. If neither is the case and they can be varied along the train, the following general conclusions may be drawn:

The best design of a countercurrent washing train using most separators, particularly hydrocyclones, is such that the flow ratios decrease along the train, so that:

1 the overall solids recovery is high,
2 the solids concentration is always highest at the end of the train (i.e. in the system underflow),

3 the solute concentration in system overflow is high,
4 the wash liquid requirement is low.

The actual design depends on how sensitive are the grade efficiency curves of the individual stages to the changes in the flow ratios. The overall grade efficiency of the train G, which determines the amount of the solids lost in the system overflow, may be calculated from the individual efficiencies of the stages G_i as for a series connection on underflow with overflow recycle, as shown in detail in section 15.4.1.

15.6.4 Mass transfer from the solids

The mass balance calculations outlined in section 15.5 assume that the mass transfer of the solubles from the solids into the suspending liquid is complete. This is reasonably true if the solids are non-porous and if enough time and shear are provided in the pipework, in the separator or in its feed sump for the mass transfer to take place before the solids leave the unit with the underflow.

Mass balance calculations are further complicated if the above assumptions are not true, such as with porous materials or if the mixing sumps are not large enough to accommodate the mass transfer. The net result, as shown in the case study in ref. 15, is that the liquid in the pores of individual particles has more solubles than the surrounding liquid. This affects not only the mass balances but also the analyses of the samples taken from a working washing train.

Note that additional contact time and shear for better mass transfer may be 'engineered' into the system (if a larger feed sump for some reason is not an available option) by using the stop–start method. The otherwise continuous system connected normally in a countercurrent mode is interrupted and, using a suitable system of valving, the individual stages are isolated whilst the pumps are still going. In each stage both separator outputs are recycled into the feed sump so that the suspension is pumped around between the sump and the separator whilst intensive mass transfer takes place between the solids and the liquid. This goes on for a pre-set time after which the system switches back to normal, countercurrent connections. Countercurrent washing can also be combined with solvent extraction using this method.

15.6.5 The sequence of decisions for the design of a countercurrent washing train

1 Choose each stage cut size to be well below the minimum size of the feed solids to be washed.
2 Establish the R_f ratio at which each stage should operate. If the solids are fine and difficult to separate, use higher R_f ratios at the front of the train and decrease them along the train, with the minimum at the end.
3 Establish solids concentration and solubles concentration in the feed.

4 Design the separators to achieve the above cut sizes.
5 Determine whether a sump is needed in each stage and, if yes, what volume.
6 Establish solubles concentration in wash liquid.
7 Determine the number of stages to obtain the required washing efficiency.
8 Establish wash-water requirement from volumetric balance calculations and make sure that each underflow has enough liquid to carry the solids, with the highest solids concentration at the end of the train!
9 Determine the number of separators needed in parallel in each stage, according to the liquid flow rates calculated.

15.7 Applications, case studies

15.7.1 Starch washing

Countercurrent separator systems can be found in many diverse industries. One example is in the production of potato, corn or wheat starch. Here, washing usually means removal of one solid from another, i.e. gluten from starch. The gluten has to be sheared off the starch particles and hydrocyclones are ideally suited to this duty. The density of the solids is low, however, (around 1500 kg/m^3) and this combined with low particle size necessitates the use of small diameter (10 mm) cyclones in parallel arrangements. The number of stages used is often high (eight or nine, up to 24 in extreme cases).

Figure 15.16 gives a typical nine-stage wheat starch washing system, which normally has to employ an additional separator (or a series) on the system overflow. Its function is to return the finest starch fractions present in wheat (down to 3 microns or so) which the first washing stage is not capable of separating efficiently. A sedimenting centrifuge is sometimes used in this role but a three-stage overflow series of small diameter hydrocyclones may also be used. A well-designed arrangement with the recycles usually plumbed in (i.e. no intermediate sumps) is capable of excellent washing efficiency coupled with minimum solids losses to overflow and good thickening to 23 to 24 Baumé (this is a slurry density measurement using hydrometers; 24 Baumé corresponds to about 40% by volume for starch).

One consulting visit to a wheat processing plant revealed an arrangement similar to that in *Figure 15.17*. The washing train set up by the manufacturer failed to produce the thickening performance expected and only 17 Baumé was achieved no matter how much the wash liquid supply was reduced. As a desperate remedy, the user installed an additional three-stage hydrocyclone thickening series on the system underflow as shown in *Figure 15.17* that then produced the desired underflow density of 24 Baumé.

This extra thickening arrangement should not have been required if the washing train was set up properly. The problem was that the minimum liquid flow to carry the solids down the train was somewhere within the train and not

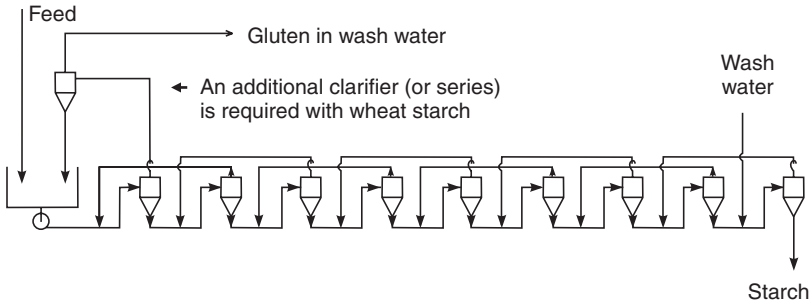

Figure 15.16 A line diagram of a typical starch washing plant

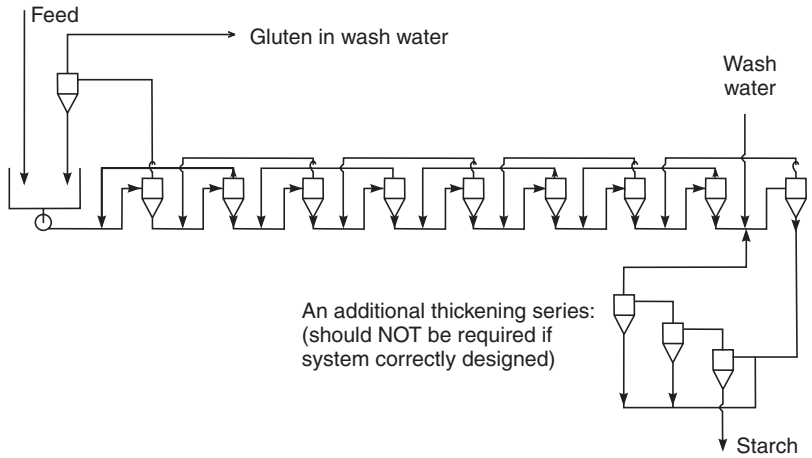

Figure 15.17 A line diagram showing an additional thickening series from the starch washing case study

at the end of it. Attempts to starve the system of wash liquid failed because this simply reduced liquid flows everywhere in proportion and it did not move the bottleneck but merely increased starch losses to overflow. Analysis of the system function with mass balance simulator software revealed a simple remedy: more liquid added to the solids at the front of the train moved the point of thickest underflow to the end of the train. A corresponding reduction in wash liquid addition then brought the system underflow to the desired concentration level, thereby obviating the need for the additional thickening series.

15.7.2 Hydrogel washing

Removal of solubles from the feed solids is achieved using washing arrangements sometimes known as countercurrent decantation. This may be used

either when the solids represent the product, like gypsum in the phosphoric acid process, or when the solvent is the product, like the leaching residues (leached uranium, copper, etc.[17,18]). Hydrocyclones here compete strongly with the conventional means of decantation in gravity thickeners but offer lower installed costs and greater ease of control.

Reference 15 gives a case study of a pilot test series to wash solubles off a solid product (silica gel), illustrating the problems in testing such a system and the complexity of countercurrent washing arrangements in general. Only a summary of the most important aspects is given below.

Silica hydrogel has a porous structure containing water, which can normally only be removed from the pores by drying. In the manufacture of the hydrogel, an intermediate material is produced which contains large amounts of electrolyte and this has to be removed by washing. The electrolyte is contained in an aqueous solution in the hydrogel pores. The composition of the hydrogel feed to the washing system is (weight %):

18% SiO_2
12% Na_2SO_4
3% H_2SO_4
67% H_2O

The test washing plant was based on three hydrocyclone stages (four units were used in some experiments) connected in series for countercurrent washing as depicted in *Figure 15.1*. The train was constructed from commercially available portable test rigs with suitable modifications to the pipework. The majority of the wash water was added to the last stage, but additional water was added to the first unit so that the flows could be balanced under the operating conditions used.

All the experiments were based on single 2 inch nominal diameter (i.d. 44 mm), narrow cone angle hydrocyclones using 14 mm diameter vortex finders (overflow orifice) and either 8 mm or 6 mm diameter spigots (underflow orifice). In order to simplify the installation and operation of the washing train, the hydrocyclone in each stage was operated under the same conditions, e.g. the same pressure drop (50 psig = 3.4 bar) across the hydrocyclone.

The mass flow rates of the individual streams were measured by the 'bucket-and-stopwatch' method. The solids concentrations of the hydrogel slurries were determined by filtering a known quantity and dewatering the cake as much as possible by air displacement, followed by drying. The flow ratios were nearly constant in all the stages for a particular experiment.

The total solids recovery (total efficiency) in the different stages was evaluated and reported in ref. 15. The mass balances were checked by using the individual total efficiencies to predict the overall solids recovery of the train. For the experiment No. 3881/68 (listed in *Table 15.4*) for example, the predicted overall system recovery of 83.4% was in good agreement with the measured value of 81.7%.

The ultimate test of the comparison between the measurements and the computer predictions is the washing efficiency, i.e. the solute concentration (measured as ppm Na_2O) in the system underflow.

Table 15.4. Comparison of measured and predicted Na_2O concentration in product underflow (filtrate)

Experiment No.	*3881/68*	*3881/15*	*4357/20*	*1950/64*	*G69/2*	*G610/70*
measured ppm	770	1515	1978	445	175	135
predicted ppm	884	1475	1330	444	110	230

Table 15.4 shows that there is good agreement between the predicted and experimental values from the hydrocyclone system. Therefore, a computer model is very useful in mapping out the operating conditions required to give a particular product and in assessing the likely effect of the changes to the system on the washing efficiency.

Problems involved in collecting and interpreting data

Several aspects of this case study are worth mentioning because they highlight some of the difficulties involved in acquiring and interpreting data on the complex washing train.

1 Flow rate measurement. It is difficult to make accurate flow measurements in a complex system such as a washing train of this type, since the flow rates are large (up to 1 litre per second) and the system can be easily disturbed from its steady state condition. The best technique was found to be the bucket-and-stopwatch method, and to average the results of two to three measurements. The sampling time for the overflow streams was usually less than 10 seconds and so large errors can arise if care is not taken.
   Measurement on intermediate streams causes a disturbance to the system and a choice then has to be made as to whether to allow the system to settle down again or continue taking measurements and samples. The former option can take in excess of 30 minutes to make a full set of measurements and in that time the steady state position could have shifted, e.g. a change in the hydrogel feed rate to the system. The latter option took only 5 minutes and was deemed the most suitable of the two methods. All data in this study were obtained by this route.
2 The washing model assumes that equilibrium is achieved in each stage between the solute level in the hydrogel and the wash liquor. This is also the objective in the real system so as to ensure efficient washing, and the operating conditions, e.g. solids particle size, wash liquor temperature, residence time, etc., are chosen to achieve as closely as possible, within

the constraints of a viable commercial process, a system at equilibrium. If perfect mixing is achieved in the sumps and the residence time is long enough for equilibrium then the solute concentration in the filtrate from the underflow and overflow streams of any stage should be identical. Any imbalance will nearly always result in higher concentrations of solute in the underflow stream since this has a higher solids concentration. This effect can be seen in the data[15]. However, the agreement between experimental and predicted washing efficiencies suggests that some imbalance can be tolerated, provided it does not become too large.

3 If mass transfer at any stage is incomplete, the results of the analyses of the samples (especially if there is a delay in carrying out the analyses) may not reflect the exact conditions in the system at the time of sampling. In general, it is not possible to carry out immediate analysis of the samples and since any imbalance will quickly be corrected after the sample has been taken, this error cannot be easily eliminated. It is worth noting that a typical experiment on such a system where several sets of samples might be taken can result in 30 to 40 filtrations and drying tests and from 60 to 80 chemical analyses being carried out.

4 In porous systems and where the analysis of the solid is based on the total sample weight, the measured solute level will be lower in the solid than the wash liquor associated with it in the slurry. For the silica hydrogel system, which is initially 82% liquid and 18% SiO_2, the concentration of soda in the hydrogel system will be lower by a factor of 0.82. Inspection of the data in ref. 15 reveals that this is indeed approximately the case with the measured values. The effect is complicated by the fact that as solute is removed this factor (on a weight basis) changes and that the silica structure can shrink with time reducing the pore volume of the hydrogel.

As can be seen from the above study, the comparison between predicted and actual results is quite good considering the difficulties in obtaining accurate data and the assumptions made in the mass balance calculations. In the real system, the solids that are lost to the system overflow take away some solubles and this may reduce the concentration in the system underflow a little (although the predicted values do not appear to be consistently higher or lower than the measured values).

Figure 15.18 gives a summary of one experiment from this study that demonstrates well the capability of the arrangement in this application. The required near-complete separation of solids in the 44 mm hydrocyclones used was not a problem and therefore no additional separator on system overflow was needed in this case. Furthermore, all three stages could be set to have the same split ratios R_f of 26% (underflow to feed). The washing efficiency was about 97% but intermediate sumps had to be provided for mass transfer from within the porous solids to take place.

It should be noted that the wash liquid added did not have to be completely free of soda, and its flow rate was set only to give sufficient liquid flow in all

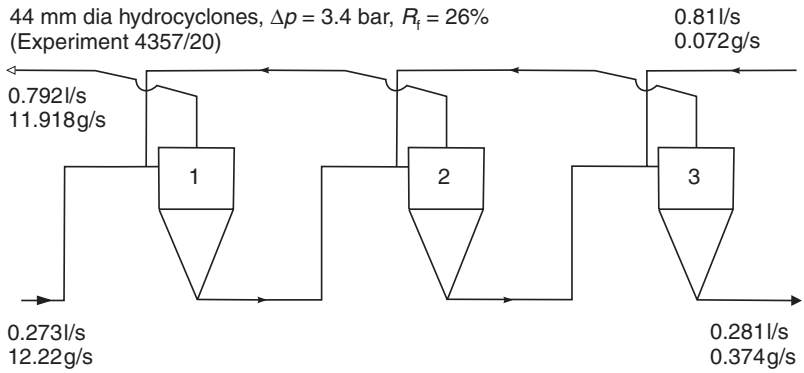

Figure 15.18 Overall balance of solubles (values in g/s) and volumetric flows (values in l/s) for Experiment 4357/20 of the hydrogel washing study[9]

underflows, i.e. about the same as in the feed (0.273 l/s). A closer examination reveals that the wash liquid feed could have been further reduced slightly, to 0.777 l/s to give precisely 0.273 l/s in the system underflow. It can be shown that if the flow ratios are the same in all stages, the underflow rates in all stages will be same if the ratio of wash feed to liquid flow in the system feed is equal to $(1 - R_f)/R_f$.

Overall, it was concluded[15] that even in this case of highly porous solids, good agreement between predicted and actual experimental data was achieved. The study highlighted the difficulties with taking representative samples and making meaningful measurements. Following the experimental study, the company has since utilized the system successfully on a commercial scale.

15.7.3 Countercurrent decantation with gravity thickeners

When sedimentation is to be used for the separation stage in countercurrent washing, gravity thickeners are an obvious choice. The largest user worldwide of this system is probably the Bayer process for alumina. The process has two outlets: the white end and the red end. The white end is the product aluminium oxide and the red end is the red mud, i.e. the insoluble residue (coloured by the high iron content) left from the caustic digestion of bauxite in the Bayer process. Both of these solids outlets involve a great deal of washing in order to remove the caustic from the solids before they leave the plant. In the white end, the washing cleans the product and in the red end, it cleans the waste material before its discharge into the environment. In both cases, the washing recovers a valuable solute (caustic) which, after the necessary concentration, is reused in the process.

The white material, the product oxide, is relatively coarse and easily washed by cake washing, by displacement, immediately after the final

vacuum filtration stage whilst still on the filter (this may be a horizontal rotating pan filter, for example). The red mud is somewhat finer but flocculated. The slurry has a high caustic concentration and to prevent scaling problems, the washing has to be done at high, close-to-boiling temperatures. A multi-stage (from four to nine stages) countercurrent washing with gravity thickeners is usually used. Theoretically, the material is coarse enough for filtration but that is virtually impossible due to the scaling problems, except perhaps for the last stage where the caustic concentration is already acceptably low. The result is a set of huge thickeners, which in the case of aughinish alumina are built above ground and have to be lagged to conserve the heat.

Clearly, great savings can be had if the number of stages needed for the required washing efficiency is reduced. As shown in section 15.6 practically the only way of doing this is to reduce the flow ratio in some or all of the

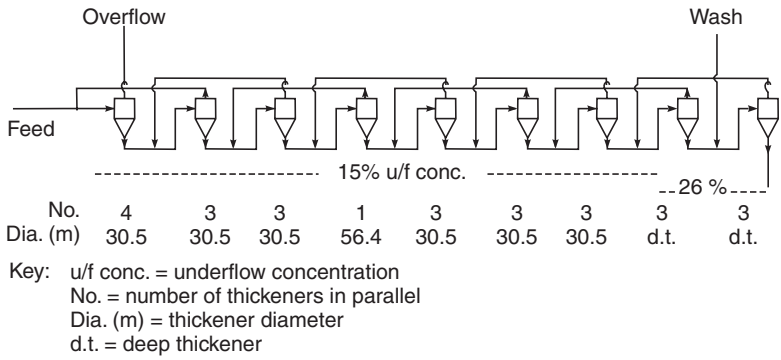

Figure 15.19 A schematic diagram of a nine-stage countercurrent decantation with gravity thickeners[19]

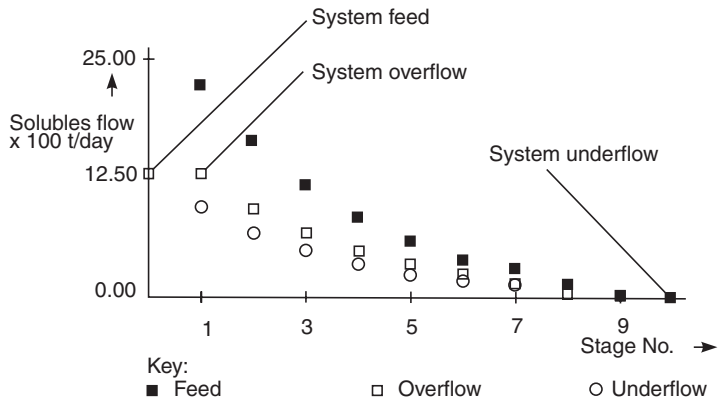

Figure 15.20 Solubles mass flow rates in the washing train of *Figure 15.19*[19]

stages. Probably the best known investigator in this field is Chandler[19] who experimented with using rakeless deep thickeners which, due to their better compression of solids before discharge, can run at flow ratios R_f significantly lower than in conventional thickeners. This led not only to a lower number of stages necessary for a given washing efficiency but also to smaller units for the same capacity: four deep bed vessels could be fitted into the space occupied by one conventional unit[19]. Chandler recognized the relative unimportance of the overflow clarity (except for the first stage) in comparison with the dewatering ability of each stage (i.e. low R_f ratio), in achieving high washing efficiencies.

Figure 15.19 shows a schematic diagram of Chandler's nine-stage system in Jamaica[19] which is a classical countercurrent arrangement with the first seven stages having conventional thickeners and the last two, deep thickeners, achieving much higher underflow concentrations. Chandler had correctly placed these low R_f ratio units at the back end of the washing train.

Solubles flows shown against stage numbers in *Figure 15.20* show the expected decline along the train, with a clear discontinuity where the last two, deep vessel, thickeners take over. Practically all the caustic entering the train leaves in system overflow and, as is one of the great advantages of countercurrent washing, at a concentration much higher than would be possible if the washing was co-current (thus requiring much less evaporation to bring it up to the concentrations needed in the process).

15.7.4 Countercurrent washing of filter cakes

There are a great number of academic papers in the literature concerned with a study of countercurrent cake, reslurry washing systems where each stage is a separate filter. The whole thing was started by Fitch in the early 1960s[14], who laid down the principle and the basic theory. It is, however, very expensive to use a multitude of filters, each with its own separate accessories such as pumps, receivers, pipework and valving. The only exception is the possibility of using a single vacuum disc filter[21] if individual discs (or bunches of discs) are equipped with separate troughs, cake discharge chutes, filtrate receivers and also separate feed pipes. Multi-stage countercurrent, reslurry washing can thus be carried out in one filter.

The cake can, however, be washed *in situ*, without the need for reslurrying and repeated filtration. Instead, a whole washing train of, say, three stages can be placed on just one horizontal vacuum belt filter (or two stages on a high-duty vacuum drum filter[20]).

Pierson in chapter 17 of this book (*Figure 17.12*) gives an example of a test of countercurrent washing on a single belt filter and claims it possible on other horizontal vacuum filters such as the rotary tipping pan. *Figure 15.21* shows the system schematically. Essentially this is the same as *Figure 15.1* except that the three stages are now three subsequent parts of the cake surface. At the far end of the belt (third stage), the fresh wash liquid is sprayed or

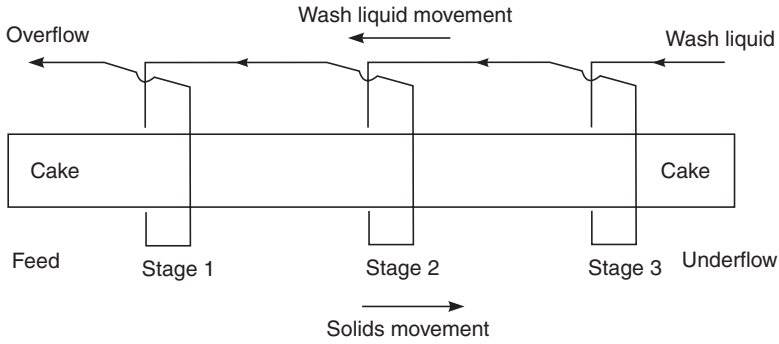

Figure 15.21 A schematic diagram of countercurrent washing of cake on a horizontal vacuum belt filter

flooded onto the belt and the filtrate is collected from under that area, to be fed backwards and sprayed onto the immediately previous cake surface (stage 2), whilst its own filtrate is fed onto the first stage. The filtrate collected from under the first stage represents the system overflow, i.e. the wash effluent.

Pierson's small-scale test in *Figure 17.12* was first published in the first edition in 1977 but since then a feed control system has been developed to enable forming of constant cake thickness irrespective of the speed with which the belt travels. This linked together with monitoring of the strength of the mother liquor and that of the system overflow (final wash liquor) (usually by conductivity measurements) allows the process to be practised on a large-scale filter[20]. This system has a great potential of further development and application because the equipment is not overly expensive, yet by combining cake washing with countercurrent washing it has a potential of really low wash water use.

15.8 Conclusions

The use of countercurrent washing is spreading in many areas of chemical, mineral and food processing. Very little is known, however, about the optimum operating conditions and design of such washing trains, and many installations can be much improved if some basic rules and recommendations are followed.

The chapter evaluates the process of countercurrent washing from the point of view of washing efficiency, wash liquid requirement and separation of the solids. It also lays down the basic rules for the best operation and design of such systems. Computer models are used to carry out the mass balances and to illustrate the performance of different systems under different operating conditions. Some examples of applications are also given.

15.9 Appendix—Leaf testing for countercurrent washing of filter cakes[2]

Laboratory leaf testing for obtaining data for countercurrent washing of cakes on vacuum filters is more involved than a standard leaf test and requires additional equipment. For each stage in the proposed countercurrent washing system, a separate leaf apparatus is required (i.e. two stages will require two leaves, three stages require three leaves, etc.).

Standard leaf testing should be done before attempting the countercurrent washing steps, to determine the proper cloth, slurry volume, vacuum levels, wash volume and final dewatering time.

Figure App. 15.1 illustrates the steps required to accomplish a three-stage countercurrent wash in a laboratory test. It is easiest to understand the principle behind this test by visualizing a continuous horizontal vacuum belt filter in operation (an indexing type is referred to here but the same applies to the models with continuous belt movement). The slurry enters the feed zone and the cake is formed (Step 1). The cloth indexes (follow Leaf C in the figure) and the formed cake move into the first wash area (Step 2). Another

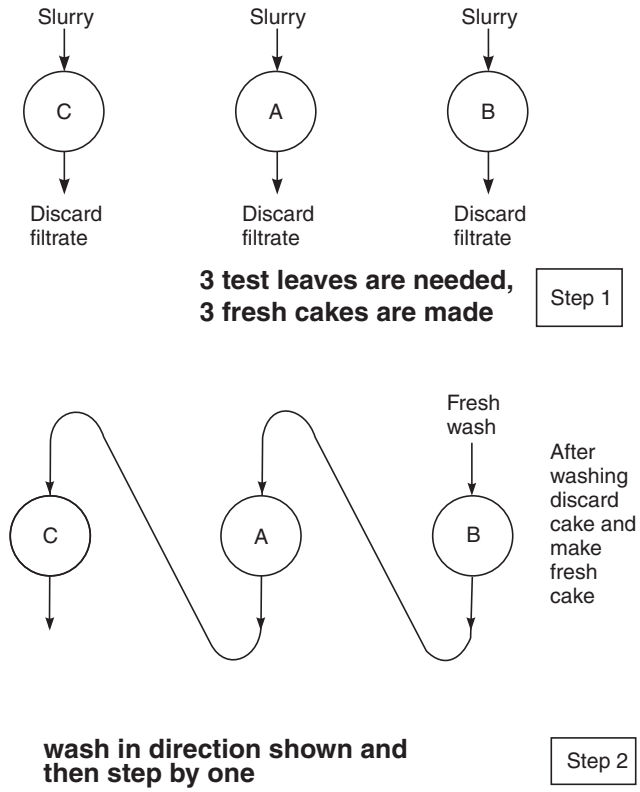

Figure App. 15.1 (*contd.*)

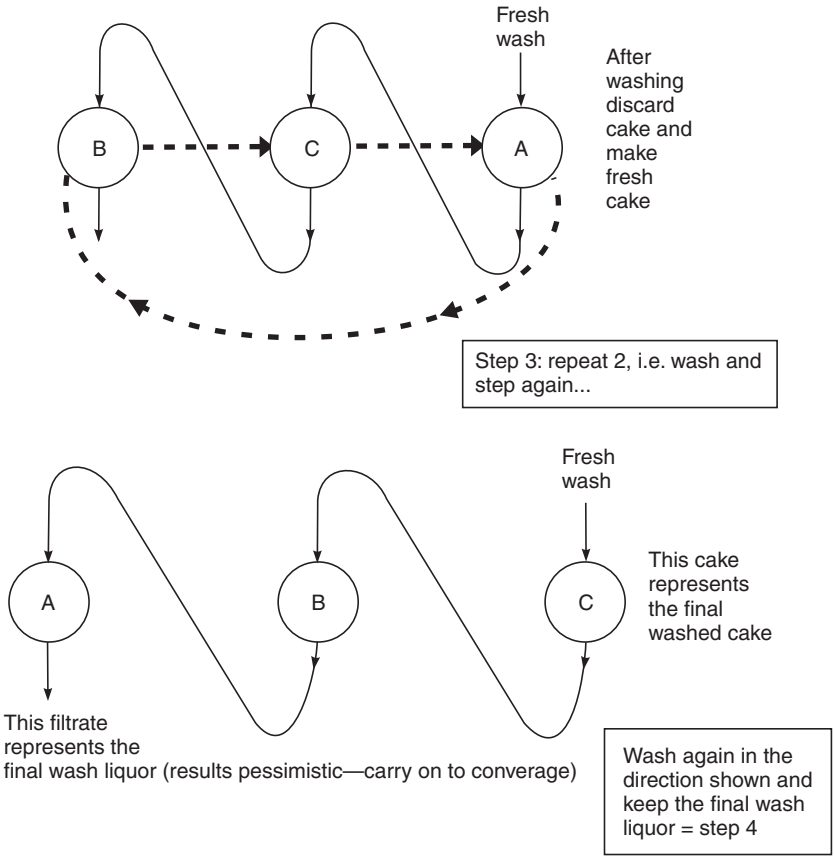

Figure App. 15.1 A schematic diagram of leaf testing for countercurrent washing of filter cakes[2]

index and Leaf C move into the second wash area (Step 3). After the third index Leaf C is washed by the fresh wash liquor prior to final cake dewatering and the final index discharges the cake. If the final wash liquor is required (from Leaf A, Step 4), it is necessary to reform the cake on Leaves A and B after it is discharged so that all washing operations of the filter will be performed during each step.

References

1. White, D. A. and Bashir, S., 'Counter current washing of ion exchange flocs—theory and optimisation', *Solid–Liquid Separation Practice III*, I.Chem.E. Symposium Series No. 113, The Institution of Chemical Engineers, Rugby, 41–50 (1989)
2. K-S ADPEC leaf testing with countercurrent washing, Komline-Sanderson Engineering Corporation, Peapack, New Jersey, published in the Short course manual,

Separation of Solids from Liquids, CfPA, East Brunswick, New Jersey, October 17–20 (1977)
3. Potucek, F. and Milichovsky, M., 'Effect of dilution and thickening on efficiency of pulp washing', Proceedings of the 22nd Conference of the Society of Slovak Chemical Engineers, Vyhne, 30 May–1 June, (1995)
4. Tomiak, A., 'Predicting performance of countercurrent filtration washing systems', *Filtration & Separation*, July/August, 354–360 (1979)
5. Tomiak, A., 'Application of Norden's efficiency factor method for pulp washing calculations
6. Svarovsky, L., 'Counter-Current Washing of Solids', Chapter 15, in *Solid–Liquid Separation*, 3rd edn, Ed. L. Svarovsky, Butterworths, London, 533–540 (1990)
7. Povarov, A. J., Gidrociklony, Gasgortechizdat, Moscow, 1961 (in Russian)
8. Kelsall, D. F., Stewart, P. S. B. and Restarick, C. J., 'A practical multiple cyclone arrangement for improved classification', Paper E5, Proc. First European Conference on Mixing and Centrifugal Separation, Cambridge, 9–11 September 1974, BHRA Fluid Engineering, Cranfield (1974)
9. Svarovsky, L., *Hydrocyclones*, Vol. 1, Holt, Rinehart and Winston, London, (1984)
10. Imre, M. and Holtzwarth, R., 'Simulation of washing with hydrocyclone networks', in *Hydrocyclones '96*, D. Claxton, L. Svarovsky and M. Thew (Eds), Mechanical Engineering Publications Ltd, London, 43–47 (1996)
11. Svarovsky, J. and Svarovsky, L., 'Computer-aided design of hydrocyclone networks', in *Hydrocyclones '96*, D. Claxton, L. Svarovsky and M. Thew (Eds), Mechanical Engineering Publications Ltd. London, 31–41 (1996)
12. 'Computer-Aided Design of Separator Networks, a computer program', *Catalogue of In-Company Short Courses, Books and Particle Technology Software*, Fine Particle Software, The Lares, Maple Avenue, Cooden, Bexhill-on-Sea, TN39 4ST, (2000)
13. 'Counter-Current Washing, a computer program', *Catalogue of In-Company Short Courses, Books and Particle Technology Software*, Fine Particle Software, The Lares, Maple Avenue, Cooden, Bexhill-on-Sea, TN39 4ST, (2000)
14. Fitch, B., 'Countercurrent filtration washing', *Chemical Engineering*, January 22 119–124 (1962)
15. Svarovsky, L. and Potter J. K., 'Counter-current washing with hydrocyclones', Paper J2, 3rd International Conference on Hydrocyclones, Oxford, 30 September to 2 October, 1987, BHRA, Cranfield, 235–247 (1987)
16. Svarovsky, L., 'Thermodynamics of solid–liquid separation', Part II, Chapter 23, in *Solid–Liquid Separation*, 3rd edn, Ed. L. Svarovsky, Butterworths, London, 697–704 (1990)
17. Trawinski, H., 'Counter-current washing of thickened suspensions by repeated dilution and separation by sedimentation', *Verfahrenstechnik*, **8** No. 1, 28–31 (1974)
18. Trawinski, H., 'Counter-current washing of leaching products in thickeners and hydrocyclones, including the mathematical calculation', *Aufbereitungs-Technik*, **18** No. 8, 395–404 (1977)
19. Chandler, J. L., 'Deep thickeners in countercurrent washing', IChemE Symposium on Solids/Liquids Separation Practice, Leeds, 2–5 April, 177–182 (1984)
20. Buttner, R. and Langeloh, T., 'Current trends in filtration, Drum filter design', *The Chemical Engineer*, 9 April, 17–19 (1992)
21. Stahl, W., 'Cost/performance comparisons between disc and drum filters', *Filtration & Separation*, January/February, 38–40 (1978)

16 Separator series and networks

L. Svarovsky

FPS Institute, England and University of Pardubice, Czech Republic

16.1 Introduction

Series connections of separators are a common way of improving the performance of single-stage, one-pass installations. They are used with various types of separators, ranging from gravity or centrifugal separators to filters. For hydrocyclones in particular, due to their low capital and running costs, multiple series arrangements are an obvious choice. As to which particular layout and arrangement should be used very much depends on the actual application and separator in question.

There is a multitude of different arrangements depending on whether the series connection is in the direction of overflow or underflow (i.e. the direction to follow from the first stage) and whether there are any recycles involved. Different applications require different arrangements: sometimes there is a choice between two or more possibilities whilst at other times there is only one and the choice is in the number of stages to be used.

There are five basic reasons for connecting separators into networks. Series arrangements or recycles can be used:

1 to lower the cut size (with the consequence of higher solids recovery and cleaner overflow),
2 to improve thickening (with dilute feeds where a single stage cannot suffice),
3 to improve the sharpness of cut (beyond what a single stage can achieve, in size or density separation),
4 to wash solids in co-current or countercurrent systems,
5 to reduce abrasion (for the same performance, a two-stage system can use lower inlet velocities than a single-stage).

Chapter 9 of ref. 1 gives a comprehensive review of the available systems, with a particular emphasis on two-stage, basic arrangements. Here, the subject is taken much further, mostly to systems comprising three or more

stages. Each section first looks at available systems and analyses their effect on separation generally, and then derives and discusses their specific use.

It is now widely accepted that the best way to analyse the separation performance of dynamic separators such as gravity settling vessels, sedimenting centrifuges or hydrocyclones is by using the grade efficiency curve. Many filters also show a grade efficiency curve but, as this curve usually depends on the amount of solids deposited on the filter, the concept is only useful for rating clean filter media.

The grade efficiency is a kind of 'transfer function' which is derived from the effect the separator has on the particle size distribution of the feed solids as they pass from the feed to the underflow. The curve describes the probability that particles of different sizes have to separate into the underflow. One can derive this curve for an individual separator or for a whole network of them. The evaluation in the following is based on observing how, for given grade efficiencies of the individual stages, any particular arrangement affects the shape and position of the overall grade efficiency of the system.

The shape and position of the grade efficiency curve can be characterized in many ways. Here we concentrate on three characteristics depicted in *Figure 16.1*. These will be mostly assessed visually from graphs although some quantitative comparisons will also be made. The three characteristics are as follows:

1 The position of the actual cut size x_{50}. This has a direct bearing on the overall solids recovery or clarification power of the system. If the cut size reduces, more solids are recovered from the feed into the underflow and the overflow becomes cleaner (and finer).

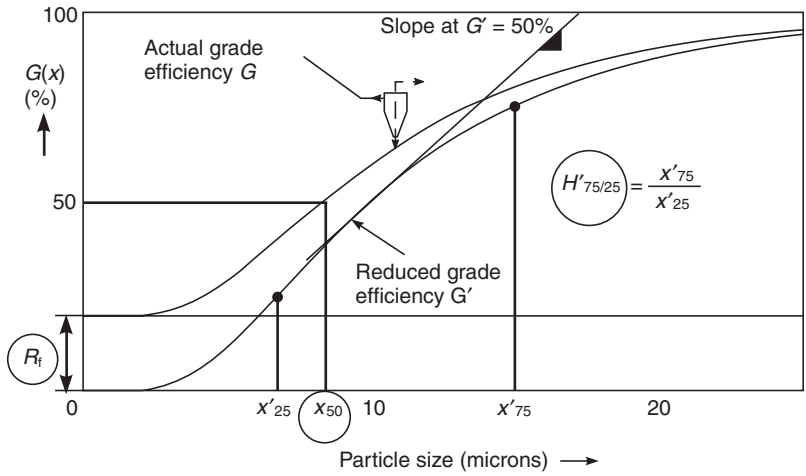

Figure 16.1 Schematic diagram depicting the three criteria used in assessing the separational performance of separators and networks (circled values)

2 The amount of 'underflow by-pass' which is shown as the intercept on the y-axis at $x = 0$. It is the flow ratio R_f and is a measure of the volumetric amount of underflow relative to that of the feed. If a system has a greater R_f than that of any individual stage, its underflow will carry more liquid and the suspension will be more dilute. In addition, more liquid in underflow will mean more of the fine particles brought into the underflow with the liquid. This would be good news in solids recovery applications but disastrous in those classification duties where the coarse product is required to be free of fines. Where the fine product is of interest, its quality is virtually unaffected by R_f—only the yield is.
3 The sharpness of cut as measured by the sharpness index $H'_{75/25}$ derived from the reduced grade efficiency curve (or by $H_{75/25}$ derived from the actual grade efficiency curve). This index is one of the many possible measures of the classification sharpness (see chapter 8) and is defined as a ratio of particle sizes $x'_{75\%}/x'_{25\%}$(or x_{75}/x_{75}). Alternatively, the slope of the reduced grade efficiency curve at x'_{50} is used as another measure of sharpness of cut. A lower value of $H'_{75/25}$ or higher value of the slope will indicate better performance in classification duties. The effect of sharpness of cut on other separation duties such as recovery or thickening is relatively small.

The last point needs explaining a little further. There are two reasons for deriving the sharpness index from the 'reduced' grade efficiency curve rather than from the actual one. Firstly, the sharpness of cut is always to some degree affected by R_f and this way the effect is removed. Secondly, as can be seen later, the sharpness index for the actual grade efficiency curve sometimes cannot have a value because the whole of the curve may be greater than 25% and x_{25} cannot be determined.

The relative merits of the different arrangements will be assessed in the following, largely visually, by comparing curves. *Figure 16.1* is one such plot where efficiency is plotted against particle size. For comparing sharpness of cut, I shall be also plotting reduced grade efficiency versus dimensionless particle size, i.e. x/x'_{50} as in *Figure 16.4*, for example. This forces all curves in that plot through the same point at 50% thus allowing easy visual comparison of the slopes.

16.2 Series connections on overflow

A simple three-stage series arrangement on overflow is shown schematically in *Figure 16.2*.

This system may or may not use intermediate pumps. If it does not, the additional back pressure on the overflows of stages 1 and 2 has to be compensated for by throttling the underflow orifices of these stages. Otherwise, the underflow rates would be much greater than for the same cyclones operated under balanced conditions.

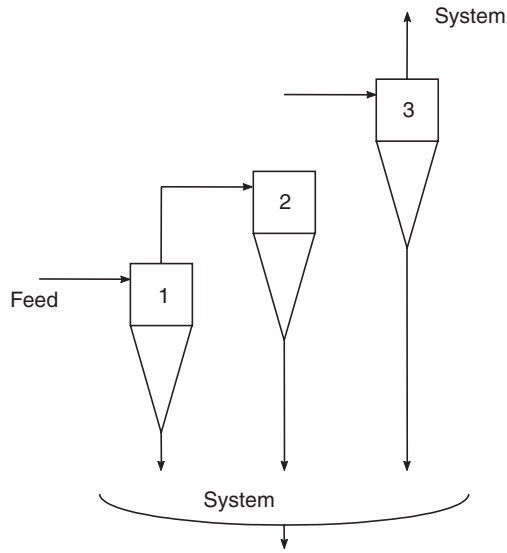

Figure 16.2 A simple three-stage series arrangement on overflow

If, for the sake of an illustrative example, we assume that all stages have identical grade efficiency curves and R_f ratios as shown in *Figure 16.1*, then the system grade efficiencies for two-stage and three-stage arrangements would be as shown in *Figure 16.3*. The figure also shows, for comparison, the grade efficiency curve of a single stage from which the two others were computed using the following formula (given for a three-stage system):

$$G(x) = G_1 + G_2 + G_3 - G_1G_2 - G_2G_3 - G_1G_3 + G_1G_2G_3 \qquad (16.1)$$

where G_i is the grade efficiency of stage i for $i = 1$ to 3 and $G(x)$ is the grade efficiency of the whole arrangement.

This equation is derived using mass balances, from total mass recoveries in the first instance. An analogous expression must then also apply to grade efficiencies—see section 16.5.1 for an example of the derivation.

Figure 16.3 clearly shows that the simple overflow series reduces the cut size. It does so by repeating the separation process and separating a little more every time. It is good practice to 'tighten up' on the separation along the series train, by reducing the stage cut size gradually. Some contribution to the cut size reduction, in our example in *Figure 16.3*, is also due to each stage removing another lot of liquid into the underflow and a corresponding proportion of fines with it.

The question is how much is the cut size of the system actually reduced. The reduction in the cut size of the whole arrangement, as opposed to that of the first (single) stage, is simply a function of the number of stages. If the cut size in each stage is the same, the flow ratio is low, i.e. $R_f \rightarrow 0$ (which is often

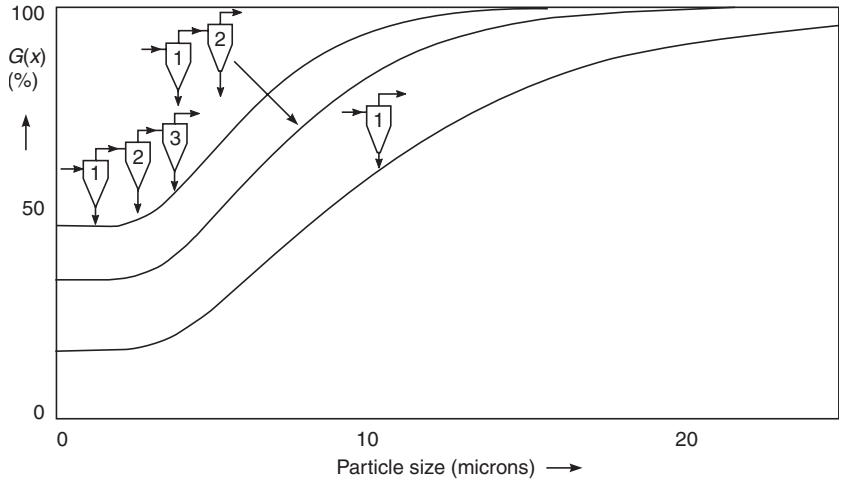

Figure 16.3 The grade efficiency curves of single-stage, two-stage and three-stage series on overflow

the case in clarification duties) and the geometric standard deviation (i.e. the steepness) of the grade efficiency curve is 1.8 (a typical value for hydrocyclones), then the rate of decrease in cut size with the number of stages is as follows. Note that for non-zero R_f values the reductions would be greater.

Table 16.1 The reduction in cut size with the number of stages in an overflow series

No. of stages	*1*	*2*	*3*	*4*	*5*	*6*
System cut size, relative to one stage	1	0.73	0.62	0.56	0.52	0.49

As can be seen from *Table 16.1*, there is a law of diminishing returns at play here: it does not make much sense to use more than, say, three stages of identical cut size in each stage in series because the further stages would separate very little indeed. The usual way to tackle this is to gradually tighten up on the cut size in the direction of the flow either by some design changes in the geometry used or by changes in the operating conditions (e.g. increasing the pressure drop in each stage).

It is also obvious from *Figure 16.3* that if flow ratio R_f is the same in all stages, the overall R_f is much greater. In other words, if unchecked, the overflow series will produce very dilute underflows. Technically, it is of course possible to limit this effect by reducing R_f along the train, as less

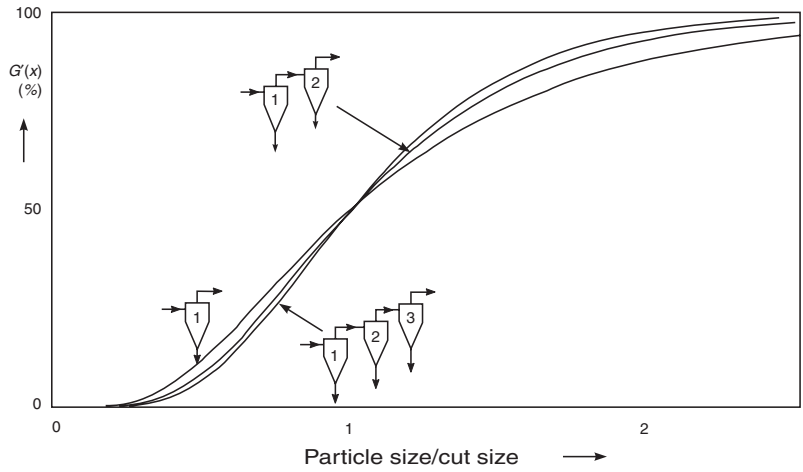

Figure 16.4 The reduced grade efficiency curves of single-stage, two-stage and three-stage series on overflow, plotted against dimensionless particle size

and less solids are separated in further stages (and correspondingly less and less liquid is needed in each underflow).

What happens to the sharpness of cut is not very clear from *Figure 16.3*. For that, it is better to plot the reduced grade efficiency $G'(x)$ in which the effect of flow splitting (R_f ratio) is removed (see equation 2.8 in ref. 1), and plot this against dimensionless particle size, *Figure 16.4*. As the curves steepen from the single-stage arrangement to the three-stage one, it is clear that the simple overflow series sharpens classification. This is mainly beneficial if the fine product is of main interest because the greater amounts of liquid passed into the underflow by this arrangement pollute the coarse product with fine particles. A further discussion of this may be found in section 16.3 where simple series on overflow and underflow are compared.

The question is how much is the sharpness of cut of the system actually improved. The increase in the sharpness of cut of the whole arrangement, as opposed to that of the first (single) stage, is clearly a function of the number of stages. If the cut size in each stage is the same, the flow ratio is low (or zero if we deal with the reduced grade efficiency $G'(x)$) and the geometric standard deviation of $G'(x)$ is 1.8 (a typical value for hydrocyclones), then the approximate increase in the sharpness of cut with the number of stages is as shown in *Table 16.2* follows (consult *Figure 16.1* for the definitions of sharpness of cut).

In summary, the simple overflow series may be used to reclassify the fine product or to lower the cut size of the system. Its main applications are, therefore, classification of solids, clarification of liquids and recovery of solids. The main disadvantage is in that it increases the R_f ratio: the system value is always greater than that of any one stage in it.

Table 16.2 Sharpness of cut improvement with number of stages, in a series arrangement on overflow

No. of stages	*1*	*2*	*3*	*4*	*5*	*6*
Dimensionless slope of $G'(x)$ at x_{50}	0.67	0.86	0.93	0.98	1.02	1.05
$H'_{75/25}$ relative to the value at $N = 1$	1	0.87	0.82	0.78	0.76	0.75

16.2.1 Overflow series with partial overflow recycle

A partial overflow recycle can be added to the overflow series arrangement as a means of lowering the cut size further. A possibility exists to do this in a multi-stage series but I have only seen it in practice applied to a single-stage system as shown in *Figure 16.5*. This is quite common in some clarification duties such as cleaning of metalworking coolants.

Hydrocyclones are particularly well suited for this arrangement. Not only the recycle reduces the cut size through the hydrocyclone being in series with itself, so to speak, but as an additional benefit it dilutes the feed for the cyclone and this also improves the cyclone efficiency. However, how much is the cut size of the system reduced? Equation 16.2 relates system $G(x)$ to the grade efficiency of the cyclone and the relative flows Q and q (meaning as per *Figure 16.5*), for negligible R_f of the cyclone (such as for a hydrocyclone operated with a grit pot).

$$G(x) = \frac{G_1}{G_1 + (1 - G_1)\frac{q}{Q}} \tag{16.2}$$

To illustrate the effect, *Figure 16.6* plots the grade efficiency curves for three values of Q/q.

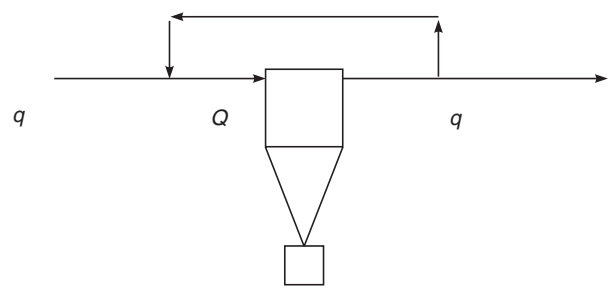

Figure 16.5 A schematic diagram of partial overflow recycle in a one-stage system (sometimes called multiple pass arrangement). The cyclone is shown to be installed with a grit pot (no underflow)

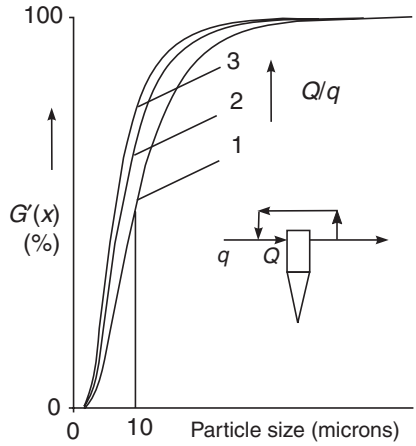

Figure 16.6 The grade efficiency curves for three values of Q/q in a multiple pass system ($R_f = 0$)

The reduction in the cut size of the whole arrangement, as opposed to that of the single-pass arrangement, is clearly a function of the recycle ratio Q/q: if the cut size of the hydrocyclone remains the same (i.e. greater recycle ratios are matched by a greater number of identical cyclones in parallel), the flow ratio R_f is low (which is often the case in clarification duties) and the geometric standard deviation (i.e. the steepness) of the grade efficiency curve is 1.8 (a typical value for hydrocyclones), then the rate of decrease in cut size with the recycle ratio Q/q is as shown in *Table 16.3*.

There is a law of diminishing returns at play here: it does not make much sense to use Q/q of more than, say, three or four: see section 16.5.2 for a further study of this.

A word of caution is appropriate regarding the use of overflow recycles in particle separation applications. As Zeitsch has shown in a whole chapter devoted to this problem[2], there is a real danger that fines may accumulate in the recycle and eventually plug the whole system. This is because the recycled stream contains material appreciably finer than the system feed and the separator may not be able to remove the extra fines at a sufficient rate. Fortunately, in case of hydrocyclones this potential problem is alleviated

Table 16.3 Reduction in cut size with recycle ratio in multiple pass systems

Ratio Q/q	*1*	*2*	*3*	*4*	*5*	*6*
System cut size relative to the value at $Q/q = 1$	1	0.78	0.67	0.61	0.57	0.53

because their cut size reduces for feeds that are more dilute. Thus the inevitable dilution of the feed with the recycle stream lowers the cut size and this improves the separation of all sizes including the fines. Careful mass balance calculations to check this potential problem are still recommended.

A closer inspection of Example 1 in section 16.5.2 reveals that the system R_f ratio increases with the recycle (if a hydrocyclone with continuous underflow is used). In fact, this increase had to be compensated in the example by a corresponding reduction in the cyclone R_f so that the system value was to remain at 10%.

As to the sharpness of cut, the multiple pass system does improve it a little (see *Table 16.4*) but nowhere near as well as a simple overflow system—compare with *Table 16.2*.

Table 16.4 Reduction in sharpness index $H_{75/25}$ with recycle ratio in multiple pass systems (for cyclone $R_f = 0$)

Ratio Q/q	*1*	*2*	*3*	*4*	*5*	*6*
$H_{75/25}$ relative to the value at $Q/q = 1$	1	0.98	0.96	0.94	0.92	0.91

How do the two clarification systems (a simple overflow series and a multiple pass system) compare? The recycle ratio Q/q is directly comparable with the number of separators N in the overflow series but here it can represent the number of parallel separators. As the pumping energy is equivalent between the two alternative systems, direct comparison of the above two tables (*Tables 16.1* and *16.3*) is possible. As can be seen, the multiple pass system reduces the system cut size less than the simple series arrangement. This is because, unlike in the series arrangement, not the entire overflow in the multiple pass system is subjected to further separation. The series arrangement is therefore better but the overall R_f flow ratio is increased less in the multiple pass system.

16.2.2 Overflow series with underflow recycles

Underflow recycles in conjunction with the overflow series are quite common in practice. However, the recycles are full, not partial, as was the case in the previous section. With three stages, there is a choice of where the recycles are returned to, as shown in *Figure 16.7*.

The equations for the system grade efficiencies in *Figure 16.7* are given below. *Figure 16.8* shows these graphically, for our standard case of the geometric standard deviation of $G'(x)$ equal to 1.8 (a typical value for hydrocyclones), and R_f and x'_{50} of each stage equal to 20% and 10 microns respectively.

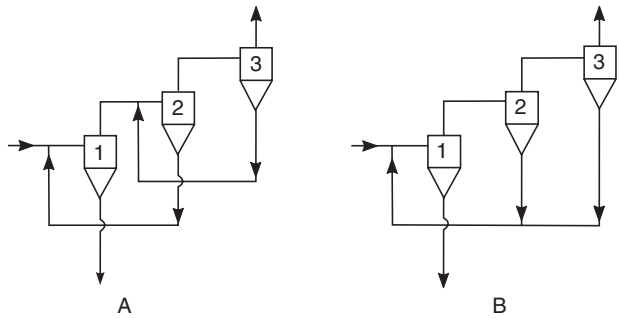

Figure 16.7 The choice of underflow recycles in a three-stage series on overflow: A, the recycles return into the feeds of the immediately preceding stages; B, both recycles return to the feed of stage 1

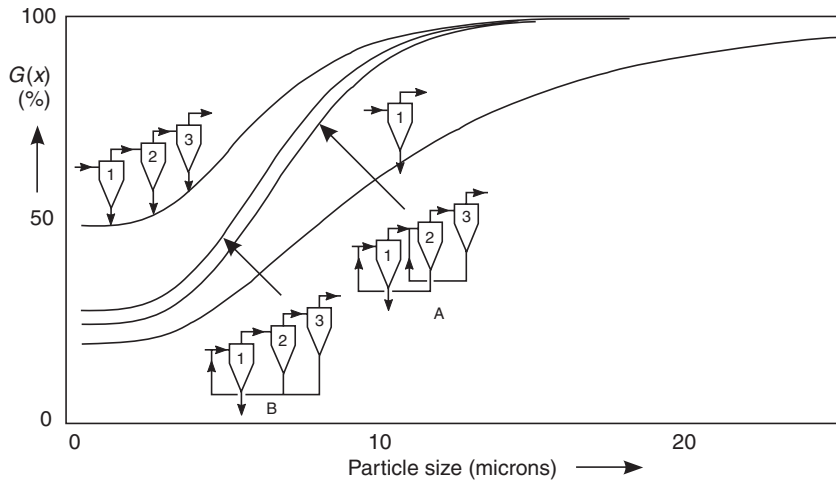

Figure 16.8 A graph depicting the grade efficiencies for the two cases A and B together with a simple three-stage overflow series. The curve for a single separator used in the arrangements is also shown

For case B: overflow series with underflow recycles from 2 and 3 back to feed 1:

$$G(x) = \frac{G_1}{1 - G_2 - G_3 + G_1G_2 + G_1G_3 + G_2G_3 - G_1G_2G_3} \tag{16.3}$$

For case A: overflow series with underflow recycles from 2 to feed 1 and from 3 to feed 2:

$$G(x) = \frac{G_1 - G_1G_3 + G_1G_2G_3}{1 - G_2 - G_3 + G_1G_2 + G_2G_3} \tag{16.4}$$

Closer inspection of *Figure 16.8* reveals that the underflow recycles generally reduce the amount of liquid passed into the system underflow (if comparing with a simple overflow series where the individual stage R_f ratios are not suitably reduced). This is at the expense of the system cut size, however, which coarsens with the recycles. Both of the two cases A and B are suitable for thickening and clarification (with case B being a little more efficient in removing solids), with stage 1 being the thickening stage and the following two used for clarification. *Figure 16.9* summarizes the relative merits of the two alternative systems and compares them with a simple overflow series.

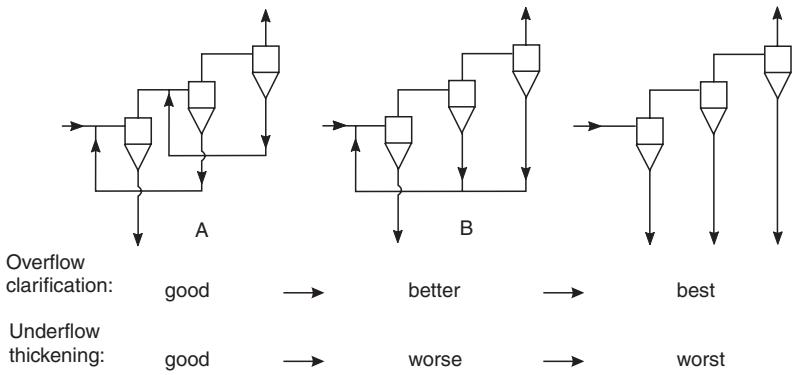

Figure 16.9 Comparison of the two recycling arrangements A and B with a simple overflow series

When fitted with hydrocyclones in practice, the first stage is operated with a concentrated underflow (i.e. as a thickener), under which conditions it would overflow some solids (as its cut size would be coarser than for the same cyclone operated at a more dilute feed and less concentrated underflow). The second and third stages would then be operated as clarifiers, with their respective underflows relatively dilute and returned into the network.

In industrial practice, the arrangements in *Figure 16.7* are used whenever good solids recovery is required coupled with good thickening performance. An example is in washing of wheat starch where the low density ($1500\,kg/m^{-3}$) and fine size (down to 2 microns) of some of the starch particles cause appreciable losses of starch in the system overflow. A counter-current washing system similar to *Figure 16.27* (except that up to 12 stages may be used) is often used and typically fitted with 10 mm hydrocyclones operated at high pressure. Since the cut size of the first stage cannot be lower than about 5 microns and its overflow, unlike that of the following stages, is not protected by recycles, it is quite common to fit an additional separator on the system overflow. This may be a disc centrifuge or a hydrocyclone clarifier/thickener system in *Figure 16.7* (A or B). Good thickening is required because the water recycled with the collected solids into the washing train contains gluten and its return is undesirable.

As to the sharpness of cut, both of the recycling arrangements A and B sharpen the cut in comparison with a simple overflow series but there is very little difference between them. Thus, for example, for a three-stage system, the sharpness index $H'_{75/25}$ varies as follows:

for each stage ($\sigma_g = 1.8$):	2.21
for a simple three-stage series:	1.80
for arrangement A:	1.63
for arrangement B:	1.62

16.3 Series connections on underflow

In direct analogy with the overflow series, one can also operate separators in series in the direction of underflow (*Figure 16.10*) but usually for very different reasons.

This system may or may not use intermediate pumps. If it does not, the additional backpressure on the underflows of stages 1 and 2 has to be compensated for by throttling the overflow orifices of these stages. Otherwise, the overflow rates would be much greater than for the same cyclones operated under balanced conditions.

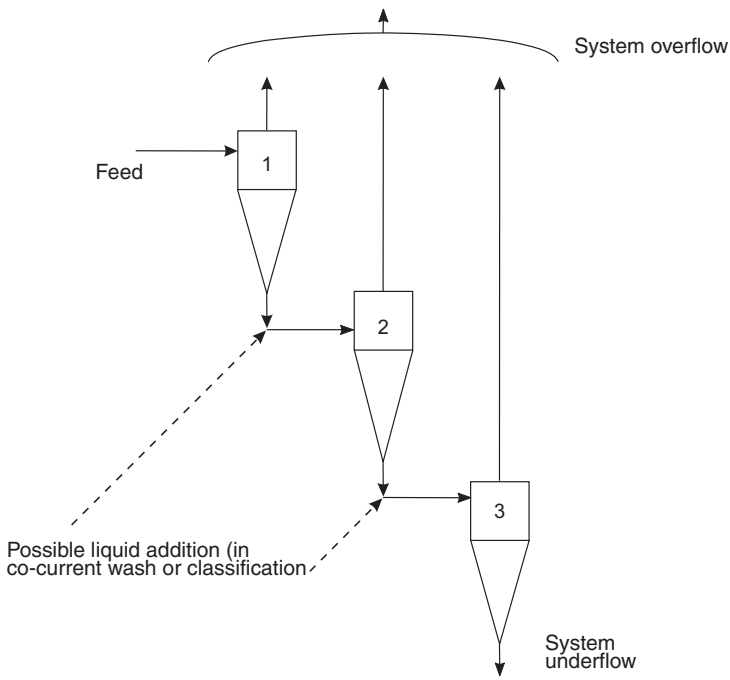

Figure 16.10 A simple three-stage series on underflow

If, for the sake of an illustrative example, we assume that all stages have identical grade efficiency curves and R_f ratios as shown in *Figure 16.1*, then the system grade efficiencies for two-stage and three-stage arrangements would be as shown in *Figure 16.11*. The figure also shows, for comparison, the grade efficiency curve of a single stage from which the two others were computed using the following formula (given for a three-stage system):

$$G(x) = G_1 G_2 G_3 \tag{16.5}$$

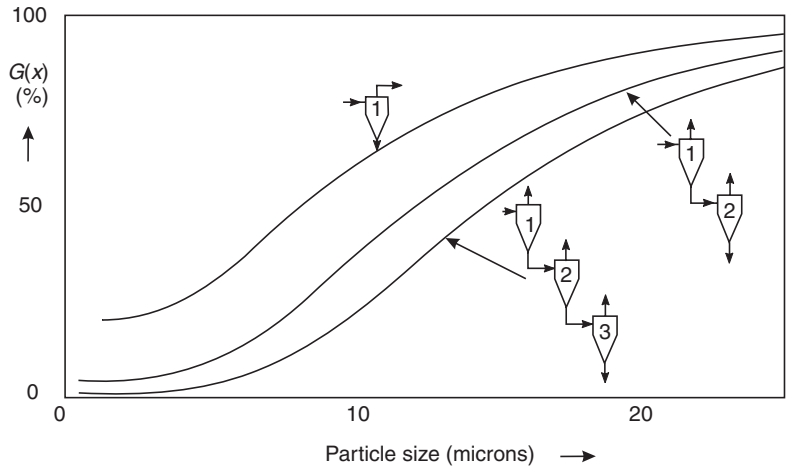

Figure 16.11 The grade efficiency curves of single-stage, two-stage and three-stage series on underflow

Looking at *Figure 16.11* one can see that the opposite happens to what we could see for the overflow series at the beginning of this section. Here, the cut size coarsens with increasing number of stages and the system R_f ratio reduces. No one would dream of using this arrangement (at least not without modification) when particle recovery is important. The arrangement is very useful, however, when it comes to thickening or co-current washing. Co-current washing simply consists of a series of separators in the direction of the underflow, with addition of wash liquid between stages as suggested in *Figure 16.10*. This makes a heavy demand on the amount of wash liquid to be used and recycles can be used to reduce this—see the following section.

As can be seen from *Figure 16.12*, the arrangement sharpens the cut and it is useful in classification particularly when the coarse product is of interest or importance.

The last conclusion is qualitatively the same as that for the overflow series in that they both sharpen the cut. Even quantitatively, when using a symmetrical sharpness index derived from the reduced grade efficiency curves, one obtains very much the same results for the underflow series as contained in

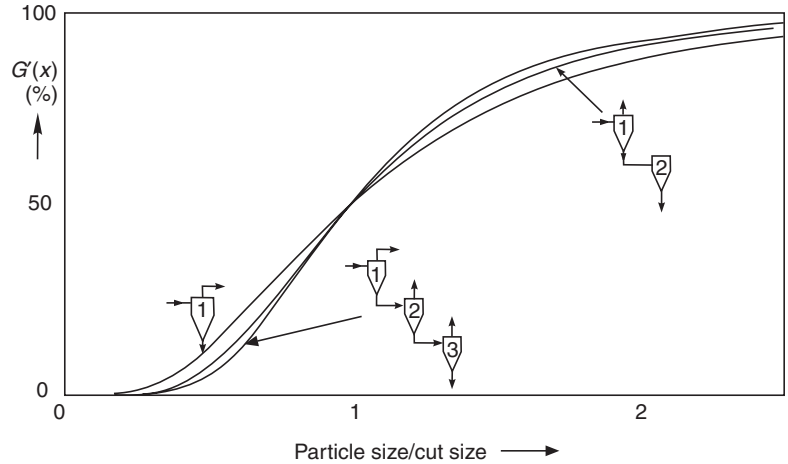

Figure 16.12 The reduced grade efficiency curves of single-stage, two-stage and three-stage series on underflow plotted against dimensionless particle size

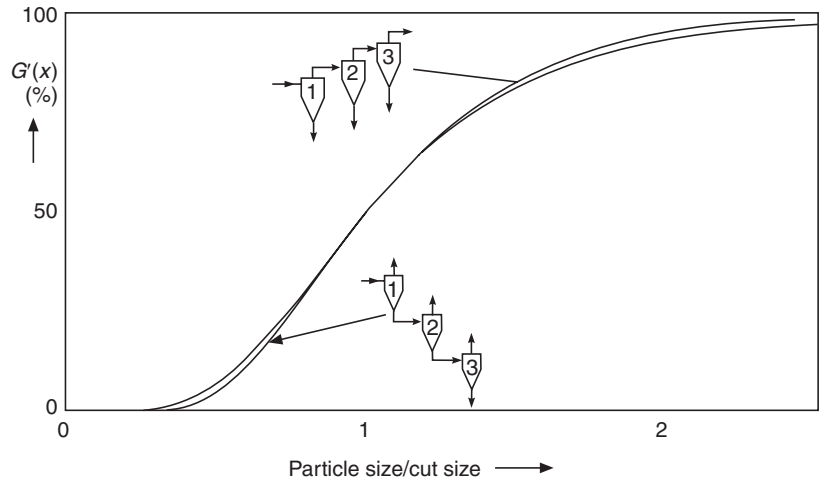

Figure 16.13 Comparison of sharpness of cut for the overflow and underflow series (both plotted against dimensionless particle size)

Table 16.2 for the overflow series. So, if both systems sharpen the cut, where is the difference? *Figure 16.13* gives the clue: note that whilst the slope of the grade efficiency curve at 50% (i.e. at the cut size) is roughly the same for either the overflow or the underflow series, the shape of the rest of the curves is different.

The overflow series gives a steeper $G'(x)$ in the coarser part, above the cut size, and this means that it gives a cleaner fine product than the underflow series. In the fines region, however, it is less steep and thus misplaces more of

Table 16.5 Comparison of asymmetric measures of sharpness of cut for two-stage overflow and underflow series

	single stage	*two-stage overflow*	*two-stage underflow*
x'_{75}/x'_{50}	1.49	1.41	1.35
x'_{50}/x'_{25}	1.49	1.35	1.41

the fines into the coarse product. The reverse is true about the underflow series: its $G'(x)$ is steeper in the fines region which is critical to the quality of the coarse product, whilst it is less steep in the coarse region and this makes the fine product unclean. The effect can be demonstrated by measuring the sharpness of cut separately above and below the cut point; thus for two stages, for example, using the sizes at 25, 50 and 75% (see also *Figure 16.12*).

Furthermore, the existence of underflow may amplify the difference. The above comparison was made for a hypothetical case of negligible flow ratio R_f because it was derived from the reduced grade efficiency curves. The difference between the two series arrangements, in their suitability for producing cleaner fine or coarse products, is further increased by the fact that the overflow series in *Figure 16.2* is bound to have a higher overall flow ratio R_f than the underflow series in *Figure 16.10*. This is particularly true when small diameter hydrocyclones are used, which have to have higher individual R_f ratios than larger units. The R_f ratio lifts the bottom part of the grade efficiency curve and increases the amount of fines misplaced into the coarse product. This makes the overflow series quite unsuitable for producing clean coarse fractions.

It can be concluded, therefore, that whether the series connection is used in the direction of the overflow or the underflow depends very much on which of the two fractions (coarse or fine) represents the product. The product is the material of interest, which should be 'clean', i.e. free of misplaced material. The overflow series in *Figure 16.2* is used for 'refining', i.e. for cleaning the fine product whilst the underflow series in *Figure 16.10* is used to clean or 'wash' the coarse product. Both arrangements steepen up the grade efficiency curve, i.e. sharpen the cut, and the more stages there are, the sharper the cut.

16.3.1 Underflow series with overflow recycle

This arrangement is a separator series in the underflow direction where overflow recycles are made to the feeds of the preceding stages as shown in *Figure 16.14*. It can be used for a whole host of applications ranging from thickening, solids recovery, classification or washing, sometimes several of these at the same time.

A special case of this separator series is the countercurrent washing system and this is capable of thickening at the same time. In this arrangement, as

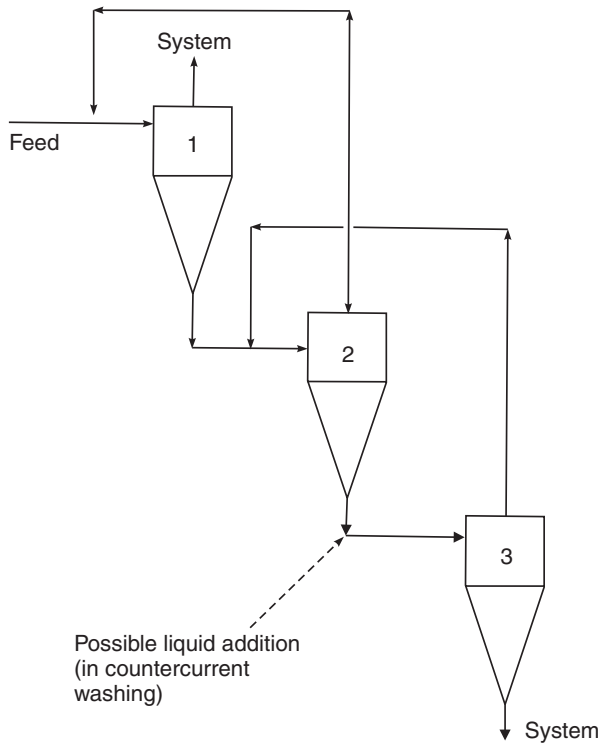

Figure 16.14 A three-stage series on underflow with recycles

indicated in *Figure 16.14* and shown especially in *Figure 17.1*, the wash liquid is introduced into the feed of the last stage and the feed solids and the wash liquid move through the separator series in opposite directions. The wash liquid is gradually more contaminated with the mother liquor while the concentration of the mother liquor in the solids stream reduces. The solids leave the washing train as a slurry in the system underflow whilst most of the decanted wash liquid leaves through the system overflow. Due to its great importance in the processing industries, the whole of chapter 15 is dedicated to countercurrent washing.

The arrangement in *Figure 16.14* may be also used for thickening, solids recovery or classification. As with a single separator, the actual function of the arrangement depends on what it is designed and set to do. In other words, it depends on where the system cut size is set in relation to the particle size distribution of the feed solids.

In washing, thickening and recovery applications we try to set the cut size of the system below the finest particle size present in the feed, so that any loss of particles into the system overflow is minimized. The problem is that, as was shown in the previous section, the underflow series that is needed for

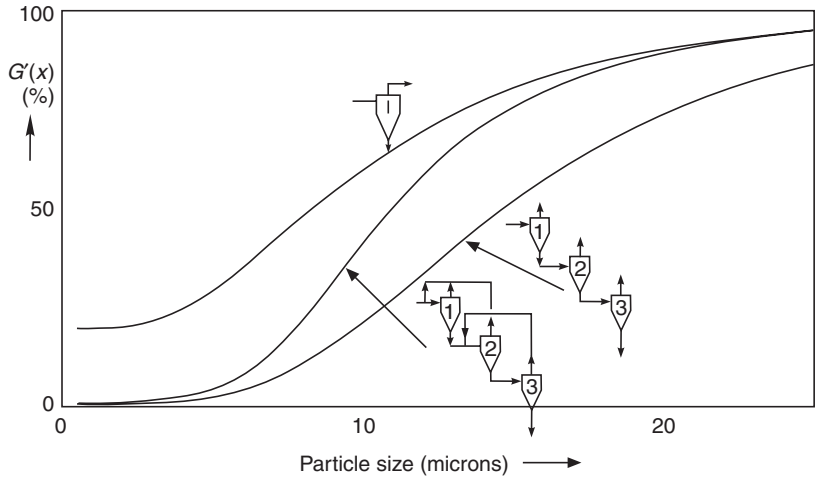

Figure 16.15 Grade efficiency of underflow series with recycles compared with those of a simple underflow series and a single stage

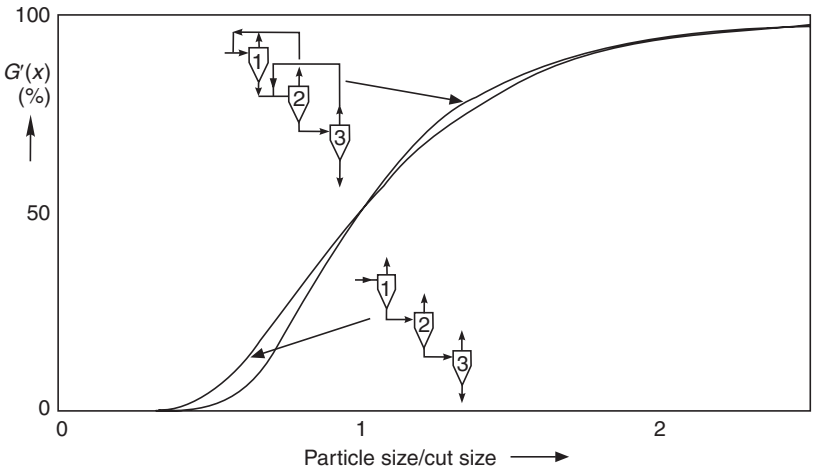

Figure 16.16 Reduced grade efficiency of underflow series with recycles compared with that of a simple underflow series (both plotted against dimensionless particle size)

thickening actually coarsens the cut. The advantage of the recycles here is, as can be seen in *Figure 16.15*, that they bring the cut size lower, part of the way down towards what it would be for a single stage. Yet, the flow ratio R_f is almost as low as for a single stage.

When the system cut size (even with the recycles) cannot be set sufficiently low it may be necessary to use an additional separator on the system overflow

to return the escaping solids back in the feed—refer to the case study on washing of wheat starch in chapter 15 for an example.

In classification, the system cut size is purposely set within the size distribution of the solids, depending on where the cut needs to be made. The arrangement in *Figure 16.14* is capable of improvement in the sharpness of cut compared with that of a single-stage separator as shown in *Figure 16.16*.

Note that both *Figures 16.15* and *16.16* have been plotted using the following equation which relates the system grade efficiency to that of the individual stages, for the arrangement in *Figure 16.14*:

$$G(x) = \frac{G_1 G_2 G_3}{1 - G_1 - G_2 + G_1 G_2 + G_2 G_3} \tag{16.6}$$

16.4 Series connections on both outlets

There are many different arrangements possible, which have stages in both directions, overflow and underflow. Only two of the most important three-stage systems are discussed below.

16.4.1 A three-stage, balanced arrangement for classification

It was concluded in section 16.3 that the overflow series was good for classification of the fine product and the underflow series was good for the coarse product. If both products are of interest and there is to be a minimum of misplaced material in either of these, it follows that an arrangement with stages in both directions is needed. The simplest of such arrangements is a three-stage set-up shown in *Figure 16.17*.

The arrangement can be set up to cut at the same particle size as the front cyclone but the grade efficiency will be significantly steeper. This can be accomplished either by setting the cut sizes of all three cyclones the same or by balancing the cut sizes of stages 2 and 3 in such a way that the system cut size stays equal to that of stage 1. The overall grade efficiency can be calculated from those of the individual stages using equation 16.7:

$$G(x) = \frac{G_1 G_3}{G_1 G_3 + (1 - G_2)(1 - G_1)} \tag{16.7}$$

Typically, sharpness index $H_{75/25}$ of 2.4 for a single cyclone can be reduced to 1.6 using this arrangement. Example 3 in section 16.5.2.3 can be seen for further analysis of this arrangement where the sharpness index can be further reduced to 1.35 but with larger and more costly equipment. Note from *Figure 16.17* that if the underflow from the previous stages is to be further classified, it must be diluted in order to obtain good sharpness of cut and the required cut size.

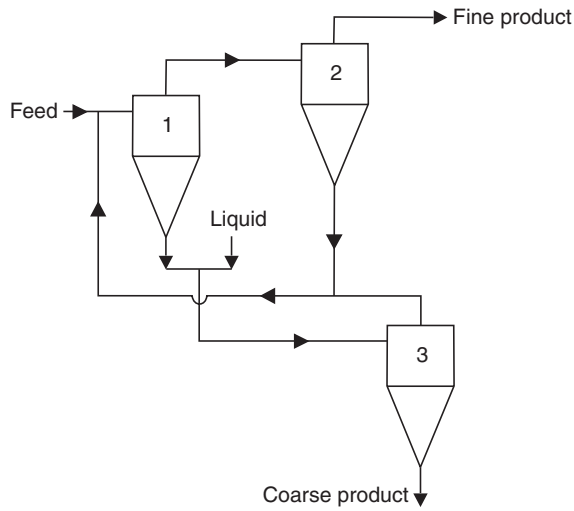

Figure 16.17 A schematic diagram of a reclassification arrangement

16.4.2 A two-stage thickening followed by clarification

This system is useful in thickening when the feed is quite dilute and the required thickening cannot be achieved in one stage. The two thickening stages in the direction of underflow, Nos 1 and 3 in *Figure 16.18*, are followed by a clarifier 2 on overflow of stage 3, with its underflow returned to the feed of stage 1. The solids recovery of stage 1 is reasonable because its underflow is not very concentrated. Stage 3 on the other hand has very thick underflow, which coarsens the cut, and the overflowing solids are returned by the clarifier in stage 2. The underflow of stage 2 is too dilute for the thickened product and has to be returned to the overall system feed.

The equation relating the grade efficiency of the system to those of the individual stages is as follows[1]:

$$G(x) = \frac{G_1 G_3}{1 - G_1 G_2 (1 - G_3)} \tag{16.8}$$

If, for the sake of an illustrative example, we assume that all three stages have identical grade efficiency curves and R_f ratios as shown in *Figure 16.1*, then the system grade efficiency can be calculated from equation 16.8. This is plotted in *Figure 16.19* and compared with the performance of a single stage, a simple two-stage thickening and a two-stage thickening with overflow recycle. As can be expected, the two-stage thickening coarsens the cut but the clarification stage brings it back part of the way towards the cut size of the first stage in a way very similar to that when overflow recycle is used (refer to *Figure 16.15*). The sharpness of cut is improved by adding the clarification

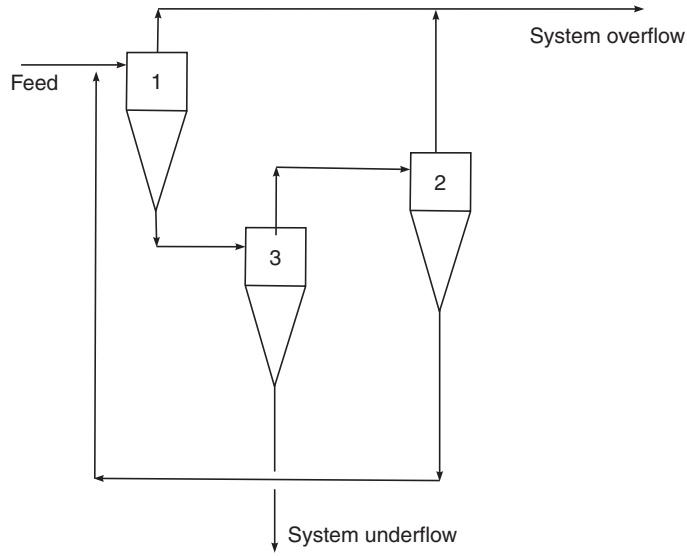

Figure 16.18 Arrangement for two-stage thickening of dilute feeds

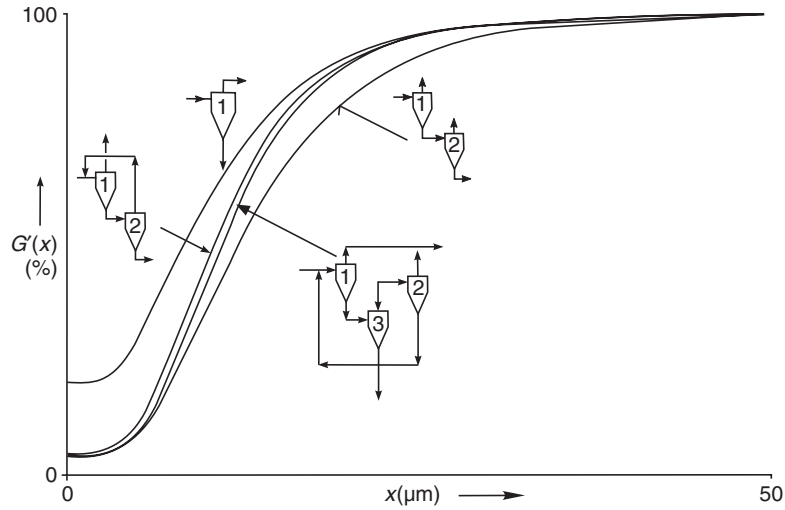

Figure 16.19 Comparison of grade efficiency curves for a single stage, a simple two-stage series on underflow, a two-stage series with an overflow recycle and a two-stage thickening followed by clarification

stage, yet the R_f value stays low. As can be seen in *Figure 16.19*, there is very little difference between two-stage thickening with overflow recycle and that with a clarification stage. *Table 16.6* allows direct comparisons:

Table 16.6 Comparison of two-stage thickening systems

	$x_{50}(\mu m)$	$x'_{50}(\mu m)$	$R_f(\%)$	$H'_{75/25}$
single stage	8.3	10.0	20.0	2.21
two stage with overflow recycle	10.3	10.7	4.76	1.93
two stage with clarifier stage	11.0	11.3	4.13	1.88
simple two stage	12.2	12.6	4.00	2.05

As can be seen, the two-stage system with a clarifier thickens and classifies a little better but the two stage with overflow recycle reduces the cut size to a little lower value.

It should be noted that, in practice, the settings of the individual stages would be different from each other to suit the conditions in the particular application. This is one of the arrangements that can be optimized using software for mass balance calculations.

16.4.3 A two-stage clarification followed by thickening

This is a simple two-stage overflow series with the second stage operating with a more dilute underflow (in order to have a lower cut size) than the first. The second stage, therefore, has to have a thickening device attached to its underflow, which has to achieve at least the same degree of thickening as the first stage. *Figure 16.20* shows a schematic diagram of this arrangement, which happens to have recently been patented for gas cyclones used in a domestic vacuum cleaner[3]. Stage 3 does not have to be a cyclone of course; it may be a filter or any thickening device. If its efficiency is high, its overflow need not be recycled like it is shown in *Figure 16.20* but it may go straight into the system overflow.

The performance of this arrangement is described by equation 16.9 which for $G_3 = 1$ reduces to a simple two-stage series on overflow (equation 16.1 where $G_3 = 0$) and for $G_2 = 1$ gives $G(x) = 1$.

$$G(x) = \frac{G_1 - G_1G_2 + G_2G_3}{1 - G_2 + G_2G_3} \tag{16.9}$$

Figure 16.20 does not show pumps. A common pump usually placed before the first stage can drive stages 1 and 2. If stage 2 is a conventional reverse flow cyclone, stage 3 has to be driven by a separate pump. In the above-mentioned case of the patent by BHRg[3], stage 2 is a uniflow cyclone and this allows stage 3 to be driven by stage 2 by feeding stage 3 from a tangential off-take from the underflow of stage 2 (usually used for pressure recovery) where static pressure is high, and by returning the recycled overflow into the centre of the vortex in stage 2 where pressure is low.

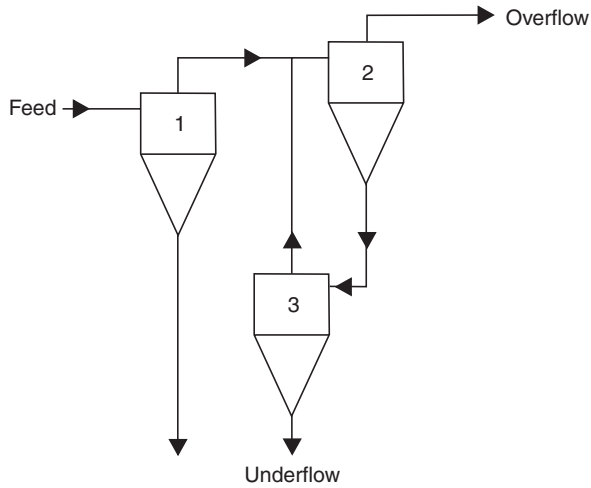

Figure 16.20 A schematic diagram of a two-stage clarification followed by thickening

16.5 Mass balance calculations

Generally, the calculation of mass balances for separator networks is time consuming and often complex, particularly when recycles are involved. This is because the size distribution of the particulate matter present has to be calculated in each stream. Furthermore, overall recovery or efficiency calculations involve a non-algebraic step of integration. There are two ways of dealing with this: either by using a short-cut method or by doing full mass balances around the network. The former was used widely in the era before personal computers and it still has some value today for quick relative comparisons. The full mass balances are best done with a computer although manual calculations are possible for some simple arrangements.

16.5.1 A short-cut method for system efficiency calculations

If the concentrations and particle size distributions of the solids within the network itself do not have to be known then the system can be considered as a single separator and its efficiency can be calculated from that of the individual stages within it. The system efficiency thus obtained can then be used in simple one-pass predictions of particle losses to overflow and other overall separation performances of the train. This allows direct comparisons of alternative systems, as shown in the worked example in section 16.4.1.

If the grade efficiency curves are known for all stages in a system, an equation for the grade efficiency of the whole system may be derived from mass balance around the arrangement. Reference 1 gave, for the first time,

such equations for many different series arrangements comprising of no more than three stages. An even more comprehensive list of such equations, for three-stage systems, may be found earlier in this section. Here an example is given of how such equations are derived.

Example of derivation of overall efficiency from that of the individual separators

Task: Derive an equation for the grade efficiency of the thickening and clarification arrangement shown in *Figure 16.21*, from the grade efficiencies of the two stages.

Solution:

The mass flow rates of solids in a minimum number of streams needed for full mass balances are given notation. Usually the system feed and the individual underflow streams are best for this, as shown in *Figure 16.21*. Equations relating the overall and individual total efficiencies are then written with the notation selected (using the definition of total efficiency as mass flow rate of solids in the underflow to that in the feed):

$$E_{\mathrm{T}} = \frac{M_{1\mathrm{u}}}{M_{\mathrm{f}}} \tag{16.9}$$

$$E_{\mathrm{T1}} = \frac{M_{1\mathrm{u}}}{M_{\mathrm{f}} + M_{2\mathrm{u}}} \tag{16.10}$$

$$E_{\mathrm{T2}} = \frac{M_{2\mathrm{u}}}{M_{\mathrm{f}} - M_{1\mathrm{u}} + M_{2\mathrm{u}}} \tag{16.11}$$

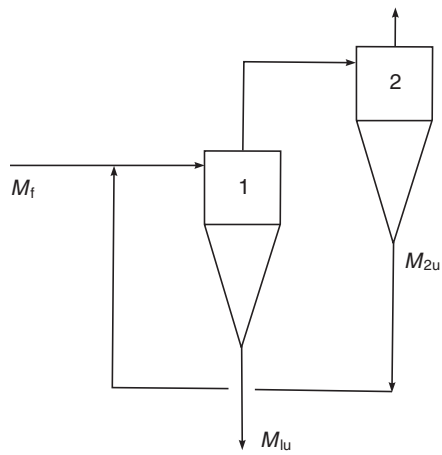

Figure 16.21 Arrangement for thickening and clarification in the example derivation

All of the mass flow rates annotated as M in the above three equations can now be eliminated, to give a relationship between the total efficiencies:

$$E_T = \frac{E_{T1}}{1 - E_{T2} + E_{T1}E_{T2}} \tag{16.12}$$

Now what holds for total efficiencies must also hold for grade efficiencies, hence

$$G(x) = \frac{G_1}{1 - G_2 + G_1 G_2} \tag{16.13}$$

and this is the final result. It is of course a special case of equations 16.3 and 16.4 for $G_3 = 0$.

Having obtained a grade efficiency curve $G(x)$ for the network, to represent it as if it were a single separator, it is then a simple matter to derive the total mass recovery of the system. This involves integration of the product $f(x)\ .\ G(x)$ with x as shown in an example below (where $f(x)$ is the differential form of the particle size distribution in the feed), or alternatively

$$E_T = \int_0^1 G(x)\,\mathrm{d}F \tag{16.14}$$

if the feed size distribution is in the cumulative form $F(x)$.

Let us demonstrate the method in an example. In *Table 7.2* in section 7.7, partially reproduced in *Table 16.7*, the grade efficiency $G(x)$ of a three-stage countercurrent washing system was derived from the grade efficiencies of the individual stages.

As shown in *Table 16.7* and *Figure 16.22*, integration of $G(x) \cdot f(x)$ with x gives $E_T = 86.8\%$, which is the expected recovery for the three-stage countercurrent washing arrangement in question. Here is a summary of the steps in the short-cut method for system recovery determination:

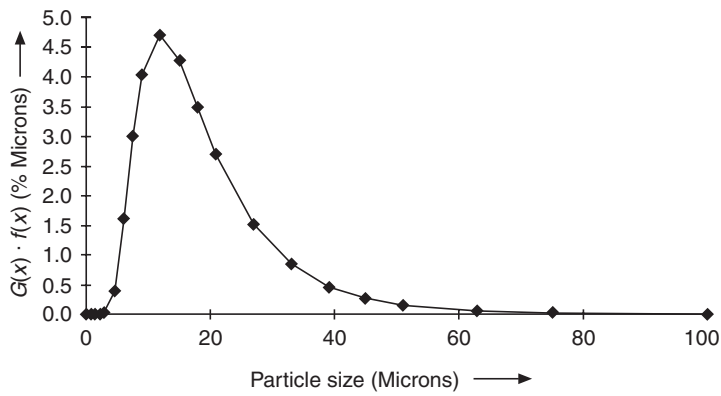

Figure 16.22 A plot of $G(x) \cdot f(x)$ from *Table 16.7*; the area under the curve represents E_T

Table 16.7 Example of total recovery calculation from $G(x)$ and $f(x)$ (using data from Table 7.2)

x micron	*f(x)* % / micron	*G(x)* %	*G(x) . f(x)* % / micron	*integral increments* %
0	0	0	0.0	
0.75	0	0.02	0.0	0.00
1.5	0.02	0.11	0.0	0.00
2.25	0.16	0.8	0.0	0.00
3	0.53	3.64	0.0	0.01
4.5	1.85	21.81	0.4	0.32
6	3.36	47.4	1.6	1.50
7.5	4.52	66.32	3.0	3.44
9	5.17	77.95	4.0	5.27
12	5.26	89.58	4.7	13.11
15	4.52	94.56	4.3	13.48
18	3.59	96.96	3.5	11.63
21	2.74	98.22	2.7	9.26
27	1.52	99.32	1.5	12.60
33	0.84	99.7	0.8	7.04
39	0.46	99.86	0.5	3.89
45	0.26	99.93	0.3	2.16
51	0.15	99.96	0.1	1.23
63	0.05	99.99	0.0	1.20
75	0.02	100	0.0	0.42
100	0	100	0.0	0.25
				$86.81\% = E_T$

1 Establish the particle size distribution (by mass) of the solids in the feed to the system (in either differential or cumulative form).
2 Establish the proposed grade efficiency curves in all stages.
3 Derive or find an equation applicable to the proposed system to calculate the system grade efficiency from those of the constituent stages, and calculate the system $G(x)$.
4 Calculate the overall recovery E_T by integrating $G(x) \cdot f(x)$ with x (or $G(x)$ with F as per equation 16.14).
5 Now that E_T is known, it is possible to calculate other values of the predicted performance of the system, such as the concentrations or particle size distributions in the system overflow and underflow (consult examples in chapter 3)—the methods are the same as for single separators because the system is now treated as a single stage. If particle sizes and/or concentrations are needed in any of the streams within the network then a full mass balance calculation is needed and this is dealt with in the following section.

16.5.2 A computerized method

The short-cut method described in the preceding section does not produce data on particle concentrations and flows in between stages. This information is needed for efficient equipment design. The problem is that if more than one stage is used in series for a given task, many or an infinite number of possibilities exist for the settings and sizes of the individual stages. Some way of weighing or optimizing the settings is needed. Not only does this require separate mass balance calculations for all alternatives but also new tools for comparison of the results. Manual calculations of detailed particle mass balances in networks are tedious and complicated. This is one area where computers come into their own.

The use of computers for particulate mass balance calculations is an obvious and necessary step in designing particle technology plants, and much commercial software exists to this end. Particle separators are included in such programs but only as one of many other unit operations catered for. The available software ranges from large solid processing plant simulators such as JKMetSim, SPEEDUP or METSIM to smaller but dedicated packages developed especially for separation applications by Alcan Chemicals Europe[4] or by Fine Particle Software (FPS)[5,6]. The latter offer more specialist features allowing direct comparisons between alternative separation and washing systems.

FPS identified the need for a more specialized and dedicated software package intended specifically for the design and optimization of separator networks with features and treatment unique to that aspect of particle technology[6]. This section reviews the development of this new software and gives examples of its use with hydrocyclones in particular. Naturally, the separate treatment of separator networks can be incorporated in larger CAD software for plant design.

16.5.2.1 Method of calculation

The distribution of particle size can be expressed by mass, surface or number. Errors are inherent in the theoretical conversion of one to another and so this is to be avoided. As mass balances call for size distributions by mass, we have assumed that, in keeping with current practice, size distributions in the feed to the networks would be specified by mass. Consequently, only mass distributions are handled in our program and in the following.

Particle size distributions are continuous functions for all practical purposes and should preferably be represented as such. One problem is that the measurement of particle size and its distribution (assuming that the feed to the separation plant is a real size distribution and has to be measured) is done at a finite number of points, usually resulting in a ‘histogram’. This step-like representation of the differential form of size distribution is commonly used, for example in mineral processing. The error in such a representation decreases with increasing number of classes or ‘channels’. In practice the

conventional and most obvious method for mass balance calculations is to take the discretized feed 'histogram' and perform the calculations in the same class intervals all the way around the plant. The mass balances following this method will hold (i.e. balance) by definition but the overall recoveries calculated by integration might involve a small error depending on the number of size classes adopted.

For an improved and more realistic representation of the feed size distribution, there are two options available:

1 Curve fitting of the whole size distribution with one of the many multiple-parameter specialized functions proposed in the literature for particle size distribution data.
2 Sequential curve fitting of parts of the distribution (two or three adjacent points) usually with second- or third-order polynomials, for example cubic splines. This is best done with size distributions in cumulative form where the measured points should lie on, or be closely represented by, the fitted curve.

The 'whole curve' fitting method has been widely used in mineral processing and other areas of particle technology, and some of the particle generation processes such as grinding are known usually to produce certain forms of distribution function in preference to others. Special graph papers exist to allow manual fitting of a set of measured points, for example the Rosin–Rammler–Intelmann or the log–probability papers. With the widespread use of computers today, software exists for this fitting. The FPS program[7] mimics the manual graph paper fitting and applies it to seven two- and three-parameter functions used widely in particle technology such as the Harris, Rosin–Rammler, Weibull and log–probability distribution functions. The parameters for the best-fitting function are computed by minimization of the squared errors in the graphical co-ordinates of the graph paper for that function.

The 'whole curve' fitting method has attracted a lot of attention in the literature and continues to do so today. The latest effort in its use for reducing the amount of data handled by computer models of particulate processes[8] is to find the necessary parameters from the moments of the particle size distribution function instead of finding the best fit from the closeness of the measured points to the fitted function, as is more usual in practice.

The advantages of the 'whole curve' fitting method include:

1 easier handling through a small number of parameters instead of the much greater number of measured points,
2 some physical meaning of the derived parameters (e.g. one a measure of the central tendency and one of the spread of the distribution),
3 under some circumstances, analytical solutions to the integrals may exist in overall recovery calculations.

The main disadvantage is that most of the functions used and proposed are advantageous only for mono-modal distributions. They can be used for multi-modal distributions by resolving them into mixtures of mono-modal functions but the number of resulting parameters grows accordingly (one set of parameters for each of the functions plus the 'composition' fractions). In our experience, the 'whole curve' fitting method works well for a one-stage separator with a mono-modal feed but the same function form is unlikely to fit either of its two product streams. Furthermore, the particle size distribution in either product stream may become bimodal under some circumstances (although the feed is mono-modal) and catering for this eventuality is cumbersome and rather open-ended in a separator networks program given the possibility of many stages in the network.

The sequential curve fitting of adjacent points such as the cubic spline method offers no saving in the number of points to be handled and stored in between stages but can be useful in splitting the size distribution into more size classes than originally measured (e.g. by sieving) in order to use the discretized method of mass balance calculation that requires a greater number of points. It could also be used in the step-by-step integration or differentiation involved in overall recovery calculations and grade efficiency testing respectively. The FPS programs for grade efficiency testing[9] and classification of particulate materials in a one-stage separator[10] use second-order polynomial fitting. The linear interpolation between points is a trivial version of sequential curve fitting.

In the program described here, FPS has adopted the discretization method with a step-like 'histogram' representation of particle size distributions around the plant, in the same number of classes as set for the feed. FPS believe that the computational complication in using any curve fitting (whether 'whole curve' or sequential) does not justify the improvement in the accuracy of overall recoveries calculated. This is particularly true when the number of size classes used exceeds 100 and most modern particle size analysers give a great number of measurement points. If the user has a much smaller number available (such as obtained from sieving) then the curve-fitted parameters can be entered from a bounded log–normal distribution and this is then 'chopped up' into the required number of points by the program. Alternatively, the user may generate additional points by interpolation (linear, cubic spline or other).

In common with established practice, the separation performance of each separator in a network is characterized by the grade efficiency curve. The probability nature of grade efficiency curves makes them well fitted by a log–normal function, only modified in the case of significant underflow in wet separator systems. This is conventionally handled by the 'reduced grade efficiency' concept described elsewhere[1]. Thus, any separator is characterized by a cut size (the 50% point on the grade efficiency curve), the geometric standard deviation (this is a measure of the sharpness of cut) and the underflow-to-throughput ratio (a measure of the flow splitting taking place in the separator, again see ref.1 for details).

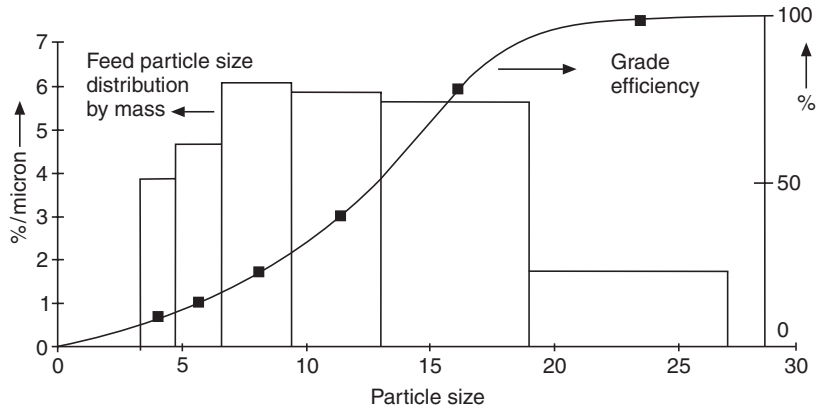

Figure 16.23 A graphical illustration of the method used for processing the feed size distribution with the grade efficiency curve

As the flow passes through a separator, the feed size distribution is processed by the grade efficiency curve/function of the separator. In keeping with established practice, each size class is split into the underflow and overflow as specified by the grade efficiency taken at its mid-point as shown in *Figure 16.23*. Note that in order to illustrate the point more clearly, *Figure 16.23* has a small number of size classes.

16.5.2.2 Program description

The program assists the designer with drafting and assessing alternative systems of separators through a graphical interface. In the current version, flow rates, solids concentrations and particle size distributions are considered (pressure drops and pumps are not included). Thus, the program will provide the information needed for sizing the pipework, pumps or separators, but will not do the sizing itself. Also, it will not optimize systems but it will free the designer to consider alternatives and do manual design and/or optimization.

Figure 16.24 shows the main display screen of the program. Any network can be drawn on screen using pick-up tools from a pictorial menu. These include the following pieces of 'equipment', which can be rotated and scaled:

Separator	specified by the flow ratio and a log–normal reduced grade efficiency
Sump	for joining streams
Feed line	specified by a flow rate, solids concentration and particle size distribution of the solids (this is in turn specified either by a table of cumulative % undersize or by three parameters of a bounded log–normal distribution)

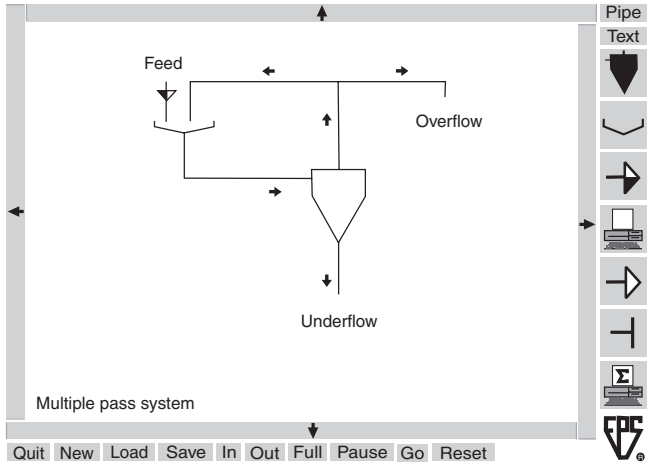

Figure 16.24 Main display screen of the Separator Networks program (showing a multiple pass system)

Instrumentation	for on-screen display of data selected from the information pages of any component of the system, be it a pipe, sump, separator, etc.
Clean liquid supply	for supplying dilution or washing liquids (specified by flow rate only)
Flow splitter	for splitting flows, in partial recycles; specified by a flow ratio
Overall plant performance monitor	for evaluation of overall plant performance; must be connected to system overflow. Information available includes overall efficiencies, cut sizes, sharpness of cut and grade efficiency curves (all of these either actual or reduced) and the overall flow ratio
Other tools:	
Pipe	for connecting the equipment in the above list
Text	for on-screen legends, plant titles, notes, etc.

For each piece of equipment, a data page can be accessed containing given and derived information such as flow rate, concentration, particle size distribution, etc. In addition, the 'instrumentation' and 'plant monitor' can be connected to equipment already on screen.

As soon as the network is drawn, connected and feed items specified, the program starts iterating and this can be observed on screen if suitable instrumentation is strategically positioned within the schematic diagram of the network and connected to chosen items. The start-up can be watched as if in real time when the network is connected, loaded from disk or by pressing the 'Reset' button. Changes to input data can be made at any time and the effect of any changes observed.

16.5.2.3 Examples of use

Example 1: A multiple pass system

Figure 16.24 shows a single-stage separator with a partial overflow recycle. This is sometimes called a 'multiple pass system' and is often used in the cleaning of metal working fluids, with a hydrocyclone as the separator. For this specific application the program can be used to demonstrate the effect of the recycle on the overall recovery of the system, by varying the splitter flow ratio from, say, 100% (no recycle) to 10% (90% recycle). However, as the increasing amount of recycle flow would cause a corresponding increase in the hydrocyclone underflow rate it is necessary to control the underflow orifice in order to keep the system underflow rate constant. Thus, the system flow ratio (underflow to throughput, by volume) is the same in the four cases shown in *Figure 16.25*.

As would be expected, the increased recycle flow improves overall recovery of the system but at the cost of increased size of the separator and also proportionately greater pumping costs. *Figure 16.26* demonstrates this in a plot of system recovery against feed flow to the hydrocyclone (this is directly related to the installed cost of the separator). It should be noted that this arrangement, if a hydrocyclone is used as the separator, leads to

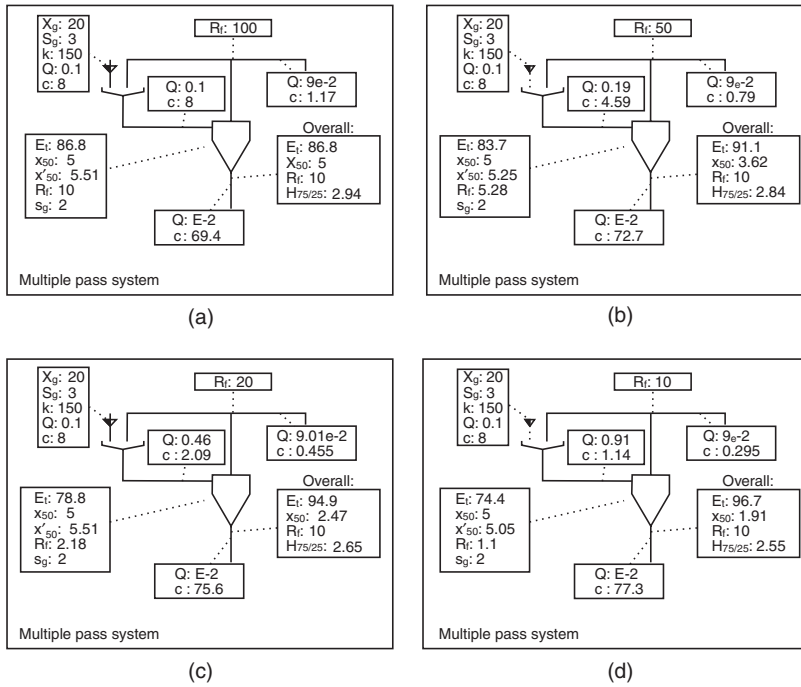

Figure 16.25a–d Sequence of four main displays for Example 1, with recycle rates from 0 to 90% (i.e. the splitter flow ratio from 100 to 10%)

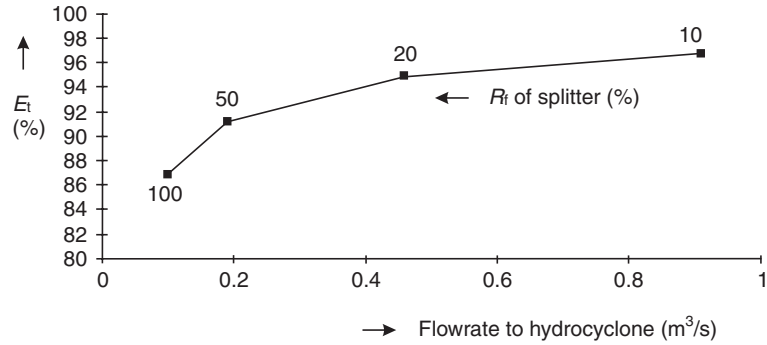

Figure 16.26 A plot of overall plant recovery as a function of recycle rate, Example 1

an additional increase in recovery due to the dilution of the feed by the recycle.

Example 2: A countercurrent washing system

One of the most complicated systems for mass balance calculations is a multi-stage countercurrent washing system. *Figure 16.27* shows an example of a nine-stage system, with an additional separator on the system overflow as is used to minimize product losses in washing of wheat starch. The most suitable separator in this specific application is a 10 mm hydrocyclone operated at a

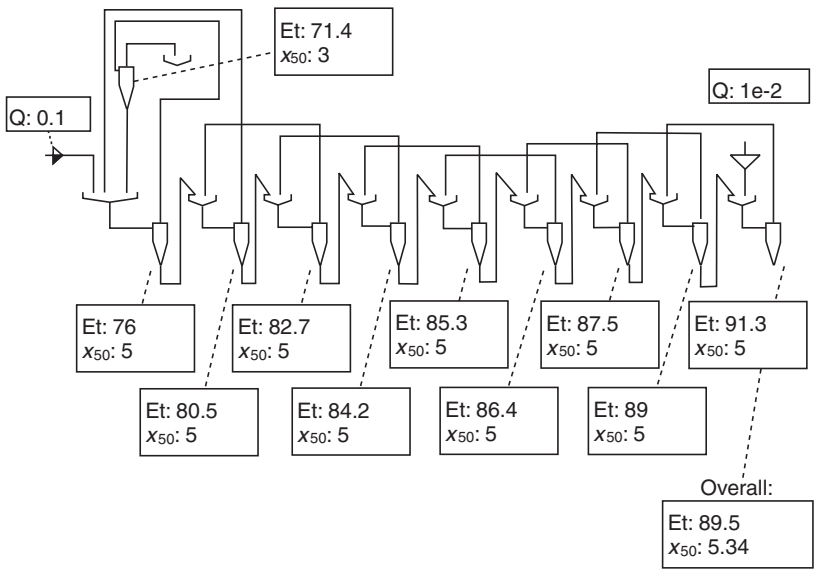

Figure 16.27 Networks display for Example 2 (nine-stage countercurrent wash)

high pressure drop. Due to the low minimum particle size of wheat starch, however, some loss of starch to system overflow is inevitable. It is usual, therefore, to install an additional separator in the system overflow: a disc centrifuge or a set of hydrocyclones in a series on overflow.

In *Figure 16.27* we used 'instrumentation' and a 'performance monitor' to display on screen the recoveries of the individual separators as well as the overall recovery respectively. On reset, the flow of material can be watched to progress down the train and the mass balances to converge in about 2 minutes (on a 486 machine, at 33 MHz, with 100 classes of particle size in each stream) or only a few seconds on a Pentium. The settings of individual stages can be set to produce a compromise between a good recovery of solids and high washing efficiency of the train, with the thickest underflow to be at the end of the train, i.e. in the system underflow.

Note that hydrocyclones are not the only suitable separators for countercurrent washing in a large number of stages. Where enough space is available, gravity thickeners can also be used.

In conclusion the discretization method of computing mass balances in separator networks can cope with the large number of streams and data handled even in the most complicated separator system such as multi-stage countercurrent washing and can do so in reasonable time.

Example 3

This example demonstrates how the current version of the program can be used for manual optimization of a whole arrangement. The reclassification system shown in *Figure 16.28* is often used to sharpen the cut in classification, when both the coarse product and the fine product are important.

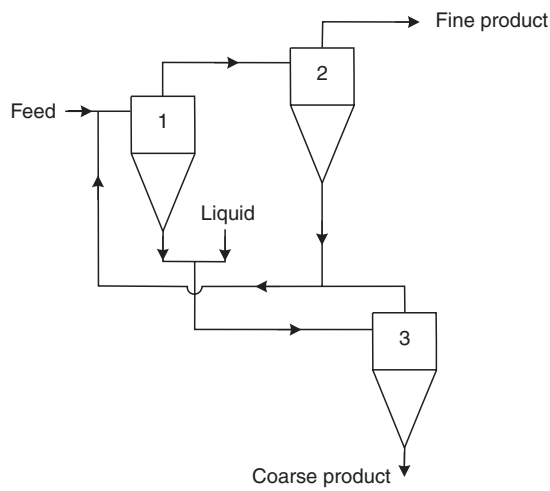

Figure 16.28 A schematic diagram of a reclassification arrangement used in Example 3

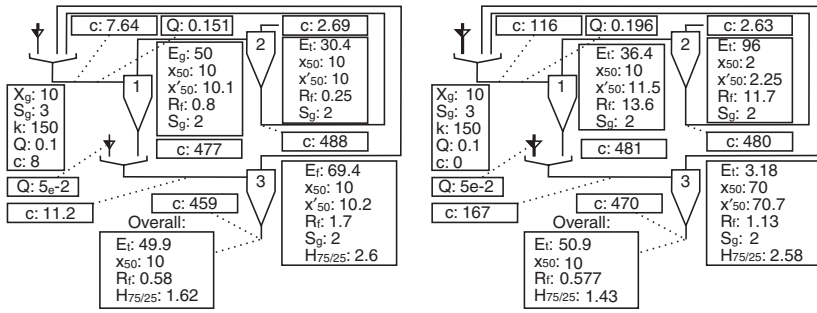

Figure 16.29a, b Two extreme settings of the optimization in Example 3

The separator in stage 1 is not efficient enough for classification, i.e. it misplaces too much of the fine particles into the coarse product and of the coarse particles into the fine product. This performance in classification is characterized by the so-called sharpness of cut derived from the shape of the grade efficiency curve. In this section we measure the sharpness of cut by the sharpness of index $H_{75/25}$ defined as the ratio of the particle sizes at 75% and 25% on the grade efficiency curve.

In the arrangement in *Figure 16.28* another separator (stage 2) is used to take out the misplaced coarse particles from the fine product and these (in the underflow of stage 2) are then returned to the feed of the whole arrangement. Likewise, the coarse product is reclassified by another separator in stage 3 and its overflow is returned to the system feed. The problem in designing an arrangement like this is to know the best settings for the cut sizes of stages 2 and 3. As the cut size of stage 1 is usually set to where the cut is needed by the classification process, the only clear requirement for stages 2 and 3 is that their joint action is not to alter the cut size of the whole arrangement but only to improve the sharpness of cut.

Figure 16.29 shows two extreme settings in our example of classification at 10 microns. *Table 16.8* gives the results at several intermediate settings also, all calculated with the FPS program using a constraint that the underflow concentration of all three stages must not exceed 481 kg/m^3. In *Figure 16.28a*, both stages 2 and 3 are set at 10 microns, same as for the front stage 1: this is often done intuitively in practice and, although it does improve the sharpness of cut, it is not necessarily the best set-up as demonstrated in *Table 16.8*.

If the cut size of stage 2 is set a little finer than 10 microns, say to 5 microns, the cut size of stage 3 has to be coarser than 10 microns (20.5 microns actually) in order to compensate and keep the overall cut size of the whole arrangement to 10 microns. As can be seen from *Table 16.8* (second row), this further improves the sharpness of cut from $H_{75/25}$ equal to 1.62 for a 10–10–10 setting to 1.41 at a 10–5–20.5 setting. As can be seen from *Table 16.8* and *Figure 16.30*, the cut size of stage 2 can be further reduced until the sharpness

Table 16.8 Table of results for Example 3: the cut size of the first stage is 10 microns, the overall cut size is also 10 microns, the underflow concentration in all stages is less than 481 kg/m^3

cut size No. 2 microns	*cut size No. 3* microns	$H_{75/25}$ *overall* —	*c to No. 1* kg/m^3	*Q to No. 1* m^3/s	*c·Q to No. 1* kg/s
10	10	1.62	7.64	0.151	1.15
5	20.5	1.41	15.6	0.154	2.40
4	26	1.37	22.7	0.156	3.54
3	37	1.35	42	0.163	6.85
2.44	49	1.37	68.9	0.174	12.0
2	70	1.43	116	0.196	22.7

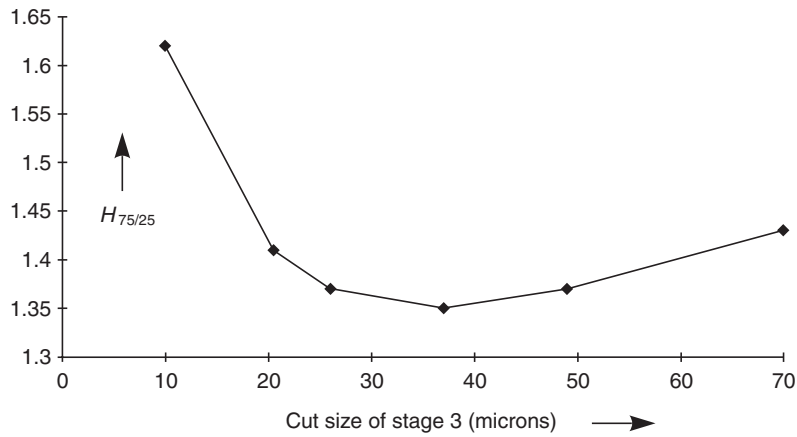

Figure 16.30 A plot of the sharpness index $H_{75/25}$ as a function of the cut size of stage 3, Example 3.

index passes through a minimum of 1.35 (at a setting of 10–3–37) and starts to rise again.

It follows, therefore, that if the sharpness index is used as the objective function, manual optimization with the FPS program can produce the settings of the cut sizes of individual stages for the best overall performance of a classification arrangement. It is interesting to observe from *Table 16.8*, where we also included the values of concentration c and flow rate Q in the feed to the first stage, that both c and Q increase as the settings get further from the initial 10–10–10 setting (the mass flow rate of solids to No. 1 stage $c \cdot Q$ increases from 1.15 to 12.0). This means that there is a price to pay for the improvement in the sharpness of cut shown in this example, in that the flow

capacity of stage 1 has to be greater and the pressure drop higher to compensate for the higher solids concentration in the feed. Economic criteria such as capital and running costs would also have to be taken into account in the optimization.

References

1. Svarovsky, L., *Hydrocyclones*, Holt Reinhart & Winston, London (1984)
2. Zeitsch, K., 'Problems with fine particle recycling', in Chapter 16, *Solid–Liquid Separation*, 3rd edn, L. Svarovsky (Ed.), Butterworths, London, 541–558 (1990)
3. UK Patent Application GB 2330786 A, date of publication 5.5.1999
4. Imre, M. and Holtzwarth, R., 'Simulation of washing with hydrocyclone networks', in *Hydrocyclones '96*, D. Claxton, L. Svarovsky and M. Thew (Eds), Mechanical Engineering Publications Ltd, London, 43–47 (1996)
5. Svarovsky, J. and Svarovsky, L., 'Computer-aided design of hydrocyclone networks', in *Hydrocyclones '96* D. Claxton, L. Svarovsky and M. Thew (Eds), Mechanical Engineering Publications Ltd, London, 31–41 (1996)
6. 'Computer-Aided Design of Separator Networks, a computer program', *Catalogue of In-Company Short Courses, Books and Particle Technology Software*, Fine Particle Software, The Lares, Maple Avenue, Cooden, Bexhill-on-Sea, TN39 4ST (2000)
7. 'Interactive Data Plotting', *Catalogue of In-Company Short Courses, Books and Particle Technology Software*, Fine Particle Software, The Lares, Maple Avenue, Cooden, Bexhill-on-Sea, TN39 4ST (2000)
8. Hounslow, M. J. and Wynn, E. J. W., 'Short-cut Models for Particulate Processes', *Computers Chem. Engng*, **Vol. 17**, No. 5/6, 505–516 (1993)
9. 'Grade Efficiency Testing', *Catalogue of In-Company Short Courses, Books and Particle Technology Software*, Fine Particle Software, The Lares, Maple Avenue, Cooden, Bexhill-on-Sea, TN39 4ST (2000)
10. 'Classification of Particulate Materials', *Catalogue of In-Company Short Courses, Books and Particle Technology Software*, Fine Particle Software, The Lares, Maple Avenue, Cooden, Bexhill-on-Sea, TN39 4ST (2000)

Bibliography

Svarovsky, J. and Svarovsky, L., 'Computer-aided design of separation networks', Powder Handling and Processing, Vol. 7, No. 3, 303–306, (July/September 1995), also in Processing Part I, Trans Tech Publications, Clausthal-Zellerfeld, ISBN 0 87849 121 X, 119–122 (2000)

17

The selection of solid–liquid separation equipment

H. G. W. Pierson

Pierson & Company (Manchester) Ltd, Bozeat, Wellingborough, Northants

17.1 Introduction

The selection of solid–liquid separation equipment is dependent on such a vast number of different factors, and the choice is so very wide, that it is clearly impossible to give a formula whereby one can select the right piece of equipment without any factor of error.

This chapter should, therefore, be seen as an attempt to assist the chemical engineer in his short-listing exercise, for which it is probably more important to know which pieces of equipment are not suitable. In most cases it appears that more time and money is spent in finding that a certain piece of equipment is unsuitable rather than in finding which piece is suitable. In the end this may lead a company to turn to old, well-known, well-tried principles, thereby often settling for second best.

We would feel that we have achieved something if this chapter enables a chemical engineer to spend most of his time and budget on those pieces of equipment which are likely contenders rather than the reverse.

17.2 Sedimentation or filtration?

If one ignores impingement, it would be true to say that all mechanical solid–liquid separation systems are based on one of two principles: sedimentation or filtration (see *Figure 17.1*).

With sedimentation one must remember that substantially the only driving force is the difference in specific gravity between the phases. The apparent difference can be increased by, for instance, applying a centrifugal force or by increasing the mass of individual particles through flocculation, but the basic difference is a given factor which cannot be altered. Sedimentation is,

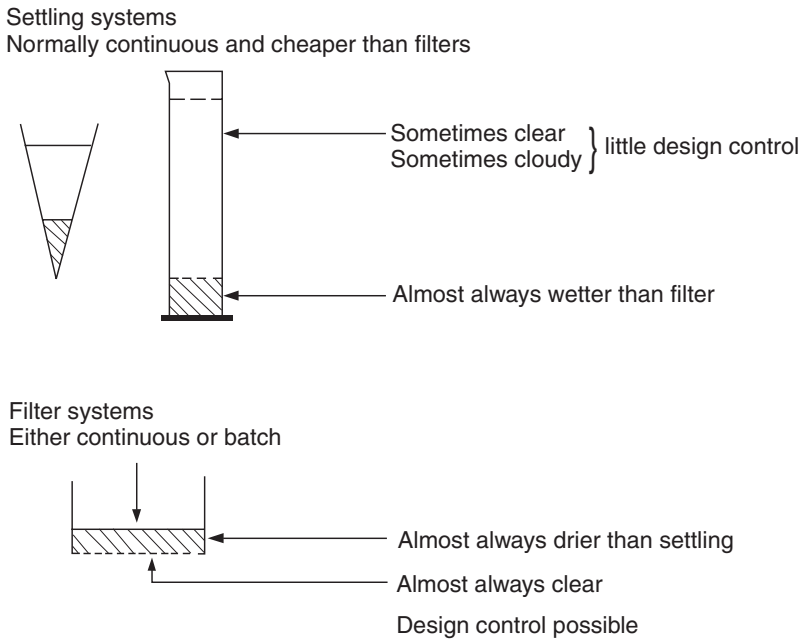

Figure 17.1 Schematic illustration of settling and filtration

therefore, a process which, from the onset, can have limiting factors which are beyond the design control. Sedimentation systems on the other hand tend to be relatively cheap, and are ideally suitable for continuous, and certainly automatic, operation.

Filtration, on the other hand, gives an almost unlimited amount of design control since it relies on a man-made septum, so chosen that it will retain those particles which must be separated. Filtration systems, however, are far less suitable for continuous production, sometimes not even for automatic production, and tend to be more expensive per volume treated than sedimentation systems.

From this it follows that one must first of all look at sedimentation. In this respect it is important to note that even if sedimentation does not achieve exactly the separation required it may still be a valuable first step in a process and may be followed by filtration. A typical example of this is the well-known clarification of water in water works. Here sedimentation with or without flocculation is first carried out, and the still somewhat hazy overflow is then passed through polishing filters. To achieve the end result purely by sedimentation or purely by filtration would be prohibitively expensive. The combined procedure, however, is both practical and reliable.

Since filtration and separation are still to a very large extent an art rather than a science it is important that right from the beginning one obtains a ‘feel’ for the material. We suggest therefore that before taking any actual

measurements one observes the sample and memorizes how it behaves. Does the material form a precipitate, does it spontaneously flocculate, do the eddy currents travelling upwards disturb the flocs, or do they simply move them out of the way, does a small stirring action upset the whole pattern, etc.? These somewhat nebulous facts are very important in the final choice since it will enable one to decide whether or not the specific mechanical details of otherwise identical pieces of equipment are acceptable or not.

17.3 Sedimentation equipment

Figures 17.2, 17.3, 17.4 and *17.5* show the settling times for different sludge volumes in the various types of sedimentation systems. It is important to note that the equipment listed is merely representative of whole groups. These

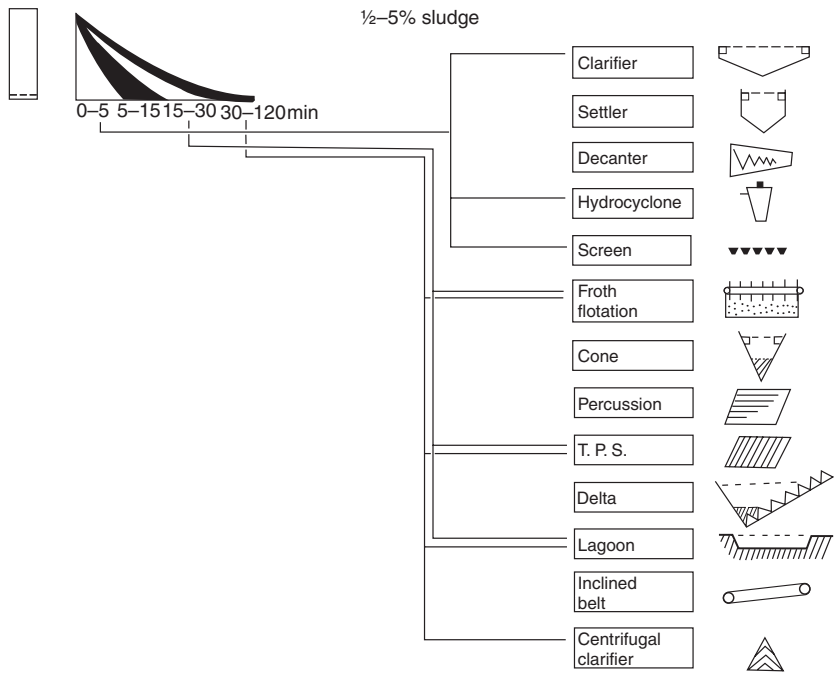

Figure 17.2 Settling times for $\frac{1}{2}$ to 5% (v/v) sludge in various types of equipment. Decanter—In this instance only a centrifugal decanter is meant. Cone—Typically a deep cone settlement system without vertical side walls. Percussion—Percussion screens or shaking tables, while originally mainly used for the classification of solids, can act as very efficient simple liquid–solid separators. Delta decanters—A truly triangular sedimentation system with a screw conveyor taking away the sludge. Particularly suitable for very fast settling coarse material

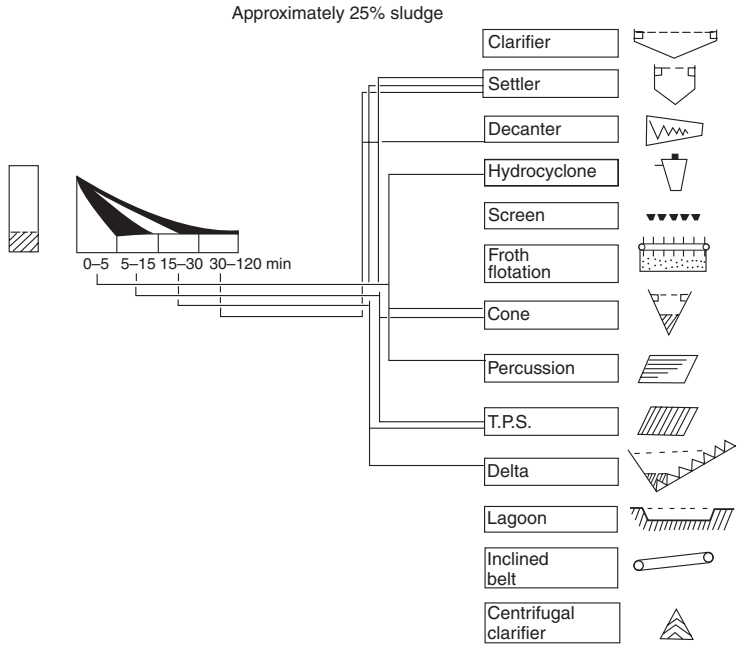

Figure 17.3 Settling times for a 25% (v/v) sludge in various types of equipment

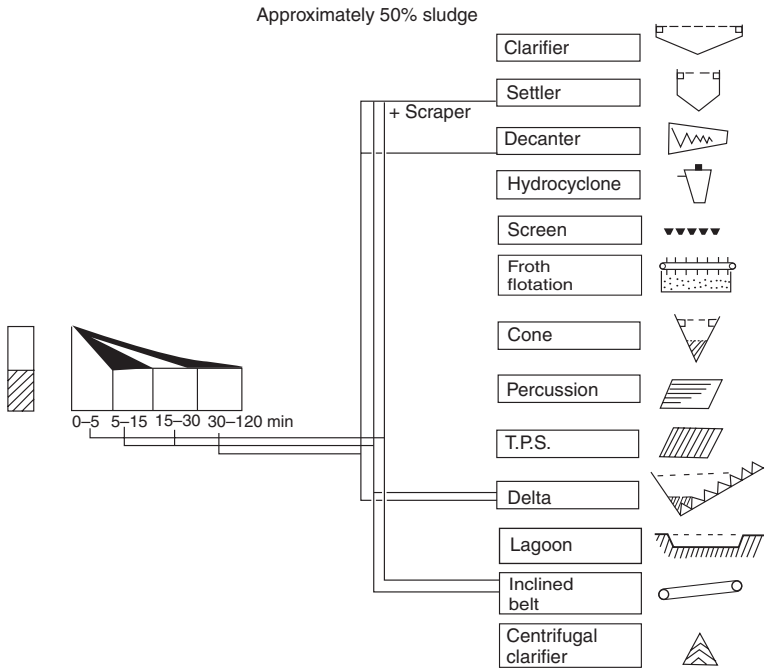

Figure 17.4 Settling times for a 50% (v/v) sludge in various types of equipment

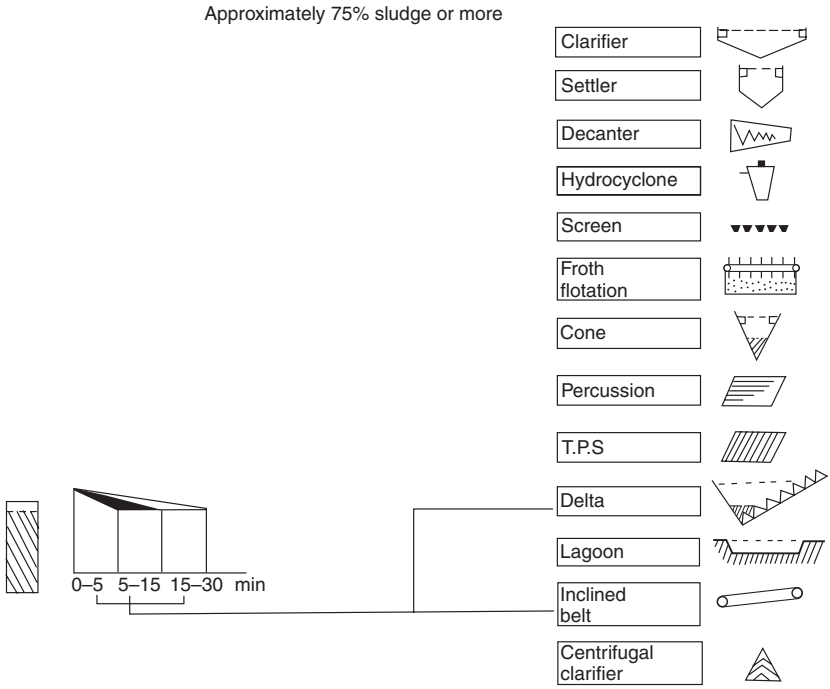

Figure 17.5 Settling times for a 75% (v/v) sludge in various types of equipment

figures are, therefore, meant purely as a short listing. Having selected a few likely groups one will then have to go further into specific design and mechanical details to see which particular type of any one group would be most suitable. That this is a task which can only be carried out successfully by an expert with an intimate knowledge of the pieces of equipment hardly requires further labouring.

Of the various groups shown two should be mentioned specifically, as they are somewhat anomalous. First of all the screen is not a sedimentation system *per se* but is listed here since there is a good chance that a slurry which behaves as indicated would also be amenable to screening, in which case this may be a preferred method. Similarly, the inclined belt, being somewhat of a hybrid, could be considered by some to be a filter using its own solid mass as a medium. The same, of course would apply for inclined vibrators.

Whereas an expert would be able to design and calculate the performance of most pieces of equipment from laboratory tests a word of warning should be sounded about centrifugally operated systems, which include hydrocyclones. In our experience these pieces of equipment are best tested on a pilot scale rather than on a laboratory scale.

17.4 Filtration equipment

Filtration is a very much more complex process than sedimentation since the large degree of design control that one has also, of course, allows a far greater number of parameters to be varied. For a true evaluation it will, therefore, be necessary to have access to a reasonably well equipped filtration laboratory. For the purpose of this chapter, however, we will review purely the short-listing and basic evaluation and assume that only the most simple laboratory equipment is available.

A prerequisite for any filtration tests is the Buchner funnel with filter flask and the filter leaf. In addition a good vacuum source is required. This should preferably be better than the simple water tap system.

Since all filtration techniques depend on passing a slurry through a septum at a pressure differential, it is clear that a basic vacuum test will in most cases at least establish filterability. It is clearly a complete method for determining the possibility of using vacuum filters and even for pressure filters the basic parameters can be plotted (*Figure 17.6*).

To establish what effect greater pressure differentials have one will have to rely on proper test equipment and, of course, the same would apply to compression filtration.

We stress that, before starting any filtration tests, the following basic principles must be adhered to:

1 *Filter medium*
Use only the material which will be used under plant conditions.
2 *Filter cloth*
If cloth is to be used remember that the wetter the cake the smoother and possibly thinner, the cloth should be.

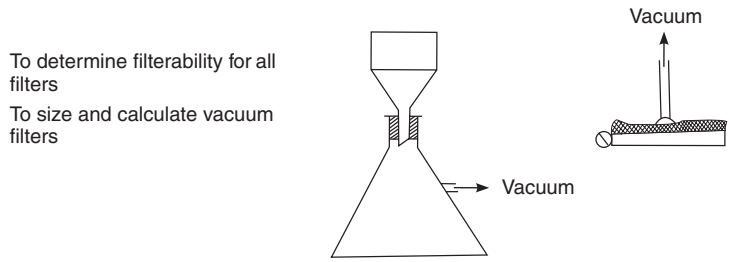

Pressure filtration	Feasibility test	Pump + strainer + cloth(s) 1. Pressure leaf 2. Single plate and frame
Compression filtration or cake compression	Feasibility test	Rolling pin or vice Hydraulic pad

Figure 17.6 Schematic illustration of basic filtration tests

3 *Actual tests*
(a) Sample must be representative.
(b) The filter area should never be less than 15 cm diameter.
(c) Test against actual cake thicknesses.

On the last point it is appreciated that formulae exist which should enable one to extrapolate from a thin cake tested under laboratory conditions to a thicker cake expected on a full scale plant. In our opinion these formulae are virtually useless.

Filters can be subdivided into numerous different groups.

A first distinction is the difference between those filters which filter through the actual cloth, paper, or screen etc. and those which filter through the cake. The cake filters have the advantage that one can normally use a support which is less prone to blinding or bleeding than for the non-cake filters, but, of course, a prerequisite is an adequate amount of solids in the feed.

A further obvious distinction is between vacuum filters (negative pressure) and pressure filters (positive pressure) (see *Figure 17.7*). As the vacuum filters are limited to a maximum practical pressure differential of about $6.8-8.2 \times 10^4\ \mathrm{Nm}^{-2}$ (10 to 12 p.s.i.), theoretically they have a lower capacity. Since most pressure filters, however, rely on a thicker cake and, therefore, a greater cake resistance, the net result is not always so much in favour of pressure filtration. It is important, therefore, actually to check these figures and not assume higher throughput with a higher pressure.

Regarding the actual cake, it must be borne in mind that the way in which the solids are applied to the screen determines to a large extent the ultimate pressure differential. It is, therefore, necessary to select a screen and a feeding

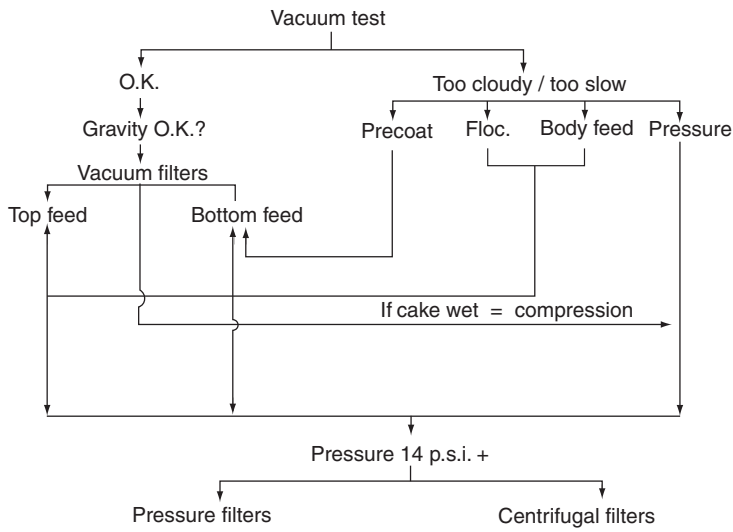

Figure 17.7 Schematic illustration of filter selection from vacuum tests

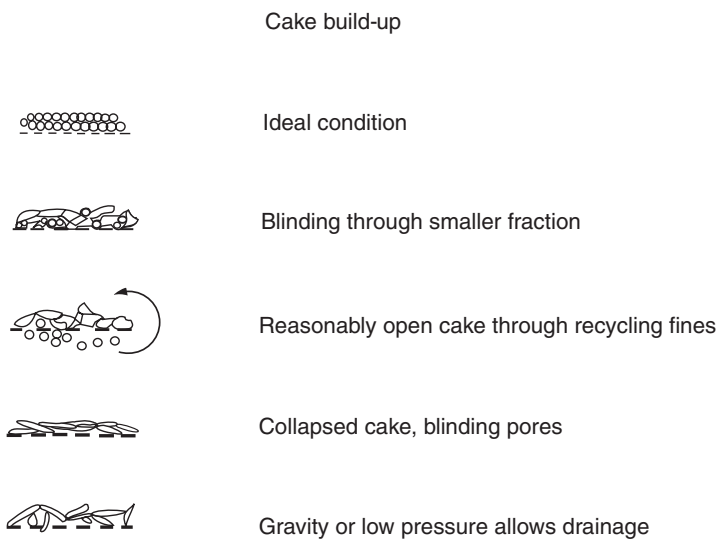

Figure 17.8 Types of cake build-up

mechanism to suit the slurry conditions. Blinding occurs in practically all filters. If the blinding occurs in the cake itself then only chemical treatment of the slurry prior to filtration or varying the pressure differentials can cure this problem. If the blinding occurs in the support screen, cloth or paper then there may be some merit in using a support with a pore size larger than that of the smallest fraction, and allowing the largest fraction first to form a bed, recycling the runnings which will contain the fine particle fraction, through the cake (*Figure 17.8*).

When the vacuum tests have been carried out and the results are known, one can use *Figure 17.7* to select likely pieces of equipment. If the vacuum tests are very successful one must first look at gravity filtration and see whether or not this would be adequate. If not, one must calculate the possibilities of using either top feed or bottom feed vacuum filters and work out the necessary costs, capital and running costs, for the particular problem.

If the vacuum tests are not successful because the rate is too slow or, if the tests are successful but the equipment for vacuum filtration would be too large or too costly, or simply because filtration is not achieved, then one has to look at four possible alternatives. These are: a bottom feed vacuum filter with precoating; flocculating the feed or adding body feed, either for bottom feed or top feed vacuum filters; or pressure filtration in all its ramifications, either with or without flocculation or body feed. In certain cases one can even look at precoating pressure filters. In this respect, of course, pressure filters can equally well be centrifugal filters, or compression filters.

Since the solids are often of importance, not only as an end product but also as a costly item to dispose of if they are not wanted, many filters are being classified by the form in which they dispose of the cake. A very broad breakdown is given in *Table 17.1*. In the table the arrows indicate whether or not the cake discharge tends to be a dry or a wet cake.

Table 17.1 Filter selection by cake quality

Dry cake	*Wet cake/sludge*	*Thin sludge/slurry*
Vacuum filters		
(Precoat rotary)*	⟵ Pressure leaf	Sand bed
Filter presses	Candle ⟶	Mixed media
Spinning leaf ⟶	Gravity ⟶	Screens
Disposable belt*		Laminar flow
Cartridge		Edge
Centrifugal filter		Reverse osmosis
Compression filter		

* Solids cannot normally be recovered

No mention of filters would be complete without reference to cake washing. Particularly with the burden of effluent costs becoming greater every day and the cost of water rising, more and more companies are being forced into better and more efficient methods of cake washing. In this respect the filter press is particularly important at present since historically it has been used extensively for cake washing applications. Whereas a filter press will give a very well washed cake in most cases it will only do so at the cost of a tremendous amount of water. Possibly for this reason many companies are looking at continuous vacuum filters and, specifically, rotary vacuum filters, for cake washing.

One must remember the great difference between a rotary drum filter and a rotary belt filter. As shown in *Figure 17.9* the loss factor, or, in other words, the area of the drum which is not used for filtration is very much greater for a belt filter than for a drum filter. This has led to many mistakes being made since rotary vacuum filters are quoted in square feet of filter area, by which the manufacturer means the total area of the drum. As can be seen from *Figure 17.9* for an identical drum circumference and face the drum filter offers a far greater effective filter area than the rotary vacuum belt filter. Or, in other words, for a given effective filtration area the rotary belt filter will have to be a larger machine than the drum filter.

A further point which is often ignored with rotary filters is the necessity to have a certain ratio between pick-up time and filtration time. *Figure 17.10* shows, for example, that in a case where the pick-up time is 60% of the total time an ordinary rotary vacuum drum or belt filter could run at, for instance,

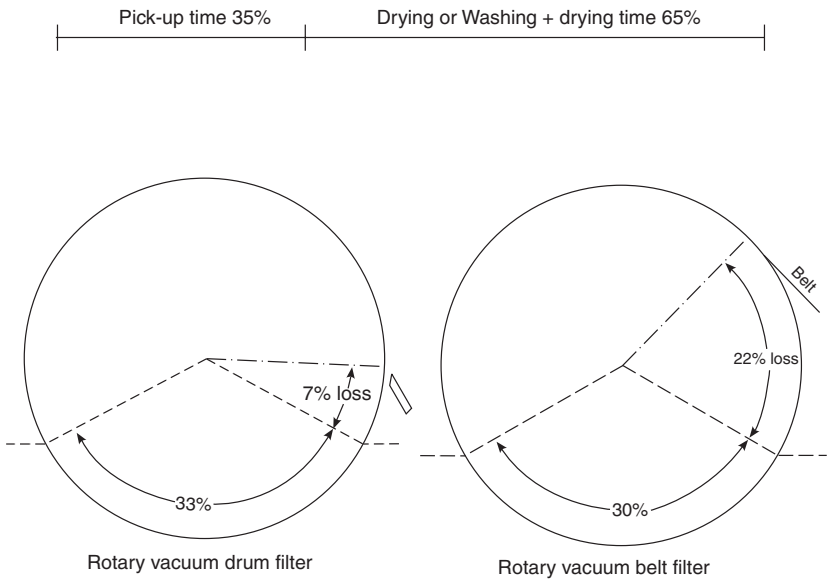

Figure 17.9 The loss factor in two types of rotary vacuum filter

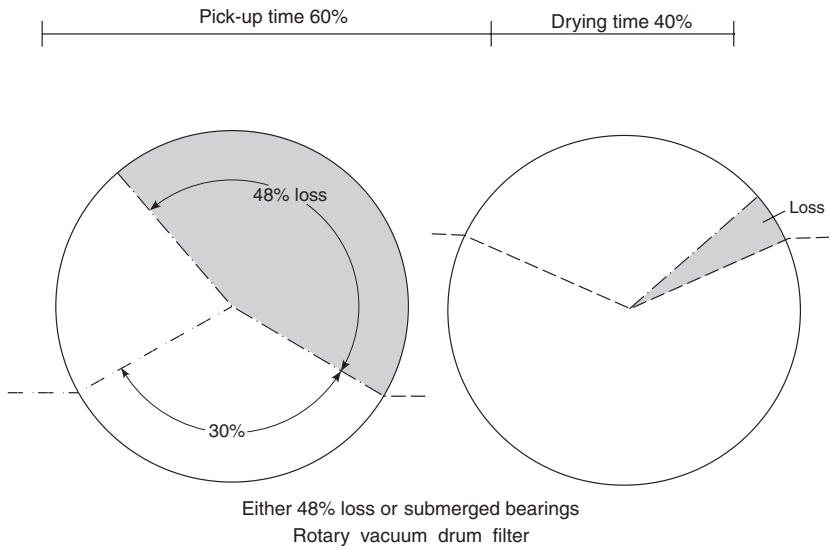

Figure 17.10 Reduction of the loss factor in a rotary drum filter with submerged bearings

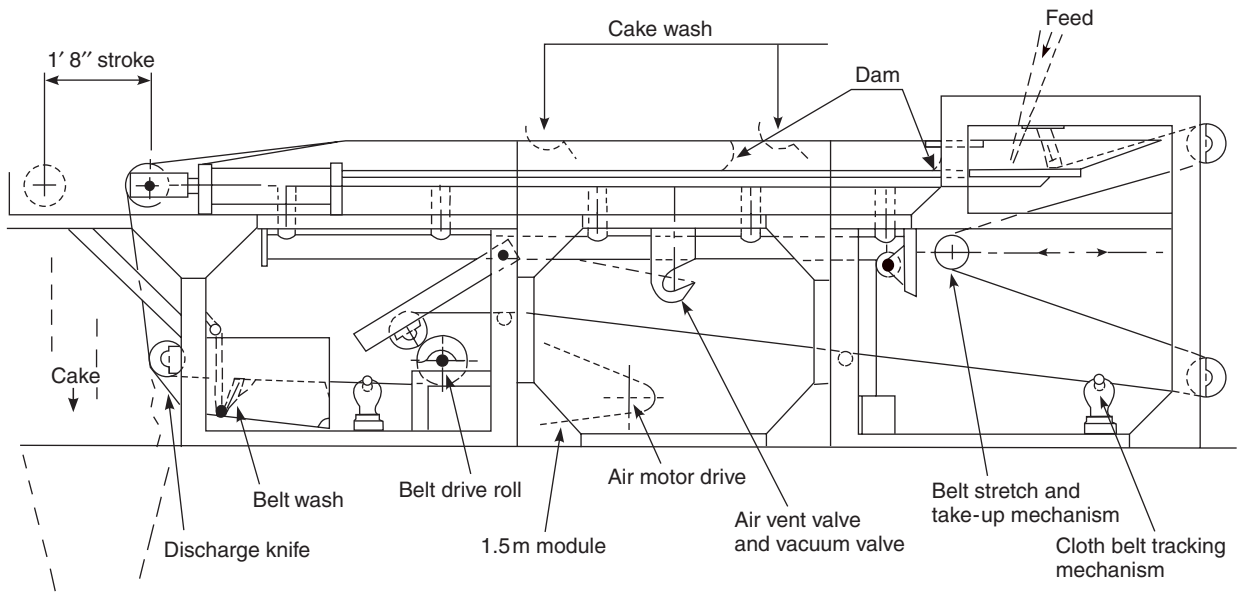

Figure 17.11 Horizontal belt filter

a 48% loss factor. This could only be reduced if one uses a machine which has submerged bearings, which is very much more expensive. Since the ratio tends to vary somewhat between various makes it must be stressed that these loss percentages may not be absolute but should be taken only as an indication.

A rotary vacuum filter, therefore, requires very careful selection and a very careful study before a decision is made. If one wishes to wash with a rotary vacuum filter then the problem is even more aggravated since the natural configuration of the filter does not present a very good surface for washing. This, in itself, can again alter the ratio and it is not uncommon to find that one is reduced either to using two or three filters, or to using machines which are vastly larger than the theoretically required filter area.

These problems do not exist in the horizontal belt filter, of which in the last few years quite a number of very successful machines have been introduced. This filter is basically constructed as an endless belt so it does not have the same dead time factors, is not affected by differences between cake formation and drying time, and in all cases presents a far better washing surface than a rotary filter (see *Figure 17.11*). If one wishes to take cake washing to the ultimate efficiency then one must consider countercurrent washing, which is virtually only possible on a belt filter or any other type of filter which has a continuous horizontal filter surface such as, for instance, the rotary tipping pan (see *Figure 17.12*).

With a growing interest in energy conservation, it is obvious that more and more filters will be required which produce cakes of the greatest possible dryness. For this purpose membrane pressure filters tend to be the best solution. Semi-automatic and automatic units are available. Since they all rely on a flexible membrane the limiting factor appears to be more in the choice of rubber than anything else. It is important to remember, however, that if cake washing has to be carried out prior to ultimate drying the membrane press can be a disadvantage since the very compacting of the cake which frequently occurs quite often prevents effective cake washing.

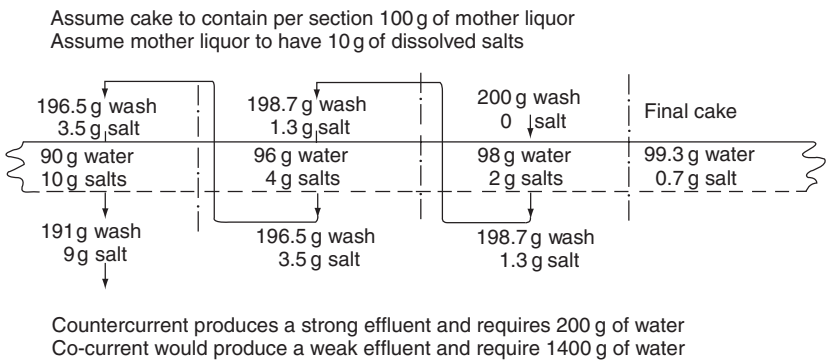

Figure 17.12 Countercurrent washing on a horizontal filter

This chapter attempts to do nothing more than to give a very broad outline of the possibilities, and above all the limitations, of different groups of equipment. We hope that it will enable the chemical engineer to make, relatively quickly, an approximate choice of equipment in order to assess whether or not a given project is financially effective. The ultimate selection and final design of the complete plant can only be made after a very detailed study of the problem as a whole and of the individual pieces of equipment which are short-listed.

17.5 A note from the editor

This excellent and very practical chapter from H. G. W. Pierson, although originally written some years ago, is still of great value today. The subject lends itself well to computerization in an expert system and, indeed, many such developments have taken place since the advent of the generic program in the 1980s, see below. None of that has challenged, however, the appeal and applicability of advice like that given in this chapter, by a practitioner well skilled in communicating the essentials.

The very first expert system for selection of equipment for solid–liquid separation was designed (and since then marketed) by Fine Particle Software in 1985[1]. It has been part of a suite of computer programs given to each participant of an annual short course on Solid–Liquid Separation in the *Course Manual*, out of which this book has grown. Since 1985, several other companies and universities have designed their own expert systems, some of which go further than just producing a shortlist of possibly suitable hardware but actually lead to sizing of equipment on the basis of the results of specialized tests carried out by the program user. ICI, for example, designed their own in-house expert system[2,3], so have the University of Lappeenranta in Finland[4] and the University of Exeter in the UK[5,6,7]. No doubt others exist unknown to the editor.

Expert systems in solid–liquid separation have now gone out of fashion somewhat and the pre-selection of equipment now tends to be built into much larger design software. In any case, computerized advice, although helpful to complete beginners as a first approach, is no substitute for experience and in-depth knowledge of the subject.

References

1. 'Equipment selection in solid–liquid separation, a simple expert system', *Catalogue of In-Company Short Courses, Books and Particle Technology Software*, Fine Particle Software, The Lares, Maple Avenue, Cooden, Bexhill-on-Sea, TN39 4ST (2000), also on website: http:/ /members.aol.com/lsvarovsky/
2. Cardew, P. and Jones, S., 'Equipment selector's crystal ball', *The ICI Engineer*, Issue 10, Autumn, 23 (1989)

3. McBriar, I., 'SLS Advisor—New release', *The ICI Engineer*, Issue 15, May, 19 (1992)
4. Nystrom, L. and Oja, M., 'Expert systems for method and equipment selection', Centre for Separation Technology, University of Lappenranta, research topics on website: http:/ /www.lut.fi/research_fields.htm#tesu, email: Lars.Nystrom@lut.fi
5. Wakeman, R. J. and Tarleton, E. S., 'Solid/liquid separation equipment simulation and design—an expert systems approach', *Filtration & Separation*, July/August, **29**(4), 268–274 (1991)
6. Wakeman, R. J., 'Selection of equipment for solid/liquid separation processes', *Filtration & Separation*, April, 337–341 (1995)
7. Tarleton, E. S. and Wakeman, R. J., 'A philosophy for the selection, scale-up and process simulation of filters,' Proceedings Volume II, World Filtration Congress 8, European Federation of Chemical Engineering Event No. 607, organised by The Filtration Society and Elsevier Science, The Brighton Centre, Brighton, UK, 3–7 April 2000, 747–750 (2000)

18

Particle–fluid interaction, thermodynamics of solid–liquid separation Part I—Particle–fluid interaction

L. Svarovsky

FPS Institute, England and University of Pardubice, Czech Republic

Nomenclature

A	Projected area of a particle facing the flow; or the face area of a packed bed
C, c	Solids concentration
C_1	Minimum solids concentration at which zone settling occurs
C_D	Particle drag coefficient
$f(\epsilon)$	Function of voidage (voidage function)
F_D	Drag force on a particle
g	Gravity acceleration
G	Separation factor (number of gs)
K	Permeability of a packed bed
L	Depth of a packed bed
m	Particle mass
Q	Volumetric flow rate
R	Radius of particle position; or medium resistance
R_o	Initial radius of particle position
Re	Reynolds number for the flow in a packed bed
Re_p	Particle Reynolds number
S_o	Volume-specific surface of the bed
t	Time
u	Particle–fluid relative velocity
u_c	Terminal settling velocity in a centrifuge
u_g	Terminal settling velocity under gravity
v	Superficial velocity in a packed bed
V	Filtrate volume collected

w	Angular speed
x	Particle size
x_c	Top size limit in a centrifuge
x_g	Top size limit under gravity
x_{sv}	Mean particle size in a packed bed
α	Specific cake resistance
Δp	Static pressure drop across a packed bed
ϵ	Voidage of a packed bed
μ	Liquid viscosity
ρ	Liquid density
ρ_s	Solid (particle) density
τ	Particle relaxation time

18.1 Introduction

This chapter reviews some fundamentals on which much of the rest of this book is based. Particle–fluid interaction (Part I), whether in suspensions or in packed beds, plays an important role both in sedimentation and in filtration. Thermodynamics underlie it all, of course, and Part II of this chapter gives an overview of the practical help that thermodynamics can offer in this subject.

18.2 Motion of particles in fluids

In this first section, the fundamentals of particle–fluid interaction are reviewed, with particular emphasis on the concepts used in scale-up of equipment in particle–fluid separation.

If a particle moves relative to the fluid in which it is suspended, there exists a force opposing the motion, known as the drag force. Knowledge of the magnitude of this force is essential if the particle motion is to be studied. The conventional way to express the drag force, F_D, is according to Newton:

$$F_D = C_D \cdot A \cdot \frac{\rho u^2}{2} \tag{18.1}$$

where u is the particle–fluid relative velocity, ρ is the fluid density, A is the area of the particle projected in the direction of the motion and C_D is a coefficient of proportionality known as the drag coefficient. Newton assumed that the drag force is due to the inertia of the fluid and that C_D would then be constant.

Dimensional analysis shows that C_D is generally a function of the particle Reynolds number:

$$\frac{u \cdot x \cdot \rho}{\mu} = \mathrm{Re}_p \tag{18.2}$$

(where x is particle size) and the form of the function depends on the regime of the flow. *Figure 18.1* shows this relationship for rigid spherical particles in

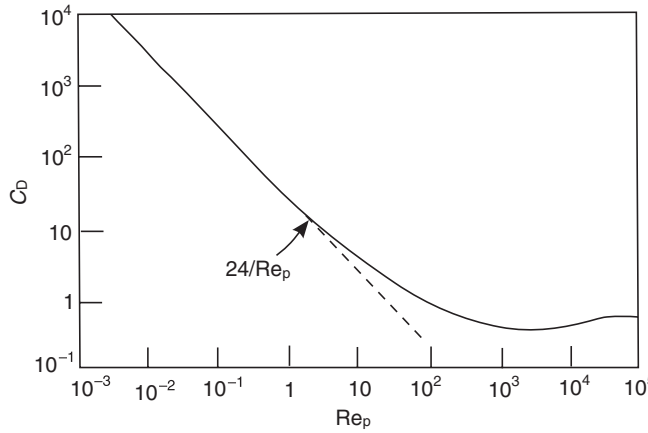

Figure 18.1 Drag coefficient versus particle Reynolds number for spherical particles

a log–log plot. At low Reynolds numbers, under laminar flow conditions when viscous forces prevail, C_D can be determined theoretically from Navier–Stokes' equations and the solution is known as Stokes' law:

$$F_D = 3\pi\mu ux \tag{18.3}$$

This is an approximation which gives best results for $Re_p \rightarrow 0$; the upper limit of its validity depends on the error which can be accepted. The usually quoted limit for Stokes' region of $Re_p = 0.2$ is based on the error of approximately 2%.

Elimination of F_D between equations 18.1, 18.2, and 18.3 gives another form of Stokes' law:

$$C_D = \frac{24}{Re_p} \quad (Re_p < 0.2) \tag{18.4}$$

and this is shown in *Figure 18.1* as a straight line. For Reynolds numbers greater than about 1000, the flow is fully turbulent with inertial forces prevailing and C_D becomes constant and equal to 0.44 (Newton's region). The region in between $Re_p = 0.2$ and 1000 is known as the transition region and C_D is either described in a graph or by one or more empirical equations.

In solid–fluid separation, the greatest concern is with the fine particles which are most difficult to separate. This means that Re_p is low, almost inevitably less than 0.2 due to low values of x and u and, therefore, only the Stokes region need be considered here.

18.2.1 Gravity settling at low concentrations

A single particle settling in a gravity field is subjected primarily to drag force, gravity force and buoyancy, which have to be in equilibrium with the inertial

force, i.e.

$$\underset{\text{inertial force}}{m\frac{\mathrm{d}u}{\mathrm{d}t}} = \underset{\text{gravity force}}{m \cdot g} - \underset{\text{buoyancy}}{m\frac{\rho}{\rho_s}g} - \underset{\text{drag force}}{F_D} \tag{18.5}$$

(taking the downward forces as positive), where m is the particle mass, g is the acceleration due to gravity, ρ_s is particle density and t is time.

If equation 18.5 is divided by m and Stokes' law in equation 18.3 is introduced for F_D, the following equation of motion is obtained:

$$\frac{\mathrm{d}u}{\mathrm{d}t} = g \quad \frac{\rho_s - \rho}{\rho_s} - \frac{u}{\tau} \tag{18.6}$$

where the constant $\tau = m/3\pi\mu x$ is known as the particle relaxation time and is for spherical particles

$$\tau = \frac{x^2\rho_s}{18\mu} \tag{18.7}$$

Equation 18.6 can be solved with the following result:

$$u(t) = \frac{\rho_s - \rho}{\rho_s}\tau \cdot g\left(1 - \exp\left(\frac{-t}{\tau}\right)\right) \tag{18.8}$$

This is an exponential relationship which with increasing time, t, approaches

$$u_g = \left(\frac{\rho_s - \rho}{\rho_s}\right)\tau g \tag{18.9}$$

and this is known as the terminal settling velocity under gravity. Equation 18.9 can also be written as:

$$u_g = \frac{x^2(\rho_s - \rho)g}{18\mu} \tag{18.10}$$

by elimination of τ using equation 18.7.

It can be shown that the terminal velocity is in the case of fine particles approached so fast that in practical engineering calculations the settling is taken as a constant velocity motion and the acceleration period is neglected. This is shown in the following example.

Example 18.1

Determine the time in which a solid particle of 5 μm diameter and a density of $2500\,\mathrm{kg\,m^{-3}}$ will reach 99% of its terminal settling velocity when falling under gravity from a stationary position, in water of viscosity $\mu = 0.001\,\mathrm{Ns\,m^{-2}}$.

Solution

Assuming Stokes' law, equations 18.8 and 18.9 give:

$$\frac{u(t)}{u_g} = \left(1 - \exp\left(\frac{-t}{\tau}\right)\right) \tag{18.11}$$

and this has to be equal to 0.99 to find the time t_{99}. Particle relaxation time is, from equation 18.7,

$$\tau = \frac{(5 \times 10^{-6})^2 \times 2500}{18 \times 0.001} = 3.472 \times 10^{-6}\,\text{s}$$

and the time from equation 18.11 for $u(t)/u_g = 0.99$

$$t_{99} = -\tau \ln 0.01 = 0.016 \times 10^{-3}\,\text{s}$$

Checking Re_p for Stokes' region requires knowledge of the instantaneous particle velocity at the time $u(t_{99})$ and, from equation 18.8, this is

$$\begin{aligned} u(t_{99}) &= 0.99 \times u_g \\ &= 0.99\,\frac{\rho_s - \rho}{\rho_s}\,\tau \cdot g \\ &= 0.99\,\frac{1500}{2500} \times 3.472 \times 10^{-6} \times 9.81 \\ u(t_{99}) &= 20.23\,\mu\text{m}\,\text{s}^{-1} \end{aligned}$$

and the particle Reynolds number at t_{99} is then from equation 18.2:

$$\text{Re}_p(t_{99}) = \frac{20.23 \times 10^{-6} \times 5 \times 10^{-6} \times 1000}{0.001} = 1.012 \times 10^{-4} < 0.2$$

This is, of course, well within the Stokes' region. Note that for a particle ten times larger, i.e. 50 μm, both t_{99} and $u(t_{99})$ increase by a factor of 10^2 for 1.6×10^{-3} s and $20.23 \times 10^{-4}\,\text{m}\,\text{s}^{-1}$ respectively, and $\text{Re}_p = 0.1012$ which is still in the Stokes' region.

It is obvious from this example that the times needed for acceleration to a velocity which is very close to the terminal settling velocity are very short indeed and negligible for practical purposes.

Equation 18.10 is the basis of simple scale-up calculations for non-flocculent systems within the restrictions of Stokes' law. It can also be applied to non-spherical particles provided that the size is measured by sedimentation which leads to the equivalent Stokes' diameter.

It should be pointed out that there is also a bottom limit of particle size (usually about 1 μm) below which Stokes' law cannot be assumed to apply in gravity sedimentation. This is due to Brownian diffusion which becomes significant below 1 μm and leads to settling rates lower than those predicted by Stokes' law.

18.2.2 Hindered settling at high concentrations

As the concentration of the suspension increases, particles get closer together and begin to interfere with each other. If the particles are not distributed uniformly the overall effect is a net increase in settling velocity because the return flow due to volume displacement will predominate in particle sparse regions. This is the now well-known effect of cluster formation which is only significant in nearly mono-sized suspensions. With most practical, widely dispersed suspensions clusters do not survive for long enough to affect the settling behaviour and, as the return flow is more uniformly distributed, the settling rate steadily declines with increasing concentration. This is referred to as hindered settling and can be theoretically approached from three starting premises:

1 as a Stokes' law correction by introducing a multiplying factor;
2 by adopting 'effective' fluid properties for the suspension, different from those of the pure fluid;
3 by determining the bed expansion from a modified Carman–Kozeny equation.

The three approaches above yield essentially identical results in the form

$$\frac{u_p}{u_g} = \epsilon^2 f(\epsilon) \tag{18.12}$$

where u_p is the hindered settling velocity of a particle, u_g is the terminal settling velocity of a single particle as calculated from Stokes' law (equation 18.1), τ is the volume fraction of the fluid (voidage), and $f(\epsilon)$ is a 'voidage function' which for Newtonian fluids have different forms depending on the theoretical approach adopted. The differences between the available expressions for $f(\epsilon)$ are not great and are frequently within experimental accuracy. The most important forms are as follows:

(i) from the Carman–Kozeny equation (see section 18.3.1)

$$f(\epsilon) = \frac{\epsilon}{10(1-\epsilon)} \tag{18.13}$$

(ii) from Brinkman's theory[1] applied to Einstein's viscosity equation[2]:

$$f(\epsilon) = \epsilon^{2.5} \tag{18.14}$$

and (iii) from the well-known Richardson and Zaki equation[3]

$$f(\epsilon) = \epsilon^{2.65} \tag{18.15}$$

For irregular or non-rigid particles (e.g. flocs) the Einstein constant (2.5) and the Richardson and Zaki exponent (2.65) can be considerably larger than for spheres.

Strictly speaking, the above correlations apply only to the cases when flocculation is absent, such as with coarse mineral suspensions. Suspensions of fine particles, due to the very high specific surface of the particles, often flocculate and therefore show different behaviour. With increasing concentration of such suspensions at a particular concentration C_1, an interface can be observed and this becomes sharper at $C > C_1$. The slurry is then said to be in the zone settling region. The particles below the interface, if their size range is not more than 6:1, settle 'en masse', i.e. all settle at the same velocity irrespective of their size. There are two possible reasons for this: either the flocs become of similar size and settle at the same velocity or the flocs are locked into a loose plastic structure and thus sweep down as a 'web'. Interestingly enough the settling rates of the interface (and of the solids below it) of many practical suspensions can still be described by the Richardson and Zaki equation but the value of u_g must be determined by extrapolating the experimental log–linear plot for $\epsilon = 1$. The value of this intercept has in fact been used for the indirect size measurement of the flocs. The slope of the plot determines the exponent.

The concentration C_1 at which zone settling can first be observed depends very much on the material and its state of flocculation and no guidance can be given on this. Addition of flocculation (or dispersing) agents drastically changes this concentration and its value can only be determined by experimental evaluation. If the concentration is increased further still, a point is reached when the flocs become significantly supported mechanically from underneath as well as hydraulically and the suspension is then known to be in compression or compression settling. The solids in compression continue to consolidate and the rate of consolidation depends not only on the concentration but also on the structure of the solids which, in turn, depends on the pressure and flow conditions. This is a very complex problem closely related to cake filtration and the mechanical squeezing of cakes. For intermediate concentrations between those of zone settling and fully established uniform compression there is sometimes also a phenomenon called channelling which particularly occurs in slowly raked large-scale thickeners. Under these conditions a coarser structure of pores becomes interconnected in the forms of channels.

Most authors who have studied the consolidation process of solids in compression have used the basic model of a porous medium with point contacts which yields a general form of the mass and momentum balances. This must be supplemented by a model describing filtration and deformation properties. Probably the best model to date is that of Kos[4], which uses two parameters to define the characteristic behaviour of suspensions. His model can potentially be applied to four processes: sedimentation, thickening, cake filtration and expression.

18.2.3 Centrifugal sedimentation at low concentrations

Particle terminal settling velocity under centrifugal acceleration can be calculated from Stokes' law by substituting g in equation 18.1 by Rw^2 (where w is the angular speed and R is the radius of particle position) and the same assumptions apply as under section 18.2.1. There is one important difference here however: particle motion is no longer at constant velocity but as the particles move radially outwards they are continuously accelerated (Rw^2 increases). Similarly as under gravity, particle inertia is neglected and the particles are always assumed to move at their respective terminal velocities; this is an acceptable assumption in most practical cases. The top size limit of acceptability of Stokes' law is reduced here due to higher accelerations. It can be shown that if a separation factor G is defined as a number of gs, i.e.

$$G = \frac{Rw^2}{g} \tag{18.16}$$

then the top size limit of Stokes' law, x_c, for a centrifuge can be calculated from the limiting size under gravity x_g

$$x_c = x_g / \sqrt[3]{G} \tag{18.17}$$

Under gravity acceleration the distance covered by a particle in a given time is simply $U_g t$; under centrifugal acceleration (as the motion is accelerated) the following expression is obtained from integration of the terminal velocity expression

$$u_c = \frac{dR}{dt} = \frac{x^2 \Delta\rho R w^2}{18\mu} \tag{18.18}$$

from R_o (the initial radius) to R (radius after time t):

$$\frac{R(t)}{R_o} = exp \frac{x^2 \Delta\rho w^2 t}{18\mu} \tag{18.19}$$

The settling time of a given particle size x from R_o to R can be calculated from the above equation.

18.2.4 Centrifugal sedimentation at high concentrations

Centrifugal sedimentation at high concentrations is not hindered as much as in the case of gravity sedimentation because higher concentrations exist within the settling suspension only for a fraction of the total settling time rather than for all the time as under gravity. This is due to the continuous dilution effect: as particles settle radially they spread out and thus the concentration at a given radius falls steadily with time. However, the settling is still hindered, if only for some time, from the start and this has to be taken into account as it prolongs the settling times. Surprisingly, this effect was neglected until relatively recently, when Baron and Wajc[5] published a full study of the effect.

They concluded that some settling in the centrifugal field leads to much the same behaviour as under gravity, i.e. to the formation of a visible interface between the supernatant liquid and the settling suspension, and that the concentration below the interface is the same right down to the sediment level. However, this concentration is not constant but decreases with time because of the above-mentioned dilution effect, until it comes out of the zone settling regime and the interface ceases to be visible. The total settling times are naturally much longer than those obtained at lower concentrations. The analysis derived by Baron and Wajc is much too complicated to be reported here, but the important feature of it is that it uses the experimental settling flux curve obtained under gravity which, in principle, allows scale-up of sedimenting centrifuges from gravity experiments. Further development in this area is anticipated.

18.3 Flow through packed beds

18.3.1 Carman–Kozeny equation and its limitations

Flow through packed beds under laminar conditions can be described by a model in which the flow is assumed to be through capillaries whose surface equals that of the solids comprising the bed. The capillary volume is set equal to the void volume of the bed. The model leads to the well-known Carman–Kozeny equation[6] as follows:

$$\frac{Q}{A} = \frac{\Delta p}{\mu L} \frac{\epsilon^3}{5(1-\epsilon)^2 S_o^2} \tag{18.20}$$

where Q is the volumetric flow rate, A is the face area of the bed, L is the depth of the bed, Δp is the applied pressure drop, ϵ is the voidage of the bed (porosity), S_o is the volume-specific surface of the bed, and μ is the liquid viscosity.

The constant 5 is valid for lower porosity ranges and particles not too far from spherical in shape; it generally depends on particle size, shape and porosity. Unfortunately, although the above equation has been found to work reasonably well for incompressible cakes over narrow porosity ranges, its importance is limited in cake filtration because it cannot be used for most practical compressible cakes. Its value is mostly in illustrating the high sensitivity of the pressure drop to the cake porosity and to the specific surface of the solids. A major criticism of the Carman–Kozeny equation is that it incorrectly tends to infinity when the voidage approaches 1.

18.3.2 Darcy's law and the basic cake filtration equation

Darcy's law[7] combines the constants in the last term of equation 18.20 into one factor, K, known as the permeability of the bed, which is a constant

$$K = \frac{\epsilon^3}{5(1-\epsilon)^2 S_o^2} \tag{18.21}$$

for incompressible solids, but for compressible cakes it depends on the applied pressure, the approach velocity, and the concentration and, therefore, it presents serious problems in cake filtration testing and scale-up. There are some materials such as highly flocculated beds for which the above linear relationship between the face velocity and pressure drop does not hold and the flow is then called non-Darcian.

The modern filtration theory tends to prefer the Ruth form of Darcy's law as:

$$\frac{Q}{A} = \frac{\Delta p}{\mu R} \tag{18.22a}$$

where R is known as the bed resistance. In cake filtration the bed resistance consists of the medium resistance in series with the resistance of the deposited cake (assuming no penetration of solids into the filtration medium) and the general filtration equation is then written as:

$$\frac{Q}{A} = \frac{\Delta P}{\alpha \mu \frac{cV}{A} + \mu R} \tag{18.22b}$$

where α is the specific cake resistance, μ is the liquid viscosity, c is the solids concentration in the feed, V is the filtrate volume collected since the commencement of filtration, and R is the medium resistance. This equation is the basis of cake filtration analysis. The feed liquid flow rate and filtrate volume, V, are usually assumed to be related as,

$$\frac{\mathrm{d}V}{\mathrm{d}t} = Q \tag{18.23}$$

There is a hidden assumption in the above relationships that the volume of the solids and the liquid retained in the cake is negligible. This is reasonable at low concentrations but can lead to errors at higher solids concentrations and moisture contents of cakes. The usual way to correct for this is by using a 'corrected' value of the concentration, c, in equation 18.22b.

18.3.3 Alternatives to the Carman–Kozeny equation

As was briefly pointed out in section 18.3.1, the Carman–Kozeny equation does not work well towards the limit of $\epsilon = 1$; Carman[6] himself stated that the equation should not be used for $\epsilon > 0.8$. Several researchers have attempted to derive a model with a more realistic and general outcome. Perhaps the most significant attempt is that by Rudnick[8] who used a free-surface cell model by Happel[9] in which each particle is assumed to be a sphere at the centre of a cell, the volume of which is such that the porosity of each cell is the same as that of the bed. If the tangential stresses at the boundaries of adjoining cells are set to zero, an exact solution of the general Navier–Stokes' equations exists, assuming that the inertial terms are negligible.

The solution leads to an equation similar to the Carman–Kozeny equation (18.20) except that the term

$$\frac{\epsilon^3}{(1-\epsilon)^2}$$

is now replaced by a more complicated one of ϵ, as follows:

$$10\frac{3.45(1-\epsilon)^{1/3}+4.5(1-\epsilon)^{5/3}-3(1-\epsilon)^2}{3(1-\epsilon)+2(1-\epsilon)^{8/3}} \tag{18.24}$$

The two equations compare favourably in the lower porosity range, say below 0.6, but the Rudnick equation predicts correctly finite flow rates through very highly porous beds.

18.3.4 Ergun equation

With increasing Reynolds number, the flow in some of the passages in the bed becomes turbulent, the Carman–Kozeny equation is no longer valid and must be corrected by adding a turbulent term. In turbulent flow, the pressure drop is no longer proportional to the flow velocity but increases with the square of the velocity. As a part of the flow in the bed, in the smaller passages, is still laminar, the overall pressure drop is a sum of two components, laminar and turbulent.

The laminar term is derived from the Carman–Kozeny equation (equation 18.20)

$$\frac{\Delta p}{L} = 5\frac{Q}{A}\mu\, S_o^2\frac{(1-\epsilon)^2}{\epsilon^3} \tag{18.25}$$

whilst the turbulent term, derived using a similar model, is

$$\frac{\Delta p}{L} = 0.292\left(\frac{Q}{A}\right)^2\rho S_o\frac{1-\epsilon}{\epsilon^3} \tag{18.26}$$

The two terms combined lead to the well-known Ergun[10] equation in the following form:

$$\frac{\Delta p}{L} = 4.17\frac{Q}{A}\mu S_o^2\frac{(1-\epsilon)^2}{\epsilon^3} + 0.292\left(\frac{Q}{A}\right)^2\rho S_o\frac{1-\epsilon}{\epsilon^3} \tag{18.27}$$

where the constant of 5 in the Carman–Kozeny term becomes 4.17 in the Ergun equation. Equation 18.27 is often written in a form where specific surface S_o is replaced by $6/x_{sv}$ where x_{sv} is the mean surface volume diameter of the particles making up the bed. This step is not always necessary, however, and it involves an assumption that the particles are spherical; it is best, whenever possible, to use the actual (measured) specific surface of any real particle system.

The relative importance of the two terms in equation 18.27 depends on the Reynolds number which describes the flow in the passages in the bed. This may be defined using x_{sv} as the mean particle size in the bed:

$$\mathrm{Re} = \frac{v x_{sv} \rho}{\mu} \tag{18.28}$$

where v is the superficial velocity equal to Q/A with A being the face area of the bed. For Re less than about 1, the second (turbulent) term in equation 18.28 becomes negligible compared with the first, whilst for Re greater than about 1000 the turbulent flow term dominates.

Highly turbulent flow in fixed beds is only possible, however, if the bed is constrained so that the individual grains within it cannot move. If the bed is not constrained and the flow through it is upwards, the bed becomes fluidized.

18.4 Particles in non-Newtonian liquids

This chapter up to now has been about the so-called Newtonian liquids, which have a constant viscosity dependent only on temperature. Particle processing or separation can also take place in non-Newtonian liquids or slurries, where the viscosity may change with the rate of shear and sometimes also with time, and the model may contain a zero shear viscosity as a parameter. Such liquids are handled, for example, in plastics and synthetic fibre manufacture, in polymer processing, in enhanced oil recovery, in biochemistry and biotechnology, and in petrochemicals. Particle–fluid interaction in such liquids has only been studied in the past 30 years or so and much fundamental research is still going on. A short reference to some of the latest work is given in the following, with references quoted for the reader to follow up any specific interests. The topic is divided into three sections, concerned with gravity settling of individual or dilute particles, settling of slurries and flow through packed and fluidized beds.

18.4.1 Gravity settling of individual or dilute particles

As for settling of single particles in Newtonian liquids, the fundamental hydrodynamic characteristic for particle motion in non-Newtonian fluids is again the drag coefficient. Its prediction allows calculations of terminal settling velocities. Note that equation 18.10, which applies to low particle concentrations (below 0.5% by volume) in Newtonian liquids at low Reynolds numbers, can, in principle, also be used non-Newtonian fluids where viscosity μ then becomes the apparent viscosity but, depending on the type of the non-Newtonian behaviour (=model), its determination may require an iterative procedure. Each model redefines the particle Reynolds number so that, for example, for a power law fluid characterized by constants n and K

(i.e. when shear stress τ and rate of shear γ are related as $\tau = K\gamma^n$) equation 18.2 becomes $\mathrm{Re}_p = x^n u^{2-n}\rho/K$.

Prior to 1993 the results of theoretical and experimental studies on the flow of non-Newtonian fluids past a sphere have been reviewed by Chabra[11]. Since then a number of research studies have been published, most notably by Machac and co-workers at the University of Pardubice[12–15]. They investigated experimentally the drag coefficients and settling velocities of spherical particles in power law and Herschel–Bulkley model fluids[12], in Carreau model fluids (spherical in ref. 13 and non-spherical in ref. 14) and also the effect of the wall in a rectangular cell, for power law fluids[15].

18.4.2 Settling of slurries

Chabra *et al.*[16] have shown that the Richardson and Zaki equation (represented by equations 18.12 and 18.15) can be used for prediction of sedimentation velocities with power law fluids in the range of flow index $0.8 \leq n \leq 1$. This was to some extent confirmed by an experimental investigation using a conductivity meter[17] although much larger discrepancies were found than for Newtonian fluids, attributed to the observed development of local non-homogeneities.

The main two currently available general models for the relative motion between a fluid and an assembly of spherical particles are the cell model[17] and the capillary model[18]. Both of these models, however, assume a uniform spatial distribution of particles and their application is based on the use of various viscosity models. In practice, however, non-homogeneous or aggregative sedimentation has been observed[20,21] which renders these models invalid. The intensity and duration of the non-homogeneities observed experimentally (by image analysis) depended on the initial solid concentration and on the rheological properties of the liquid. Aggregative sedimentation was found to prevail at low initial solids concentrations and was enhanced by increasing pseudoplasticity and elasticity of the liquid[20,21].

18.4.3 Flow through packed and fluidized beds

As the use of non-Newtonian fluids in industry is increasing, the interest and research in the fundamentals of flow through packed and fluidized beds for non-Newtonian fluids are also growing. The latest example is the recent work of Machac and co-workers on purely viscous[22] and viscoelastic[23] fluids. The application of their work to cake filtration is discussed in section 9.9 of chapter 9.

The most fundamental and also practical tasks in fluidization are to describe the transition from a fixed bed to a fluidized bed, and to predict the fluidized bed expansion as a function of the flow rate and of the rheological behaviour of the fluid. For the fluidization with Newtonian liquids, the bed expansion is usually well described by the Richardson and

Zaki equation (represented by equations 18.12 and 18.15 where u is the superficial velocity in the bed). This means that the plot of $\log(\epsilon)$ vs $\log(u/u_t)$ is linear. In non-Newtonian liquids, however, this plot has been found not always linear and the anomaly is called 'a fall of expansion rate'. In this context the expansion rate is the ratio characterizing the slope of the above-mentioned plot, i.e. $\mathrm{d}\log\epsilon/\mathrm{d}\log u$, and this falls off with increasing superficial velocity u. Mikulasek[24] and Machac *et al.*[25] studied this phenomenon for polymer solutions, suspensions of china clay and Boger fluids (elastic fluids with constant viscosity such as starch sugar syrup) and found that the shape of the expansion curves differed according to the liquid used. The most pronounced anomalies were observed for shear thinning and simultaneously elastic polymer solutions. The fall of the expansion rate is evidence of a reduction of the bed resistance coefficient due to the changes of the flow pattern caused by anomalous flow properties of polymer solutions. The fluidization becomes unstable with increasing flow rate, and channelling and particle circulation occurs in the bed.

The transition from a fixed bed into a fluidized bed state and the expansion of spherical particle beds fluidized with polymer solutions were investigated in creeping and transient flow regions[25]. Empirical equations based on the Carreau viscosity model were suggested for predicting bed expansion and for estimating maximum voidage of the expanded beds. The reduction of expansion weakens with the increasing Reynolds number. When a critical value of Re, which depends on liquid elasticity, is exceeded, the bed expansion curve shapes are identical with those for fluidization with Newtonian liquids and can be predicted with a Richardson and Zaki-type equation.

It was also found that the ratio of minimum fluidization velocity and terminal settling velocity did not depend significantly on rheological properties of the fluid. Simple relationships were proposed for the estimates of minimum fluidization velocity in both creeping flow and transient flow regions. In experimental investigations, the effect of the rectangular column walls on the bed behaviour can be strong, as shown in a more recent study[26]. The shapes of the expansion curves obtained were similar to those observed in cylindrical columns and they were independent of the construction of the liquid distributor.

References

1. Brinkman, H. C., *Appl. Sci. Res.*, **A1, 27** (1947); **A1**, 81 (1948); **A2**, 190 (1949)
2. Einstein, A., *Ann. Phys. Leipzig*, **19**, 289 (1906); **34**, 591 (1911)
3. Richardson, J. F. and Zaki, W. N., *Chem. Eng. Sci.*, **3**, 65 (1954)
4. Kos, P., *Second World Filtration Congress* (London, 18–20 September 1979), pp. 595–603
5. Baron, G. and Wajc, S., 'Fluidized settling in centrifuges, Synopsis 686', *Chem. Eng. Technol.*, **4**, 333 (1979)

6. Carman, P. C., *Flow of Gases through Porous Media*, Butterworths, London (1956)
7. Darcy, H. P. G., *Les Fontaines Publiques de la Ville de Dijon*, Victor Dalamont (1856)
8. Rudnick, S. N., 'Fundamental factors governing specific resistance of filter dust cakes', S. D. Thesis, Harvard School of Public Health, Boston, MA (1978)
9. Happel, J., 'Viscous flow in multiparticle systems', *Assoc. Ind. Chem. Eng.*, **4**, 197 (1958)
10. Ergun, S., *Chem. Eng. Prog.*, **48**, 93 (1952)
11. Chabra, R. P., *Bubbles, Drops and Particles in non-Newtonian Fluids*, CRC Press, Boca Raton, Fl. (1993)
12. Machač, I., Ulbrichova, I., Elson, T. P. and Cheesman, D. J., 'Fall of spherical particles through non-Newtonian suspensions', *Che. Eng. Sci*., **50**, 3323 (1995)
13. Machač, I., Šiška, B. and Machacova, L., 'Terminal falling velocity of spherical particles moving through a Carreau model fluid', *Chem. Eng. Proc*., accepted for publication in early 2000
14. Machač, I., Lecjaks, Z. and Šiška, B., 'Fall of non-spherical particles in a Carreau model fluid' (in Czech), 46th Conference CHISA'99, Srni 1999, paper B5.7
15. Machač, I. and Lecjaks, Z., 'Wall effect for a sphere falling through a non-Newtonian fluid in a rectangular duct', *Chem. Eng. Sci*., **50**, 143 (1995)
16. Chabra, R. P., Unnikrishnan, A. and Unnikrishnan Nair, V. R., *Can. J. Chem. Engng*., **70**, 716 (1992)
17. Šiška, B., Machač, I. and Lecjaks, Z., *Sedimentation of spherical particles in non-Newtonian liquids* (in Czech), Zborník 23. konferencie SSCHI, Závažná Poruba 1996
18. Kawase, Y. and Ulbrecht, J. J., *Chem. Engng. Comm*., **13**, 55 (1981)
19. Brea, F. M., Edwards, M. F. and Wilkinson, W. G., *Chem. Engng. Sci*., **31**, 329 (1976)
20. Šiška, B., Machač, I., Dolecek, P. and Lecjaks, Z., 'Sedimentation of spherical particles in non-Newtonian fluids in a column of rectangular cross-section', 12th International Congress CHISA, Prague (1996)
21. Šiška, B., Machač, I., Lecjaks, Z. and Cakl, J., 'A study of batch sedimentation of spherical particles in non-Newtonian fluids using image analysis', 13th International Congress CHISA, Prague (1998) (poster)
22. Machač, I., Cakl, J., Comiti, J. and Sabiri, N. E., 'Flow of non-Newtonian fluids through fixed beds of particles: Comparison of two models', *Chem. Eng. Proc*., **37**, 169–176 (1998)
23. Cakl, J. and Machač, I., 'Pressure drop in the flow of viscoelastic fluids through fixed beds of particles', *Collect. Czech. Chem. Commun*., **Vol. 60**, 1124–1139 (1995)
24. Mikulasek, P., 'Flow of non-Newtonian liquids through a fluidized bed of spherical particles' (in Czech), PhD Thesis, Faculty of Chemical Technology, University of Pardubice (1991)
25. Machač, I., Mikulasek, P. and Ulbrichova, I., 'Non-Newtonian fluidization of spherical-particle beds', *Chem. Eng. Sci*., **Vol. 48**, No. 11, 2109–2118 (1993)
26. Machač, I., Šiška, B., Lecjaks, Z. and Bena, J., 'Fluidization of spherical particle beds with non-Newtonian fluids in columns of rectangular cross-section', *Chem. Eng. Sci*., **Vol. 52**, No. 19, 3409–3414 (1997)

Particle–fluid interaction, thermodynamics of solid–liquid separation Part II—Thermodynamics of solid–liquid separation

L. Svarovsky

FPS Institute, England and University of Pardubice, Czech Republic

Nomenclature

A	Helmholtz free energy
c	Volumetric concentration of the solids (as a fraction)
E_s	Entropy index
g	Gravity acceleration
H	Total settling height
h	Height of the settled sediment
k	Boltzmann constant
N	Total number of particles in the system
N_1	Number of particles
N_2	Number of sites in the fluid
R_f	Underflow-to-throughput ratio, by volume
S	Overall entropy
S_{susp}	Entropy of the suspension
s	Specific entropy, per volume of suspension
T	Absolute temperature
U	Internal energy
V_p	Volume of a particle
V_o	Volume of the supernatant liquid in a settled system
V_1	Volume of the packed sediment
W	Number of distinguishable arrangements (multiplicity)
x	Particle size (diameter of a sphere)
Δ	Denotes a difference in the variable
$\Delta\rho$	Density difference between that of the solids and of the liquid

18.5 Introduction

The science of thermodynamics is widely used in systems involving heat or chemical change. This part of chapter 18 sets out to show that even in a cold, non-reacting system such as solid–liquid separation, thermodynamics can be very useful. The concepts of entropy and free energy can be used in:

1 developing criteria for separation efficiency;
2 obtaining a criterion to indicate whether the separation is to occur at all;
3 making estimates of sediment porosity.

The state of the art and applications in the above-mentioned aspects of solid–liquid separation are reviewed and an outline of further work and development is given.

The use of thermodynamics is well accepted and indeed essential in those areas of particle technology which involve heat and/or flow of gases. Properties of a dust-laden gas, for example, deviate from those of a perfect gas as a consequence of the finite particle volume. Internal energy, enthalpy and specific heats of a particulate system, needed in applications involving heat, are the suitably weighted means of the respective properties of the constituents (except that enthalpy of the particulate phase suspended in a gas also depends on the pressure). Another example[1] is the effect of the presence of particles on both the equilibrium and 'frozen' velocities of sound in a gas.

In contrast to the above, very little use is made of thermodynamics of 'cold' systems which do not involve flow of gases such as solid–liquid separation, yet the principles of thermodynamics underlie this subject too and can be made use of in practice.

18.6 Some notes on entropy

The concept of entropy as a general measure of the disorder of a system is, of course, highly relevant in solid–liquid separation because the degree of restoration of the order (the reduction in entropy) describes the success of the separation process. Fundamentally, entropy is a measure of the way in which the total energy of the system is distributed amongst its constituent atoms.

In order to be able to evaluate the relative reduction in entropy during or after the separation process, we have to be able to calculate the entropy of the suspension as a function of the solids concentration. The necessary relationship may be derived in analogy with a molecular model for an ideal solution as used in chemical thermodynamics[2], summarized in the following. A very small solid particle is treated simply as if it were a large molecule.

Assuming, in the first instance, mono-sized particles, completely interchangeable with pockets of fluid of the same size without affecting the

internal energy of the system, the number of distinguishable arrangements (the so-called 'multiplicity') is

$$W = \frac{(N_1 + N_2)!}{N_1!\, N_2!} \tag{18.29}$$

where N_1 and N_2 are the number of sites of particles and fluid respectively.

From molecular thermodynamics, the entropy, S, is proportional to the natural logarithm of the multiplicity W, i.e.

$$S = k \ln (W) \tag{18.30}$$

where k is really the Boltzmann constant but we shall take it as 'a constant' for the time being as we are merely after a relative measure of entropy at this stage.

Stirling's approximation for equation 18.29, used with equation 18.30, gives the entropy of a suspension

$$S_{\text{susp}} = -k\left[N_1 \ln\left(\frac{N_1}{N_1 + N_2}\right) + N_2 \ln\left(\frac{N_2}{N_1 + N_2}\right)\right] \tag{18.31}$$

In the above equation, S is used for S_{susp} because it is an extensive property for a given number of sites $N_1 + N_2$. If we now divide the right-hand side of equation 18.31 by $k(N_1 + N_2)$ we obtain entropy in arbitrary units, say specific per unit volume of suspension, s:

$$S_{\text{susp}} = -\frac{N_1}{N_1 + N_2} \ln\left(\frac{N_1}{N_1 + N_2}\right) - \frac{N_2}{N_1 + N_2} \ln\left(\frac{N_2}{N_1 + N_2}\right) \tag{18.32}$$

For the mono-disperse system, the concentrations by number in the above equation are the same as the volume, so we can write

$$S_{\text{susp}} = -c \ln c - (1 - c) \ln (1 - c) \tag{18.33}$$

where c is the concentration of particles by volume, as a fraction. Better still, if the maximum entropy (at $c = 0.5$) is to be equal to 1:

$$S_{\text{susp}} = -c \ln_2 c - (1 - c) \ln_2 (1 - c) \tag{18.34}$$

where $\ln_2$ denotes logarithm to the base 2, i.e. $\ln_2 (x) = 1.44 \ln (x)$.

Equation 18.34 is the basis of the use of the 'entropy index' defined in the following section; it should be borne in mind, however, that, strictly speaking, equation 18.34 is derived for a mono-sized suspension of fine particles only.

18.7 Entropy index

In an ideal world, solid–liquid separation separates the solids and the liquid in a suspension into a stream of dry solids going one way and a stream of pure liquid going the other way. The entropy of the whole is reduced from a given

starting value according to the initial solids concentration c in equation 18.34, down to zero ($S_{susp} = 0$ for $c = 0$).

In a real world, we always have to accept some liquid with the separated solids (in the filter 'cake' or in the system 'underflow') and some, usually fine, solids with the liquid (in the 'filtrate' of 'overflow'). In other words, neither the separation of the solids nor that of the liquid is perfect. In evaluating the efficiency of a separation process, therefore, both the separation of the solids and the separation of the liquid must be considered. In most practical applications, the emphasis on either of these two is different and they are kept separate: in thickening, for example, the goal is the separation of the liquid and the (complete) separation of the solids is secondary. In solids recovery or liquid clarification, the completeness of the separation of the solids has priority over the separation of the liquid.

If we wish to consider both the separation of the solids and that of the liquid with equal emphasis, entropy gives us an ideal tool. The efficiency of the overall separation can thus be evaluated as a fraction or percentage decrease in the entropy of the system, taking the initial entropy of the suspension (from equation 18.34) as being 100%. This definition of separation efficiency has been called the 'entropy index' and has been used widely in the Russian scientific literature[3,4].

Mathematically, the entropy index is defined as

$$E_s = \frac{S_{feed} - (S_{underflow} + S_{overflow})}{S_{feed}} \tag{18.35}$$

where S is the total entropy in the respective streams, with the origin $S = 0$ for complete separation. In terms of our specific entropy s, i.e. the entropy per unit volume of slurry, the values of entropy must be weighted by their respective volumetric contributions, and the above equation then becomes

$$E_s = \frac{s_{feed} - R_f s_{underflow} - (1 - R_f) s_{overflow}}{s_{feed}} \tag{18.36}$$

where R_f is the underflow-to-throughput ratio by volume and the values of s are evaluated from equation 18.34.

The entropy index as defined in equation 18.36 is potentially very useful in the fundamental evaluation of any separation processes, not just in solid–liquid separation. Besides the Russian references[3,4], Ogawa *et al.*[5] derived the same entropy index (but using mass fractions rather than volumetric ones) from information theory and proposed its use for the evaluation of any separation process.

The use of entropy in particle technology is not restricted to evaluations of separation efficiency. A unit-less definition of entropy virtually identical with that in equation 18.6 but in terms of probability of events, as used in information theory and proposed by Shannon[6], has been applied in geology to histograms and cumulative curves by Sharp and Fan[7] to define a sorting index for particle size analysis. Sharp[8] applied the information entropy to

define a measure of parity between the mean and the standard deviation of a distribution whilst, more recently, Full *et al.*[9] used it to define optimum class intervals of histograms or frequency plots. Entropy also has a great potential in the evaluation of the quality of mixing in powder mixing applications which are really the reverse of separation or classification.

There are two problems, however, with using equations 18.30 and 18.34 blindly, as many authors seem to do. Firstly, the multiplicity W in equation 18.30 is the total number of combinations if the phase space were to be discrete, i.e. the particle centres constrained to lattice points. For a real, continuous-phase space, W should be replaced[10] by a full $3N$-dimensional configurational integral (N being the number of particles) which has no simple solution mainly due to the lack of an adequate equation of state for liquids. Secondly, and notwithstanding the first point, equation 18.34 applies to mono-sized systems only but seems to be applied indiscriminately to all two-phase systems, including polydisperse ones. Strictly speaking, one should go back to equation 18.30 and consider the effect of the presence of particles of different sizes on their respective 'free volumes' or configuration combinations. This is bound to have some bearing on the entropy index as the size distributions of the solids in the feed, overflow and underflow are so very much different in most solid–liquid separators. More work is needed in this area.

18.8 Criterion of separation

Besides its use in assessing separation efficiency, entropy, in conjunction with internal energy, can also be used in deriving a criterion of separation[11,12]. This is in analogy with chemical thermodynamics: the value of the criterion will decide whether separation will take place spontaneously or not at all. Only a summary of the derivation is given in the following.

The Helmholtz free energy, ΔA, for a non-flow process, is calculated from the change in internal energy, ΔU, and the change in entropy, ΔS

$$\Delta A = \Delta U - T\Delta S \tag{18.37}$$

where T is the absolute temperature.

For a spontaneous process A decreases, so the condition for separation to take place is

$$-T\Delta S < -\Delta U \tag{18.38}$$

(as both changes are normally negative), i.e. if we define

$$\text{separation criterion} = \frac{\Delta U}{T\Delta S} \tag{18.39}$$

the separation will take place if the value is greater than 1 and it is impossible if the value is less than 1.

The problem now is how to calculate the changes in entropy and in internal energy for a specific case and arrive at values which are not merely relative (in arbitrary units such as in the previous section) but absolute, measured from a standard state. Attempts have been made to calculate the values of the criterion for some special cases[11,12] and only a relatively simple case of gravity settling is described here for illustration.

In the calculation of the change of entropy, ΔS, the following assumptions are made:

1 mono-disperse system;
2 complete separation;
3 negligible liquid in sediment;
4 analogue of 'regular solution', without excess free energy of mixing of particles and liquid molecules;
5 dilute suspension.

The result is[11]

$$\Delta S = -kN \ln (V_o/V_l) \tag{18.40}$$

where N is the number of particles, k is the Boltzmann constant, V_o is the volume of the supernatant liquid and V_l is the volume of the packed sediment.

For mono-disperse, non-interacting particles, the change in internal energy, ΔU, is equal to the change in the potential energy of the settling system. Taking the heights from *Figure 18.2* (H is total settling height, h is the height of the sediment after separation), the change in internal energy can be calculated as

$$\Delta U = -NV_p \Delta\rho g(H/2 - h/2) \tag{18.41}$$

where V_p is the single particle volume and $\Delta\rho$ is the density difference between the solids and the liquid.

Assuming that V_l/V_o is approximately equal to the volumetric concentration of the solids (for dilute suspensions) and taking a spherical particle of

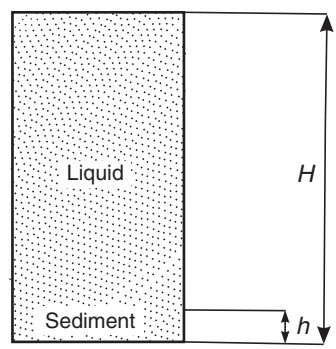

Figure 18.2 Definition of settling heights for equation 18.41

diameter x, the sedimentation criterion may be calculated from equations 18.39, 18.40 and 18.41:

$$\text{sedimentation criterion} = \frac{\pi g \Delta \rho x^3 H(1-c)}{12kT \ln(1/c)} \tag{18.42}$$

It is rather surprising to find that the value of the criterion which decides whether the settling will or will not take place depends on the absolute value of the settling distance, H. Taking an example of a 1-μm particle settling through 20 cm at $\Delta\rho = 1600\,\text{kg m}^{-3}$ and 20 °C, the value of the criterion is 436663. To bring this value below 1, one would need a particle less than 0.013 μm in size, which would not settle under gravity in the above system; this is quite a credible value considering that it has been derived solely from thermodynamics without any input from the theories of settling or diffusion.

The separation criterion may also be derived for polydisperse systems[11] in terms of summations, and this makes it possible to establish the likelihood of the separation of any particular fraction of the particle population.

In general, the evaluation of the separation criterion is subject to much the same criticisms as is the entropy index. In this case, however, the problem is even more difficult due to the fact that absolute changes in entropies and internal energies are needed. More work is needed to establish these quantities for particulate suspensions, with the inevitable particle–particle interactions and excess free energies of mixing. Textbooks on thermodynamics are remarkably silent on the subject of thermodynamics of particulate systems and suspensions.

18.9 Estimates of sediment porosity

Reasoning very similar to that in deriving the separation criterion can also be used for making estimates of sediment porosity. The liquid content in the sediment is not neglected this time, however, and the equilibrium condition of the separation criterion equal to 1 is used[11], i.e. when no more settling can take place in the sediment. This is the least researched area, however, requiring much more realistic assumptions about the thermodynamics of real, polydisperse systems than in the cases of the entropy index and separation criterion. The only study on this subject known to the author[11] does not include the effect of the interaction energies of the particles with one another, an omission hardly acceptable for particles in close proximity in the sediment. The potential in this area is great, however, and a serious study is needed.

18.10 Conclusions

The thermodynamics of suspensions is a subject much neglected in textbooks, yet there are many potential uses, particularly in solid–liquid separation. A

review of the state of the art has revealed at least three important applications where thermodynamics can make a real and practical contribution. The available literature shows a sizeable Russian lead but their initial proposals and ideas need fine tuning. It is hoped that this review will stimulate further work in this area.

References

1. Rudinger, G., *Fundamentals of Gas-Particle Flow, Handbook of Powder Technology*, Vol. 2, Elsevier, Amsterdam (1980)
2. Pitzer, K. S. and Brewer, L., *Thermodynamics*, McGraw-Hill, New York (1961)
3. Agranonik, R. Ya., Shishmakov, S. Yu. and Shamanaev, Sh. Sh., 'Application of the entropy index to evaluate the efficiency of separator operation', *Chem. Petrol Eng.*, **19**, 227–229 (1984)
4. Sulla, M. B. and Fikhtman, S. A., 'Application of the entropy index to evaluate the efficiency of thickening equipment', *Vodosnabzhenie i Sanitarnaya Tekhnika*, **11**, 11–13 (1972)
5. Ogawa, K., Ito, S. and Kishino, H., 'A definition of separation efficiency', *J. Chem. Eng. Jpn.*, **11**, 44–47 (1978)
6. Shannon, E., *Bell System Technol. J.*, **379**, 623 (1948)
7. Sharp, W. E. and Fan, P., 'A sorting index', *J. Geol.*, **71**, 76 (1963)
8. Sharp, W. E., 'Entropy as a parity check', *Earth Res.*, **1**, 27 (1973)
9. Full, W. E., Ehrlich, R. and Kennedy, S., 'Optimal definition of class intervals of histograms or frequency plots'. In *Morphological Analysis, Particle Characterisation in Technology* (J. K Beddow, Ed.), Vol. II, Chap. 11, CRC Press Inc., Boca Raton, FL (1984)
10. Woodcock, L., private communication (1988)
11. Figurovskii, N. A. and Sokolov, N. V., 'Thermodynamics of sedimentation', *Russian J. Phys. Chem.*, **55**, 111–112 (1981)
12. Kutepov, A. M. and Sokolov, N. V., 'Thermodynamics of separation processes', *Theor. Found. Chem. Eng.*, **76**, 287–291 (1982)

Index